IES Recommended Practice 012.1

Handbook

for

Dynamic Data Acquisition and Analysis

Prepared by:

Harry Himelblau
Jet Propulsion Laboratory
California Institute of Technology
4800 Oak Grove Drive
Pasadena, CA 91109-8099

Allan G. PierSol
Piersol Engineering Company
23021 Brenford Street
Woodland Hills, CA 91364-4830

James H. Wise
Jet Propulsion Laboratory
California Institute of Technology
4800 Oak Grove Drive
Pasadena, CA 91109-8099

Max R. Grundvig
The Aerospace Corporation (retired)
947 Quail Ridge Road
Washington, UT 84780

Institute of Environmental Sciences
940 East Northwest Highway
Mount Prospect, IL 60056
Tel: (708) 255-1561
FAX: (708) 255-1699

This page is left for IES Material on the back of the ~~cover~~ title page.

FOREWORD

This Handbook was prepared by the Jet Propulsion Laboratory (JPL), California Institute of Technology, for the Space arid Missile Systems Center, U.S. Air Force Materiel Command, through an agreement with the National Aeronautics and Space Administration. Support was also provided by The Aerospace Corporation. The original intent was to publish this document as a Military Handbook. Subsequently, the sponsor decided against dissemination in this form and turned the Handbook over to JPL for publication elsewhere. Since the Institute of Environmental Sciences (IES) had long been interested in using the document as a Recommended Practice, the authors considered it appropriate to turn the document over to the IES for that purpose. The Air Force has released the copyright to JPL control with the stipulation that the U.S. Government retain an unrestricted license for its use.

The authors received substantial assistance in the preparation of this Handbook from a number of reviewers. The most important of these reviewers were as follows: Larry Bement and James Schoenster of NASA Langley Research Center; Robert Bohle of Kistler Instrument Corp.; Anthony Chu of Endevco; Charles Coe of NASA Ames Research Center; John Favour and Clark Beck of Boeing Aerospace Corp.; Dennis Foti of Metrum Information Storage; Arnold Galef, George Scott, Charles Wright, and Glenn Wasz of TRW Space and Electronics Group; Gerry Kahre, Marc Hoskins, Dan Powers, David Sherry, and Paul Spas of McDonnell Douglas Space Systems Co,; Dennis Kern of JPL; Ronald Merritt of NAWC/China Lake; James Nagy of PRC/Patuxent; Dennis Nelson and David Small wood of Sandia National Laboratories; Peter Rentz of Syscon Corp.; Karl Siwiecki and James Lally of PCB Piezotronics; Strether Smith and William Hollowell of Lockheed Research Laboratory; Vladimir Valentekovich of Wyle Labora tones; Joseph Weatherstone and William Brennan of Brüel & Kjaer Instruments; and Scott Walton of ACSTA/Aberdeen.

Some reviewers read every word of several drafts, while others concentrated on sections that embodied their areas of expertise. Some furnished illustrations previously unknown to the authors, whereas others performed research to resolve controversial technical issues. Of particular value were independent studies of the pyroshock measurement problem performed by Dan Powers of McDonnell Douglas Space Systems Co., with the close support of Richard Chalmers of the Naval Ocean Systems Center, Howard Gaberson of the Naval Facilities Engineering Services Center, and Anthony Chu of Endevco. The results of those studies contributed substantially to the discussions and recommendations for the pyroshock data acquisition and analysis procedures presented in Appendix A of the Handbook.

Although not identified here, other reviewers made significant though less comprehensive suggestions. All made substantial contribution to the list of references, which is considered the heart of the Handbook.

TABLE OF CONTENTS (Continued)

3.3 Signal Conditioners ---------- ---------- 94
3.3.1 Strain Gage Conditioners ------- ---------- ---94
3.3.2 Amplifiers - ---------- ---------- ---96
3,3,3 Filters---------- ---------- 100
3.3.4 Power Supplies ---------- ---------- ---- 103
3.3.5 Cabling ---------- 103
3.4 Multiplexers and Demultiplexers ---------- -------- 106
3.4.1 FrequencyDivision Multiplexing- ---------- --- 107
3.4.2 TimeDivision Mutliplexing ------ ---------- -112
3.4.3 Demultiplexers ---------- ----------119
3.5 Communication Links ---------- ----------121
3.5,1 LandLines ---------- ---------- --------121
3.5,2 RadioFrequencyTelemetry ---------- ------121
3,6 Data Recording, Playback and Storage ---------- -----123
3.6.1 DataCapacity ---------- ----------124
3.6.2 FrequencyResponse ---------- ----------124
3.6.3 Recording Modes ---------- ---------- ---125
3.6.4 FDM Recording ---------- ---------- -126
3.6.5 TDM Recordin ---------- ---------- -126
3.6.6 Ancillary Data Recording ---------- 130
3.6.7 Tape C· yang ---------- ---------- ---131
3.6.8 Tape Storage ---------- ---------- --- 131
3.7 Analog-t-Digital Converters---- ---------- ------- 133
3.7.1 Instruments ---------- ---------- ----133
3.7.2 Sampling RateandAliasing ------ ---------- - 136
3.7.3 Anti-Aliasing Filters and Errors ---------- 137
3.7.4 Other ADC Errors ---------- ---------- ---- 139
3.7.5 Multi-ChannelDigital Conversion ---------- ----- 140
3.7.6 Digital-to-Analog Converters ----- ---------- - 141
3.8 System calibration ---------- ---------- ---------141
3.8.1 Laboratorycalibration -------- ---------- --- 141
3.8.2 End-to-End Electrical Calibration-- ---------- - 144
3.8.3 End-to-End Mechanical Calibration ---------- --- 148
3.8.4 Linearitycalibrations --------- ---------- --- 152
3.9 SystemGain Settings ---------- ---------- ----- 153
3,9.1 Stationary and Steady-State Data with On-line Control ---------- 153
3.9.2 NonstationaryandTransientData- ---------- ---154
3.10 Record Keeping (Log Sheets) ---------- 155
3.11 References ---------- ---------- ----- 156

TABLE OF CONTENTS

Page

LIST OF TABLES ---------- x
LIST OF FIGURES ---------- xi
LIST OF SYMBOLS ---------- xx
LIST OF ABBREVIATIONS ---------- xxi

1 INTRODUCTION ---------- 1
1.1 Historical Background ---------- 1
1.2 Purpose ---------- 1
1.3 Inclusions and Exclusions ---------- 1

2 DYNAMIC MEASUREMENT PLANNING ---------- 3
2.1 Introduction ---------- 3
2.2 Measurement Numbers, Locations, and Directions ---------- 7
2.3 Frequency Ranges ---------- 9
2.4 Dynamic Ranges ---------- 10
2.5 MeasurementDurations ---------- 13
2,6 Multi-Channel Measurements ---------- 14
2.7 Time Codes ---------- 15
2.8 Error Budgets ---------- 15
2.8.1 Error Source Identification and Qualification ---------- 16
2.8.2 ErrorBudget Preparation ---------- 16
2.8.3 System ErrorCalibration ---------- 16
2.8.4 System Error Utilization ---------- 17
2.9 Instruments and/or Software Selection and Vendor Evaluation ---------- 17
2.10 MajorCausesofErrors ---------- 18
2.11 References ---------- 20

3 DATA ACQUISITION ---------- 25
3.1 Introduction ---------- 25
3.2 Transducers ---------- 25
3.2.1 SensingElements ---------- 25
3.2.2 Single-Degree-of-Freedom System ---------- 31
3.2.3 Measurement Parameters ---------- 34
3.2.4 Environmental Effects ---------- 46
3.2.5 Physical properties ---------- 59
3.2.6 MotionTransducers ---------- 63
3.2.7 PressureTransducers ---------- 82
3.2.8 Strain Gages ---------- 86
3.2.9 ForceTransducers ---------- 92

TABLE OF CONTENTS (Continued)

4 DATA VALIDATION AND EDITING ---------- -.. -,---------- 165
4.1 Introduction ---------- ---------- -------- 165
4.2 Identification of Physical Events - ---------- ---------165
4.2.1 Random Versus Periodic Signals-- ---------- -- 165
4.2.2 Time-Varying Signals --------- ---------- ---- 168
4,3 Visual Inspection of Analog Time Histories ---------- -- 170
4.3.1 Signal Clipping ---------- 170
4.3.2 Excessive Background Noise--- ---------- ------ 172
4.3.3 Intermittent Noise ---------- ---------- -----174
4.3.4 Powerline Pickup ---------- ---------- ---176
4.3.5 SpuriousTrends ---------- ---------- ---178
4.3.6 Signal Drop-Outs ---------- ---------- ---180
4,4 Visual Inspection of Digital Time Histories ---------- --- 181
4.4.1 Signal Clipping ---------- ---------- -182
4.4,2 Excessive Background Noise-- ---------- -------182
4.4,3 WildPoints ---------- ---------- ---182
4.4.4 SpuriousTrends ---------- ---------- -- 183
4.4.5 Other ADC Malfunctions ------ ---------- ----- 184
4.5 Visual Inspection of Analyzed Data ---------- ------- 184
4.5.1 ProbabilityDensityPlots ------- ---------- ---- 184
4.5.2 Narrowband Spectral Analysis-- ---------- ----- 186
4.6 Corrective Editing of Time Histories ---------- ------- 189
4.6.1 Corrections for Excessive Background Noise ---------- 189
4.6.2 Removal ofIntermittentNoise Spikes andWildPoints ---------- 190
4.6.3 Removal ofSpuriousTrends ---- ---------- ---191
4.6.4 Removal ofTemporary SignalDmp-Outs --- ----------191
4.7 Identification of Periodic Components ---------- ------ 193
4.7,1 Narrowband Spectral Analysis - - - ---------- ---- 193
4.7.2 Band-Limited Probability Density Analysis ---------- ----- 193
4.8 Identification of Nonstationary Trends ---------- ------194
4.8.1 BasicConsiderations -------- ---------- ------ 194
4.8.2 Test Statistic ---------- ---------- -----195
4.8.3 Decision procedure ---------- ---------- ---- 196
4.8,4 Illustration ---------- ---------- ------ 197
4.9 Reference s---------- ---------- --------198

TABLE OF CONTENTS (Continued)

5 DATA ANALYSIS ---------- 201
5.1 Introduction ---------- 201
5.2 TimeHistories ---------- 201
5,2.1 Instantaneous Values ---------- 201
5.2.2 Average Values ---------- 203
5.2.3 SynchronousAveraging ---------- 205
5.2.4 Filtered Signals ---------- 206
5.3 Data Classification ---------- 207
5.3.1 TimeDependence ---------- 207
5.3.2 Randomness ---------- 209
53.3 Normality ---------- 210
5.4 Single Channel Spectral Analysis-Periodic andRandomData ---------- 210
5.4.1 FFT Algorithms ---------- 211
5.4.2 PeriodicData ---------- 214
5.4.3 Stationary Random Data ---------- 218
5.4.4 NonstationaryData ---------- 224
5.4.5 Proportional Bandwidth Spectra ---------- 225
5.5 SingleChannelSpectralAnalysis- TransientData ---------- 227
5.5.1 FourierSpectra ---------- 227
5.5.2 Energy Spectra ---------- 229
5.5.3 Shock Response Spectra ---------- 231
5.6 Dual ChannelAnalysis- ---------- 237
5.6.1 Cross Spectra ---------- 237
5.6.2 Coherence ---------- 241
5.6.3 Frequency Response ---------- 243
5.6.4 Cross Correlation ---------- 246
5.6.5 CorrelationCoefficient ---------- 247
5.6.6 UnitImpulseResponse ---------- 248
5.7 Other Analyses ---------- 248
5.7.1 ProbabilityDensity ---------- 248
5.7.2 Parametric SpectralAnalysisProcedures ---------- 250
5.7.3 Miscellaneous Signal Processing Procedures ---------- 251
5.8 References ---------- 252

TABLE OF CONTENTS (Continued)
APPENDICES

A PYROSHOCK DATA ACQUISITION AND ANALYSIS ---------- 259
A.1 Introduction ---------- ---------- -------- 259
A.2 Summary of Data Acquisition and Analysis Problems ---------- 260
A.2.1 Transducers ---------- ---------- -- 261
A.2.2 Signal Conditioners ---------- ---------- ---- 265
A.2.3 Electrical Lowpass Filter ------ ---------- ---- 267
A.2.4 Mechanical Lowpass Filters ---- ---------- ---- 267
A.2.5 Data RecorderS and Storage ---- ---------- ---- 268
A.2.6 Anti-Aliasing Filters and Analog-to-Digital Converters ---------- 268
A.2.7 Analysisprocedures ---------- ---------- 269
A.3 Guidelines and Recommendations ---------- -------- 271
A.3.1 MeasurementLocations ------- ---------- ---- 271
A.3.2 Accelerometers ---------- ---------- ---- 272
A.3.3 Signal Conditioners ---------- ---------- ---- 275
A.3.4 DataRecorders ---------- ---------- ---- 275
A.3.5 Data Sampling and Editing ------ ---------- -- 276
A.3.6 DataAnalysis ---------- ---------- ----- 277
A.4 Other Pyroshock Measurement Procedures ---------- - 283
A.5 References ---------- ---------- -------- 284

B NONSTATIONARYRANDOMVIBROACOUSTICDATAANALYSIS ---------- 287
B.1 Introduction ---------- ---------- --------- 287
B.2 NonstationaryTime Intervals ---------- ---------- 287
B.3 Maximax Spectrum ---------- ---------- -------- 288
B.4 Nonstationary Aeroacoustic Data Analysis ---------- --- 288
B.4.1 General DataAnalysisProcedure - ---------- --- 291
B.4.2 Averaging procedures ------- ---------- ----- 292
B.4.3 GeneralAveragingTimeSelection Procedure ---------- ---- 292
B.4.4 Procedures for Titan IV and Space Shuttle Lift-Off Acoustic Data ------- 293
B.5 NonstationaryVibration DataAnalysis ---------- ----- 294
B.5.1 General Data Analysis Procedure ---------- ----- 296
B.5.2 FrequencyResolution Bandwidth-- ---------- 296
B.5.3 Averaging Procedures -------- ---------- ---- 298
B.5.4 General AveragingTime Selection Procedure ---------- ----- 298
B.5.5 Procedures for Titan IV and Space Shuttle Lift-OfTVibrationData ------- 299
B.6 Alternate Nonstationary Data Analysis Procedures ---------- 300
B.7 References ---------- ---------- ---------- 301

LIST OF TABLES

Page

3.1 Qualitative Comparison of Piezoelectric Accelerometer Designs ----------69

3.2 Proportional Bandwidth FM Subcarrier Channels- ----------108

3.3 Constant Bandwidth FM Subcarrier Channels ----------109

3.4 Reference Frequencies for Tape Speed Control and Flutter Compensation ------- 110

3.5 Constant-Amplitude Tape Speed Control Signals ---------- 111

3.6 Optimum Frame Synchronization Patterns for PCM Telemetry ----------116

3.7 Magnetic Tape Speeds and Recording Time ----------124

3.8 Direct Record and Reproduce Parameters ---------- 125

3.9 Wideband and Double-Density FM Record Parameters ---------- 127

3.10 Predetection Carrier Parameters ---- ---------- -----128

3.11 Maximum Recommended Bit Rates for Postdetection Recording ---------- 128

3.12 Maximum Recommended Bit Rates for Serial High Density Digital Recording ---- 129

3.13 Decimal Digits and Peak Signal-to-Noise Level for Analog-to-Digital Converters --- 135

4.1 Percentage Points for the Reverse Arrangements Distribution ---------- 196

LIST OF FIGURES

Page

2.1 Vibration Measured on S-IVB Stage of the Uprated Saturn 1 Space Vehicle during Apollo-Saturn Flight SA-203 ---------- 4

2.2 Typical Instrumentation Systems for Data Acquisition and Analysis ---------- 5

2.3 Diagram of Data Acquisition System for Wind Tunnel Aerodynamic Noise Test ---- 6

3.1 Data Acquisition Instrument Selection Guide ----------26

3.2 Some Typical Data Acquisition Instrument Configurations ----------27

3.3 Circuit Diagram of a Whetstone Bridge for Strain Sensitive Materials, including Metallic and Semiconductor (Piezoresistive) Strain Gages and Transducers --------- ---------- 28

3.4 Normalized Response of a Linear Single-Degree-of-Freedom System to Sinusoidal Force or Base Acceleration Excitation ---------- 32

3.5 Phase Angle Between the Sinusoidal Response and Excitation for a Linear Single-Degree-of-Freedom System- ---------- -- 33

3.6 Range of Single-Degree-of-Freedom System Responses Normally Used in Accelerometer and Pressure Transducer Design ---------- 33

3.7 Range of Single-Degree-of-Freedom System Phase Angles Normally Used in Accelerometer and Pressure Transducer Design ---------- 34

3.8 Normalized Relative Velocity Response of a Linear Single-Degree-of-Freedom System to Sinusoidal Velocity Base Excitation ---------- 35

3.9 Typical Frequency Response for a Family of Similarly-Designed Condenser Microphones ---------- ---------- 37

3.10 Typical Frequency Response for a Piezoelectric Accelerometer, Normalized to the Sensitivity at 100 Hz -- ---------- 38

3.11 Useful Operating Range for a Piezoelectric Accelerometer ----------40

3.12 Diagrammatic Representation of Transverse Sensitivity for a Piezoelectric Accelerometer -------- ---------- - 41

LIST OF FIGURES (Continued)

3.13 Diagrammatic Representation of Transverse Sensitivity Well Below Transverse Resonance for a Piezoelectric Accelerometer ---------- 42

3.14 Typical Frequency Response of a Piezoelectric Accelerometer in a Transverse Direction Relative to the Intended Direction ---------- 42

3,15 Directional Response of an Electret Microphone ----------44

3.16 Typical Microphone Frequency Response for Two Free-Field Directions and Random Incidence ------ ---------- ----------44

3.17 Frequency Response of a Microphone or Pressure Transducer to Normal Boundary Layer Turbulence at Grazing Incidence ---------- 45

3.18 Temperature Sensitivity of Five Different Piezoelectric Ceramics, Normalized to the Sensitivity at 68 deg F ---------- ---------47

3.19 Temperature Sensitivity of a Typical Piezoelectric Material in tie Vicinity of a Curie Point ----"---------- 47

3.20 Temperature Effects on the Frequency Response of a Piezoresistive Accelerometer with Oil Damping ---- ---------- ----48

3.21 Temperature Effects on the Frequency Response and the Sensitivity at 1 kHz for a Free-Field Condenser Microphone ---------- 49

3.22 Methods of Protecting an Accelerometer from High or Low Temperatures ------- 50

3.23 Condenser Microphone with Water-Cooled Protective Cap ---------- 50

3.24 Temperature-Compensated Strain Gage, Which Uses the Same Thermal Expansion Coefficient as the Structure, Connected into One Arm of a Wheatstone Bridge Circuit -- ----------51

3.25 Average Thermal Expansion Coefficient (from 68 deg F to Final Temperature) for 2024-T4 Aluminum ---------- 51

3.26 Typical Temperature-Induced Apparent Strain for Three Commonly-Used Strain Gage Metal Alloys- ---------- 52

3.27 Typical Temperature-Induced Gage Factor Variation for Three Commonly-Used Strain Gage Metal Alloy s ---------- 52

LIST OF FIGURES (Continued)

3.28 Compensating Bridge Circuit, Comprised of Two Strain Gages Connected in Adjacent Arms with One Gage Exposed to Static and/or Dynamic Strain and Both Exposed to the Same Temperature ---------- 53

3.29 Typical Accelerometer Output After Sudden Immersion in Ice Water ---------- 54

3.30 Static Pressure Effects on the Frequency Response and the Sensitivity at 250 Hz (Normalized to the Sensitivity at Standard Atmospheric pressure) for Two Condenser Microphones ---------- 55

3.31 Connector Encapsulation by a Sealant to Prevent Moisture penetration ---------- 56

3.32 Multiple Layer Sealing of a Strain Gage to Prevent Liquid and Moisture Penetration ---------- 56

3.33 Structure-Accelerometer Interaction Which Causes Structural Stiffening and Accelerometer Base Strain ---------- 58

3,34 Cross-Section of a Vibration-Compensated Piezoelectric Microphone ---------- 60

3.35 Large and Small Strain Gages Measuring Spatial-Average Strains over their Grid Areas ---------- 61

3.36 Circuit Diagram of a Piezoelectric Transducer and Voltage Amplifier ---------- 64

3.37 Circuit Diagram of a Piezoelectric Transducer and Charge Amplifier ---------- 64

3.38 Circuit Diagram of a Piezoelectric Transducer with Integral Electronic Amplifier and External Power Supply ---------- 65

3.39 Cut-Away View of a Single-Ended Compression Piezoelectric Accelerometer ---------- 66

3.40 Cross-Section of an Inverted Isolated Compression Accelerometer with Integral Electronic Amplifier ---------- 66

3.41 Cut-Away View of a Ring Shear Piezoelectric Accelerometer ---------- 67

3.42 Cut-Away View of a Miniature Ring Shear Piezoelectric Accelerometer with a Center Mounting Hole ---------- 67

LIST OF FIGURES (Continued)

3.43 Cut-Away View of a Plate Shear Piezoelectric Accelerometer ---------- 68

3.44 Disassembled View of a Plate Shear Piezoelectric Accelerometer ---------- 68

3.45 Cress-Section of a Beam Bender Piezoelectric Accelerometer for Bi-directional Measurements ------- ---------- 69

3.46 Method of Measuring Rotational Acceleration with a Matched Pair of Translational Accelerometers- ---------- -----70

3.47 Cantilever-Mass Piezoresistive Accelerometer Using Four Semiconductor Strain Gages ---------- 70

3,48 Twin Cantilever-Mass Piezoresistive Accelerometer Using Monolithic Semiconductor Strain Gage Sensing Elements ---------- 71

3.49 Disassembled View of a Servo-Accelerometer ---------- 72

3.50 Circuit Diagram of a Servo-Accelerometer ---------- 73

3.51 Cut-Away View of a Velocity Pickup ----- ---------- 74

3.52 Schematic Diagram of a Laser Doppler Vibrometer ---------- 75

3.53 Useful Operating Range for a Laser Doppler Vibrometer ---------- 76

3,54 Extended Cube Mounting Block of Matched Accelerometers for Measuring In-Plane Motion and Bending-Induced Rotations ---------- 78

3.55 Typical Effects of Various Mounting Techniques on the Frequency Response of Accelerometer ---------- - 80

3.56 Cross-Section of a Pressure Gage Using Diaphragm/Beam-Loaded Metallic Strain Gages ---------- ---------- 82

3.57 Cut-Away View of a Miniature Piezoresistive Pressure Transducer and Enlarged Cross-Section of Silicon Diaphragm Showing Semiconductor Strain Gage Locations ---------- --- 84

3.58 Cut-Away View of a Condenser Microphone- -------- u ---------- 85

3.59 Cross-Section of an Electret Microphone ---------- `---------- 85

LIST OF FIGURES (Continued)

3.60 Various Metallic Foil Strain Gage Sizes Shapes and Configurations ---------- 87

3.61 Typical Semiconductor or Piezoresistive Strain Gages ---------- - 88

3.62 Typical Metallic Crack Detection or Crack Propagation Gages ---------- 88

3.63 Arrangement of Four Matched Strain Gages for Measuring Direct (Tension-Compression) Internal Loads While Canceling Measurements of Bending and Insensitive Torsion Loads ---------- 89

3.64 Arrangements of Four Matched Strain Gages for Measuring Bending Internal Loads in One Plane While Canceling Measurements of Bending in the Other Plane, and Insensitive to Direct and Torsion Loads ---------- 89

3,65 Arrangements of Four Matched Strain Gages for Measuring Torsion Internal Loads While canceling Measurements of Direct and Bending Loads --------- ---------- ---90

3.66 Metallic Strain Gage Patterns for Diaphragm Pressure Gages ---------- 90

3.67 Miniature Semiconductor or Piezoresistive Strain Gages for Installation in Accelerometers and Pressure Transducers ---------- 91

3.68 Cress-Section of a Piezoelectric Force Transducer with Integral Electronic Amplifier ------- ---------- --- 93

3.69 Cut-Away View and Sensing Element Connections of a Triaxial Piezoelectric Force Transducer with a Center Mounting Hole ---------- ---------- 94

3.70 Circuit Diagram of a Typical Strain Gage Signal Conditioner ---------- 95

3.71 Typical Slew Rate Limiting of an Amplifier- ---------- 97

3.72 Shield Coupling of an Amplifier with Floating Shield ---------- 98

3.73 Circuit Diagram of a Guarded Differential Amplifier with Ground Locations at Each End of the Circuit ----------98

3.74 Circuit Diagram of a Differential Strain Gage Amplifier with Ground Locations at Each End of the Circuit ----------99

LIST OF FIGURES (Continued)

3.75 Circuit Diagram of a Differential Charge Amplifier with Ground Locations at Each End of the Circuit- ---------- 99

3.76 ElectricalF ilterTypes ---------- ----------100

3.77 Triboelectric Noise Itineration in a Coaxial Cable ---------- 104

3.78 IRIG Standard Pulse Code Modulation Frame Structure ---------- 113

3.79 IRIG Standard Pulse Code Modulation Binary Codes ---------- 115

3.80 IRIG Standard 50 Percent Duty Cycle Pulse Amplitude Modulation with Amplitude Synchronization ---------- 117

3.81 IRIG Standard 100 Percent Duty Cycle Pulse Amplitude Modulation with Amplitude Synchronization ---------- 118

3.82 Recommended Temperature and Humidity Ranges to Avoid Magnetic Tape Deterioration ---------- 132

3.83 Schematic Diagram for a Simple Analog-to-Digital Converter ---------- 133

3.84 Illustration of Aliasing due to an Inadequate Digital Sampling Rate ---------- 136

3,85 Illustration of Aliasing Error in the Computation of an Autospectral Density Function ----- ---------- ---- 137

3.86 Illustration of Linear Phase Shift due to Time Delay between Two Instrumentation Channels or Tracks with a Common Input Random Signal ---------- ---------- --- 143

3.87 Illustration of Coherence due to Lack of Phase Lock between Two Instrumentation Channels or Tracks with a Common Input Random Signal ---------- ---------- 143

4,1 Outline of Data Evaluation and Editing Procedures- ---------- 166

4.2 Illustration of Periodic, Random, and Mixed Signals ---------- 167

4.3 Illustration of Transient and Nonstationary Random Signals ---------- 169

4.4 Identification of Physical Events in Space Shuttle Launch Vibration Signal ------- 169

LIST OF FIGURES (Continued)

4.5 Illustration of Clipped Periodic, Random, and Transient Signals ---------- 171

4,6 Illustration of Excessive Instrumentation Noise in Periodic, Random, and Transient Signals -------- ---------- ---------- 173

4.7 Illustration of Intermittent Noise in Periodic, Random, and Transient Signals ----- 175

4.8 Illustration of Power Line Pickup in Periodic, Random, and Transient Signals ---- 177

4.9 Illustration of Spurious Trend in Periodic, Random, and Transient Signals ------ 179

4.10 Illustration of Drop-Outs in Random Signals ---------- 181

4.11 Illustration of Excessive Digital Due to Inadequate Input Signal Level to ADC ----- 183

4,12 Influence of Signal Clipping and Intermittent Noise on Probability Density Plots --- 185"

4.13 Influence of Power Line Pick-up and Signal Drop-Outs on Probability Density Plots ------ ---------- ------187

4.14 Influence of Instrumentation and Power Line Pickup Noise on Spectral Density Plots ------ ---------- ---------- 188

4.15 Noise Floor Correction Factors for Spectral Density Estimates of Random Signals ---------- ---------- ---------- 190

4,16 Selection of Time Segments for Spectral Analysis of Signals with Dropouts ----- 192

4.17 Sequence of Short Time-Averaged RMS Value Estimates of a Random Signals ----198

5.1 Outline of Data Analysis Procedures ---------- 202

5.2 Normalized Random Errors for Mean and Mean Square Value Estimates -------- 204

5.3 Signal-to-Noise Level Enhancement with Synchronous Averaging ---------- 206

5.4 Rectangular (Untapered) Window for Spectral Analysis of Stationary Signals ----- 213

5.5 Harming Window for Spectral Analysis of Stationary Signals ----------213

5.6 Frequency Correction for Periodic Component in Line Spectrum ---------- 217

5.7 Amplitude Correction for Periodic Component in Line Spectrum ----------218

LIST OF FIGURES (Continued)

5.8 Frequency Resolution Bias Error for Peaks in Spectral Density Estimates -------- 221

5.9 Normalized Random Error for Autospectral Density Estimates ---------- 223

5.10 Exponential Window for Spectral Analysis of Transient Signals ---------- 228

5.11 Mechanical Analog for Shock Response Spectrum Computation ---------- 232

5.12 Time Delay Bias Error for Cross-Correlation, Cress-Spectral Density, and Frequency Response Magnitude Estimates ------- ------- ------- ----.239

5.13 Normalized Random Error for Cross-Spectral Density Estimates ---------- 240

5.14 Time Delay Bias Error for Coherence Estimates ---------- 242

5.15 Normalized Random Error for Coherence Estimates ---------- 243

5.16 Normalized Random Error for Frequency Response Estimates ---------- 245

5.17 Normalized Random Error for Cross-Correlation Estimates ---------- 247

5.18 Probability Density Functions of Peak Values in Gaussian Random Signals versus Spectral Parameter α ---------- 251

A.1 Typical Pyroshock Acceleration Signal Measured with 20 kHz Bandwidth ------- 259

A.2 Near-Field Pyroshock Velocity Signal Measured with 1 MHz Sampling Rate- ----- 260

A.3 Pyroshock Acceleration Signal Measured with 80 kHz Bandwidth Showing Accelerator Case Resonance ------- ---------- ----262

A.4 Pyroshock Acceleration Signal with Zero-Shift due to Overload of Accelerometer Piezoelectric Element - ---------- --- 263

AS Pyroshock Acceleration Signal with Zero-Shift due to Acceleration Malfunction and/or Amplifier Saturation ---------- ---263

A.6 Accelerometer Mounting Procedure for In-Plane Pyroshock Measurements ------ 264

A.7 Pyroshock Acceleration Signal with Zero-Shift due to Amplifier Saturation ------ 266

A.8 Maximax Shock Response Spectra for Sinusoidal Forcing Function versus Number of Half-Cycles-- ---------- ---------- 270

LIST OF FIGURES (Continued)

A.9 Typical Maximax Acceleration Shock Response Spectrum for Pyroshock on Heavy Aluminum Structure-- ---------- ----------271

A. 10 Pyroshock Acceleration and Velocity Signals for Valid and Invalid Measurements ---------- ---------- ----278

A. 11 Pyroshock Acceleration and Velocity Signals, and Positive and Negative Acceleration Shock Response Spectra for Valid Data ---------- ------281

A. 12 Pyroshock Acceleration and Velocity Signals, and Positive and Negative Acceleration Shock Response Spectra for Invalid Data ---------- 282

B. 1 Running Averages of Overall SPL Inside Titan IV Payload Shroud During Lift-Off ---------- 290

B.2 Procedure for Estimating Time-Varying Autospectral Density Function --------- 294

LIST OF SYMBOLS

a(t)	acceleration signal time history
B	Frequency bandwidth, Hz
B_{hp}, B_r	Half-power point bandwidth
c	Damping coefficient
c_L	Longitudinal wave velocity
c_B	Bending wave velocity
c	Capacitance, various constants
$C_{xy}(f)$	Co-spectrum of x(t) and y(t)
d	Diameter
D	Modulus of rigidity
E[ ]	Expected value of [ ]
$E_{xx}(f)$	Energy spectrum of x(t)
f	Cyclical frequency (Hz)
f_c	Cut-off frequency
f_n	Undamped natural frequency
f_N	Nyquist frequency
f_r	Resonance frequency
F(t)	Force time history
$F_x(f)$	Fourier spectrum of x(t)
$G_{xx}(f)$	Auto- (power) spectrum of x(t)
$G_{xy}(f)$	Cross-spectrum of x(t) and y(t)
$h_{xy}(\tau)$	impulse response function
$H_{xy}(f)$	Frequency response function
i	index
j	$\sqrt{-1}$
k	Spring constant, index
K	RC time constant
L	Length
L_x	Sound or fluctuating pressure level
m	Lag number, mass
M	Step size, Mach number
n	index
n_d	Number of disjoint averages
N	Number of data values
p	Integer
p(t)	Periodic signal time history
p(x)	Probability density of x(t)
$p_p(x)$	Probability density of peaks
$P_x(f)$	Spectrum of periodic signal
Q	Quality factor [1/(2ζ)]
$Q_{xy}(f)$	Quad-spectrum of x(t) and y(t)
R	Resistance, radius, sampling rate
$R_{xy}(\tau)$	Cross-correlation of x(t) and y(t)
$S_x(f_n)$	Shock response spectrum of x(t)
t	Time, thickness
T	Averaging time, block duration
T_r	Measurement duration
u(t)	Tapering function, displacement time history
u(f)	Fourier transform of u(t)
u	Peak displacement
U_0	Propagation velocity
v	Voltage
x(t),y(t)	Signal time histories
z	Impedance
α	Spectral parameter, level of signif.
δ	Relative displacement
Δd	Separation distance
Δf	Frequency resolution, frequency difference
ε	Normalized error
$\phi_{xy}(f)$	Phase between x(t) and y(t)
$\gamma^2_{xy}(f)$	Coherence between x(t) and y(t)
λ	Wave length
μ_x	Mean value of x(t)
θ, ϕ	Phase angles
$\theta_{xy}(f)$	Cress-spectrum phase
ρ_s	Surface mass density
$\rho_{xy}(\tau)$	Correlation coefficient function
σ_x	Standard deviation of x(t)
τ	Time delay, rise time
ψ_x	rms value of x(t)
ζ	Damping ratio
*	Complex conjugate
^	Estimate of

LIST OF ABBREVIATIONS

ADARK)	Analog/Digital/Adaptable/ Recorder Input/Output
AC	Alternating current
ADC	Analog-to-digital converter
AGC	Automatic gain control
ANSI	American National Standards Institute
Bi-ϕ	Bi-phase
CE	Capacitance element
CWB	Constant bandwidth
DAC	Digital-to-analog converter
DEMUX	Demultiplexer
Dc	Direct current
DR	Dynamic range (dB)
EDs	Electrodynamic system
EMR	Electromagnetic radiation
EOS	Electro-optical system
FDM	Frequency division multiplexing
FFT	Fast Fourier transform
FLsc	Flexible linear shaped charge
FM	Frequency modulation
HDDR	High density digital PCM recorder
IF	Intermediate frequency
IRIG	Inter-Range Instrumentation Group
LDV	Laser Doppler vibrometer
MIL-STD	Military standard
Mux	Multiplexer
NASA	National Aeronautics and Space Administration
NIST	National Institute of Standards and Technology
NRZ	Non-return to zero
PAM	Pulse amplitude modulation
PBW	Proportional bandwidth
PCM	Pulse code modulation
PE	Piezoelectric element
PM	Phase modulation
PR	Piezoresistive element
PSK	Phase shift keyed
PSNR	Peak signal-to-noise ratio (linear)
Ps/N	Peak signal-to-noise level (dB)
RCR	Telemetry receiver
RF	Radio frequency
RNRZ	Randomized non-return to zero
RSS	Root sum of squares
RZ	Return to zero
S/C	Signal conditioner
Scs	Servo-control system
SDF	Single-degree-of-freedom
SNR	Signal-to-noise ratio (linear)
SIN	Signal-to-noise level (dB)
SPL	Sound pressure level (dB)
SRB	Solid Rocket Booster
SRS	Shock response spectrum
SS	Strain sensitive
SSME	Space Shuttle Main Engines
TDM	Time division multiplexing
TFE	Telemetry front end
TSC	Tape speed control
TTL	Transistor-transistor logic
Vc	Variable capacitance
Vco	Voltage control oscillator
XDR	Transducer
XMR	Telemetry receiver

THIS PAGE IS INTENTIONALLY LEFT BLANK

1. INTRODUCTION

1.1 Historical Background. The original motivation for this Handbook came from personnel of The Aerospace Corporation (TAC), who are technical advisors to the Air Force Space and Missile Systems Center. Over the preceding two decades, TAC had observed a seemingly endless series of errors and anomalies in the acquisition and analysis of structural dynamic and aeroacoustic data. To evaluate the scope of data analysis errors alone, TAC arranged a "round robin", where identical magnetic tapes dubs of short time-limited stationary random signals were sent to several data processing centers for a 1/3 octave band analysis with their normally-used equipment. Ten centers responded with analyzed data that revealed discrepancies of nearly 20 dB at some frequencies [1.1, 1.2]. Rather than continue to accept this situation, Don Wong of TAC arranged to have the Air Force fund the development of a Handbook that would help reduce the variability and eliminate the errors commonly found in measured dynamic data, The Jet Propulsion Laboratory (JPL) was selected to prepare the Handbook, as well as perform any research required to achieve the Handbook objectives. Harry Himelblau of JPL was appointed the Task Manager for the preparation of the Handbook. He was assisted by Allan PierSol of the PierSol Engineering Co., James Wise of JPL, and Max Grundvig, who was brought out of retirement from TAC for this assignment. Additional assistance was provided by the numerous reviewers acknowledged in the Foreword.

1.2 Purpose. The purpose of this Handbook is to provide guidelines for acquiring and analyzing structural (or mechanical) shock and vibration, and acoustic and aerodynamic noise data from flight and ground tests for all categories of aerospace vehicles. The guidelines may also be used for dynamic measurements on a variety of ground and sea transportation vehicles, industrial machinery, and civil engineering structures (e.g., the response of buildings to earthquake loads). The objectives of the guidelines are to ensure the accuracy and reduce the errors and variability often associated with the acquisition and analysis of dynamic data. Specific procedures are provided unless they are highly dependent on the particular applications or instruments utilized The ultimate goal is to make accurate measurements of the dynamic phenomenon of interest, without that or any other phenomenon influencing the measurement process.

1.3 Inclusions and Exclusions. Most dynamic analyses involve the transformation of data from the time domain to the frequency domain. The main reason for employing this transformation is that most structures have frequency-dependent resonant responses. Many potential structural failures, such as those due to fatigue, crack propagation, and single peak load exceedance, are highly dependent on these resonances.

Most current measurement systems employ mainly analog instruments for data acquisition and mainly digital instruments for data analysis, although some old analog spectrum analysis equipment may still be in use. In general, these guidelines are written assuming current instrumentation is utilized.

In many cases, errors are encountered because certain traditional methods have been followed even though they can produce erroneous results, e.g., computing vibration spectra using a frequency resolution bandwidth insufficiently narrow compared to the bandwidth of critical structural resonances, or the misapplication of random data analysis procedures to periodic and/or transient data. Utilization of this Handbook is intended to avoid most of these types of problems. Certain errors, however, cannot be avoided by the application of these guidelines. These are the human errors that no set of guidelines can avoid, e.g., misidentification of measurement or channel numbers, incorrect or mislabeled calibration data, or erroneously reported instrumentation gain settings. Only adequate care, planning, communication, and documentation, coupled with personal motivation, can circumvent these errors. Excluding on-line. analysis, errors usually have much more serious consequences during data acquisition than during data analysis. Errors in data analysis can usually be corrected by a reanalysis of recorded data, unless there is a serious deficiency in the analysis instruments or in the knowledge and/or training of analysis personnel. On the other hand, errors in data acquisition may necessitate an extremely costly retest, or the complete loss of the information.

There are some special cases of dynamic measurements that will not be covered by this Handbook because of their unique nature and/or the rapid advances currently taking place in the state-of-the-art of their technology. These topics include modal testing or system identification, power and intensity measurements, mechanical impedance measurements, equipment health monitoring, determination of system stability, and a wide variety of biodynamics, human hearing and speech measurements. Even in these cases, some portions of the Handbook maybe useful. The technical literature generally provides adequate sources of information on these topics.

1.4 References.

1.1 Himelblau, H., and Piersol, A. G., "Summary of Guidelines for Dynamic Data Acquisition and Analysis", *Proc., 64th Mock and Vibration Symp.*, Vol. I, pp. 121-132, Oct. 1993.

.2 Tanner, C. S., "Shuttle Acoustics Data Reduction Methods", *Aerospace Corporation Rept TOR-0082(2463-03)-1, 30 Oct. 1981.*

2. DYNAMIC MEASUREMENT PLANNING

2,1 Introduction. Some of the most important measurement activities should take place long before data are acquired Planning for data acquisition and analysis should be initiated as early as possible, preferably during the proposal stage of a new program. There are several issues that should be addressed during this planning, particularly the ultimate uses of the data, the selection of the number and type of transducers and their frequent y ranges, i.e., the maximum and minimum frequencies to be measured, and whether the transducer is to measure more than one event or condition. For example, a single accelerometer on a space vehicle may be used to measure the structural responses induced by the engine ignition overpressure and acoustic noise during liftoff, and the boundary layer pressure fluctuations during the transonic and maximum (fluid) dynamic pressure (max q) flight conditions, all with different magnitudes and spectra. These various events are illustrated in Figure 2,1, which shows a typical high frequency flight vibration measurement [2.1]. The instantaneous and rms time histories are shown at the top. Four random vibration spectra from 20 Hz to 3 kHz are shown below, corresponding to four important flight events: liftoff, transonic, and at the beginning and end of upper stage engine burn. The time histories do not show the quasi-static acceleration because the instrumentation system did not respond to signals at frequencies below 10 Hz.

The summation of the channel maximum frequencies of all selected measurements is called the total or system data bandwidth. Two of the most important parameters for selecting instruments for data acquisition are the total data bandwidth and the number of measurements. Another important part of the planning is determining the possible need for multi-channel measurements, e.g., microphone pairs required to define or confirm the time-dependent spatial distribution of the fluctuating pressure loading on a structure. Such paired measurements require special considerations to minimize relative time or phase errors within critical instruments of the data acquisition and analysis system.

Careful consideration should be given to the tradeoff between the overall cost of the measurement program and the potential consequences of an insufficient number of measurements, e.g., not enough data to help determine the cause of flight failures, or insufficient amount data to determine or verify design or test criteria. Obviously, relatively few measurements may suffice when a comprehensive measurement program has been previously carried out on a similar vehicle or structural configuration. On the other hand, a substantial y greater number of measurements maybe required when dynamic loads are suspected to have caused a failure. In many cases, the use of ground tests with high-quality simulation and a comprehensive measurement program can substitute for extensive flight tests to establish environmental and load criteria, with a modest number of supplemental flight test measurements to confirm or modify the ground test results.

Detailed knowledge of the various instruments of the measurement system is required for their selection and utilization. Figure 2.2 shows block diagrams for a typical dynamic data analysis system, and for two of the most common types of d ynamic data acquisition systems. A telemetry

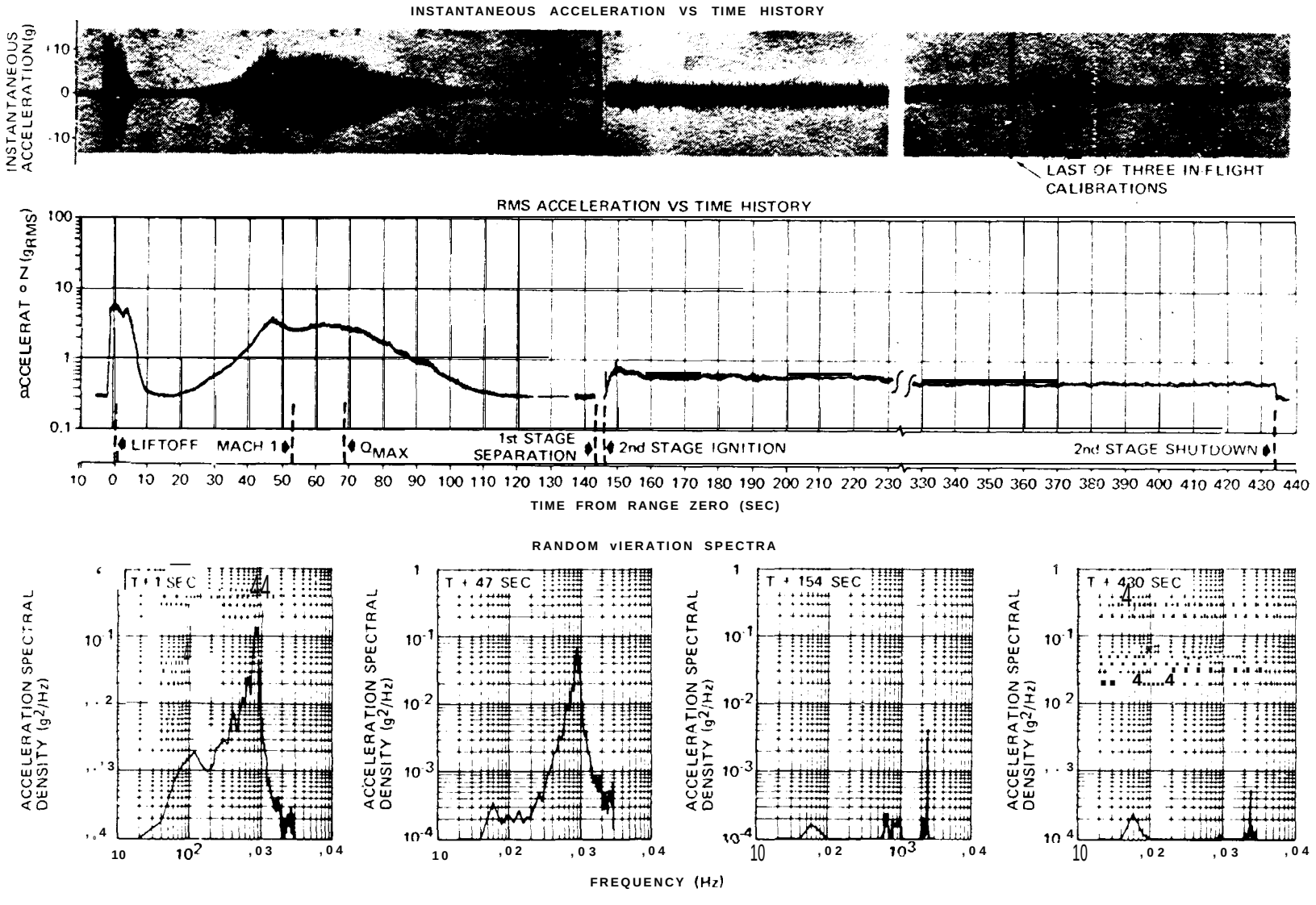

Figure 2.1. Vibration Measured on S-IVB Stage of the Uprated Saturn I Space Vehicle during Apollo-Saturn Flight SA-203. Spectral Analyses were Performed using a Frequency Resolution Bandwidth of 40 Hz and a Time Duration of 1 sec [2.1].

system, such as shown in Figure 2,2a, can be used on a wide variety of vehicles, where the transducers (XDR), signal conditioners (S/C) and power supplies, multiplexer (MUX), and a telemetry transmitter (XMR) are located on the vehicle, and the telemetry receiver (RCR), demultiplexers (DEMUX), tape recorders (TAPE) (used for data storage), and accessories are located in a ground station. In particular, telemetry systems are used on expendable launch vehicles and payloads, small aircraft when there is insufficient room for onboard recording, and for ground or flight tests of rotating machinery when the use of slip rings is inadequate or impractical, Hardwire systems, such as shown in Figure 2.2b, are commonly used for ground tests, and on larger aircraft where sufficient room exists for onboard recording. The Space Shuttle has used hardwire systems with on-board tape recording for dynamic data acquisition. Data analysis is usually performed after the time the data are acquired, and often at a facility remote from the data acquisition location, requiring the tape or a dub to be transferred to the data analysis facility. Data analysis is commonly performed on a wide variety of stand-alone analyzers, or by software on computers ranging in size from a personal computer (PC) to a mainframe, as indicated in Figure 2.2c. Figure 2.2 shows by asterisk the several possible locations of an analog-to digital converter (ADC). Of course, there are many variations of the systems outlined in the simple block diagrams of Figure 2.2. For example, Figure 2,3 shows the dynamic data acquisition system for recording 120 fluctuating pressure measurements of aerodynamic noise on a scale model in a wind tunnel [2.2].

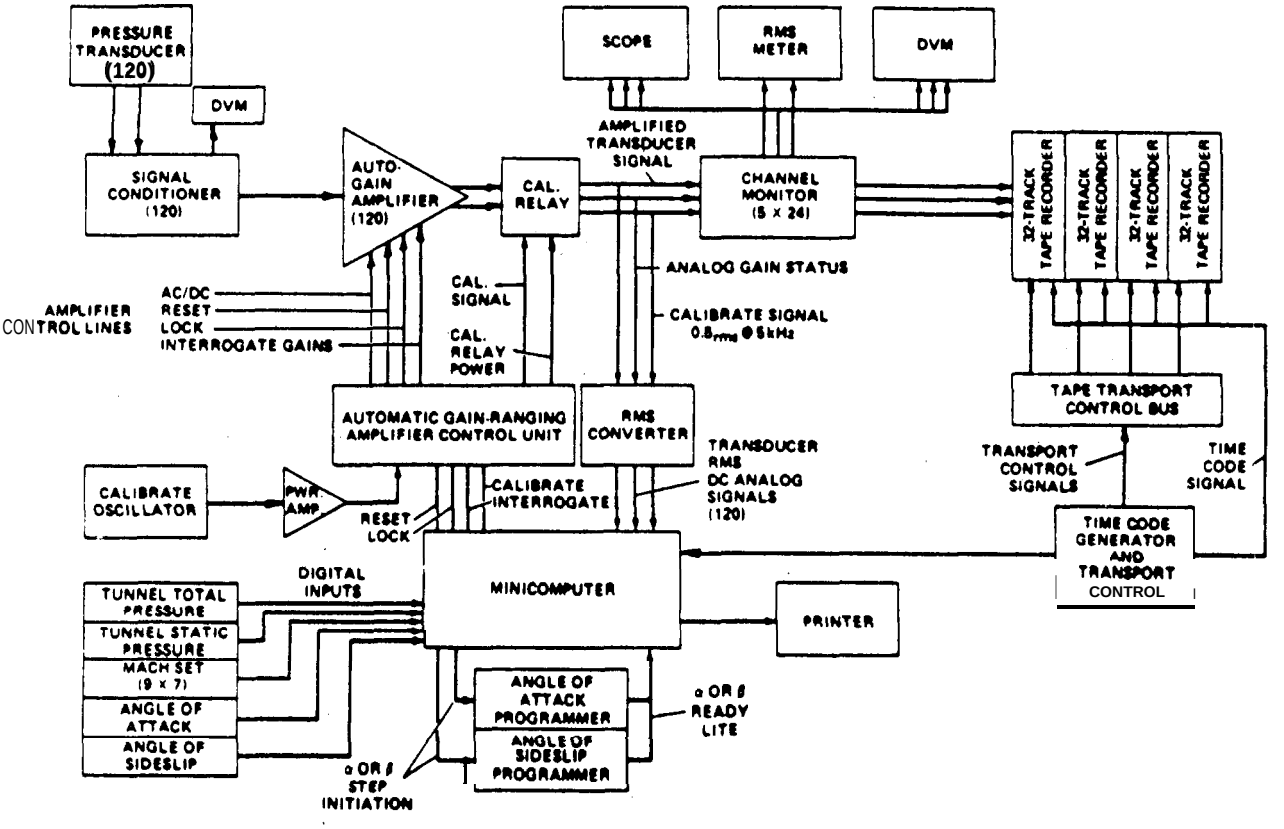

Figure 2.3. Diagram of Data Acquisition System for Wind Tunnel Aerodynamic Noise Tests [2,2].

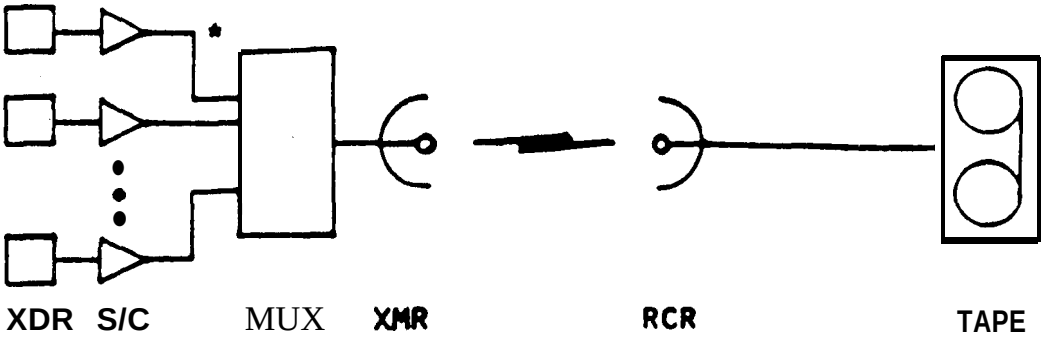

(a) Typical Telemetry System for Dynamic Data Acquisition.

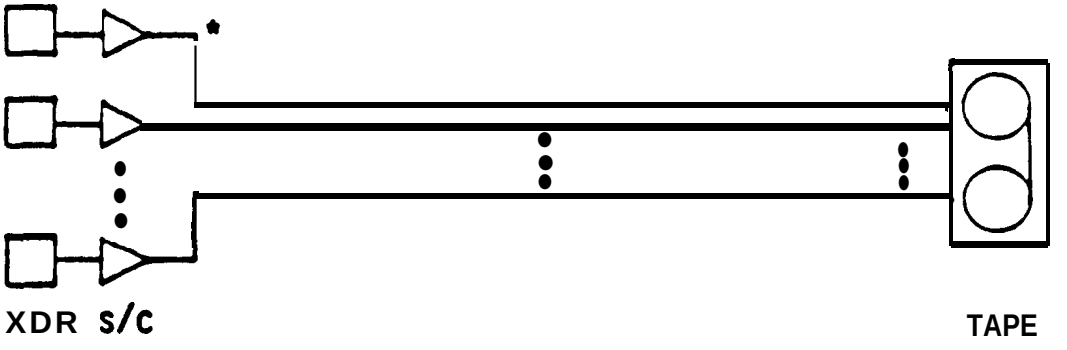

(b) Typical Hardwire System for Dynamic Data Acquisition.

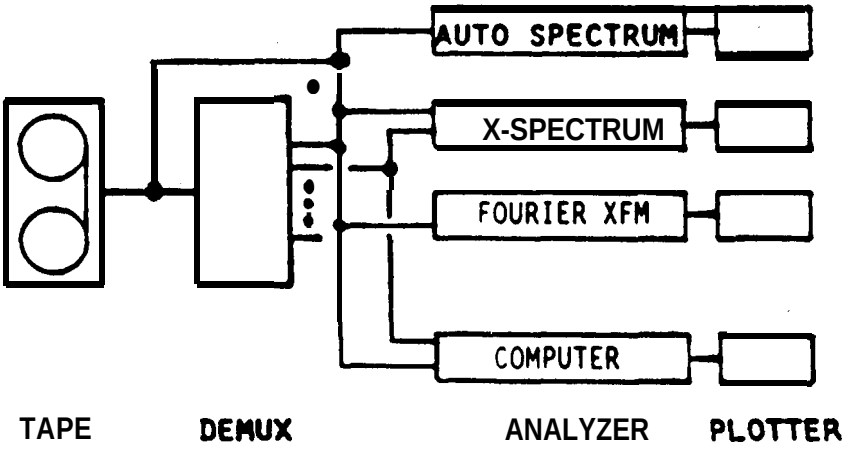

(c) Typical System for Dynamic Data Analysis.

*An analog-to-digital converter (ADC) may be located at any asterisk

Figure 2.2. Typical Instrumentation Systems for Data Acquisition and Analysis.

system, such as shown in Figure 2,2a, can be used on a wide variety of vehicles, where the transducers (XDR), signal conditioners (S/C) and power supplies, multiplexer (MUX), and a telemetry transmitter (XMR) are located on the vehicle, and the telemetry receiver (RCR), demultiplexers (DEMUX), tape recorders (TAPE) (used for data storage), and accessories are located in a ground station. In particular, telemetry systems are used on expendable launch vehicles and payloads, small aircraft when there is insufficient room for onboard recording, and for ground or flight tests of rotating machinery when the use of slip rings is inadequate or impractical, Hardwire systems, such as shown in Figure 2.2b, are commonly used for ground tests, and on larger aircraft where sufficient room exists for onboard recording. The Space Shuttle has used hardwire systems with on-board tape recording for dynamic data acquisition. Data analysis is usually performed after the time the data are acquired, and often at a facility remote from the data acquisition location, requiring the tape or a dub to be transferred to the data analysis facility. Data analysis is commonly performed on a wide variety of stand-alone analyzers, or by software on computers ranging in size from a personal computer (PC) to a mainframe, as indicated in Figure 2.2c. Figure 2.2 shows by asterisk the several possible locations of an analog-to digital converter (ADC). Of course, there are many variations of the systems outlined in the simple block diagrams of Figure 2.2. For example, Figure 2,3 shows the dynamic data acquisition system for recording 120 fluctuating pressure measurements of aerodynamic noise on a scale model in a wind tunnel [2.2].

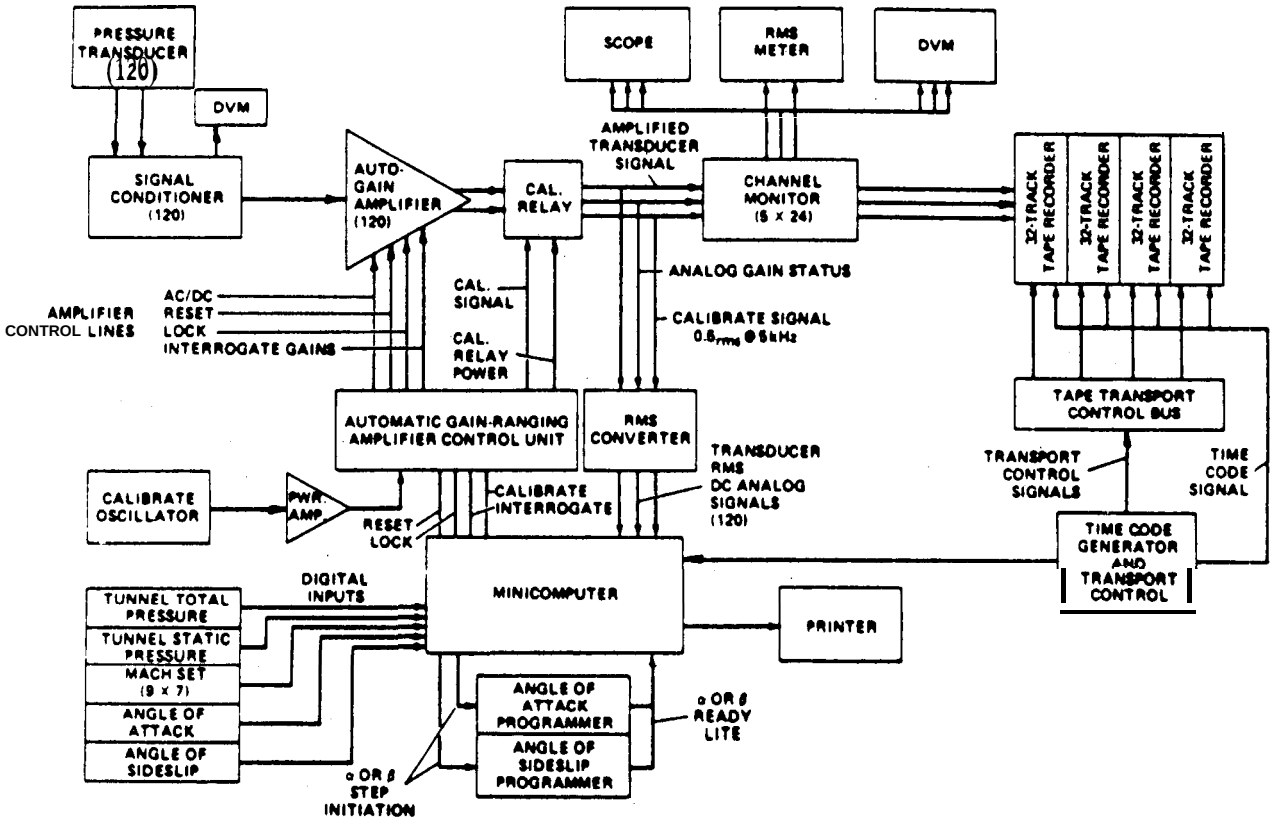

Figure 2.3. Diagram of Data Acquisition System for Wind Tunnel Aerodynamic Noise Tests [2,2].

2.2 Measurement Numbers, Locations, and Directions. The initial task in dynamic measurement planning is the selection of the transducer locations and directions, which determines the total number of measurements. The experience and knowledge of instrumentation personnel and the user(s) should be important factors in this selection.

For aerospace applications, low frequency (usually below 100 Hz) strain gages and accelerometers are generally installed based on critical locations and directions computed from dynamic or combined static and dynamic analyses using elaborate finite element models [2.3-2,6], and/or experience gained from previous programs. High frequent y (usually above 20 Hz) accelerometers are often located on external structures, or internally near critical hardware. For high frequency accelerometers to be located on external (and often internal) structures, a mix of uni-directional (or uniaxial) and sets of three orthogonal hi-directional (or triaxial) accelerometers is usually selected with most of the uniaxial accelerometers sensing the normal or transverse dynamic response of the structural surface in order to measure the maximum response value. For wide frequency strain gages located on external (and often internal) structures, their number and directions are usually based on computed dynamic responses using finite element models of these "local" structures, or on predictions from simple plate or shell theory, e.g., [2.7-2.9]. For all strain gage measurements, care must be taken to intentionally include or exclude the effects of local strain distributions (i.e., stress concentrations), depending on the subsequent utilization of the strain data. For high frequency accelerometers to be located near aerospacehardware/structural interfaces, triaxial measurements are usually made to help generate or verify dynamic design and test criteria, Renewed interest has been observed in making force measurements at the structure/hardware interface to improve criteria development [2. 10-2. 12]. For all types of measurements, each transducer should be as small and lightweight as possible, consistent with the product of the anticipated (static and/or dynamic) magnitude times the sensitivity of the transducer. The sensitivity is defined as the ratio of the transducer electrical output to the magnitude of the measured input.

For low frequency, it is fairly common to spatially arrange a group of transducers to determine the global response of the structure [2.5, 2.6], often using multi-channel measurements described in Section 2.6. On the other hand, local structure response is often obtained at high frequencies, with little or no coherence observed among measurements, For a new aerospace vehicle, it is common to divide regions of similar structures and/or external environments into vibroacoustic zones, with a few measurements selected for each zone to beused to establish zonal vibroacoustic design and test criteria [2. 1]. For example, the Shuttle Orbiter has over 60 vibration zones. As a result, the number of high-frequency measurements is often a function of vehicle size. Sources that cause high-magnitude vibration, such as reciprocating and rotating machinery, and jet and rocket engines, often receive a large number of measurements.

Pressure transducers are used to measure pressure fluctuations Some measure quasi-static or combined quasi-static and dynamic pressures, whereas others measure dynamic pressures only.

These devices are often installed flush with the external surface to measure engine-induced acoustic noise, as well as aerodynamic pressure fluctuations called aerodynamic noise. In most cases, engine-induced acoustic noise fields change gradually between 'measurement locations, requiring relatively few measurements, On the other hand, aerodynamic noise can often change drastically even between closely-spaced transducers, especially in the transonic regime at vehicle Mach numbers from 0,7 to 1.3, due to separated flow that results from shock wave-boundary layer interactions. This situation often requires a significant number of measurements to define adequately the spatially-distributed fluctuating pressure loads.

The determination of acoustic and aerodynamic (i.e., aeroacoustic) noise can be characterized as an experimental rather than a theoretical art, due mainly to an inability to quantify analytically the basic sources of the noise (e.g., the volume distribution of fluctuating fluid shear stresses) after decades of attempts. As a result, it is common to perform ground tests using vehicle scale models to measure aeroacoustic noise early in a new program. For example, scale model vehicles with scale model engines, and scale models of nearby facilities, such as launch pads, are sometimes used to define engine-induced acoustic noise on vehicle external surfaces. Similarly, wind tunnel tests of scale model vehicles are sometimes used to define aerodynamic noise on vehicle external surfaces, usually in transonic and max q regimes and under flight conditions involving high angles of attack and yaw. A comprehensive scale model program can significantly reduce the need for flight aeroacoustic measurements. However, scale models usually require miniature microphones with very high maximum frequencies to provide full scale data with a nominal frequency range. For example, a 4% model requires a data acquisition system with a maximum frequency of 50 kHz to provide full scale data up to 2 kHz,

Internal acoustic noise fields are usually measured whenever significant loads or vibratory responses are anticipated for internal structures, or if the cavity is used for human habitation.

If the testis costly or impossible to rerun and/or if the non-dynamic environments applied to the transducers are not adequately known, and if the test results are highly dependent on accurate dynamic data, redundant adjacent transducers may be required to ensure that the desired data are obtained even if some transducers fail. Also, if the magnitude of the quasi-static and/or dynamic load or environment is difficult to predict, redundant transducers with different sensitivities may be needed to ensure that the desired test data are obtained.

If the above selection procedure results in too many measurements, a careful reevaluation should be initiated. Consideration should be given to spreading many of the measurements over several flights or ground tests. Lastly, a priority list should be made to assist in the selection if a fewer number of measurements are approved. In most cases, it is cheaper to make a large number of measurements in a ground test than a flight test, On this basis, consideration should be given to an increased emphasis on ground testing for dynamic measurements.

In many cases, individual measurements are more important than a collection of measurements that cannot be directly correlated because of the large degree of independence between the various sources of dynamic excitation.

2.3 Frequency Ranges. After measurement numbers, locations and directions have been selected, the next task is to establish the frequency range for each measurement, i.e., the maximum and minimum frequencies to be recorded and analyzed. For those transducers used to determine combined static and dynamic loads (usually strain gages and low frequency accelerometers), the minimum frequency is obviously zero, i.e., DC. However, under many circumstances, not all low frequency accelerometers need go down to zero frequency, when other DC accelerometers can be used for interpolation. Definition of pressure fields may also require measurement down to or close to zero frequency. For example, the transient pressure from engine ignition often has a substantial very low frequency component whose phase relationship to high frequency components can be vital to load definition. Also, high intensity aerodynamic pressure fluctuations, sometimes called buffet at low frequencies, are usually accompanied by substantial low frequency pressures, which should also be measured for proper environmental definition.

The selection of the maximum frequency is often the most challenging part of this task. It usually has the greatest impact on the total data or system bandwidth and on the various instruments of the measurement system. The maximum frequency is usually selected to equal (a) the maximum significant frequency of the anticipated environment or load, or (b) the maximum frequency that can be simulated in laboratory tests, or (c) the maximum frequency achievable by the data acquisition system. Alternative (a) is recommended over the other two. Experience from previous programs, when available, and theoretical analyses should be of great assistance in establishing the maximum significant frequency.

Before completing a list of the desired frequency ranges, consideration should also be given to available instrumentation options. For example, it may be desired to make six flight vibration measurements up to 2 kHz, using IRIG standard telemetry for data acquisition with constant bandwidth frequency modulation (FM) subcarriers (used for frequency division multiplexing) [2.13]. Later, it may be found that the data analysis facility only has the capacity for six C channels (O -1.6 kHz) or three D channels (O- 3.2 kHz). The user may then be required to decide which alternative to use, i.e., to get by without data in the 1.6-2 kHz range for the six desired measurements, or lose three of the measurements while obtaining the desired range (and more) for the remaining measurements. In addition, it is often worthwhile to consider the frequency ranges used in common aerospace practice, which is based for the most part on past experience and failures, e.g., (a) 0-100 Hz (or sometimes less) for low frequency shock, vibration and strain, due mainly to vehicle transient events, (b) 10 Hz -2 kHz for high frequency vibration and strain, (c) 10 Hz -10 kHz for high frequency aeroacoustics, and (d) 100 Hz- 1MHz for near field pyroshock (i.e., within a 6 inch distance from the pyrotechnic source to the transducer) and a lesser high frequency limit (100 Hz to 10 kHz) as the

source-to-transducer distance increases. A few measurements in the later two categories have a substantial impact on the total data bandwidth and, therefore, on the data acquisition system. However, it would be a serious mistake to arbitrarily use these frequency ranges when technical considerations justify their modification. It is recommended that Appendix A be reviewed before the planning of pyroshock measurements is initiated.

2.4 Dynamic Ranges. The dynamic range of a measurement system is defined as

$$DR = 10\log_{10}\left(\frac{x_{max}}{x_{min}}\right)^2 \quad \text{(dB)} \qquad (2.1)$$

where x_{max} is the maximum instantaneous value of the signal that can be transmitted by the system without distortion, and x_{min} is the minimum detectable value of the signal generated by the transducer at the output display. The minimum detectable signal is dependent upon

(a) the magnitude of undesired electrical noise in the measurement system,
(b) the quantization of the measurement by an analog-to-digital converter (digital noise), -
(c) low magnitude distortion of the signal, and/or
(d) interference from other measurements.

Factor (a) usually dominates to produce the background noise floor for the analog instruments of a measurement system, and (b) produces the theoretical noise floor of analog-to-digital converters, The theoretical measures for the dynamic range of analog-to-digital converters, and a discussion of practical limitations, is presented in Section 3.7.1.3.

For analog systems, it is common to express the dynamic range of instruments in terms of a peak signal-to-noise ratio given by

$$PSNR_m = \left(\frac{x_{max}}{\sigma_n}\right)^2 \qquad (2.2)$$

where σ_n is the standard deviation of the background noise (or the rms value of the background noise if the mean value is zero). The dynamic range of the measurement system may also be defined in terms of an rms signal-to-noise ratio given by

$$SNR_m = \left(\frac{\sigma_x}{\sigma_n}\right)^2 \qquad (2.3)$$

where σ_x is the standard deviation of the signal (or the rms value of the signal if the mean value is zero), However, this latter description is meaningful only if the specific characteristics of the signal are defined. It is often assumed that $x(t) = X_s \sin(2\pi f_s t)$, so that $X_s = x_{max} = \sqrt{2}\,\sigma_x$.

It is common practice to express signal-to-noise ratios for measurement systems in dB to obtain what will henceforth be called signal-to-noise levels. The peak signal-to-noise level is then given by

$$PS/N_m = 10\log_{10}(PSNR_m) = 10\log_{10}\left(\frac{x_{max}}{\sigma_n}\right)^2 \quad \text{(dB)} \tag{2.4}$$

while the rms signal-to-noise level is defined as

$$S/N_m = 10\log_{10}(SNR_m) = 10\log_{10}\left(\frac{\sigma_x}{\sigma_n}\right)^2 \quad \text{(dB)} \tag{2.5}$$

For example, S/N_m =40 dB corresponds to SNR_m = 10,000. Some sources, e.g. [2.14], provide alternate definitions of dynamic range and/or signal-to-noise ratio, which use the ratio on the right hand side of Equations (2,1) - (2.3) without the ratio squared, When these definitions are used, the ratio must be squared to obtain the correct DR, PS/N_m or S/N_m.

Another useful ratio is the actual signal-to-noise ratio of a specific measurement, as opposed to the maximum signal-to-noise ratio provided by the measurement system. The actual signal-t-noise ratio, which can never exceed the system signal-to-noise ratio without clipping, is denoted in terms of the actual peak signal-t-noise ratio and level by

$$PSNR_a = \left(\frac{x_{ma}}{\sigma_n}\right)^2 \text{ or } PS/N_a = 10\log_{10}\left(\frac{x_{ma}}{\sigma_n}\right)^2 \quad \text{(dB)} \tag{2.6}$$

or in terms of the actual rms signal-to-noise ratio and level by

$$SNR_a = \left(\frac{\sigma_{xa}}{\sigma_n}\right)^2 \text{ or } S/N^* = 10\log_{10}\left(\frac{\sigma_{xa}}{\sigma_n}\right)^2 \quad \text{(dB)} \tag{2.7}$$

The determination of the maximum anticipated instantaneous value, x_{ma}, for a measurement is usually the most challenging task associated with the selection of system gain settings to optimize the actual signal-to-noise ratio of a measurement. This value is usually selected to equal (a) the maximum anticipated instantaneous value of a transient or a periodic signal, or (b) the product of a crest factor times the standard deviation of a maximum anticipated random signal, whichever is greater. The crest factor, or peak-to-standard deviation ratio, of a random signal may be as low as three for a short duration random signal, or in excess of six for a very long duration random signal or a signal representing the response of a highly nonlinear structure to random excitation.

The value of x_{max} for the data acquisition system is usually selected to be a little more than the anticipated value of x_{ma}, say by a factor of $\sqrt{2}$ or 3 dB, to leave a little spread (or "head room") for the lack of a precise estimate of x_{ma}, or for flight-to-flight variations. On the other hand, a much greater spread, say 6 to even 10 dB, is often used for the first few flights to compensate for even

less confidence in the estimate. Of course, everything else being equal, the additional spread reduces the useful PS/N_a of the measurement. Usually the greatest need for a large system dynamic range (DR) is when it is intended to measure widely diverse multiple events, such as low frequency structural response to gust loading as well as stage separation, or high frequency structural response to aerodynamic noise at max q as well as pyroshock. In many cases, it may be impossible to measure multiple events properly with only one measurement channel. An example is shown in Figure 2.1, where S/N_a is an adequate 24, 21 and 20 dB for the liftoff, transonic and max q events, respectively, but only 6 and 4 dB at the beginning and end, respectively, of the second stage engine burn. See Section 4.6.1 for excessive background noise corrections.

Usually a single instrument of the system is responsible for limiting the dynamic range, e.g., high noise floor of the signal conditioner, or the PS/N_m of the subcarrier used for the frequency division multiplexing (FDM) of several signals prior to telemetering, or tape recoding. Often the electrical noise of the signal conditioner can be reduced by better grounding or shielding, but a system change may be required to improve the PS/N_m of the FDM subcarrier. For example, the PS/N_m of an IRIG standard FM subcarrier is approximately 45 dB. However, once the DR of the critical instrument is determined, the DR for the other instruments need only to exceed that of the critical instrument by a reasonable amount, say 6 dB, to avoid additional degradation of the system DR.

In certain cases, if the load or environment to be measured is of low magnitude, there may be a problem in achieving both the desired useful amplitude range and frequency range. For a particular transducer design, a wide frequency range may only be achieved at the expense of transducer sensitivity, even with amplification, and vice versa. Thus, this situation may have a substantial influence on the selection of both the frequency range and dynamic range. In other cases, it may be impossible to measure the low-magnitude condition, e.g., turbulent flow-induced aerodynamic noise applied to certain regions of a wind tunnel model may be less than the acoustic noise transmitted from other wind tunnel sources [2. 15]. To determine the magnitude of these sources, another pressure transducer can be located in the laminar flow region of the model (usually near the nose). Spectral comparison can then be used to determine if and where the desired aerodynamic noise spectrum exceeds that of the tunnel noise, and is therefore valid data for flight vehicle design.

In many cases, orders for needed instruments are placed by the purchasing department with the various instrument vendors shortly after the completion of measurement planning, especially for long-lead items. Once placed, proposed changes to these purchase orders are likely to meet with great resistance. When signal conditioners are purchased, one of the characteristics specified is the amplifier gain setting (see Sections 3.3 and 3.9), which is determined by the user's estimate of the various values of x_{ma}. Later, loads or response analyses, or ground or early flight tests may show the need for changes in the various values of x_{ma}. If the signal conditioners have been ordered with unadjustable fixed-gain amplifiers, there may not be enough time to reorder, return, make the required changes, deliver and reinstall the signal conditioners before the next test, or the purchasing

department may want to show its reluctance to reorder without program management approval, who by then are probably working on several higher priority problems, potentially causing an extended delay. Either will probably result in (a) delay of the next test, or (b) much data lost due to signal clipping or saturation, or insufficient PS/N_a. See Sections 4.3-4.6 for details on Alternative (b). To avoid these problems, it is recommended that all signal conditioners be ordered initially with (1) manually-adjustable fixed-gain amplifiers, over a gain range of ± 10 dB or more (referenced to the original x_{ma}), so that gain settings may be changed if necessary or (2) computer-controlled amplifiers with continuous gain-ranges or autoranging. Even in large test programs, the relative cost difference should be small for Alternative (l). The higher initial cost of Alternative (2) is offset by the elimination of time-consuming manual adjustments (which could be substantial with many measurements) and the risk of human error.

2.5 Measurement Durations, It is sometimes necessary and always desirable to measure dynamic loads and/or environments during the complete period of excitation. If this is impossible with the data recording and storage instruments selected, then at least the loads and/or environments should be measured during periods of significant excitation, and when the excitation changes. For example, a duration-limited instrumentation system for a space vehicle should acquire data for the entire period of powered ascent, and maybe turned off until shortly before upper stage engine ignition. If the engine bum duration is still too long for the capacity of the data recording instrument, then it may have to be turned off again until shortly before engine cutoff if the risk is acceptable.

In most cases, the factor limiting the total duration of data acquisition is the capacity of the data storage instrument (e.g., magnetic tape or disk). IRIG standard tape recorders used for dynamic measurements usually accommodate 10,5 in, or 14 in. diameter reels, with resulting tape lengths of about 4600 ft and 9200 ft, respectively. The total recording duration can be calculated from

$$T_t = \frac{L_t}{5V} \text{ (minutes)} \tag{2.8}$$

where L_t is the total tape length in feet, and V is the tape speed in in./sec (ips). Using an IRIG standard tape speed of 60 ips, as is often used for wideband and frequency division multiplex (FDM) dynamic data recording, a total duration of 15 rein, 20 sec and 30 rein, 40 sec is obtained for the 10.5 in. and 14 in. tape reels, respectively. Pretest and (whenever possible) post test calibrations (or cals) should be included on the tape with the dynamic data, once the minimum time is determined for each cal period. (One minute each for recording a DC step cal, an AC sine cal, and background noise is often used). Little time may then be left for the dynamic data. Of course, if the useful frequency ranges of the measurements can be achieved with a slower tape speed (30 or 15 ips), then a substantially longer recording duration may be obtained. If the signals are to be tape recorded using FM recording (as discussed in Section 3.6.3.2) and if the frequency range of the cal can be recorded with a much slower tape speed, then a longer data recording duration at a higher speed can be achieved

When it is necessary to use higher tape speeds for FM recording, a simple solution to the duration problem may be to record the cals on one tape and the dynamic data on another, taking care not to change any gain settings between the cals and the data. However, this may not be used for direct, e.g., amplitude modulation (AM), recording, due to potential tape-to-tape magnetic density variations, unless it can be verified that both tapes came from the same batch. Another solution is to use twice as many (or three times as many) tape recorders, first recording data on the first recorder (or first set), then recording data on the second recorder (or second set) with a little overlap, etc. This obviously complicates the data acquisition process and substantially increases the cost.

2.6 Multi-Channel Measurements. In most cases, the dynamic response of a spatially-distributed aerospace structure is caused by an external distributed load over its various surfaces, or by multi-point loading. In many of these cases, it is necessary or desirable to determine or verify the spatial distribution of these loads, or the dynamic response they produce. In addition, sometimes it is desirable to establish the frequency response function between a load and a response at a single or at different locations. In other cases, it is desired to ascertain the transit time of a wave or waves between two locations. Other applications are given in [2.16]. For all of the above, multiple channel measurements are required.

Examination of the analytical equations which govern the dynamic response of distributed structures shows that the response is dependent on the loading expressed in terms of parameters which are dependent on location pairs [2.1,2.16,2.17]. Thus the analysis of multiple channel measurements is actually performed in terms of dual channel analysis, considerably simplifying the data analysis, but not the data acquisition.

The capability of the instrumentation system to measure dual channel data accurately must be evaluated prior to the acquisition of multi-channel data. The two parts of this evaluation are the determination of(a) magnitude, and (b) relative phase or time delay. The evaluation of the system for dual channel magnitude turns out to be identical to that for individual measurements, i.e., by conventional single channel calibration (see Section 3.8). The evaluation of the instrumentation system for dual channel phase or time delay requires that the same calibration signal be applied to all multi-channel simultaneously, so that the relative phase between charnels over the selected spectrum can be observed. The most common calibration in present use is the simultaneous application of an electrical random signal, usually with a white spectrum (constant autospectral density function described in Section 5.4.3), over the frequency range of interest (see Section 3.8). The between-channel coherence and cross-spectrum phase of this signal is later measured for all desired dual channels. Unity coherence and zero phase of this calibration signal over the desired frequency range indicates that accurate dual channel analysis of the measurements should be expected. A coherence less than unity shows that there is some distortion, interference, or noise on one or both channels that must be reduced, no matter what the phase is. Obviously, zero phase is preferred, However, the situation is not lost even when the phase is other than zero, as long as the coherence

is unity. All that is necessary is to have the dual channel data, once it is acquired and analyzed, corrected with the phase data obtained from this calibration. See Section 3,8 for details.

It should be emphasized that it is currently impractical to control relative phase between measurements recorded on separate tape recorders, no matter what measures are taken to try to synchronize the recorders (although such techniques have been proposed, e.g. [2. 18]). Thus it is mandatory that acquisition of multi-channel data intended for dual channel analysis be limited to a single tape recorder, using either wideband recording or multiplexing. For wideband recording, the applicable signals should be recorded on adjacent tracks (odd or even) of the same head stack. If the number of multi-channel measurements exceeds the capacity of a single recorder, then one or more measurements must be recorded on two (or more) tape recorders to maintain a proper phase reference for later analysis. Therefore, if it is necessary or desirable to obtain multi-channel data for dual channel analyses, the measurement plan must make provisions for unambiguous phase determination during the data acquisition of these measurements, and the application of a single calibration to all multi-channels simultaneously.

2.7 Time Codes. For all flight tests and nearly all ground tests, it is necessary to record an unambiguous time code on all recorders used for dynamic data acquisition. A properly formatted time code can be used to detect, and sometimes correct, time errors in the recording process, as well as be used in the selection and implementation of spectral analysis intervals during data analysis. In most cases, one of the standard IRIG time formats is selected for the time code [2.19]. For dynamic measurements, this is usually IRIG B. See Section 3.6.6 for details.

2.8 Error Budgets. A simple concept that is often ignored during the data acquisition and analysis planning is called the "error budget", which consists of a clear definition and tabulation of all potential errors in the data acquisition and analysis instrumentation, including the statistical estimation errors in the final analysis of random data signals. An error budget is valuable in four basic ways, as follows:

(1) It forces the planner to think about all possible sources of error before data are acquired and analyzed, and in so doing greatly reduces the risk that the experiment will fail to provide the desired information due to obscuring uncertainties in the results.

(2) It immediately identifies the primary sources of errors (the "weak links") in the system instrumentation and, hence, allows the consideration of pre-experiment changes in specific instruments to minimize the overall potential error in the experimental results.

(3) For the case of random data, it allows the logical selection of the measurement durations that will be needed for the data analysis to assure that the statistical sampling errors are consistent with the potential error due to the data acquisition and analysis instruments.

(4) It permits the objective estimation of an overall system potential error in the final results of the experiment.

Although an error budget is probably most useful during measurement planning, it can provide valuable information anytime during the measurement program.

2.8,1 Error Source Identification and Quantification. The first step in preparing an error budget is to identify and quantify the potential errors associated with each instrument in the data acquisition and analysis system, and for the case of random data, the statistical sampling errors in each data analysis procedure To assist this task, Section 3 details potential error sources and quantifies certain error values for a wide range of data acquisition instruments, including (a) transducers, (b) signal conditioners, (c) multiplexer and demultiplexers, (d) communication links, and (e) data recording, playback, and storage devices. Section 3 covers not only intrinsic errors, but also the environmentally-induced errors, e.g., the influence of temperature on the accuracy of an accelerometer. Section 4 presents procedures for identif ying and, in some cases, suppressing various errors in data signals after they have been acquired, Section 5 summarizes the statistical sampling errors (both random and bias) in the analysis of random data signals. Beyond the information in this Handbook, definitive details on the errors to be expected in various data acquisition and analysis instruments are often provided in the manufacturers' specs and literature. Finally, there are a number of textbooks which develop and discuss error expressions for various types of instruments [2. 14, 2.20- 2.22], See [2,23] for an illustration of the identification and quantification of errors for the Space Shuttle dynamic data acquisition and analysis system.

2.8.2 Error Budget Preparation. Using a flow chart for the system instrumentation, the error budget should be prepared by making a detailed listing of each instrument and its potential error contributions. This may include several error sources for each instrument. For example, error sources for an accelerometer may include, (a) frequency linearity, (b) amplitude linearity, (c) installation effects, (d) base strain sensitivity, (e) transverse vibration sensitivity. It is important that the listed errors include estimates for all environmental-induced errors [e.g., (d) and (e) above], particular y for measurements made under extreme conditions. The error budget preparation must be very carefully examined to assure that no significant error sources are omitted. It will be complete only when every link in the flow chart for the data acquisition and analysis system has been assigned an error value. If the error for one or more links in the flow chart is missing, it should be approximated based upon good engineering judgment.

2.8.3 Systern Error Calculation. The total system error should be computed by taking the square root of the sum of squares (called the RSS error) for the individual errors listed in the error budget. In computing an RSS error, it is important that the constituent errors be defined on a common basis. For example, many data acquisition instrument errors are quoted in terms of a "percent of full scale", while most data analysis statistical sampling errors are presented in terms of a "percent of reading". The errors must be converted to a common format before computing the RSS.

2,8.4 System Error Utilization. Once the system RSS error has been computed, if it is too large to allow a meaningful interpretation of experimental results, the various elements in the error budget should be reviewed to establish where and how the constituent errors can be reduced to bring the RSS error down to an acceptable level. Remembering that the RSS computation involves a sum of squared error terms, it follows that attention should be focused on the largest error sources, since they dominant in the RSS computation, For example, if there were six error sources, where one was 5% and the other five were 1% each, totally eliminating all five of the 1% error sources would reduce the RSS error only from about 5.5% to 5.0%. This same reduction in the RSS error could be accomplished by reducing the single 5% error source to 4.5%.

For the case where the acquired data are random in character, meaning there will be statistical sampling errors in the data analysis, the RSS error for the data acquisition instruments is a key factor in the selection of the measurement durations for the later data analysis. Specifically, the duration of the acquired data signals directly influences the statistical accuracy of the data analysis results, as well as the duration and, hence, the cost of the experiment. If the RSS for the data acquisition instrumentation were, say 20%, it would clearly serve no purpose to spend the money needed to collect sufficient data to allow an analysis with a statistical sampling error of 5%. In this fashion, the error budget plays a key roll in the selection of measurement durations during the data acquisition and analysis planning. See [2.2 1] for further discussions of error budgets.

2.9 Instruments and/or Software Selection and Vendor Evaluation. Once the requirements have been determined for the number and type of measurements, their locations and directions, their frequency and dynamic ranges, and measurement durations, plus the need for multi-channel data and special types of data analysis, then available on-site instruments and/or software should be examined to ascertain that the requirements can be satisfied, It may be found that no single instrument can meet all the requirements, e.g., dynamic or frequency range. Then consideration should be given to the potential use of two or more instruments, or modification of the requirements. Occasionally, only one type of instrument can satisfy a unique requirement, e.g., water-cooled accelerometers for measuring vibration at high temperature, or vibration-compensated microphones for measuring aeroacoustic noise near structures responding with high magnitude vibration. Deficiencies should be identified and plans made to correct them, including the potential purchase of new instruments and/or software.

The process of determining if commercial instruments and/or software can satisfy user requirements should then be initiated using the most knowledgeable and experienced instrumentation and user personnel available. This process should start with the careful examination of instrument manufacturers' catalogs and specification (spec) sheets, and/or software developers' descriptions and spec sheets (plus instructions on their utilization on certain computer), to identify the applicable characteristics and inherent limitations of the candidate instruments and/or software. Other important factors should also be considered: environmental effects, size and weight, mounting provisions, power

requirements, ease of operation, and various precautions that may be needed in instrument utilization. The user should be aware that even the most respected vendors may permit excessive optimism to creep into their catalogs, descriptions, and spec sheets, e.g., software that works perfectly in one application may be seriously deficient in another application. Hence, it is recommended that the process of determining if available instruments and/or software satisfy user requirements be continued by contacting current and previous users of the product concerning their evaluation, It is not uncommon for users from competing organizations to discuss these products freely and openly. However, concentration on current and past designs can tend to perpetuate obsolete technology, which can in the long run hinder the future development of better instruments and software.

Most instrument manufacturers and software developers are happy to provide detailed data on their products, services and applications, usually by knowledgeable and experienced personnel, However, some may be unwilling to provide unbiased information on the relative merits of competitors' products. Another data source is the instrumentation consultant, who usually can be counted on to provide an independent assessment of competing products. Manufacturers, developers and consultants should all be knowledgeable of the current state-of-the-art.

In addition, business-related factors should have an important influence on vendor evaluation and selection: price and delivery, quality control, calibration services, past performance, financial stability, innovation, ability and willingness to make modifications, and overall cooperation. Vendor facilities should be visited to verify current capabilities.

Standards are available for many instruments of the data acquisition and analysis system. IRIG (or Inter-Range Instrumentation Group) and military standards are available for telemetry, muxs and demuxs, tape recorders, time codes, calibration system, and even the magnetic tape [2.13,2,19, 2.24- 2.26]. Nearly all test ranges have instruments built to IRIG standards in their ground stations. If the user's instrumentation requirements fall outside of the IRIG instruments capabilities, then a special non-IRIG system will need to be considered or developed and validated, usually at considerable expense and delay, or the requirements will need to be modified. In addition, there are a variety of ANSI standards for other instruments, such as transducers and their calibration, spectral analysis, and procedures for a variety of vibration and acoustic measurements [2.27 - 2.51]. When this process is finally completed, presentations to and discussions with program managers and customer representatives should be made to obtain their concurrence with the instrumentation plan and cost, or to establish alternatives.

2.10 Major Causes Of Errors. As a closing comment related to measurement planning, it may be useful to note what are considered the most common causes of errors and variability y in dynamic data acquisition and analysis:

(1) No end-to-end calibration, especially important in flight and major ground tests, permitting a large number of potential error sources to influence the determination of instrumentation calibration factors,

(2) Advanced purchase of a large number of incorrectly-set unadjustable fixed-gain amplifiers, resulting in uncorrectable cases of signal loss due to saturation, or serious contamination by background noise.

(3) Ignoring the effects of non-dynamic environments and other dynamic loads on dynamic transducers and signal conditioners, such as base bending of accelerometers, vibration response of microphones, and moisture penetration into signal conditioners, causing unknown errors in the measured output.

(4) Failure to properly evaluate the effects of the installation or mounting on the transducer response to the dynamic load or environment to be measured, causing an erroneous output,

(5) Locating low pass filters after signal conditioners, rather than ahead of them, allowing high frequency components to saturate the conditioners and invalidate the data at all frequencies.

(6) Lack of an anti-aliasing filter prior to analog-to-digital conversion, leading to Nyquist foldover, despite all warnings to the contrary.

(7) When nonstationary flight data are analyzed, the initiation of time windows manually by data processing personnel rather than by a time code-activated switch, resulting in erroneous spectra caused by uncontrollable time translations.

(8) Selecting a frequency resolution bandwidth wider than structural resonant bandwidths in random vibration data analysis, causing significant errors in the accurate determination of spectral peaks.

(9) Making pyroshock accelerometer measurements too close to the pyrotechnic source, allowing intense high frequency response components, including a possible accelerometer resonant response, to saturate the transducer and/or signal conditioner, and invalidate the resulting data at all frequencies.

(10) Human errors, often due to the lack of proper planning, training, communication, attention to details, and/or personal motivation in the data acquisition and analysis process, which can often be circumvented by direct user involvement in all aspects of these activities. One possible solution to this problem is to put all measurement functions, from instrument selection through processing data plots, under one organization made responsible by management for the accuracy of resulting data.

2.11 References.*

2.1 Himelblau, H., Fuller, C. M. and Scharton, T. D., "Assessment of Space Vehicle Aeroacoustic Noise-Induced Vibration Prediction, Design, Analysis and Testing", *NASA CR-1596,* July 1970.

2.2 Coe, C. F., and Brownson, J. J, "Instrumentation Applications to Space Shuttle Models and Thermal Protection System Tiles Tested in NASA-Ames Wind Tunnels", *IEEE Publ. 81CH1712-9,* Sept. 30, 1981.

2.3 Przemieniecki, J. S., *Theory of Matrix Structural Analysis,* McGraw-Hill, NY, 1968 (reprinted by Dover, Mineola, NY, 1985).

2.4 Craig, R. R., *Structural Dynamics: An Introduction to Computer Methods,* Wiley, NY, 1981.

2.5 Chwastyk, T. F., and Rapp, D. G., "A Quantitative Method for Evaluating Sensor Layouts," *Shock and Vibration Bull., No. 57, Pt.* 1, pp. 21-54, Jan. 1987.

2.6 Bert, R. L., "Effective Location of Pickups for Transient Measurements," *Proc., 61st Shock and Vibration Symp.*, Vol II, pp. 197-208, Oct. 1990.

2,7 Leissa, A, W., "Vibration of Plates", *NASA SP-160, 1969* (Ace. N70-1 *8461).*

2.8 Leissa, A. W., "Vibration of Shells", *NASA SP-288,* 1973 (Ace. *N73-26924).*

2,9 Blevins, R. D., *Formulas for Natural Frequency and Mode Shape,* Van Nostrand Reinhold, NY, 1979 (reprinted by Krieger, Melbourne, FL, 1984). "

2.10 Smallwood, D. 0., "The Application of Unloaded (Free) Motion Measurements and Mechanical Impedance to Vibration Testing", *Proc., Inst. Envir. Se.,* pp. 71-82, Apr. 1976.

2.11 Scharton, T. D., "Force Specifications for Extremal Dual Controlled Vibration Tests," *Proc., 61st Shock* and *Vibration Symp.*, Vol. I, pp. 105-115, Oct. 1990.

2,12 Scharton, T. D., "Force Limited Vibration Testing at JPL," *Proc., 14th Aerospace Testing Seminar,* Mar. 1993.

2.13 Telemetry Group, Range Commanders Council, "Telemetry Standards", *IRIG Std* 106-9.?, Jan. 1993,

2,14 Doebelin, E. O., *Measurement Systems: Application and Design, 4th* ed., McGraw-Hill, NY, 1990.

2,15 Dods, J, B., and Hanly, R, D., "Evaluation of Transonic and Supersonic Wind-Tunnel Background Noise and Effects on Surface Pressure Fluctuation Measurements", AIAA *Paper* 72-1004, Sept. 1972.

2.16 Bendat, J. S. and Piersol, A. G., *Engineering Application of Correlation and Spectral Analysis,* 2nd cd., Wiley, NY, 1993.

2.17 Lin, Y. K., *Probabilistic Theory of Structural Dynamics,* McGraw-Hill, NY, 1967 (reprinted by Krieger, Melbourne, FL, 1985).

2.18 Wise, J. H., and McGregor, J. W., "Synchronization of Data Recorded on Different Recorders", *NASA Tech Briefs,* Vol. 10, No. 2, p. 56, Mar./Apr. 1986.

2.19 Telecommunications Group, Range Commanders Council, "IRIG Standard Time Formats", *IRIG Std* 200-89, Mar. 1989 (DTIC No, AD A206580).

2.20 Taylor, J. L., *Fundamentals of Measurement Error,* Neff Instr. Co., Monrovia, CA, 1988.

2.21 Taylor, J. L., *Computer-Based Data Acquisition Systems,* 2nd ed., Instr. Soc. Amer., Research Triangle Park, NC, 1990.

2.22 Mark, A., et al, "Metrology-Calibration and Measurement Process Guidelines", *NASA RP - XxXX,* Draft 1992.

2.23 Wise, J. H., "DATE Dynamic Data Error Analysis", Proc., Shuttle Payload Dynamic Environments and Loads Prediction Workshop, *JPL Dec. D-1347,* Vol. I, pp. 97-111, Jan. 1984.

2.24 Telemetry Group, Range Commanders Council, "Telemetry Applications Handbook", *IRIG Dec.* 119-88, Feb. 1988 (DTIC No. AD A193741).

2.25 Anon, "Helical Digital Recording Format for 19-MM Magnetic Tape Cassette Recorder/ Reproducers", *MIL-STD-2179A,* Dec. 24, 1987.

2.26 Anon, "Military Standard, Calibration System Requirements", *MIL-STD-45662A,* Aug. 1, 1988.

2.27 Anon, "American National Standard, Pickups for Shock and Vibration Measurements Method for Specifying the Characteristics of", *ANSI Std Z24.21-1957 (R 1990).*

2.28 Anon, "American National Standard, Methods for the Calibration of Shock and Vibration Pickups", ANSI *Std S2.2-1959 (R 1990).*

2.29 Anon, “American National Standard, Techniques of Machinery Vibration Measurement”, *ANSI Std S2.1 7-1980 (R 1986).*

2.30 Anon, “American National Standard, Mechanical Vibration of Rotating and Reciprocating Machinery - Requirements for Instruments for Measuring Vibration Severity”, ANSI *Std* S2.40-1984 *(R 1990).*

2,31 Anon, “American National Standard, Guide to the Mechanical Mounting of Accelerometers”, ANSI *Std S2,61-1989.*

2,32 Anon, “American National Standard, Measurement of Sound Pressure Levels, Methods for”, *ANSI Std* **S1.13-1971** *(R* 1986).

2.33 Anon, “American National Standard, Calibration and Tests for Electrical Transducers used for Measuring Shock and Vibration, Selection of”, *ANSI Std* S2.12-1969 *(R 1989).*

2.34 Anon, “American National Standard, Method for the Calibration of Microphones”, *ANSI Std SI.1O-I966 (R1986).*

2.35 Anon, “American National Standard, Specifications for Laboratory Standard Microphones”, *ANSI Std S1.12-1967 (R1977).*

2.36 Anon, “American National Standard, Requirements for the Performance and Calibration of Reference Sound Sources”, *ANSI Std* S12.5-1985.

2.37 Anon, “American National Standard for Acoustical Calibrators”, *ANSI Std* S1.40-1984,

2.38 Anon, “American National Standard, Methods for Analysis and Presentations of Shock and Vibration Data”, ANSI *Std S2,1O-1971 (R1982).*

2.39 Anon, “American National Standard, Specification for Octave-Band and Fractional-Octave-Band Analog and Digital Filters”, *ANSI Std S1.11-1986.*

2,40 Anon, “American National Standard for Sound Level Meters”, *ANSI Std 5’2.4-1983.*

2.41 Anon, “Amendment to S 1.4-1983”, *ANSI Std S1.4A-1985.*

2.42 Brenig, A., et al, “Catalog of Acoustical Standards" *ASA Stds Cat. 7-1988.*

2.43 Anon, “American National Standard, A Guide for the Dynamic Calibration of Pressure Transducers”, *ANSI Std MC* 88.1-1972 *(R1987).*

2,44 Anon, "Electrical Transducer Nomenclature and Terminology”, *ANSI Std* S37.2-1975 *(R1982).*

2.45 Anon, "Guide for Specifications and Tests for Piezoelectric Acceleration Transducers for Aerospace Testing", *ANSI Std RP 37.2-1982.*

2,46 Anon, "Specifications and Tests for Strain Gage Pressure Transducers", *ANSI Std* S37,3-1975 *(R1982).*

2.47 Anon, "Specifications and Tests for Strain Gage Linear Acceleration Transducers", *ANSI Std S373-1975 (R1982).*

2.48 Anon, "Specifications and Tests for Strain Gage Force Transducers", *ANSI Std S37.8-1 9 7 7 (R1982).*

2.49 Anon, "Specifications and Tests for Piezoelectric Pressure and Sound-Pressure Transducers", *ANSI Std S37.1O-1975 (R1982).*

2.50 Anon, "Specifications and Tests of Potentiometric Pressure Transducers", *ANSI Std S37.6-1976 (R1982).*

2,51 Anon, "Specifications and Tests of Potentiometric Displacement Transducers", ANSI *Std S37.12-1977 (R1982).*

* Recent revisions of IRIG and ANSI standards may supersede those listed in these references. Information on IRIG documents [2.13, 2.19, 2.24] may be obtained from the following organizations:

U.S. Government Agencies
Secretariat
Range Commanders Council
Atm: STEWS-SA-R
White Sands Missile Range,
NM 88002-5110
Phone: (505) 678-1107

All Others
National Defense Logistics Agency
Defense Technical Information Center
Atm: FDRA
Cameron Station
Alexandria, VA 22304-6145
Phone: (202) 274-7633

Information on ANSI standards maybe obtained from the following three organizations:

Standards Secretariat [2.27-2.42]
Acoustical Society of America
120 Wall Street, 32nd Floor
New York, N Y 10005-3993
Phone: (212) 248-0373

Standard Secretariat [2.43]
American Society of Mechanical Engineers
34s East 47th street
New York, NY 10017
Phone: (800) 843-2763

Instrument Society of America [2.44-2.51]
POB 3561
Durham, NC 27702
Phone: (919) 549-8411

3. DATA ACQUISITION

3.1 Introduction, This section presents guidelines for the acquisition of dynamic data. Factors to be considered in the selection and usage of data acquisition instruments are discussed in the following sections and outlined in Figure 3.1. Some typical instrumentation configurations are shown in Figure 3.2,

3.2 Transducers. An instrumentation transducer converts the physical phenomenon of interest to an equivalent electrical signal for subsequent processing, and is the key instrument of the data acquisition system *[3.* 1- *3.3].* Transducers commonly used to measure dynamic loads and environments include accelerometers and velocity transducers, various pressure transducers, strain gages, and force transducers.

3.2.1 Sensing Elements. The nerve center of a transducer is its sensing element, which converts relative displacement or velocity to an electrical signal. The same type of sensing element is often used in different types of transducers. Hence, a short survey of the various sensing elements is appropriate before their transducer applications are described

3.2.1.1 Piezoelectric Materials. A piezoelectric (PE) material generates an electrical charge proportional to the instantaneous applied dynamic force or relative displacement, i.e., it is electrically self-generating. Many models of accelerometers and microphones employ PE materials [3.1 - 3.14]. PE materials may be naturally polarized single crystals (e.g., quartz, tourmaline, lithium niobate, Rochelle salt) or man-made artificially-polarized ferroelectric polycrystalline ceramics (e.g., barium titanate, lead zirconate, lead metaniobate, or combinations). The ceramics have a higher charge sensitivity and moldability to various shapes, whereas the crystals mayor may not have a higher voltage sensitivity and can be cut to various sizes and shapes. Both can be directionally polarized, e.g., made sensitive to shear rather than direct (tension/compression) loading. All PE materials are usable up to very high frequencies (above 1 MHz). However, they cannot hold a charge indefinitely under a static load because of susceptibility to leakage, although the amount of leakage is dependent on the type of PE material and the following electronics. Thus, they cannot provide a DC response. The low frequency limit of PE transducers is controlled mainly by the characteristics of the cable type and capacitance, and signal conditioning electronics. Because a PE material generates its own electrical signal, a "power supply is not needed for signal generation. PE materials are sensitive to humidity, salt spray, chemical contamination, dust, dirt, temperature changes, and have low and high temperature limits.

3.2.1.2 Strain-Sensitive Materials. A strain-sensitive (SS) material changes its electrical resistance in proportion to the instantaneous spatial-average strain applied over the surface area of the material. All strain gages and internal load measurements, and many accelerometers and pressure transducers use SS materials [3.1 -3.5, 3.14- 3.21]. There are two categories of SS materials:

Transducers (3.2)

- Sensing Elements (3.2.1)
- Single DOF System (3.2,2)
- Measurement Parameters (3.2,3)
- Environmental Effects (3.2.4)
- Physical Properties (3.2.5)
- Motion Transducers (3.2.6)
- Pressure Transducers (3.2.7)
- Strain Gages (3.2.8)
- Force Transducers (3.2.9)

Signal Conditioners (3.3)

- Strain Gage Conditioners (3.3. 1)
- Amplifiers (3.3.2)
- Filters (3.3.3)
- Power Supplies (3.3.4)
- Cabling (3.3.5)

Multiplexers and Demultiplexers *(3.4)*

- Freq. Division Multiplexing (3.4.1)
- Time Division Multiplexing (3.4.2)
- Demultiplexers (3.4.3)

Communication Links (3.5)

- Land Lines (3.5. 1)
- Radio Frequency Telemetry (3.5.2)

Recording, Playback. and Storage (3.6)

- Data Capacity (3.6. 1)
- Frequency Response (3.6.2)
- Recording Modes (3.6.3)
- FDM Recording (3,6.4)
- TDM Recording (3.6.5)
- Ancillary Signal Recording (3.6.6)
- Tape Copying (3.6.7)
- Tape Storage (3.6.8)

Analog-to-Digital Converters (3.7)

- Instruments (3.7, 1)
- Sampling Rate and Aliasing (3.7.2)
- Anti-Aliasing Filters (3.7.3)
- Other ADC Errors (3.7.4)
- Multiple-Channel Digital Con. (3.7.5)
- Digital-to-Analog Converters (3.7.6)

System Calibration (3.8)

- Laboratory Calibration (3.8.1)
- End-to-End Electrical Cal. (3.8.2)
- End-to-End Mechanical Cal. (3.8.3)
- Linearity Calibration (3.8.4)

System Gain Settings (3.9)

- Stationary and Steady State Data (3.9.1)
- Nonstationary and Trans. Data (3.9.2)

Record Keeping (Log Sheets) (3.10)

Figure 3.1. Data Acquisition Instrument Selection Guide..

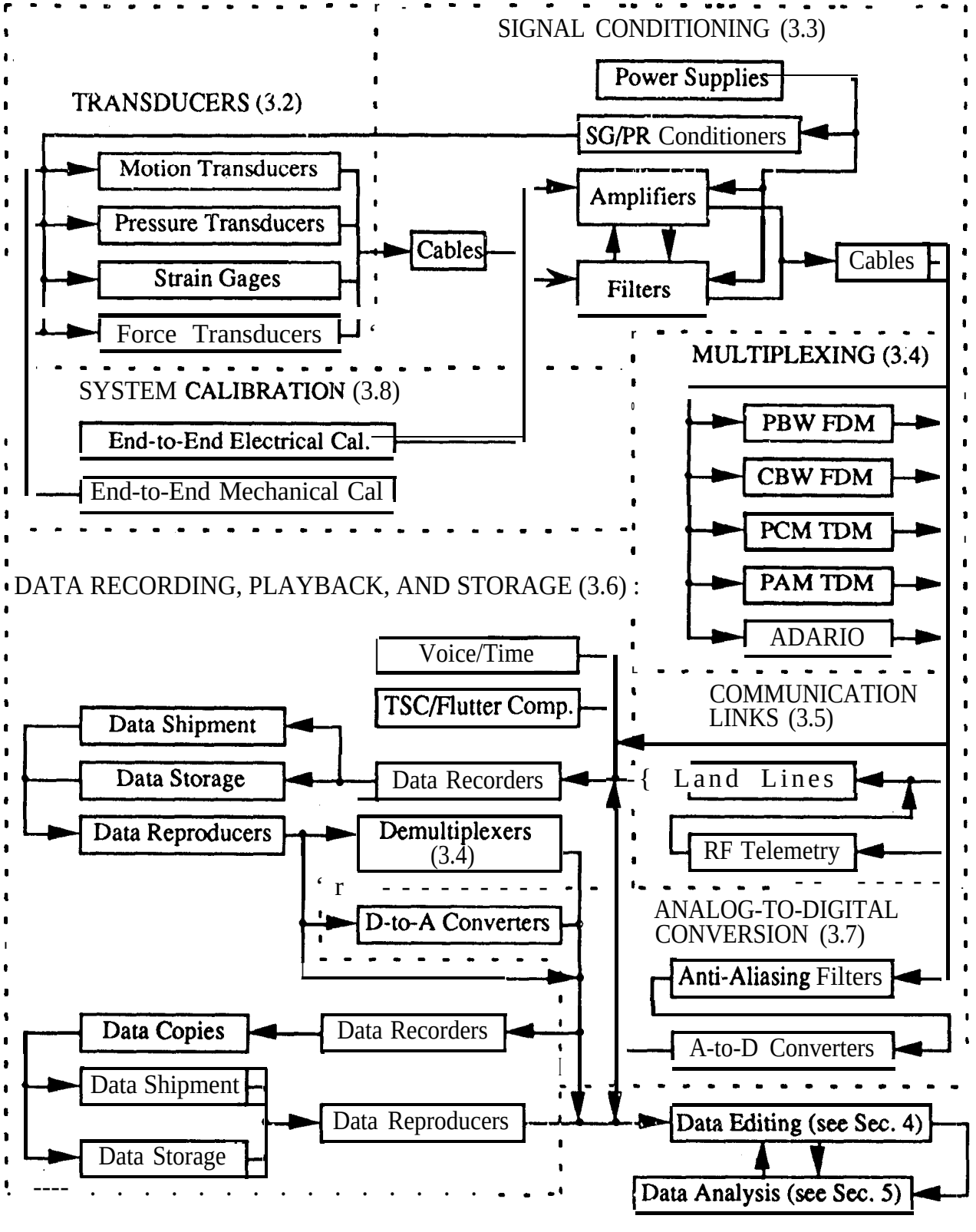

Figure 3.2 Some Typical Data Acquisition instrument Configurations.

metallic and semiconductor. The most common metallic materials are Constantan (a copper-nickel alloy), Karma (mainly nickel-chrome) and occasionally Isoelastic (mainly iron-nickel-chrome), whereas the most common semiconductor material is nearly pure monocrystalline silicon with intentional trace impurities. There are two types of silicon: the p-type (positive) usually with boron as the trace impurity, and the n-type (negative) usually with arsenic as the trace impurity. The metallic materials and p-type semiconductor show an increase in resistance with an increase in mechanical- and/or thermal-induced tensile strain, whereas the n-type semiconductor exhibits a decrease in resistance with an increase in mechanical-induced strain and an increase in resistance with an increase in thermal-induced tensile strain. This latter property can provide a substantial advantage in the utilization of semiconductor materials, as described in Section 3.2.4.1. When the SS material is a semiconductor, it is usually called piezoresistive (PR). SS materials do not generate an electrical signal. This must be furnished by a power source, usually in the signal conditioner. In nearly all cases, the electrical configuration of the power source, the material(s), and the

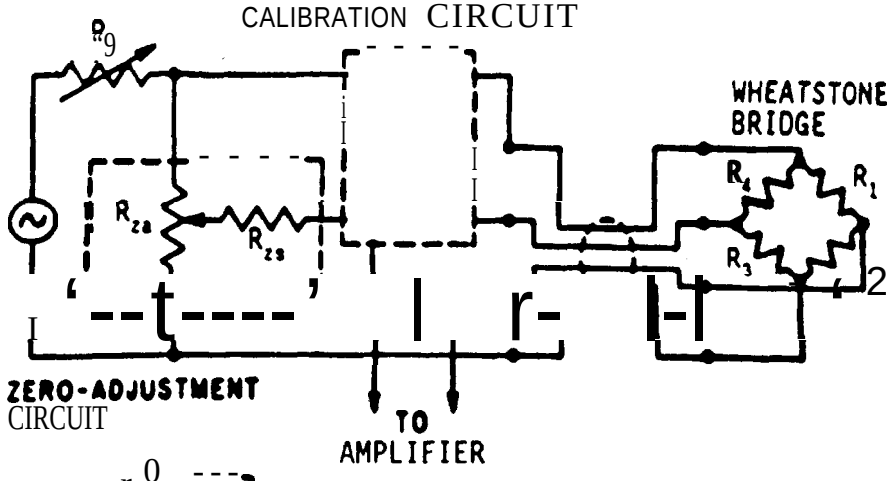

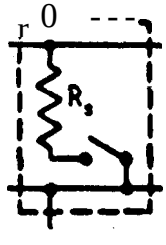

Shunt Calibration Circuit for Metallic Strain Gages and Transducers, and for Semiconductor Strain Gages and Transducer with Two Active Arms (R_1 and R_2) and Two Fixed Resistor Arms (R_3 and R_4)

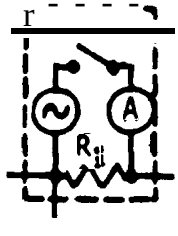

Voltage Insertion Calibration Circuit for Semiconductor Strain Gages and Transducers with Four Active Arms. (Insert voltage power supply is ungrounded.) ,

Figure 3.3. Circuit Diagram of a WheatStone Bridge for Strain Sensitive Materials, including Metallic and Semiconductor (Piezoresistive) Strain Gages and Transducers [3.15].

signal output is in the form of a Wheatstone bridge (actually invented by Samuel Christie), as shown in Figure 3.3. SS materials are installed in one, two, or four arms of the bridge, denoted by RI through R_4 in Figure *3.3,* depending on the transducer application. If loaded SS materials are installed in either one or two arms of the bridge (called active arms), then unloaded SS materials and/or fixed resistors should be installed in the remaining (dummy) arms. All SS materials cover a very wide frequency range that extends from zero (DC) to a high frequency that greatly exceeds the maximum frequency of interest, e.g., O -1 GHz, as long as the SS material is uniformly loaded. SS materials are sensitive to temperature changes, but the effects are concentrated in the frequency range near DC. In fact, SS materials are commonly used as temperature sensors. However, temperature compensation often can be successfully achieved with care. When installed, SS materials nearly always need to be protected from high humidity and other climatic environments,

3.2.1.3 Capacitance Elements. A conventional capacitance element (CE) is comprised of two parallel conductive plates separated by a small distance. An electrical DC voltage applied across the plates, called a polarizing voltage, causes an electric field to be developed in the intervening space (called the dielectric). One of the two plates is the fixed reference, while the other plate moves in proportion to the dynamic response, resulting in a capacitance change that is sensed by the system electronics. To provide linearity, the maximum dynamic displacement must be small compared to the gap between the plates. To make the CE more sensitive, it is common to replace the second plate, whose dynamic response is controlled by its bending resistance, by a thin diaphragm, whose response is controlled by membrane or in-plane resistance. The polarizing voltage is nearly always supplied by a power source in the signal conditioner. As a displacement-sensing element, the CE is equally sensitive to displacement at any frequency, including DC. However, the dynamic displacement of the load usually decreases with increasing frequency, limiting the practical frequency range. In addition, the CE cannot hold a constant charge indefinitely because of leakage.

The condenser microphone is the most common transducer in aerospace usage that employs a conventional CE, although other transduce including accelerometers have been developed [3.1, 3.5, 3.8, 3.9, 3.12, 3.13, 3.22, 3.23]. To avoid letting atmospheric pressure changes cause a static bias between the plates of the microphone, the air gap is nearly always vented to the atmosphere. For this reason, a CE microphone will not measure pressure down to zero frequency. Conventional CEs are generally insensitive to temperature changes, but will be sensitive to humidity if condensation occurs, due to the influence of humidity on charge leakage. To avoid the degrading effects of humidity, conventional CEs may be heated locally and should be stored with a desiccant between usage. Special protection must be provided for long-term outdoor applications.

Another type of CE is the electret, which does not require a polarization voltage [3.3, 3.9,3. 12]. Polarization is provided by a pre-polarized polymer containing a trapped charge bonded to the molecules of the polymer. The polymer material is either deposited onto the backplate or is contained in a thin film stretched across the air gap. The electret CE is insensitive to humidity.

3.2.1.4 Electrodynamic Systems. An electrodynamics system (EDS) uses a moving coil of wire in a fixed (non-moving) or a moving DC magnetic field, which cuts lines of magnetic flux to generate an electric current from the coil. Since the instantaneous current is proportional to the rate at which the coil cuts the flux lines, the electrical output is proportional to the relative velocity between the coil and the magnetic field [3. 1,3.2, 3.23]. The velocity pickup is a typical EDS.

3.2.1.5 Servo-Control Systems. A servo-control system (SCS) employs a combination of electrical and mechanical elements in an attempt to prevent a mass from moving relative to its case when it is exposed to structural motion [3.1, 3.2, 3.23]. Specifically y, the instantaneous acceleration applied to the mass causes an instantaneous displacement from its equilibrium or neutral position, which is sensed by a displacement transducer whose instantaneous electrical output signal is used in a servo control loop to restore the mass to its neutral position. This electrical signal, which is proportional to the acceleration of the mass, is the output of the SCS. The power source 'is incorporated in the signal conditioning section of the SCS. This principle of operation has been used extensively in aerospace guidance and navigation applications. A typical SCS is very sensitive in the low frequency range, including zero frequency. As with many other sensing elements, extending the range to mid frequencies can be accomplished at the expense of reduced sensitivity.

3.2.1,6 Electro-Optical Systems. There are a variety of electro-optical systems (EOSs) that use a beam of visible or laser light (sometimes through an optical fiber) to sense relative motion, either displacement or velocity, between a fixed reference and a point on a structure responding to dynamic loading [3, 1, 3.23]. For one such EOS, called a laser Doppler vibrometer (LDV) and described in Section 3.2.6.5, the instantaneous structural velocity causes a Doppler shift in the frequency between the incident and the reflected beams of light [3.24- 3.29]. An electrical circuit converts the Doppler shift into an instantaneous electrical signal that is proportional to the instantaneous velocity of the reflecting surface. Fringe-counting interferometers are another type of EOS. The shift of the constructive/destructive interference pattern between the incident and reflected light beams, or the number of wavelengths that the reflecting surface moves, is counted and translated into an instantaneous electrical signal which is proportional to the instantaneous displacement. Other EOSS differentiate between the intensities of the incident and reflected light beams. EOSS are generally very sensitive and thus capable of measuring very small motions of the structure, as long as the fixed reference itself does not move. As a result, EOSS are usually restricted to laboratory use. The frequency range of a velocity sensing system may include or exclude DC, depending on system operation. A displacement-sensing system is equally sensitive to displacement at an y frequency, including zero frequency. However, the dynamic displacement of the load or environment usually decreases with increasing frequency (with the exception of pyroshock), limiting the practical frequency range to low and mid frequencies.

Other EOSS are used primarily for measuring mode shapes in modal testing, and are therefore outside the scope of this Handbook. These include holography, surface scanning interferometers, and

3.8, where the ordinate is $(\dot{\delta}_s/\dot{U}_s)$ for a sinusoidal base velocity excitation $\dot{u}(t) = \dot{U}_s \sin(2\pi f_s t)$, and $\dot{\delta}_s = |\dot{x} - \dot{u}|$, is the relative velocity amplitude between the mass and the base [3.4]. The phase angle ϕ between the relative velocity response and the velocity excitation in Figure 3.8 is the same as that shown in Figure 3.5,

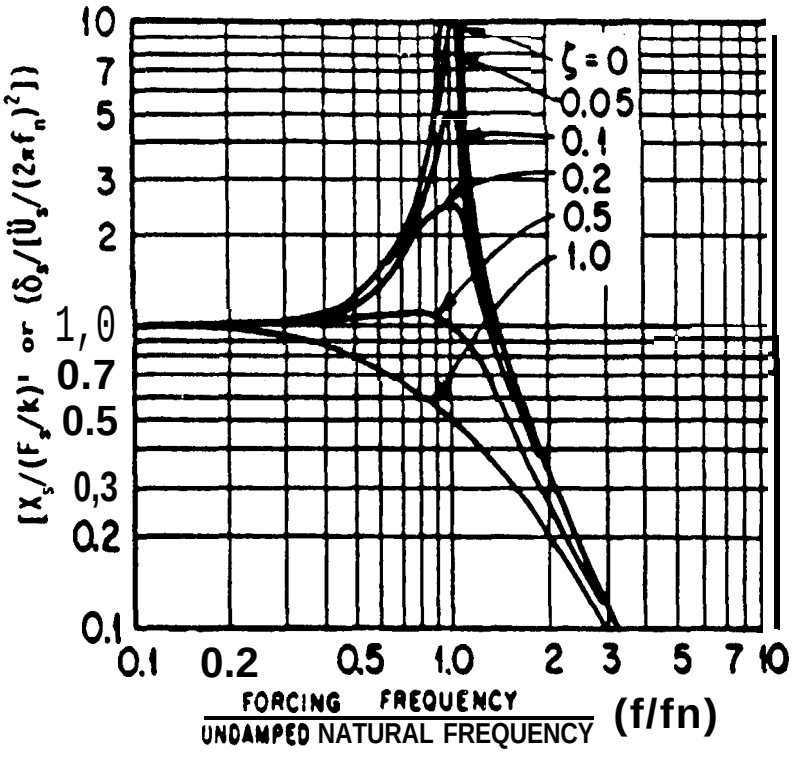

X_s = displacement response amplitude of the mass
F_s = amplitude of sinusoidal force excitation
δ_s = $|x-u|_s$ = relative displacement amplitude between the mass and the base
$\dot{U}_s$ = amplitude of sinusoidal base acceleration excitation
k = spring rate or stiffness
f = excitation frequency
f_n = undamped natural frequency
ζ = viscous damping ratio or fraction of critical damping

Figure *3.4,* Normalized Response of a Linear Single-Degree-of-Freedom System to Sinusoidal Force or Base Acceleration Excitation [3.4].

a system for determining modal stress distributions by sensing the thermal emissions from the structural surface.

3,2,1,7 Other Types of Sensing Elements. There are a wide variety of other sensing elements available for utilization in transducers, e.g., eddy current, differential transformer, variable reluctance, fiber optic, and potentiometer devices. However, they are seldom currently used for dynamic measurements in aerospace applications *[3.1, 3,2,* 3.23, 3.30, *3.31].* The primary reason for the lack of aerospace utilization is nearly always excessive size and weight, limited sensitivity, and/or useful frequency range.

3.2,2 Single-Degree-of-Freedom System. With the exception of strain gages applied directly to structures, force transducers, and electro-optical systems, the basic design feature of a transducer used for making dynamic measurements is the linear single-degree-of-freedom (or SDF) system, where the electrical transducer output is proportional to either the absolute or relative displacement or velocity response of the system. Specifically, pressure fluctuations on pressure transducers can be idealized by a force excitation applied to the mass of the SDF system, whereas motion to accelerometers and velocity pickups can be idealized by the motion excitation applied to the base or foundation of the SDF system. The former and latter models are sometimes called fixed reference and seismic transducers, respectively, All elementary vibration texts introduce the SDF system. The normalized frequency response for the SDF system below or near resonance is shown in Figure 3.4, where the ordinate is $[X_s/(F_s/k)]$ for a sinusoidal force excitation $F(t) = F_s\sin(2\pi f_s t)$ or $\{\delta_s/[\ddot{U}_s/(2\pi f_n)^2]\}$ for a sinusoidal base acceleration excitation $u(t) = \ddot{U}_s\sin(2\pi f_s t)$, where F_s and $\ddot{U}_s$ are the force and base acceleration amplitudes, respectively. The abscissa is the ratio of the sinusoidal excitation frequency f_s to the system undamped natural frequency f_n, k is the spring rate (or stiffness), X_s is the displacement response amplitude of the mass, and $\delta_s = |x-u|_s$ is the relative displacement amplitude between the mass and the base. The family of curves shown in Figure 3.4 correspond to different values of the viscous damping ratio ζ (or fraction of critical damping) [3.4]. The phase angle ϕ between the displacement response and the force excitation is shown in Figure 3.5 as a function of frequency ratio. and damping [3.32]. The negative value of ϕ denotes that the response lags behind the excitation in time, The phase angle θ between the relative displacement response and the acceleration excitation may be calculated from $\theta = 180° +\$$, where $(-180' \leq \phi \leq O)$. Thus θ is always positive. Only small portions of the total ranges, shown in logarithmic coordinates in Figures 3.4 and 3.5, are normally utilized in pressure transducer and accelerometer design. These portions, at frequencies below resonance, are detailed in linear coordinates in Figures 3,6 and 3.7 [3.4, 3.33].

The electrical output of a velocity pickup is proportional to the relative velocity response of the system. Motion to the pickup can be idealized by the motion excitation applied to the base of the SDF system. The normalized frequency response near and above resonance is shown in Figure

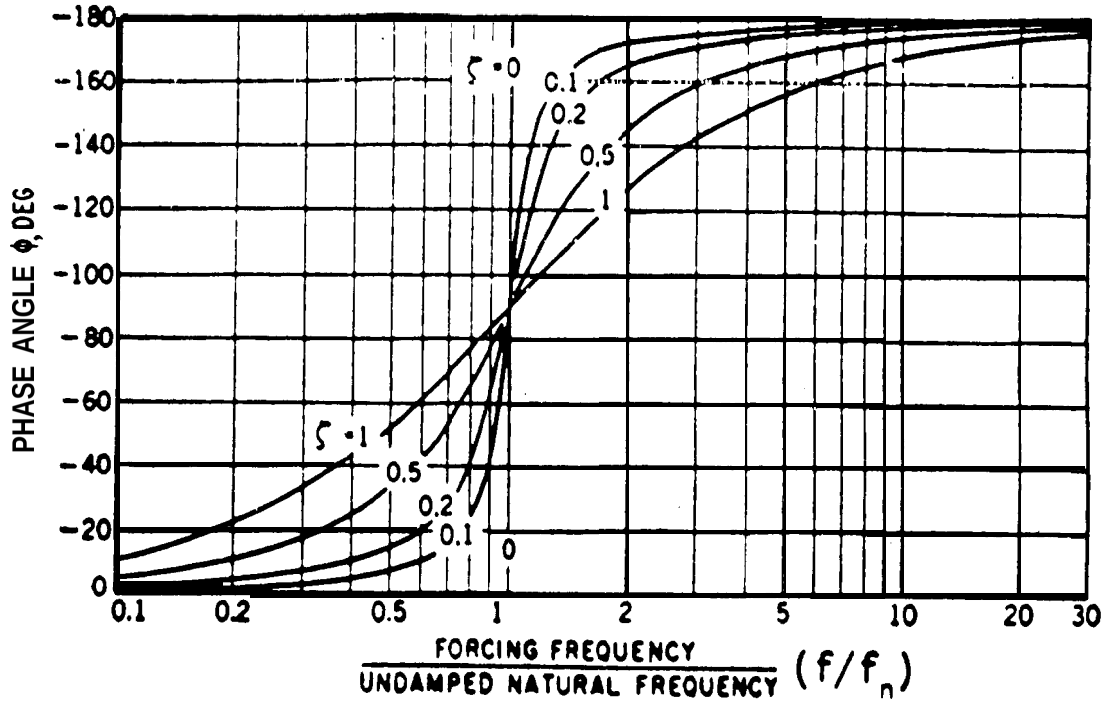

Figure 3.5. Phase Angle Between the Sinusoidal Response and Excitation for a Linear Single-Degree-of-Freedom System [3.32].

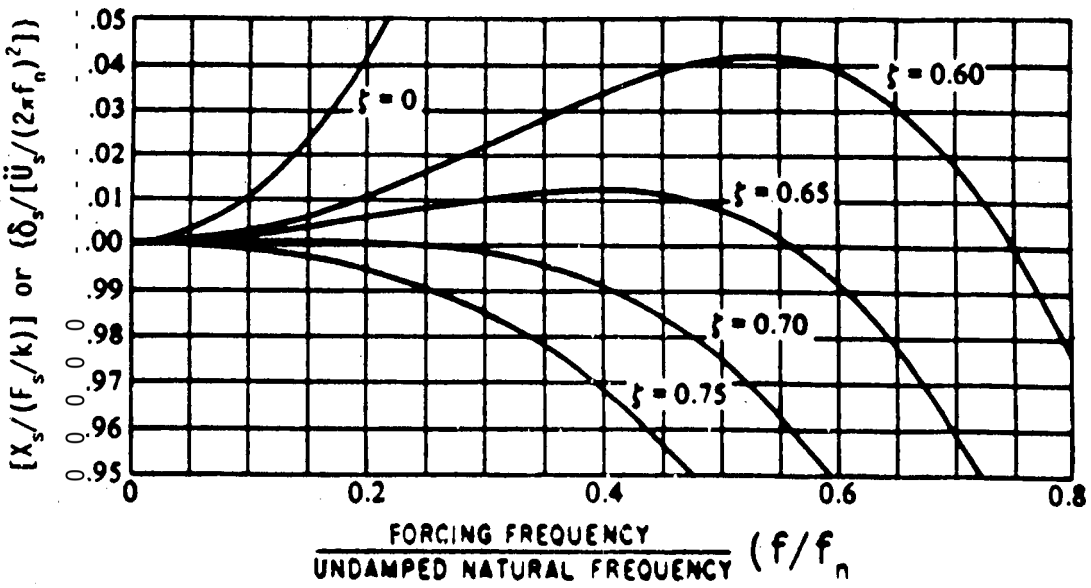

Figure 3.6. Range of Single-Degree-of-Freedom System Responses Normally Used in Accelerometer and Pressure Transducer Design [3.33].

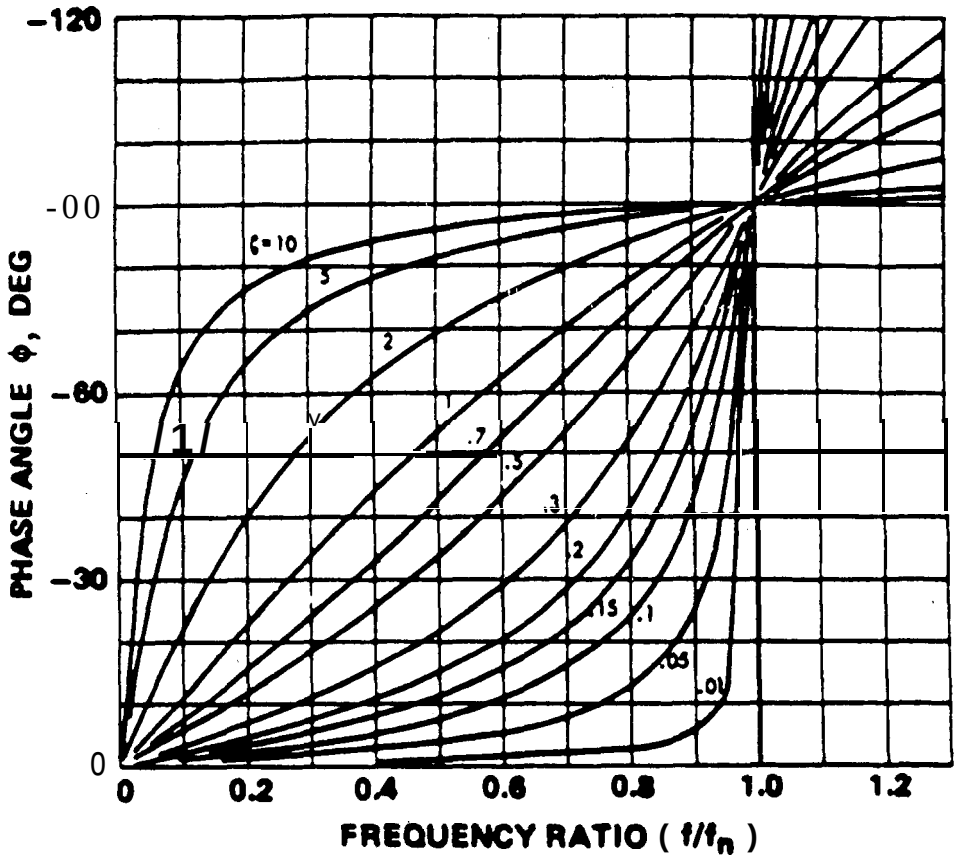

Figure 3.7. Range of Single-Degree-of-Freedom System Phase Angles Normally Used in Accelerometer and Pressure Transducer Design [3,4].

It is important to mention that when the SDF system is used as a fixed reference transducer, it is assumed that there is no base motion; when it is used as a seismic transducer, it is assumed that no force is applied to" the mass. Hence, a transducer using the fixed reference feature must be designed to avoid base motion, whereas one using the seismic feature must be designed to avoid direct force or pressure applied to the mass.

3.2.3 Measurement Parameters. *The* selection of transducers for measuring loads and environments should take into account all the factors or parameters that can affect the accuracy and reliability of the measurements. Depending on the type and installation of the transducer, and the total environmental exposure, some of these parameters may have a severe effect on accuracy and reliability, whereas the effects of others maybe negligible [3.1 - 3,23]. These measurement parameters are summarized in the following sections. A more detailed source of data is usually available from manufacturers' catalogs and specification sheets. It is also recommended that manufacturers, previous and current users of candidate transducers, and/or consultants be contacted concerning their evaluation of these measurement parameters.

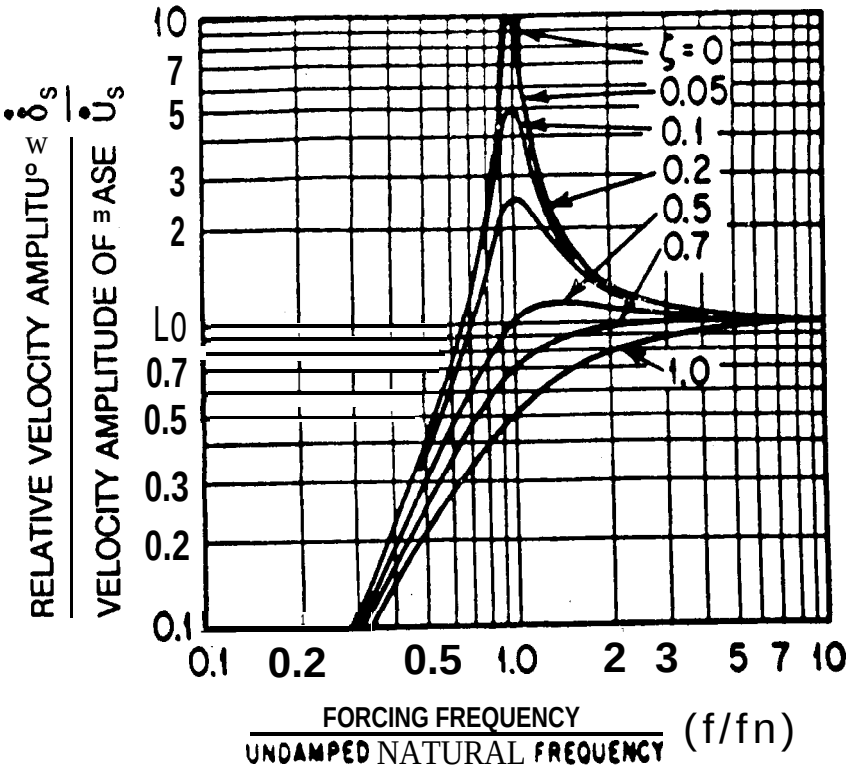

Figure 3.8. **Normalized Relative Velocity Response of a Linear Single-Degree-of-Freedom System** to Sinusoidal Velocity Base Excitation [3.33].

Typical environmental effects are described in Section 3.2.4. It is recommended that the user(s) ascertain under what specific conditions the measurement parameters and environmental effects were determined

3.2.3.1 **Transducer Sensitivity**. The sensitivity is the ratio of the transducer **electrical** output to the physical input (static **and/or** dynamic) magnitude. A high sensitivity is usually **desirable** when the load or environment is small, and vice versa. It is recommended that sensitivity calibration be performed on every transducer in accordance with Section 3.8.11. Tight control of transducer sensitivity is critical if the transducer output is **connected** directly to a recording instrument. However, if the transducer output is first connected to a variable gain signal conditioner, tight tolerance on sensitivity is unnecessary.

The maximum output of the transducer will equal the maximum value of the load or environment times the transducer sensitivity. To fully utilize the dynamic range of the measurement system, as described in Section 2.4, the maximum output should be made slightly less than the maximum instantaneous value of the signal that the system can transmit without distortion.

If the load or environment to be measured is not of high magnitude, sensitivity can become an important factor for a less-sensitive small and/or light weight transducer. In this case, amplification from the following signal conditioner can be used to provide the desired output as long as care is taken to avoid a substantial increase in background electrical noise,

Because strain gages rely on external power rather than generate their own electrical signals, the sensitivity is given in terms of a gage factor, defined as the ratio of the load-induced resistance change to the original (or unloaded) resistance, divided by the strain. Metal gages have (uniaxial) gage factors of about 2 through 5, whereas piezoresistive gages have factors that range from about 50 to nearly 200 for p-type silicon, and from about -100 to over -150 for n-type silicon, In Wheatstone bridge applications, the sensitivity in terms of bridge output can be doubled by using active strain gages in two arms, or can be quadrupled by using active gages in four arms, rather than by using only a single (active) gage in one arm with dummy gages and/or fixed resistors in the remaining arms *[3,3 -3.5, 3.15 -3,2* 1]. The variety of applied voltages, available gage resistances and gage factors provides a wide range for measuring static and/or dynamic strains.

3.2.3.2 Useful Frequency Range. Over the useful range, the sensitivity of a transducer should not vary more than a (usually small) specified amount from the nominal value. A plot of transducer sensitivity versus frequency is usually called the frequency response of the transducer. The minimum and maximum frequency limits are often specified where the frequency response is either 1 dB (12%) or 0.5 dB (6%) below or above the nominal value, It is recommended that frequency response calibration be performed on each transducer in accordance with Section 3.8.1.1. For transducers capable of measuring static and dynamic loads (e.g., strain gages and piezoresistive pressure transducers and accelerometers), the minimum frequency limit is usually zero frequency. For other transducers, the minimum frequency limit is usually dependent on the transducer design and/or its electrical compatibility with its cabling and/or its signal conditioner. For example; the low frequency cut-off or 3 dB down point for a piezoelectric transducer is given by [3.5, 3.7, 3.14, 3.34]

$$f_{1c} = \frac{1}{2\pi RC} \tag{3.1}$$

When the following signal conditioner is a voltage amplifier, described in Section 3.3.2.1: $C = C_t + CC + C_a$, and $R = 1/(R_t^{-1} + R_c^{-1} + R_a^{-1})$, where C_t, CC and C_a are the capacitances of the transducer, coax cable and amplifier input, and R_t, R_c and R_a are the resistances of transducer leakage, coax cable and connector leakage, and amplifier input, respectively. For a charge amplifier, described in Section 3.3.2.2: $C = C_f$ and $R = R_f$, where C_f is the capacitance of the amplifier feedback capacitor, and R_f is the shunt resistance across the feedback capacitor.

For accelerometers, which use the SDF design feature, the maximum frequency limit is usually determined as a function of the mounted resonance frequency and the viscous damping ratio of the sensing element, For example, Figures 3.4 and *3.6* show that the maximum frequency limit should be less than 0.2 or 0.3 of the undamped natural frequency, for a SDF system with no damping, to achieve a flat frequency response within + *0.5* dB or + 1 dB, respectively. For some SDF-based transducers, it is difficult to obtain both a high sensitivity and a high maximum frequency limit. Specifically, as observed in the ordinate of Figure 3.4, a high sensitivity for base acceleration excitation, proportional to $(\delta_s/\ddot{U}_s)$, can only be achieved with a low resonance frequency. Similarly, a high sensitivity for force excitation, proportional to (X_s/F_s), can only be achieved with a low stiffness, resulting in a low resonance frequency. For example, Figure 3.9 shows the various combinations of transducer sensitivities and useful frequency ranges for a, family of condenser microphones [3.9, 3,22, 3.35]. However, the use of the SDF system does not guarantee a nearly flat frequency response. Figure 3.10 shows the frequency response for a typical piezoelectric accelerometer within the useful range, normalized to the sensitivity at 100 Hz. In addition, the maximum frequency limit may be reduced by the method of attachment, as described in Section 3.2.6.6. Resonances of the transducer structure have sometimes been observed well below the SDF resonance, as illustrated in Appendix A, which may further limit the useful frequency range.

For velocity pickups, which also use the SDF design feature, the minimum frequency limit is usually determined as a function of the mounted resonance frequency and the viscous damping ratio of the sensing element. For example, Figure 3.8 shows that the minimum frequency limit

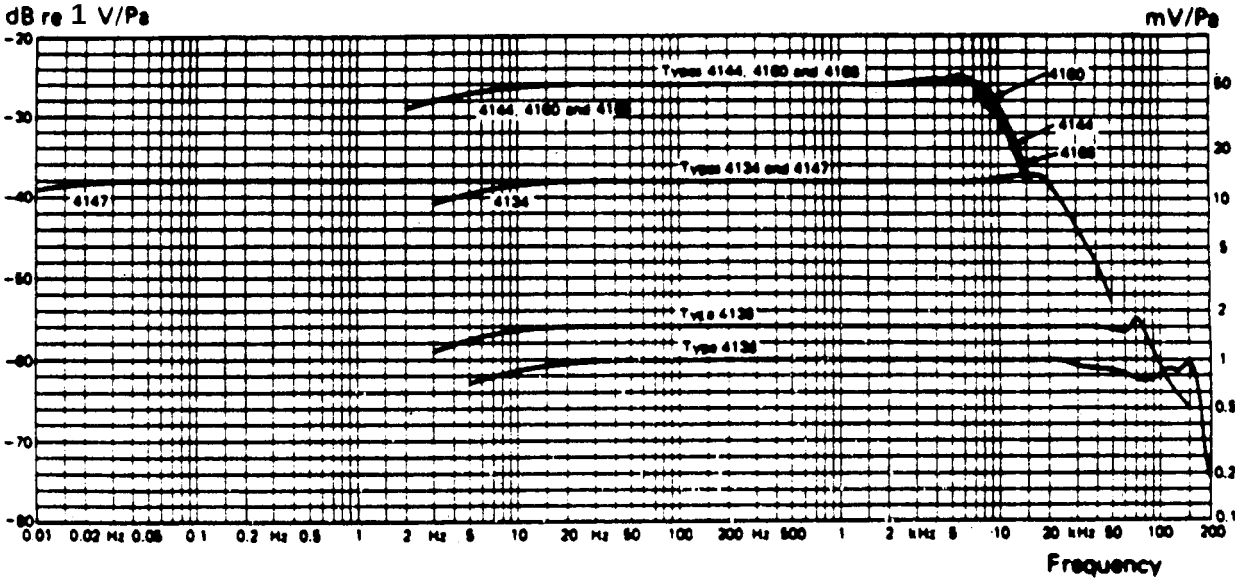

Figure 3.9. Typical Frequency Response for a Family of Similarly-Designed Condenser Microphones (Courtesy Bruel & Kjaer) [3.22, 3.35].

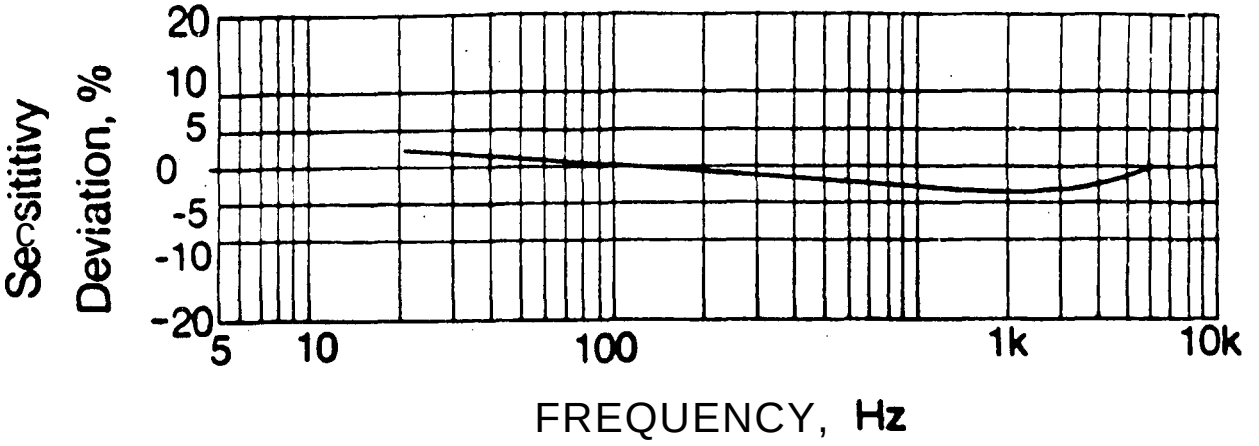

Figure 3,10. Typical Frequency Response for a Piezoelectric Accelerometer, Normalized to the Sensitivity at 100 Hz (Courtesy Endevco) [3.5].

should be more than 3.0 or 4.1 times the undamped natural frequency, for a SDF system with no damping, to achieve a flat frequency response within+ 1 dB or + 0.5 dB, respectively. The maximum frequency limit is dependent on the particular transducer design.

As mentioned in Section 3.2.1.2, uniformly-loaded strain gages, which are directly applied to structures, can exhibit exceedingly high maximum frequency limits, e.g., 1 GHz. However, there are structural and gage size considerations that may limit the maximum frequency when measuring strains associated with various waves propagating from a source, such as a pyrotechnic device, along a structure to a location of interest. For a strain gage to be uniformly loaded during wave propagation (i.e., to avoid strain cancellation along the length of the gage), the structural wavelengths must be appreciably longer than the gage length, say $\lambda_s > 8L_g$ where λ_s is the structural wavelength and L_g is the gage length. Longitudinal (or direct tension-compression) waves maintain the same waveform as they propagate through the structure, even though they maybe attenuated with distance from the source. For longitudinal waves: $\lambda_s = \lambda_L = (c_L'/f)$, where λ_L is the longitudinal wavelength, c_L' is the constant longitudinal wavespeed in a plate, and f is the frequency. For most metallic aerospace structures, $c_L' \approx 17{,}000$ ft/sec $\approx 200{,}000$ in./sec (ips). The longitudinal wavespeed for most composite structural materials, such as graphite epoxy, is much higher. Combining the above equations, the maximum frquency limit for longitudinal waves is $f_{mu} = (c_L'/8L_g)$. Bending waves are dispersive, i.e., the waveform changes with distance from the source. For bending waves, $\lambda_s = \lambda_B = (c_B/f)$, where the frequency-dependent bending wavespeed is $c_B = (2\pi f)^{1/2} (D/\langle\rho_s t\rangle)^{1/4}$, D is the modulus of rigidity and $\langle\rho_s t\rangle$ is mass per unit area of the structure [3.36, 3.37]. Therefore, the maximum frequency limit for bending waves is $f_{mu} = (\pi/32\, L_g^2)\, (D/\langle\rho_s t\rangle)^{1/2}$. Note that a small change in gage length has a significant effect on the useful frequency range. For metallic aerospace structures <u>without</u> stiffeners, the quantity

$(D/<\rho_s t>)^{1/2} = (c_L' t/12^{1/2})$, where t is the structural thickness. In most cases, the maximum frequency limit for longitudinal waves exceeds that for bending waves.

Sometimes a single transducer that responds down to zero frequency is used to provide data on the quasi-static and dynamic load or environment separately (rather than combined), using a lowpass filter to measure the quasi-static component and a highpass or a bandpass filter to measure the dynamic component. Depending on the magnitude and frequency range, a different amplifier gain setting is used for each component to maximize the signal-to-noise ratio. An amplifier with bias adjustment can zero out a DC component to maximize the dynamic range of the dynamic component.

There are some occasions where the user(s) and/or instrumentation personnel may find it necessary to measure dynamic loads and/or environments in frequency ranges well above and/or below the previously-described conventional limits [3.38 - 3.42]. This situation may occur when the test schedule does not permit the purchase of instruments that are appropriate for the desired frequency range. Under these circumstances, it may be possible to use currently available, though inadequate, instruments and then to correct the resulting data for measurement system deficiencies, For example, it may be desired to obtain dynamic data at frequencies above the resonances of available transducers. After the data are acquired, the resulting time histories can be transformed into their Fourier spectra and divided by the system frequency response function to obtain corrected spectra, which can then be inverse transformed back into corrected time histories for further processing, However, it is essential that the system not be used beyond the linear magnitude range; otherwise no valid correction can be made. Also, the original signal must significantly exceed the background noise so that the procedure does not erroneously "correct" the noise floor. In many cases, the correction process turns out to be more expensive than the cost of appropriate instruments that need no correction. Thus, this process is not generally recommended.

3.2.3.3 Magnitude Characteristic. Three factors comprise the amplitude or magnitude characteristics of a transducer: linearity, minimum limit, and maximum limit. Linearity is defined as the amount of invariance of the transducer sensitivity with input magnitude. The minimum limit is the lower instantaneous magnitude of acceptable linear behavior. For modem transducers, all of which are designed to avoid friction in their sensing elements, the minimum limit is nearly always caused by the background electrical noise floor, The maximum limit is the upper instantaneous magnitude of acceptable linear behavior. The maximum limit is usually determined by mechanical hardening of the stiffness element(s) of the transducer, hard bottoming on mechanical stops, which often causes electrical saturation, or by mechanical failure. Figure 3.11 shows the useful operating range of a particular piezoelectric accelerometer, which combines the useful frequency range with the linear magnitude range of the transducer [3.4, 3.10]. Note that this accelerometer has a dynamic range of over 140 dB, roughly double the range anticipated for most accelerometers.

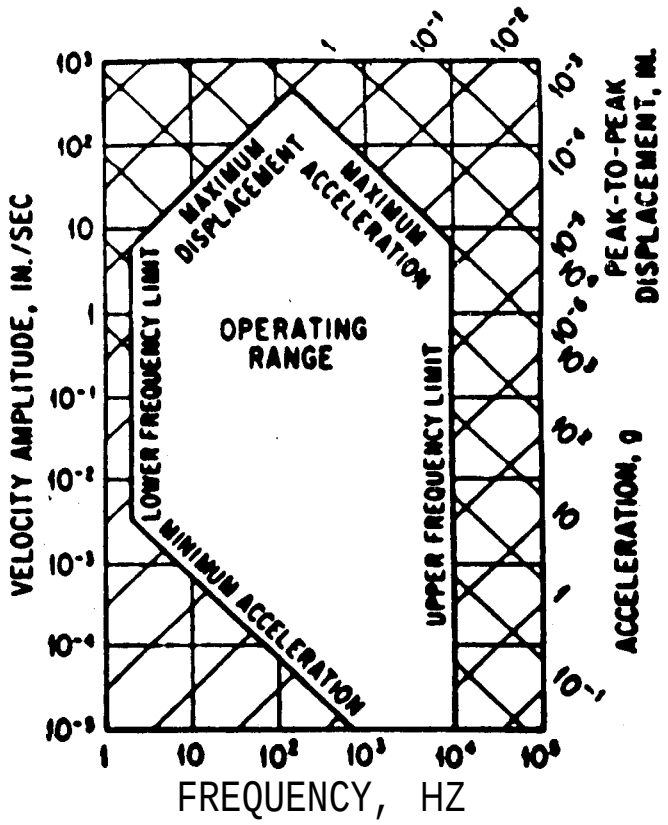

Figure 3.11. Useful Operating Range for a Piezoelectric Accelerometer [3.4,3.10].

3.2.3,4 Phase Shift. Phase shift is a description of the frequency-dependent time delay between the transducer electrical output and the physical input, and is therefore important to the potential distortion of the time history or waveform of the physical input. Phase shift is often observed with transduce that use the SDF design feature, where the phase shift is a function of frequency ratio and viscous damping ratio, as shown in Figures 3.3 and 3.5. For transducers with low darnping, say $\zeta \leq 2\%$, the phase angle is small (i.e., less than 2.5 deg) for a maximum frequency limit of 0,6 of the transducer resonance frequency. However, as discussed in Section 3.2.3.2, the maximum frequency limit must be further restricted to 0.2 or 0,3 of the resonance frequency to achieve flat frequency response within 0.5 dB or 1 dB, respectively, with damping of $\zeta \leq 2\%$. Undistorted waveforms can be maintained even with large phase shifts as long as the phase angle is proportional to frequency. Figure 3.7 shows that a transducer with a damping of{= 0.7 has a nearly linear phase shift up to the resonance frequency. However, Figure 3.6 shows that the maximum frequency limit must be further restricted to less than 0.55 of the undamped natural frequency to achieve a nearly flat frequency response with this damping. Hence, except for strain and force gages, most transducers are designed to have damping of either near zero or 70% of critical to minimize phase distortion. Minimizing phase distortion is especially important for transient data analysis, including shock response spectra computations [3.43].

Relative phase shift between transducers is usually critical for dual channel analyses, even when the phase shift is sufficiently linear to avoid intra-channel distortion problems. For example, inter-channel phase distortion will occur between a microphone with $\zeta \approx 0.01$ and an accelerometer with $\zeta \approx 0.7$, providing a phase shift proportional to frequency up to the limits described above, However, so long as the individual phase responses are known, the effects of phase distortion may be corrected later during dual channel computations.

3.2.3.5 Directional Sensitivity. For transducers designed to measure structural motion along a specific axis, such as accelerometers, transverse sensitivity is the transducer electrical output in response to structural motion along axes other than the specific axis of interest. Transverse sensitivity is sometimes referred to as cross-axis or lateral sensitivity, and should be as low as possible. The design of the transducer usually determines the amount of transverse sensitivity and the most and least sensitive transverse directions, as illustrated in Figures 3.12 and 3.13 for piezoelectric accelerometers [3.4 -3.7, 3.10, 3.14]. See [3.5, 3.14] for a thorough discussion. Accelerometers may also exhibit transverse resonances, as shown in Figure 3.14 [3.6, 3.7, 3.44]. It should be noted that manufacturers generally do not measure transverse sensitivity to rotational motions, although it is sometimes claimed that certain transducer designs make rotational sensitivity low. Rotational sensitivity may become a problem if a motion transducer is subjected simultaneously to

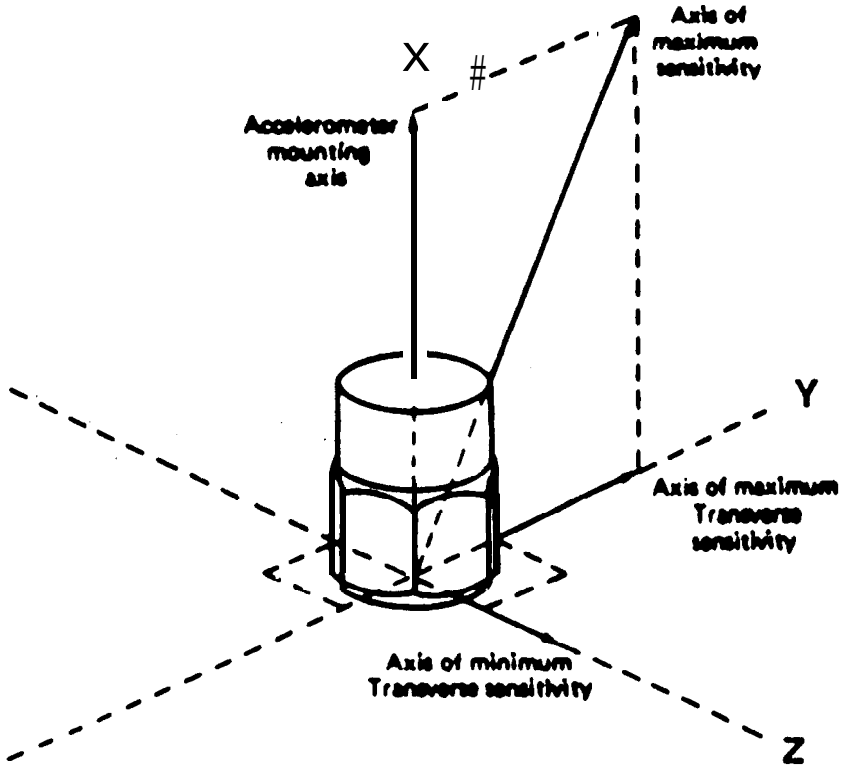

Figure 3.12. Diagrammatic Representation of Transverse Sensitivity for a Piezoelectric Accelerometer [3.6, 3.7].

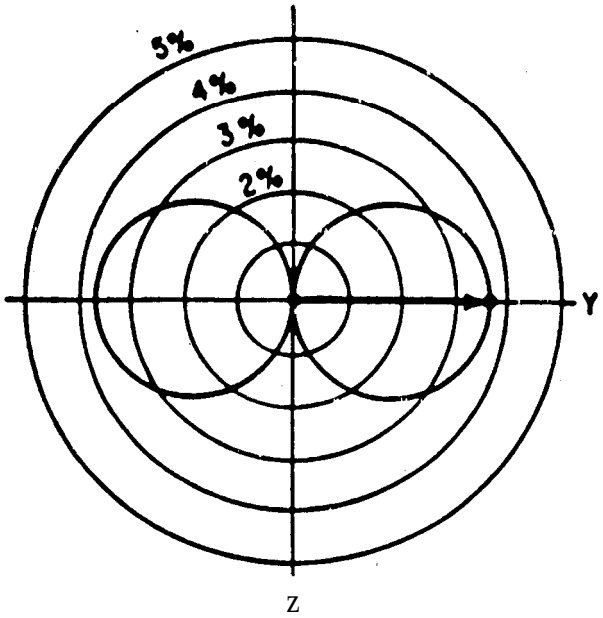

Figure 3.13. Diagrammatic Representation of Transverse Sensitivity Well Below Transverse Resonance for a Piezoelectric Accelerometer [3.4, 3.5,3.10].

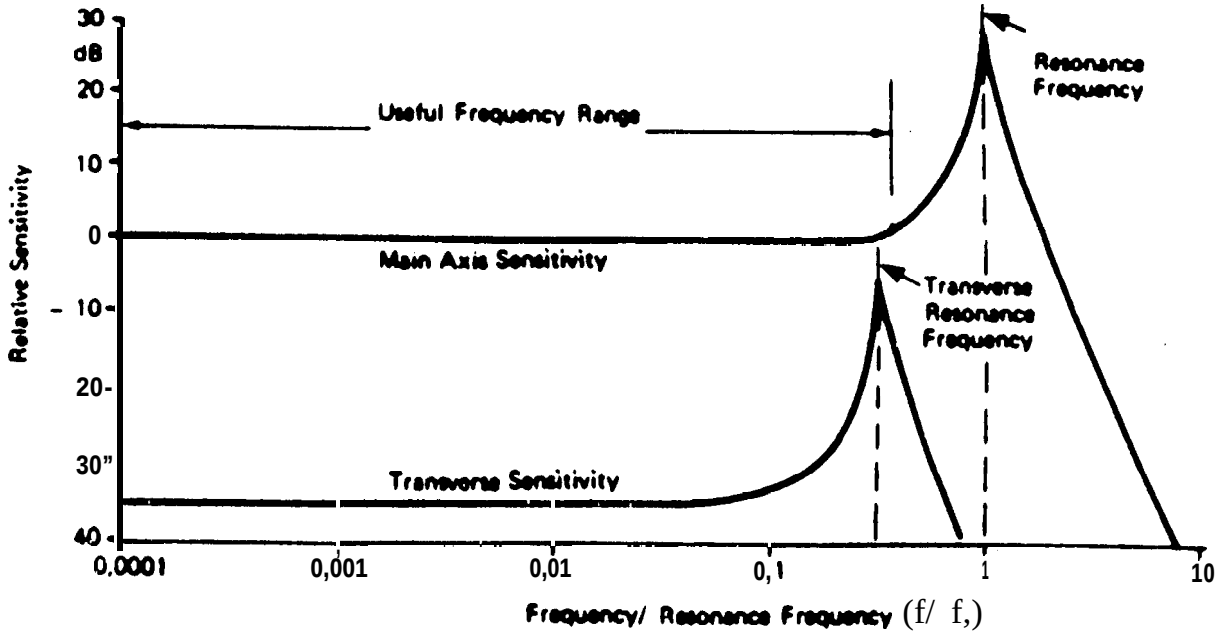

Figure 3.14. Typical Frequency Response of a Piezoelectric Accelerometer in a Transverse Direction Relative to the Intended Direction [3.6, 3.7, 3.44].

low magnitude translational motion in the specified direction, and high magnitude rotational motion, e.g., if the transducer is located on a structure at a point that corresponds to a node line of a responding dominant mode (where high rotational motion occurs). Concerned users are usually left on their own to evaluate rotational sensitivity.

Since the transverse output is the product of the transverse input times the transverse sensitivity, just as the desired transducer output is the product of the desired physical input times the transducer (uniaxial) sensitivity, the transverse sensitivity is important only if the transverse output is unacceptably high compared to the desired uniaxial output.

For pressure transducers, directional response is the relative transducer sensitivity as a function of the spherical angle of incidence T between the direction of pressure wave propagation and the direction of maximum sensitivity, which corresponds to the direction normal or perpendicular to the sensing surface (i.e., diaphragm or plate) of the transducer. This sensitivity is different if the pressure transducer is surrounded by a baffle that is flush mounted with the transducer sensing surface (or positioned close to the baffle), since pressure doubling will occur for all hemispherical angles of incidence except for grazing incidence (θ = 90 deg), as long as $R > \lambda_a$, where R is the effective distance from the edge of the baffle to the center of the transducer, and λ_a is the aeroacoustic wavelength given by $\lambda_a = (U_o/f)$, f is the frequency, and U_o is the speed of propagation. For acoustic noise, the propagation speed is identical to the speed of sound in air, i.e., $U_o = C_a$. At standard room temperature (T= 20°C = 68°F) and sea level pressure [P_a = 1 atm = 101325 Pa = 14.696 psi = 760 mm Hg (torr) = 1013.25 mbar], c_a = 344 m/sec ≈ 1128 ft/sec [3.8, 3.45- 3.48]. For aerodynamic noise, which usually occurs at grazing incidence, $U_\infty = M_\infty c_a$ and $U_o = U_\ell = M_\ell c_a$, where M_∞ and M_ℓ are the Mach numbers of the free-stream and the local flow, respectively. At altitudes of 20k c H < 35k ft (transonic through max q altitude range for most launch vehicles), $c_a \approx 1037 - 4.27\times10^{-3}$ (H - 20k) ft/sec.

For acoustic noise measurements at low and mid frequencies, where the acoustic wavelength is long compared to the size of a typical transducer, say $\lambda_a > 8d$, where d is the diameter of the transducer sensing element, a uniform angular response is usually observed (except for the aforementioned grazing incidence for a baffled transducer). The transducer is then called omnidirectional and is equally usable for all internal or external acoustic fields at low and mid frequencies. At high frequencies, however, significant directional behavior is observed. For microphones and pressure transducers without a baffle, highly directional response occurs because of reflections and diffraction caused by the presence of the transducer itself, especially for the transducer backside, as shown in Figure 3.15 for a typical microphone [3.8, 3.9, 3,12, 3.22, 3.35]. Other high frequency effects include (a) the SDF response described in Sections 3.2.2 and 3.2.3.2, and (b) pressure cancellation across the surface of the sensing diaphragm or plate when $\lambda_a \geq d \sin\theta$. The lowest frequency of cancellation therefore occurs for grazing incidence. Because of the different microphone installations, manufacturers traditionally provide directional response data for three types of

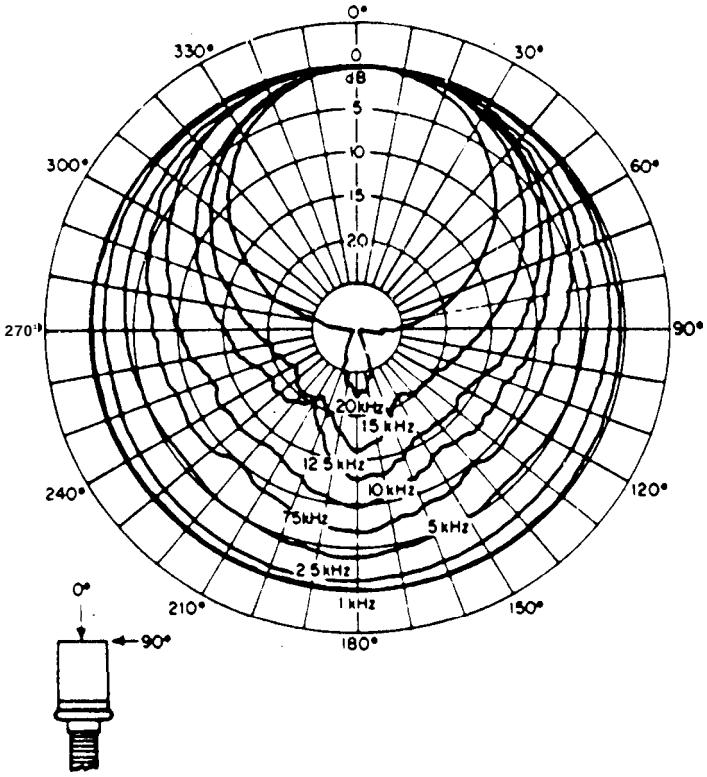

Figure 3.15. Directional Response of an **Electret** Microphone (Courtesy **GenRad)** [3.8].

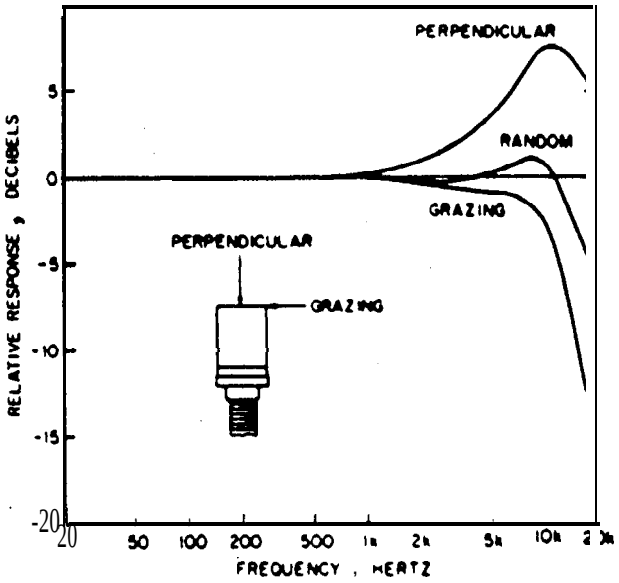

Figure 3.16. Typical Microphone Frequency Response for Two Free-Field Directions and Random Incidence [3.8, 3.12].

incidence, namely, perpendicular, grazing, and random, as shown in Figure 3.16 [3.8, 3.9, 3.12, 3.13,3.22, 3.35, 3,49]. Random incidence is the average response for all angles of incidence, as would be encountered in a reverberant sound field. Some microphones have been specially designed for certain angles of incidence.

For some applications, the directional properties of an acoustic field needs to be determined, which may be accomplished with the aid of a directional microphone. One type of directional microphone positions an omnidirectional microphone at the focus of a parabolic reflector, called a parabolic microphone, while another is attached to one or more long tubes, called a line, rifle or shotgun microphone [3.50, 3.5 1]. These configurations lose their directivity at low frequencies when the acoustic wavelength exceeds the structural dimensions.

For aerodynamic noise measurements of normal boundary layer using flush-mounted pressure transducers or microphones at grazing incidence, the free-stream aerodynamic wavelength should greatly exceed the transducer diaphragm diameter, say $\lambda_\infty > 25d$, to avoid pressure cancellation [3.52 - 3.54]. For higher frequencies, the amount of cancellation is also a function of the boundary layer displacement thickness δ^*, as shown in Figure 3.17. This figure may also be used for correcting measured spectra of normal boundary layer turbulence. Studies have shown that pressure cancellation is not a problem when measuring more severe aerodynamic noise from separated flow caused by shock wave-boundary layer interactions. Thus, no spectral correction is necessary.

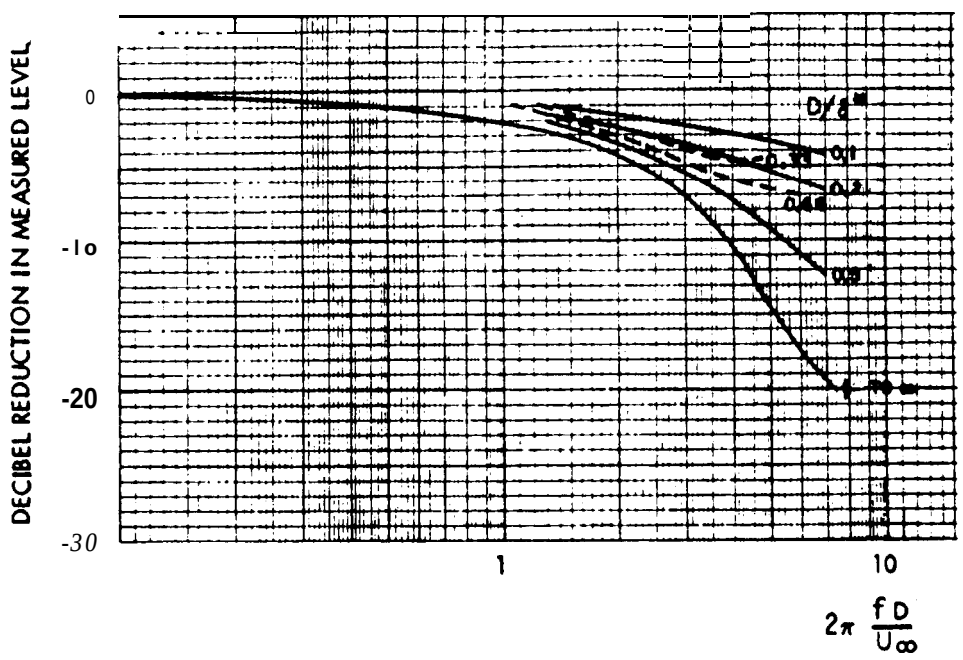

Figure 3.17. Frequency Response of a Microphone or Pressure Transducer to Normal Boundary Layer Turbulence at Grazing Incidence [3.53].

Depending on its material and design, and the material and strain field of the structure on which it is mounted, a strain gage will usually exhibit transverse response, whose sensitivity coefficient is the ratio of the transverse gage factor to the axial gage factor. In fact, the transverse response will be zero only if the gage is mounted in the maximum principal direction of a uniaxial stress field on a structure whose material is identical to that used for calibrating the same type of strain gage, achieving the same Poisson's ratio.

In most aerospace applications, structural failure under dynamic or combined static and dynamic loading usually occurs due to fatigue, which is initiated at one (or sometimes more than one) critical location on the surface under a biaxial strain field, where the strain gages should be mounted. However, a different biaxial field usually exists for static loading and in each of the dynamic modes. Therefore, a uniaxial strain gage is insufficient to measure potential failure conditions. A detailed finite element dynamic or combined static and dynamic analysis, or a three-gage rosette, is required to determine the maximum and minimum principal strains and stresses, and their directions, at the critical location(s). A three-gage rectangular rosette is generally preferred to a delta rosette because of the ease of using the data in subsequent calculations, and correction for transverse sensitivity *[3.* 16- *3.21].* Unfortunately, the use of the three-gage rosette triples the number of measurements to be made, but is necessary for the determination of equivalent uniaxial dynamic or combined stress(es) for subsequent fatigue analyses. These analyses may utilize one or more of the following techniques for combining biaxial stresses or strains: (a) maximum principal, (b) maximum shear, (c) von Mises, or (d) Sines' or Langer's method [3,55 - 3,57]. A two-gage T-rosette should be avoided unless the detailed finite element model is used to determine the principal directions.

3.2.4 Environmental Effects. There are a variety of climatic and induced environments that can affect the performance of a transducer, including temperature, pressure, humidity, corrosion, contamination, certain types of radiation, and static and dynamic loading. For certain types and designs of transducers, some of these environments are critical, while others have only a negligible influence, Thus, the user should carefully review all applied environments to determine if they will affect the measurements, and if the data can be corrected for them, Manufacturers' catalogs and specification sheets, as well as manufacturers, previous and current users, and/or consultants should be consulted concerning their recommendations, as discussed in Section 2.9.

3.2.4.1 Temperature. Ambient temperature and pressure are seldom a problem for transducers used in indoor laboratory tests, except under special circumstances (e.g., a vibration test of a feedline with a cryogenic fluid), because transducers are usually designed for room temperature and sea level atmospheric pressure conditions, Nearly all transducers are affected by high and low temperatures, as is often encountered in flight or major outdoor ground tests (e.g., a rocket engine static firing), causing potential changes in transducer sensitivity, zero or DC shift, natural frequency and damping. Piezoelectric (PE) transducers are particularly susceptible, with temperature

especially affecting sensitivity over the operating range, as shown in Figure 3.18 for several types of PE materials used for accelerometers and microphones [3.5], Like many other solids, PE materials exhibit crystallographic phase changes at certain temperatures called Curie points, Above or below a Curie point, the sensitivity usually changes dramatically, as shown in Figure 3.19. or the material may lose its polarization entirely and thus develop no charge, making the transducer useless [3,5]. When disconnected, a PE transducer may develop a high voltage across its crystal or

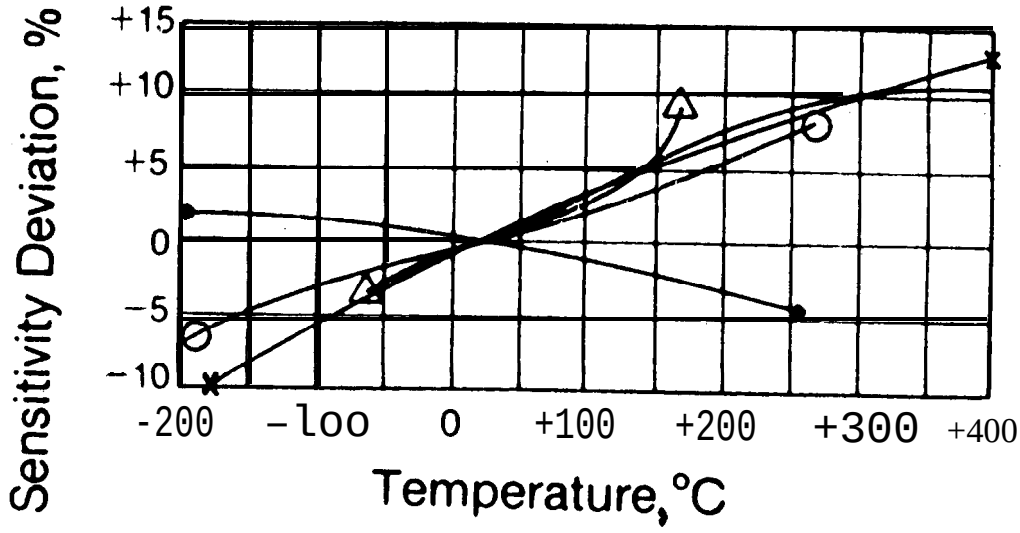

Figure 3.18. Temperature Sensitivity of Five Different Piezoelectric Ceramics, Normalized to the Sensitivity at 68 deg F (Courtesy Endevco) [3.5].

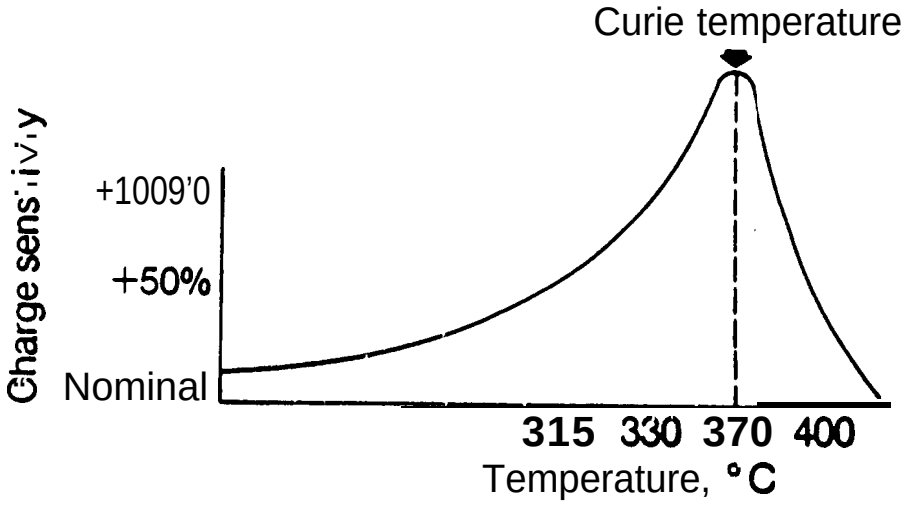

Figure 3.19. Temperature Sensitivity of a Typical Piezoelectric Material in the Vicinity of a Curie Point [3.5].

ceramic sensing element when the transducer is subjected to high temperature, The transducer output should be shorted before connecting it to its signal conditioner to avoid damaging the input stage,

High sensitivity, low natural frequency accelerometers that utilize gas or oil to achieve high damping ($\zeta \approx 0.7$), and thus extend the useful frequency range (as discussed in Sections *3.2,2, 3,2.3.2* and *3.2.3.4), may* exhibit substantial changes in damping with temperature, as shown in Figure 3.20, adversely affecting the maximum frequency limit for both flat response and linear phase shift [3.4, 3.5, 3.10]. It is common for piezoresistive transducers to exhibit a zero shift when exposed to change in temperature because of a slight shift in resistance between the active arms of the WheatStone bridge. Condenser microphones are also affected, with some variations shown in Figure 3.21 [3.22, 3.35]. Some transducers are designed to operate only at high or low temperature. Manufacturers' catalogs and specification sheets should be consulted to identify the transducers most applicable for certain conditions. Under extreme temperatures, static and/or dynamic measurements (e.g., pressure fluctuations in the combustion chamber of a jet or rocket engine, or the vibration response of the inner wall of a feed-line passing cryogenic propellants) sometimes require external heating or cooling.

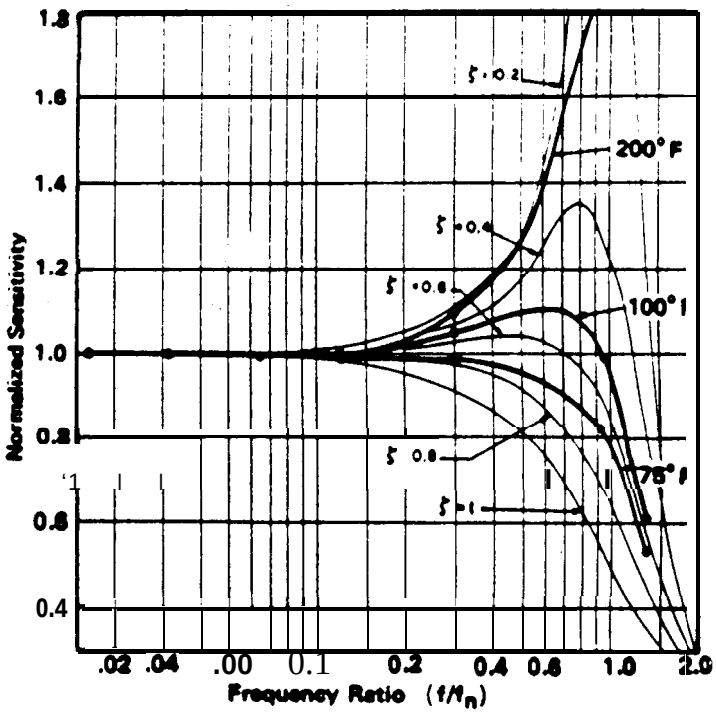

Figure 3.20. Temperature Effects on the Frequency Response of a Piezoresistive Accelerometer with Oil Damping (Courtesy Endevco).

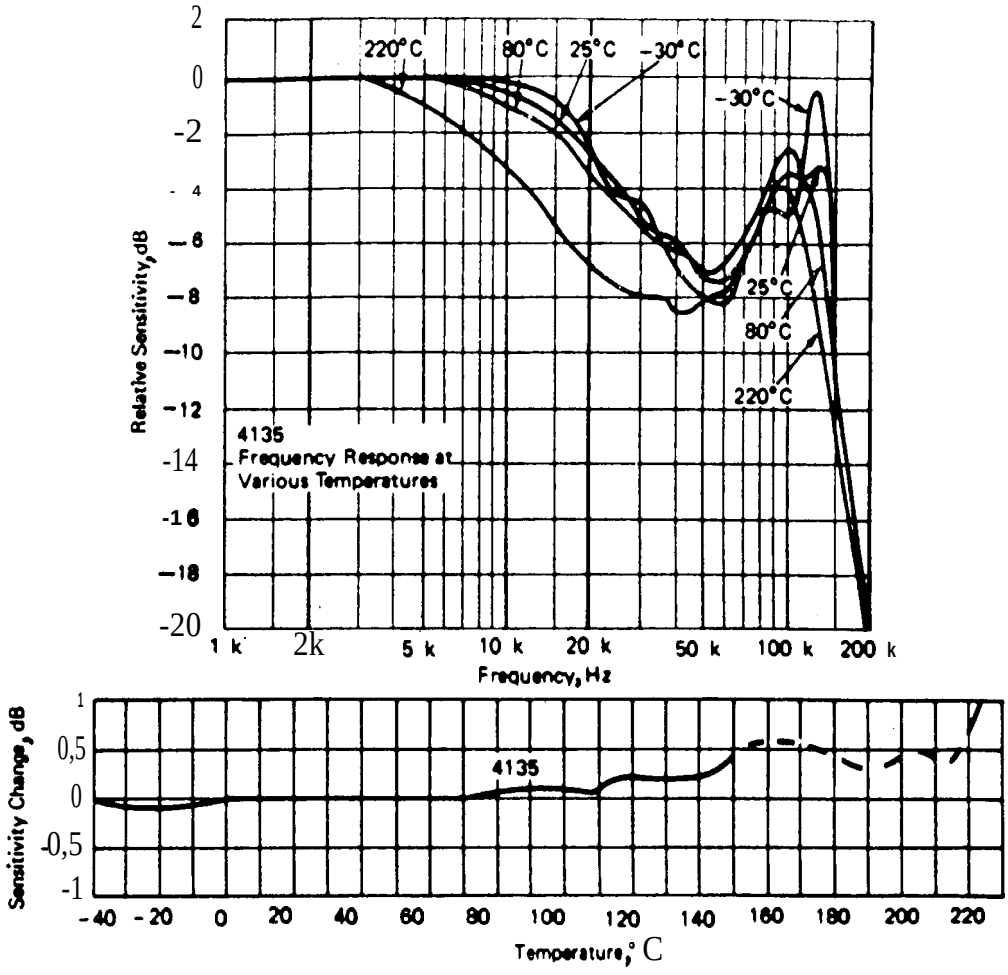

Figure 3.21. Temperature Effects on the Frequency Response and the Sensitivity at 1 kHz for a Free-Field Condenser Microphone (Courtesy Bruel & Kjaer) [3.22, 3.35].

Figure 3.22 shows a typical accelerometer protected against a hot or cold structure with an insulator and a radiator [3.6, 3.7]. External air cooling or heating can be added to increase convective heat transfer. (Note that the insulator may affect the maximum frequency limit, and the radiator may affect the transverse sensitivity). A cutaway view of a condenser microphone with a special water-cooled cap, designed for combustion temperatures, is shown in Figure 3.23.

A pressure transducer maybe connected by a hollow metal or ceramic tube to a hot or cold open space that exceeds the transducer temperature limit where the aeroacoustic measurement is needed. The tube may also be cooled or heated by an external jacket to provide additional protection, Unfortunately, this tube will exhibit an organ pipe-type resonance that could limit the useful frequency range. For a uniform tube diameter from the transducer diaphragm to the open end, and

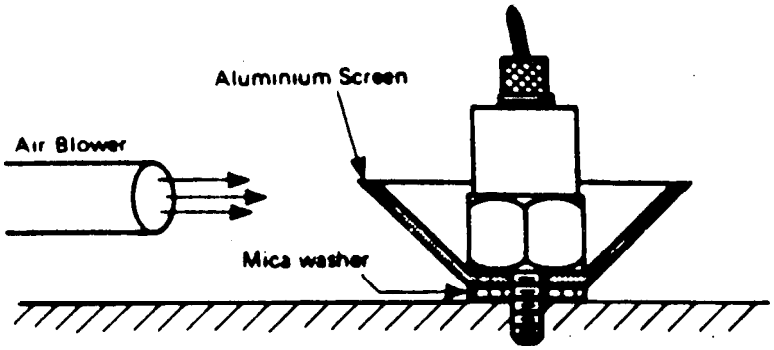

Figure *3.22.* Methods of Protecting an Accelerometer from High or Low Temperatures [3.6, 3.7].

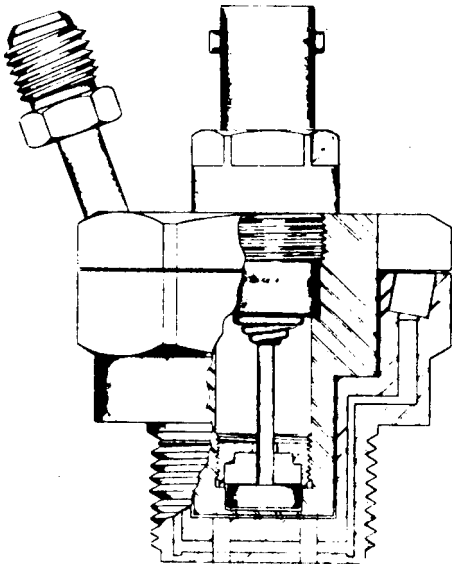

Figure 3.23. Condenser Microphone with Water-Cooled Protective Cap (Courtesy **Whittaker**).

tubing and diaphragm stiffness much greater than that of the fluid (usually air) the tube, an approximate flat frequency response of pressure transmission for the tubing installation can be achieved up to *20%* of the organ pipe resonance frequency f_t, given by $f_t = c_a/4\ell_t$, where c, = speed of sound in the fluid at temperature and ℓ_t = the length of the tube [3.48, 3.58]. Thus, if the maximum frequency limit has been selected, the tubing should be no longer than

$$\ell_{max} \leq \frac{c_a}{20 f_{max}} \tag{3.2}$$

The installation should be carefully calibrated at the service temperature.

All dynamic transducers designed to measure DC response, including strain gages, are particularly sensitive to temperature changes, usually occurring at low frequencies (below 5 Hz). Unless restrained, most materials expand when exposed to higher temperature, and vice versa This characteristic applies to both a strain gage and the structure on which it is mounted. In both cases, the pertinent material property is the thermal expansion coefficient. If a strain gage is available with the same coefficient as the structure, then with proper installation, thermal compensation should be achievable (unless it is desired to measure the thermal-induced apparent strain). Such a temperature-compensated strain gage is shown in Figure 3.24, connected into one arm of the WheatStone bridge to measure mechanically-induced strain only. Fixed precision resistors occupy the remaining unloaded or dummy arms of the bridge, and are usually located in the signal conditioner. However, the thermal expansion coefficient for typical aerospace structures is almost never constant, as illustrated in Figure 3.25 for 2024 aluminum. Thus complete compensation is unlikely.

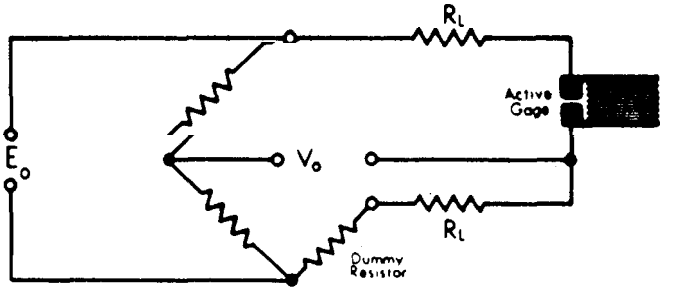

Figure 3.24. Temperature-Compensated Strain Gage, Which Uses the Same Thermal Expansion Coefficient as the Structure, Connected into One Arm of a Wheatstone Bridge Circuit (Courtesy Measurements Grp).

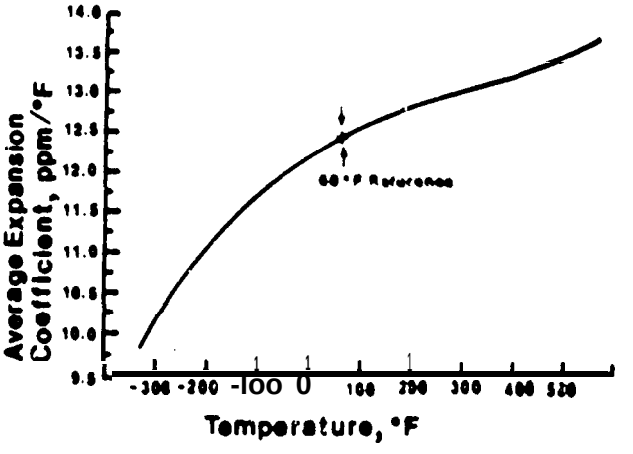

Figure 3.25. Average Thermal Expansion Coefficient (from 68 deg F to Final Temperature) for 2024-T4 Aluminum (Courtesy Measurement Grp).

Fortunately, materials commonly used for strain gages have two temperature-dependent parameters (i.e., the temperature coefficient of resistance or resistivity and the thermal expansion coefficient), that can be adjusted to provide temperature compensation. Figure 3.26 shows the amount of compensation achievable with three typical strain gage metallic materials [3. 15- 3.21]. The gage factor, which affects all frequencies, is also temperature sensitive, as shown in Figure 3.27 for metallic materials.

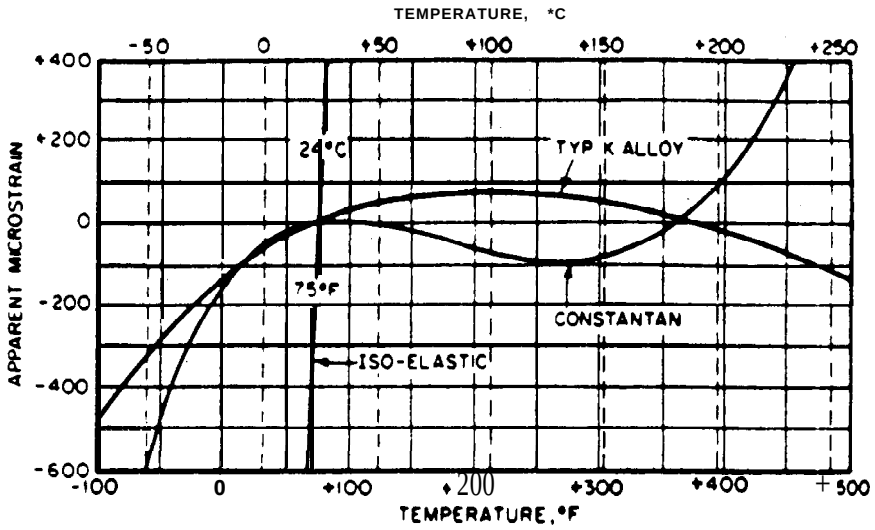

Figure 3,26. Typical Temperature-Induced Apparent Strain for Three Commonly-Used Strain Gage Metal Alloys [3.15 - 3.21].

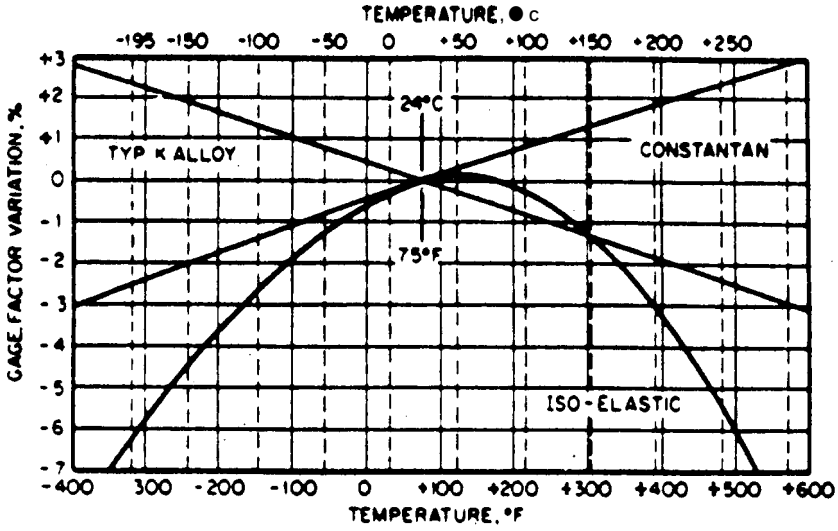

Figure 3,27. Typical Temperature-Induced Gage Factor Variation for Three Commonly-Used Strain Gage Metal Alloys [3.15 - 3.21].

If the amount of compensation is inadequate, even with a temperature-compensated strain gage, other techniques are possible, A second strain gage, with nearly identical properties to the fret, may be mounted in a mechanically-unloaded region of the structure (e.g., an appendage) but close enough to the first gage to be exposed to the same temperature. If the second gage is connected into the Wheatstone bridge in an arm adjacent to that of the first gage, as shown in Figure 3.28, additional temperature compensation can be obtained since the resistance change is the same in both arms [3, 15- 3,21]. This use of the Whetstone bridge is referred to as a compensating bridge circuit. The combined use of positive and negative silicon gages provides an additional advantage. A p-type and an n-type gage maybe mounted beside each other on the structure and thus be exposed to the same mechanical loading and temperature. connecting a p-type gage into one arm, and a properly-matched n-type into an adjacent arm, the Wheatstone bridge output can be nearly doubled while simultaneous y providing temperature compensation, as indicated in Section 3.2.1.2. Temperature compensation, when all four arms of the Wheatstone bridge are active or mechanically loaded, is discussed in Section 3,2.6.2.

Temperature compensation for a strain gage mounted on an isotropy material, such as a multi-layered composite with adjacent layers running in different directions, is nearly impossible because the thermal expansion coefficient is nonuniform.

The thermal response of strain gages can seriously interfere with the measurement of static or very low frequency dynamic loads unless considerable cam is taken [3.59]. However, if strain data are needed only at higher frequencies, it is common practice to use highpass faltering to avoid most residual thermal response problems. Under special circumstances, strain gages have been known to be the cause of higher frequency thermal-induced dynamic strain. When the strain of cryogenic propellant tanks has been measured, with the gage directly exposed to the electrically non-conducting liquid, gas bubble formation has been observed at the gage due to power dissipation, Rapid temperature changes result when the insulating bubbles break loose from the surface, causing a higher frequency gage output. A protective coating, lower applied voltage, or a higher gage resistance can be used to avoid bubble formation.

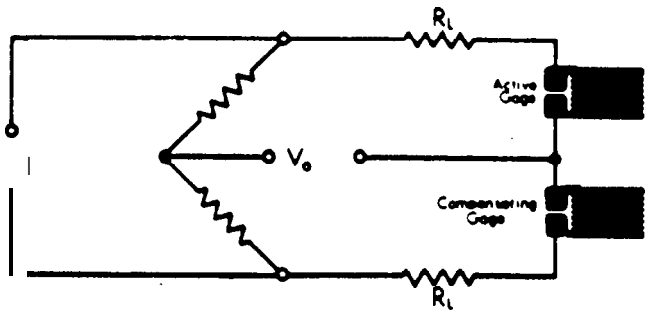

Figure 3.28. Compensating Bridge Circuit, Comprised of Two Strain Gages Connected in Adjacent Arms with One Gage Exposed to Static and/or Dynamic Strain and Both Exposed to the Same Temperature [3,15 - 3.21].

Lastly, it is recommended that all transducers and their methods of attachments be calibrated at applicable temperature(s) to determine or ascertain transducer sensitivity, zero shift, and other measurement parameters unless available data indicates that these precautions are unnecessary.

3.2.4.2 Thermal Shock. Transducers which are sensitive to temperature differences are usually susceptible to transient temperatures (or thermal shock), with the effect usually observed below 5 Hz. Figure 3.29 shows the output time history of a typical PE accelerometer, initially at 82 deg F, to sudden immersion in ice water [3.5]. Note that the dominant response occurred below 0.3 Hz. Two potential causes of transducer response to transient temperature are (a) non-uniform stress applied to the sensing element(s), caused by differential thermal expansion or contraction, and (b) sensing material response to temperature change, in PE transducers called the pyroelectric effect. The magnitude of the response is determined by the input temperature time history, the design of the transducer, and the material used for the sensing element.

Heat sinks are sometimes used in the path of heat transmission to minimize the effects of temperature change. In addition, other temperature control methods are described in Section 3.2,4.1. .

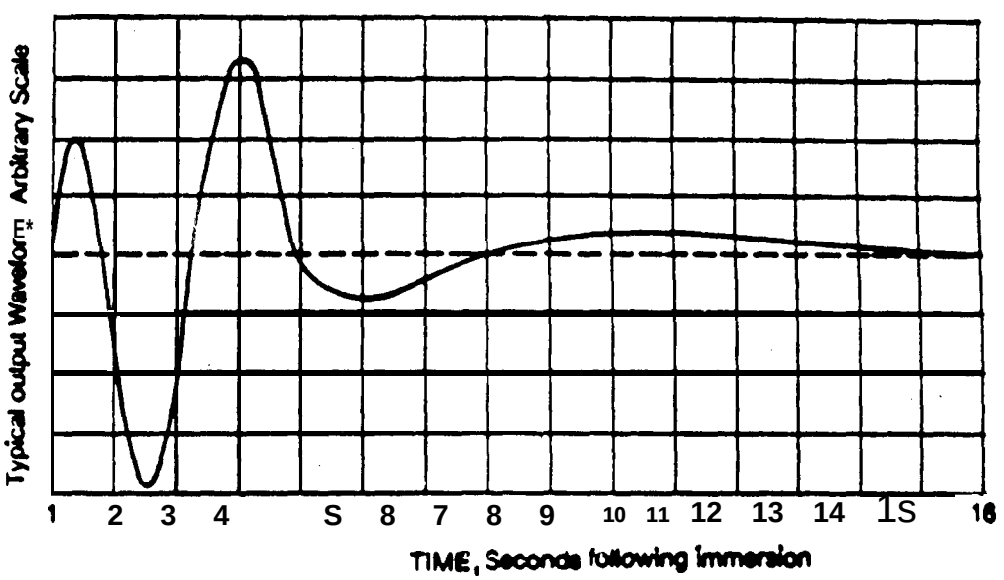

Figure 3.29. Typical Accelerometer Output After Sudden Immersion in Ice Water [3.5].

3.2.4.3 Pressure. Atmospheric pressure variations can have a substantial influence on microphone performance. Figure 3.30 shows the effects of (a) low pressure (relative to sea level conditions) *on the* frequency response of two types of condenser microphones, and (b) high and low static pressure on low and mid frequency transducer sensitivity [3.3s], The cause of these effects is the air inside the microphone cavity. Even though the cavity is vented to the outside, air increases both the stiffness and apparent mass of the diaphragm (at different rates) over the fre-

quency range, and the damping at the fundamental resonance. Some piezoelectric microphones may also be susceptible to low static pressure, but for a different reason. During manufacture, the diaphragm is pulled over the sensing element by a hard vacuum applied to the inside of the microphone, which is then hermetically sealed. A low external static pressure can permit the diaphragm to separate from the sensing element under aeroacoustic loading, causing the diaphragm to respond nonlinearly and making the transducer useless.

A microphone used during the vertical ascent of a space vehicle will have a reduced sensitivity with altitude and thus with time. If the microphone is simultaneously subjected to structural vibration, the microphone output will be increasingly a function of vibration response rather than the acoustic loading, as discussed in Section *3.2.4.8. Some* relief can be achieved by using the vibration canceling microphone described in Section 3.2.7.3. In general, accelerometers are not sensitive to atmospheric pressure.

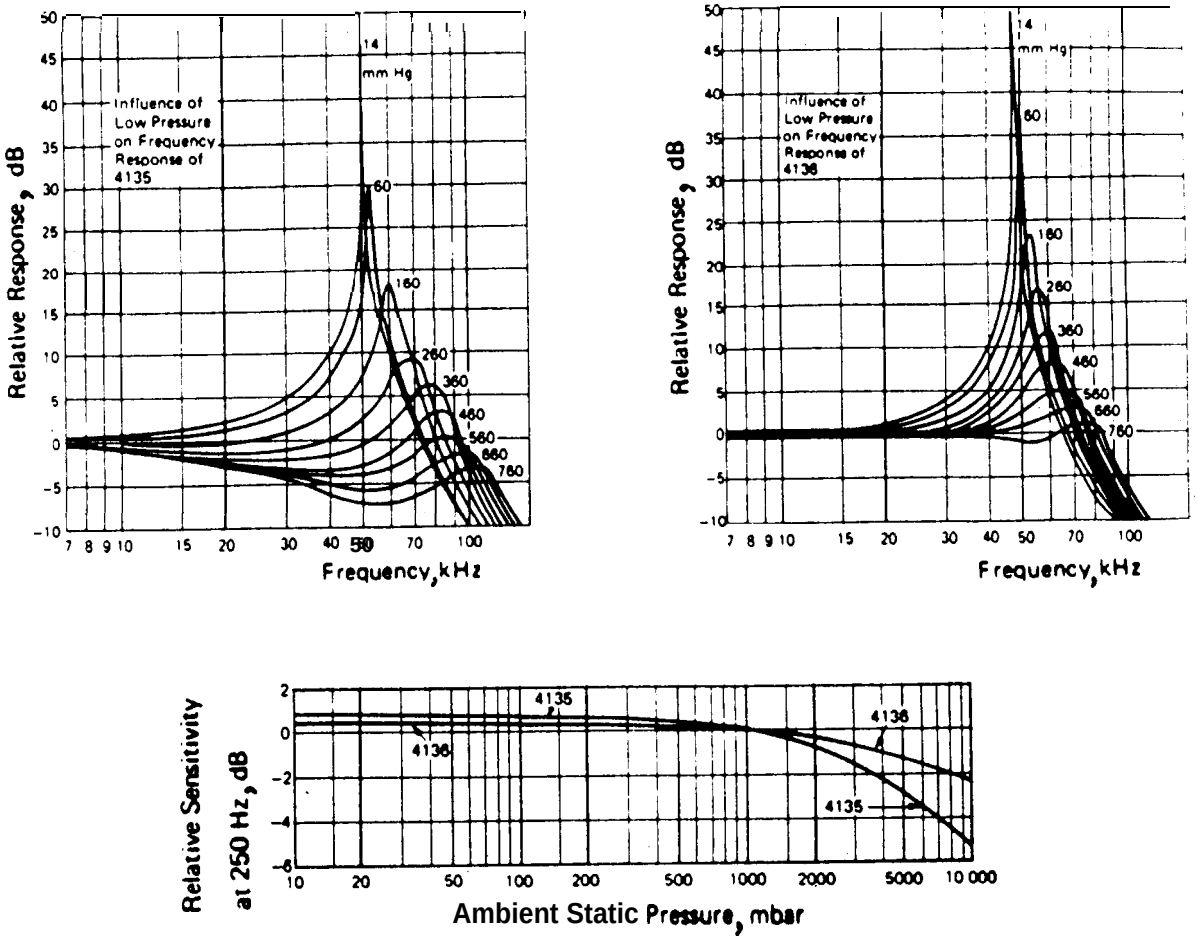

Figure *3.30.* Static Pressure Effects on the Frequency Response and the Sensitivity at 2S0 Hz (Normalized to the Sensitivity at Standard Atmospheric Pressure) for Two Condenser Microphones (Courtesy Bruel & Kjaer) [3.23].

3.2.4.4-. Because of its effects on charge leakage, high humidity can seriously degrade the transducer sensitivity and increase the background noise of condenser microphones that use an air gap for a dielectric. However, microphone manufacturers usually provide coupled preamplifiers with heaters to prevent moisture, or recommend limited outdoor exposure and microphone storage with desiccants between usage. Nearly all piezoelectric and piezoresistive transducers are sealed against moisture. However, those piezoelectric transducers with high output impedance may be affected by moisture penetration at the cable connector during high humidity conditions, requiring connector encapsulation with a chemically-compatible elastomer, as shown in Figure 3.31. Strain gages are also degraded by high humidity or by conducting liquids that reduce the electrical resistance between the gage and the structure or within the gage itself [3.16- 3.21], Thus, a leak-proof barrier is required for these conditions, as illustrated in Figure 3,32. To avoid sealing in moisture, the barrier should be installed under low humidity conditions, or with the structure heated in the vicinity of the gage.

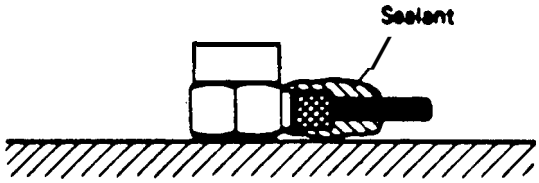

Figure 3.31. Connector Encapsulation by a Sealant to Prevent Moisture Penetration [3.6].

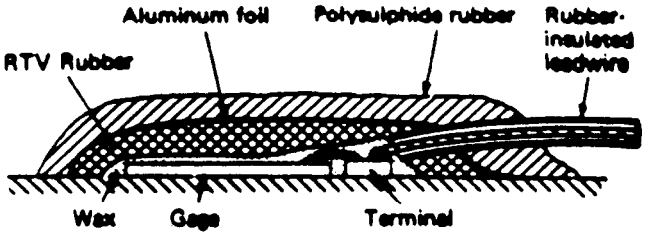

Figure 3.32. Multiple Layer Sealing of a Strain Gage to Prevent Liquid and Moisture Penetration [3.18].

3.2.4.5 Corrosion. Static and/or dynamic measurements maybe severely compromised by a corrosive environment that could attack transducer materials. Corrosive agents include water, salt water, hydraulic fluids, hydrazine, nitrogen tetroxide, and engine exhaust gases. Two methods of possible corrosion prevention are (a) the selection of corrosion-resistant transducer materials, or (b) the protection of transducers with corrosion-resistant coatings. In the latter case, the effects of the coating on transducer performance should be established. If the materials of commercial transducers or available coatings are not suitable, then it may be necessary to order transducers with special materials. Such an order should be placed with the manufacturer well before the intended usage to allow adequate lead time for the manufacturing process and pre-usage testing.

3.2.4,6 Contamination. Contamination composed of dust or small solid particles, and sometimes water droplets, is generally not a problem for sealed accelerometers, but maybe for microphones if the particles are borne by the wind or aerodynamic flow. For acoustic noise measurements over extended periods, fine particles can be trapped between the diaphragm and the protective cap of a microphone, or clog the vent of a condenser microphone. Aerodynamic noise must be measured without a protective cap to avoid disturbing the flow. Small particles often cause such transducers to fail due to impact during flight and wind tunnel testing. Microphones on forward-facing surfaces are more vulnerable than others to particle-induced failure. Thus, it is not uncommon to double the number of microphones at critical locations for a comprehensive wind tunnel test program, in each case using one as the primary transducer and the other (adjacent to the primary) for backup, to be used in case the primary is damaged If the primary microphone fails, the backup is cabled into the remainder of the data acquisition system at the earliest opportunity, usually before the next test run. This technique reduces the time between test runs without losing critical data, but leads to a higher initial cost of transducers and their installation and checkout.

3.2.4.7 Electromagnetic, Visible and Nuclear Radiation. Transducers may also be exposed to other possible deleterious environments, including electromagnetic (usually radio frequency or RF) and nuclear radiation, and strong magnetic and electric fields. For example, pyrotechnic detonation is usually accompanied by a pulse of electromagnetic radiation, as described in Appendix A. The design and materials of the transducer determines its susceptibility. Some pressure transducers are known to be sensitive to sunshine, other bright light sources, and rocket engine plumes. The diaphragms of some very small pressure transducers are so thin that they are almost transparent. Exposure to direct sunlight can cause a response of the piezoresistive sensing elements on the back side of the diaphragm. In these cases, diaphragms have been lightly spray-painted to make them more opaque and thus less light-sensitive but with a slight decrease in their resonance frequencies *[3.60]*. For strain gages, the bonding materials used for mounting the gage to the structure maybe affected by radiation. Stray electric and magnetic fields may have substantial effects on the entire data acquisition system, especially those with long cable runs, as discussed in Section 3.3.5. An accelerometer (especially piezoelectric) may need to he mounted to the structure using an insulated or isolated stud or washer, as described in Section 3.2.6.6. However, even carefully designed and installed isolation may affect the maximum frequency limit of the accelerometer.

To ascertain the need for protecting a transducer, measurements maybe required to determine the characteristics of the various radiation environments. Then manufacturers' catalogs and specification sheets should be reviewed to determine the effects. In addition, current and previous users of identical or similar transducers subjected to similar exposure should be contacted. If the environmental effects are excessive, manufacturers should be contacted concerning the availability of resistant techniques, or models not listed in the catalog. Adequate lead time in purchasing these models will probably be required to avoid delays.

3.2.4.8 Vibroacoustic Excitation. Accelerometers are generally insensitive to direct aeroacoustic excitation because of the noise reduction provided by their sealed cases, unless the case is used to preload the sensing element. Similar to transverse sensitivity discussed in Section 3.2.3.5, accelerometers and force transducers may be sensitive to the static and/or dynamic bending that accompanies the transverse deformation and/or motion of the structure, e.g., as shown in Figure 3.33 for an accelerometer. Structural bending at the attachment of an accelerometer or force transducer will induce strain throughout the transducer, especially if the transducer has a large attachment area. Good accelerometer or force transducer&sign can substantially reduce the transfer of strain to the sensing element, and/or preclude an electrical output from the sensing element under the transferred strain. For an accelerometer, this effect is called base strain. To standardize the evaluation of base strain sensitivity, ANSI has specified that the accelerometer be mounted near the root of a cantilever beam whose resonance frequency is approximately 5 Hz. When the beam is excited, the accelerometer output must be determined when the maximum instantaneous beam bending strain is 250 $\mu\varepsilon$ (equivalent to a minimum radius of curvature of 10^3 in.) [3.61]. However, this value should be used with caution because base strain sensitivity is likely to be nonlinear. In addition, an isolated stud or washer or cemented accelerometer pad can significantly attenuate the bending transfer between the structure and the accelerometer base, as well as provide electrical isolation. However, the maximum frequency limit may be affected, as previously mentioned in Section 3.2,3.1.

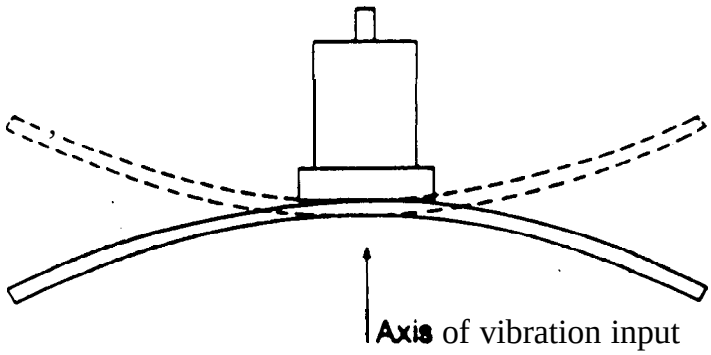

Figure 3.33. Structure-Accelerometer Interaction Which Causes Structural Stiffening and Accelerometer Base Strain [3.5].

An accelerometer or force transducer with a large and stiff base can appreciably stiffen the structure under the transducer, especially when installed on thin- skinned aerospace structure at mid and high frequencies, causing structural mode shapes to be modified in the vicinity of the accelerometer or force transducer, thus likely to change the measured force or motion. An isolated stud or washer can significant.ly attenuate the base-induced stiffness applied to the structure, as well as provide electrical isolation. The maximum frequency limit may be affected, as previously mentioned in Section 3.2.3.1.

Even when base bending does not occur, an in-plane structural stress concentration at the accelerometer location have been shown to cause an erroneous accelerometer output [3,62].

Unless they are mechanically isolated, pressure transducers may be susceptible to direct structural excitation because they exhibit the SDF responses of Section 3.2.2, with the electrical output proportional to (a) the absolute displacement response under force (or pressure) excitation, or (b) the relative displacement response under base acceleration excitation. For the useful frequency range described in Section 3.2.3.2, the double ordinate of Figure 3.4 can be used to calculate the electrical output V_{ss} of the pressure transducer from structural excitation (assuming the transducer is rigid and rigidly mounted to the structure):

$$V_{ss} = \rho_d g t_d \left(\frac{V_{sp}}{p_s}\right)\left(\frac{\ddot{U}_s}{g}\right) \tag{3,3}$$

where ρ_d and t_d are the mass density and thickness of the sensing diaphragm or plate, respectively, (V_{sp}/p_s) is the aeroacoustic sensitivity of the transducer (i.e., V_{sp} is the electrical output due to the applied pressure magnitude p_s), $\ddot{U}_s$ is the structural acceleration at the transducer location, and g is the gravitational constant. Thus, a pressure transducer with a less dense or thinner diaphragm will be less sensitive to structural excitation for a given aeroacoustic sensitivity. For pressure transducers subjected directly to severe structural excitation, consideration should be given to using a vibration-compensated pressure transducer, shown in Figure 3.34, to measure low-to-moderate aeroacoustic levels.

3.2.5 Physical Properties. The transducer physical properties of concern are their size, weight and stiffness,

3.2.5.1 Size. In 'most cases, a small transducer is beneficial in minimizing its effects on the potential disturbance of the dynamic environment or the dynamic response of the structure. For example, an accelerometer with a small base has less influence on structural modal responses, especially at mid and high frequencies, as discussed in Section 3.2.4.8. A small pressure transducer produces less potential disturbance of an external or internal acoustic field at high frequencies, and less chance of pressure cancellation over the surface of the diaphragm for both acoustic and aerodynamic noise measurements, as discussed in Section 3.2.3.5. Actually, in most cases, smaller diameter pressure transducers provide more accurate measurements of aerodynamic noise over the entire spectrum, not just at high frequencies as might be expected, under conditions of normal boundary layer turbulence [3.54]. However, small transducers are usually less sensitive, which may cause a compromise with size except under a high magnitude load or environment, as discussed in Section 3.2.3.1.

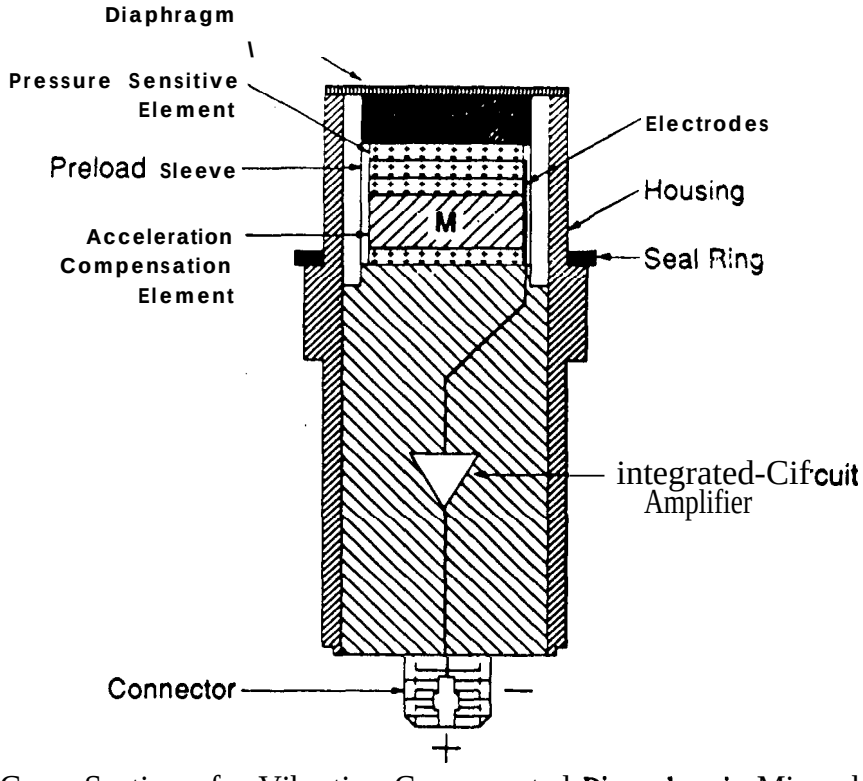

Figure 3,34, Cross-Section of a Vibration-Compensated **Piezoelectric** Microphone (Courtesy PCB) [3.11].

The size of a strain gage should be dependent on the specific measurement objective. For some measurements, the objective is the determination of the maximum strain in a local region (called a stress concentration). Here the gage should be as small as possible to avoid averaging over strain gradients that usually exist in the vicinity of the maximum strain, as illustrated in Figure 3.35 [3. 15]. For other measurements, the objective is to determine the average strain over a local region, so the preferred gage is much larger to minimize the effects of any **local** stress concentrations. For strain measurements at very high frequencies, such as those generated by pyroshock, small strain gages may be required to avoid problems associated with spatial strain averaging over the gage length, as described in Section 3,2.3.2.

3.2.5.2 **Weight.** For most accelerometers and pressure transducers, size and weight are roughly proportional, so the discussion of Section 3.2.5.1 on size also applies to weight. The **mass** of even a lightweight accelerometer, or a mounting bracket between the accelerometer and the structure, can have an appreciable effect on the measured environment, natural frequencies, and mode shapes of a lightweight structure, such as an electronic assembly or a small electromechanical device. However, the unloaded dynamic environment at the mounting point can be calculated **from** the measured (or accelerometer-loaded) dynamic environment using the well-known impedance ratio [3,63, 3.64] given by

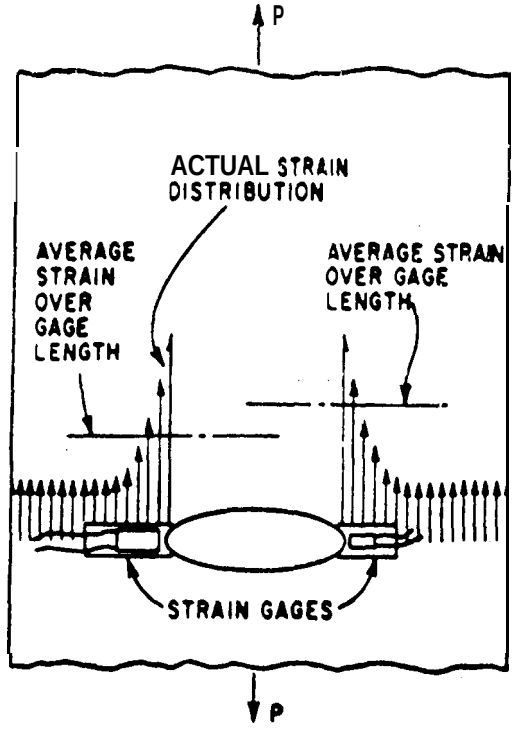

Figure *3.35,* Large and Small Strain Gages Measuring Spatial-Average Strains over Their Grid Areas [3.15].

$$R_z(f) = \frac{Z_1(f) + Z_2'(f)}{Z_1(f) + Z_2''(f)} \tag{3,4}$$

where $2_1(f)$ and $Z_2'(f)$ are the mechanical (driving point) impedance of the structure and the accelerometer, respectively, at the accelerometer mounting point, and $Z_2''(f) = O$ for the assumption of no accelerometer. The mechanical impedance of the structure must be measured *in situ*, i.e., as the structure is normally installed [3.65]. For frequencies sufficiently below the resonance frequency of the accelerometer, $Z_2'(f) = j2\pi m_a f$, where m_a is the mass of the accelerometer. For periodic, random and transient signals, the dynamic environment for the unloaded structure is

$$P_x''(f) = |R_z(f)|\, P_x'(f) \tag{3.5}$$

$$G_{xx}''(f) = |R_z(f)|^2\, G_{xx}'(f) \tag{3.6}$$

$$F_x''(f) = R_z(f)\, F_x'(f) \tag{3.7}$$

where $P_x(f)$, $G_{xx}(f)$, and $F_x(f)$ are the periodic line spectrum, random autospectral density, and transient Fourier spectrum of Sections 5.4.2, 5.4.3 and 5.5.1, respectively, and the prime and double prime superscripts denote the measured and unloaded dynamic environments, respectively. However, when so much instrumentation is added that the instrumentation weight is no longer a negligible percentage of the total structural weight, then a finite element analysis of the system, with and without the instrumentation, must be performed to determine the effects of instrumentation weight on structural response. Large cable bundles often affect structural weight and damping. Separating the individual cables often reduces the damping.

3.2.5.3 Stiffness. The stiffness, mass (and sometimes damping) of a force transducer can have an appreciable effect on the measured dynamic force. However, the true dynamic force that would have been obtained by an infinitely-stiff massless transducer at the same measurement location can be calculated from the measured dynamic force using another impedance ratio [3.66], i.e.,

$$R_F(f) = \frac{[Z_{s1}(f) + j2\pi m_1 f]^{-1} + [Z_{s2}(f) + j2\pi m_2 f]^{-1} + [\{k/(j2\pi f)\} + c]^{-1}}{Z_{s1}^{-1}(f) + Z_{s2}^{-1}(f)} \tag{3.8}$$

where $Z_{s1}(f)$ and $Z_{s2}(f)$ are the mechanical (driving point) impedance of the structure on each side of the force transducer, respective y, ml and m_2 are the mass of the transducer on each side of the force sensing element(s), and k and c are the stiffness and damping coefficient of the sensing element(s). Utilization of Equation (3.8) requires that the maximum frequency be limited to satisfy the conditions that (a) the masses ml and m_2 are essentially rigid, and (b) the stiffness k and damping c of the sensing element(s) can be represented by a massless linear spring-viscous darnper combination. These conditions are easily satisfied if the maximum frequency limit does not significantly exceed the mass-spring-mass resonance of the force transducer given by

$$f_r = \frac{1}{2\pi}\left[\frac{k(m_1 + m_2)}{m_1 m_2}\right]^{1/2} \tag{3.9}$$

The mechanical impedance of the structure must be measured in situ, i.e., as the structure is normally installed [3.65]. For periodic, random and transient signals, the true dynamic force at the measurement location is therefore

$$P_F''(f) = |R_F(f)| P_F'(f) \tag{3.10}$$

$$Gin''(f) = |R_F(f)|^2 G_{FF}'(f) \tag{3.11}$$

$$F_F''(f) = R_F(f) F_F'(f) \tag{3.12}$$

where $P_F(f)$, $G_{FF}(f)$, and $F_F(f)$ are the periodic line spectrum, random autospectral density, and transient Fourier spectrum of Sections 5.4.2, 5.4.3 and 5.5.1, respectively, and the prime and double prime superscripts denote the measured and true dynamic force, respectively. However, when more than one compliant force transducer is used, a finite element analysis of the system, with and without force transducers, must be performed to determine the effects of the transducers on structural response.

3.2.6 Motion Transducers. The most widely used motion transducers for dynamic data acquisition are accelerometers, although velocity pickups and laser vibrometers are also sometimes employed.

3.2.6.1 Accelerometers. An accelerometer is a transducer that senses the instantaneous mechanical or structural acceleration applied to its base and, alone or with other electrical components, generates an instantaneous electrical signal related to the applied motion. Four types of accelerometers are commonl y used for static and/or dynamic data acquisition in aerospace applications: (1) piezoelectric, (2) piezoresistive, (3) variable capacitance, and (4) servo [3.67]. Their characteristics and installation are summarized in the following sections, All accelerometers exhibit the SDF responses described in Section 3.2.2.

The useful frequency range for accelerometers is discussed in Section 3.2.3.2. If the accelerometer selected has low damping, e.g., $\zeta < 0.1$, care must be taken to ensure that the transducer resonance is not sufficiently excited (even though the resonance frequency is significantly above the maximum frequency limit) to (a) cause the sensing element to fail or the transducer to respond nonlinearly (e.g., hard bottom), and/or (b) generate an excessive electrical output that could cause the following signal conditioner to respond nonlinear y, such as amplifier saturation. Nonlinear response not only affects signal fidelity at resonance, but also throughout the spectrum as well. Thus, the resulting data is likely to be worthless. However, if the transducer responds linearly while providing an excessive resonant output, then a lowpass filter may be used between the transducer and signal conditioner to attenuate the output. Such filters are described in Section 3.3.3. An important example is pyroshock measurement, discussed in Appendix A.

3.2.6.1.1 Piezoelectric Accelerometers. PE accelerometers are transducers that use the PE crystal(s) or ceramic(s), described in Section 3.2.1.1, as the spring between a base and mass (idealized by the SDF system of Section 3.2.2) to sense dynamic structural accelerations applied to the base. When a dynamic force or relative displacement is applied to the crystal(s) or ceramic(s), a charge is instantaneously generated on the surface that is proportional to the force or displacement. PE accelerometers have a wide range of measurement parameters and configurations designed for specific applications. Most PE accelerometers have very low damping ($\zeta < 0.005$) and, therefore, are useful only to about 20% of their PE SDF resonance frequencies. In addition, the accelerometer case or housing also has resonances that could cause an undesired signal at higher frequencies, but they could be less than the SDF resonance.

The minimum frequency limit for a PE accelerometer is dependent on the characteristics of the signal conditioner that follows the sensing element(s). Specifically, if the signal conditioner is a voltage mode amplifier, shown in Figure 3.36, the low frequency cut-off is determined by the RC time constant of the crystal or ceramic sensing element(s), amplifier and connecting cable, as discussed in Sections 3,2.3.2 and 3,3.2.1. On the other hand, if the signal conditioner is a charge mode amplifier, shown in Figure 3.37, the low frequency cut-off is determined by the feedback capacitance and resistance of the amplifier, discussed in Sections 32.3,2 and 3,3,2.2. A minimum frequency limit of 1 Hz is commonly obtained. In Figures 3.36 and 3.37, the resistance that shunts across (or is parallel to) each capacitance is not shown. The maximum frequency limit usually varies inversely with the sensitivity and size of the accelerometer, as described in Section 3.2.3.2.

The signal conditioner is either separate from or integral with the accelerometer. Integral voltage or charge mode electronics may increase the size and weight of the accelerometer, but provide a low

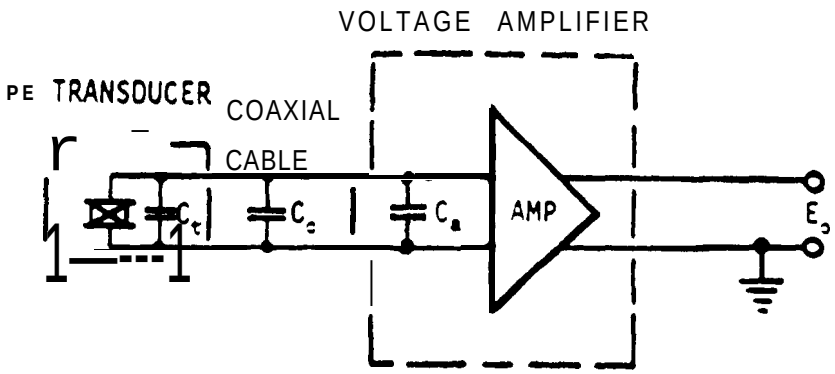

Figure 3,36. Circuit Diagram of a Piezoelectric Transducer and Voltage Amplifier.

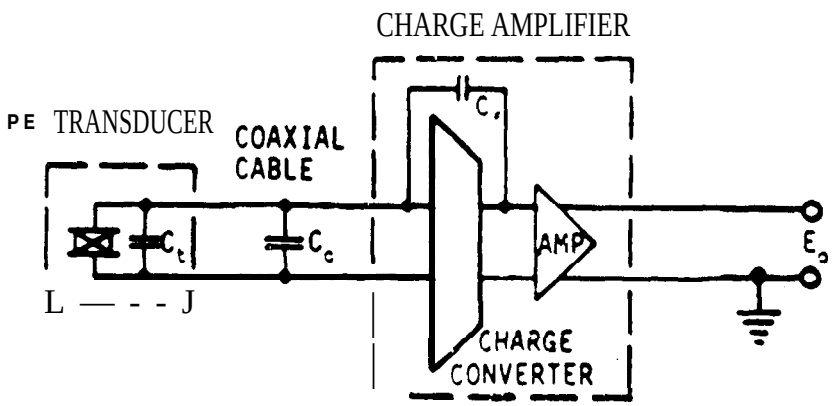

Figure 3.37. Circuit Diagram of a Piezoelectric Transducer and Charge Amplifier.

impedance output that may be used to drive long cables. The increased weight of integral electronics and the surrounding structure may be an important consideration for very small, lightweight accelerometers, as indicated in Section 3.2.5.2, but is usually unimportant for larger, heavier transducers, The coupling between preamplifiers and cabling is described in Sections *3.3.2.4* and 3.3.5. *DC* power is usually supplied to the integral electronics through the signal output cable, as shown in Figure 3.38 *[3.68]:* Current sensitive integral electronics should be supplied with the manufacturers rated current. Otherwise, the thermal performance may be degraded due to circuit heating. Higher than rated currents may be required to drive high frequency signals through very long cables. For certain integral electronic circuits, high currents may reduce transducer sensitivity and increase the background noise floor. Separate charge mode electronics require a special high impedance, low noise coaxial cable from the accelerometer, although the cable may be long. Further cable and signal conditioner details are described in Sections 3.3.5 and 3.3,2, respectively,

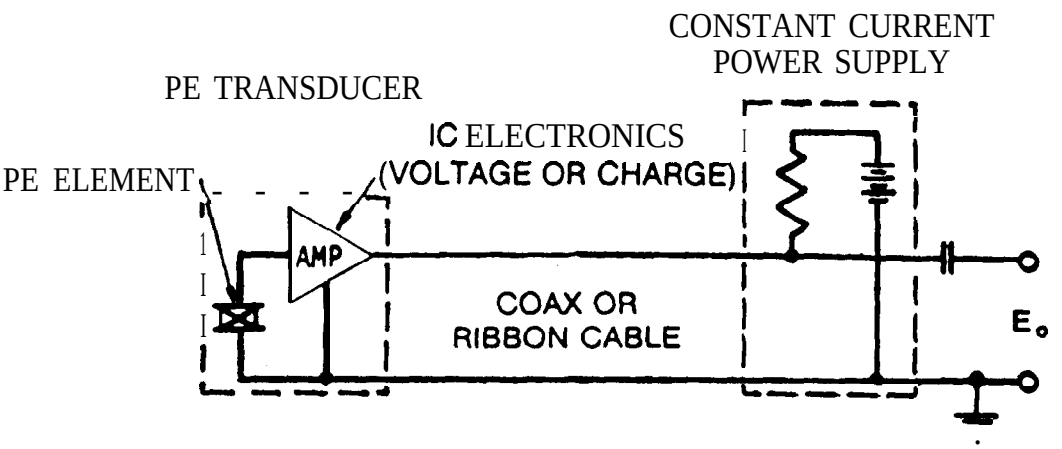

Figure 3.38 Circuit Diagram of a Piezoelectric Transducer with Integral Electronic Amplifier and External Power Supply (Courtesy PCB) [3,68].

In one design of PE accelerometer, the tension/compression-polarized ceramic or crystal is mechanically preloaded in compression by a stud and nut, as shown in Figure 3,39 [3.4, 3.6, 3.7, 3.10]. This design is called single-ended compression. When variable pressure is applied to the wafer under dynamic excitation, a charge is generated on its surface that is proportional to the applied acceleration. This design is often susceptible to base strain and thermal transients, as described in Sections 3.2.4.8, 3.2.4.1 and 3.2.4.2. Also, if the sensing element were preloaded by the top of the accelerometer case and used in a severe acoustic environment, the acoustically-induced signal could be a large or even dominant percentage of the total output, as described in Section 3.2.4.8, It probably would be impossible to separate the acoustically-induced signal from the desired acceleration. Other PE accelerometer designs have been developed to achieve a better compromise among size, weight, minimizing base strain effects and maximizing case resonance frequencies. For example, the inverted compression accelerometer of Figure 3.40 is designed to minimize base strain effects while compromising the other features such as size and weight [3.11],

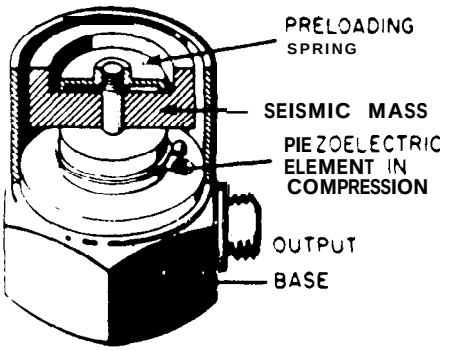

Figure 3,39. Cut-Away View of a Typical Single-Ended Compression Piezoelectric Accelerometer (Courtesy Bruel & Kjaer) [3.4, 3,6, 3.7].

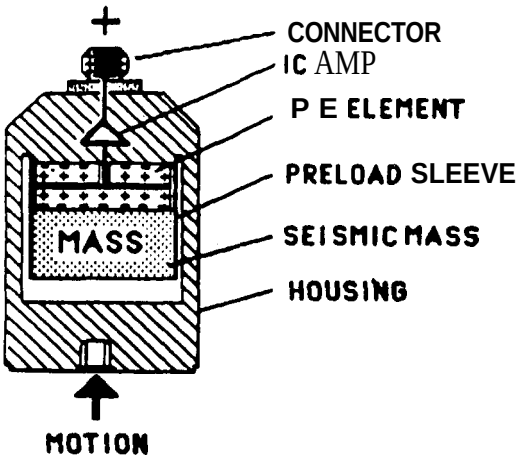

Figure 3.40 Cross-Section of a Typical Inverted Isolated Compression Accelerometer with Integral Electronic Amplifier (Courtesy PCB) [3.11].

Several designs of shear PE accelerometers are available. One type, called a ring shear, consists of a center post oriented in the intended direction of measurement, a concentric cylindrical shear-polarized ceramic or crystal attached to the post, and a concentric cylindrical mass attached to the outer surface of the sensing element, as shown in Figure 3.41 [3.4, 3.5, 3,10]. If the central post is made hollow, as shown in Figure 3.42, a simple mounting method is provided by fastening through the case into the structure [3.5]. Another type, called a plate shear, uses flat plate sensing elements, as shown in Figures 3.43 and 3.44 [3,4, 3,5, 3,6, 3.7, 3.10, 3.11]. The plate shear accelerometers shown include a pedestal between the base and the sensing elements. When exposed to dynamic excitation in the intended direction, the ceramic or crystal is stressed in shear. Transverse sensitivity is minimized by directional polarization. Some shear designs provide excellent protection against base strain, thermal effects, and acoustic noise, and can be constructed smaller and lighter. However, some ring shear designs have been found to be susceptible to base

strain, with the magnitude dependent on accelerometer orientation, and base thickness and elastic modulus [3.62]. The strain-induced signal can affect the acceleration-induced signal in magnitude and phase. Plate shear sensing elements can be used to reduce the rotational sensitivity of ring sensing elements.

The bimorph or beam bender uses a pair of tension/compression-polarized sensing elements in a single or double cantilever configuration, as shown in Figure 3.45 [3.69], to measure translational and/or rotational accelerations.

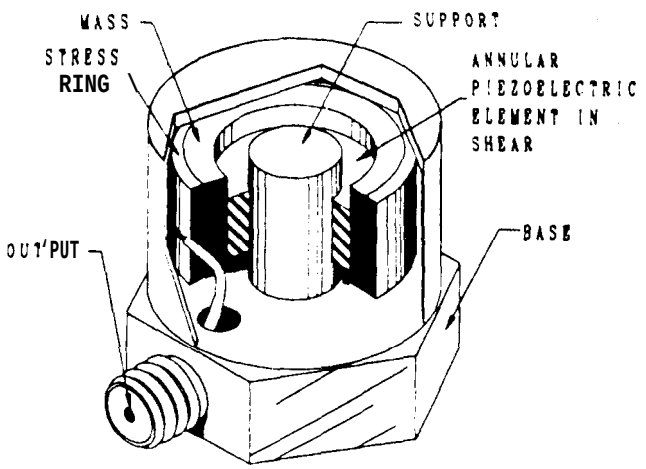

Figure 3.41. Cut-Away View of a Typical Ring Shear Piezoelectric Accelerometer (Courtesy Endevco) [3.5].

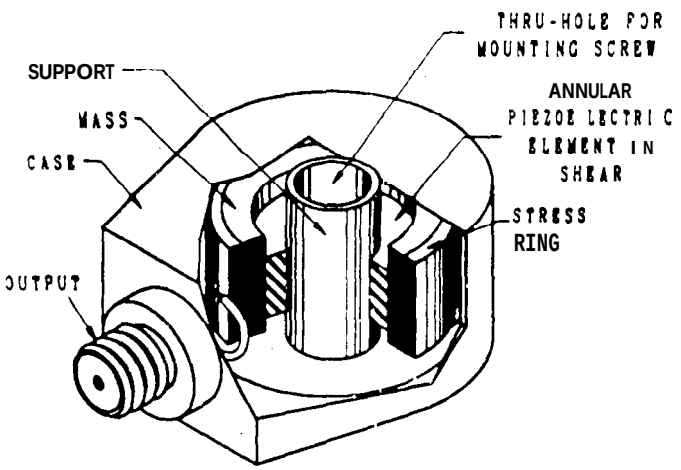

Figure 3.42. Cut-Away View of a Typical Miniature Ring Shear Piezoelectric Accelerometer with a Center Mounting Hole (Courtesy Endevco) [3.5].

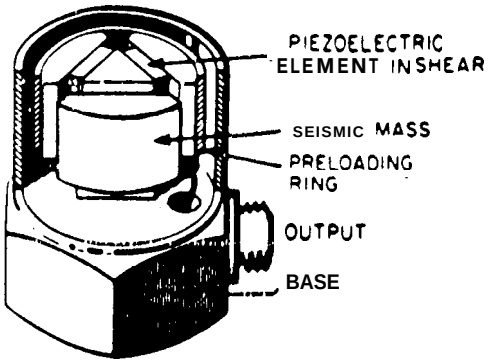

Figure 3.43. Cut-Away View of a Typical Plate Shear Piezoelectric Accelerometer (Courtesy Bruel & Kjaer) [3.4, 3.6, 3.7].

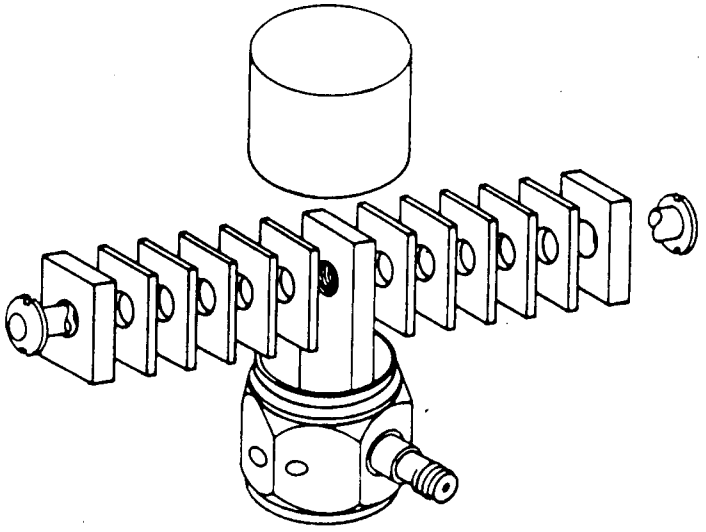

Figure 3.44, Disassembled View of a Plate Shear Piezoelectric Accelerometer (Courtesy Endevco) [3.5].

A qualitative, subjective comparison of the above PE accelerometer designs, furnished by accelerometer manufacture, is presented in Table 3.1. Many manufacturers offer several of these designs with or without integral electronics, which are discussed in Section 3.3.2 and described earlier in this section.

For very small accelerometers, the weight of the connector and the stiff end of the cable may not be a negligible percentage of the accelerometer weight. Most manufacturers offer a cable integrated directly into the accelerometer base or case to reduce this percentage. The integrated cable can be much more easily damaged than the conventional connector and cable during accelerometer installation and removal, but can be much less susceptible to moisture penetration during high humidity conditions, as mentioned in Section 3.2.4.4.

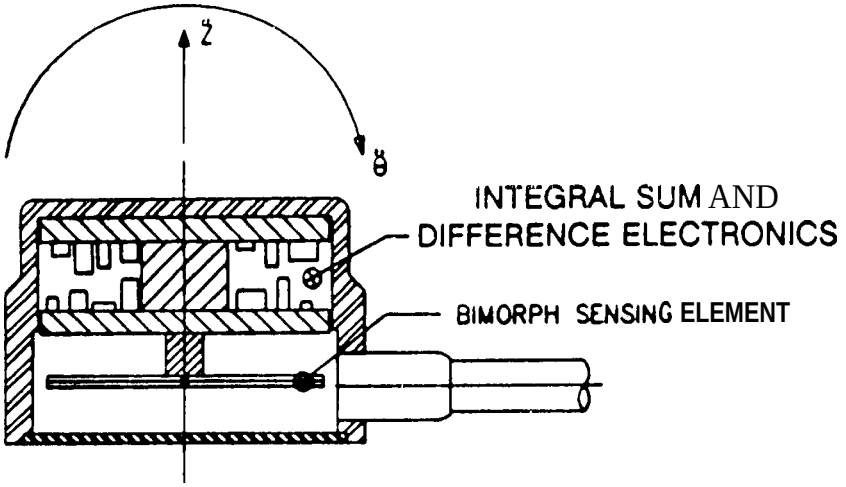

Figure 3.45 Cross-Section of a Beam Bender Piezoelectric Accelerometer for Bi-directional Measurements (Courtesy Kistler) [3.69].

Table 3.1. General Comparison of Piezoelectric Accelerometer Designs.

Parameters	Sensor Designs				
	Single-Ended Compression	Inverted Compression	Plate Shear	Ring Shear	Bimorph Bender
Ruggedness	" B	B	B	A	D
Small Size	C	D	C	A	B
Low cost	B	B	c	C	A
Shape Flexibility	C	C	C	B	C
Wide Bandwidth	B	B	B	A	D
Thermal Transient	C	B	A "	B	C
Base Strain Sensitivity	D	B	B	C	B

A- Best; B- Good; C- Fair; D-Poor

This table shows relative ratings of the five generic designs found in most piezoelectric accelerometers, There may be important exceptions. Thus, the accelerometer user should treat this table as a pointer rather than a definitive selection guide.

Under certain circumstances, translational (or linear) accelerometers may also be used to measure rotational (or angular) dynamic excitation. Figure 3.46 shows a carefully matched pair of PE accelerometers attached to abeam that is sufficiently rigid up to the desired maximum frequency limit of the measurement [3.5]. When wired correctly, the output signal is the difference between the individual accelerometer outputs. Careful calibration of the pair is required to avoid problems of mismatching and transverse sensitivity.

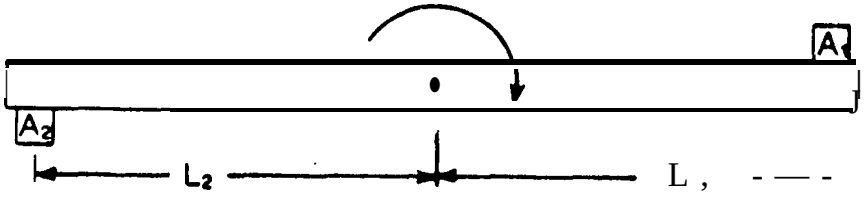

Figure 3.46. Method of Measuring Rotational Acceleration with a Matched Pair of Translational Accelerometers [3.5].

3.2.6.1.2 Piezoresistive Accelerometers. PR (or semiconductor strain gage) accelerometers, such as shown in Figures 3.47 and 3.48, use strain-sensitive materials described in Section 3.2.1.2 [3.5]. Both accelerometers shown use mechanically-loaded or active gages for all four arms of the Wheatstone bridge, with the two "tension" gages of Figure 3.48 located in Arms R_1 and R_3 of Figure 3.3, and the two "compression" gages located in Arms R_2 and R_4. This arrangement

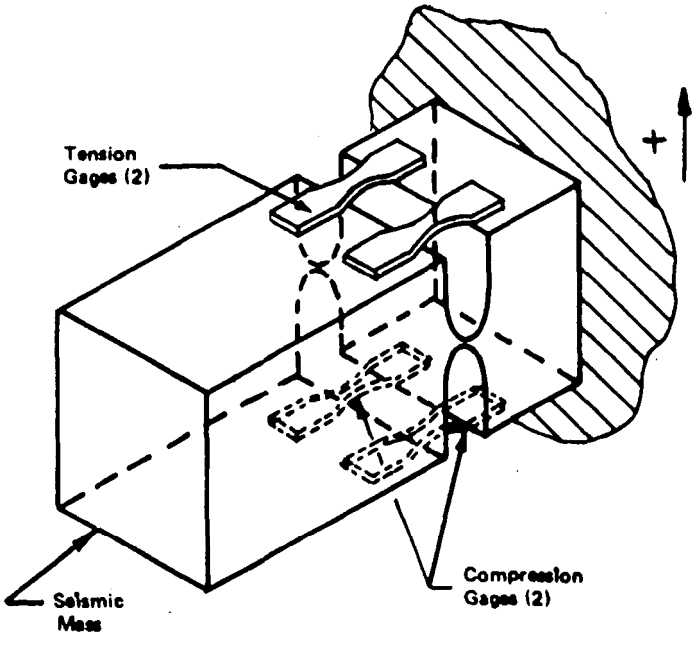

Figure 3.47. Cantilever-Mass Piezoresistive Accelerometer Using Four Semiconductor Strain Gages (Courtesy Endevco).

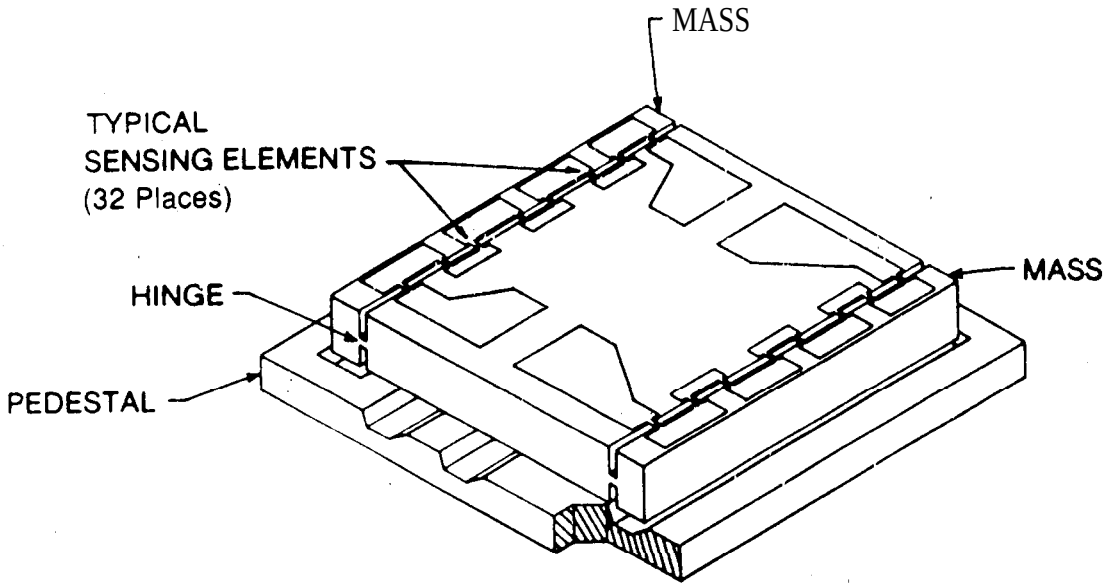

Figure 3.48. Twin Cantilever-Mass Piezoresistive Accelerometer Using Monolithic Semiconductor Strain Gage Sensing Elements (Courtesy Endevco) [3.5].

quadruples the transducer sensitivity over a single gage in a single arm, as discussed in Section 3.2.3.1, and provides temperature compensation as long as all four gages are matched and exposed to the same temperature simultaneously, as discussed in Section 3.2.4.1. PR accelerometers are capable of zero frequency (i.e., DC) response, which is particularly important for transient measurements when a significant static acceleration (i.e., velocity change) may add to the dynamic acceleration. Unfortunately, DC shift may be encountered, The maximum frequency limit can reach 150 kHz. The PR accelerometer is not self-generating and requires a well-regulated power source, but has the advantage of a low impedance output. The PR accelerometer is not capable of as high a sensitivity as the PE transducer, but is usually smaller and lighter.

PR accelerometers can be gas or oil damped, so they can be used up to a higher percentage of their resonance frequency, as described in Section 3.2.2. However, the damping may vary significantly with temperature, as discussed in Section 3.2.4,1 and illustrated in Figure 3.21. If a low enough temperature is reached, the liquid will freeze and the transducer will become inoperative.

PR accelerometers are usually supplied with a specified length of shielded cable. Long cables can cause a reduction of accelerometer sensitivity because the resistance in long power supply cables to the Whetstone bridge can reduce the voltage to the transducer, and resistance in long signal cables from the bridge can reduce the voltage to the signal conditioner. In addition, all cables have capacitance associated with them. If the cable is long, the combined capacitance and resistance becomes a distributed lowpass filter that can attenuate the signal at higher frequencies.

A simple and accurate DC calibration can be performed on a PR accelerometer simply by inverting it in the earth's gravitational field. However, insensitive transducers maybe calibrated over only a small portion of their dynamic range using this method. Very sensitive transducers may be calibrated below 1g by rotation to different angles relative to earth's gravitational field using a rotating tilt tabk and an inclinometer.

3.2.6.1.3 Variable Capacitance Accelerometers. Vc accelerometers, whose principle of operation is described in Section 3.2.1.3, provide zero frequency (i.e., DC) response, but arc limited to a maximum frequency of about 1 kHz. They can be very sensitive and accurate, with high acceleration over-range capacities. Integral electronics within the accelerometers can provide low impedance Outputs to drive long cables with little interference. The VC accelerometer was developed for measuring low level static and low frequency dynamic accelerations. To extend the limited frequency range, gas or oil darnping can be incorporated, as described in section 3.2.2. However, the damping may vary significantly with temperature, as discussed in Section 3.2.4.1 and illustrated in Figure 3.20. If a low enough temperature is reached, the liquid will freeze and the transducer will become inoperative

3.2.6.1.4 Servo-Accelerometers. The servo-accelerometer is very sensitive and accurate, and has a DC response, but it is relatively heavy and has a limited frequency range (generally less than 200 Hz). This range can be extended to higher frequencies (about 500 Hz), sometimes by simply changing the value of an external resistor, at some sacrifice of transducer sensitivity. The servo-accelerometer is used primarily for aerospace inertial guidance applications. It requires a very stable and accurate power supply to maintain its mass at its null position while the acceleration tends to displace it, as described in Section 3.2.1.4. Magnitude limits extend from 10 μg to about 50 g. Special temperature control is usually required. Closed-loop servo-accelerometers are recommended over open-loop designs because of their insensitivity to power supply voltage variations,

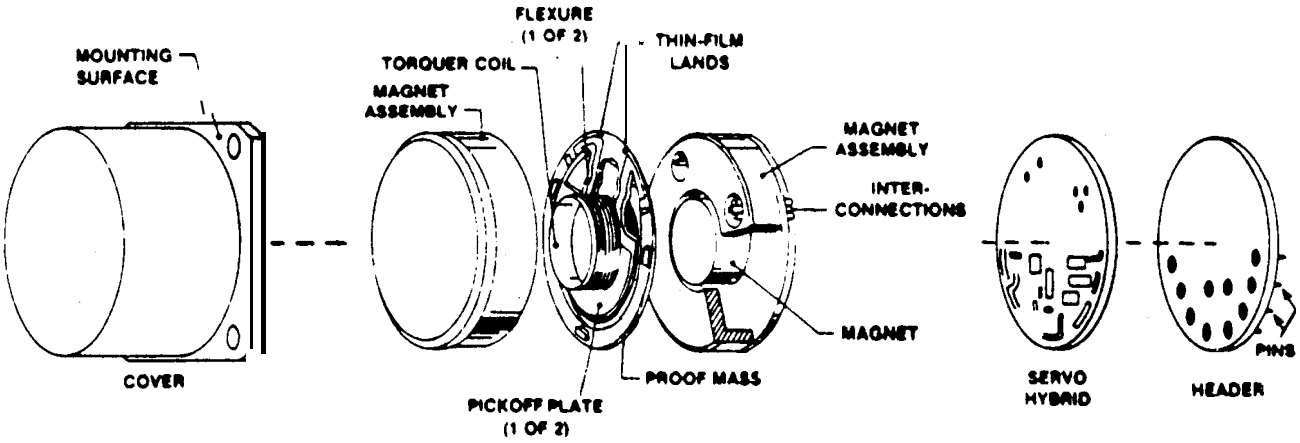

Figure 3.49. Disassembled View of a Servo-Accelerometer (Courtesy Sundstrand) [3.1].

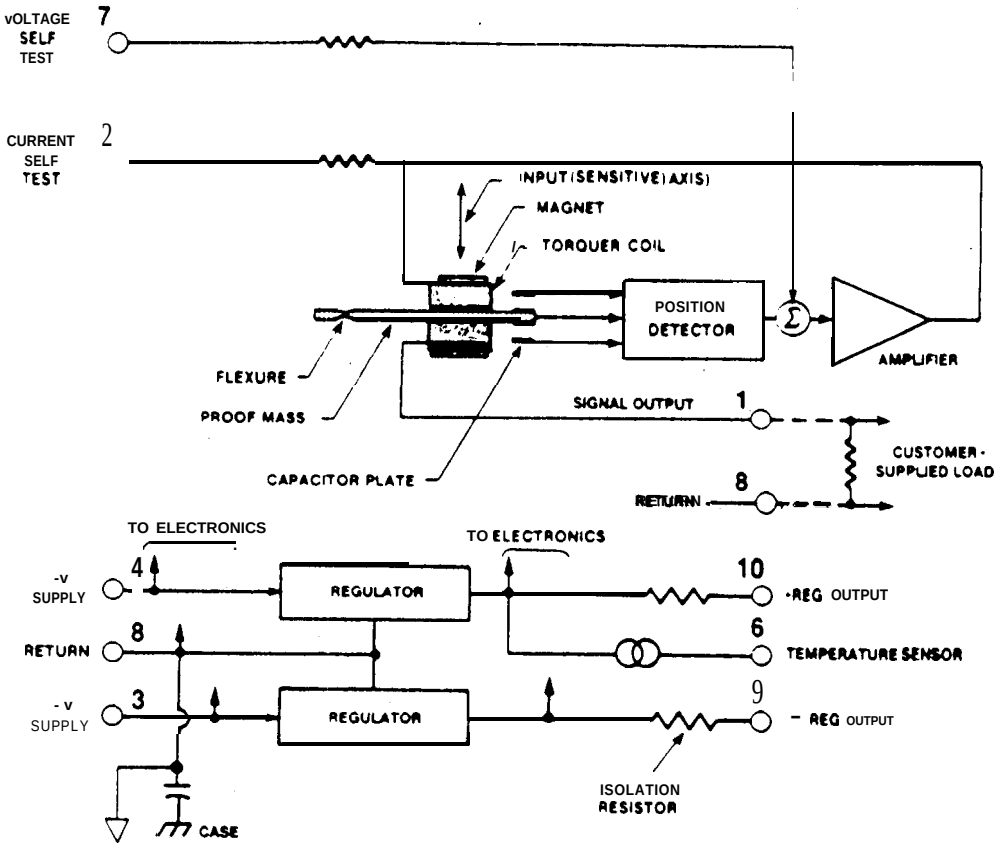

Figure 3.50. Circuit Diagram of a Servo-Accelerometer (Courtesy Sundstrand) [3. 1].

nonlinearity, scale factor thermal shifts, and zero shift. A disassembled view and a block diagram of a typical servo-accelerometer are shown in Figures 3.49 and 3.50 [3.1].

Servo-accelerometers are also being used for micro-gravity measurements. Such transducers presently under development show promise for extremely sensitive applications, perhaps as low as 10 ng from DC to about 2 Hz, and weighing less than an ounce with dimensions less than an inch. These devices also will be able to survive launch environments without mechanical constraints.

3.2.6.2 Velocity Transducers. Velocity measurements may be made using either an electrodynamic system (EDS) or a laser Doppler vibrometer (LDV).

3.2.6.2.1 Velocity Pickups. Velocity pickups, such as shown in Figure 3.51, are transducers that use an electrodynamics system (EDS), described in Section 3,2.1.4, with a spring(s) connecting a base, which contains a magnet, to a mass, which is integral with the moving coil (idealized by the SDF system of Section ,3.2.2), to sense dynamic structural velocities applied to the base. Sometimes a damper is incorporated into the pickup, as shown in Figure 3.51.

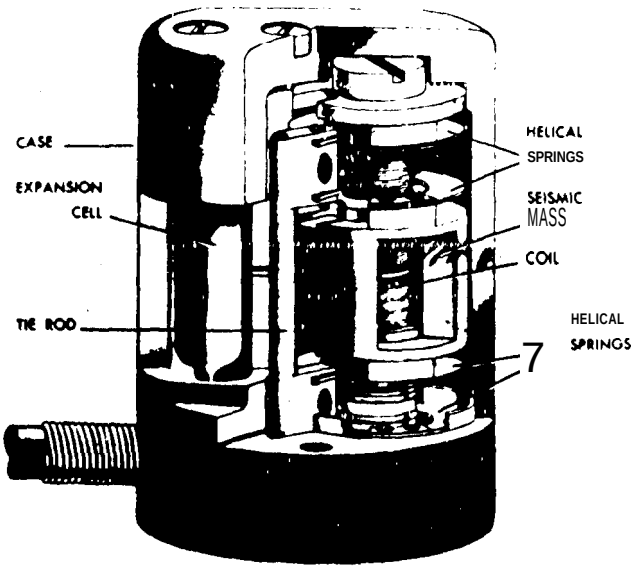

Figure 3.51. Cut-Away View of a Velocity Pickup (Courtesy IMO).

The useful frequency range for velocity pickups is discussed in Section 3.2.3.2. If the pickup selected has low damping, e.g., $\zeta < 0.1$, care must be taken to ensure that the transducer resonance is not sufficiently excited (even though the resonance frequency is significantly below the minimum frequency limit) to (a) cause the transducer to respond nonlinearly, especially hard bottom, and/or (b) generate an excessive electrical output that could cause the following signal conditioner to respond nonlinearly, such as amplifier saturation. Nonlinear response not only affects signal fidelity at resonance, but also throughout the spectrum as well, Thus, the resulting data are likely to be worthless. However, if the transducer responds linearly while providing an excessive resonant output, then a highpass filter may be used between the transducer and signal conditioner to attenuate the output. Such filters are described in Section 3.3.3.

3.2.6.2.2 Laser Doppler Vibrometers. The LDV is a non-contact system that measures the Doppler shift of a laser beam reflected from a target on a moving or vibrating surface. The output is proportional to the instantaneous velocity of the target in the direction of the beam, as described in Section 3.2.1.5. The system must have a fixed (or non-moving) reference, which generally restricts it to laboratory tests, where a fixed foundation can be obtained. For a normal-incident laser beam, the instantaneous Doppler shift $\Delta f_D(t)$ is

$$\Delta f_D(t) = \frac{2\,x(t)}{\lambda_\ell} \tag{3.12}$$

where x(t) is the instantaneous target velocity, and λ_ℓ is the light wavelength (λ_ℓ = 633 nm for the popular He-Ne laser). One such system is illustrated in Figure 3.52, where the dynamic velocity can range from 1 μ to 10 m/sec (40 μ to 400in./sec) with a frequency range from 1 Hz to 500 kHz [3.27, 3.28]. Measurements maybe made at distances ranging from 10cm to 0.5 m (4 to 20 in.) from the target. Since the system has an analog output that is a linear function of the instantaneous target velocity, the integral of the output yields target displacement while the derivative yields target acceleration. The acceleration range is shown in Figure 3.53. A variety of similar systems have been developed to cover either higher [3.24- 3.26] or lower [3,29] velocities or frequencies.

The LDV appears advantageous for measuring dynamic motion transverse to the structural surface when the acceleration magnitude increases approximately proportional to frequency, such as pyre-shock described in Appendix A.

There are three types of technical considerations associated with LDV measurements: (1) installation, (2) calibration, and (3) instrumentation noise. There can be various installation problems, including the positioning of the LDV relative to the location of the desired target, and optical alignment. Although the electronics can be absolutely calibrated, the optics usually cannot. Thus the calibration is generally restricted to the range of the accelerometer used as the transfer standard transducer identified in Section 3.8.1.1, which is usually only a small portion of the LDV magnitude and frequency range.

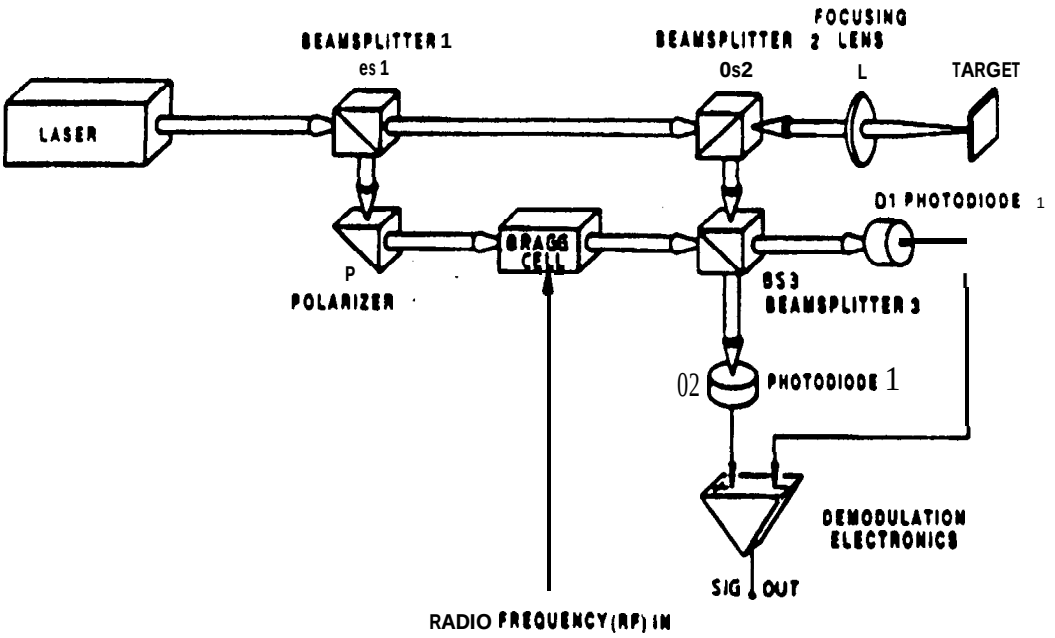

Figure 3.52. Schematic Diagram of a Laser Doppler Vibrometer (Courtesy Polytec).

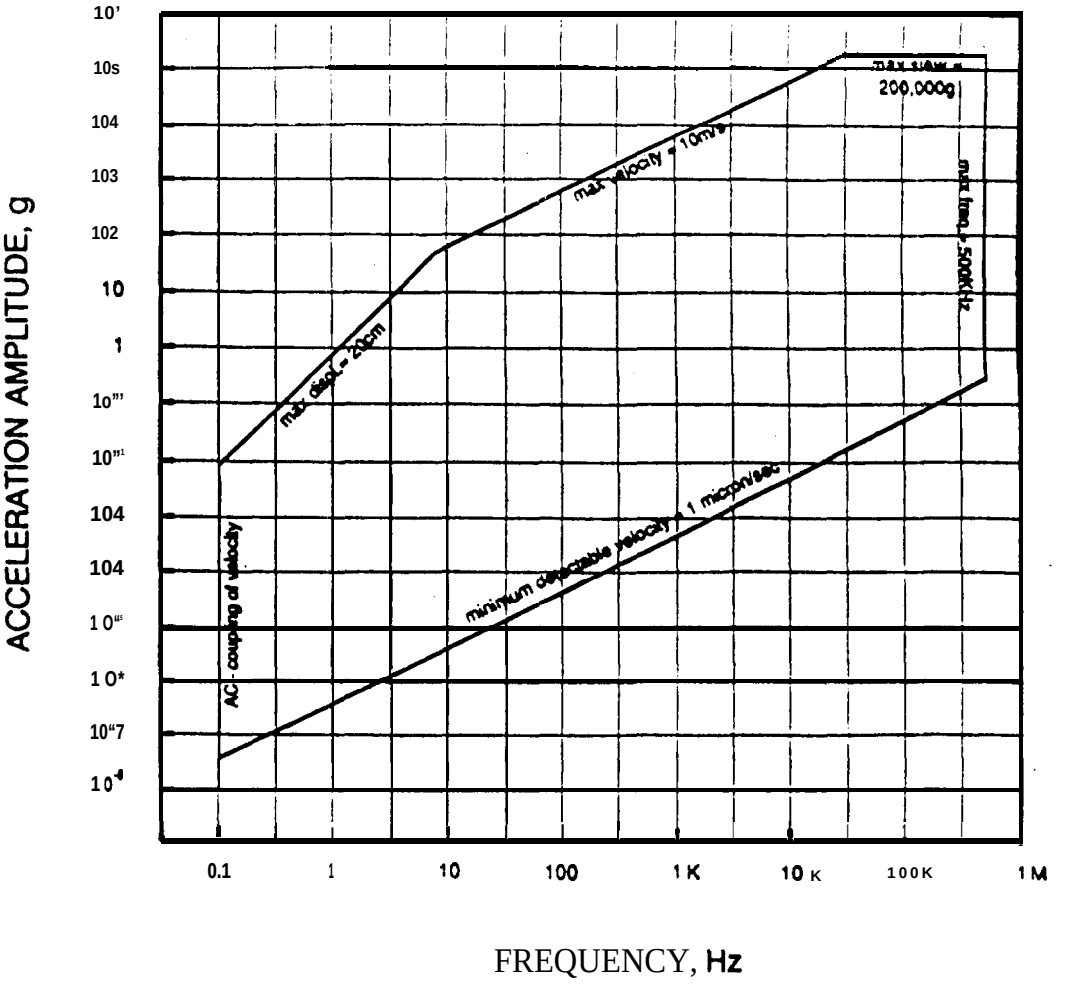

Figure 3.53. Useful Operating Range for a Laser Doppler Vibrometer [3.28].

There are several categories of potential LDV noise sources. Motion of the fixed reference or of fiber optic cables (if used) can cause spurious noise. Structural in-plane or rotational motion of the target can cause noise if the topography of the target surface is not flat with respect to the wavelength of the laser beam over the total motion to be measured. Because the LDV measurement technique is based upon coherent light scattering, non-uniform topography can cause spurious or complete loss of reflectivity. Complete reflectivity loss will cause signal drop-out, described in Section 4.3.6 and illustrated in Figure 4.10 (b). It is recommended that the target surface be sufficiently polished to avoid back-scatted light intensity variations with target topography and motion. Attaching corner cube reflectors is not recommended, while retro-reflective tape may be acceptable for low magnitude vibration or shock applications. The foregoing problems are further discussed in [3.27, 3.28].

3.2.6.3 Motion Transducer Installation. The method of mounting or attaching an accelerometer or velocity pickup to a structure is highly dependent on the intended direction and frequency range, the anticipated magnitude of the static and/or dynamic load or environment, the size of the transducer, climatic environmental effects, mechanical restrictions, and certain load-carrying capacities of the structure at the measurement location [3.4- 3.7, 3.41, 3.70- 3.72]. It is recommended that the transducer be fastened directly to the structure by bolt(s) or stud(s) when high magnitudes and/or frequencies are expected. When attaching a piezoelectric accelerometer with a bolt or stud, a deep socket with a groove cut into its side to provide clearance for a side connector, if required, is recommended. A torque wrench should be used to obtain the transducer manufacturer's recommended installation torque. It is critical that both mounting surfaces be flat and smooth, and the mounting hole be normal to the surfaces in accordance with the manufacturer's criteria. A very thin layer of oil or grease between the surfaces is recommend for high frequency measurements.

The ideal location for measuring in-plane motion is at an edge or 90' bend of the structure, if (a) the edge or bend is close to the intended measurement location, (b) the edge or bend is normal to the intended in-plane direction, (c) the edge or bend is thick enough to enable a bolt or stud to be installed, and (e) there is sufficient room for the transducer and mounting tools. If these four conditions are not all satisfied, then a mounting block will be required to obtain the intended in-plane measurements. The conventional cube mounting block permits one, two or three orthogonal transducers to be attached, and in turn is attached to one side of the structure. However, if dynamic structural bending accompanies the in-plane motion, as often occurs in practice, mounting block rotation (or rocking) may be caused by the bending motion, resulting in increased in-plane motion at the in-plane transducer location, as described in Appendix A. This in-plane component can cause errors in excess of 100% when compared to the true in-plane motion of the structure, particularly at higher frequencies. Three techniques have been developed to avoid this situation [3.41, 3.73]: (1) the dual mounting block, composed of identical blocks and in-plane transducers on opposite sides of the structure, (2) the wedge or triangular mounting block, and (3) the extended cube (really a rectangular prism, not a cube). The first two techniques are described in Appendix A. The third technique, shown in Figure 3.54, requires a larger mounting block compared to the conventional cube. Unfortunately, all three techniques require twice as many matched transducers to measure true in-plane motions, using instantaneous signal sums or differences to electrically determine the in-plane components. Fortunate] y, the second technique can also be used to electrically determine the transverse component, whereas the first and third techniques can also be used to electrically determine mounting block rotations [3.41, 3.73]. In all cases, mounting blocks increase the weight and stiffen the structure locally, but substantially reduce the effects of base bending strains on the transducers, as discussed in Section 3.2.4.8.

When electrical isolation or insulation is required between an accelerometer and the structure to avoid ground loops, as discussed in Section 3.3.5.3, an insulated or isolated mounting stud or washer should be used. This may cause a reduction of the maximum frequency limit, as most

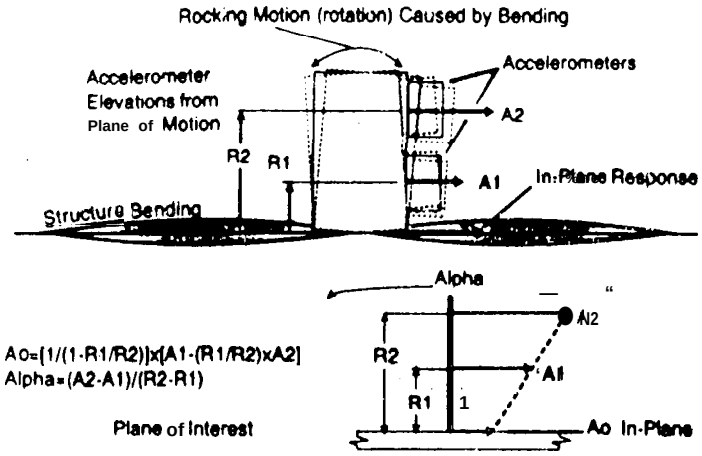

Figure 3.54. Extended Cube Mounting Block of Matched Accelerometers for Measuring h-Plane Motion and BendingInduced Rotations [3,41].

commercially-available accelerometer isolated studs have a 30 kHz or more mounted resonance, which limits data accuracy at and above those frequencies. Isolated studs cause less stiffening of the structure by the accelerometer, as described in Sections 3.2.4 .1,3.2.4.7 and 3.2.4.8.

In many cases, mounting holes will not be permitted in the structure because of insufficient structural thickness, structural integrity (i.e., strength) or criticality considerations. A variety of adhesives must be considered, including cyanoacrylate, epoxy and high strength dental cements [3.5 - 3,7,3.70- 3.72]. Generally, matching surfaces must be cleaned with a hydrocarbon solvent, such as acetone, prior to applying the adhesive, keeping the solvent away from the cables and connectors. The cements are generally moisture-resistant and strong, especially when applied in a thin layer, but are not recommended for long-term use under high humidity, or for pyroshock application as discussed in Appendix A. When the transducer is installed, the transducer should be quickly pressed into the adhesive to achieve a thin adhesive layer. The resulting excess adhesive surrounding the transducer should then be removed to avoid providing a weak compliant bond at the transducer perimeter in case the bond under the traducer fails. Thus, the failed bond can be immediately observed and any resulting data discarded [3.41]. Most cements must be cured, with the curing time prior to use highly dependent on the cement composition, thickness and temperature. Each cement has its useful temperature and humidity ranges. Dental cement is popular for contoured structural surfaces, although the bond strength and maximum frequency may be limited. Also, a small mounting block can have one surface contoured to match the structural surface, and the opposite surface flat to permit bolting of the transducer. Often, narrow deep V-grooves are cut into the mounting block on the contoured-surface side to increase the integrity of the bond. Many cements are good electrical isolators, and may be used for avoiding ground loops. After usage, most accelerometer bonds are easily broken in shear (usually by twisting the accelerometer with a

wrench), though it may sometimes be difficult or impossible to remove cement-mounted accelerometers without damage or failure. Some manufacturers have recommended procedures for their removal. Once removed, the structural and transducer surfaces may be difficult to clean, although a solvent may work best. Sometimes thin plastic tape is used between the transducer and structure to minimize this problem. Some manufacturers make cement-on pads to which accelerometers may be bolted, When these are used, the final orientation of a side connector must be considered before the pad is cemented in place.

Other techniques, such as double-backed tape, beeswax and magnets are much easier to apply, but are limited to low and mid frequencies and/or much lower accelerations. The thin application of adhesive in double-backed tape or beeswax is preferred to achieve the highest possible frequency limit. Obviously, magnets can be used only when the structure is magnetic. The intervening magnet can be bolted to the transducer, or held by magnetic force if applicable. The additional weight of the magnet maybe a substantial percentage of the transducer weight. A hand-held probe maybe used, but is restricted to qualitative measurements at low and mid frequencies and low accelerations (below 1 g). Except for occasional survey purposes, its use is not recommended.

The effects of various laboratory mounting techniques on the frequency response of a piezoelectric accelerometer having a mounted resonance frequency of about 30 kHz is illustrated in Figure 3.55, based on data from one manufacturer [3,6, 3.70, 3.71]. The recommended maximum temperature is also shown when applicable. In special circumstances, such as the measurement of high intensity pyroshock, a combination of a mounting stud and adhesive is recommended, as discussed in Appendix A.

It is usually desirable to check the adequacy of the adhesive bond, as well as the installation of transducer cable connectors, prior to their use under actual dynamic loading. Traditionally this is performed by a tap test, i.e., impacting the structure or mounting block near the transducer in rough simulation of the dynamic environment. Unfortunately, large variability has been observed with this method. A tool has been suggested to avoid this variability, composed of a modified spring-loaded center punch plus an adapter for transferring the center punch dynamic load to the structure and/or mounting block in close proximity to the transducer(s) [3.41]. The built-in spring is designed to provide a repeatable dynamic environment. A softer or harder spring maybe used to achieve a lesser or greater environment, respectively. Readout from the signal conditioner can be used to check the adequacy of the adhesive bond, cable connector and even the signal conditioner gain setting.

It is usually prudent to take enough photographs to verify the location and orientation of the transducers.

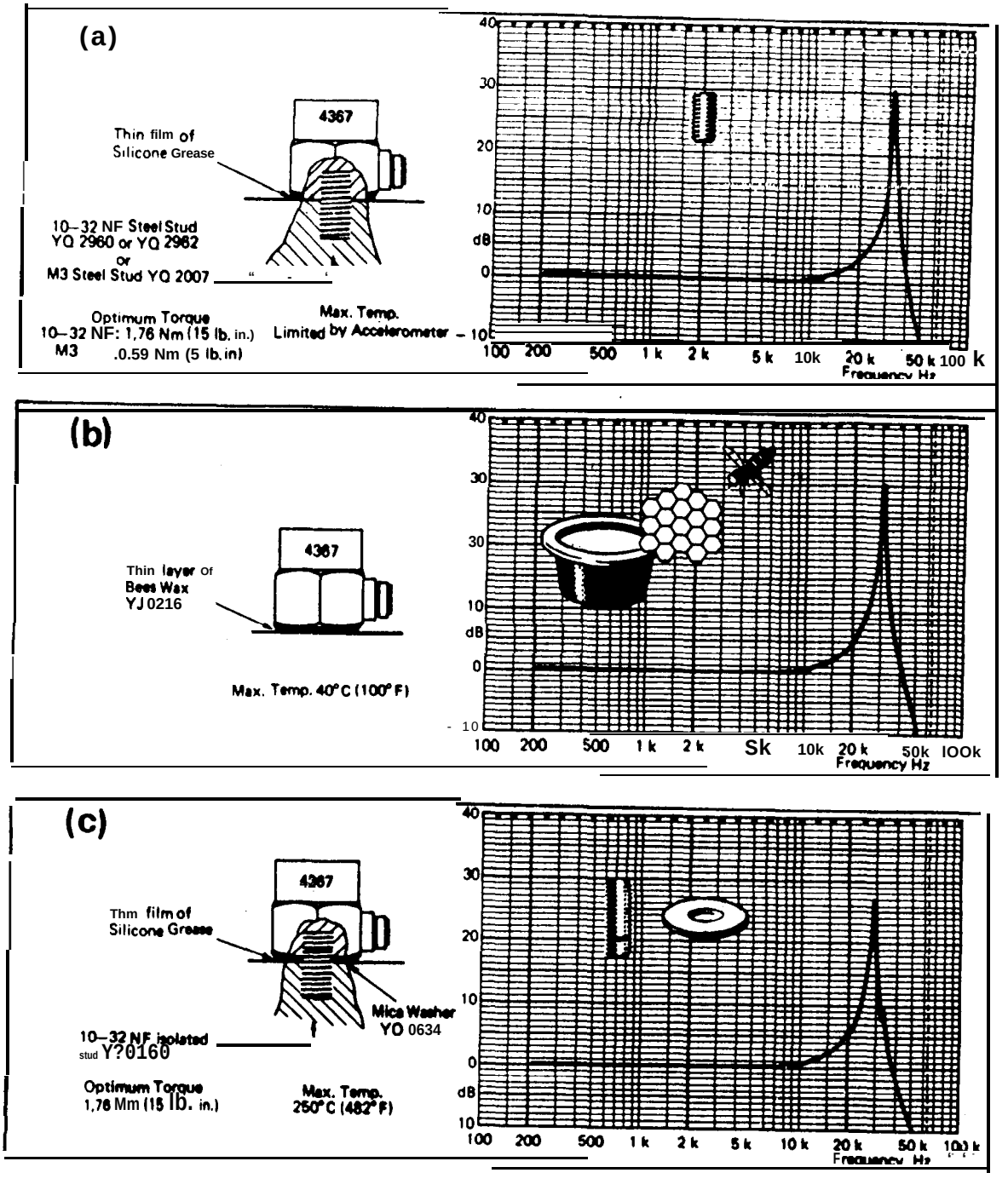

Figure 3.55. Typical Effects of Various Mounting Techniques on the Frequency Response of **Accelerometers.** Maximum Temperature Limits **are also** Shown **(Courtesy Bruel & Kjaer)** [3.6].

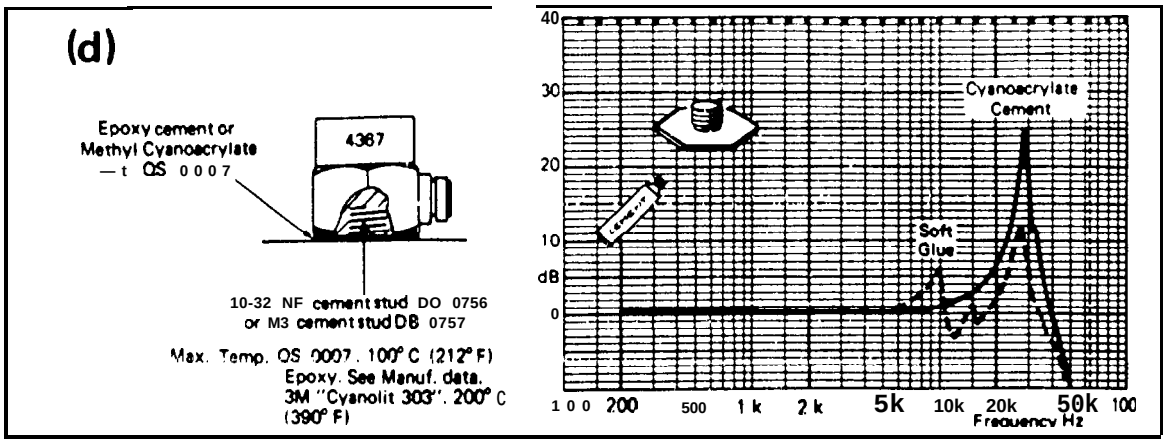
(d)
Epoxy cement or
Methyl Cyanoacrylate
— t QS 0007
4367
10-32 NF cement stud DO 0756
or M3 cement stud DB 0757
Max. Temp. QS 0007. 100° C (212° F)
Epoxy. See Manuf. data.
3M "Cyanolit 303". 200° C
(390° F)
Cyanoacrylate
Cement
Soft
Glue
40
30
20
10
dB
0
100 200 500 1 k 2 k 5k 10k 20k 50k 100
Frequency Hz

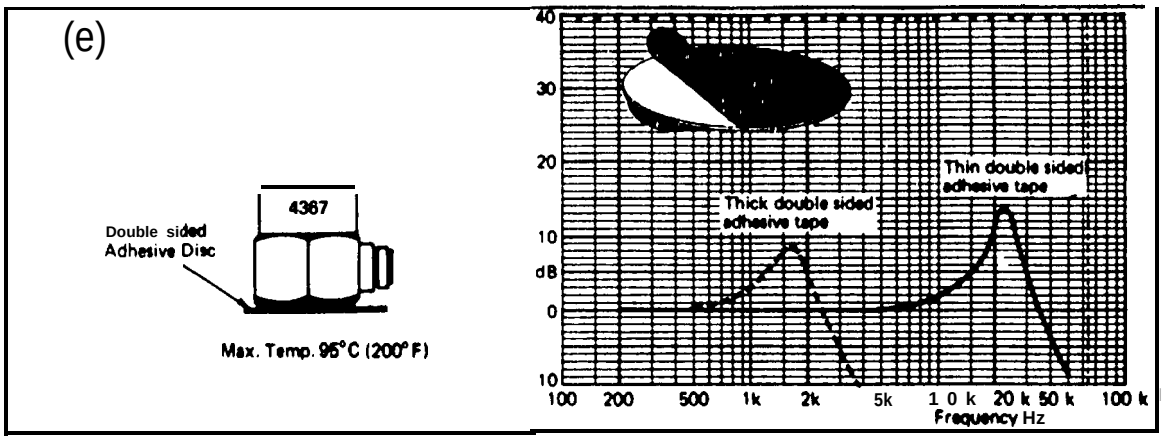
(e)
4367
Double sided
Adhesive Disc
Max. Temp. 95°C (200° F)
Thin double sided
adhesive tape
Thick double sided
adhesive tape
40
30
20
10
dB
0
10
100 200 500 1k 2k 5k 10 k 20 k 50 k 100 k
Frequency Hz

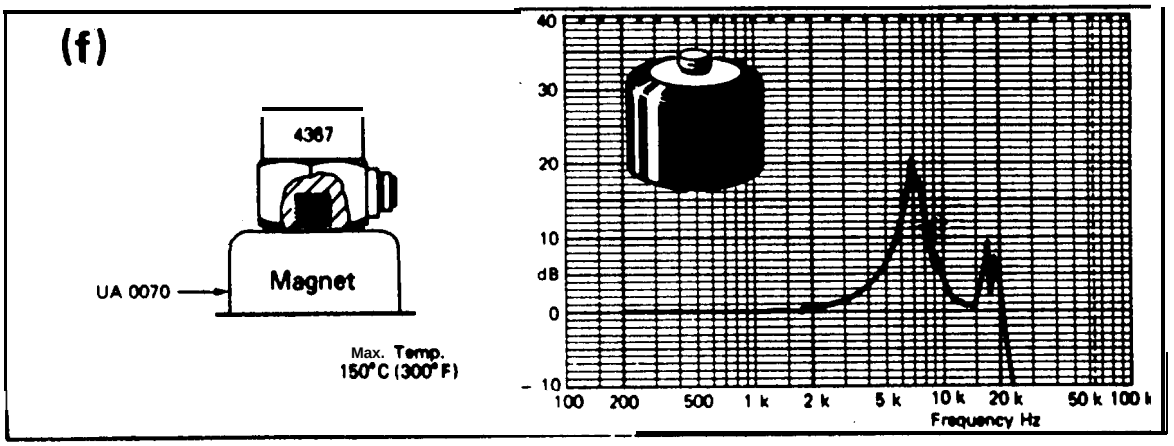
(f)
4367
UA 0070
Magnet
Max. Temp.
150°C (300° F)
40
30
20
10
dB
0
- 10
100 200 500 1 k 2 k 5 k 10 k 20 k 50 k 100 k
Frequency Hz

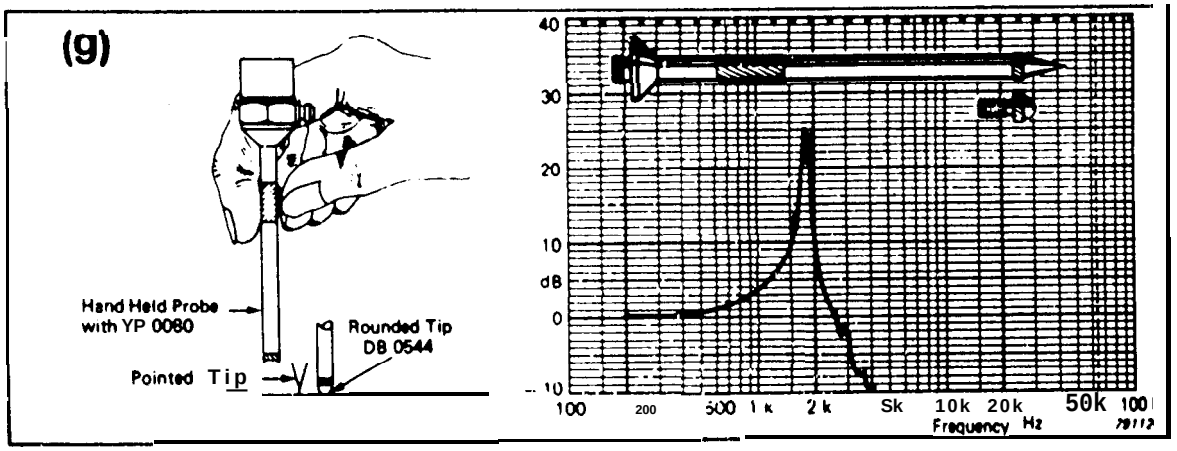
(g)
Hand Held Probe
with YP 0080
Rounded Tip
DB 0544
Pointed Tip
40
30
20
10
dB
0
- 10
100 200 500 1 k 2 k Sk 10k 20k 50k 100
Frequency Hz

3.2.7 Pressure Transducers. A pressure transducer used for aerospace applications senses the motion of a circular diaphragm that deforms under instantaneous pressure and, alone or with other electrical components, generates an instantaneous electrical signal related to the applied pressure. Four types of pressure transduce are commonly used for static and/or dynamic data acquisition in aerospace applications: (1) metallic strain gage pressure transducers, (2) piezoresistive pressure transducers, (3) piezoelectric microphones, and (4) condenser (or electrostatic) microphones, including the electret. Strain gage and PR pressure transducers are both capable of measuring static pressures. However, there may be high sensitivity to temperature changes in the response below 5 Hz, as discussed in Section 3.2.4.1. In addition, some pressure transducers are susceptible to freezing. All pressure transduce USC the SDF design feature described in Section 3.2.2.

The useful frequency range for pressure transducers is discussed in Section 3.2.3.2. If the transducer selected has low damping, e.g., $\zeta < 0.1$, care must be taken to ensure that the transducer resonance is not sufficiently excited (even though the resonance frequency is significantly above the maximum frequency limit) to (a) cause the transducer to respond nonlinearly, especially hard bottom, and/or (b) generate an excessive electrical output that could cause the following signal

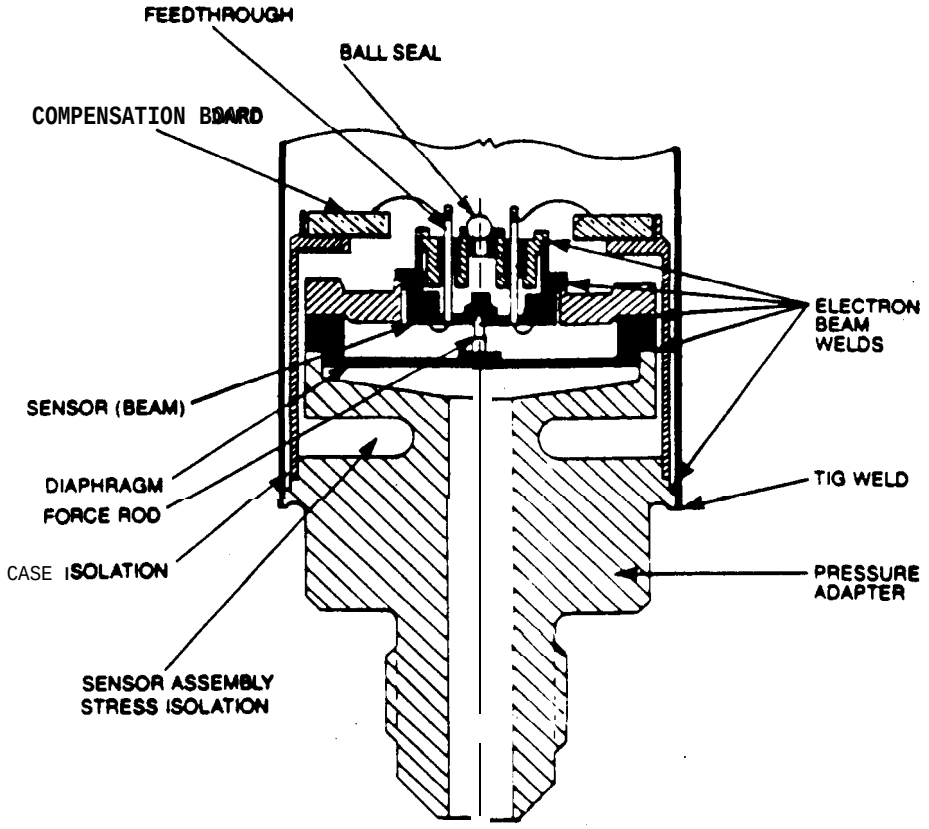

Figure 3.56. Cross-Section of a Pressure Gage Using Diaphragm/Beam-Loaded Metallic Strain Gages (Courtesy IMO).

conditioner to respond nonlinearly, such as amplifier saturation. Nonlinear response not only affects signal fidelity at resonance, but also throughout the spectrum as well. Thus, the resulting data are likely to be worthless. However, if the transducer responds linearly while providing an excessive resonant output, then a lowpass filter may be used between the transducer and signal conditioner to attenuate the output. Such filters are described in Section 3.3.3.

3.2.7.1 Metallic and Piezoresistive Pressure Gages. Fairly large and rugged pressure transducers called pressure gages, such as shown in Figure 3.56, utilize metallic strain gages or PR sensing elements in a Wheatstone bridge arrangement, described in Section 3.2.1.2, often with lower sensitivities to measure high-magnitude static and dynamic pressures [3.74]. The maximum frequency limit can be over 15 kHz, with the limit varying inversely with the sensitivity and size of the gage.

3.2.7.2 Piezoresistive Pressure Transducers. Very small pressure transducers, such as shown in Figure 3.57, utilize PR sensing elements in a Wheatstone bridge arrangement with moderate-to-high sensitivities to measure pressures over a very wide frequency range, e.g., up to 300 kHz. Their small size (e.g., diameters down to 0.03 in.) make them ideal for making measurements with scale models in wind tunnel aerodynamic noise and rocket engine acoustic noise model tests [3.75 - 3.77].

3.2.7.3 Piezoelectric Microphones. Most PE microphones use a thin metallic foil as the diaphragm, pressed against a ceramic or crystal sensing element, as shown on the top of Figure 3.34 and discussed in Section 3.2.1.1. During its manufacture, a hard vacuum may be applied to the inside of the microphone, which is then hermetically sealed, to ensure that the diaphragm fits tightly to the sensing element. This permits the microphone to be impervious to moisture and operate over a wide range of static pressures in excess of a hard vacuum. If isolation from structural excitation is inadequate, vibration-canceling PE microphones are available. A typical compensating accelerometer inside the microphone is shown in the center portion of Figure 3,34. The useful frequency range for both types of PE microphones extends from about 1 Hz to about 100 kHz, with the maximum frequency limit varying inversely with the sensitivity and size of the microphone.

3,2.7.4 Condenser Microphones. A conventional condenser (or capacitor or electrostatic) microphone, such as shown in Figure 3.58, uses a thin diaphragm, a fixed backplate and an air dielectric to form the sensing element, as described in Section 3,2.1.3 [3.8, 3.9, 3.12, 3.13, 3.22, 3.35, 3.49]. The useful frequency range extends from about 3 Hz to over 50 kHz, with the maximum frequency limit varying inversely with the sensitivity and often with the size of the microphone. The power supply for the polarization voltage and signal amplifier are usually supplied with the transducer. Condenser microphones have stable characteristics over long periods of time and a relatively wide temperature range, but are susceptible to electrical leakage degradation if used in high humidity without protection, as discussed in Section 3.2.4.4.

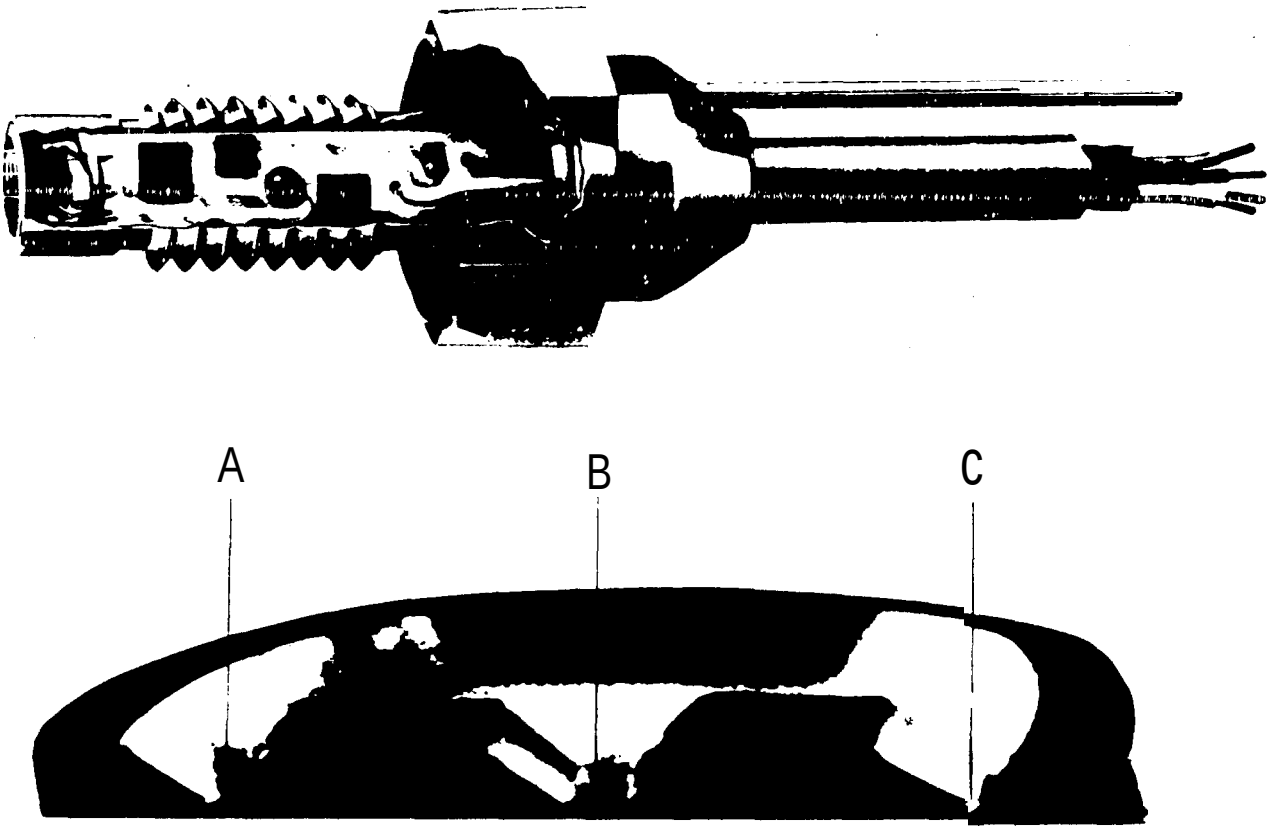

Figure 3.57. Cut-Away View of a Miniature Piezoresistive Pressure Transducer and Enlarged Cross-Section of Silicon Diaphragm Showing Semiconductor Strain Gage Locations (Courtesy Endevco).

A variation of the condenser microphone is the electret, also called a prepolarized microphone. This type of microphone employs an electrically charged polymer to create the field in the air gap, In one design, the polymer material is deposited onto the backplate, as shown in Figure 3.59 [3.8, 3.9, 3.12, 3.13]. In another design, a polymer film is the diaphragm, i.e., stretched across the air gap in front of the backplate. A metallic coating is applied to the outside of the film. Such microphones are useful in high humidity applications, However, the prepolarized charge can degrade with time. In addition, the maximum frequency limit of the second design may also degrade with time as the polymer film creeps under the tension load, especially at higher temperatures. The useful frequency range for electret microphones extends from about 5 Hz to about 20 kHz.

3.2.7.S <u>Pressure Transducer Installation</u>. A major requirement for the installation of any pressure transducer is the avoidance of additional static loading on the diaphragm, whose consequences extend from as little as a minor sensitivity change to as much as catastrophic failure. Obviously, a

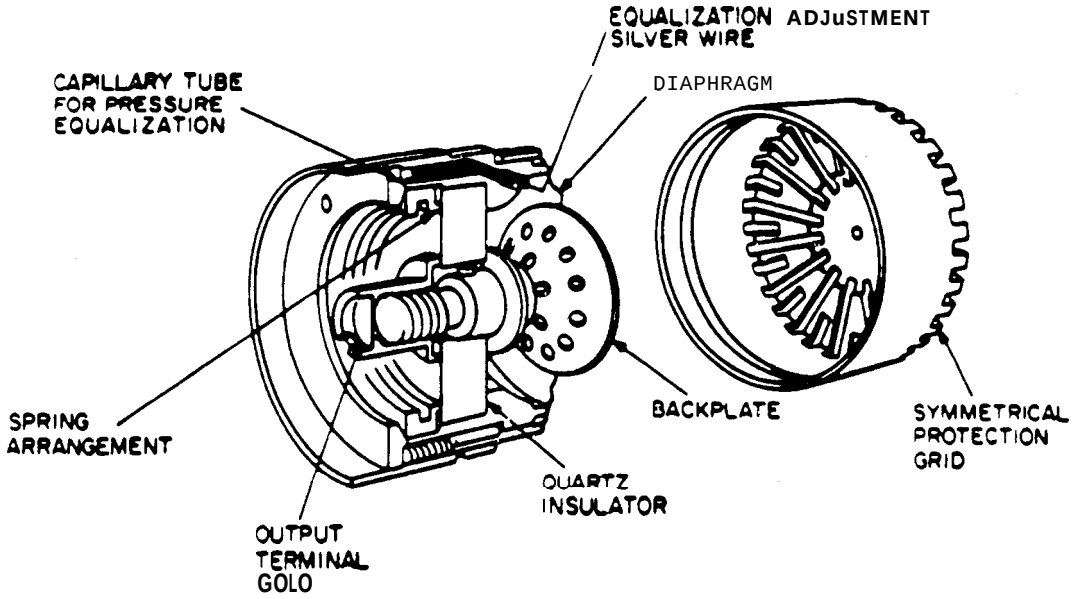

Figure 3.58. Cut-Away View of a Condenser Microphone (Courtesy **Bruel** & **Kjaer)** [3.22, 3.35].

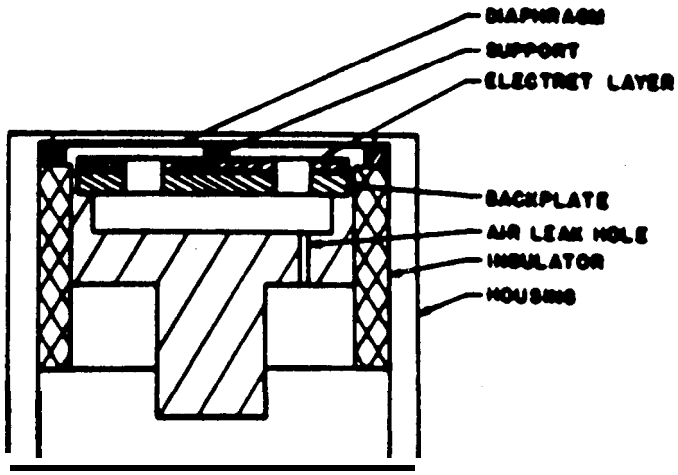

Figure 3.59. Cross-Section of an **Electret** Microphone (Courtesy **GenRad)** [3.8, 3.13].

resilient support is the recommended installation configuration to avoid diaphragm loading, unless it causes a substantial increase to the structural-induced response of the transducer, as discussed in Section 3.2.4.8, or unless the diaphragm is mechanically isolated from the remainder of the transducer. Most transducer manufacturers recommend one or more types of installation. In addition, the type of installation is highly dependent on the purpose of the **measurement.** Tubing is sometimes used to transmit pressures from the intended point **of** measurement to the pressure trans-

ducer, usually to avoid subjecting the transducer to excessive temperatures, as described in Section 3.2,4.1. It is usually prudent to take enough photographs to verify the location and orientation of the transducers.

If the objective is to measure external aerodynamic noise, either during flight or a wind tunnel test, the transducer must be installed so the diaphragm is flush mounted to the structural surface to avoid disturbing the flow. In addition, the protective cap (if normally provided) must be removed. Actually, a slightly recessed diaphragm (e.g., submerged by 0.005-0.010 in.) has been found to provide the least amount of flow disturbance, without creating a cavity resonance [3.75, 3.78]. Care must be taken to avoid inadvertent damage to the delicate diaphragm during transducer installation, calibration and pre- and post-test operations. Rain can also damage delicate diaphragms. After installation, it is common practice to cover each diaphragm with a sheet metal shield, using tape for easy shield installation and removal, except for testing and calibration. Similarly, for transducers using tubing, the tube opening should be shielded to avoid debris getting inside the tubing. "Hands Off" warning signs are also helpful. Pressure transducers used to measure external acoustic noise may be installed with their diaphragms flush mounted, or they may be externally located adjacent to the surface as long as (a) the acoustic wavelength λ_a sufficiently exceeds the diaphragm diameter d, say $\lambda_a > 8d$, as discussed in Section 3.2.3.5, and (b) the acoustic wavelength λ_a also sufficiently exceeds the distance D_d from the center of the diaphragm to the nearest point on the surface, say $\lambda_a > 8D_d$. If these higher frequency conditions cannot be achieved (e.g., by using a smaller transducer diameter), then the diaphragm must be flush mounted. At even shorter wavelengths, transducer directivity and pressure cancellation effects occur, as described in Section 3.2.3.5.

3.2.8 **Strain Gages**. There is a wide variety of strain gages available for aerospace applications. Gage(s) may be applied directly to structures to measure strain(s) at a single location, or in a Wheatstone bridge arrangement for measurement of internal loads or of transducer responses. Two categories of strain sensitive materials are available, metallic and piezoresistive (PR), as discussed in Section 3.2.1.2 [3.1 -3.5, 3.14- 3.21].

3.2.8.1 **Structural Applications**. Figures 3.60 and 3.61 show the great variety of metallic and PR gages available for direct installation on structures. In addition, each gage configuration is often available in a variety of sizes, some very small. Gages are usually bonded to or encapsulated by a plastic carrier, such as polyamide, epoxy, and/or fiberglass for a stronger, more convenient and precise installation. In many cases, strain gages must be installed in hard-to-reach locations. To accommodate this situation, a variety of tabs is provided for leadwire attachment. Certain gages cannot be installed on surfaces with sharp curvatures or contours without failure. In these cases, the gage manufacturer should be contacted regarding recommended substitutes.

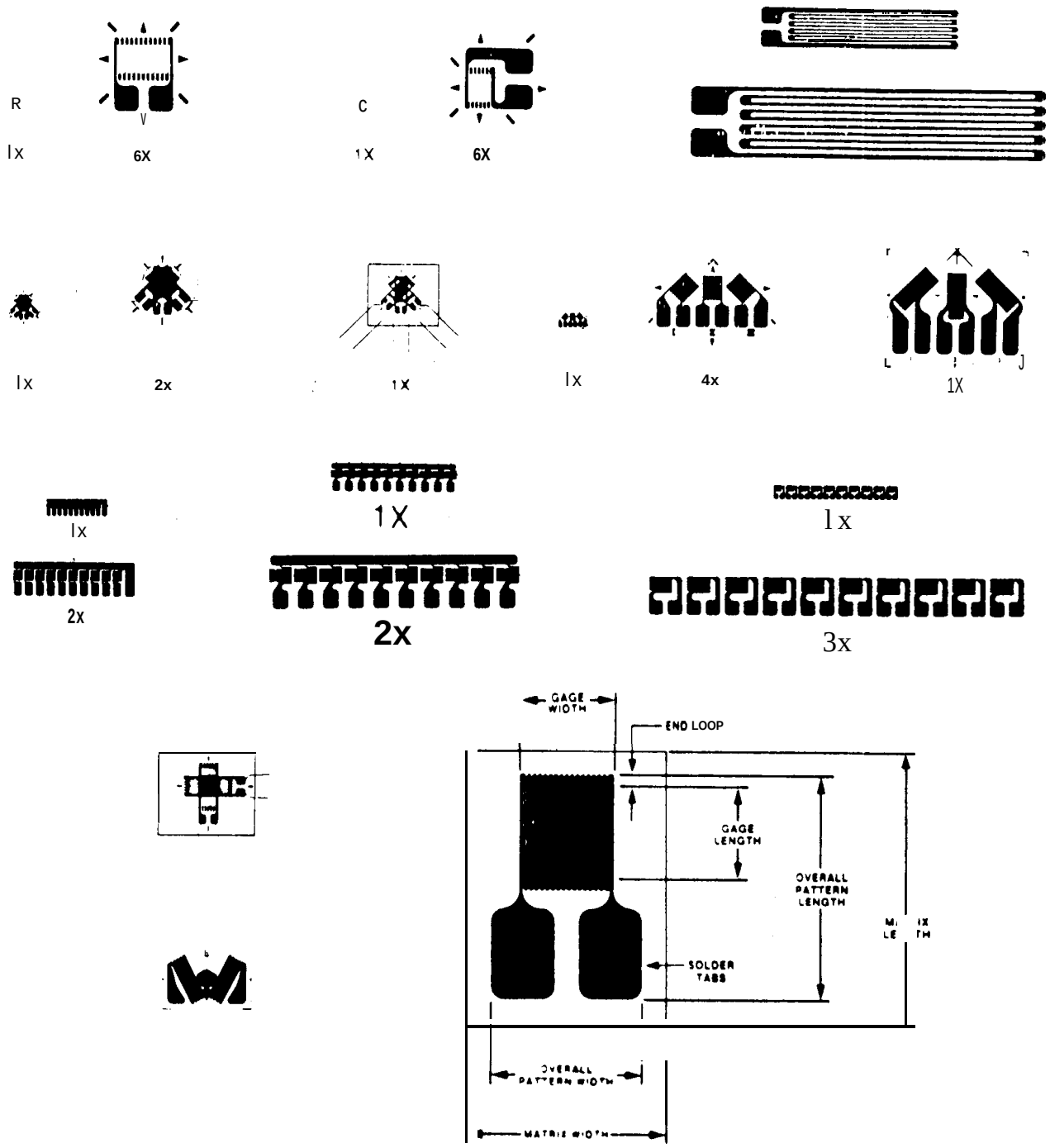

Note: "_X" means that the gage shown is __ times its actual size.

Figure 3.60. Various Metallic Foil Strain Gage Sizes Shapes and Configurations. First Row: Single-Element Gages; Second Row: Stacked and Single-Plane Three-Element 45-Degree Rosettes; Third Row: Strip Gages; Last Two Rows: Two-Element 90-Degree Rosette, Stress Gage; Nomenclature Shown on Enlarged Gage (Courtesy Measurements Grp).

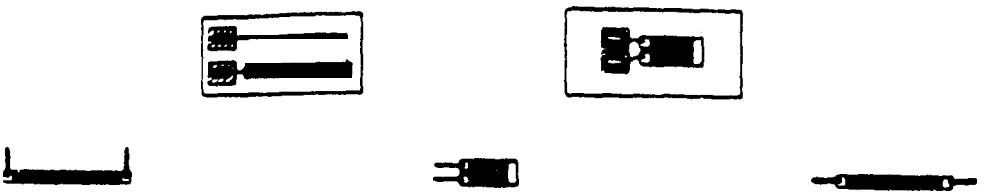

Figure 3.61. Typical Semiconductor or Piezoresistive Strain Gages (Courtesy Kulite).

Most but not all gages are intended to measure strain "at a point". Two different rosette configurations are shown in Figure 3.60, one with the three strain gages overlaid or stacked and the other with the three gages adjacent to each other in a single plane. The stacked configuration has the advantage of measuring all three strains at the same point, which is important in regions of high strain gradients (i.e., stress concentrations), as discussed in Section 3.2.5.1. However, some loss of strain transfer through the rosette thickness to the outer two gages will occur. On the other hand, the single-plane configuration has the advantage of superior strain transfer from the structure to all three gages, but the disadvantage of not measuring the strains at the same point. Thus the rosette should be selected on the basis of the amount of anticipate strain gradient. In many cases, the exact location of the maximum strain is unknown. In other cases, it is desired to measure the strain distribution in a region. In both cases, the strip gages of Figure 3.60 are available to provide this information with relative case of installation. In addition, crack detection and crack propagation gages, such as shown in Figure 3.62, are available in different sizes to monitor the progress of anticipated fatigue crack growth.

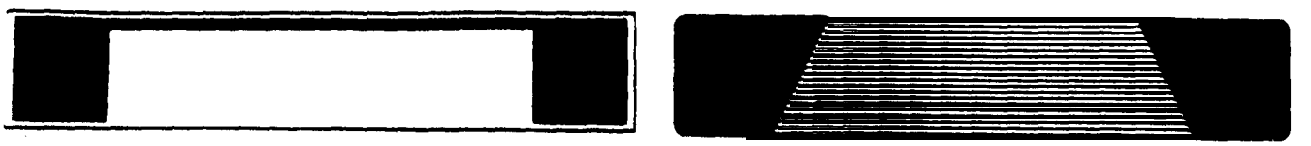

Figure 3.62. Typical Metallic Crack Detection or Crack Propagation Gages (Courtesy Measurements Grp).

3.2.8.2 Load Cell Applications. Combinations of strain gages maybe used with specially designed structural members to form load cells designed to measure any one of the three types of internal loads, direct (tension-compression), bending and torsion, as shown schematically in Figures 3.63-3.65, respectively [3.79]. These load cells may be fabricated specially for the specific application, or may be purchased commercially. In each case, the proper installation of four matched gages in the arrangement shown in these figures permits the desired load to be measured while simultaneously providing temperature compensation, as discussed in Section 3.2.4.1, and canceling any influence from the other two types of loading. In Figures 3,63-3.65, the gage numbers

correspond to the numbered arms of the Whetstone bridge shown in Figure 3,3. In Figure 3.64, note that the left-right symmetry permits cancellation of any bending output orthogonal to the loading direction shown. In Figure 3.65, note that the load cell is cylindrical to provide uniform torsional strain to the gages over their lengths. For a single structural member to be used for measuring all load components, i.e., axial, bending in both transverse orthogonal planes, and torsion, a cylindrical load cell is required to provide uniform torsional strain. Moreover, in all cases, the structural member must be carefully designed to avoid stress concentrations that would lead to erroneous outputs [3,80]. Finally, the wavelength of each dynamic load component must be appreciably longer than the load ceil length, say $\lambda_\ell \geq 8 L_\ell$, similar to that described in Section 3.2.3.2 for individual strain gages, to ensure a uniform distribution of loads over the structural member, Satisfying this wavelength condition provides the maximum frquency limit for the load cell and a. minimum of additional compliance to the structure.

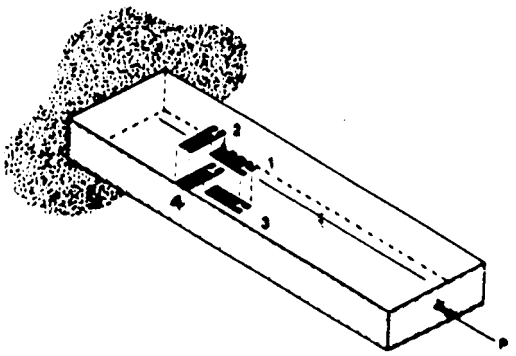

Figure 3.63. Arrangement of Four Matched Strain Gages for Measuring Direct (Tension-Compression) Internal Loads While Canceling Measurements of Bending and Insensitive to Torsion Loads [3.79].

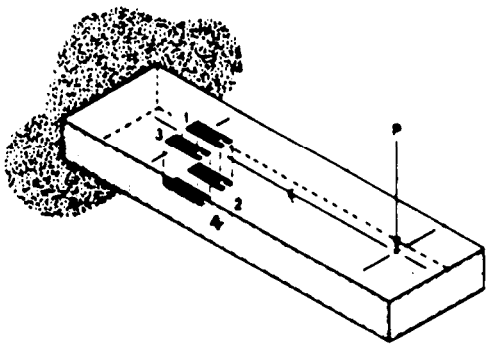

Figure 3.64. Arrangements of Four Matched Strain Gages for Measuring Bending Internal Loads in One Plane While Canceling Measurements of Bending in the Other Plane, and Insensitive to Direct and Torsion Loads [3.79],

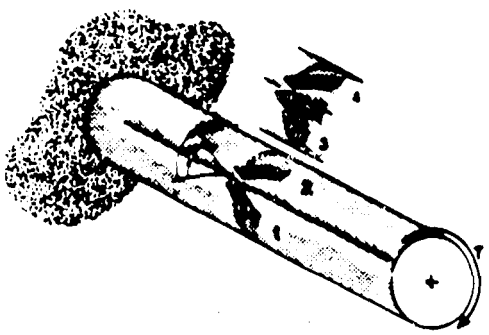

Figure 3.65. Arrangements of Four Matched Strain Gages for Measuring Torsion Internal Loads While Canceling Measurements of Direct and Bending Loads [3.79].

3.2.8.3 Transducer Applications. Figures 3.66 and 3.67 show a few of the metallic and PR gages available for installation in pressure transducers and PR accelerometers, described in Sections 3.2.7.1, 3.2.7,2 and 3.2.6.1.2, respectively. Much smaller sizes are available than those shown in these figures. These transducers and their gages are designed for repeated use. Transducers with unbended (i.e., free) wire strain gages are seldom used, due mainly to transducer insensitivity or limited useful frequency range.

3.2.8.4 Strain Gage Installation. A metallic or PR gage can be satisfactorily attached to almost any structural material if the structural surface is properly prepared at the gage location, the recommended adhesive is properly applied, and the gage is carefully installed, all in strict accordance

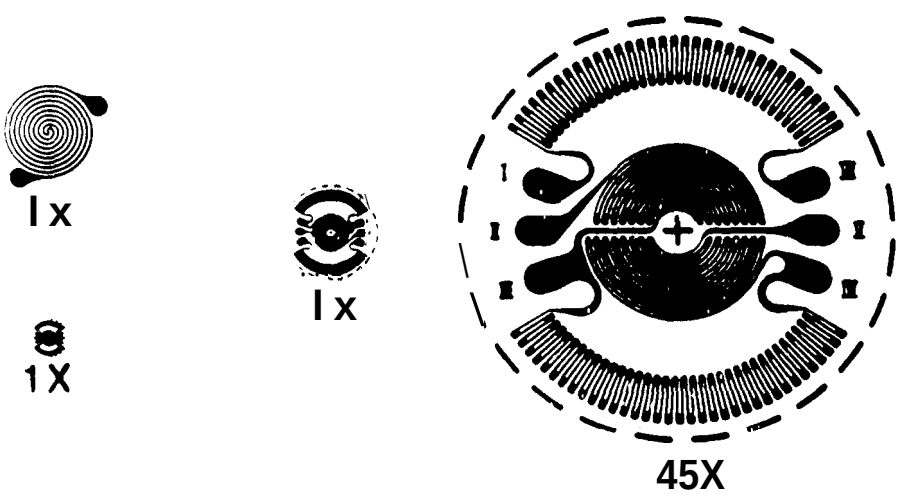

Figure 3.66. Metallic Strain Gage Patterns for Diaphragm Pressure Gages (Courtesy Measurement Grp).

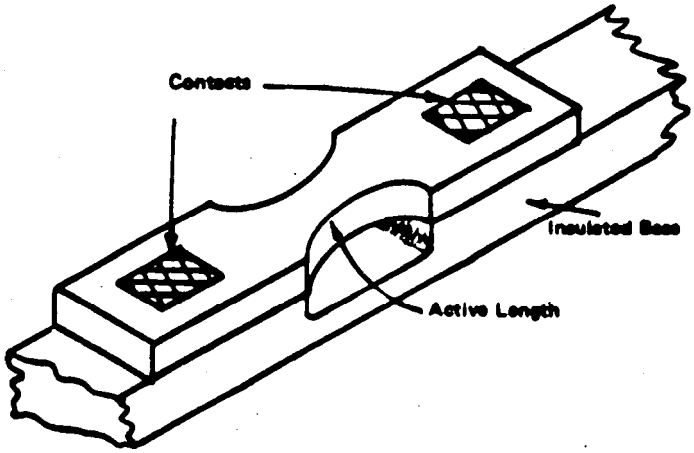

Figure 3.67. Miniature Semiconductor or Piezoresistive Strain Gages for Installation in Accelerometers and Pressure Transducers (Courtesy Micro Gage and Endevco).

with the manufacturer's instructions [3. 15- 3.21]. To quote [3.18]: "The singularly unimpressive feat of bonding a strain gage to a specimen is perhaps one of the most critical steps in the entire process of measuring strain with a bonded resistance strain gage. The improper use of an adhesive costing a few dollars per test can seriously degrade the validity of an experimental stress analysis which may cost thousands of dollars."

The surface surrounding the gage location must first be prepared to receive the adhesive. The surface must be chemically clean, have roughness compatible with the adhesive, have visible lines for properly locating and orienting the gage, and have the appropriate pH value to allow proper adhesive curing, in order for the structure to transfer the correct strain uniformly to the gage. In most cases, there are five basic steps in surface preparation, performed in the following order: (1) solvent decreasing, (2) surface abrading, (3) gage line layout, (4) surface conditioning, and (5) surface neutralizing. All forms of contamination must be avoided, no matter what circumstances are encountered.

A variety of adhesives are available for attaching the strain gage to the prepared surface, including cyanoacrylate, epoxy and ceramic cements, and cellulose nitrate. The cements are generally moisture-resistant and strong, especially when applied in a thin layer. Most cements must be cured, with the curing time prior to use highly dependent on the cement composition, thickness and temperature. Each cement has its useful temperature and humidity ranges. The electrical resistance between the gage and the structure should always be measured to verify the acceptability of the isolation at the gage installation.

After the strain gage is installed, using the manufacturer's procedure for aligning the gage at the intended location, consideration should be given to provide moisture protection, as discussed in Section 3.2.4.4. It is usually prudent to take enough photographs to verify the location and orientation of the gages. After usage, it is common practice to leave the strain gages on the structure rather than remove them. Sometimes it is impossible to install a strain gage in the desired location. If this circumstance occurs, consideration should be given to performing a finite element analysis of a large enough region of the structure surrounding the desired location to enable an analytical comparison of strain at the desired location with that at a nearby location where a strain gage can reasonably be installed. This should permit scaling of the measured data for structural wavelengths λ_s which exceed the relative distance M between the two locations, say~28 Δd.

3.2.9 Force Transducers. Two main types of force transducers are available for static and/or dynamic data acquisition in aerospace applications: (1) piezoelectric, and (2) strain gage [3.67]. Force transducers do not use SDF design features but rather are frequency limited by transducer masses and sensing element stiffnesses while strain gage transducers may be further restricted by wavelength considerations, as discussed in Sections 3.2.3.2 and 3.2.5.3. It is desirable to select a force transducer that provides a negligible mass to the structure.

Piezoelectric force transducers are charge devices that do not provide a constant DC response, as described in Section 3.2.1,1. They have a wide range of sensitivities and configurations designed for specific applications, The minimum frequency limit may extend down to about 1 Hz. The output signal is conditioned by electronics that are separate from or integral with the transducer, as discussed for PE accelerometers in Section 3.2.6.1.1. PE force transducers use ceramic(s) or crystal(s) as the sensing element(s), which is sandwiched between the two mounting surface masses, as shown in Figure 3.68 [3.6]. The sensing element is preloaded in compression. When variable pressure is applied to the element under dynamic excitation, a charge is generated on its surface that is proportional to the applied instantaneous force. This design is susceptible to base strain and thermal transients. If the base is stressed by the static or dynamic deformation of the structure to which it is attached, an extraneous signal can be produced, as described in Section 3.2.4.8. Thermal transients can have the same effect, as discussed in Sections 3.2.4.1 and 3.2,4.2.

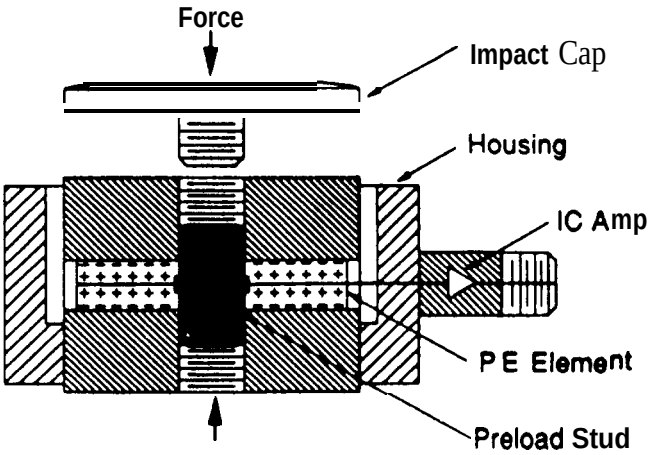

Figure 3.68. Cross-Section of a Piezoelectric Force Transducer with Integral Electronic Amplifier (Courtesy PCB) [3.11].

PE force transducers with multiple elements are available to measure triaxial forces, as shown in Figure 3.69, with one set of elements in compression and two sets in shear [3.81]. Other PE transducers are available for measuring both force and moment [3.82]. The outputs from matched pairs of single PE force transducers may also be wired up to measure dynamic torques or moments. The use of a combination of strain gages for measuring forces, torques and other internal loads is described in Section 3.2.8.2. It is usually prudent to take enough photographs to verify the location and orientation of the transducers.

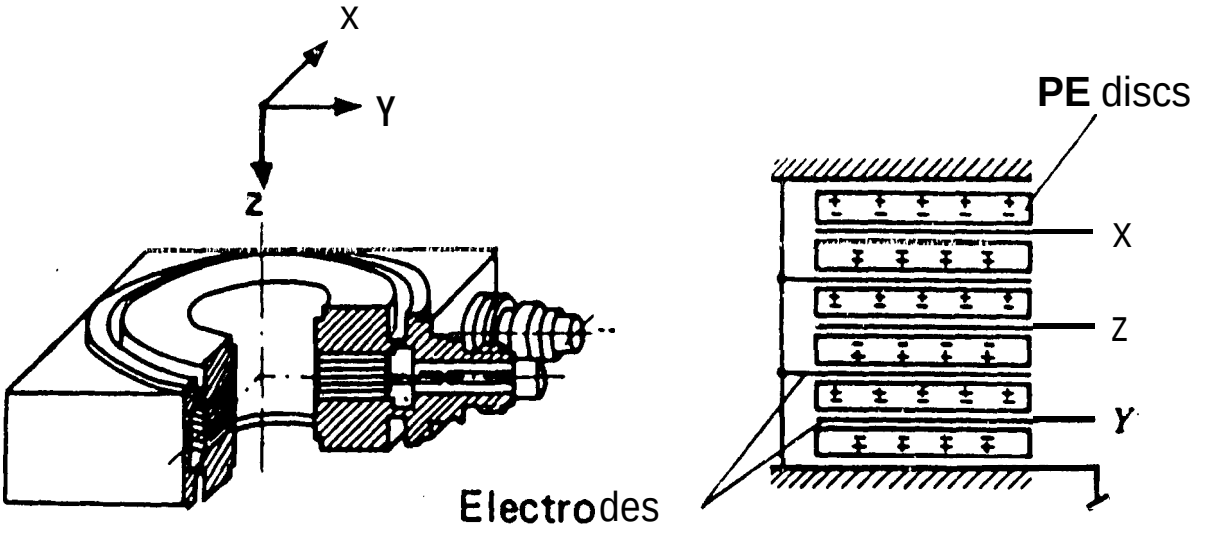

Figure 3.69, Cut-Away View and Sensing Element Connections of a Triaxial Piezoelectric Force Transducer with a Center Mounting Hole (Courtesy Kistler) [3.80].

3.3 Signal Conditioners. All transducers must have their output signals conditioned to accommodate the requirements of cabling, recording and transmission instruments. Signal conditioners include amplifiers, filters, differentiators and integrators, power supplies, and cabling [3.1 -3.3, 3.34]. More than one of the signal conditioning functions can be incorporated in one instrument. Digital as well as analog signal conditioning is used for dynamic data acquisition [3.83]. In all cases, the locations of signal conditioning instruments and cabling must be selected to ensure that the various natural and induced environments do not exceed the specified capabilities of the instruments. It is important that instrumentation power be turned on during initial vehicle or laboratory radio frequenc y (RF) check-out or operation to assure that no RF interference occurs to the data acquisition system later,

3.3,1 Strain Gage Conditioners. Strain gages are not self-generating transducers and therefore require a source of power, as discussed in Section 3.2.1.2. A typical strain gage signal conditioner diagram is shown in Figure 3.70. The following discussion is applicable to all types of strain gage conditioners, including piezoresistive conditioning.

Two types of power supplies are used: constant voltage and constant current. Constant voltage supplies are used when the cabling between the transducer and the signal conditioner is relatively short, and the danger of background noise pickup, as well as resistance and temperature variations, are negligible. Constant current supplies are used when these conditions can create errors. In addition, constant current supplies are more linear than constant voltage supplies when the percentage of Whetstone bridge resistance variation is relatively high. If the voltage is monitored at a remote bridge, then cable lengths greater than 25 ft may be used with constant voltage supplies.

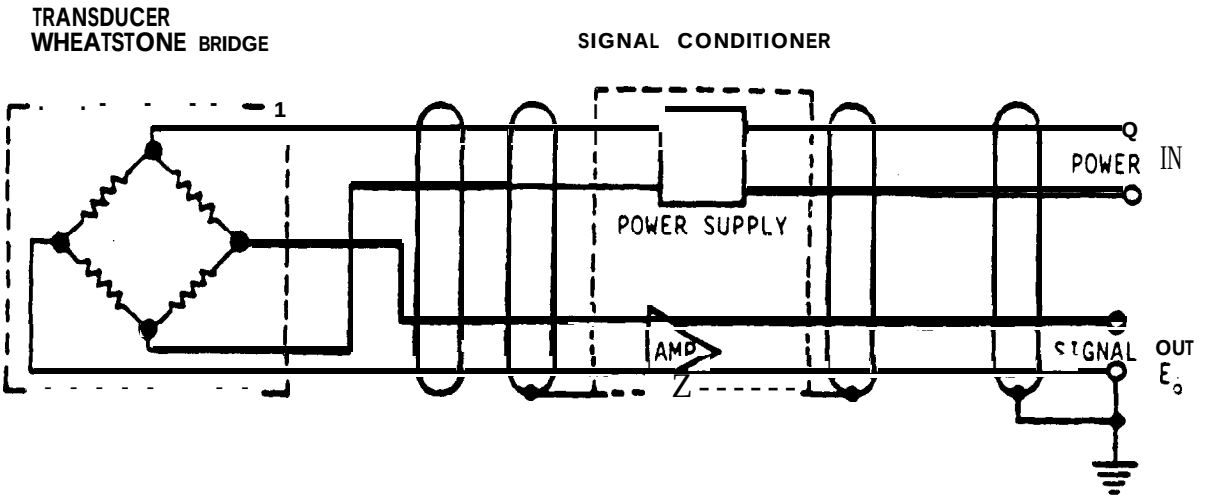

Figure 3.70. **Circuit Diagram of a Typical Strain Gage Signal Conditioner.**

Power supplies for strain gage conditioning must have the following characteristics:

(a) They must be stable with very little ripple to eliminate errors in the output signal.
(b) The primary power source must be well regulated over the expected variations in transducer loads, have good DC isolation, have low capacitive coupling to AC power, and have ripple and background noise filtered out at the noise source.
(c) The circuit must be stable overtime and expected temperature variations.
(d) For constant current systems, transducers must be compensated and **calibrated** over their total operational ranges.
(e) For constant voltage systems, external voltage sensing leads connected directly to the transducer should be provided when long cables are required, so that voltage can be maintained at a constant value when the wire temperature and the excitation voltage vary.
(f) If a single primary power supply is used for several signal conditioners, the individual strain gages must be isolated to prevent noise pickup in **all** channels due to a **fault** in one of them. When an AC power **source** is used, shielded isolation transformers should be incorporated in the power supply to avoid ground loop noise problems.
(g) They should not use switching regulators.

Strain gages circuits may be excited with an AC carrier. AC supplies must be just as well regulated as DC supplies, and the carrier frequency should be at least five, and preferably ten, times the maximum frequency limit of Section 3.2.3.2. Features shown in **Figure** *3.3 are* considered essential for a strain gage conditioner, including the ability to (a) zero balance the strain gage bridge, **(b)** adjust the excitation voltage, (c) monitor the excitation and data signals, and (d) calibrate the transducer remotely, preferably using plus and minus multi-point calibration.

An amplifier is required in the strain gage conditioner to adjust the output voltage to meet the magnitude and impedance requirements of following instruments of the system, Calibrated gain controls should be provided to permit the adjustment of gain in known, calibrated increments. The input impedance of the amplifier should be significantly higher than the source impedance of the transducer to prevent loading errors in the transducer output. Where both sides of the signal must be isolated, differential amplifiers should be used. When single-ended amplifiers are used, the system should be grounded only at the last point in the system to prevent ground loops.

3.3.2 Amplifiers. Amplifiers are used to increase the magnitude of the signal. In addition, they can (a) transform the signal from one form to another (e.g., a charge amplifier converts a charge output from a piezoelectric transducer to a voltage output), (b) provide a calibrated gain change to maintain a calibration when a different gain is required, (c) provide a zero shift or level offset, and (d) provide an impedance change to match the output impedance of one instrument to the input impedance of another, which can prevent loading of electrical circuits and consequent signal degradation. When the signal exceeds the dynamic range of the amplifier, signal limiting or clipping occurs, resulting in distortion. Low magnitude signals may be corrupted by the background noise floor, and must be amplified to take full advantage of the dynamic range.

Although amplifiers have inherent limitations in their frequency response, they maybe limited further by filters, as discussed in Section 3.3.3. If data are desired out to the filter cut-off frequency (usually defined as that frequency where the filter gain is 3 dB below its nominal gain), the effect on data magnitude and phase must be understood. Depending on the type of filter, the roll-off can be down by as much as 0.5 dB atone-half the filter cut-off frequency, causing significant magnitude errors, Filter phase distortion can produce errors in measured time histories and subsequent shock response spectra computations [3.43], and make interchannel phase matching difficult.

The slew rate of an amplifier is its rate of voltage change, Slew limiting will occur when the maximum allowable rate is exceeded, causing signal distortion errors including DC offset or zero shift. The amplifier may be operating within its frequency range, but may be incapable of delivering sufficient current to drive the cable and instrument at its output. When this occurs, the signal is distorted, such as shown in Figure 3.71 for a sine wave. If the signal output voltage is reduced sufficiently for the amplifier to operate below its slew limit, then the distortion disappears. To avoid slew limiting, the maximum signal frequency should not exceed [3.5]

$$f_{max} = \frac{I_s}{2\pi V_s C} \tag{3.13}$$

where I_s and V_s are the maximum output current and rated output voltage, respectively, of the amplifier, as normally specified for a sine wave, and C is the total capacitance of the output cable and the following instrument, i.e., $C = C_c + C_I$. If the amplifier has an insufficient current output

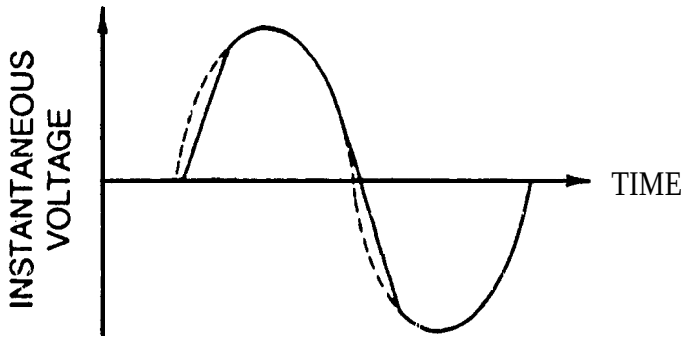

Figure 3.71. Typical Slew Rate Limiting of an Amplifier (Courtesy Endevco).

to avoid slew limiting over the desired frequency range, a line-driver amplifier with high current output may be used.

When some amplifiers are severely overloaded at their input, they can be driven into saturation and may take as long as several seconds to recover. They can also exhibit a low frequenc y decaying sinusoid in the output that is directly attributable to the saturation. In the case of a charge amplifier, the charge converter can be saturated by an unfiltered resonant response of the transducer. The saturation will not be seen at the amplifier output because of filtering, but a decaying low frequency can be seen when the charge converter recovers. This can cause a false low frequency peak in the spectrum computed from the signal [3.43], Some other overloaded amplifiers only clip the signaL Unfortunately, subsequent filtering removes all evidence of this distortion.

3.3.2.1 Voltage Amplifiers. Voltage amplifiers, such as shown in Figure 3.36, are used when the objective is to change the gain and/or source impedance of the signal [3.34]. They are usually provided with a calibrated gain control to adjust the gain to a predetermined value. The signal calibration is changed in logical, known steps, which eliminates the need to recalibrate the system when a gain change is required. If the amplifier has a DC response, a control can be provided which permits the adjustment of a zero voltage signal to its true null position, or to bias the signal to a different voltage (e.g., biasing for input to a telemetry system). DC amplifiers may also display zero drift, which can be suppressed by stable electronics and close monitoring.

3.3.2.2 Charge Amplifiers. A charge amplifier differs from a voltage amplifier by the presence of a charge converter input stage, and is used to condition the signal from charge generating elements, such as piezoelectric transducers, as shown in Figure 3.37 [3.34]. This is accomplished with a feedback capacitor between the output of an operational amplifier and its input. The charge converter generates a feedback voltage that opposes the charge from the transducer and maintains the input at zero charge. The voltage at the converter output is proportional to the instantaneous charge generated by the transducer, and is then amplified by a voltage ampli.tier section. Since virtually no current flows in the cable between the transducer and charge converter, longer cables can be used.

However, care must be taken to use cabling that minimizes any triboelectric voltages that can be generated in the cable between high impedance instruments, as explained in Section 3.3.5.1, If susceptibility to radiated noise is anticipated, remote charge amplifiers (preferably differential) should be used. Some charge amplifiers reverse signal polarity when the gain range is changed

3.3.2,3 Differential Amplifiers. Conventional amplifiers with two conductor signal leads can produce parasitic voltages that appear on both the high and ground (common) signal leads. Differential amplifiers reject common mode instrumentation background noise. Figure 3.72 represents a simplified amplifier where the shield can couple unwanted signals into the amplifier through stray capacitances Cl, C_2, and C_3. If the shield floats, C_3 can be a source of noise. If the shield is grounded, then the noise is transmitted through C_1 and C_2. A differential amplifier, such as shown in Figure 3.73, can be used to reject common mode noise. The shield is grounded at the source and must enter the amplifier case, but is isolated from it. The differential inputs are amplified, but common mode noise EC is rejected.

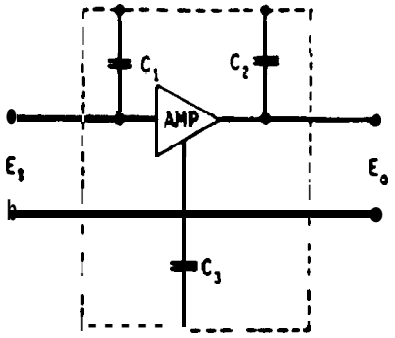

Figure 3.72. Shield Coupling of an Amplifier with Floating Shield.

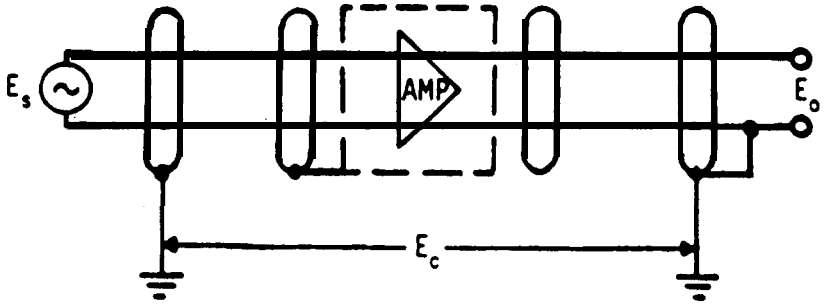

Figure 3.73. Circuit Diagram of a Guarded Differential Amplifier with Ground Locations at Each End of the Circuit.

The circuit diagram for a strain gage bridge differential amplifier is illustrated in Figure 3.74. It is very similar to that of a standard *differential* amplifier, except there are two excitation leads in addition to two signal leads. Charge amplifiers may also be employed in the differential mode, as

shown in Figure 3,7S, The low side of the signal lead should be grounded at the input to the final readout point in all differential instruments, The transducer and amplifier inputs are both grounded. Common mode noise EC between the two ground points is rejected. The shield should be grounded at the transducer as well as the last point of the data acquisition system. The high and low sides of the signal line should be isolated from the shield, and the low side grounded at the last point with the shield,

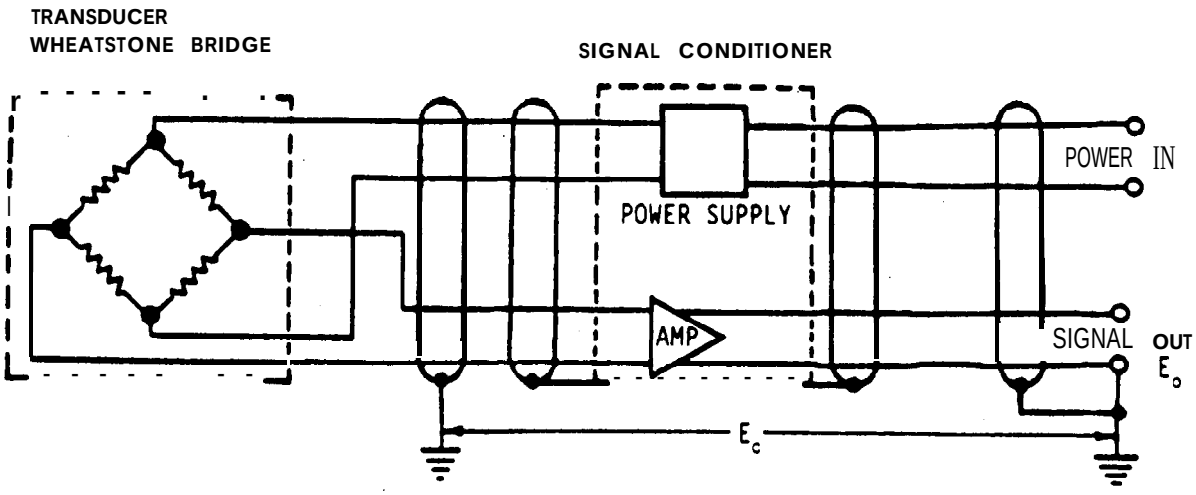

Figure 3.74. Circuit Diagram of a Differential Strain Gage Amplifier with Ground Locations at Each End of the Circuit.

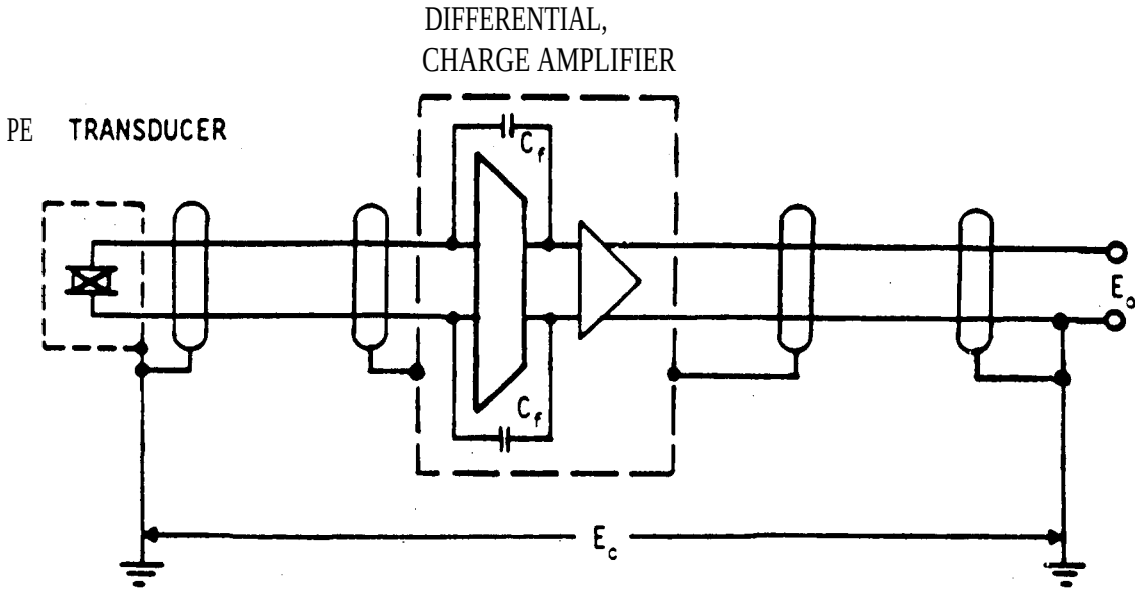

Figure 3.75. Circuit Diagram of a Differential Charge Amplifier with Ground Locations at Each End of the Circuit.

3.3,2.4 Preamplifiers. Preamplifiers are used to convert weak signals from high source impedance transducers into usable voltages with a low source impedance. They can take the form of a voltage, charge, or line-driver preamplifier. A preamplifier can be integral with the transducer, or external and connected to the transducer with a short cable. Integral preamplifiers are usually size limited with limited linedriver capability, making them susceptible to distortion from slew limiting as described in Section 3.3.2. Because of the low output impedance, preamplifiers are less susceptible to the coupling of undesirable external background noise into the system through cables between transducers and signal conditioning amplifiers. Noise coupling is a function of impedance and cable length. Therefore, a line-driver amplifier may be used as the output of the preamplifier to minimize noise. Line-driver amplifiers are usually limited in their frequency response and dynamic range, compared to higher quality remote charge amplifiers. All parameters must be examined to determine the best compromise.

3,3.3-. The objective of filtering is to limit the bandwidth of the signal. The purpose of limiting the bandwidth is to reduce the effects of background noise, and/or undesirable system characteristics (e.g., transducer resonances, aliasing) outside the desired frequency range [3,34]. As shown in Figure 3.76, highpass filters attenuate the low frequencies and pass the highs. Conversely, lowpass filters attenuate the high frequencies and pass the lows. Bandpass falters are a combination of lowpass and highpass, thereby passing the frequencies between the low and high cutoff frequencies. Band rejection filters eliminate a narrow band of frequencies within the band of

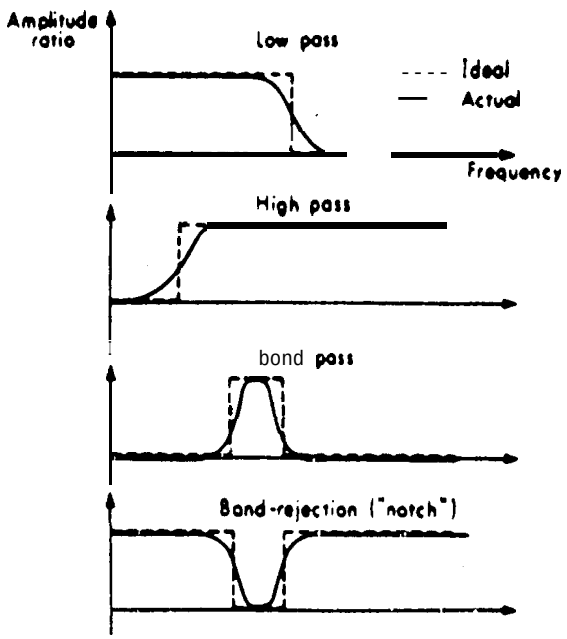

Figure 3.76. Electrical Filter Types [3.1].

interest. The type of filter and the steepness of the filter cut-off slope area function of the number and location of the poles and zeros of the filter circuit.

3.3.3.1 **Analog Filters**. Linear phase filters exhibit a constant time delay over the passband, thereby preserving phase relationships between all frequencies within the band. This type of filter does not create signal magnitude distortion, as occurs in nonlinear phase filters, nor does it exhibit excessive overshoot from a step function input. The frequency response shows minimum ripple, but the filter roll-off starts at about half the cut-off frequency. Filter roll-off beyond cut-off is not as steep as for other filters, which limits its ability to prevent data aliasing in a digital analyzer (see Section 3.7.2). ButterWorth, or maximally flat, filters are probably the most commonly used. They have a flat passband response with some ripple and overshoot when excited by a step function input. They are reasonably flat to about 80% of their cut-off frequency, but exhibit phase distortion in the region of cut-off. Elliptic, called Cauer or "brick wall", filters have the sharpest rejection (on the order of 100 dB/octave), but exhibit high overshoot from a step function input and substantial phase distortion (as high as 120 deg at cut-off). They are primarily used prior to digital analysis as anti-aliasing filters because of their steep slope beyond cut-off. The sampling rate can be as low as 2.5 times the cut-off frequency (whereas the Nyquist frequency is two times the cut-off frequency). When analog filters are selected, it is important to remember that the closer that the selected filter approximates the ideal amplitude response, the further the phase response will be from the ideal, and vice versa [3.34]. See [3.2, 3.5, 3.34, 3.43, 3.84] for a more detailed discussion of the different types of analog filters available.

3.3.3.2 **Digital Filters**. Digital filters are used in digital analysis systems where the data have already been sampled into the digital domain [3.83, 3,85]. Good control of filter parameters, such as ripple, roll-off, and phase coherence, can be achieved, and the characteristics can be easily modified to suit changes in conditions. Digital falters are most commonly used prior to data decimation (Section 5.2.4.3) and zoom transform (Section 5.4.3.8) operations. See [3.85] for details of digital filter design.

3.3.3.3 **Pre-Filters**. As discussed in Section 3.2, all nearly-undamped piezoresistive and piezoelectric transducers have a maximum frequency limit of only about 24)% of the resonance frequency of their sensing element. Typically, the damping of the sensing element for these types of transducers is less than 0.5%, producing a response at resonance that exceeds the flat response at lower frequencies by a factor in excess of 100. Hence, if the dynamic environment being measured includes significant excitation at the resonance frequency of the transducer, as sometimes occurs in pyroshock measurements (see Appendix A or [3.40, 3.41]), an intense high frequency signal output will be generated that may saturate the first amplifier or charge converter stage in the signal conditioner, or force a very low input gain setting that will cause the lower frequency portion of the signal to be obscured by the instrumentation background noise. Even when the sensing element resonance is not excited, the same problem can occur if the measured dynamic environment in-

eludes intense high frequency components above the frequency range of primary interest [3.86]. Thus the pre-filter allows gain optimization at lower frequencies where the dynamic excitation may be less. The problem is compounded by the fact that a saturated amplifier commonly outputs a low frequency signal that may appear reasonable and, hence, obscure evidence of saturation. Another phenomenon that has been observed is a measurable difference in the positive- and negative-going amplifier slew rates at the transducer resonance frequency. Even in the absence of amplifier saturation, the different slew rates can create a signal envelope that appears to analysis instruments as a low frequency component. See [3.43, 3.86] for more detailed discussions of these effects.

For those shock and vibration measurements with nearly-undamped piezoresistive and piezoelectric accelerometers, where it is anticipated that the measurement will include intense high frequency excitation above the frequency range of primary interest, it is recommended that a lowpass pre-filter be inserted prior to the input to the signal conditioner. This filter must be passive. For piezoresistive transducers that produce a voltage output from a low impedance source, such passive pm-filters can be introduced with little trouble. For piezoelectric transducers, which have charge-generating sensing elements, the pre-filter must be inserted in series in the cable between the transducer and the charge amplifier, e.g., in a small T-circuit box that may also be used for insert voltage calibrations. (Of course, this is impossible if the transducer has an integrated charge converter). For example, a 6 dB/octave RC pre-filter can be achieved for a particular cutoff frequency by utilizing the input capacitance (C_a) of the charge amplifier and the resistor (R_c) in the cable. Because the distributed capacitance of the cable between the transducer and the charge amplifier forms part of the filter, there maybe some difficulties in matching the phase response between channels when cable lengths are not equal. Hence, the falter components must be chosen for a particular application. Commercial pm-filters are usually one or two poles, with a cut-off rate of 6 or 12 dB/octave, respectively. This is adequate in many cases to reduce the high frequency portion of the signal to values that can be handled by amplifier stages without saturation or slew rate errors. Nevertheless, data should be examined for evidence of unexpected low frequencies indicative of saturation or slew rate problems. Also, such pre-filters are not always effective in suppressing the intense high frequency components in some pyroshock signals (see Appendix A).

3.3.3.4 Mechanical Filters. A mechanical filter is a small structural resilient element that may be attached between an accelerometer and the structure, or may be built into the accelerometer assembly, for the purpose of isolating the accelerometer from high frequency loading that might cause the accelerometer to respond at its resonance(s), as discussed in Section 3.2.6.1 [3.6, 3.7]. Since mechanical filters use the SDF design feature of Section 3.2.2 in the intended measurement direction, magnitude and phase distortion may occur unless the filter responds linearly and has a damping ratio of $\zeta \approx 0.7$. Thus, filter performance may be degraded by temperature variations, as described in Section 3.2.4.1 for damped accelerometers. Under high magnitude near-field pyroshock, significant nonlinear behavior and poor falter transient response characteristics may invalidate the measurement, as discussed in Appendix A.

3.3.4 **Power Supplies**. Power supplies for general instrumentation purposes should have the following features:

(a) They should be well regulated to supply constant voltage or current, depending on the circuit.
(b) They should be shielded to prevent background noise pickup in nearby circuits.
(c) hey should be well regulated to minimize power line contamination of the data.
(d) When a common power source supplies several channels, individual power supplies should be isolated to prevent noise pickup in all channels by a fault in one of them.
(e) Reserve power should be available in all supplies to prevent overloading when the power load is at its peak.

Special considerations related to power supply applications for strain gage conditioning have been discussed in Section 3.3.1.

3.3.5 **Cabling**. Cables are required for transmitting electrical signals from the transducer to the remainder of the system [3.87]. Each situation presents a unique set of problems. Therefore, cable types must be chosen to suit the application. In many cases, there is more than one solution to a cabling problem, and the best compromise must be selected for the operating environment and parameters. Cable selection should depend upon (a) cable length, (b) the impedance of the transducer, cable and electronics, (c) magnetic and capacitive background noise coupling, (d) the physical environment, and (e) the type of transducer and signal conditioner. Cable jackets must be chosen to preclude deterioration due to temperature, ultraviolet radiation and, where applicable, space flight-induced high energy particles and atomic oxygen. The effects of cable capacitance on slew limiting are described in Section 3.3.2.

Care should be taken that cables and connectors are not damaged during installation on instruments, as follows:

(a) Cables should be aligned so that the pins do not bend when installed. Most multi-pin connectors are keyed to help pin and connector alignment.
(b) The connector nut must be turned onto the mating connector without twisting the cable, and the transducer should not be turned while the connector nut is held stationary.
(c) The connector nut should not be over-tightened (e.g., finger tighten only).
(d) Care should be taken to assure that the connectors are not contaminated with dirt, water or conductive material which might decrease the shunt resistance of the cable.
(e) The cable bend radius should not be less than the manufacturer's recommendation.
(f) For applications where moisture can be a problem, drip loops should be used to prevent moisture from entering a connector.
(g) Cables must not affect the structure or the transducer by mechanically loading them.

(h) Cables should be light, flexible, not provide tension which can affect their motion, nor exert force on the transducer.

(i) Cables should be tied down within 3 in. of their termination to prevent cable whip and subsequent damage to the conductors.

(j) Prior to use, low noise cables used with piezoelectric transducers should be tested in accordance with [3.88],

See Appendix A for special considerations related to pyroshock measurements.

The center punch tool suggested in Section 3.2.6.3 can be used to check the cable connector at the transducer under consistent conditions, as well as the adequacy of any adhesive used for attaching the transducer to the structure.

During system checkout, all cables should be "wiggled" to the limits of their anticipated displacement to determine if excessive background or intermittent noise is produced by the cables or their connectors. Cables or connectors exhibiting excessive noise must be replaced or secured (i.e., better tied down). In addition, every effort should be made to suppress triboelectric noise, as discussed in the next section.

3,3.5.1 Triboelectric Noise. Triboelectric noise can be generated when a coaxial cable, used to connect a high impedance piezoelectric transducer to a charge amplifier, is mechanically distorted by flexing, squeezing, bending, and/or dynamic loading, so as to cause separation of the shield from the center conductor insulation, as illustrated in Figure 3.77 [3.4, 3.5]. Triboelectric noise may be minimized by the use of low noise cable that has a conductive coating between the shield and inner insulator. Electrostatic charges then have a leakage path to the shield and eventually to ground. While this works well, care must be taken when the cables are terminated with a connector. No conductive coating can be permitted to come in contact with the center conductor when the insulator is stripped off. Appropriate cleaning agents should be used to eliminate any loose conductive coating that might create a leakage path to the center conductor, However, it is required that the cleaning agent not become a vehicle to transport the conductive coating to the center con-

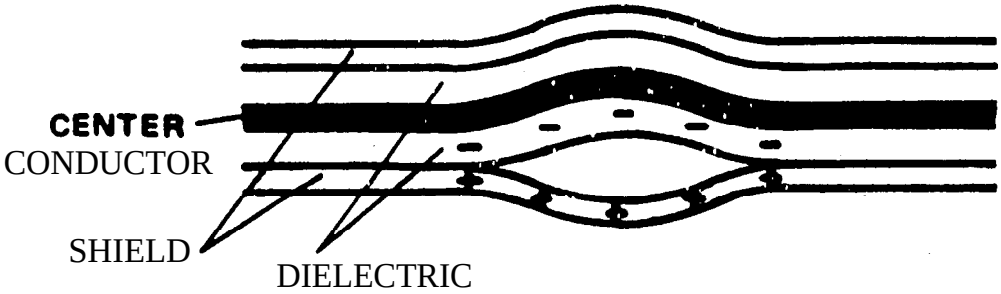

Figure 3.77. Triboelectric Noise Generation in a Coaxial Cable [3.4, 3.5].

ductor. Some users buy raw cables and connectors, and make their own cables to reduce costs. Because of the variability of assembly skill level, this practice often contributes to cable failures and malfunctions.

3.3.5.2- Gage and Piezoresistive Transducer Cables. Strain gages and piezoresistive transducers use multi-conductor cables because they not only carry the signal, but also carry the source of power. A minimum of four conductors p] us a shield, and up to as many as ten conductors, are required. The additional conductors maybe required for monitoring transducer excitation voltage, inserting shunt resistors for calibration, and eliminating zero shift. In addition to the overall shield, each pair may be individually shielded. The source impedance of strain gage circuits is much less than that for piezoelectric transducers, but there is still a danger of noise pickup, especially in long cables and high electromagnetic environments. The conductors should be shielded twisted pairs to minimize electromagnetic pickup.

3.3.5.3 Grounding. Grounding is the establishment of a path of electrical conduction between a circuit and a designated reference point, which is usually at zero potential, to which all system voltages are referenced, This reference point is dependent upon the system and could be the earth, a vehicle or test structure, an equipment case, or a bus structure defined as "ground". In an ideal case, the "ground" would be the zero potential reference for all signals and power. Frequently in practice, separate circuit paths to ground are provided for power returns, digital signals, and analog signals to minimize electromagnetic interference, which is seen in systems as background noise. In the case of low level analog signals from transducers, it is important to establish a single point ground except for differential instruments [3. 1, 3.3, 3,5, 3.89, 3.90]. Because a remotely grounded transducer may beat a different potential than the last instrument, the resulting "ground loop" could introduce background noise into the data. For acquiring dynamic data using telemetry transmission (e.g., from an aerospace vehicle in flight to a ground station), such as shown in Figure 2.2a, the last instrument is the telemetry antenna. On the ground, the last instrument is the tape recorder. For a hardwire system, such as shown in Figure 2.2b, the last instrument is the tape recorder or, in some cases, the readout instrument. For a data analysis system, such as shown in Figure 2.2c, the last instrument is usually the computer or the plotter. In measurement systems, the grounds should terminate at the input to the last instrument and should be carried through all intervening instruments to the ground terminating point. A unique electro-optic signal conditioner has been developed for piezoelectric transducers when single point grounding cannot be achieved [3.91].

When dynamic measurements are made during system RF operations, one or more cables may act as tuned antennae. This situation maybe avoided by changing the length(s) of the cable(s), or by using multi-point grounds. However, the utilization of multi-point grounds could cause ground" loops, as discussed previously. In locations where RF interference is of concern, flat straps or flat braid should be used for grounding, which reduces the RF impedance of the ground path.

3.3.5.4 **Shields**. Shielding is the process by which radiated electromagnetic energy can be confined within a specific volume, or by which incident electromagnetic radiation can be prevented from penetrating a specific region. Shielding maybe implemented in the form of partitions within enclosures, complete enclosures, cable connectors, and cable treatment. There are two basic types of shields: (a) electrostatic shields, and (b) magnetic shields [3.1, 3.3, 3.5, 3.89, 3.90].

Electrostatic shields are usually the easiest to implement and primarily involve the imposition of an electrically conductive surface, at ground potential, between the region of concern and the electrostatic field sources. Effectiveness is dependent upon high reflective loss and additional attenuation due to absorption of the wave within the shielding material. The electrostatic shielding of transducer cables typically consists of conductive braid and/or foil surrounding the center conductors, The cable shield is usually grounded at the output end. In severe electric field environments, two concentric and isolated shields should be used.

Magnetic shields short circuit the magnetic flux lines and oppose time-varying magnetic fields with eddy current fields. They are made from high permeability materials, are as thick as possible, have a minimum of joints and holes, and the joints are further protected with magnetically-shielded gaskets. Good magnetic shields are also good electrostatic shields, but the contrary is not true. Magnetic shields usually take the form of shielded enclosures, such as fully enclosed cable trays and instrument cases. Where there is likely to be sources of strong magnetic fields, e.g., motors, transformers and solenoids, the adverse emissions should be constrained by magnetic shielding. These sources are usually high power instruments, such as power supplies, power cables, small motors, solenoids, or current sources within the system. High current power leads and returns should be located in the same bundle and twisted. Data cables should not be laid in the same cable trays as current-carrying cables because of the magnetic field surrounding the current cables. Since field strength is a function of distance from the source, two parallel leads in a data cable can be influenced by the field to two different values, This is a source of magnetically-induced noise. A solution to noise in parallel cables, as in a cable tray, is to use twisted pair cable. The individual leads alternate position relative to the power cable and tend to average the amount of noise, resulting in the minimum effective noise signal. The interference decreases with the square of the distance from the source. Hence, when conditions permit, a good solution is to lay signal cables as far from power sources as possible. The transducer should not be overlooked when the system is required to be magnetically shielded.

3.4 **Multiplexers and Demultiplexers**, The process of mixing many measurements to form a single signal for transmission and/or recording is referred to as “multiplexing” [3.34]. Two forms of multiplexing are described herein: Frequency Division Multiplexing (FDM) and Time Division Multiplexing (TDM). A multiplexer and a demultiplexer are commonly referred to as a “roux” and a "demux", respectively.

3.4.1 Frequency Division Multiplexing. Analog data may be multiplexed using FDM. The total number of data channels that can be multiplexed on a single link by FDM is, however, limited by the total frequency bandwidth available. In FDM systems, two or more data channels make use of separate subcarriers that occupy defined center frequencies and bandwidths in the modulation baseband of the radio frequency (RF) carrier. Each of the subcarriers conveys data in frequency modulation (FM) form, and is prevented from interfering with other subcarriers and their data by the use of bandpass filters and guard bands. Two types of FM subcarrier formats are recommended, conforming to the IRIG Standard 10693 [3.92]. These are referred to as Proportional Bandwidth (PBW) and Constant Bandwidth (CBW) multiplexer. The data bandwidth of a PBW format is proportional to the subcarrier center frequency while the data bandwidth of a CBW format is constant, regardless of subcarrier center frequency. The number of data channels may be increased by modulating one or more of the subcarriers with a TDM format such as PCM or PAM (see Section 3.4.2).

The selection and grouping of subcarrier channels depend upon the data bandwidth requirements of the application and the necessity to ensure adequate guard bands between channels. (Guard bands are "dead" spaces on the baseband to accommodate the finite slopes of demux bandpass filters used to avoid interference between adjacent data channels.) Combinations of PBW and CBW channels may be used within the limits of maximum subcarrier deviation. PBW systems are commonly used in data systems where a combination of measurements of varying bandwidths are desired. For dynamic data applications where relative phase between data channels must be preserved, the matched filter characteristics of CBW systems are preferred. Tables 3.2 and 3.3 list the IRIG standard PBW and CBW channels, respective] y [3.92]. Due to specific requirements for inter-channel phase relationships, dynamic range and intermodulation distortion, consultation with instrumentation personnel knowledgeable of multiplexer systems is recommended.

When FDM data are to be recorded on an analog tape, there will be a need for tape speed servo control (TSC) and flutter compensation signals to reduce the signal errors induced by tape speed differences during recording and playback, as discussed in Section 3.6.6.2. It is recommended that the TSC and flutter compensation signals be selected from Tables 3.4 or 3.5 and mixed with the data subcarriers for transmission and data recording [3.92].

The number of subcarrier channels that maybe used simultaneously to modulate an RF carrier is limited by the RF channel bandwidth and by the output signal-to-noise ratio (SNR) that is acceptable for the application. As channels are added, the individual subcarriers add energy to the total already existing in the baseband. To accommodate additional channels, either all subcarrier channel modulation indices may need to be decreased and/or some or all subcarrier voltages may need to be reduced to stay within the available total SNR of the system. In these cases the signal maybe degraded by background noise and drop-outs. The number of subcarrier channels must be within

Table 3.2, Proportional Bandwidth FM Subcarrier Channels [3.92].

Channel	Center frequency, Hz	Lower deviation limit,[a] Hz	Upper deviation limit,[a] Hz	Nominal frequency response, Hz	Nominal rise time, msec	Maximum frequency response,[a,b] Hz	Minimum rise time,[b] msec
±7.5% Subcarrier deviation channels							
1	400	370	4313	5	58	30	11.7
2	560	518	602	9	44	42	8.33
3	730	675	785	11	32	55	6.40
4	960	888	1,032	14	2s	72	4.86
5	1,300	1,202	1,398	20	18	98	3.60
6	1,700	1,572	1,828	25	14	128	2.74
7	2,300	2,127	2,473	35	10	173	2.03
8	3,000	2,775	3,225	45	7.8	225	1.56
9	3,900	3,607	4,193	59	6.0	293	1.20
10	5,400	4,995	5,805	81	4.3	405	0.864
11	7,350	6,799	7,901	110	3.2	551	0.635
12	10,500	9,712	11,288	160	2.2	788	0.444
13	14,500	13,412	15,588	220	1.6	1,088	0.322
14	22,000	20,350	23,650	330	1.1	1,650	0.212
15	30,000	27,750	32,250	450	0.78	2,250	0.156
16	40,000	37,000	43,000	600	0.58	3,000	0.117
17	52, S00	48,562	56,438	790	0,44	3,938	0.089
18	70,000	64,750	75,250	1,050	0.33	5,250	0.067
19	93.000	86,025	99,975	1,395	0,25	6,975	0.050
20	124,000	114,700	133,300	1,860	0.19	9* 300	0,038
21	165,000	152,624	177,325	2,475	0.14	12,375	0.029
22	225,000	208,125	241,875	3,37s	0.10	16,875	0.021
23	300,000	277,500	322,500	4,500	0.08	22,500	0.016
24	400,000	370,000	430,000	6,000	0.06	30,000	0.012
25	560,000	518,000	602,000	8,400	0,04	42,000	0,008,
±15% Subcarrier deviation channels[c]							
A	22,000	18,700	25,300	660	0.53	3,300	0.106
B	30,000	25,500	34,500	900	0.39	4,500	0.078
C	40,000	34,000	46,000	1,200	0.29	6,000	0.058
D	52,500	44,625	60,375	1,575	0.22	7,875	0.044
E	70,000	59,500	80,500	2,100	0.17	10,500	0.033
F	93,000	79,050	106,950	2,790	0.13	13,950	0.025
G	124,000	105,400	142,600	3,720	0.09	18,600	0.018
H	165,000	140,240	189,750	4,950	0.07	24,750	0.014
1	225,000	191,250	258,750	6,750	0.05	33,750	0.010
"J	300,000	255,000	345,000	9,000	0.04	45,000	0.008
K	400,000	340,000	460,000	12,000	0.03	60,000	0.006
L	560,000	476,000	644,000	16,800	0.02	84,000	0.004
±30% Subcarrier deviation channels[d]							
AA	22,000	15,400	28,600	1,320	0.265	6,600	0.053
BB	30,000	21,000	39,000	1, ?.00	0.194	9,000	0.038
CC	40,000	28,000	52,000	2,400	0.146	12,000	0.029
00	52,500	36,750	60,250	3,150	0.111	15,750	0.022
EE	70,000	49,000	91,000	4,200	0.083	21,000	0.016
FF	93,000	65,100	120,900	5,580	0,063	27,900	0,012
GG	124,000	86,800	161,200	7,440	0.047	37,200	0,009
HH	16 S,000	115,500	214,500	9,900	0.035	49,500	0.007
II	225,000	157,500	292,500	13,500	0.026	67,500	0.005
JJ	300,000	210,000	390,000	18,000	0.019	90,000	0.004
KK	400,0043	280,000	520,000	24,000	0.015	120,000	0,003
LL	560.000	392,000	728.000	33,600	0,.010	168,000	0.002

[a] Rounded off to the nearest Hz.

[b] The indicated maximum data frequency response and minimum rise time is based on the maximum theoretical response that can be obtained in a bandwidth between the upper and lower frequency limits specified for the channels. (See Appendix B of [3.92] for 'determining possible accuracy-versus-response trade-offs).

[c] Channels A through L may be used by omitting adjacent lettered and numbered channels. Channels 13 and A may be used together with some increase in adjacent "channel interference.

[d] Channels AA through LL may be used by omitting every four adjacent double-lettered and lettered channels and every three adjacent numbered channels. Channels AA through LL may be used by omitting every three adjacent double-lettered and lettered channels and every two adjacent numbered channels with some increase in adjacent channel interference,

Table 3.3. Constant Bandwidth FM **Subcarrier** Channels [3.92].

A CHANNELS Deviation limits = ± 2 kHz Nominal frequency response = 0.4 kHz Maximum frequency response = 2 kHz	B CHANNELS Deviation limits = ± 4 kHz Nominal frequency response = 0.8 kHz Maximum frequency response = 4 kHz	C CHANNELS Deviation limits = ± 8 kHz Nominal frequency response = 1.6 kHz Maximum frequency response = 8 kHz	D CHANNELS Deviation limits = ± 16 kHz Nominal frequency response = 3.2 kHz Maximum frequency response = 16 kHz	E CHANNELS Deviation limits = ± 32 kHz Nominal frequency response = 6.4 kHz Maximum frequency response = 32 kHz	F CHANNELS Deviation limits = ± 64 kHz Nominal frequency response = 12.8 kHz Maximum frequency response = 64 kHz	G CHANNELS Deviation limits = ± 128 kHz Nominal frequency response = 25.6 kHz Maximum frequency response = 128 kHz	H CHANNELS Deviation limits = ± 256 kHz Nominal frequency response = 51.2 kHz Maximum frequency response = 256 kHz
Center frequency (kHz)	Center frequency (kHz)	Center frequency (kHz)	Center frequency (kHz)	Center frequency (kHz)	Center frequency (kHz)	Center frequency (kHz)	Center frequency (kHz)
8	16	32	64	128	256	m	1024
16	32	64	128	256	512	1024	2048
24	48	96	192	384	768	1536	3072
32	64	128	256	512	1024	2048	
40	80	160	320	640	1280	2560	
48	96	192	384	768	1536	3072	
56	112	224	448	m	1792	3584	
64	128	256	512	1924	2048		
n	144	288	576	1152	2304		
80	160	320	640		2560		
88	176	352	704	1408	2816		
96	192	384	768	1536	3072		
104	208	416	832				
112	224	448	896	1792	3584		
120	240	480	960		3840		
128	256	512	1024				
136	272	544	1088	2176			
144	288	576	1152				
152	304	608	1216	2432			
160	320	640	1280				
168	336	672	1344				
176	352	704	14a	2816			

The constant bandwidth channel designation shall be the channel center frequency in kilohertz and the channel letter indicating deviation limit; for example, 16A, indicating fc = 16 kHz, deviation limit of ± 2 kHz. See appendix F for former subcarrier nomenclature.

The indicated maximum frequency is based upon the maximum theoretical response that can be obtained in a bandwidth between deviation limits specified for the channel. See discussion in appendix B for determining practical accuracy versus frequency response trade offs.

Prior to using a channel outside the enclosed area, the user should verify the availability of range assets to support the demodulation of the channel selected. Very limited support is available above 2 MHz.

Table 3,4. Reference Frequencies for Tape Speed Control and Flutter Compensation [3.92].

Reference Frequency (kHz ±0.01%)
960'
480'
240'
200
100
50
25
12.5
6.25
3.125

If the reference signal is recorded *on a* separate tape track, any of the listed reference frequencies may be used provided the requirements for compensation rate *of* change are satisfied.

If the reference signal is mixed with the data signal, consideration must be given to possible problems with intermodulation sum and difference frequencies. Also, sufficient guard band must be allowed between the reference frequency and any adjacent data subcarrier.

'These frequencies are for flutter compensation only and not for capstan servo speed control. In addition, the 240 kHz reference signal may be used as a retranslation frequency in a constant-bandwidth format.

Table 3.5. Constant-Amplitude Tape Speed Control Signals [3.92]1.

Tape Speed mm/s	ips	Frequency[2] kHz			
6096	(240)	400	±0.01%	800	±0.01%
3048	(120)	200	±0.01%	400	±0.01%
1524	(6 0)	100	±0.01%	200	±0.01%
762	(30)	50	±0.01%	100	tool%
381	(1 5)	25	±0.01%	50	±0.01%
190.5	(7-1/2)	12. s	±0.01%	25	±0.01%
95.5	(3-3/4)	6.5	±0.01%	12.5	±0.01%
47.6	(1-7/8)	3.125	±0.01%	6.25	±0.01%

'May also serve as discriminator flutter-correction reference signal (see table 3.4).

[2]Either set of speed-control signals may be used primarily with wide-band systems, but only the higher set of frequencies is recommended for double-density systems. When interchanging tapes, care should be taken to ensure that the recorded speed-control signal is compatible with the reproduce system's speed-control electronics.

NOTE

Caution should be used when multiplexing other signals with the speed-control signal. In the vicinity of the frequency of the speed-control signal (fsc ±10 percent), the level of individual extraneous signals including spurious, harmonics and noise must be 40 dB or more below the level of the speed-control signal. A better procedure is to leave one octave on either side of the speed-control signal free of other signals.

the restriction of the bandwidth of the baseband carrier system. By limiting the number of channels, particularly at higher frequencies, the input subcarrier signal magnitude to the transmitter can be increased. Thus, a higher modulation index (ratio of the carrier deviation frequency to the data frequency) and dynamic range can also be achieved. It is therefore the user's responsibility to determine acceptable tradeoffs between the number (and frequencies) of subcarrier channels and acceptable subcarrier SNR. Performance is also influenced by other considerations, such as hardware capabilities. See [3.92, Appendix B] for a mare detailed discussion.

3.4.2 Time Division Multiplexing. An increase in data channel capacity can be achieved at the expense of per-channel bandwidth by transmitting a short sample of each measurement to form a single signal. This process is referred to as TDM. In TDM systems, several analog or digital data signals may be filtered, sampled, and assembled (commutated) into a single signal for transmission on a common communication link, and subsequently recorded on one tape track. There are currently three IRIG standard TDM formats: (a) Pulse Code Modulation (pCM), (b) Pulse Amplitude Modulation (PAM), and (c) the recently-standardized ADARIO format (Analog/Digital/Adaptable/ Recorder Input/Output). PCM is usually preferred over PAM for dynamic measurements.

TDM requires that all signals be sampled prior to transmission and/or recording. The sampling rate R must be compatible with the user's frequency range requirements described in Sections 2.3 and 3.7. The user's maximum frequency limit f_{max}, assumed achievable by the transducer (see Section 3.2.3.2) and signal conditioner (see Section 3.3), must be exceeded by the Nyquist cut-off frequency associated the anti-aliasing filter of the sampling circuit, i.e., $R > 2 f_{max}$. Sampling at least 2.5 times the maximum frequency using appropriate lowpass falters is recommended for frequency domain processing of long duration stationary random or periodic signals (see Sections 5.4.2.2 and 5.4.3.2). This rate will be inadequate for transients or highly nonstationary signals when it is necessary to sample peak values with negligible error [3.43]. For example, Appendix A recommends a sampling rate of 10 times the maximum frequency for the computation of shock response spectra for pyroshock unless digital interpolation is used (see Section A.3.5).

3.4.2.1 Pulse Code Modulation. PCM data are transmitted as a serial bit stream of binary coded words. Each word consists of a sequence of bits to represent a discrete magnitude of the data, an assembly of event or discrete condition indicator bits, or a portion of a longer fragmented word that cannot be contained within the PCM word format restrictions. The sample rate must also be compatible with the PCM frame rate so that the sample rate for each signal is a multiple or submultiple of the minor frame rate as described in Section 3.4,2.1.5.

3.4.2.1.1 Word and Frame Structure. PCM frame formats are divided into two classes. The basic, or Class I, format is most commonly used and routinely supported by the test ranges and most contractor data reduction facilities. The more complex, or Class II, formats are permitted when measurement requirements cannot be satisfied within one or more of the Class I format constraints.

Since the Class II formats are not routinely supported by most range and contractor facilities, it is recommended that the user observe Class I format restrictions. Thus, the following discussion is limited to listed Class I format restrictions [3.92].

The PCM frame contains a known number of bit intervals of equal duration. The duration and number of bit intervals per frame remains fixed from frame to frame for the duration of the test or flight. Figure 3,78 shows the graphical PCM frame structure [3,92],

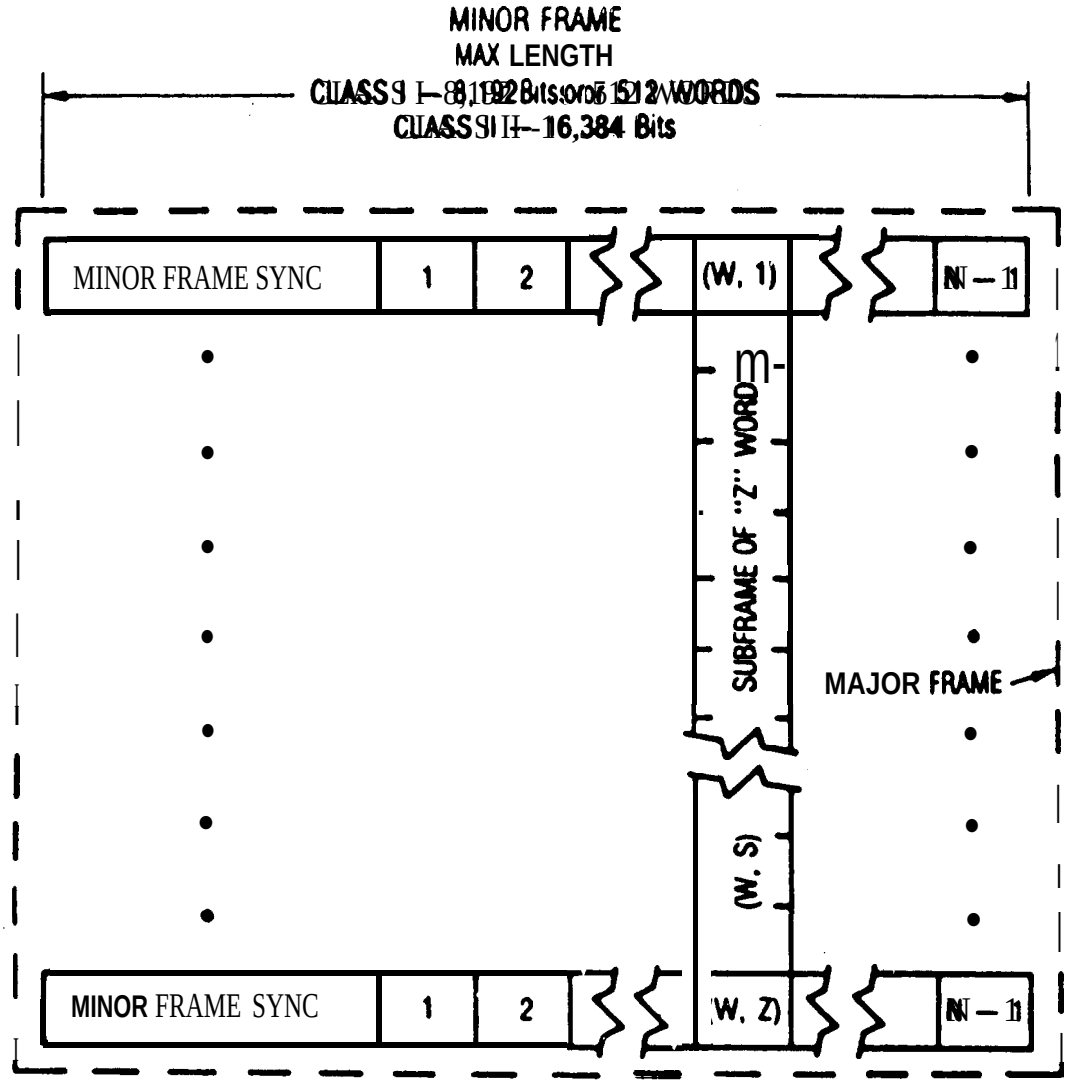

• BY DEFINITION A MAJOR FRAME CONTAINS N • Z WORDS.
"Z" = THE NUMBER OF WORDS IN LONGEST SUBFRAME. (Max.256)
"N" = THE NUMBER OF WORDS IN MINOR FRAME.
• MINOR FRAME SYNC IS CONSIDERED ONE WORD, REGARDLESS OF LENGTH.

Figure 3.78. IRIG Standard Pulse Code Modulation Frame Structure [3.92].

3.4.2.1.2 PCM Binary Bits. The permissible PCM code conventions for representing serial binary "ones" and "zeros" are identified and shown graphically in Figure 3.79 [3.92]. Only one code is used in a single PCM bit stream. The transmitted or recorded bit stream is continuous and contains sufficient transitions to assure bit acquisition and continued bit synchronization. The bit rate is at least 10 bits/see but not greater than 5 Mbits/see (a Class I restriction). During any data acquisition period, the bit rate must not differ from the specified nominal bit rate by more than 0,1%. The bit jitter must not exceed ± 0.1 bit interval referenced to the expected transition time with no jitter. The expected transition time is based on the average bit period during the immediately preceding 1000 bits.

3.4.2.1.3 PCM Words. Individual words may vary in length from 4 to 16 bits (a Class I restriction). Subwords (syllables) maybe combined to form a larger word (up to 16 bits). Words of different length may be multiplexed in a single minor frame. The length of a WOKI in any identified word position within a minor frame must remain constant. It should be noted, however, that equipment restrictions at some facilities maybe limited to a fixed word length for all words in the minor frame. To provide a consistent notation, the first word following the synchronization word is numbered "one" and each subsequent word is numbered sequentially within the minor frame.

It should be noted that PCM encoding always takes place slightly after the occurrence of the physical event or instantaneous signal value. Due to this time delay, the information content of the PCM "wed" occurs prior to the time of its sampling and commutation into the PCM frame. The word position in the PCM frame represents the commutation time. Some PCM multiplexer-encoders have a "simultaneous sample and hold" feature that permits several closely related analog signals to be sampled simultaneously, allowing the ADC to sample each held measurement sequentially. If phase relationships between two or more signals is critical, it is important that the data analyst be aware of the time relationship of the actual sampling process.

3.4,2.1.4 Minor PCM Frames. The minor frame is defined as the data structure, in time sequence, from the beginning of a minor frame synchronization pattern to the beginning of the next minor frame sync pattern. The length of the minor frame must not exceed 8,192 bits or 512 words (a Class I restriction). Each minor frame should contain a frame counter that is a natural binary count corresponding to the minor frame number in which the frame count word occurs. The frame count word normally follows immediate y after the minor frame sync pattern (i.e., in Word 1). The frame counter should be of nominal word length and be reset after reaching a maximum predetermined value, normally after the last minor frame in the major frame. The minor frame sync pattern normally consists of a fixed digital word of at least 16 but no more than 33 bits, Recommended sync patterns are listed in Table 3.6 [3.92].

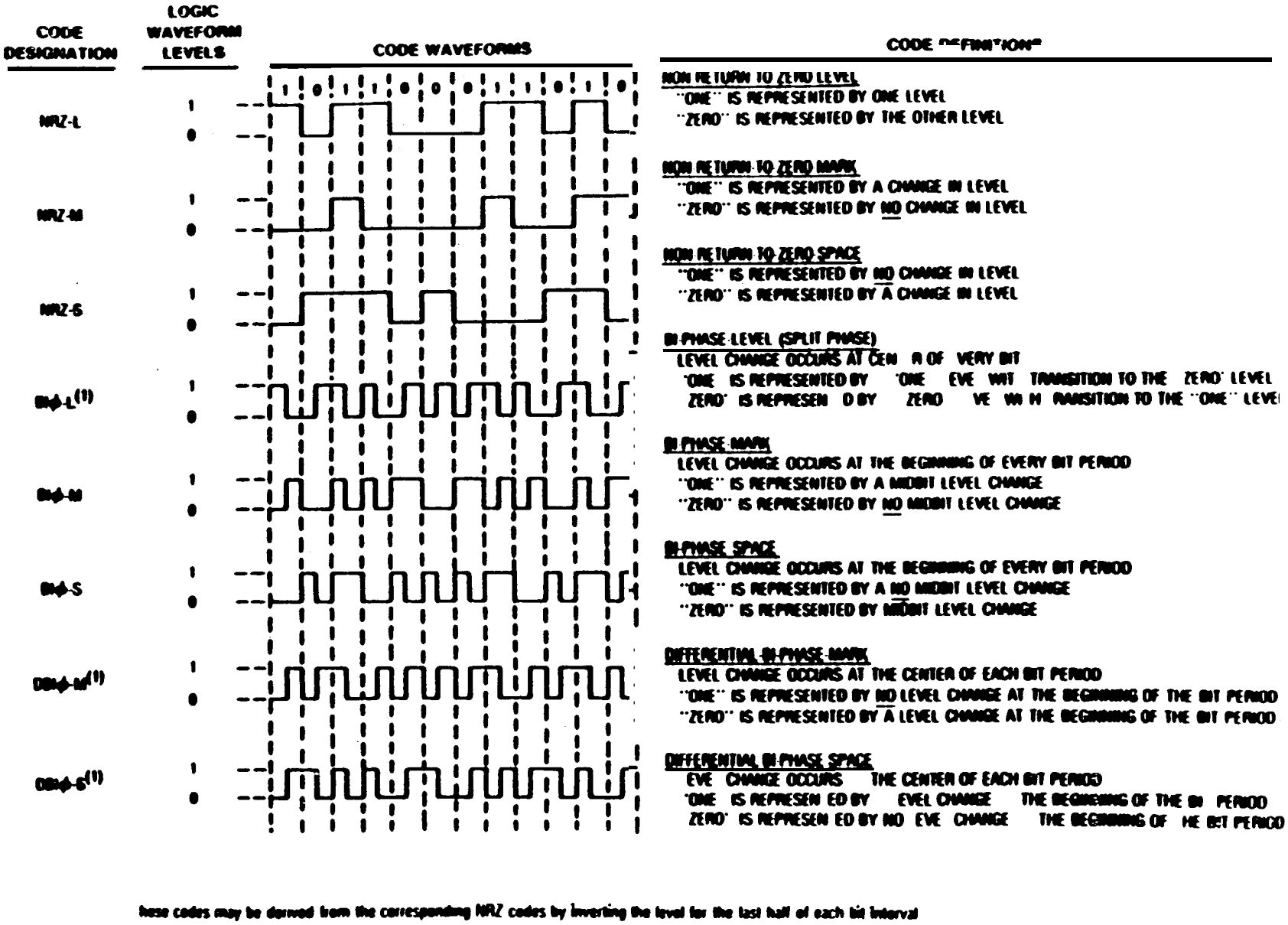

Figure 3.79. IRIG Standard Pulse Code Modulation Binary Code [3.92].

Table 3,6, Optimum Frame Synchronization Patterns for PCM Telemetry [3.92].

Pattern Length	Patterns										
7	101	100	0								
8	101	110	00								
9	101	110	000								
10	110	111	000	0							
11	101	101	110	00							
12	110	101	100	000							
13	111	010	110	000	0						
14	111	001	101	000	00						
15	111	011	001	010	000						
16	111	010	111	001	000	0					
17	111	100	110	101	000	00					
18	111	100	110	101	000	000					
19	111	110	011	001	010	000	0				
20	111	011	011	110	001	000	00				
21	111	011	101	001	011	000	000				
22	111	100	110	110	101	000	000	0			
23	111	101	011	100	110	100	000	00			
24	111	110	101	111	001	100	100	000			
25	111	110	010	110	111	000	100	000	0		
26	111	110	100	110	101	100	110	000	00		
27	111	110	101	101	001	100	110	000	000		
28	111	101	011	110	010	110	011	000	000	0	
29	111	101	011	110	011	001	101	000	00000		
30	111	110	101	111	001	100	110	100	000	000	
31	111	111	100	110	111	110	101	000	010	000	0
32	111	111	100	110	101	100	101	000	010	000	00
33	111	110	111	010	011	101	001	010	010	011	000

3.4.2.1.5 Major PCM Frames. A major PCM frame consists of an integer number of minor frames that are required in order to include one sample of every parameter in the PCM data stream format. The number of minor frames in a major frame must not exceed 256 (a Class I restriction).

Data words are commutated into the PCM format at rates that arc multiples (supercommutation) or submultiples (subcommutation) of the minor frame rate. Supercommutated data words are equally spaced in time within the minor frame format. A subframe is defined as one cycle of the parameters from a commutator whose rate is a submultiple of the minor frame rate. An independent subframe is defined as a subframe that is not synchronous with and not an integer submultiple of ocher subframes in the major frame. An independent subframe has its own subframe counter. A dependent subframe is defined as a subframe that is synchronous with and thus an integer submultiple of, or equal in length to, an independent subframe in the major frame. Supercommutation of data words within a subframe is permitted and must, as in the minor frame, occur as equally spaced multiple samples of the same parameter in the subframe.

3.4.2.2 Pulse Amplitude Modulation. PAM data are transmittal as TDM analog pulses with the amplitude of the information channel pulse representing the value of the sampled analog signal. PAM waveforms may be modulated on an FM subcarrier and mixed with other analog signals in a FDM system.

3.4.2.2.1 PAM Frame and Pulse Structure. Each frame consists of a constant number of time-sequenced channel intervals. The maximum frame length is 128 channel time intervals, including the channels devoted to synchronization and calibration. The pulse and frame structure conforms to either Figure 3.80 (RZ-PAM, 50% duty cycle) or Figure 3.81 (NM-PAM, 100% duty cycle) [3.92]. The channels are allocated equal and constant time intervals within the frame. Each channel contains a sample pulse that begins at the start of the interval and has an amplitude determined by the amplitude of the measurement. Each frame is identified by the presence of a synchronization interval. The sync pattern interval for RZ-PAM is two channel intervals and for NRZ-PAM is five channel intervals. The amplitude pattern within the sync interval must conform to that shown in Figure 3.80 or 3.81, respectively.

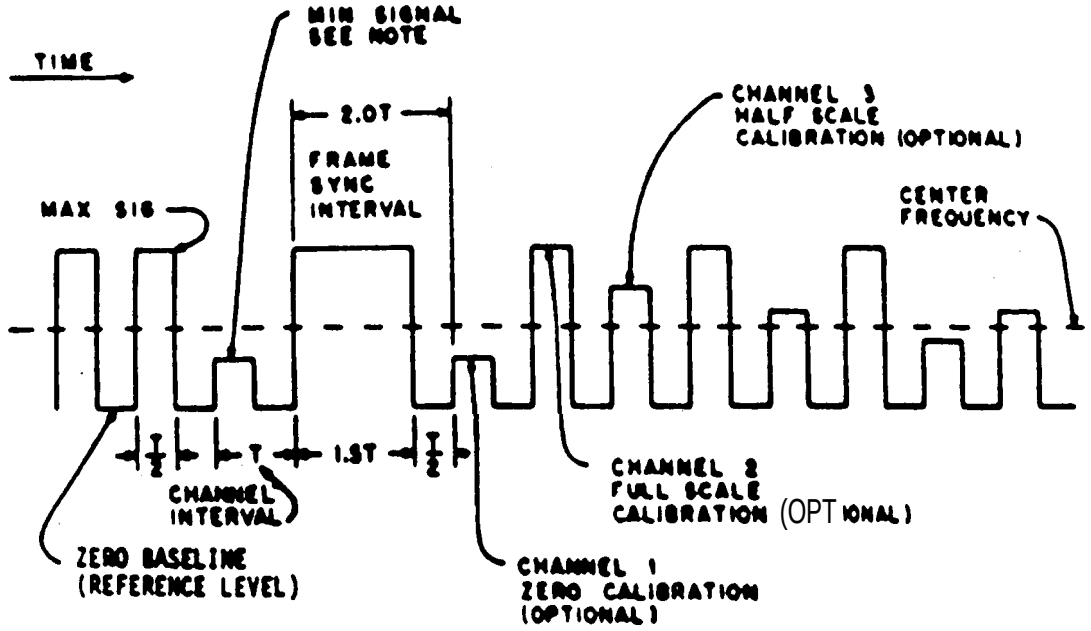

NOTE

A 20 to 25 percent deviation reserved for pulse synchronization is recommended.

Figure 3.80. IRIG Standard 50 Percent Duty Cycle Pulse Amplitude Modulation with Amplitude Synchronization [3.92].

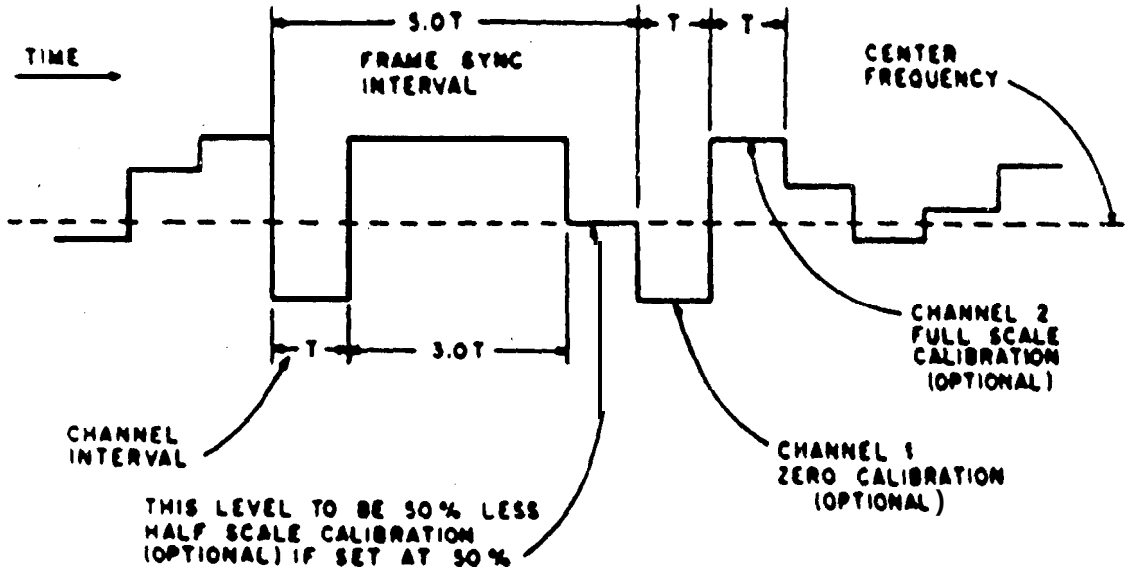

Figure 3.81. IRIG Standard 100 Percent Duty Cycle Pulse Amplitude Modulation with Amplitude Synchronization [3.92].

It is recommended that in-process calibration be used, and that Channels 1 and 2, immediately following the frame synchronization interval, be used for zero and full-scale calibration, respectively, For RZ-PAM, Channel 3 maybe used for an optional half-scale calibration. For NRZ-PAM, the channel interval preceding Channel 1 maybe used for half-scale calibration if set to SO%.

3.4.2.2,2 PAM Supercommutation and Subcommutation. Data multiplexing at sampling rates that are multiples (supercommutation) and submultiples (subcommutation) of the frame rate is permissible. The beginning of the longest submultiple frame interval is identified by the transmission of a sync pattern. All other submultiple frames have a fixed and known relationship to the identified submultiple frame. The interval of any submultiple frame, including the time devoted to synchronization, must not exceed 12$ times the interval of the frame in which it occupies a reaming position.

3.4.2.3 ADARIO. The Analog/Digi@/Adaptable/Recorder Input/Output system accommodates up to 2^{24} (i.e., 16,777,216) data blocks with each block having 2^{11} (i.e., 2048) 24-bit words [3.92]. The ADARIO format accepts up to 16 channels of synchronous data with data rates ranging from 10 kbps to 35 Mbps per channel using the NRZ-L code at TTL (transistor-transistor logic) levels. When ADARIO data are to be *recorded, the* maximum bit rate must not exceed the maximum allowable bit rate of the recorder. ADARIO preserves phase coherence between channels, and provides channel source and timing information.

3.4.3 Demultiplexers. The demultiplexing process involves the instruments and procedures used to reconstruct the data format to its original form, i.e., that which existed immediately prior to multiplexing. For FDM data (also referred to as FM), demuxing involves selective bandpass filtering, frequency detection and demodulation. For TDM data (PCM, PCM/FM, PAM or PAM/FM), demuxing involves demodulation (for PCM/FM and PAM/FM only), synchronization and decommutation. These processes are briefly described in the following sections [3.92].

3.4.3,1 FDM Data Discrimination and Demodulation. The FDM signal is input to a set of bandpass filters and discriminators, where a separate discriminator is tuned to each subcarrier center frequency. The demodulated signals are faltered within appropriate bandwidth limits and output as analog data signals for further processing.

If the FDM signal source is from tape recorder playback, it is important to recognize that tape speed differences between the original recorder and the playback recorder will appear as false data on each of the FM carriers and subcarriers. A first order correction for this effect is to control the playback recorder speed using a tape speed control (TSC) signal, which should have been recorded on the original tape and copied on each reproduced or "dubbed" tape. A second order flutter compensation is achieved by inputting the multiplexed signal, including a flutter compensation reference signal, to a reference discriminator. The reference discriminator output is an error signal that is applied to the flutter compensation input port of each discriminator where it is used to correct the demodulated data. Both TSC and flutter compensation are discussed in Section 3.6.6.2.

3,4.3.2 PCM Data Synchronization and Decommutation, The PCM waveform is perceived as a digital bit stream that appears as one of the coded formats shown in Figure 3.78. Whether received as output from a radio frequency (RF) receiver or from an analog tape playback (and demodulated from an FM subcarrier, if applicable), the PCM waveform is in reality an analog representation of a digital signal. This noise-contaminated signal is sent to a PCM bit synchronizer, where the coded binary bit stream is reconstructed from the analog signal, and a clock [3.93].

Typical operator-selected parameters are PCM binary code, bit rate and loop bandwidth. The code and bit rate must match the incoming signal. A narrow loop bandwidth selection is preferred when the SNR is low and there are long periods with few or no transitions. A wide loop bandwidth performs best when the data rate is unstable. Bit rate instability is most commonly related to tape recorder/reproducer time base error, occasionally to an unstable clock in the PCM encoder/transmitter system or, to a lesser degree, the Doppler effect associated with high velocity approaching or receding vehicles. An excessively noisy PCM signal or a poor choice of loop bandwidth can result in incorrect bit decisions or loss of synchronization. As with FM data, tape recorder/reproducer time base error can be minimized with proper use of tape speed servo control. Loss of bit sync will typically result in failure of the frame synchronizer to find the frame sync pattern at the next expected location.

The bit synchronizer data output, usually NW-L, and clock signal are required inputs to the PCM frame synchronizer along with bit rate, frame synchronization pattern and pattern length. There are typically two and often three levels of sync status: (1) search, (2) lock, and (3) sometimes check or verify. The frame sync first "searches" the incoming bit stream on a bit-by-bit basis until it finds the expected pattern. It can then be programmed to go directly to the lock mode or to an intermediate status of verify for a specified number of pattern occurrences. Other optional inputs to the frame synchronizer are (a) allowable bit errors in the sync pattern while in search, verify or lock mode, and (b) the window size (in bit periods) to check for the expected pattern when in verify or lock mode. Usually the window size is specified as O, ±1 or ±2 bit periods around the expected location of the sync pattern.

Another required input to the frame sync is the number of bits in each word of the PCM frame. This can be specified as a constant word or variable word length. If variable, the length of each word must be defined. Each word is then "decommutated" and sequentially output to a bit-parallel output port for input to a computer and/or word selector. The word selector is usually programmed to select specified words for distribution to other data processing instruments, such as digital-to-analog converters (DAC) and chart recorders. Most word selectors "hold" the last value when frame synchronization is lost.

3.4.3.3 PAM Data Synchronization and Decommutation. The PAM waveform from a receiver, tape recorder, or as a demodulated signal from an FM discriminator, is input to a PAM frame synchronizer. Inputs to the frame synchronizer are waveform structure (e.g., NRZ in Figure 3.80), frame length and position within the channel period to sample the analog value (usually at 20 to 40%).

The frame synchronizer searches the PAM waveform to locate the proper sync pattern. Care must be taken to avoid data channel assignments of PAM signals to contiguous word locations which may assume values that produce apparent sync patterns and thus result in false sync. Other potential causes of poor sync are electrical noise superimposed on the PAM signal, tape recorder/reproducer time base error, or an unstable commutator clock. Noise can originate from a variety of sources which affects analog signals, including tape recorder/reproducer flutter. Flutter compensation is achieved by use of the tape speed flutter compensation discussed in Section 3.4.3.1 for FM data. Tape recorder/reproducer time base error can be minimized with proper tape speed servo control, as described in Sections 3.4.3.1 and 3.6.6.2. Compensation for unstable commutator clocks is more difficult. Trial-and-error tests to establish average word rates can often improve the tracking capability of the frame synchronizer. Fortunately, with current technology electronics, this situation is rare. It is, however, important to be able to distinguish between frame rate jitter caused by an unstable clock and that caused by a variable speed tape drive.

Output from the frame synchronizer is a sample of the data signal and a clock signal at each word (channel) time which are sent to a word selector. The word selector is programmed to select specified words from the PAM data frame for distribution to analog chart recorders or to the ADC. The ADC is typically an 8, 10 or 12 bit converter which is interfaced to a digital computer or digital chart recorder.

3.5 Communication Links. Signal transmission from the signal conditioner between the instruments 'of the data acquisition and analysis system can be accomplished by one or more communication links. The selection of the most appropriate medium is dependent on a variety of factors which influence data integrity and cost. This Handbook is not intended to present a detailed discussion of technological issues associated with the design of the communication media. However, the selected data transmission approach may have a significant impact upon data quality.

3.5.1 Land Lines. For purposes of this Handbook, land lines consist of wire, coaxial cable, twisted shielded cable, fiber optics and commercial telephone networks. Unshielded wire should be avoided for transmission of analog signals due to interchannel modulation (or cross talk), excessive background noise, etc. Similarly, telephone networks may create problems due to background noise, unknown routing and switching, and noise effects at couplers and connectors. Coaxial cables are the most commonly used transmission medium at the present time. Fiber optic data links may be used to replace coax cable to meet low noise or security requirements. Cost effective installation and maintenance over long distances can also be limiting factors which influence signal transmission quality. See Section 3.3.5 for cable selection and installation recommendaions.

3.5.2 Radio Frequency Telemetry. Data transmission over long distances from air-to-ground, ground-to-air, air-to-air and occasionally ground-to-ground (e.g., telemetering of data from rotating machinery at short range) involves the use of RF telemetry techniques. In this sense, use of the word "air" also implies "space". The procedures and equipment for conditioning the data for transmission as a single signal are discussed in Section 3.4. The resultant complex signal, generally called the "baseband" signal, is used to modulate the transmitter's output signal or RF carrier that is radiated from the transmitting antenna. The receiving system consists of the receiving antenna, telemetry receiver and telemetry demodulation, The government has designated certain UHF bands for RF telemetry use, specifically 1.435 to 1.535 GHz in the L-Band, 2.20 to 2.29 GHz in the E-Band, and 2.31 to 2.39 GHz in the S-Band range [3.92].

3.5.2.1 PCM Telemetry System. The transmitted data are provided in either digital or analog format, as described in Section 3.4. The digital data format, called pulse code modulation (PCM), is a serial bit stream of binary-coded time division multiplexed words organized into major and minor frames as described in Section 3.4,2.1 [3,92]. The PCM signal is used to modulate the RF carrier frequency. The characteristics of the modulation, usually frequency or phase modulation,

and the performance of the transmission link are discussed in [3.93]. The performance of the transmission system is characterized in terms of bit error probability versus bit energy-to-noise power density ratio.

The signal parameters of the analog sensor output that are required to configure the telemetry system are the data bandwidth, including its cut-off frequency and roll-off rate, the dynamic range of the signal (as discussed in Section 2.4), and the desired accuracy. These parameters are used to determine the sampling rate and number of bits per sample required to satisfy the dynamic range and accuracy requirements, as discussed in Section 3.4.2.1. The sum of the bit rates of each of the desired analog measurements, when formatted into a PCM serial waveform with the format defined in [3.92], determines the transmission data rate. As a general rule, a higher transmission data bit rate necessitates a wider transmission bandwidth. As a consequence, more transmitter power is required to maintain the desired bit error probability for a fixed set of transmit and receive antennas and receiver characteristics.

3.5.2.2 FDM Telemetry System. The analog format is a composite baseband signal that consists of multiple subcarriers that have been frequency modulated (FM) by the analog transducer signals. The RF carrier is frequency modulated by the subcarrier FM signals. The performance of this type of system is based upon the received signal-to-noise ratio (SNR, as defined in Section 2.4) [3.92, 3.93]. For above-threshold operation, the received channel SNR for the ith subcarrier is

$$SNR_{di} = \frac{3}{4}\left(\frac{\Delta f_i}{f_i}\right)^2\left(\frac{\Delta f_{si}}{f_c}\right)^2\left(\frac{B_{IF}}{f_c}\right) SNR_{IF} \tag{3.14}$$

where SNR_{di} is the discriminator output SNR, SNR_{IF} is the intermediate frequency (IF) SNR, B_{IF} is the IF bandwidth, f_c is the lowpass filter bandwidth, f_i is the subcarrier center frequency, Δf_{si} is the subcarrier peak deviation, and Δf_i is the peak RF deviation. Additional information on the above equation can be found in [3.92, 3.93].

The signal parameters of the analog sensor output, required to design the telemetry system, are the data bandwidth, including its cut-off frequency and roll-off rate, the dynamic range of the signal and the desired accuracy. The number of subcarrier channels that may be used simultaneously to modulate an RF carrier is constrained by the transmission channel bandwidth, the output signal-to-noise ratio that is required, the transmitter power output capability, transmitter frequency deviation capability, and the linearity and frequency response of the subcarrier oscillators and discriminators employed. The RF transmission system can affect the data accuracy by introducing noise and intermodulation. The telemetry system needs to balance the contributions from each of these sources. The SNR of the telemetry system is degraded as the number of subcarriers increases, due to increased intermodulation, required bandwidth, and the requirement to stay within the available maximum SNR performance as the additional signals increase the total sum of the FDM subcarrier

signal magnitude. To accommodate additional channels, the power associated with individual sub carriers must be reduced to stay within the available RF signal power limits, which decreases individual SNRs. This situation may lead to data dropouts during the demodulation process.

3.6 Data Recording, Playback and Storage. The evolution of data recording technology during the last three decades has closely paralleled developments in the electronics industry. Early techniques involved the data recording on oscillographs and low frequency pen chart recorders. These recordings were often manually converted to numerical (digital) form for computation and analysis. Recent developments show promise for high density optical and laser technology using tape or disk instruments. Current systems use magnetic recording technology that interfaces to the data acquisition and communications systems in two basic ways: (1) analog and digital magnetic tape recorders, and (2) digital computers. The digital computer interface requires the use of telemetry front end (TFE) equipment, such as those discussed in Section 3.4.3. Special software is required to format the computer-acquired digital data and write these data on magnetic disks or computer-compatible digital tape recorders. These systems are facility or application dependent and are not covered in this Handbook,

Magnetic tape recorders can be roughly categorized as five general types, as follows:

(1) Low fidelity portable tape recorders, such as 4-track l/4-inch open reel recorders or audio cassette recorders.

(2) High density special application tape recorders, such as those used for radar tracking (up to 400 tracks on 2-inch tape).

(3) Rotary head helical-scan tape recorders, such as the l/2-inch single-track video and instrumentation cassette recorder. An edge track is sometimes available for voice, time code, or event recording.

(4) High fidelity instrumentation tape recorders, such as the 7-track l/2-inch, 14-track l-inch, or 28-track l-inch open reel recorders.

(5) Rotary-head helical-scan instrumentation tape recorders, such as the single-track 19-mm (3/4-inch) digital cassette recorder recently included in [3.92], although it had been previously standardized in [3.94]. Three edge tracks have been included for source/event identification, control, and time code. These recorders and cassettes are similar to but incompatible with the video recorders and cassettes summarized under Category (3).

Of the above five types, only the instrumentation tape recorders of Categories (4) and (5) are covered in IRIG Telemetry Standard 106-93 [3.92]. However, not all track configurations are available at all government test ranges and contractor facilities so it is necessary to ascertain what is

available. The discussion in this Handbook will be limited to these categories. Current information on magnetic recording appears in [3.95 - 3.97].

3.6.1 Data Capacity. The data storage capacity of a reel or cassette of magnetic tape is normally referred to as the "recording time" or duration. This depends on reel size, tape thickness, and tape speed. Of the four open reel sizes specified in [3.92], the 10.5- and 14-inch reels are the most commonly used. The tape speed should be selected to match the frequency response and recoding time requirements of the application. Table 3.7 shows tape length and recording time versus reel size and tape speed. These values are based on a nominal tape thickness of 0.001 in. (the tape thickness of 0.0015 in. is being phased out by manufacturers). Two cassette sizes are specified in [3.92], medium and large, having reading times of 24 and 55 minutes, respectively, when using a digital data rate of 240 Mbps. A tape thickness of 16pm (0.00063 in.) is specified

Table 3.7. Magnetic Tape Speeds and Recording Time.

Reel Size, in.	10.5	14	15	16
mm	266	356	381	408
Tape Length, ft	4,600	9,200	10,800	12,500
m	1,400	2,800	3,290	3,800
Tape Speed, ips	Recoding Time, minutes*			
240	3.8	7.7	9.0	10.4
120	7.7	15.3	18.0	20.8
60	15.3	30.7	36.0	41.7
30	30.7	61.3	72.0	83.3
15	61.3	122.7	144.0	166.7
7.5	122.7	245,3	288.0	333.3
3.75	245.3	490,7	576.0	666.7
1.875	490.7	981.3	1152.0	1333.3

* Based on tape thickness of 0.001 in. (0.025 mm).

3.6.2 Frequency Response. The effective frequency response of any tape recorder/reproducer system is a function of tape head assembly specifications, tape speed, and magnetic tape specifications. A current wideband top-of-the-line longitudinal tape drive of most manufacturers is a 2 MHz tape recorder operating at 120 ips using a suitabl y rated reel of tape Older 1.5 MHz machines are still in use. Models that meet a 4 MHz specification include a 240 ips speed option. Double density recording (Direct, FM, or PCM) on magnetic tape at bandwidths equal to those used in wideband instrumentation recording, but at one-half the wideband tape speeds specified in [3.92], requires special record/reproduce heads and high performance magnetic tape. Less expensive inter-

mediate band 0.6 MHz tape recorders are commonly available, but are no longer included in [3.92]. See Table 3.8 for details. For IRIG-standard helical-scan digital recorders, bit rates may range from less than 10 Mbps to as much as 256 Mbps.

3,6,3 Recording Modes. Standard wording techniques, tape speeds and tape configurations are required to provide a convenient interchange of recorded magnetic tapes between the test ranges, government agencies and contractors. Any one of the following methods of information storage or any compatible combination may be used simultaneously: (a) direct recording, (b) predetection recording, (c) FM recording, or (d) PCM recording. Double density recording maybe used when

Table 3,8. Direct Record and Reproduce Parameters [3.92].

Tap. Speed mm/s	(ips)	±3 dB Reproduce Passband kHz[1]	Direct R.Cord Bias Set Frequency (UBE) kHz[2]	Direct Record Level Set Frequency (10% of UBE) kHz
WIDE BAND			(OVERBIAS 2dB)	
6096.0	(240)	0.8-4000	4000	400
3048.0	(120)	0.4-2000	2000	200
1524.0	(60)	0.4-1000	1000	100
762.0	(30)	0.4- 500	500	50
381.0	(15	0.4- 2s0	2s0	2s
190.5	(7-1/2;	0.4- 125	12s	12. s
95.2	(3-3/4)	0.4- 62. S	62.5	6.25
47.6	(1-7/8)	0.4- 31.25	31.25	3.12
DOUBLE DENSITY			(OVERBIAS 2 dB)	
3048.0	(120)	2 -4000	4000	400
1524.0	(60)	2 -2000	2000	200
762.0	(30)	2 -1000	1000	100
381.0	(15)	a - 500	500	50
190.0	(7-1/2)	1 - 250	250	2s
9S.2	(3-3/4)	0.5- 125	12s	12. s

[1]Passband response *ref* ● rence is the output amplitude of a sinusoidal signal at the record level set frequency recorded at Standard Record Level. The record level set frequency is 10 percent of the upper band edge frequency (O. 1 UBE)

[2]When setting record bias level, a UBE frequency input signal is employed. The signal input level is set 5 to 6 dB below standard record level to avoid saturation effects which could result in ● rroneous bias level settings. The record bias current is adjusted for maximum reproduce output level and then increased until the output level decreases by the number *of* dB indicated in the table (see paragraph 4.1.3.3 of volume 111, RCC document 118-XX).

recording time is critical; however, it must be used realizing that performance parameters may be degraded [3.92]. Of the above methods, the Direct Record or FM Record may be viewed as recording modes of the tape recorder/reproducer system, whereas predetection or PCM recording relate to the source of the signal to be recorded.

3.6.3.1 Direct Recording. Direct recording is a magnetic recording technique employing a high-frequency bias signal that is linearly added to the data signal. The composite signal is then used as the driving signal to the record head. The bias signal transforms the recording of the data signal so that it is a more nearly linear process. There are two classes, (1) wideband and (2) double density, whose parameters are shown in Table 3.8 [3.92].

3.6.3.2 FM Recording. FM recording is a recording technique using frequency modulation to obtain response from DC to an upper specified frequency. FM systems forfeit the high frequency response of Direct Record systems to obtain a much flatter operating data bandwidth, a greater dynamic range, and low frequency and DC response. FM electronics maybe configured as a feature of the tape recorder and specified on an individual track basis, or can be provided external to the recorder. If the data signal is frequency modulated external to the tape recorder, the recording is usually made in the Direct Record mode and the signal is demodulated by external electronics during the reproduce (playback) process. Table 3.9 shows the FM Record parameters [3.92].

3.6.3.3 Predetection Recording. Predetection (Pre-D) signals consist of FM, phase modulation (PM) or phase shift keyed (PSK) signals that have been translated in frequency. Predetection recoding employs direct recording of the signal obtained by heterodyning the receiver intermediate frequency (IF) signal to one of the center frequencies listed in Table 3.10 [3.92]. The recorded signal is processed during playback as a Group II FM recording.

3.6,4 M Recording. An FDM signal maybe recorded in either Direct Record or FM Record mode. However, FM is rarely used because of frequency limitation. To achieve optimum recovery of the recorded signal, several ancillary data signals should also be recorded These are covered in Section 3.6,6.

3.6.5 TDM Recording. TDM data maybe recorded in either Direct Record or FM Record mode. TDM data that are carried on subcarriers are included in the signal and recorded as FDM data (see Section 3.6.4). Other signals to be recorded in conjunction with TDM data are discussed in Section 3.6.6. PAM data, as a separate signal, is recorded as an analog signal, either Director FM. PCM data maybe recorded using one of several different methods: (a) Pm-D, (b) Post detection (Post-D) or (c) serial High Density Digital Recording (HDDR). Pre-D and Post-D apply to the recorded output from the RF telemetry receiver.

Table 3.9. Wideband and Double-Density FM Record Parameters [3.92].

	Tape Speed mm/s (ips)	Carrier Center Frequency kHz	Carrier Deviation Limits[1] Plus Deviation kHz	Carrier Deviation Limits[1] Minus Deviation kHz	Modulation Frequency kHz	Response Band Limits dB[2]
	Wide-Band FM					
	Group I					
	47.6 (1-7/8)	6.7S0	9.460	4.050	dc to 1.2s0	±1
	95.2 (3-3/4)	13.500	18.900	8.100	dc to 2.s00	±1
	190.5 (7-1/2)	27.000	37.800	16.200	dc to 5.000	±1
	381.0 (15)	54.000	75.600	32.400	dc to 10.000	±1
	762.0 (30)	108.000	151.200	64.800	dc to 20.000	±1
	1524.0 (60)	216.000	302.400	129.600	dc to 40.000	±1
	3048.0 (120)	432.000	604.800	259.200	dc to 80.000	±1
Double-Density						
	Group II					
	47.6 (1-7/8)	14.062	18.281	9.844	dc to 7.810	*1, -3
	95.2 (3-3/4)	28.125	36.562	19.688	dc to 15.620	±1, -3
95.2 (3-3/4)	190.5 (7-1/2)	56.250	73.125	39.375	dc to 31.250	±1, -3
190.5 (7-1/2)	381.0 (15)	112.500	146.250	78.7S0	dc to 62.500	±1, -3
381.0 (15)	762.0 (30)	225.000	292.500	1s7.s00	dc to 125.000	±1, -3
762.0 (30)	1524.0 (60)	450.000	585.000	315.000	dc to 2S0.000	±1, -3
1524.0 (60)	3048.0 (120)	900.000	1170.000	630.000	dc to 500.000	±1, -3
3048.0 (120)	6096.0 (240)	1800.000	2340.000	1260.000	dc to 1000.000	±1, -3

[1] Input voltage levels per subparagraph 6.4.1, [3.92].

[2] Frequency response referred to l-kHz output for FM channels 13.5 kHz and above, and 100 Hz for channels below 13.5 kHz.

Table 3.10. Predetection Carrier Parameters [3.92].

Tape Speed mm/s	(ips)	mm/s	(ips)	Predetection Carrier Center Frequency[1,2] kHz A	B
Wide-Band		Double-Density			
6096	(240)	3048.0	(120)	1800	2400
3048	(120)	1524.0	(60)	900	1200
1524	(60)	762.0	(30)	450.0	600
762	(30)	381.0	(15)	225.0	300
381	(15)	109.5	(7.5)	112.5	150

[1]The predetection record/playback passband is the carrier center frequency ±66.7 percent.

[2]Use center frequencies in column B when data bandwidth exceeds the capabilities of those in column A.

Table 3.11. Maximum Recommended Bit Rates for Postdetection Recoding [3.92].

Tape Speed m/s	(ips)	mm/s	(ips)	Post-o Direct BiØ (kb/s)	Post-FM BiØ (kb/s)	NRZ (kb/s)
Wide-Band		Double-Density				
6096.0	(240)	3048.0	(120)	1800	900	1800
3048.0	(120)	1524.0	(60)	900	450	900
1524.0	(60)	762.0	(30)	450	225	4s0
762.0	(30)	381.0	(15)	225	112	225
381.0	(15)	109.5	(7-1/2)	112	56	112
190.0	(7-1/2)	95.2	(3-3/4)	56	28	56
95.2	(3-3/4)	---	---	28	14	28
47.6	(1-7/8)	---	---	14	1	14

[1]Direct recording of NRZ signals is NOT recommended unless the signal format is carefully designed to eliminate low-frequency components for any data expected.

3.6.5.1 Predetection PCM Ret_ Pre-D employs direct recording of the signal obtained by heterodyning the receiver IF signal to one of the center frequencies listed in Table 3.10 [3.92], without demodulating the PCM signal. The maximum recommended bit rates for pre-D recording of NRZ data is equal to the pre-D carrier frequency. The maximum recommended bit rate forpre-D recording of hi-phase (Biø) data is equal to one-half the pre-D carrier frequency. For bit rates greater than one-half the recommended rates, the preferred method of detection is to convert the signal to a higher frequency before demodulation.

3.6.5.2 Postdetection PCM Recording. Post-D employs the PCM signal (plus noise) at the video output of the receiver demodulator. This signal is recorded by director wideband FM recording modes without converting the PCM signal to a hi-level form. Table 3.11 lists the maximum recommended bit rates versus tape speed for these recording methods and PCM codes [3.92]. The minimum recommended bit rates are 10 kbps for post-D Direct Record Biø, and 10 bps for post-D FM Record,

3.6.5.3 Serial High Density Digital PCM Recording (HDDR). Serial HDDR is a method of direct recording PCM data as a hi-level signal [3.98]. The recommended PCM codes for serial HDDR are hi-phase level (Biø-L) and randomized non-return to zero level (RNRZ-L), shown in Figure 3.75. The recommended maximum bit packing densities are 15 kilobits/in. (kbpi) for Biø-L and 25 kbpi for RNRZ-L codes. These maximum bit packing densities translate to the maximurn recommended bit rates listed in Table 3.12 [3.92], The recommended minimum bit rates are 5 kbps and 200 kbps for Biø-L and RNRZ-L codes, respectively. The Biø-L code is recommended when the PCM bit rate does not exceed the recommended maximum, and the amount of tape required is not a severe operational constraint.

Table 3.12. Maximum Recommended Bit Rates for Serial High Density Digital Recording (HDDR) [3.92].

Tape Speed					
m/s	(ips)	mm/s	(ips)	BiØ-L (kb/s)	RNRZ-L (kb/s)
Wide-Band		Double-Density			
6096.0	(240)	3048.0	(120)	3600	6000
3048.0	(120)	1524.0	(60)	1800	3000
1524.0	(60)	762.0	(30)	900	1500
762.0	(30)	381.0	(15)	4s0	7s0
381.0	(15)	190. s	(7-1/2)	22s	375
190. s	(7-1/2)	9S.2	(3-3/4)	112	187'
9S.2	(3-3/4)	---	---	56	93'
47.6	(1-7/8)	---	---	28	46'

'Reproducing data at bit rates less than 200 kb/s is not recommended when using RNRZ-L.

3.6.6 Ancillary Signal Recording. To achieve optimum recovery of recorded data, and to support the data processing activities, several ancillary signals should also be supplied.

3.6.6.1 Tape Signature Recording. For data processing using wideband and double density recorders/reproducers, a tape signature recorded before and/or after the data provides a method for adjusting the reproducer head azimuth and equalizers. A swept-frequency or white noise signature may be recorded on those tape tracks that are used to record FDM data. A PCM signature? using the same PCM binary code, should be recorded on the same tape tracks used for recording the PCM data.

3.6.6.2 Tape Speed Control and Flutter Compensation. The average or long term tape speed must be the same between record and reproduce to avoid frequency offsets which may result in erroneous data. To minimize this problem, a reference signal should be recorded on one track of the tape to servo-control the tape speed during reproduce. This constant-amplitude and -frequency tape speed control (TSC) signal should be recorded on a separate track near the center of the tape for optimum speed correction. However, the TSC signal maybe mixed with data subcarriers and other signals if recording requirements permit and system performance is not seriously degraded, as described in IRIG Standard 106-86 [3.92]. Tables 3.4 and 3.5 list the IRIG-recommended TSC frequencies.

In addition to TSC, a high frequency signal is normally mixed with the data subcarrier signals, usually inserted near the high frequency limit of each track, for flutter compensation. This signal is used to control the center frequency of each discriminator on the applicable track during tape playback for flutter correction. IRIG-recommended flutter compensation frequencies are also listed in Tables 3.4 and 3.5 [3.92].

3.6.6.3 Time Code Rec-. Modulated-carrier time code signals (IRIG-A,-B and -C) are widely used for identifying specific dynamic events, and for assisting in subsequent data analysis operations, although other formats are available [3.99]. To ensure that the time code signal will be usable during subsequent operations, a channel bandwidth of seven or more times the time code carrier frequency should be used. The recorder tape speed must be compatible with this bandwidth, as well as the desired frequency range of the measurements. If not, another IRIG time code should be selected, or the time code signal should be recorded as a DC shift using DC shift encoding and decoding instruments. For example, when recording the IRIG-B time code (the one most frequently used), care must be taken to provide low frequency response down to DC. The Direct Record low frequency cutoff of some intermediate band and most wideband recorders is 400-800 Hz. The time code is often recorded as a frequency multiplexed signal along with voice and receiver signal strength signals.

3.6.6,4 Receiver Signal Strength Recording. Receiver signal strength information can assist in-

strumentation personnel and the data users to identify if or when dynamic data, which have been telemetered before recording, become invalid. Without this signal, for example, it is often difficult to separate valid random data from background noise that is due to weak RF receiver signal strength. Receiver signal strength data are usually muxed with voice and time code signals, and recorded as a FDM signal (see Section 3.6.4).

3.6.6.5 Voice and Event Recording. Voice and/or event signals may be recorded on the edge track or muxed with other signals (time code, signal strength) for wording as FDM data.

3.6.7 Tape Copying. The frequent playback of original tapes is not recommended. Tape recorder malfunction can stretch, break or otherwise damage a tape, causing the data to be either degraded or lost. Unintentional over-recording or erasure can also occur. The use of tape copies, called dubs, from original tapes is therefore recommended. With proper packaging and careful handling and storage (see Section 3.6.8), dub tapes can be transported world wide and stored so that data analysis can be performed remotely from the data recording facility and repeated years later if necessary. Lost or damaged dubs can usually be replaced with minor inconvenience. To achieve faithful reproduction and optimal data quality in a dubbed tape, the following copying practices are suggested:

(a) Align the reproduce head azimuth to the original tape.
(b) Adjust the reproducer equalizers correctly.
(c) Reproduce the recorded FDM or PCM tape signature from the original tape.
(d) Reproduce the recorded tape speed control and flutter compensation signal from the original tape.
(e) Convert the PCM signal from the original tape to a hi-level signal prior to recording a dub.

The PCM bit synchronizer should contain circuitry to reestablish the baseline reference PCM signal. This circuit is essential when reproducing RNRZ-L bit rates less than 1 Mbps. The PCM bit synchronizer loop bandwidth should be selected for optimum performance between 0.1 and 3% of the bit rate. If an appropriate bit synchronizer is unavailable, the tape can be copied directly, but a decrease in SNR can be expected

3.6.8 Tape Storage. Magnetic tape is subject to deterioration at extremes of temperature and humidity, as illustrated in Figure 3.82 [3.100-3.102]. In some cases the damage is reversible, but irreversible damage may occur during long-term storage in unfavorable conditions. Figure 3.82 also shows recommended storage conditions.

3.6.8.1 Environmental Degradation and Restoration. The primary mechanism of tape aging and degradation involves a chemical reaction between binders and environmental moisture [3.95 -3.97, 3.100- 3.102], as follows:

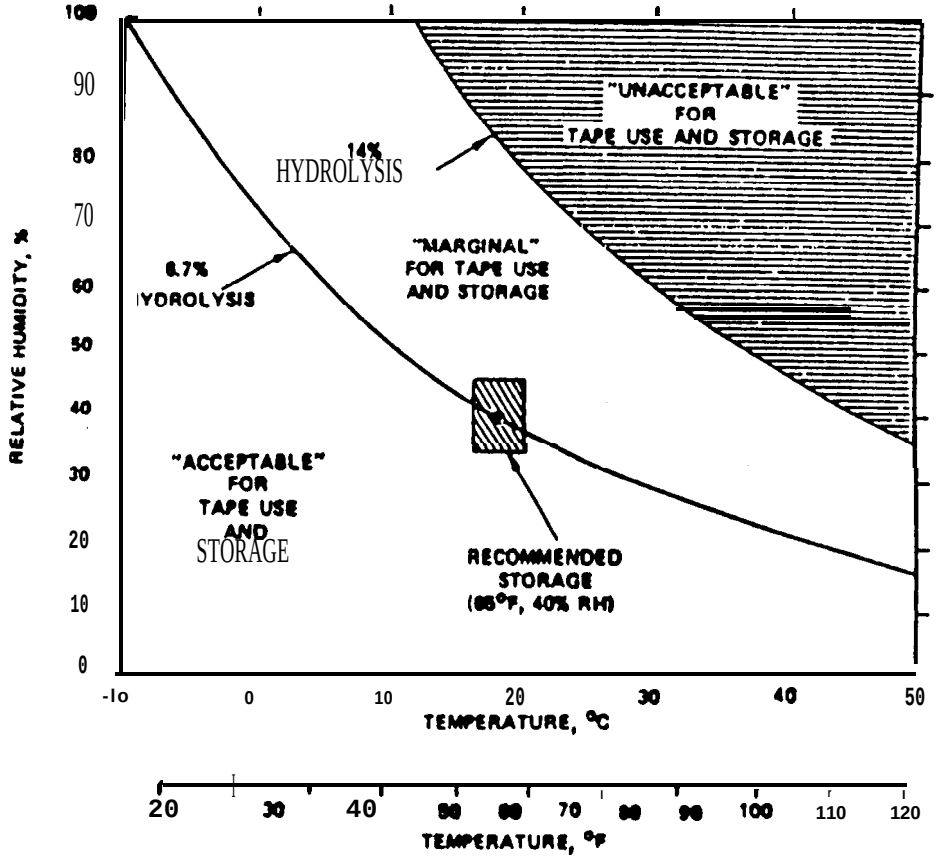

Figure 3.82. Recommended Temperature and Humidity Ranges to Avoid Magnetic Tape Deterioration [3, 102].

(a) At high humidities, abrasion is increased and other performance problems, such as tape drag and friction, may arise.

(b) At low humidities, tape binder and oxide tend to dry out, resulting in unsatisfactory oxide and binder adhesion.

(c) At high temperatures, the binder/oxide system becomes sticky (gummy) and unusable. High temperatures also accelerate atmospheric moisture hydrolysis.

(d) At low temperatures (below freezing), lubricants and plasticizers tend to migrate out of the oxide coating, resulting in gummy surface deposits.

Vacuum and heat sealing of tape in plastic air-tight bags can reduce the effects of atmospheric moisture during long term storage. Tapes that have been subjected to unfavorable conditions can often be restored to a usable state by a drying and cleaning process. The drying process should be done over 24-48 hr in a precise temperature controlled laboratory oven at 104°F. Use of a commercially available tape cleaner to remove dust and residue after drying is recommended

3.7 --to-Digital Converters. Essentially all modern analysis of dynamic data is accomplished using digital computational procedures. Hence, the analog signals from the transducers and signal conditioners (see Sections 3.2 and 3.3) must ultimately be converted to a digital format. This digital conversion may occur on-line prior to telemetry and/or data recording and storage operations, as discussed in Sections 3.4 and 3.5.2. In other cases where the data are initially acquired and stored in analog form, usually as FM tape recordings, the digital conversion may be accomplished after the data acquisition when the analog signals are reproduced for data analysis. Figure 2.2 shows some of the alternatives. In any case, a digital conversion operation must be performed by an instrument generally referred to as the analog-to-digital converter (ADC).

3,7,1 **Instruments.** A wide range of ADCs are commercially available [3.103]. For the case of special purpose digital signal analysis equipment, digital telemetry, and digital tape recorders, the ADC is an integral part of a more general instrument. For those cases where the ultimate data analysis will be accomplished on a general purpose digital computer, the ADC will probably be a separate instrument.

3.7.1.1 **Operating Principles.** Early ADCs were commonly mechanical devices that used a shaft angle-to-digital conversion procedure. Essentially all modem ADCs, however, are direct voltage-to-digital (electronic) devices. The detailed operating principles for electronic ADCs vary widely [3.1, 3.2,3.103, 3.104], but the basic elements in the simplest type of device are schematically illustrated in Figure 3.83. The input analog signal is passed through a "sample-and-hold" amplifier

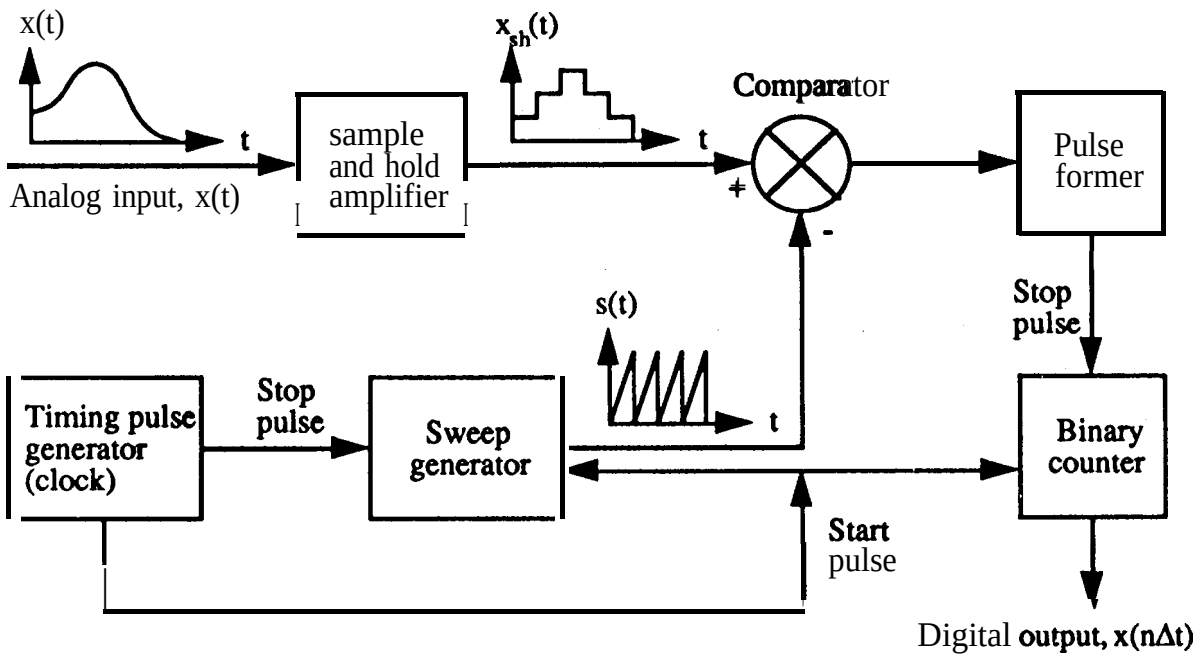

Figure 3.83. Schematic Diagram for a Simple Analog-to-Digital Converter.

to make the input signal appear as a step function with a constant time duration per step. This step version of the analog input is then compared to a repetitive ramp function produced by a sweep generator driven by a timing pulse generator or clock. A binary counter is initiated at the start of each sweep cycle, and is stopped at the instant the sweep signal value coincides with the input analog value out of the sample-and-hold amplifier. This produces a series of digital values representing the values of the input analog signal spaced al equal time increments.

3.7.1.2 Digital Formats. Commercird ADCs are usually either binary or ASCII (American Standard Code for Information Interchange) systems. A binary system maps a continuous signal onto a set of two digits, namely, O or 1, while an ASCII system maps the signal onto a set of ten digits, specifically, O to 9. Binary systems are simpler to build, but usually require machine-language programming to process data. Conversely, ASCII systems are functionally more complicated and less efficient, but have the advantage that data maybe read directly by any computer program written in a common language, such as FORTRAN. Also, ASCII systems can drive terminal and register displays directly. Essentially all special purpose signal processing instruments, where the ADC inputs directly to data analysis algorithms, use binary systems. ASCII systems are generally used only for simple "stand-alone" instruments, such as digital voltmeters.

3.7.1.3 Dynamic Range. From Section 2.4, the dynamic range (DR) of any system is generally defined as

$$DR = 10\log_{10}\left(\frac{x_{max}}{x_{min}}\right)^2 \qquad \text{(dB)} \qquad (3.15)$$

where x_{max} is the maximum instantaneous value of the signal that can be transmitted by the system without distortion, and x_{min} is the minimum detectable value of the signal at the output display. For ADCS, it is common to assume x_{min} is the digital resolution increment Ax provided by the ADC. Starting from zero, the maximum range for an ADC is $x_{max} = (2^n - 1)$ Ax, where n is the ADC word size; i.e., the number of bits (excluding a sign-bit) used by the ADC to express a number. It follows that the dynamic range of the ADC can be expressed in dB by

$$\begin{aligned} \text{ADC DR} &= 10\log_{10}(2^n - 1)^2 \qquad \text{(dB)} \\ &\approx 6n\ ;\ n > 5 \end{aligned} \qquad (3.16)$$

The dynamic range of an ADC can also be expressed in terms of a peak signal-to-noise level (PS/N), which from Section 2.4 is given by

$$Ps/N = 10\log_{10}\left(\frac{x_{max}}{\sigma_n}\right)^2 \qquad \text{(dB)} \qquad (3.17)$$

where σ_n is the standard deviation of the noise. For an ADC, the noise can be viewed as the round-off error associated with converting the instantaneous value of a continuous analog signal into a number taken from a finite set of numbers, determined by the AD(! word size. If it is assumed the round-off error (often referred to as the digital or computational noise) occurs randomly with a uniform distribution over the digital resolution interval Ax, the standard deviation of the round-off error is given by $\sigma_n = \Delta x/\sqrt{12}$, [3.105, 3.106]. From Equation (3.17), the peak signal-to-noise level is then given by

$$\text{ADC PS/N} = 10 \log_{10} [12 (2^{n} - 1)^2] \quad \text{(dB)}$$
$$\approx 6n + 11 \; ; \; n > 5 \qquad (3.18)$$

The word size for modem ADCs generally ranges from 6 to 18 bits, with 10 or 12 bits being the most common in current use, and 16 bits available in the newest instruments. The dynamic range and the peak signal-to-noise level provided by an ADC with these various word sizes are summarized in Table 3.13. The data in Table 3.13 represent the theoretical maximum DR and PS/N, respectively, that can be provided by the ADC. In practice, other factors (e.g., analog noise in the ADC) often limit the DR and PS/N to something less than these theoretical values, particularly when the word size is large. Hence, to be conservative, the word size used to estimate the DR and/or PS/N of an ADC should be one less (two less if a sign-bit is used) than the actual word size quoted for the ADC.

It is recommended that the analog-todigital conversion of acquired dynamic data be performed with an ADC that has a word size of no less than 10 bits (excluding the sign-bit, if used). This provides aDR254 dB (PS/N265 dB), which usually will be better than the net signal-to-noise level of the analog instruments in the data acquisition system preceding the ADC, particularly if an analog FM telemetry system is used to transmit the signals or an FM tape recorder is used to store the signals prior to the ADC. It should be mentioned that some of the older "on-board" Pulse Code Modulation (PCM) systems that may still be in use in the aircraft industry have only 8 bit ADCs.

Table 3.13. Decimal Digits and Peak Signal-to-Noise Level for Analog-to-Digital Converters.

Word Size (Number of Bits)	Range of Counts	Number of Decimal Digits	ADc Dynamic Range, dB	Peak Signal-To-Noise Level, dB
6	63	1.8	36	47
8	2 5 5	2.4	48	59
10	1,023	3.0	60	71
12	4,095	3.6	72	83
14	16,383	4.2	84	9 5
16	65,535	4.8	96	107

As these older systems are retired, it is recommended that they be replaced by newer systems with at least 10 bit, and preferably 12 bit, ADCs.

3.7.2 Sampling Rate and Aliasing. Analog-to-digital conversion is normally performed with a fixed time interval between sample values, denoted by At in sec. This sampling interval is clearly related to the sampling rate of the ADC, denoted by R_s in samples/see (sps), i.e., R_s = l/At. Sampling rates for current "off the shelf' ADC instruments range up to $R_s = 10^7$ sps for 12-bit words 'and $R_s = 10^6$ sps for 16-bit words.

The sampling rate R_s introduces an upper frequency limit on the resulting digital data, independent of the frequency limits that may be imposed on the analog signal by the data acquisition system prior to the digital conversion. Specifically, since at least two sample values per cycle are required to describe a frequency component in a continuous analog signal, the analog-to-digital conversion imposes an upper frequency limit of

$$f_N = 1/(2\Delta t) = R_s/2 \qquad (3.19)$$

where f_N is called the Nyquist frequency (sometimes called the folding frequency). If the sampling rate of the ADC is such that there are frequency components in the sampled analog signal above the Nyquist frequency f_N, these components will appear in the digital data at frequencies below f_N, as shown in Figure 3.84. This unwanted phenomenon is called "aliasing". The frequencies in the original data above f_N that will be aliased with fin the range $0 < f \leq f_N$ are defined relative to f_N by

$$f_{al} = (2nf_N \pm f); \; n = 1,2,3, \ldots \qquad (3,20)$$

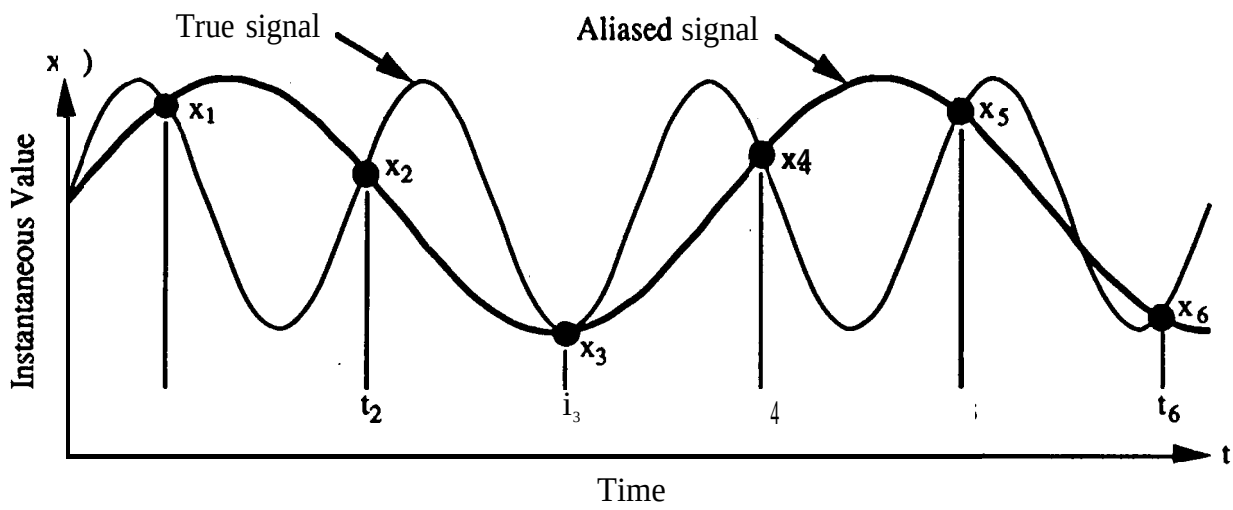

Figure 3.84. Illustration of Aliasing due to an Inadequate Digital Sampling Rate.

The consequences of aliasing in the computation of an autospectrum for a random signal (see Section 5.4.3) are illustrated in Figure 3.85. It is important to understand that once the analog-to-digital conversion is completed, there is no way to know from the digital data if aliasing occurred, Furthermore, even if it were known that aliasing occurred, there is no practical *way* to correct the digitized signal for aliasing induced errors. See [3.' 05, 3.106] for details.

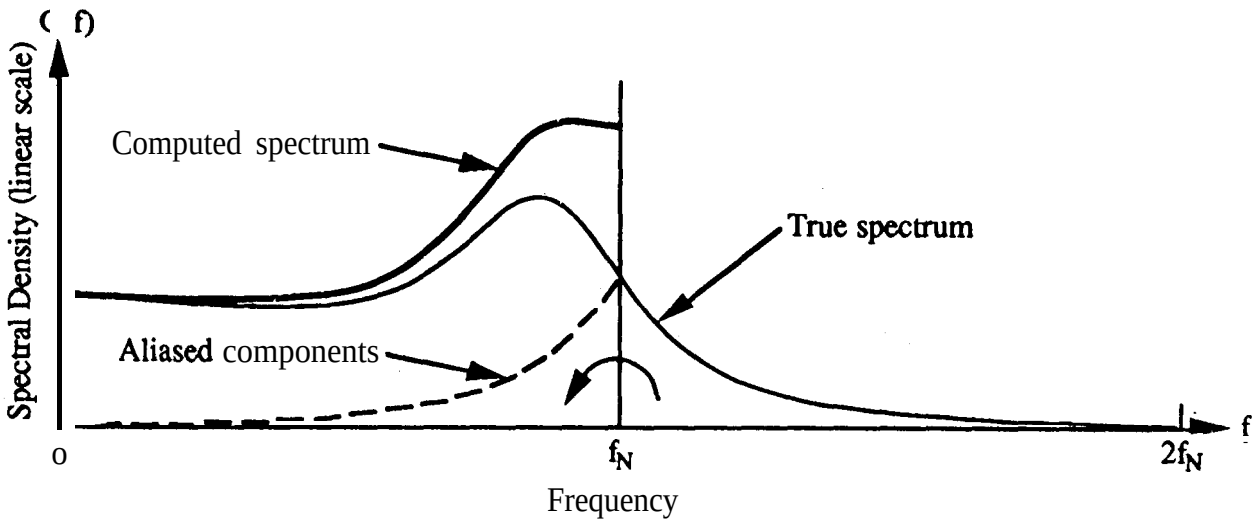

Figure 3.85. Illustration of Aliasing Error in the Computation of an Autospectral Density Function.

3.7.3 Anti-Aliasing Filters and Errors. Because of the severe distortion aliasing can introduce into digital data, it is imperative that aliasing be made negligible by assuring the analog signal being sampled has no significant frequency components above the Nyquist frequency, fixed by the ADC sampling rate. This is accomplished through the use of an analoglowpass falter at the input to the ADC, referred to as the anti-aliasing filter. Of course, the Nyquist frequency for the digital conversion of data signals may sometimes be much higher than what is believed to be the upper frequency limit of the analog instrumentation used to acquire the signals. Nevertheless, due to the possibility of unexpected high frequency components in the analog signals and the potentially disastrous consequences of aliasing, under no circumstances should analog-to-digital conversion be accomplished without an analog lowpass (anti-aliasing) filter at the input to the ADC.

3.7.3.1 cut-off Frequency. To provide a margin of safety, the upper cut-off frequency of the analog lowpass anti-aliasing filter, denoted by f_c, should be set somewhat below the Nyquist frequency f_N. The desired value of f_c relative to f_N depends on the cut-off rate of the anti-aliasing filter, the type of analysis to be performed, and the anticipated mean square value (power) in the signal above f_N. For most applications, the following recommendations apply:

(1) A lowpass anti-aliasing filter with a cut-off rate of at least 60 dB/octave should be used for the analog-to-digital conversion of all dynamic data.

(2) With a 60 dB/octave cut-off rate, the half-power point cut-off frequency of the filter should be set at $f_c \leq 0{,}6\ f_N$.

(3) If the anti-aliasing filter has a more rapid cut-off rate, a higher cut-off frequency can be used, but the bound $f_c \leq 0{,}8\ f_N$ should never be exceeded

See Section 5.5.3 for the more restrictive recommendations that apply to the digital conversion of transient signals for shock response spectrum computations.

3.7.3.2 Oversampling Procedure. In recent years, ADC systems that employ oversampling and digital anti-aliasing filters have come into wide use. These ADCS operate at a very much higher sampling rate (commonly 10^6 sps or higher) than is required for the upper frequency limit of dynamic data analysis (usually 20 kHz or less). 'he oversampled signal is then digitally lowpass filtered and decimated to obtain a digital time history with a lower sampling rate and upper cut-off frequency appropriate for the desired data analysis. Of course, a lowpass analog filter must still be used prior to the ADC to suppress aliasing in the original analog signal, but the final anti-aliasing operation is accomplished by a lowpass digital filter with a much lower cut-off frequency. Hence, the characteristics of the analog filter are not critical to the resulting digital data. This approach to the suppression of aliasing offers two advantages, namely, (a) digital filters with desirable cut-off and phase characteristics are cheaper and more stable than analog filters, and (b) the digital lowpass faltering/decimation operation will enhance the signal-to-noise level of spectra computed from the resulting digital time series [3, 107].

3.7.3.3 Magnitude Errors. It is obviously desirable for anti-aliasing filters to have a flat frequency response over the widest possible frequency range below the cut-off frequency f_c. However, compromises are sometimes required to achieve the desired phase characteristics discussed in Section 3.7.3.4. In any case, it is recommended that the frequency response of anti-aliasing filters be flat to within a maximum of ± 10% (preferable to within ± 5%) over the frequency range where the spectral properties of the signals will be computed during data analysis.

3.7.3.4 Phase Errors. Most lowpass filters produce frequency dependent phase shifts in the signals they pass, particularly at frequencies near the cut-off frequency of the filter. Hence, the lowpass filtering operation for anti-aliasing purposes may introduce phase errors that will distort the time history of the signal. If the ultimate goal of the data acquisition is, for example, a single channel autospectrum analysis, phase errors in the time history are unimportant since they do not influence the autospectrum computation (see Section 5,4.3). On the other hand, time domain analyses, such as probability density or shock response spectrum computations, and dual channel analyses, such as cross-spectrum and frequency response computations, may be adversely affected by phase errors.

To suppress such potential problems, filters that provide a constant time delay (linear phase) are theoretically desirable for anti-aliasing purposes. Bessel falters have a linear phase function below their cut-off frequency, but are not recommended because of their poor cut-off characteristics. Butterworth filters have good cut-off characteristics, but introduce a nonlinear phase, particularity near the cut-off frequency. Elliptical filters can be designed to have good cut-off characteristics and near-linear phase up to the cut-off frequency, but their frequency response above the cut-off frequency may reveal strong leakage lobes. Of course, if the final anti-aliasing operation is accomplished using digital filters, as discussed in Section 3.7.3.2, anti-aliasing filters of any type can provide a zero phase shift at all frequencies by filtering the sequence of digital values first forward and then backward in time, For certain types of analyses (e.g., the computation of shock response spectra), the potential errors introduced by the nonlinear phase characteristics of the anti-aliasing filter can be avoided by simply limiting the analysis of the signal to about two-thirds of the cut-off frequency of the filter [3.108].

In general, either Butterworth or elliptical filters are recommended for anti-aliasing purposes, although other types of filters maybe acceptable depending on the analyses that will be performed and their ultimate applications. However, what ever type of filter is selected, the recommendations in Sections 3.7.3.1 and 3.7.3.3 regarding the falter cut-off rate and frequency response apply.

For dual channel analysis, the frequency responses (both the magnitude and phase characteristics) of the anti-aliasing filters should be carefully matched. Precisely matched lowpass falter characteristics are most easily achieved using the procedure discussed in the Section 3.7.3.2, where the analog signal is originally sampled at a much higher rate than needed for the analysis, and is then digitally lowpass filtered and decimated [3,107].

3.7.4 Other ADC Errors. Beyond the digital noise and aliasing problems, there are various other potential sources of error that can be introduced by the ADC. The most important of these are as follows:

(1) Aperture error, arising from the fact that each data sample is taken over a finite period of time rather than instantaneously.

(2) Jitter, arising from the fact that the time interval between samples can vary slightly in some random manner.

(3) Nonlinearities, arising from such sources as bit drop-outs, quantization spacing, and zero discontinuity.

In modern ADC instruments that are properly maintained, the errors in the digital time history due to these miscellaneous sources should be negligible. See [3.103, 3.106] for details.

3.7,5 Multiple-Channel Digital Conversion. It is common to acquire and digitally convert two or more measurements simultaneously, often with the intention of later performing various dual channel analyses such as cross-spectral density, coherence, frequency response, and cross-correlation computations (see Section 5.6). Since the ADC will commonly have a very much higher sampling rate than required to achieve the desired Nyquist frequency for a single signal, multiple signals can usually be digitized by time division multiplexing through a single ADC. In other cases, where there are a large number of signals that must be analyzed to relatively high frequencies, parallel ADC instruments maybe required.

3.7.5.1 Digital Conversion through a Single ADC. Let R_s be the sampling rate (corresponding to a sampling interval of At) for an ADC, and R_{s1} be the desired sampling rate (corresponding to a sampling interval of At,) for each of a collection of k signals to be digitized. It follows that the k signals can be converted to digital values by sequential sampling through the single ADC as long as $kR_{s1} \leq R_s$. However, if this is done by multiplexing the signals into a single sample-and-hold amplifier, there will be a time delay of $\Delta\tau$ between the nth sample value from one digital time history to the next. For those cases where the digitized signals are to be analyzed in terms of single channel quantities only (see Sections 5.4 and 5.5), this slight offset in the time base of the various signals poses no problem. On the other hand, if the signals are to be used for dual channel analysis, such as frequency response estimates (see Section 5.6.3), the time base offset will translate into a linear phase error in the resulting computations. Of course, this phase error can be corrected by appropriate software, but a better procedure is to avoid the time base offset initially by using multiple sample-and-hold circuits in the ADC that will store the k signal values sampled simultaneously from the k channels until all are sequentially converted into digital words, It is recommended that ADCS with multiple sample-and-hold circuits be used for the digital sampling of all data signals intended for dual channel analysis of any type.

3.7.5.2 - Conversion through Parallel ADCs. Using the notation defined in the foregoing section, if $kR_{s1} > R_s$, it follows that two or more ADCS will be needed to simultaneously convert k signals into digital time histories. For those cases where the digitized signals are to be analyzed in terms of single channel quantities only (see Sections 5.4 and 5.5), the use of multiple ADCs poses no problem. However, no type of dual channel analysis should ever be attempted on two digital time histories produced by two independent ADCs. The problem here is similar to that associated with a dual channel analysis of two signals recorded on two separate tape recorders (see Section 3.5). Specifically, two independent ADCs cannot be perfectly phase coherent. Hence, even when the input to the two ADCS is a common analog signal, the digital time histories produced by the two ADCS will have a coherence that diminishes with increasing frequency.

The problem of maintaining phase coherence among two or more ADCs can be resolved by slaving the ADCs to a single master unit, so that the sample times are determined by a common timing pulse generator or clock. This procedure is commonly used in equipment with multiple ADCs, and

is strongly recommended for all data acquisition where dual channel analyses of the resulting digital time histories may be required.

3.7.5,3 Other Multiple-Channel Phase Errors. Beyond the possible time off-set problem discussed in Section 3.7.5.1, there are two other sources of relative time delays among the channels in a multiple-channel digital conversion that must be considered and corrected for later dual channel analyses. The first is the time delay in sample-and-hold amplifiers caused by different carrier signal frequencies. The second is the relative time delays caused by the different lag times of subsystems in the data acquisition system. In both cases, the resulting phase error between any two channels will be linear. Hence, it can be easily corrected in the later data analysis if it is detected and quantified by appropriate calibration procedures discussed in Section 3.8.

3.7.6 Digital-to-Analog Converters. There is sometimes a need to convert a digitized time history, or some digital analysis of that time history, back to an analog signal, This operation is easily accomplished using a digital-to-analog converter (DAC). The underlying theory governing the operation of a DAC is the sampling theorem [3.105], which may be broadly stated as follows: If an analog signal x(t) is digitally converted to N equally spaced discrete values, x_i; i = 1, 2, ..., N, such that $N \geq 2BT_r$, where B is the bandwidth of the signal and T_r is the measurement duration, then the original signal x(t) can be recovered from the digital values, x_i; i = 1,2, ..., N, by interpolation, See [3. 103, 3,104] for details on the operation of a DAC and appropriate interpolation circuits.

3.8 System Calibration. The calibration procedure for all elements of the data acquisition system may be divided into three separate categories; (a) laboratory calibrations of individual instruments, (b) end-to-end electrical calibrations of the system, and (c) end-to-end mechanical calibrations of the system.

3.8.1 Laboratory Calibration. Most organizations engaged in the acquisition of dynamic data have a specific group or instrument laboratory that is responsible for providing the necessary instrumentation. Such groups commonly have a formal procedure and schedule for the routine maintenance and calibration of individual transducers and instruments, If such a group does not exist, it is recommended that it be created as outlined in MIL-STD-45662A [3.109]. The exact details of how the transducers and instruments are maintained and calibrated should be based upon the manufacturer's recommendations, with additional guidance from established reference e.g., [3.6, 3.8, 3.22,3.109- 3.112], However, certain minimum requirements are recommended, as follows:

3.8.1.1 Transducers. It is recommended that all reusable transducers (e.g., accelerometers and pressure transducers) be calibrated against a National Institute of Standards and Technology (NIST, formerly the National Bureau of Standards) traceable reference in compliance with MIL-STD-45662A at least once a year, or after any usage or accident where possible damage or extreme

conditions beyond the advertised limits of the transducer are suspected. A more frequent calibration schedule should& used if recommended by the transducer manufacturer. For the special case of accelerometers used for pyroshock measurements, a calibration before and after each usage is suggested. The calibrations should be performed at selected amplitudes and frequencies covering the entire useful amplitude and frequency range of the transducer using procedures and equipment that control all facets of the dynamic environment, e.g., the amount of transverse excitation applied to an accelerometer being calibrated.

When transducers are newly purchased, or are recalibrated by a calibration service, a certificate should be provided that states the traceability to NIST through an identified transfer standard transducer. This certificate should arly state which portion of the calibration is simply typical for the transducer type or model, and which is actually measured on the transducer being calibrated

3.8.1.2 Other Instruments. All signal conditioners, data recording and storage devices, telemetry, and mux/demux instruments, whether analog or digital, and all independent ADCs should receive routine maintenance and calibration in accordance with the manufacturer's recommendations at least once a year. The exception to this recommendation is the tape or cassette re er/reproducer, whose electromechanical assemblies require maintenance and calibration based on usage, i.e., recording, reproducing and rewind time, and total tape length. Tape heads need regular inspection for oxide removal, head wear, and azimuth adjustment. Record and reproduce electronics should be routinely checked for carrier and/or subcarrier center frequency and band edge (or modulation index) deviations, as applicable. Tape copying and storage issues are summarized in Sections 3.6.7 and 3.6.8, respectively. Thorough discussions and recommendations for recorder maintenance and tape storage are available from manufacturers and [3.95 - 3,97].

All cables and land lines, and their connectors, should receive routine inspection, and if warranted, repair or replacement at least once a year.

Beyond the above recommendations, all signal conditioners, data recording and storage devices, telemetry, mux/demux instruments, and all independent ADCS, that are used for multiple-channel analysis should be checked at least once a year for static and dynamic time base errors between channels or tracks by the following procedure:

(1) Insert a common random signal with a nearly uniform autospectrum (see Section 5,4.3) simultaneously into all channels or tracks of the instrument. The bandwidth for the input random signal should exceed the advertised bandwidth of the instrument being calibrated.

(2) Compute the coherence and phase (see Sections 5,6.1 and 5.6.2) between the output of each channel or track of the instrument with every other channel or track.

(3) The phase between the output of each channel or track versus all other channels or tracks should be zero over the entire frequency range of the instrument. A non-zero phase between the two channels or tracks is usually caused by a fixed time delay, which will appear as a linear ramp function starting with zero phase at zero frequency, as illustrated in Figure 3.86. If possible, adjustments should be made to the instrument to make the phase zero at all frequencies. Otherwise, the phase versus frequency measured between the various channels or tracks should be recorded and used to make corrections to the phase computed during later dual channel analyses (see Section 5.6) of the data acquired using that instrument.

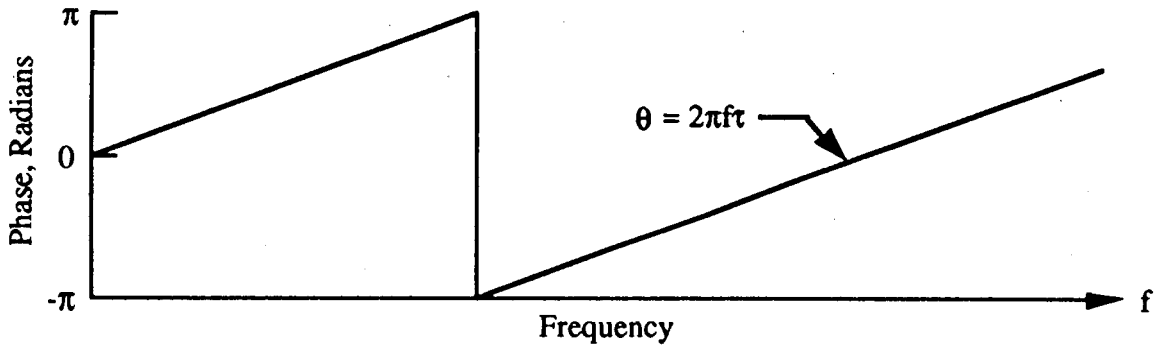

Figure 3.86. Illustration of Linear Phase Shift due to Time Delay between Two Instrument Channels or Tracks with a Common Input Random Signal.

(4) The coherence between the output of each track or channel versus all other tracks or channels should be unity over the entire frequency range of the instrument. If it is not, this is indicative of a dynamic time base error, a nonlinearity, or excessive noise in one or both channels or tracks of the instrument. For the case of analog tape recorders, a lack of perfect coherence between the tracks may be due to dynamic skew of the tape, which commonly produces a coherence plot like that shown in Figure 3.87. Problems of this type often cannot be corrected by simple adjustments, and may require an overhaul or replacement of the instrument,

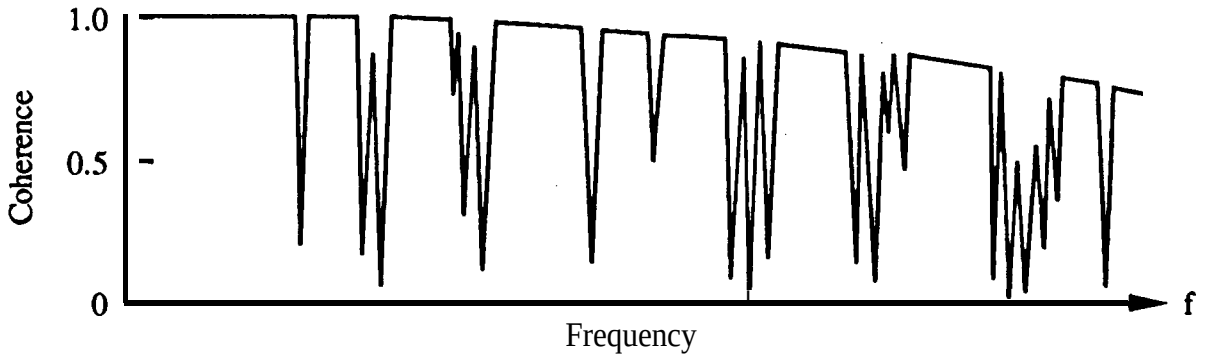

Figure 3.87. Illustration of Coherence due to Lack of Phase Lock between Two Instrument Channels or Tracks with a Common Input Random Signal..

3.8.2 **End-to-End Electrical Calibration**. An end-to-end electrical calibration means a full calibration of the instrumentation from the closest point to the transducer to the output where the analog or digital signal will normally be analyzed. It is recommended that an end-to-end electrical calibration be performed on all channels of the data acquisition system prior to each test for which the system is used. The calibration should be performed with the data acquisition system in its completed configuration, including all transducers mounted, cables installed, and all signal conditioner gains set as they will be for the actual measurements. If a different gain setting is used for the calibration, it should be recorded so that the calibration results can be later corrected for the gain used to make the actual measurements. In those cases where the squired data are to be recorded and stored for later analysis, the calibration signals should be recorded and stored in exactly the same manner, and the calibration performed on the output signals from the storage device. The lack of an appropriate end-to-end calibration is probably the most important of the major causes of errors in dynamic measurements, as listed in Section *2.10.*

End-to-end electrical calibration can be accomplished by either of two techniques:

(1) For most types of transducers (including piezoelectric), a calibration signal can be applied across a resistor inserted in the circuit between the transducer and the signal conditioner [3. 113], The voltage insertion circuit and power supply must be ungrounded. The various types of voltage insertion signals and the procedure for their application are described in Sections 3.8.2,1 through 3.8.2.4.

(2) For transducers which utilize (a) strain-sensitive materials (e.g., strain gages) in a Wheatstone bridge arrangement, and (b) signal conditioners and following electronics with a DC response, a known resistance can be applied across (Le., in parallel with) the resistor in one arm of the bridge, provided that the resistor in that arm is not a semiconductor. This shunt calibration procedure provides only a DC calibration of the system, and does not cover the remaining portions of the data bandwidth.

Both calibration techniques applied to a strain gage or piezoresistive transducer are illustrated in Figure 3.3.

3.8.2.1 **Calibration Signal**. Three types of signals maybe used for voltage insertion end-to-end electrical calibrations, as follows:

(1) A random signal with a nearly uniform autospectrum (see Section 5.4.3) over a frequency range that exceeds the bandwidth of the data acquisition system is considered the most desirable calibration signal (even when the actual data will be non-random) because it permits the rapid calibration of the system at all frequencies simultaneously, and allows a rigorous evaluation of system noise and/or nonlinearities.

(2) A sinusoidal signal at selected frequencies over the desired data bandwidth is a desirable calibration signal in that it is easy to implement and analyze, but it makes the calibration procedure more time consuming.

(3) A pulse calibration signal involving a simple step followed by a carefully controlled exponential decay may also be used to produce a nearly uniform Fourier magnitude spectrum (see Section 5.4. 1) over a frequency range that exceeds the bandwidth of the data acquisition system. Such a pulse signal allows a rapid calibration of the system at all frequencies simultaneously, but the decay rate of the pulse must be accurately determined and controlled. See [3.38] for details.

Before applying one or more of the following signal insertion procedures, the transducer manufacturer should be contacted to ascertain the appropriate calibration resistor, signal magnitude, and insertion procedures.

3.8.2.2 Electrical Calibration Procedure - Random Signal Insertion. When a wideband random calibration signal is used, it is recommended that all transducer channels be electrically calibrated by the following procedure:

(1) Insert a random calibration signal with an accurately defined autospectrum into each channel.

(2) Compute the coherence (see Section 5.6.2) between the input calibration signal and the output of that channel of the data acquisition system. The coherence should be in excess of 0.99 at all frequencies of interest. If it is not, every effort should be made to identify the reasons for the lesser coherence and correct the problem. See [3.114] for details on the common sources of poor coherence in measurement systems.

(3) Compute the frequency response (see Section 5.6.3) between the input calibration signal and the output of that channel of the data acquisition system. This frequency response establishes the voltage gain and phase of each channel of the data acquisition system. Deviations from a uniform gain and linear phase should be recorded for later corrections of the data.

(4) During the calibration of each channel, the cables in the data acquisition system for that channel should be moved about, and the output signal should be checked for noise spikes, power line pickup, and other evidence of faulty connectors, broken shields, multiple grounding points, and other motion-induced problems (see Section 4).

For those channels where dual channel analysis of the transducer signals is anticipated, the following additional calibration steps are recommended:

(5) Insert a common random signal with an accurately defined autospectrum simultaneously into all channels. This should be done in Step (1) above.

(6) Compute the coherence and phase (see Sections 5.6.1 and 5.6.2) between the output of each channel with the output of every other charnel.

(7) The phase between the output of each channel versus all other channels would ideally be zero over the entire frequency range of interest. However, due to differences in the instrumentation for the various channels, this may not occur. If not, the phase versus frequency measured between the various channels should be recorded and used to make appropriate corrections to the phase data computed during later dual channel analyses (see Section 5.6).

(8) The coherence between the output of each channel and all other channels should be in excess of 0.99 at all frequencies of interest. If it is not, every effort should be made to identify the source of the inadequate coherence and correct the problem. See [3.114] for details on the common sources of poor coherence in measurement systems.

3.8.2.3 Electrical Calibration Procedure Sinusoidal Signal Insertion. When a sinusoidal calibration signal is used, it is recommended that all transducer channels be electrically calibrated by the following procedure:

(1) Insert a sinusoidal calibration signal with an accurately defined rms value into each channel. The frequency of the sinusoidal signal should be at the reference frequency for zero dB in the frequency response calibration of the channels (usually 100 Hz).

(2) Determine the rms value of the output signal from each channel. The ratio of the output to input rms values establishes the voltage gain of each channel.

(3) Perform a spectral analysis (see Section 5.4.2) of the output signal from each channel. No harmonic (i.e., the spectral values at integer multiples of the input sine wave frequency) should have an amplitude that exceeds 5% of the fundamental amplitude. If it does, every effort should be made to identify the source of the signal distortion and correct the problem.

(4) During the calibration of each channel, the cables in the data acquisition system for that channel should be moved about, and the output signal should be checked for noise spikes, power line pickup, and other evidence of faulty connectors, broken shields, multiple grounding points, and other motion-induced problems (see Section 4).

For those channels where dual channel analysis of the transducer signals is anticipated, the following additional calibration steps are recommended:

(5) Insert a common sinusoidal signal with an accurately defined rms value simultaneously into all channels. This should be done in Step (1) above. The frequency of the sinusoidal signal should beat the reference frequency for zero dB in the frequency response calibrations of the channels (usually 100 Hz).

(6) Determine the phase between the output of each channel and the output of every other channel. This may be done using a phase meter or by a careful inspection of the two superimposed time histories on an oscilloscope.

(7) The calibration procedure should be repeated at different input frequencies to cover the frequency range of the anticipated data, and the phase should be measured and recorded between the various channels at each frequency. The phase between the output of each channel and all other channels should ideally be zero at the frequencies of the calibration signal. However, due to differences in the instrumentation for the various channels, this may not occur. If not, the phase measured between the various channels at the sinusoidal calibration frequencies should be recorded, the phase data should be interpolated over all frequencies of interest, and the result used to make appropriate corrections to the phase data computed during later dual channel analyses (see Section 5.6).

3,8.2.4 Electrical Calibration Procedure - Pulse Signal Insertion. When a pulse calibration signal is used, it is recommended that all transducer channels be electrically calibrated by the following procedure:

(1) Insert a pulse calibration signal with an accurately determined exponential decay rate that provides a well-defined Fourier spectrum into each channel.

(2) Compute the frequency response between the input calibration signal and the output of that channel of the data acquisition system. This can be done by computing the ratio of the Fourier magnitude spectra and the difference between the Fourier phase spectra for the output and input signals. This frequency response establishes the voltage gain and phase of each channel of the data acquisition system, Deviations from a uniform gain and a linear phase should be recorded for later corrections of the data.

(4) During the calibration of each channel, the cables in the data acquisition system for that channel should be moved about, and the output signal should be checked for noise spikes, power line pickup, and other evidence of faulty connectors, broken shields, multiple grounding points, and other motion induced problems (see Section 4).

For those channels where dual channel analysis of the transduce{ signals is anticipated, the following additional calibration steps are recommended:

(5) Insert a common pulse signal with an accurately defined Fourier spectrum simultaneously into all channels. This should be done in Step (1) above.

(6) Compute the phase between the output of each channel with the output of every other channel from the difference between the Fourier phase spectra for each pair of outputs.

(7) The phase between the output of each channel versus all other channels would ideally be zero over the entire frequency range of interest. However, due to differences in the instrumentation for the various channels, this may not occur. If not, the phase versus frequency measured between the various channels should be recorded and used to make appropriate corrections to the phase data computed during later dual channel analyses (see Section 5.6).

3.8.2.5 Reconciliations of Calibration Discrepancies. A check of the data acquisition system electrical calibrations should be accomplished using the following procedure:

(1) Using the laboratory calibrated gains of the individual instruments in the data acquisition system (as determined in Section 3.8.1), compute the net gain of each channel from the output of the transducer, through the data acquisition system, to the output (analog or digital) signal that will be analyzed.

(2) Compare the net gain of each channel computed from the individual instrument gains in Step (1) to the channel gain determined from the end-to-end electrical calibration in Sections 3.8.2.2 through 3.8.2.4, and determine if there is a discrepancy. If a discrepancy in excess of 5% for any channel is found, every effort should be made to identify the source of the discrepancy and correct the problem.

(3) If the discrepancy cannot be resolved, but it is confined that there were no errors made in the end-to-end electrical calibration, it is recommended that the results of the end-to-end electrical calibration be accepted as the correct system calibration. It is further recommended that, following the test, new laboratory calibrations (see Section 3.8, 1) be performed on all instruments used in the data acquisition system,

3.8.3 End-to-End Mechanical Calibration. An end-to-end mechanical calibration means a full calibration of the instrumentation from the actual physical input to the transducer to the output where the analog or digital signal will normally be analyzed. Mechanical calibrations are generally limited to data channels for accelerometers and microphones where the introduction of a known physical input is easily achieved. Specifically, calibration shakers can be used for accelerometers, although this may require removing the accelerometer from its actual mounting location for calibration purposes. Pistonphones or other pressure generating devices are available for microphones, which may or may not require removing the microphone from its mounting location, depending

upon the installation. The calibrations of remote or hard-to-reach transducers often must be accomplished during the assembly of the test configuration, which requires advanced planning. In those cases where the transducer must be removed from its final mounting location for calibration purposes, it is recommended that at least a crude functional check be performed after the final installation by applying an uncalibrated input to the transducer, e.g., tap accelerometers and speak into microphones to confirm that they are generating signals. In any case, all other instruments in the data acquisition system should be in their completed configuration; i.e., all cables installed and all signal conditioner gains set as they will be for the actual measurements. If a different gain setting is used for the calibration, it should be recorded so that the calibration results can be later corrected for the gain used to make the actual measurements. In those cases where the acquired data are to be recorded and stored for later analysis, the calibration signals should be recorded and stored in exactly the same manner, and the calibration performed on the output signals from the storage device.

End-to-end mechanical calibrations are recommended for all accelerometer and microphone channels in the data acquisition system prior to each test.' An end-to-end mechanical calibration of a given transducer channel generally constitutes a final check on the calibration of that channel, and may replace the end-to-end electrical calibration (see Section 3.8.2) of that channel in some (but not all) cases to be described shortly.

3.8.3.1 Calibration Signal and Insertion Procedure. There are theoretically three types of signals that may be used for end-to-end mechanical calibrations, namely, wideband random, sinusoidal, and step. Wideband random inputs are usually limited to accelerometers employed in laboratory tests, where a shaker can be used as the physical source of excitation. Sinusoidal excitation can be applied to accelerometers through simple field calibration shakers, and to microphones through equally simple field pistonphones [3.6, 3,8, 3.22]. Such field calibration devices for both accelerometers and microphones are commercially available. Step mechanical calibration inputs are most common for accelerometers with a DC response and relatively high sensitivity (see Section 3.2.1). For these devices, an accurate step input can be applied by simply turning the accelerometer up side down to obtain a change in the acceleration input from +1g to -lg. In some cases, a step calibration of an accelerometer can be accomplished after installation if the instrumented structure can be moved from one orientation to another in a carefully controlled way, e.g., when an instrumented launch vehicle is raised from a horizontal to a vertical position for launch. However, it should be noted that this DC calibration does not cover the remaining portions of the data bandwidth.

3.8.3.2 Mechanical Calibration Procedure · Random Excitation. For the special case of accelerometers and other motion transducers in a data acquisition system being used for a laboratory test, a wideband random mechanical calibration of the applicable transducer channels of the data acquisition system may be performed using the following procedure:

(1) Mount all accelerometers on a shaker with a transfer standard (calibration reference) accelerometer. The reference accelerometer will provide a voltage signal representing the vibration input from the shaker. All other instruments of the data acquisition system should be complete and in their final configuration.

(2) Apply a precisely defined wideband random excitation simultaneously to the accelerometers. If possible, the bandwidth for the input random excitation should cover the desired bandwidth for the measurements. However, the excitation bandwidth must never exceed the frequency range for uniform shaker table motion.

(3) Using the output of the reference accelerometer as the input calibration signal, perform the calibration detailed in Steps (2) through (8) in Section 3.8.2.2.

An end-to-end mechanical calibration with random excitation is considered optional, but if it is performed, all end-to-end electrical calibrations recommended in Section 3.8.2 for those motion transducers can be omitted, An exception is the electrical noise checks of the data acquisition system, which should always be performed with the transducer mounted in place, as detailed in Step (4) of Sections 3.8.2.2.

3.8.3.3 Mechanical Calibration Procedure - Sinusoidal Exe_. For all accelerometers or other motion transducers, and all microphones being used in a data acquisition system for either a ground or flight test, it is recommended that a sinusoidal mechanical calibration of the applicable channels of the data acquisition system be performed. For test articles that are sufficiently small to be vibrated by a single shaker, the calibration of motion transducers should be performed as follows:

(1) Mount all accelerometers on the test article with all instruments of the data acquisition system complete and in their final configuration.

(2) Apply a sinusoidal excitation to the test article with a shaker capable of producing a significant acceleration of the test article with an accurately defined rms value at a frequency less than 20% of the first normal mode frequency of the test article (so that the test article essentially responds as a rigid body).

(3) Using the known magnitude of the sinusoidal excitation as the input calibration signal, perform the calibration steps detailed in Section 3.8.2,3.

For test articles that are too large to be vibrated by a single shaker, the calibration of motion transducers should be performed using the following procedure:

(1) Mount all accelerometers on a shaker with a transfer standard (calibration reference) accelerometer. The reference accelerometer will provide a voltage signal representing the vibration input from the shaker, All other instruments of the data acquisition system should be complete and in their final configuration.

(2) Apply a sinusoidal excitation simultaneously to the accelerometers. The frequency of the sinusoidal signal should be at the reference frequency for zero dB in the frequency response calibration of the channels (usually 100 Hz). In no case, however, should the frequency of the sinusoidal excitation exceed the frequency range for uniform shaker table motion,

(3) Using the output of the reference accelerometer as the input calibration signal, perform the calibration detailed in Steps (2) through (7) in Section 3.8.2.3.

For microphones, the calibration should be performed using the following procedure:

(1) Attach sequentially to each microphone a pistonphone that delivers sinusoidal excitation with an accurately defined rms value. All other instruments of the data acquisition system should be complete and in their final configuration.

(2) Apply a sinusoidal excitation to each microphone. The frequency of the input sine wave may be fixed by the pistonphone, but if not, the frequency should beat the reference frequency for zero dB in the frequency response calibration of the microphones (usually 100 Hz).

(3) Using the known magnitude of the sinusoidal excitation as the input calibration signal, perform the calibration detailed in Steps (2) through (4) in Section 3.8.2.3.

An end-to-end mechanical calibration with sinusoidal excitation is recommended whenever a mechanical calibration with wideband random excitation cannot be performed. Although redundant, it is not recommended that the end-to-end mechanical calibration replace the end-to-end electrical calibration detailed in Section 3.8.2. The mechanical calibration in this case should be viewed as a final check on the data acquisition system.

3.8.3.4 Mechanical Calibration Procedure - Step Excitation. For those accelerometers that sense static acceleration (i.e., have a frequency response down to DC) and are sufficiently sensitive for 1g to provide a significant output without saturation, it is recommended that a step mechanical calibration of all applicable channels of the data acquisition system be performed using the following procedure:

(1) Place each applicable accelerometer, with the sensitive axis in the vertical direction, on a flat, horizontal surface of a table or other object with a benign vibration environment. With all

other instruments of the data acquisition system complete and in their final configuration, measure the DC output of that channel in the data acquisition system.

(2) Using the same mounting surface, turn the accelerometer up side down, and again measure the DC output of that channel in the data acquisition system.

(3) The difference between the measured outputs in Steps (1) and (2) constitutes an exact ±1g static calibration of the data acquisition system.

3.8.3.5 Reconciliations of Calibration Discrepancies. A check of the data acquisition system mechanical calibrations should be accomplished using the following procedure:

(1) Using the laboratory calibrated sensitivities of the transducers and the gains of the individual instruments in the data acquisition system (as determined in Section 3,8.1), compute the net gain of each channel from the physical input to the transducer, through the data acquisition system, to the output (analog or digital) that will be analyzed.

(2) Compare the net gain of each channel computed from the transducer and individual instrument gains in Step (1) to the channel gain determined from the end-to-end mechanical calibration in Sections 3.8.3.2 through 3.8.3.4, and determine if there is a discrepancy. If a discrepancy in excess of 5% for any channel is found, every effort should be made to identify the source of the discrepancy and correct the problem.

(3) If the discrepancy cannot be resolved, but it is confirmed that there were no errors. made in the end-to-end mechanical calibration, a second comparison should be made against the results of the end-to-end electrical calibration in Section 3.8.2, coupled with the laboratory calibrated sensitivity of the transducer. If a discrepancy still exists, this indicates there is a conflict between the laboratory calibrated sensitivity of the transducer and its actual sensitivity in the data acquisition system.

(4) Since a change in the sensitivity of a transducer from the laboratory calibrated values is often indicative of damage that might alter the frequency response and other critical properties of the transducer, it is recommended that such transducers be removal from the data acquisition system immediately (before the test is performed), and be replaced by different transducers that produce no conflicts in the Step (3).

3.8.4 Linearity Calibrations - Individual instruments and/or entire data acquisition systems are often checked for linearity and/or stability using the calibration procedures detailed in Sections 3.8.1 through 3.8.3, where the input (either physical or an electrical equivalent) to the instrument or system is applied at several different levels with well defined units of magnitude, and the output

voltage of the instrument or system is measured at each input level. This approach yields a calibration function in terms of volts/unit, when in fact a calibration function in terms of units/volt is desired; i.e., the calibration is essentially done backwards. If the measured calibration function is perfectly linear with no scatter, a correct calibration factor in units/volt can be determined accurately by taking the reciprocal of the slope of the measured function in volts/unit. However, if the measured calibration function deviates from a perfect linear relationship, or reveals significant scatter about a straight line, then taking the reciprocal of the slope of a straight line fitted to the measured volts/unit data can lead to an erroneous calibration in units/volt. In such cases, the following calibration procedure is recommended:

(1) Plot the input units versus the output volts at each level, i.e., let the output volts be the independent variable x_i; i = 1,2, ..., N, and the input units be the dependent variable y_i; i = 1,2, ..., N.

(2) Determine a linear approximation for the average calibration factor b in units/volts by computing the slope of the regression line for y on x using conventional least squares procedures [3,63], i.e.,

$$b = \frac{\sum_{i=1}^{N} x_i y_i}{\sum_{i=1}^{N} x_i^2} \tag{3.21}$$

3.9 System Gain Settings. After the pre-test system calibration, the gain settings for the instrumentation system must be set for the actual data measurements. For laboratory tests and those field tests where a technician can maintain on-line control of the data acquisition system, proper gain settings can be established by trial-and-error procedures during the initial collection of data signals, assuming the test produces stationary or steady state data. For those cases where on-line control of the data acquisition system is not feasible and/or the data signals are nonstationary or transient, it will be necessary to preset the gains prior to the test based upon predictions for the maximum signal magnitudes expected during the test.

3.9.1 Stationary and Steady State Data with On-Line Control. When the data signals are stationary or steady state and on-line gain adjustments can be made, the following procedure for setting data acquisition system gains is recommended:

(1) Whenever possible, all signal gain adjustments for a given test, whether accomplished manually or by an automatic gain control (AGC) circuit, should be made in the transducer signal conditioner (or an independent amplifier on the output of the signal conditioner), prior to the first instrument (usually an ADC, data recorder, or telemetry transmitter) after the signal

conditioner. The gain settings for all data acquisition and analysis equipment after the signal conditioner should be fixed to an optimum value relative to a specific voltage (usually 1 volt zero-to-peak) into the first instrument after the signal conditioner,

(2) If the need for a change in signal gain or attenuation after the transducer signal conditioner cannot be avoided, such a change should be made at the input to the first instrument where a different signal magnitude is warranted, so as to optimize the signs.1-t~noise level for the entire data acquisition and analysis system.

(3) After the start of the data acquisition, set the signal conditioner gain to produce an output voltage signal that is just below (within one unit of gain resolution, usually 3 dB) the level that will cause an overload at the input to the first instrument after the signal conditioner.

3.9.2 Nonstationary and Transient Data. When the test data signals are nonstationary or transients, or on-line gain adjustments are not feasible, the following procedure for setting data acquisition system gains is recommended:

(1) The same as Step (1) in Section 3,9.1, except AGC circuits are not recommended for use in the acquisition of nonstationary or transient data.

(2) The same as Step (2) in Section 3.9.1.

(3) For periodic and transient data, predict the maximum instantaneous value of the anticipated signal in engineering units (g, psi, etc.). For random data, predict the maximum rms value of the anticipated signal in engineering units, and multiply this value by a crest factor (usually three) to obtain an equivalent maximum instantaneous value.

(4) Add a safety factor (often called "head-room") to the maximum instantaneous value predicted in Step (3) to allow for uncertainties in the maximum value prediction. The magnitude of the head-room must be governed by the confidence associated with the maximum value prediction, but should never be less than 3 dB.

(5) Using the calibration factor for the transducer, convert the maximum instantaneous value (with head-room) predicted in engineering units in Step *(4)* into a maximum voltage out of the signal conditioner. Then adjust the signal conditioner gain to make the maximum output voltage equal the maximum input voltage to the first instrument after the signal conditioner.

(6) If a sufficient number of instrumentation channels are available, consider using two or more channels for each transducer with different signal conditioner gain settings to increase the likelihood of obtaining a measurement with a near optimum input signal level to the instrumentation system.

3.10 Record Keeping (Log Sheets). During the validation, analysis, and/or engineering interpretations of measured dynamic data, questions often arise that require a review or conflation of certain details of the data acquisition operations. This may be necessitated by observed anomalies in analyzed results, or perhaps an uncertainty about the exact location of a transducer or the conditions under which a measurement was made. In any case, an inability to check and confirm the details of the data acquisition can prove very costly, and should be minimized by accurate and thorough record keeping in the form of comprehensive log sheets for all measurements. Hence, it is recommended that each measurement of dynamic data be accompanied by a log sheet that includes, at a minimum, the following information.

(1) Test information (as applicable).
- (a) An identification of the test.
- (b) An identification of the test article.
- (c) An identification of the test engineer and other cognizant personnel.
- (d) The location of the test.
- (e) The general environmental conditions during the test (temperature, humidity, etc.).
- (f) The specific test condition during the measurement.
- (g) The date and time the measurement was obtained.
- (h) The duration of the measurement.

(2) Transducer information.
- (a) The type of transducer (accelerometer, microphone, etc.).
- (b) The transducer model number.
- (c) The transducer serial number.
- (d) The transducer sensitivity.
- (e) The exact location of the transducer (include a diagram).
- (9 The orientation of the transducer relative to the axes of the test article (include a diagram if the orientation is not along an orthogonal axis of the test article).
- (g) The cable model number or other description.
- (h) The transducer channel identification number.

(3) Signal conditioner information.
- (a) The type of signal conditioner (charge amplifier, power supply, etc.).
- (b) The signal conditioner model number.
- (c) The signal conditioner serial number.
- (d) Gain and attenuator settings.
- (e) All input and/or output filter cut-off frequencies,

(4) Data recorder and telemetry information (as applicable).
- (a) The type. of data recorder and/or telemetry unit (FM, PCM, etc.).
- (b) The data recorder and/or telemetry unit configuration.

(c) The data recorder and/or telemetry unit model number.
(d) The data recorder and/or telemetry unit serial number.
(e) The data recorder and/or telemetry unit channel or track number.
(f) The data recorder speed; e.g., the tape speed for a tape recorder.
(g) The mux channel or track number.
(h) All gain and attenuator settings,

(5) Calibration information (as applicable).
(a) End-to-end electrical calibration results, with all gain and attenuator settings.
(b) End-to-end mechanical calibration results, with all gain and attenuator settings,
(c) Phase of output signal relative to input signal.

(6) Unusual events and special circumstances.
List all unusual events that occurred during the measurement, and any special circumstances associated with the measurement that might influence the analysis of the data or its engineering interpretations.

For those cases where the acquired measurements are stored in a digital data base, the log sheet information should also be entered into the data base.

3.11 References.

3.1 Doebelin, E. O., *Measurement* Systems: *Applications and Design, 4th cd.,* McGraw-Hill, NY, 1990.

3.2 Beauchamp, K.G., and Yuen, C. K., *Data Acquisition for Signal Analysis,* George Allen & Unwin, London, 1980.

3.3 Morrison, R., *Instrumentation Fundamentals and Applications,* Wiley, NY, 1984.

3.4 Eller, E. E., and Whittier, W. H., "Piezoelectric And Piezoresistive Transducers", Ch. 12, *Shock and Vibration Handbook,* 3rd ed. (Ed: C. M. Harris), McGraw-Hill, NY, 1988.

3.5 Plankey, R. C. and Wilson, J. S., *Shock and Vibration Measurement Technology,* Endevco, San Juan Capistrano, CA, 1987.

3.6 Broch, J. T., et al, *Mechanical Vibration and Shock Measurements,* 2nd cd., Bruel & Kjaer, Naerum, Denmark, 1984.

3.7 Serridge, M., and Licht, T. R., *Piezoelectric Accelerometers and Vibration Preamplifier Handbook,* Bruel & Kjaer, Naerum, Denmark, Nov. 1987.

3.8 Peterson, A. P. G., *Handbook of Noise Measurements, 9th ed.,* GenRad, Concord, MA, 1980.

3.9 Johnson, D. L., Marsh, A. H., and Harris, C. M., "Acoustical Measurement Instruments," Ch. 5, *Handbook of Acoustical Measurements and Noise Control,* 3rd ed. (Ed: C. M. Harris), McGraw-Hill, NY, 1991.

3.10 Eller, E. E., and Whittier, R. M., "'Vibration Transducers," Ch. 7, *Handbook of Acoustical Measurements and Noise Control,* 3rd cd. (Ed: C. M. Harris), McGraw-Hill, NY, 1991.

3.11 Lally, J. F., "Introduction to Piezoelectric Sensors", *PCB Article Reprint AR-18,* PCB, Depew, NY, Oct. 1985.

3.12 Kundert, W. R., "Everything You've Wanted to Know About Measurement Microphones," Sound *and Vibration,* Vol. 12, No. 3, pp. 10-23, Mar. 1978.

3.13 Starr, E. A., "Sound and Vibration Transducers", Ch. 3, Noise *and Vibration Control (Ed:* L. L. Beranek), McGraw-Hill, NY, 1971 (reprinted by Inst. Noise Control Engrg, Washington, DC, 1988).

3.14 Dranetz, A. I., Orlacchio, A. W., and Mason, W. P., "Piezoelectric and Piezoresistive Pickups", Ch. 16, *Shock and Vibration Handbook,* 1st ed. (Ed: C.M. Harris and C. E. Creole), McGraw Hill, NY, 1961.

3.15 Wilson, E. J., "Strain-Gage Instrumentation", Ch. 17, *Shock and Vibration Handbook,* 3rd ed. (Ed: C. M. Harris), McGraw-Hill, NY, 1988.

3.16 Doyle, J. F., and Phillips, J. W., Ed., *Manual on Experimental Stress Analysis,* 5th cd., Soc. Exper. Mech., Bethel, CT, 1989.

3.17 Kobayashi, A. S., Ed., *Handbook on Experimental Mechanics,* 2nd cd., SW. Exper. Mech., Bethel, CT, 1987.

3.18 Dally, J. W., and Riley, W. F., *Experimental Stress Analysis,* 3rd cd., McGraw-Hill, *NY,* 1991.

3.19 Collins, S. J., and Buckley, G., Ed., *Application of Advanced Strain Measurement Techniques,* ASTM, Philadelphia, 1988.

3,20 Dove, R. C., and Adams, P. H., *Experimental Stress Analysis and Motion Measurement,* Chas. E. Merrill, Columbus, OH, 1964.

3.21 Perry, C. C., and Lissner, H. R., *The Strain Gage Primer,* 2nd cd., McGraw-Hill, NY, 1962.

3.22 Hassall, J. R., and Zaveri, K., *Acoustic* Noise *Measurements, 5th cd.,* Bruel & Kjaer, Naerum, Denmark, 1989.

3.23 Judd, J. E., and Ramboz, J. D., "Special-Purpose Transducers", Ch. 14, *Shock and Vibration Handbook,* 3rd ed. (Ed: C. M. Harris), McGraw-Hill, NY, 1988.

3.24 Barker, L. M., and Hollenbach, R. E., "Interferometer Technique for Measuring the Dynamic Mechanical Properties of Materials," *Rev. Scientific Instr.,* Vol. 36, No. 11, pp 1617-1620, Nov." 1965.

3.25 Barker, L. M., and Hollenbach, R. E., "Laser Interferometer for Measuring High Velocities of any Reflecting Surface," *J. Appl. Physics,* Vol. 43, No. 11, pp 4669-4675, 1972.

3,26 Pickering, C. J. D., and Halliwell, N. A., "The Laser Vibrometer: A Portable Instrument," *J. Sound and Vibration,* Vol. 107, No. 3,pp471 -485, 1986.

3.27 Valentekovich, V. M., Navid, M., and Goding, A. C., "Laser Doppler Vibrometry Measurements of Pyrotechnically Induced Shock," *Proc., 60th Shock and Vibration Symp.,* Vol. I, pp 259-271, Nov. 1989,

3.28 Valentekovich, V. M., and Goding, A. C., "Characterizing Near Field Pyroshock with a Laser Doppler Vibrometer," *Proc., 61st Shock and Vibration Symp.,* Vol. II, pp 205-221, Oct. 1990.

3.29 Lieberman, P., Czajkowski, J. and Rehard, J., "Optical System for Measurement of Pyrotechnic Test Accelerations," *J. Inst. Envir. Se.,* Vol. XxXV, No. 6, pp 25-39, Nov./Dee. 1992.

3.30 Udd, E., Ed., *Fiber Optic Sensors,* Wiley, NY, 1991.

3.31 Culshaw, B., and Dakin, J. P., Ed., *Optical Fiber Sensors,* Vol. I-III, Artech Hse, Norwood, MA, 1988-89.

3,32 Blake, R. E., "Basic Vibration Theory", Ch. 2, *Shock and Vibration Handbook,* 3rd ed. (Ed: C. M. Harris), McGraw-Hill, NY, 1988.

3.33 Meirovitch, L., *Elements of Vibration Analysis,* 2nd ed., McGraw-Hill, NY, 1986,

3.34 Veatch, D. W., and Bogue, R, K., "Analog Signal Conditioning for Flight Test Instrumentation ," *NASA Ref. Publ. 1159,* 1986. (Also AGARDograph 160, Vol. 17).

3.35 Anon, *Condenser Microphones and Microphone Preamplifiers Data Handbook,* Bruel & Kjaer, Naerum, Denmark, Rev. Sept. 1982.

3.36 Vér, I, L., and Holmer, C. I., "Interaction of Sound Waves with Solid Structures", Ch. 11, Noise *and Vibration Control (Ed:* L. L. Beranek), McGraw-Hill, NY, 1971 (reprinted by Inst. Noise Control Engrg, Washington, DC, 1988).

3.37 Vér, I. L., "Interaction of Sound Waves with Solid Structures," Ch. 9, Noise *and Vibration Control* Engineering (Ed: L. L, Beranek and I. L. Vér), Wiley, NY, 1992,

3.38 Favour, J. D., "Transient Data Distortion Compensation," *Shock* and *Vibration Bull., No. 35,* Pt *4,* pp 231-238, Feb. 1966.

3.39 Favour, J. D., "Digital Control and Analysis of Transient Waveforms in the Test Laboratory," *Proc., Intern. Symp. on Shock Analysis and Testing,* Oct. 1974.

3.40 Smith, S., and Hollowell, B., "Techniques for the Normalization of Shock Data," *Proc.,* 62nd *Shock and Vibration Symp.,* Vol. II, pp 403-411, Oct. 1991.

3.41 Hollowell, B., Smith, S., and Hansen, J., "A Close Look at the Measurement of Shock Data," *J, Inst. Envir. Se.,* Vol. XXXV, No. 5, pp 39-45, Sept./Ott. 1992.

3.42 Wright, C. P., "Try a More Liberal Sampling Model if Your Back is to the Design Wall," *Personal Engrg and Instr. News,* Vol. 9, No, 8, pp 58-61, Aug. 1992.

3.43 Wise, J. H., "The Effects of Digitizing Rate and Phase Distortion on the Shock Response Spectrum", *Proc., Inst. Envir. Se.,* pp 36-43, Apr. 1983.

3.44 Kinzel, R. L., and Tustin, W., "Accelerometer Transverse Resonance Effects," Soc. *Auto. Engrs Paper 892380,* Sept. 1989.

3,45 Franken, P. A., "The Behavior of Sound Waves", Ch. 1, *Noise and Vibration Control* (Ed: L. L. Beranek), McGraw-Hill, NY, 1971 (reprinted by Inst. Noise Control Engrg, Washington, DC, 1988).

3.46 Beranek, L. L., "Basic Acoustical Quantities: Levels and Decibels," Ch. 1, Noise *and Vibration Control Engineering* (Ed: L, L, Beranek and I. L. Vér), Wiley, NY, 1992.

3.47 Harris, C. M., "Introduction," Ch. 1, *Handbook of Acoustical Measurements and Noise Control,* 3rd ed. (Ed: C. M. Harris), McGraw-Hill, NY, 1991.

3.48 Pierce, A. D., *Acoustics,* McGraw-Hill, NY, 1981 (reprinted by Acoust. See. Amer., Woodbury, NY, 1989).

3.49 Hassall, J. R., "Noise Measurement Techniques, " Ch. 9, *Handbook of Acoustical Measurements and Noise Control,* 3rd ed. (Ed: C. M. Harris), McGraw-Hill, NY, 1991.

3.50 Eargle, J. M., *Handbook of Recording Engineering,* Van Nostrand Reinhold, NY, 1986.

3.51 Borwick, J., *Microphones: Technology and Technique,* Focal/Butterworths, pp 35, 36, 106, 107, Boston, 1990.

3.52 Corcos, G. M., "Resolution of Pressure in Turbulence", *J. Acoust. Sot. Amer.,* Vol. 35, No. 2, pp 192-199, Feb. 1963.

3.53 Bies, D. A., "A Review of Flight and Wind Tunnel Measurements of Boundary Layer Pressure "Fluctuations and Induced Structural Response", *NASA CR-626,* Oct. *1966.*

3.54 Lewis, T. L., and Dods, J. B., "Wind-Tunnel Measurements of Surface-Pressure Fluctuations at Mach Numbers of 1.6, 2.0, and 2.5 Using 12 Different Transducers", *NASA TN D-7087,* Oct. 1972.

3.55 Frost, N. E., Marsh, K. J., and Pook, L. P., *Metal Fatigue,* Clarendon Press, Oxford, UK, 1974.

3.56 Fuchs, H. O., and Stephens, R. I., *Metal Fatigue in Engineering,* Wiley, NY, 1980.

3,57 Brock, D., *Elementary Engineering Fracture Mechanics,* 3rd cd., Martinus Nijhoff, Boston, 1982.

3.58 Morse, P. M., *Vibration and Sound,* 2nd ed., McGraw-Hill, NY, 1948 (reprinted by Acoust. Sot. Amer., Woodbury, NY, 1981).

3.59 Telinde, J. C., "Strain Gages in Cyrogenic Environments," *Experimental Mechanics,* Vol. 10, No. *9,* pp 394-400, Sept. 1970.

3.60 Coe, C. F., and Cunningham, A. M., "Predictions of F-111 TACT Aircraft Buffet Response and Correlations of Fluctuating Pressures Measured on Aluminum and Steel Models and the Aircraft", NASA CR-4069, May 1987.

3.61 Anon, "Guide for Specifications and Tests for Piezoelectric Acceleration Transducers for Aerospace Testing," *ANSI Std RP 37.2-1982.*

3.62 Nagy, J. A., and Henley, C. E., "Influence of Fixture Stress Concentrations on Ring Accelerometers," *Shock and Vibration Bull. No. 37,* Pt *2,* pp *43-50,* Jan. 1968 (Also *NASA TN D-4540,* May 1968).

3.63 Belsheim, R. O., and Young, J. W., "Mechanical Impedance as a Tool for Shock or Vibration Analysis", Naval *Res. Lab Rep?* 5409, Washington, Feb. 15, 1960 (DTIC No. AD 234227).

3.64 Schloss, F., "Inherent Limitations of Accelerometers for High-Frequency Vibration Measurements", *J. Acoust. Sot,* Amer., Vol. 33, No. 4, p. 539, Apr. 1%1.

, 3.65, O'Hara, G. J., "Mechanical Impedance and Mobility Concepts", *J. Acoust. Sot. Amer.,* Vol. 41, No. 5, pp 1180-1184, May 1%7.

3.66 Rubin, S., Private Communication, Sept. 30, 1991.

3.67 Chu, A. S., "Transducer Selection", *Proc. Inst. Envir. Se., May 1994.*

3.68 Lally, R. W., "General Guide to ICP Instrumentation", *PCB Article Reprint AR-4,* PCB, Depew, NY, 1971.

3.69 Bill, B., and Wicks, A. L., "Measuring Simultaneously Translational and Angular Acceleration with the New Translation-Angular-Piezobeam (TAP) System," *Sensors and Actuators,* Vol. A21-A23, pp 282-284, 1990.

3.70 Harris, C. M., "Measurement Techniques", Ch. 15, *Shock and Vibration Handbook, 3rd* ed. (Ed: *C.* M. Harris), McGraw-Hill, NY, 1988.

3.71 Harris, C. M., "Vibration Measurement Techniques," Ch. 10, *Handbook of Acoustical Measurements and* Noise *Control,* 3rd ed. (Ed: C. M. Harris), McGraw-Hill, NY, 1991.

3.72 Landerville, J. B., and Urashima, K. P., "Accelerometer Bonding Study," *Proc.; 12th IES Aerospace Testing Seminar,* pp 95-105, Mar. 1990.

3.73 Hollowell, B., and Smith, S., "In-Plane Shock Response Measurement," *Proc., 61st Shock and Vibration Symp.,* Vol. II, pp 223-232, Oct. 1990.

3.74 Anon, *C'EC Pressure Transducer Handbook,* Imo, *San Dimas,* CA, rev. 1989.

3.75 Coe, C. F., and Brownson, J. J., "Instrumentation Applications to Space Shuttle Models and Thermal Protection System Tiles Tested in NASA-Ames Wind Tunnels", *IEEE Publ. 81 CH1712-9,* Sept. 30, 1981.

3.76 Guest, S. H., and Jones, J. H., "Space Shuttle Noise Suppression Concepts", *Proc., 13th Space Cong.,* May 1976.

3.77 Dougherty, N. S., and Guest, S. H., "A Correlation of Scale Model and Flight Aeroacoustic Data for the Space Shuttle Vehicle", *AIAA Paper 84-2351,* Oct. *1984.*

3.78 Hanly, R. D., "Effects of Transducer Flushness on Fluctuating Surface Pressure Measurements," *AIAA Paper* 75-534, Mar. 1975.

3.79 Anon, "Force and Torque Measurement", *Exper. Stress Anal. Notebook,* issue 6, Measurements Grp, Raleigh, NC, May 1987.

3.80 Dykes, B. C., "When Strain Gages Don't Give the Expected Results", *Proc. Western Regional Strain* Gage *Comm. Mtg, Sot.* Exper. Mech., Bethel, CT, Aug. 1982.

3.81 Martini, K. H., "Multicomponent Dynamometers Using Quartz Crystals as Spring Elements," *Intr.* Sot. *Amer. Trans.,* Vol. 22, No. 1, pp. 35-45, 1983.

3.82 Gautschi, G. H., "Piezoelectric Multicomponent Force Transducers and Measuring Systems," *Proc., Transducer '78 Conf.,* London, UK, 1978.

3.83 Bever, G. A., "Digital Signal Conditioning for Flight Test Instrumentation," *NASA TM 101739, Mar.* 1991 (Also AGARDograph 160, Vol. 19).

3.84 Randall, R. B., *Frequency Analysis,* 3rd cd., Bruel & Kjaer, Naerum, Denmark, 1987.

3.85 Hamming, R. W., *Digital Filters,* 2nd cd., Prentice-Hall, Englewood Cliffs, NJ, 1983.

3.86 Nelson, D. B., "Critique of Ballistic Vehicle Vibration Measurements", *SAE Paper 871741,* Oct. 1987.

3.87 Lally, J. F., "Accelerometer Cable, Wiring, and Connections", *Proc. Inst. Envir. SC.,* Vol. 2, pp. 424-437, May 1993.

3.88 Anon, "American National Standard, Calibration and Tests for Electrical Transducers Used for Measuring Shock and Vibration, Selection of," *ANSI Std* S2.12-1%9 *(R 1989).*

3.89 Morrison, R., *Grounding and Shielding Techniques in Instrumentation,* Wiley, NY, 1977.

3.90 Wilson, J., "Noise Suppression and Prevention in Piezoelectric Transducer Systems," Sound and *Vibration,* VOL 13, No. 4, pp 22-25, Apr. 1979.

3.91 Hartenbaum, B., Morrison, J., and Gord, J., "Piezoelectric Transducer Signal Conditioning: Low Noise and Ultra-High Isolation," *Proc., 36th Intern. Instr. Symp.,* Intr. *Sot.* Amer., pp 59-64, May 1990.

3.92 Telemetry Group, Range Commanders Council, "Telemetry Standards", *IRIG* Std 105-93, Jan. 1993.

3.93 Telemetry Group, Range Commanders Council, "Telemetry Applications Handbook", *IRIG Dec.* 119-88, Feb. 1988.

3.94 Anon, "Helical Digital Recording Format for 19-MM Magnetic Tape Cassette Recorder/Reproducers," *MIL-STD-21* 79A, Dec. 24, 1987.

3.95 Camras, M., *Magnetic Recording Handbook,* Van Nostrand Reinhold, NY, 1988.

3.96 Jorgensen, F., *The Complete Handbook of Magnetic Recording,* Tab Books, Blue Ridge Summit, PA, 1980.

3.97 Kalil, F., Ed., "Magnetic Tape Recording for the Eighties," *NASA Ref. Publ.* 1075, Apr. 1982.

3.98 Kalil, F., Ed., "High Density Digital Recoding," *NASA Ref. Publ. 1111*, Sept. 1985.

3.99 Telecommunications Group, Range Commanders Council, "IRIG Standard Time Formats", *IRIG Std* 200-70, Aug. 1970 (DTIC No. AD 28069).

3.100 Cuddihy, E. F., "Hydroscopic Properties of Magnetic Recording Tape", *IEEE Trans. on Magnetics*, Vol. MAG-12, No. 2, pp 126-135, Mar. 1976.

3.101 Cuddihy, E. F., "Aging of Magnetic Recording Tape", *IEEE Trans. on Magnetics*, Vol. MAG-16, No. 4, pp 558-568, July 1980.

3.102 Bertram, H. N., and Cuddihy, E. F., "Kinetics of Humid Aging of Magnetic Recording Tape", *IEEE Trans. on Magnetics*, Vol. MAG-18, No. 5, pp 993-999, Sept. 1982.

3.103 Hnatek, E. R., *A Users Handbook of D/A and AID Converters,* Wiley, NY, 1976.

3.104 Taylor, J. L., *Computer-Based Data Acquisition Systems,* 2nd cd., Instr. Sot. Amer., Research Triangle Park, NC, 1990.

3.105 Bendat, J. S., and PierSol, A, G., *Random Data: Analysis and Measurement Procedures,* 2nd cd., Wiley, NY, 1986.

3.106 Otnes, R. K., and Enochson, L., *Applied Time Series Analysis,* Wiley, NY, 1978.

3.107 Hauser, M. W., "Principles of Oversampling A/D Conversion", *J. Audio Eng. Sot.,* Vol. 39, No. 1/2, pp. 3-26, Jan./Feb. 1991.

3.108 Nelson, D. B., "Effect of Filter Frequency Response on Pyroshock Data Analysis", *Proc. Spacecraft Dynamic Environment TIM,* Vol. 2, pp. 255-283, The Aerospace Corp., El Segundo, CA, June 1990.

3.109 Anon, “Military Standard, Calibration System Requirements”, *MIL-STD-45562A*, Aug. 1988.

3.110 Mark, A., et al, “Metrology-Calibration and Measurement Processes Guidelines”, *NASA RP- XxXX*, Draft 1994.

3.111 Ramboz, J. D., Serbyn, M. R., and Lally, R. W., “Calibration of Pickups”, Ch. 18, *Shock and Vibration Handbook*, 3rd ed. (Ed: C. *M. Harris)*, McGraw-Hill, NY, 1988.

3.112 Sill, R. D., “Accelerometer Calibration: Minimizing Measurement Uncertainty”, *Endevco TP 299*, Endevco, San Juan Capistrano, CA, Mar. 1993.

3.113 Rhodes, J. E., "Piezoelectric Transducer Calibration Simulation Method Using Series Insertion”, *Endevco TP 226*, Endevco, San Juan Capistrano, CA, Apr. 1962.

3.114 Bendat, J. S., and PierSol, A. G., *Engineering Applications of Correlation and Spectral* Analysis, 2nd ed., Wiley, NY, 1993.

4, DATA VALIDATION AND EDITING

4.1 Introduction. This section presents guidelines for the validation and editing of measured dynamic signals prior to detailed data analysis operations. In some cases, dynamic measurements may be analyzed on-line, making data validation and editing prior to analysis impossible or impractical, It is more common, however, for measured signals to be recorded on either analog or digital storage devices for later analysis. In these cases, all measured signals should be validated and edited (if necessary) prior to analysis. Many of the desired data validation operations can be automated by knowledge-based computer programs to obtain a substantial reduction in labor, e.g., [4. 1]. Such automation of data validation operations is strongly endorsed for those activities where the volume of data to be processed is large. Also, the procedures recommended herein are not intended to replace more qualitative techniques that may be in use, such as audio evaluations of signal quality by the ear of an experienced analyst, An outline of the data validation and editing procedures covered in this section is presented in Figure 4.1,

Conventional wisdom suggests that all dynamic measurements that reveal anomalies during the data validation operations, which cannot be confidently corrected by an editing operation, should be rejected and not used for any engineering purpose, However, practical considerations (e.g., the cost of acquiring the measurements) often demand a more tolerant approach to the acceptance of less than perfect data signals. The recommendations to follow are made with the understanding that the difficulty associated with acquiring certain types of measurements may sometimes force an effort to extract information from signals that are of questionable quality.

4.2 Identification of Physical Events. The first step in data validation and editing is the identification in each signal of all relevant physical events associated with the measurement, To accomplish this, each measured time history, whether stored on analog tape or in a digital storage device, should be converted to a hard copy using a hard copy recorder (see Section 5.2,1) with a frequency response equal to or greater than the frequency range of interest in the data. The basic signal properties revealed in the hard copy of the time history should then be reviewed and correlated with known physical events during the measurement duration, The results of this evaluation should be detailed in the log sheet for the measurement (see Section 3.10).

4.2.1 Random versus Periodic Signals, It usually can be anticipated that some measurements will produce basically periodic signals (e.g., a measurement of the vibration response of an unbalanced rotating machine), while others should produce basically random signals (e.g., a measurement of the fluctuating pressures in a turbulent boundary layer), Illustrations of purely periodic and stationary random signals are shown in Figure 4.2(a) and (b), respectively. In many cases, a combination of periodic and random components might be anticipated, as illustrated in Figure 4,2(c). In any case, the measured time history should be visually inspected to verify that the basic characteristics of the signal are consistent with the physical mechanisms producing the signal.

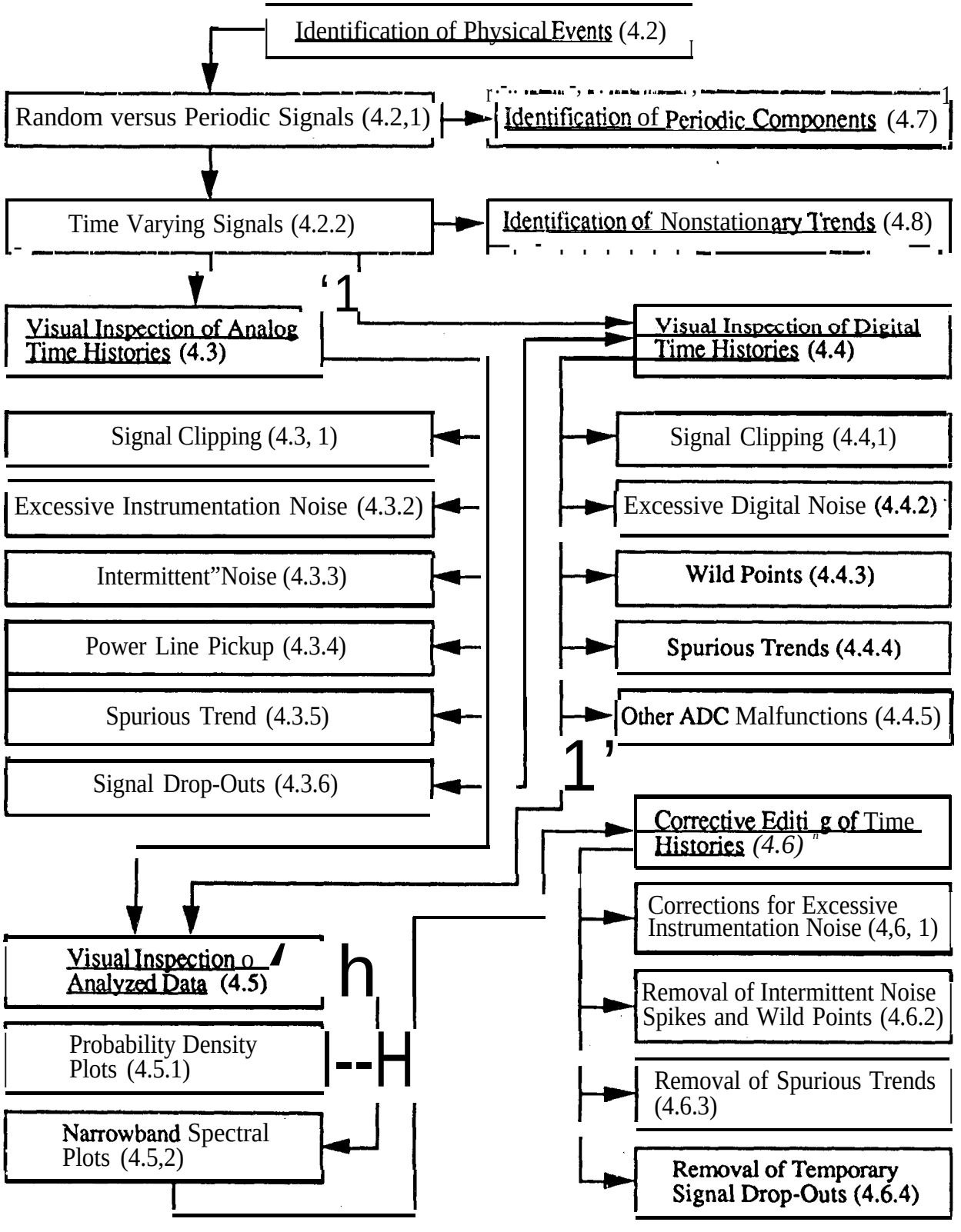

Figure 4.1. Outline of Data Validation and Editing Procedures.

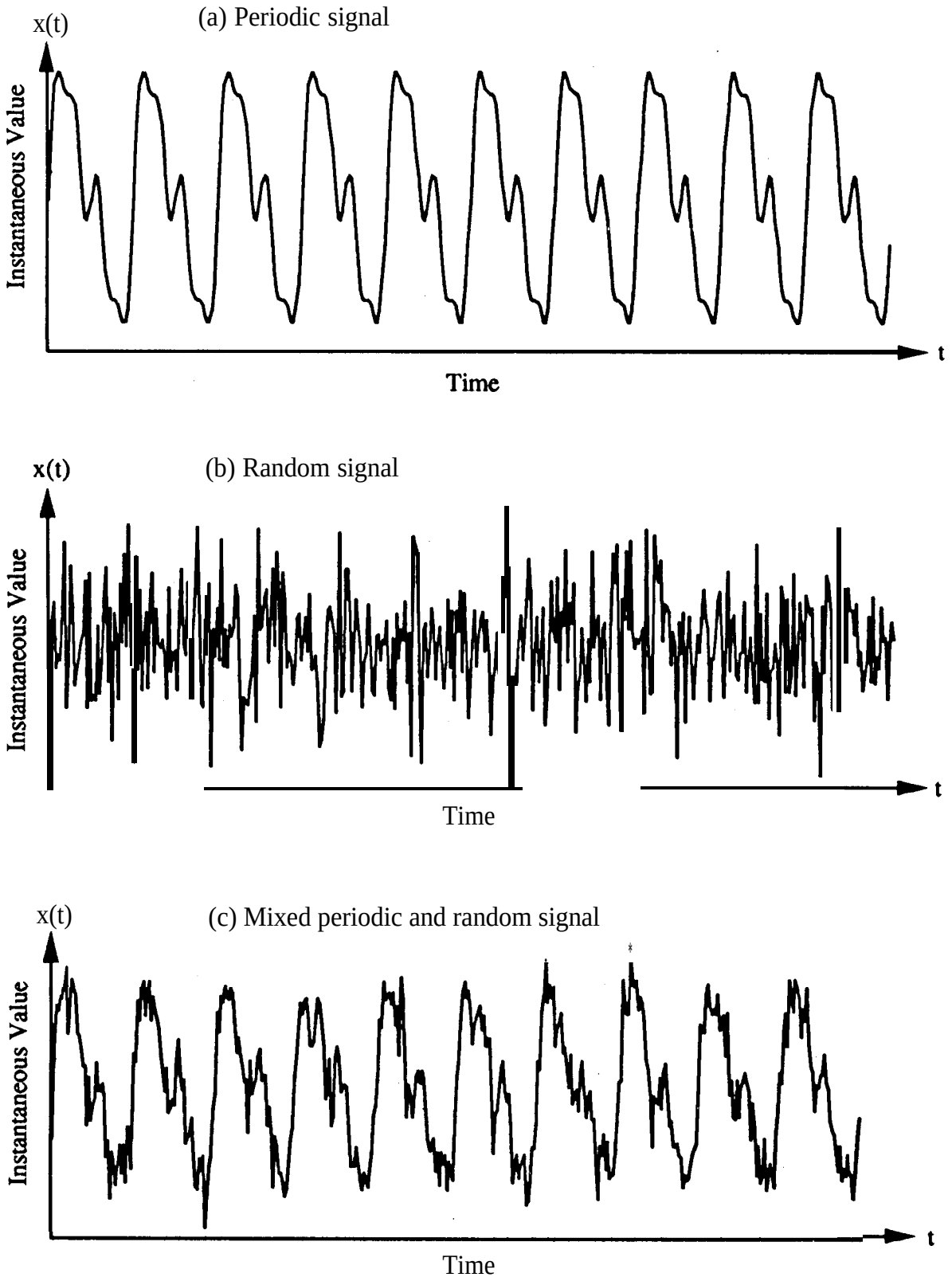

Figure 4.2. Illustration of Periodic, Random, and Mixed Signals.

Situations may arise where a measured time history, or its spectrum, reveals characteristics indicative of a periodic component in a random noise background at a frequency where a periodicity is not anticipated based upon physical considerations. In such cases, the apparent periodic component might actually be a very narrowband random signal indicative of the resonant response of a lightly damped structure or acoustic cavity to a broadband random excitation. The distinction between these two types of signals (periodic versus narrowband random) is not only relevant to physical interpretations of the data, but is also important to the selection of appropriate data analysis techniques (see Section 5). Specific procedures for distinguishing between periodic and narrowband random signals in a broadband random background are detailed in Section 4.7.

4.2.2 Time-Varying Signals. It often can be anticipated that a measurement will cover certain physical events that produce either transient signals or longer duration nonstationary signals. Transient signals are broadly defined as those which are due to momentary events that have a clear beginning and end, as illustrated in Figure 4.3(a). Typical examples of transients include the acoustic and/or structural vibration responses produced by rocket motor ignitions, space vehicle stage separations, aircraft landing loads, external store ejection shocks, and pyrotechnic events. Nonstationary signals are those which are due to longer duration events that are ongoing but have time varying characteristics, as illustrated in Figure 4.3(b). A good example of nonstationary data is the vibration response of a space vehicle during lift-off or flight through the region of maximum dynamic pressure. More practical distinctions between transient and nonstationary data from an applications (design and test) viewpoint are detailed in Section 5.3.1.4. In either case, such physical events should be identified in the time history of the measured signal as fully as possible. This is demonstrated in Figure 4.4, which shows the identification of key transient and nonstationary events in a typical vibration time history measured during a Space Shuttle launch. The identification of transient and nonstationary events is not only needed to assist the data validation, but is essential to the selection of later data analysis procedures (see Section 5 and Appendices A and B).

Situations may arise where a measured time history reveals an apparent nonstationary trend that is not anticipated based upon physical considerations, The trend may be spurious, as discussed in Sections 4.3.5 and 4.4.4, On the other hand, it might be indicative of an unexpected time varying property of the measured phenomenon, in which case the presence of a trend could have important physical implications. For the case of random signals with a slight nonstationary trend, it may be difficult to distinguish the actual trend from unusual but not statistically significant variations in the values of a stationary signaL A nonparametric test for trends, which will permit this detection of time varying rms values on a firm statistical basis, is detailed in Section 4.8. More complex nonstationarities involving a shift in the frequency content of the signal that does not alter the overall rms value can be detected by filtering the signal into two or more contiguous frequency bands, and applying the test in Section 4.8 separately to therms values in each band.

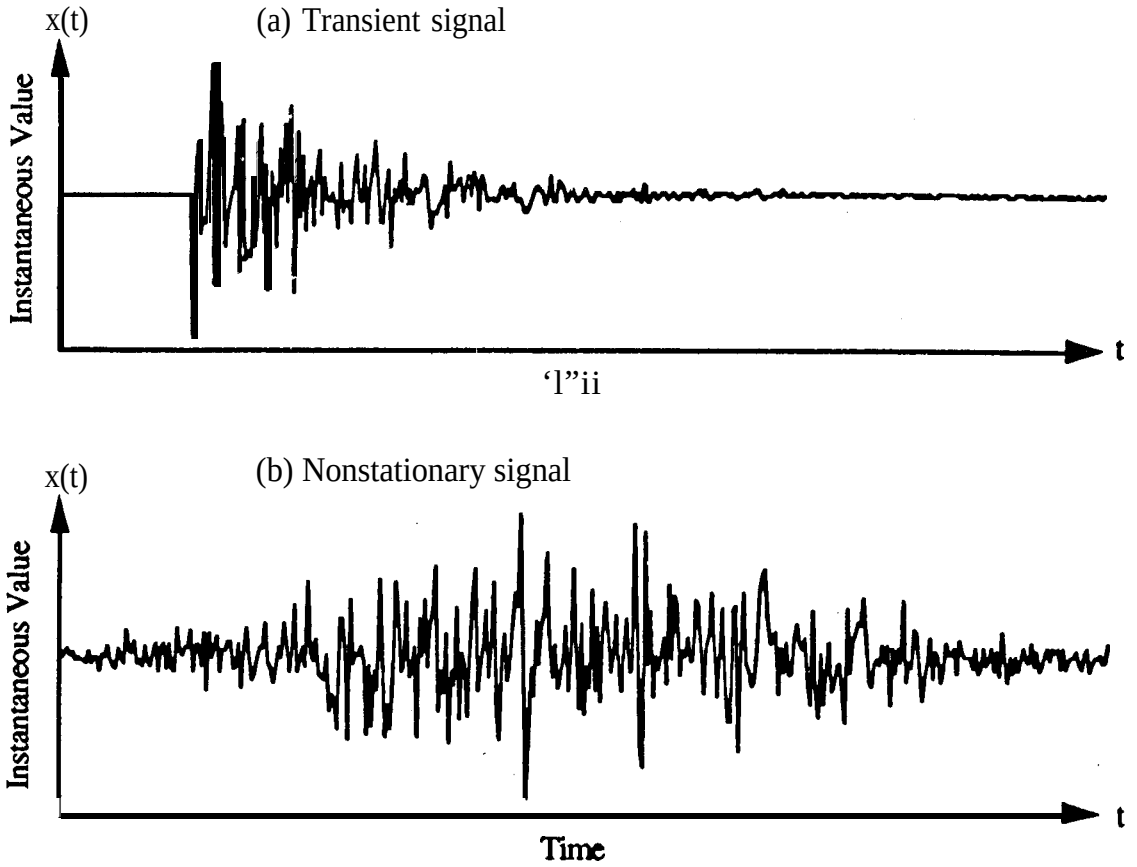

Figure 4.3. Illustration of Transient and Nonstationary Random Signals.

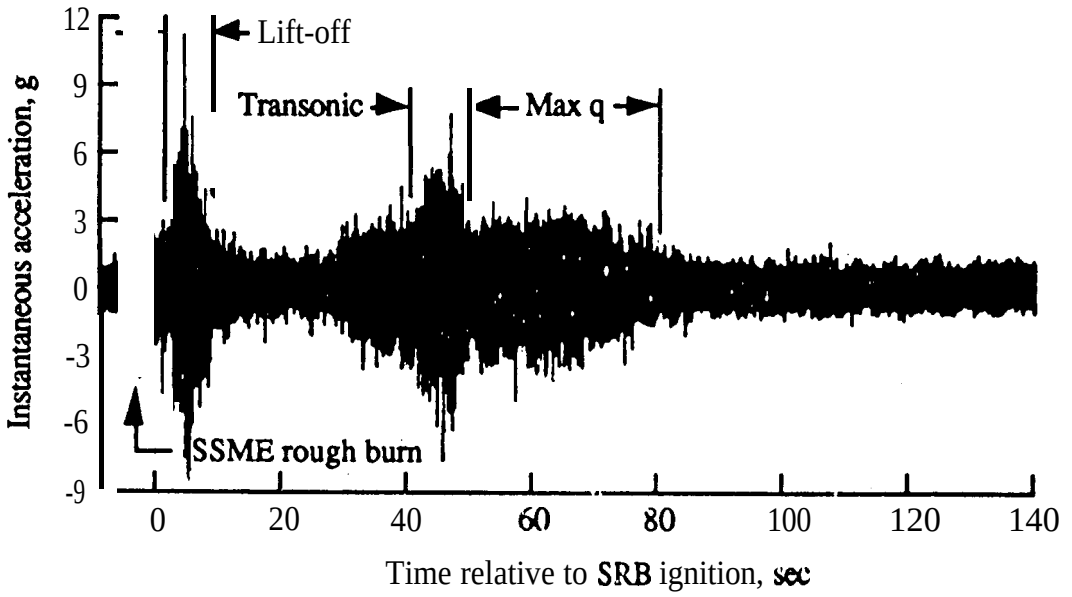

Figure 4.4. Identification of Physical Events in Space Shuttle Launch Vibration Signal.

4.3 Visual Inspection of Analog Time Histories. Using the hard copy time histories generated in Section 4.2, or an electronic display of the time histories on an oscilloscope with a signal capture mode, the instantaneous values of each measured signai should be visually inspected for the following anomalies.

4.3.1 Signal Clipping. One of the most common errors in data acquisition is the failure to provide an adequate upper limit for the dynamic range in one or more of the data acquisition instruments due to a sensitivity (gain) setting that is too high. The result is signal clipping or saturation within the data acquisition system, commonly in an amplifier, tape recorder, or telemetry channel. An inappropriate scaling of a signal output device (see Section 5.2. 1) can also cause an apparent clipping of the signal. Since this problem is easily corrected, the scaling of output devices should be checked immediately if clipping is indicated

4.3.1.1 Identification Procedure. The impact of ideal or hard clipping on the measured time histories for periodic, random, and transient data signals is illustrated in Figure 4.5. Two-sided clipping is shown in these illustrations; the clipping sometimes maybe only one-sided. It is important to note that lowpass filtering of a clipped signal will obscure the results shown in Figure 4.S, making it difficult to detect clipping of a signal after filtering operations [4.2, 4.3]. Also, signal saturation in certain types of instruments may produce a more complicated result than the idea! magnitude limiting shown in Figure 4.5, particularly when measuring intense, rapid rise-time transients such as pyroshocks. Specifically, there may be a zero shift in the signal level followed by a slow recovery that appears as a time varying trend in the mean value of the signal (see Section 3.3.2.3 and Appendix A). In the more classical cases of signal clipping, however, there will be a clear upper limit imposed on the signal values. For the special case of stationary random signals, a probability density analysis of the signal also provides a powerful tool to detect clipping, as detailed in Section 4.5.1.1.

It is clear from Figure 4.5 that the detection of signal clipping by the visual inspection of a time history is most difficult for a transient signal, particularly if it is a single pulse transient. To further assist the detection of possible clipping in transient signals, it is recommended that the peak output voltage capability of the instrumentation system be determined and compared to the peak voltage represented by the measured transient. If the peak voltage of the signal is equal to or greater than 95% of the peak voltage capabilities of the instrumentation, this would suggest that clipping might have occurred. In those cases where the value of the data provided by the signal warrants, the "over-shoot" capabilities of the instrumentation system should be determined using a laboratory simulation of the transient, and compared to the peak voltage represented by the measured transient. The term "over-shoot" is used hem to mean the linear measurement performance of the system beyond the manufacturer's specifications. No effort should ever be made to introduce nonlinear corrections to signals that have been clipped

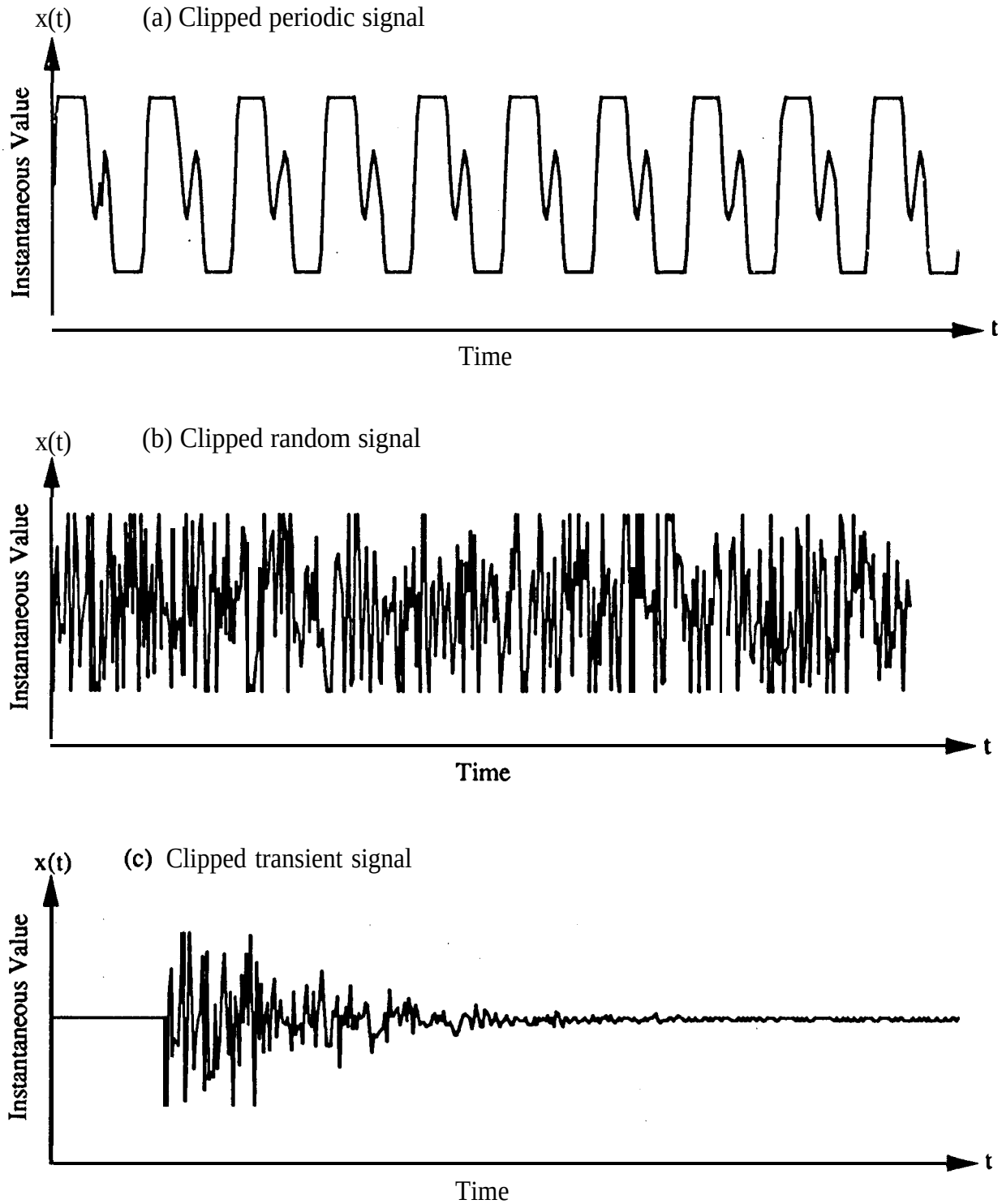

Figure 4.5. Illustration of Clipped Periodic, Random, and Transient Signals.

4.3.1.2 Data Rejection Criteria. For the case of periodic and transient signals, clipping may dramatically reduce the indicated peak magnitude of the signal. Also, clipping commonly increases the apparent high frequency content of the signal [4.4]. Hence, it is recommended that measurements of periodic and transient signals be rejected if there is any evidence of clipping revealed by the visual inspection of the analog time history outlined in Section 4.3.1.1. For the case of random signals, it is recommended that a measurement be rejected if the clipping occurs within+ 1,5 standard deviations of the mean value of the clipped signal. See Section 5.2.2 for details on the calculation of mean values and standard deviations of signals.

4.3.2 Excessive Instrumentation Noise. The other extreme of an improper upper limit for the dynamic range of the data acquisition system is where one or more of the data acquisition instruments has too low a sensitivity (gain) setting. The result is a signal that is too small relative to the instrumentation noise, i.e., an inadequate signal-to-noise level, Excluding those cases where the system is vulnerable to noise induced by external loads (e.g., microphonic or triboelectric noise), instrumentation noise can be assumed to be additive and statistically independent of the signal. Noise induced by external loads should be detected and corrected during the system calibration procedures detailed in Section 3.8.2. Also, for telemetry systems with voltage controlled oscillators (VCO) and multiplexed, it is recommended that the noise floor of the system be measured and analyzed to identify potential noise problems before the data acquisition.

4.3.2.1 Identification Procedure. The influence of excessive instrumentation noise on the measured time histories for periodic, random, and transient data signals is shown in Figure 4.6. The most powerful and effective procedure for detecting excessive instrumentation noise is to measure the output signal from the data acquisition system before and/or after the dynamic activity of interest occurs (often referred to as quiescent time histories). Of course, the quiescent time histories must be measured with exactly the same instrumentation gain settings that are used to measure the dynamic activity. This procedure provides an independent measurement of the instrumentation noise alone, which can then be directly compared to the dynamic signal measurements.

Even if quiescent time histories are not available, the presence of excessive instrumentation noise in periodic signals is usually obvious, because instrumentation noise is generally random rather than periodic in character (an exception is power line pickup discussed in Section 4.3.4). Excessive instrumentation noise is usually obvious in transient signal measurements as well, since the noise is present before and after the transient event. For stationary random signals, however, the presence of excessive instrumentation noise is usually not obvious through a visual inspection of the time history [see Figure 4.6(b)], because the noise itself is generally a stationary random signal. On the other hand, such noise will often be apparent in a spectrum of the measured data, as detailed in Section 4.5.2.1.

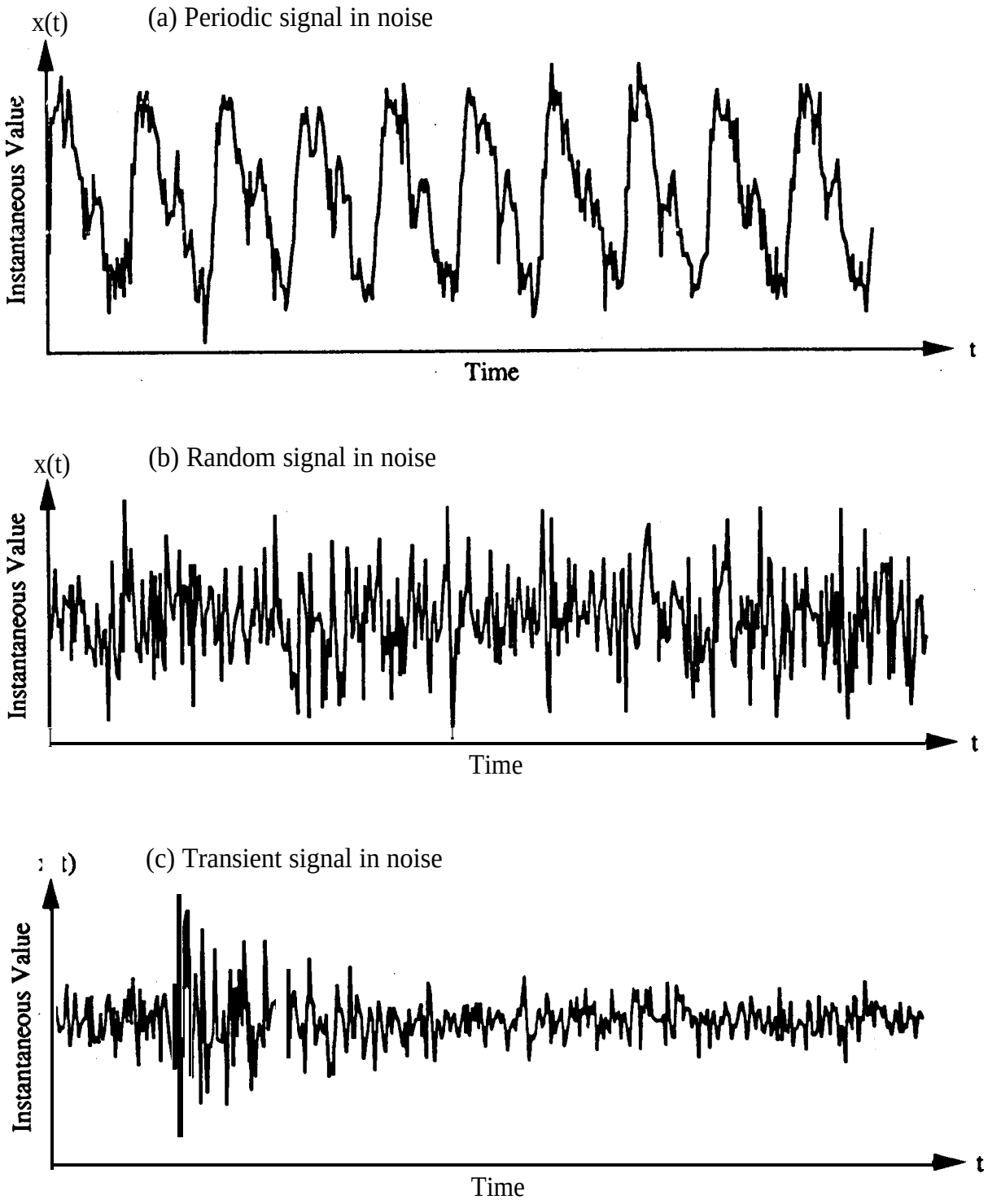

Figure 4.6. Illustration of Excessive Instrumentation Noise in Periodic, Random, and Transient Signals.

4.3.2.2 Data Rejection Criteria. For the case of periodic signals, if only a spectrum is required from the data analysis, the influence of excessive instrumentation noise can be suppressed dramatically by the narrowband filtering inherent in the computation of a spectrum (see Section 5.4.2). There is also the possibility of extracting a periodic signal from excessive instrumentation noise through the use of synchronous averaging (see Section 5.2,3). Hence, excessive instrumentation noise is not a reason to reject periodic signal measurements for spectral analysis purposes. However, it does generally rule out time domain interpretations of periodic signals, unless the noise can be suppressed by synchronous averaging procedures (see Section 5.2,3), For stationary random signals, the presence of excessive instrumentation noise presents a more difficult problem, where the decision as to whether a measurement should be rejected usually requires the computation of a spectrum (see Section 4,5.2.1). For transient signals, the criterion for rejecting a measurement due to excessive instrumentation noise is detailed in Appendix A.

4.3,3 Intermittent Noise. A special type of noise problem that sometimes arises during data acquisition is the presence of intermittent "noise spikes" in a measured time history. Of course, such noise spikes may represent real data, but more often they reflect a data acquisition system malfunction (e.g., a defective connector or shielded cable, commonly between the transducer and its signal conditioner) that produces intermittent noise when subjected to shock or vibration, The presence of noise spikes due to these sources should be detected and corrected during the data acquisition system calibration (see Section 3.8.2). However, noise spikes may also appear in FM telemetered data due to "click" (or FM) noise caused by too low a signal level at the demodulator. "Click" noise generally will not be detected during the data acquisition system calibration.

4.3.3,1 Identification Procedure. For the case of periodic data, the presence of intermittent noise spikes is usually obvious from a visual inspection of the time history, as shown in Figure 4.7(a). For random and transient signals, however, the problem may be more obscure, as illustrated in Figure 4.7(b) and (c). For the special case of stationary random signals, the detection of noise spikes can often be augmented by a probability density analysis, as detailed in Section 4.5.1.2, Special procedures for detecting noise spikes in pyroshock data are addressed in Appendix A. Additional procedure that may be helpful 'in identifying noise spikes and distinguishing them from real data are as follows:

(1) Check the log sheet for the measurement to see if a physical event occurred that would explain an extreme value at the same time a noise spike is observed in the signal (see Section 4.2).

(2) In those cases where multiple-channel measurements are made, and the source of noise spikes may be common to all channels, directly compare the time histories for all simultaneous measurements to determine if suspected noise spikes appears at exactly the same times in all measurements. Of course, the possibility that an actual physical event might have produced an extreme value in all the measurements must also be considered

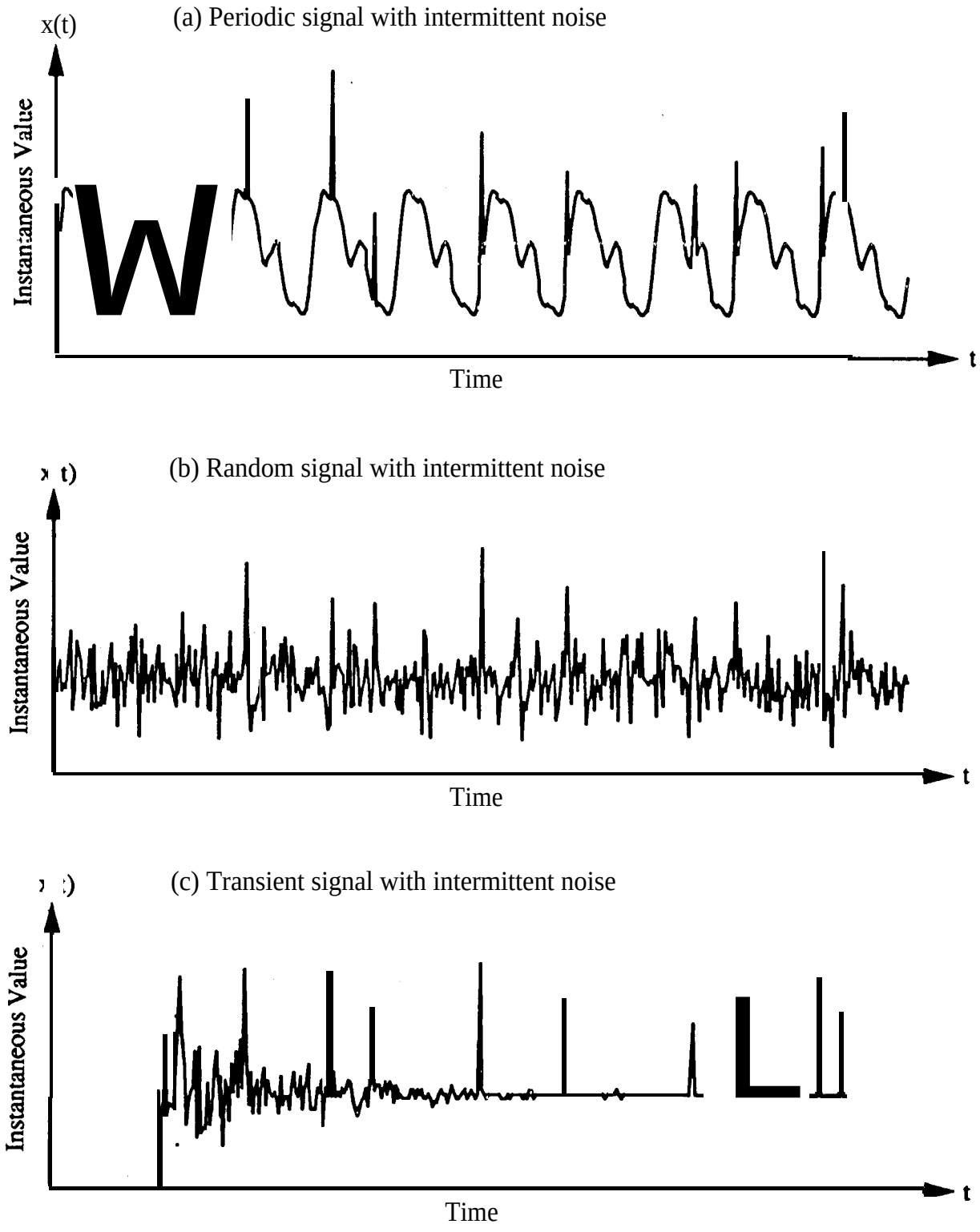

Figure 4.7. Illustration of Intermittent Noise in Periodic, Random, and Transient Signals.

(3) If the upper frequency limit of the data acquisition system substantially exceeds the upper frequency limit of the dynamic signals being measured, noise spikes will generally have a much shorter duration than actual data. Specifically, the duration of noise spikes (their "sharpness") is characteristically of the same order as the reciprocal of the uppercut-off frequency limit of the data acquisition system.

4.3.3.2 Data Rejection Criteria. Intermittent noise spikes appear in a spectral analysis as additive broadband noise, which can severely distort the spectral values of the actual signal Hence, it is recommended that all measurements with identified noise spikes in their analog time histories be rejected, unless the noise spikes can be removed by the corrective editing detailed in Section 4.6.2. For the case of stationary random signals with a wide bandwidth, even with the identification efforts detailed in Section 4.3.3.1, noise spikes in the time histories might be confused with extreme but valid signal values. Hence, it is generally recommended that all time history values in wide bandwidth random signals that exceed ± four standard deviations from the mean value of the signal be considered erroneous noise spikes. These limits maybe increased when the signal is produced by an accelerometer mounted on a structure with a hardening-spring non-linear response characteristic, or when the signal has an unusually long duration. See Section 5.2.2 for details on the computation of mean values and standard deviations of signals.

4.3.4 Power Line Pickup. The contamination of a measured signal by power line pickup (at 60 Hz within the USA, 50 Hz in most regions outside the USA, and 400 Hz in many aerospace applications) will commonly occur if the data acquisition system is not properly shielded and grounded. A break in the shielding of a signal transmission line, or the grounding of the signal transmission system at two or more points (ground loops) are the most common causes of excessive power line pickup. Although some power line pickup commonly occurs during data acquisition, the presence of excessive power line contamination of signals usually can be detected and corrected during the data acquisition system calibration (see Section 3.8,2). Power line pickup may sometimes occur in the data playback equipment. In this case, the data signals are not contaminated and the problem is easily eliminated by correcting the data playback equipment.

4.3.4.1 Identification Procedure. Power line pickup produces a periodic oscillation superimposed on the signal time history of interest, often with multiple harmonics. If the pickup is strong, the detection is easily made by visual inspection of an analog time history, as illustrated in Figure 4.8. However, a more powerful detection is provided by a spectral analysis of the signal, as detailed in Section 4.5.2.2, or by the measurement of a quiescent time history, as discussed in Section 4.3.2.1.

4.3.4.2 Rejection Criteria. Unless it is very severe, power line contamination is not a reason to reject measurements for spectral analysis purposes, although it may somewhat limit time domain interpretations of such data. If a spectrum is computed (see Section 5.4), it is recommended that all

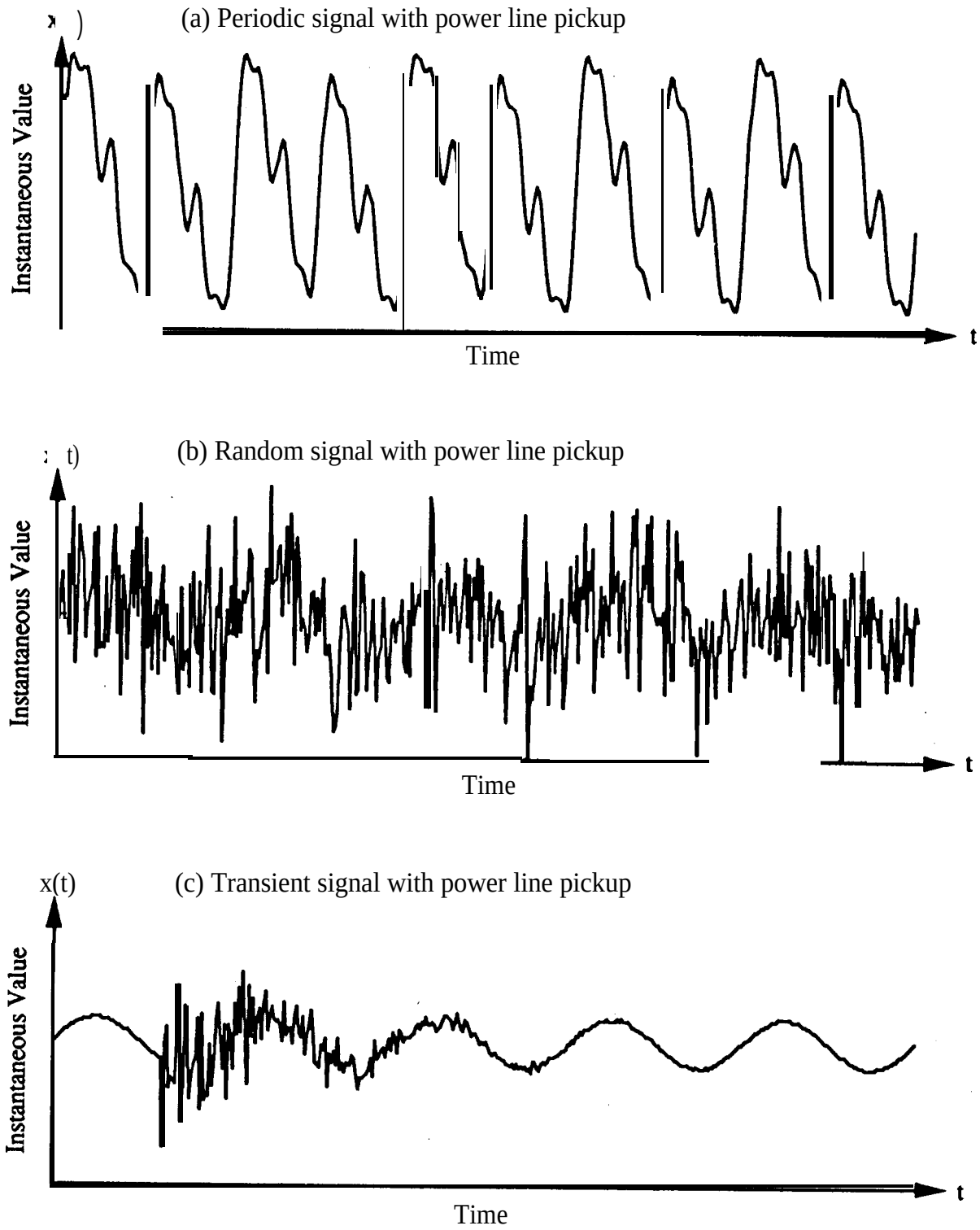

Figure 4.8. Illustration of Power Line Pickup in Periodic, Random, and Transient Signals.

spectral peaks indicative of a sine wave at the power line frequency and all multiples thereof simply be ignored. The only exception is when there is a conclusive, independent reason to believe the data actually include a periodic component at the power line frequency, e.g., a measurement that represents the vibration response of a rotating machine operating at exactly 3600 rpm or 60 Hz. There may be cases where severe power line contamination occurs early in the data acquisition system, perhaps due to a ground loop involving the transducer. This may saturate the instruments that follow in the data acquisition system, or force sufficiently low sensitivity gain settings on the instruments to cause the signal to be buried in the instrumentation noise. In such cases, all meaningful information is lost and the measurement should be rejected.

4.3.5 Spurious Trends. Measured time history signals sometimes reveal a relatively slow variation in the mean value as a function of time, often with a period that is longer than the measurement duration. Of course, such trends may be physically meaningful if the signal being measured has a time-varying mean value, and the frequency response for the data acquisition system covers static or DC values. In many cases, however, such trends are spurious. For the case of pyroshock data, they commonly occur due to a severe saturation of a signal conditioner or the sensing element in a piezoelectric transducer, and generally render the data worthless (see Appendix A). In other cases, spurious trends may occur when a signal is integrated, e.g., when a vibration response measured by an accelerometer is converted to a velocity signal. The integration of an accelerometer output will commonly produce a low frequency trend due to low frequency noise and/or a zero offset in the measurement system. Spurious trends may also arise due to environmental (usually temperature) induced drifts in analog data acquisition instrumentation.

4.3.5.1 Identification Procedure. Spurious trends in otherwise valid measurements are usually obvious in the signal time history, as long as the lower frequency limit (f_l) of the data acquisition system and/or the data signal is substantially higher than the reciprocal of the duration (T_r) of the measurement; i.e., $f_l >> 1/T_r$. Illustrations of obvious trends in periodic, random, and transient data signals are shown in Figure 4.9. If it is desired to automate the detection of possible trends in time history measurements, this can be accomplished using the trend detection algorithm detailed in Section 4.8.

For those cases where a very low frequency, long duration dynamic signal (e.g., wind velocity versus time) is measured using a DC coupled analog data acquisition system, it may be difficult or impossible to distinguish a low frequency trend due to drift in the data acquisition system from valid low frequency variations in the data signal. The only way to effectively suppress this problem is through the selection of a DC coupled data acquisition system that has been very carefully designed for minimum drift.

4.3.5.2 Data Rejection Criteria. In most cases where a trend is not due to saturation of an amplifier or piezoelectric transducer element, the presence of the trend in the data signal will only distort

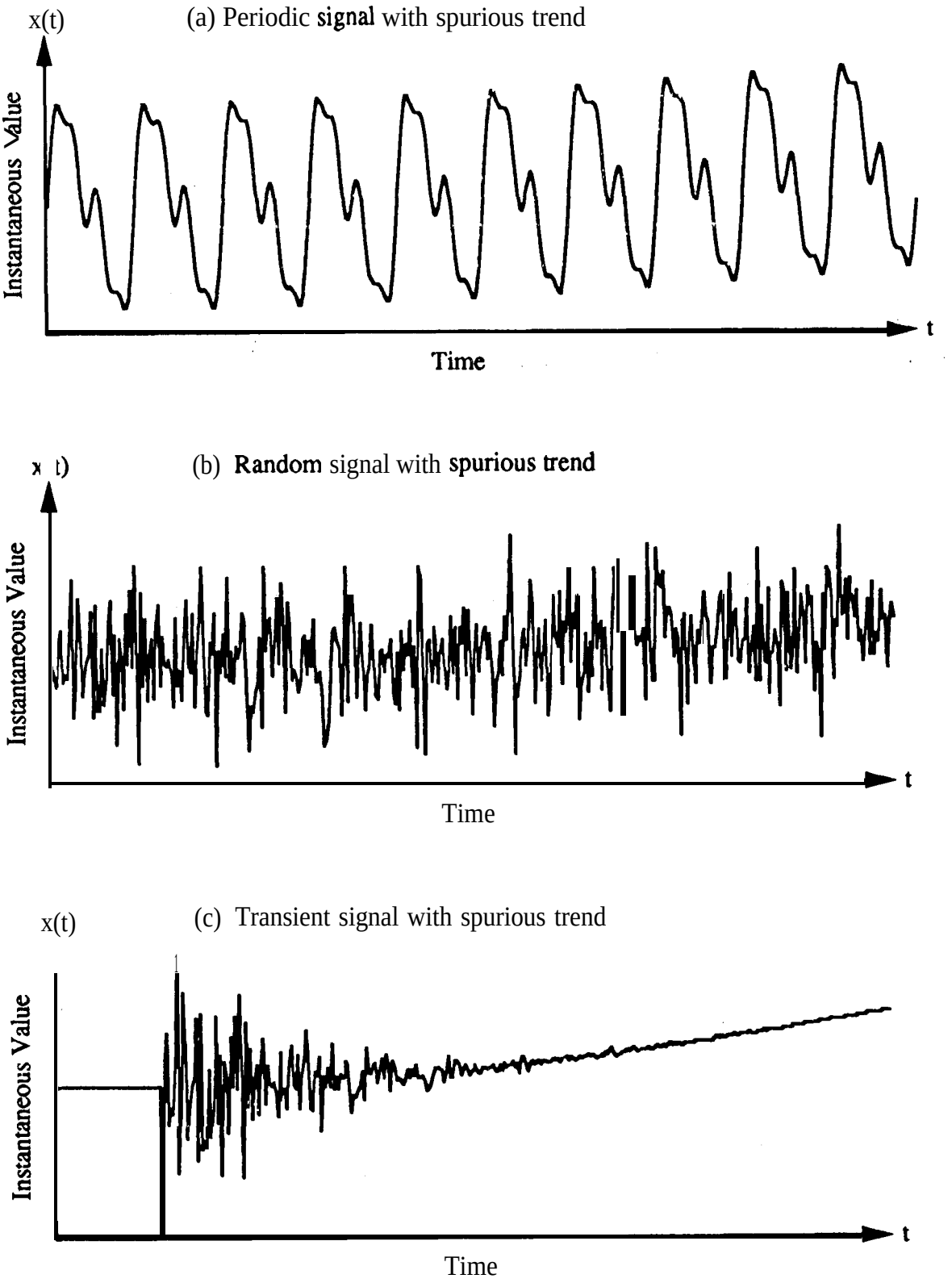

Figure 4.9. Illustration of Spurious Trend in Periodic, Random, and Transient Signals.

the low frequency content in a computed spectrum. Hence, assuming the lowest frequency f_l of interest in the signal is substantially higher than the reciprocal of the measurement duration T_r (say $f_l > 10/T_r$), a valid (detrended) signal can usually be recovered by highpass filtering operations [4.5, 4.6], Even when $f_l = 1/T_r$, monotonic trends can still be removed by the regression analysis procedures discussed in Section 4.6.3. However, for the special case of pyroshock data signals, if a spurious trend or "zero shift" due to saturation of a piezoelectric transducer or amplifier is identified, it is recommended that the measurement be rejected (no corrective editing or trend removal should be attempted) for the reasons discussed in Appendix A.

4.3,6 Signal Drop-Outs. Sometimes a measured signal will diminish rapidly into the instrumentation noise floor for no apparent reason. The signal may or may not return later in the measurement. Such signal drop-outs often represent a malfunction of the transducer or some other instrument in the data acquisition system. A permanent signal drop-out usually indicates a catastrophic malfunction, e.g., an accelerometer detaches from the structure or a signal conditioner loses power. A temporary drop-out, where the signal level ultimately recovers, usually indicates amalunction due to a momentary saturation of a transducer or signal conditioner, or a tape drop-out. Temporary or permanent drop-outs may also occur in telemetered data when the transmitter antenna moves to a position which is physically shielded or excessively remote from the receiver antenna. Reentry plasma routinely causes signal dropouts.

4.3.6.1. Identification Procedure. Permanent and temporary signal drop-out are illustrated in Figure 4.10. Such drop-outs are easily detected by a visual inspection of the signal time history, with one exception. Specifically, for the case of transient data, a drop-out might occur during the transient event so as to distort or perhaps obscure the transient signal in a manner that is not obvious by visual inspection of the time history. Such an occurrence is best identified by knowing the exact time a transient should appear on the time history, as discussed in Section 4.2.2. In those cases where multiple-channel measurements are made, and the source of tip-outs is common to all channels, a direct comparison of the time histories for two or more simultaneous measurements can also be helpful in identifying dropouts.

4.3.6.2. Data Rejection Criteria. If a measured time history reveals a permanent signal drop-out sometime after the start of the measurement, the signal prior m the drop-out can be accepted for analysis, unless there is evidence of a measurement problem prior to the drop-out. If the signal drop-out is temporary, those portions of the signa! time history covering the time intervals of the drop-outs should be deleted from the data. The remainder of the measurement can be analyzed with proper treatment of the discontinuities caused by the deletion of drop-outs, as detailed in Section 4.6.4. An important exception is a temporary drop-out in the output of any type of piezoelectric transducer. Such a drop-out might reflect an over-stress of the piezoelectric element, which will often change the sensitivity of the element and, hence, change the calibration factor for the measurement following the drop-out.

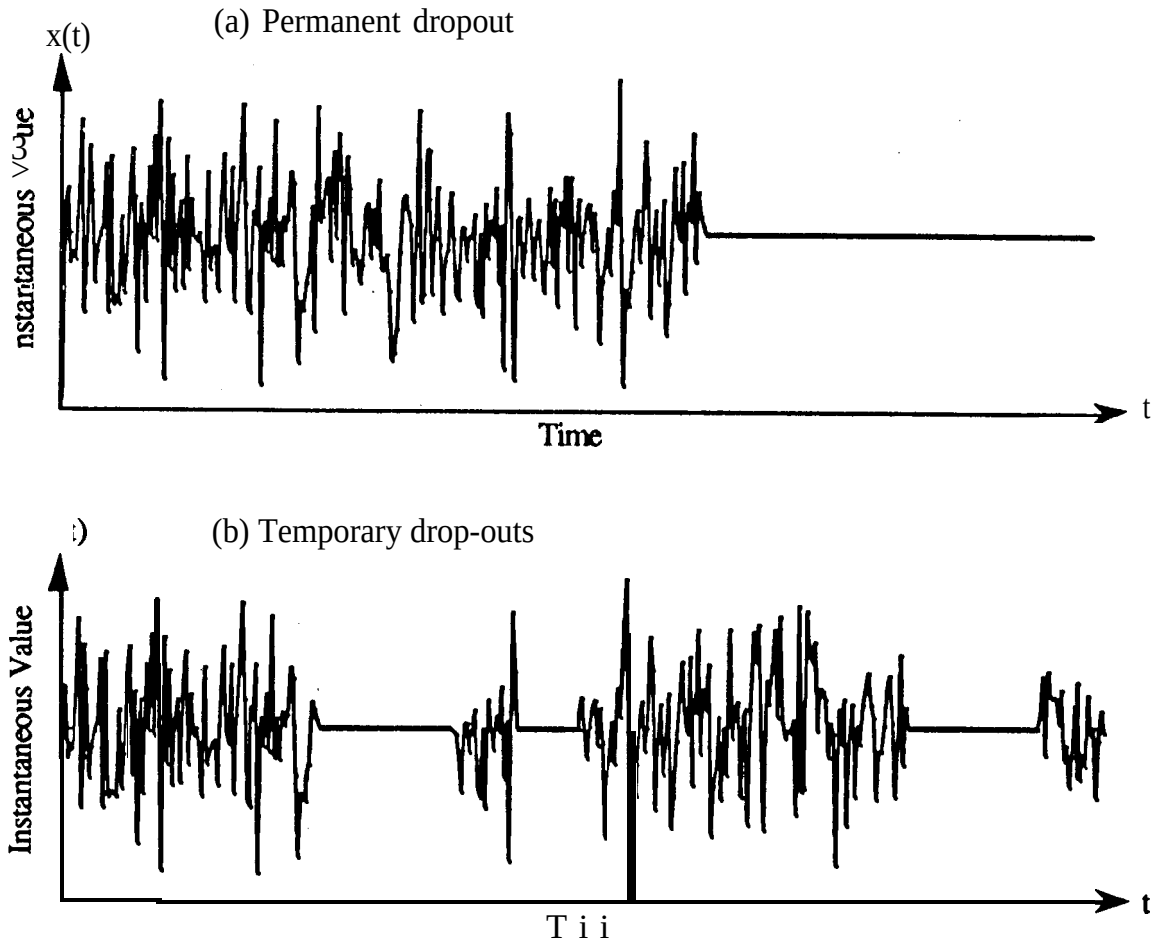

Figure 4.10. Illustration of DropOuts in Random Signals.

4.4 Visual Inspection of Digital Time Histories. Most analyses of dynamic measurements are accomplished by playing back analog tape recordings of the data signals into specialized digital signal processing instruments, where the signal digitization and analysis operations are combined. In this case, no further data validation or editing of the signal time histories, beyond those detailed in Section 4.3, is practical. In some cases, however, the analog recordings of the measured signals are digitally converted and stored on a digital magnetic tape or disk for later data analysis by appropriate software programs. In a few cases, the data from the transducers may be digitally converted and recorded on-line, without the recoding of any analog time history information.

For those cases where the data signals are digitized and recorded in a digital format on-line, each recorded signal should be played back onto a hard copy using a digital hard copy recorder (see Section 5.2. 1.2) with a frequency response equal to or greater than the frequency range of interest in the data, The instantaneous values of each measured signal should be visually inspected for the same anomalies detailed in Section 4.3, exactly as if they were analog recorded time histories. For those cases where the signals are first recorded on analog tape, and are then converted and stored

in a digital format prior to analysis, each digitally recorded signal should be played back onto a hard copy as described above. Beyond the visual inspections of the analog recorded signals described in Section 4.3, the instantaneous values of each digital signal should be visually inspected for the following additional anomalies that might be introduced by a malfunction or incorrect use of the analog-to-digital converter (ADC).

4.4,1 Signal Clipping. Just as clipping or saturation may occur in one or more of the various analog instruments in the data acquisition system (see Section 4.3.1), so clipping can occur in the ADC if the instantaneous signal value is too large relative to the upper limit of the ADC dynamic range,

4,4.1.1 Identification Procedure. ADC clipping will distort the signal time history as previously illustrated in Figure 4.5. For the case of stationary random signals, further identifications of signal clipping are provided by a probability density calculation, as detailed in Section 4,5.1.1.

4,4.1.2 Data Rejection Criteria. If the digital data are acquired by the digital conversion of an analog recording, and clipping appears in the digital time history but not in the analog time history, this firmly identifies the ADC as the source of the clipping. In such cases, it is recommended that the analog signal be redigitized with a lower input sensitivity to the ADC. If the digital data are acquired on-line, and clipping is identified in the digital time history, the data rejection criteria detailed in Section 4.3.1.2 apply.

4.4,2. Excessive Digital Noise. If the maximum instantaneous signal value is too small relative to the dynamic range of the ADC, the signal will be obscured by the digital noise of the ADC (see Section 3,7. 1.3).

4.4.2.1 Identification Procedure. Unlike analog instrument noise problems, excessive digital noise is easily identified in digital time histories, even for random signals. Specifically, the signal will usually appear as a series of well defined steps in the time history, as shown in Figure 4.11. Digital noise will also be revealed in a spectrum for the signal, as detailed in Section 4.5.2.1.

4.4.2.2 Data Rejection Criteria. If the digital data are acquired by the digital conversion of an analog record, and excessive digital noise appears in the digital time history but not in the analog time history, it is recommended that the analog signal be redigitized with a higher input sensitivity to the ADC. If the digital data are acquired on-line, and digital noise is identified in the digital time history, the data rejection criteria detailed in Section 4.3.2.2 apply.

4.4.3 Wild Points. On occasions, the output of an ADC may include one or more erroneous values due to a momentary malfunction of the ADC or a failure of the formatting equipment. Such digital data errors are called “wild points”.

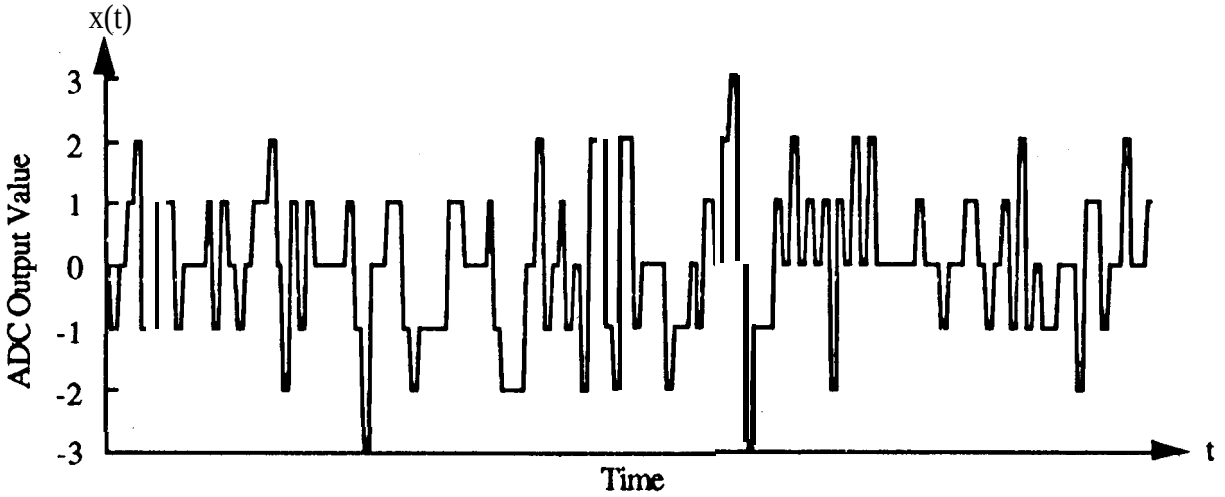

Figure 4.11. Illustration of Excessive Digital Noise Due to Inadequate Input Signal Level to ADC.

4.4,3.1 Identification Procedure. Wild points generally appear in a digital time history much like the intermittent noise spikes illustrated in Figure 4.7. Hence, the identification procedures in Section 4,3.3.1 apply to wild points as well. The detection of wild points can be further enhanced by applying a sine wave to a separate "check-channel" in the ADC. Wild points in an otherwise sinusoidal signal are obvious. Hence, assuming the malfunction causing a wild point influences all ADC channels, wild points can be easily detected by simply comparing the outputs of the ADC data channels with the sinusoidal output of the check-channel.

4.4.3.2 Data Rejection Criteria. It is important that wild points be detected and removed from the digital time history prior to analysis, because they can severely distort the results of certain types of analysis, particularly any form of spectral analysis. The procedures for removing wild points from digital time histories are the same as those detailed for intermittent noise spikes in Section 4.6.2.

4.4,4 Spurious Trends. On rare occasions, a drift in the ADC circuits may cause a trend to appear in the digital time history. If it is desired to automate the detection of possible trends in digital time history measurements, this can be accomplished using the trend detection algorithm detailed in Section 4.8.

4 . 4 . 4 . 1 Identification P r -. ADC drifts will cause a trend in the signal time history similar to that previously illustrated for analog signals in Figure 4.9.

4,4.4.2 Data Rejection Criteria. If the digital data are acquired by the digital conversion of an analog recording, and a trend appears in the digital time history but not in the analog time history, this firmly identifies the ADC as the source of the trend. In such cases, it is recommended that the analog signal be redigitized with a repaired or new ADC. If the digital data are acquired on-line,

and a trend is identified in the digital time history, the trend should be removed from the signal using a highpass digital filter or the detrending operation based upon the criteria detailed Section 4.3.5,

4,4,5 Other ADC Malfunctions. Most other ADC malfunctions are catastrophic, i.e., they result in either a total loss of ADC output values, or they produce output values with a format that cannot be read by later data analysis programs. Such problems dictate a major repair or replacement of the ADC. To help suppress these problems, regular testing of the ADC is recommended. Also, the user should be fully familiar with the ADC capabilities, including the filters built into the ADC system.

4,5 Visual Inspection of Analyzed Data. The best approach to the detection of spurious data signals is through a visual inspection of the time histories prior to a detailed data analysis. However, this is not possible for the case of on-line data analysis. Furthermore, even when stored time histories are available, there are certain types of anomalies, particularly in random signals, that are not easily detected by visual inspection of time histories alone, Some of these anomalies in random signals are easily detected (as long as the signals are stationary) in the results of certain data analysis procedure, in particular, probability density analysis and narrowband spectral analysis.

4.5.1 Probability Density Plots. For the case of stationary random data, if a probability density analysis (see Section 5.7. 1) is performed as part of the normal data analysis requirements, then an inspection of the probability density plot is recommended to identify the following data anomalies that may have been missed during the visual inspection of time histories, For those cases where stationary random signals are analyzed on-line (no time histories are available for visual inspection prior to analysis), the computation of probability density plots solely for data validation purposes should be considered,

4,5.1.1 Signal Clipping. Signal clipping due to an inadequate upper limit on the dynamic range of one or more instruments in the data acquisition system (see Section 4.3.1), including the ADC (see Section 4.4.1), will appear in a probability density plot as peaks on the tails of the computed probability density. This is illustrated for the case of an otherwise stationary random signal (assured to be approximately Gaussian) in Figure 4.12(a) and (b). The detection of clipping can be enhanced by plotting the probability density values on a logarithmic scale. The data rejection criteria are the same as detailed in Section 4.3.1.2.

4.5.1.2 Intermittent Noise. Intermittent noise spikes in an otherwise stationary random signal due to a defective connector or cable shield, or "click" noise (see Section 4.3.3), will appear in a probability density plot as unduly long extensions of the tails of the plot, as illustrated in Figure 4.12(c). Sometimes the noise spikes occur with only positive or negative values, in which case the probability density will display an unduly long tail in only one direction. If the computed proba-

4.5.1.3 Wild Points. Wild points in a digital time history due to a malfunction of the ADC will appear in a probability density plot exactly like intermittent noise spikes, The data rejection criterion given in Section 4,S. 1.2 applies,

4,5,1.4 Power Line Pickup. Power line pickup in an otherwise stationary random signal (see Section 4,3.4), if it is sufficiently intense relative to the random signal, will appear in a probability density plot as a valley centered at the mean value, as illustrated in Figure 4. 13(a) and (b). However, the rms value of the power line pickup must be at least equal to therms value of the random signal it contaminates before the anomaly shown in Figure 4.13(b) is obvious. A narrowband spectral analysis provides a far more powerful tool for the detection of power line pickup. The data rejection criteria are the same as detailed in Section 4.3.4.2.

4.5.1.5 Signal Drop-Outs. Signal drop-outs in an otherwise stationary random signal (see Section 4,3.6) will appear in a probability density plot as a sharp peak at the mean value of the signal (at zero voltage assuming the data acquisition system is AC coupled). This is illustrated in Figure 4.13(c), Even a single, short duration drop-out will usually cause a discernible peak in the probability density at the zero value, making a probability density plot a powerful tool for detecting signal drop-outs. The data rejection criteria are the same as detailed in Section 4.3.6.2.

4.5.2 Narrowband Spectral Analysis For all measured data signals (periodic, random, and transient), a narrowband spectral analysis of some form (see Sections 5.4 and 5.5) will usually be performed as part of the normal data analysis requirements. An inspection of the spectra is recommended to identify the following data anomalies that may have been missed during the visual inspection of time histories. For those cases where stationary random signals are analyzed on-line (no time histories are available for visual inspection prior to analysis), the visual inspection of narrowband spectral plots is imperative, since there is no other procedure available to detect certain types of data anomalies.

4.5.2.1 Excessive Instrumentation Noise. For the case of stationary random data, the contamination of the signals by excessive instrumentation noise is difficult to detect by a visual inspection of time histories prior to analysis (see Section 4.3.2). However, such noise is easily identified in a narrowband autospectrum. Specifically, instrumentation noise tends to have a relatively flat spectrum (i.e., the spectral values at all frequencies are similar in magnitude), while the signals produced by dynamic measurements, particularly structural vibration measurements, usually have spectra that cover a wide dynamic range (i.e., spectra with distinct peaks and notches). Hence, the appearance of constant spectral values at most frequencies is usually indicative of excessive instrumentation noise, as illustrated in Figure 4. 14(a) and (b). For data validation purposes, if the spectrum of a measurement is similar to that shown in Figure 4.14(b) and does not reveal spectral values that exceed the background value by at least 10 dB, it is recommended that the measurement be rejected unless corrective editing operations can be performed, as detailed in Section 4.6.1.

bility density reveals values in excess of ± four standard deviations from the mean value, it is recommended that the measurement be rejected, unless the noise spikes can be removed by the corrective editing discussed in Section 4.6.2. These limits may be increased when an accelerometer is mounted on a structure with hardening-spring non-linear response characteristics, or when the data are sampled over an unusually long duration.

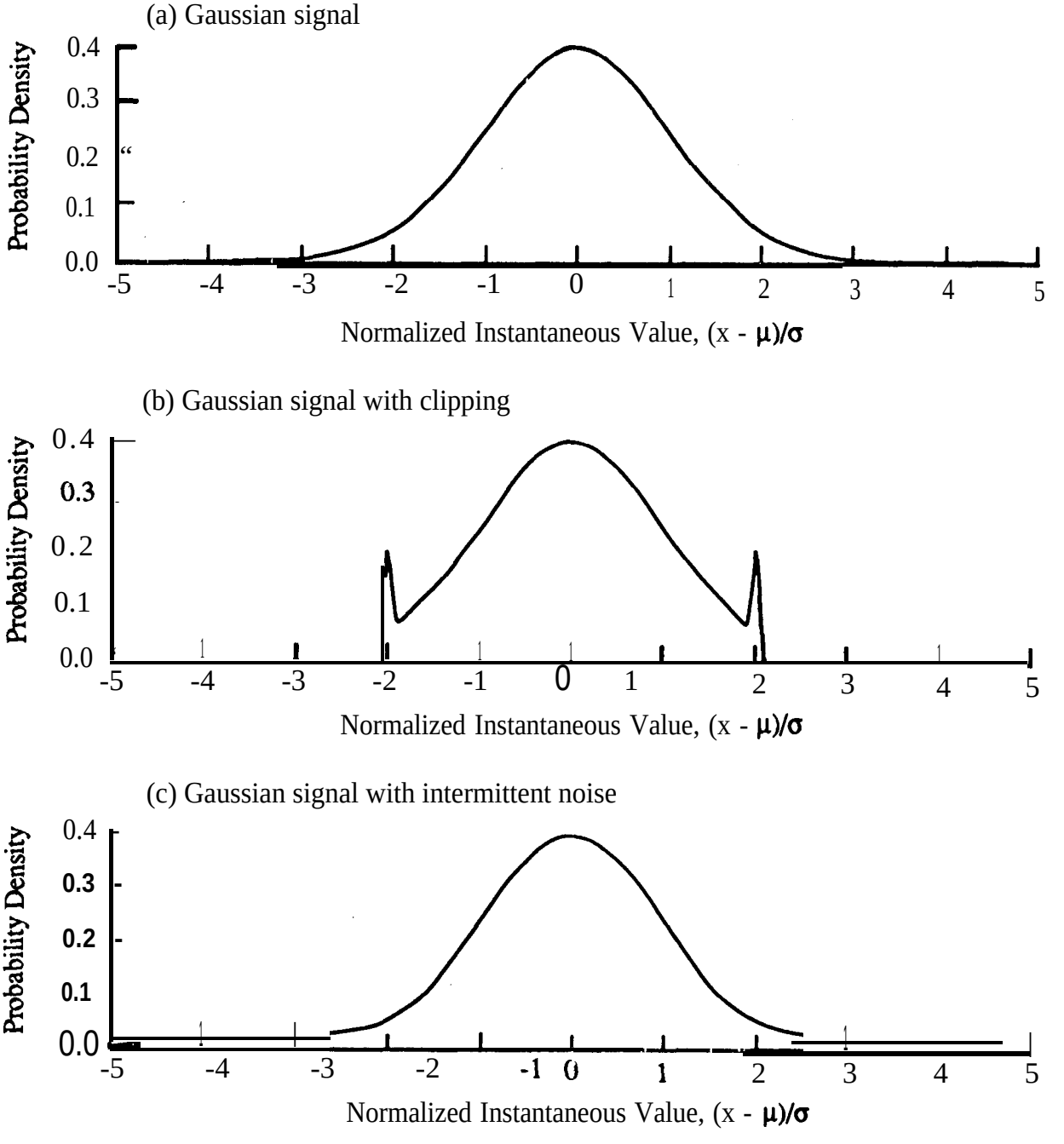

Figure 4.12. Influence of Signal Clipping and Intermittent Noise on Probability Density Plots.

However, if there are spectral values that exceed the background noise by at least 10 dB, then the computed spectrum of the measurement can be used for restricted interpretations at those frequencies where a 10 dB or greater margin exists. The frequency range of acceptable results can be further expanded by the corrective editing operations discussed in Section 4.6.1.

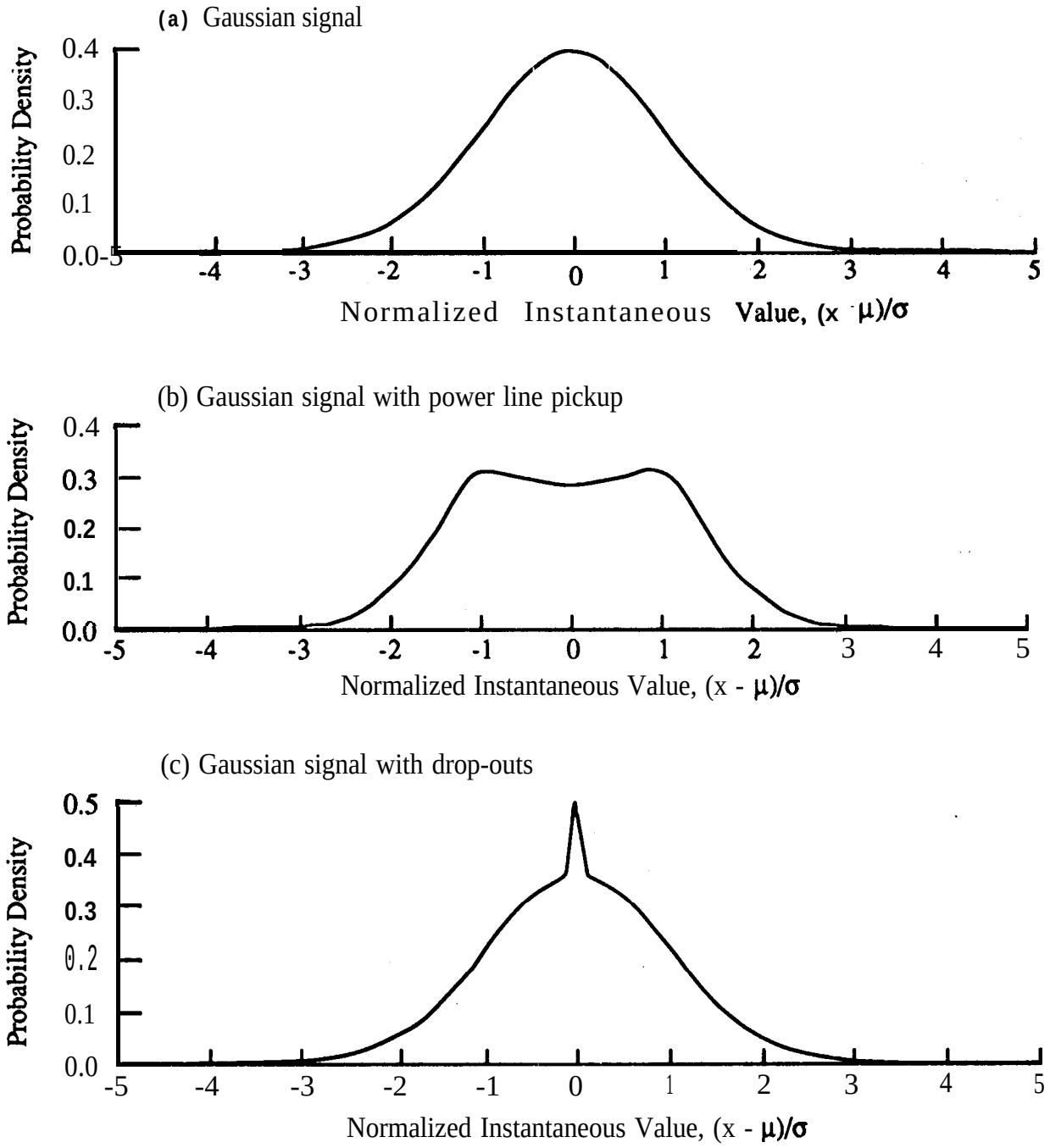

Figure 4.13. Influence of Power Line Pickup and Signal Drop-Outs on Probability Density Plots.

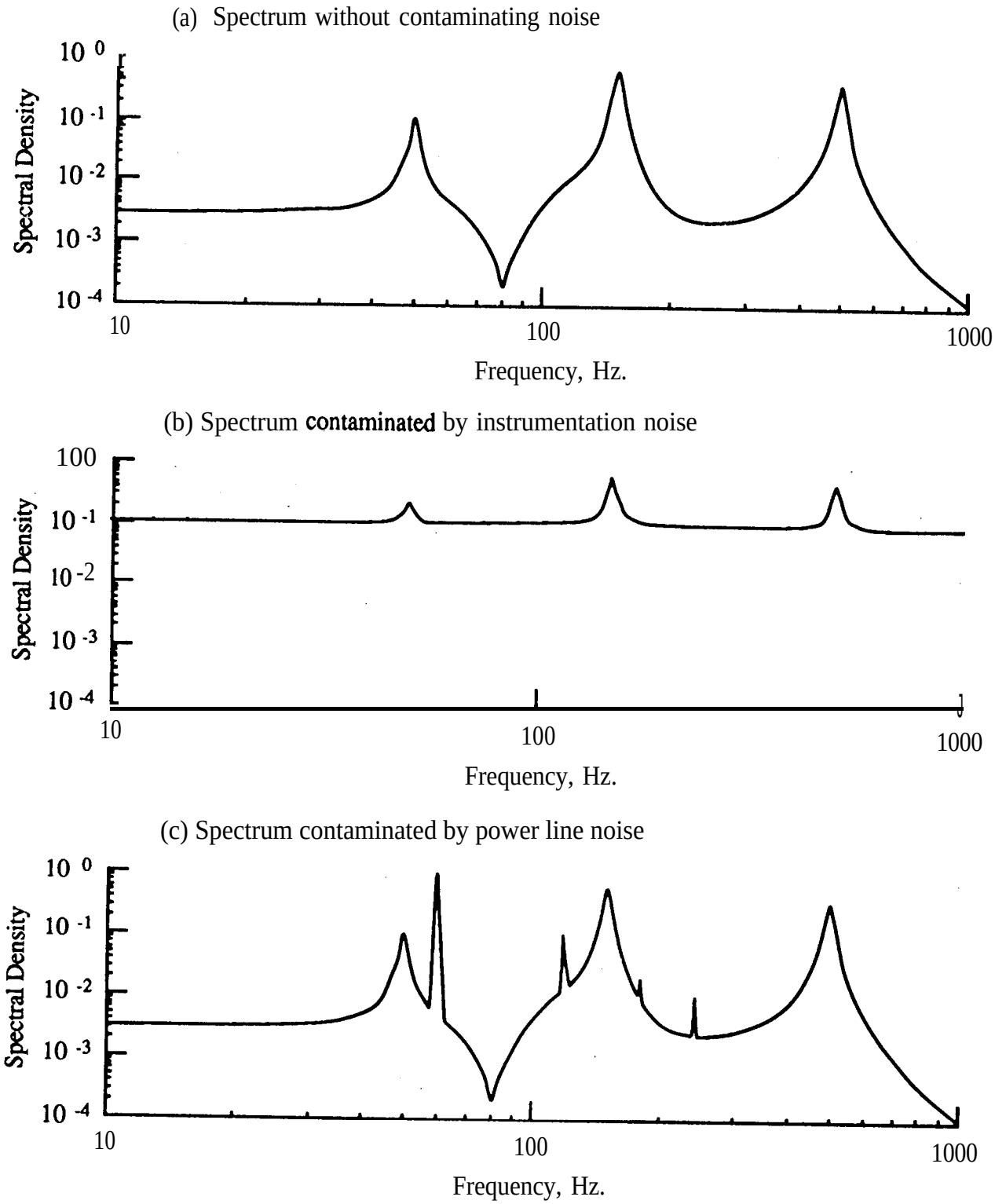

Figure 4.14. Influence of Instrumentation and Power Line Noise on Spectral Density Plots.

4.5,2.2 Power Line Pickup. The presence of small amounts of power line pickup may not be apparent from a visual inspection of the time histories for measured signals (see Section 4.3.4) or in a probability density plot (see Section 4.5.1.4). However, power line contamination will be clearly apparent in a narrowband spectral analysis, since it appears as a sharp spectral peak at exactly the power line frequency (e.g., 60 Hz). In the more severe cases of power line contamination, the harmonics of the power line frequency will also appear in the spectrum, as indicated in Figure 4.14(c). As discussed earlier in Section 4.3.4. if power line pickup occurs early in the data acquisition process and is strong, it can cause saturation of later data acquisition instruments and make all analyses of the measured signal suspect. In many cases, however, it only destroys that information in the signal at exactly the power line frequency and all multiples thereof. For data validation purposes, the recommendations in Section 4.3.4.2 apply.

4.6 Corrective Editing of Time Histories. For those measurements where digital time histories are stored prior to analysis, digital modifications of the measured signals to remove certain types of data anomalies should be considered. These corrective editing operations require the exercise of personal judgment based upon experience. In particular, it is important that the editing operations not add subjective information to the raw data, which might lead to conclusions based upon more information than is actually available from the data. For these reasons, it is recommended that all corrective editing be directed by the most experienced analyst available within the organization responsible for the data validation and editing process.

4.6,1 Corrections for Excessive Instrumentation Noise. For the case of random signals only, if excessive instrumentation noise is detected in the spectrum of the measurement (see Section 4.5.2, 1), it is recommended that the computed spectral values of the measurement be corrected by the following procedure:

(1) Identify all frequency intervals where the autospectral density values appear to be at least 3 dB above (twice the value of) the background noise autospectral density values [see Figure 4.14(b)].

(2) In all the frequency ranges identified in Step 1, determine the level (in dB) of the computed autospectral density value relative to the background noise autospectral density value as a function of frequency.

(3) Based upon the ratios determined in Step (2), reduce the computed autospectral density values, as detailed in Figure 4.15.

No effort should be made to corrector use the remainder of the autospectrum of the measurement where the spectral values are less than 3 dB above the values produced by the instrumentation noise.

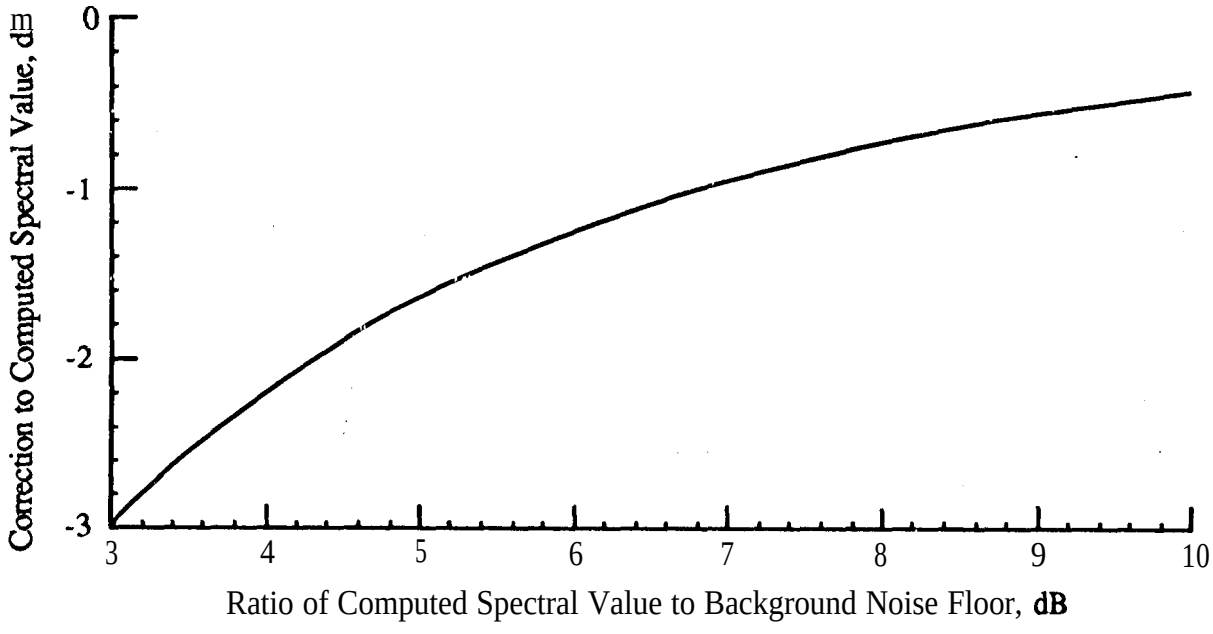

Figure 4,15. Noise Floor Correction Factors for Spectral Density Estimates of Random Signals.

4,6.2 **Removal of Intermittent Noise Spikes and Wild Points**. If intermittent noise spikes are detected in a measurement during the visual inspection of the time history (see Section 4.3.3), or from a probability density computation (see Section 4.5.1.2), it is recommended that such noise spikes be removed from the digital time history by the following procedure:

(1) Remove all digital time history values defining each noise spike, The number of digital values N_n defining each noise spike will be a function of the digital sampling rate R_s (in samples/sec) and the upper cut-off frequency of the data acquisition system, which is usually determined by the cut-off frequency f_c (in Hz) of the anti-aliasing filters. As a rule of thumb, $N_n \approx \frac{R_s}{2f_c}$.

(2) Replace the removed values for each spike with new values determined by a suitable interpolation between the last value before and the first value after the spike. For example, if the signal is periodic, an interpolation based upon data values observed in a previous period of the signal should be used. For random and transient signals, a linear interpolation should suffice, although more elaborate interpolation routines can be used.

(3) If the data where acquired with oversampling (see Section 3.7.3.2), the oversampled time histories can be edited using a linear interpolation, The final interpolation will occur when the time histories are digitally filtered and decimated prior to analysis.

It is imperative that all removed data values are replaced by interpolated values to assure that the time base for all other values of the digital time history is not altered, Furthermore, it is imperative that the editing operation not leave any extreme discontinuities in the edited time history. The above procedure also applies to the removal of wild points introduced by the ADC (see Section 4.4.3), except wild points often involve only a single data value, and in any case are unrelated to the bandwidth of the data acquisition system.

4.6,3 Removal of Spurious Trends. If a spurious trend is detected in a measurement during the visual inspection of the time history (see Section 4.3.5) or by a trend detection algorithm (see Section 4.8), it is recommended that the trend be removed from the digital time history. For those cases where the spectral content of the signal is of no interest at frequencies below $f = 10/T_r$ Hz, where T_r is the measurement duration in sec, the trend can be removed with a conventional high-pass digital filter (see Section 5.2.4.2) having a cut-off frequency of no less than $f = 10/T_r$ Hz. This will be true in all cases where the autospectrum of a random signal is computed by subdividing the total measurement duration T_r into $n_d \geq 10$ segments, each of length T, as described in Section 5.4.3. In those rare cases where the spectral content of a signal at frequencies down to $f = 1/T_r$ Hz is of interest, as may arise if the measurement duration is not segmented for spectral computations, linear and other simple monotonic trends can still be removed from the signal by the following procedure:

(1) Make a "least squares" fit to the digital time history by conventional regression analysis procedures [4.5, 4.6] using a polynomial with an order of three or less.

(2) Subtract the values of the "least squares" polynomial determined in Step (1) from the digital values of the measured signal time history.

Trend removal should never be applied to pyroshock data in an effort to remove a zero-shift from the signal, for the reasons detailed in Appendix A.

4.6.4 Removal of Temporary Signal Drop-Outs. For periodic and stationary random signals, if temporary signal drop-outs are detected during the visual inspection of a measured time history signal (see Section 4.3.6), those time intervals covering the drop-outs can be deleted from the digital time history data, and the remaining portions of the measured signal before and after the drop-outs usually can be analyzed. (Note the important exception for measurements involving piezoelectric transducers discussed in Section 4.3.6.2). However, it is important to avoid an FFT computation over any time segment of the edited signal that includes a discontinuity due to the editing. Specifically, for the case of stationary random signals, it is recommended that a spectral analysis of the edited measurements be performed as follows:

(1) Divide the edited time history signal into the n_d disjoint segments needed for a spectral analysis (see Section 5.4.3) in a manner that does not allow a discontinuity due to the editing to occur within any segment, as illustrated in Figure 4.16(a).

(2) If a large number of drop-outs are edited from the signal, the procedure in Step (1) may result in a substantial loss of information in the analysis. This problem can be suppressed by selecting overlapped segments, as illustrated in Figure 4.16(b). If this alternate approach is used for the spectral analysis of random signals, it must be remembered that the variance of the resulting spectral estimate is no longer inversely proportional to the number of data segments (see Section 5.4.3.7).

(3) For those cases where spectral analyses are performed on multiple measurements from the same experiment, it is important that the same time segments be used for the analysis of all the measurements for comparative purposes.

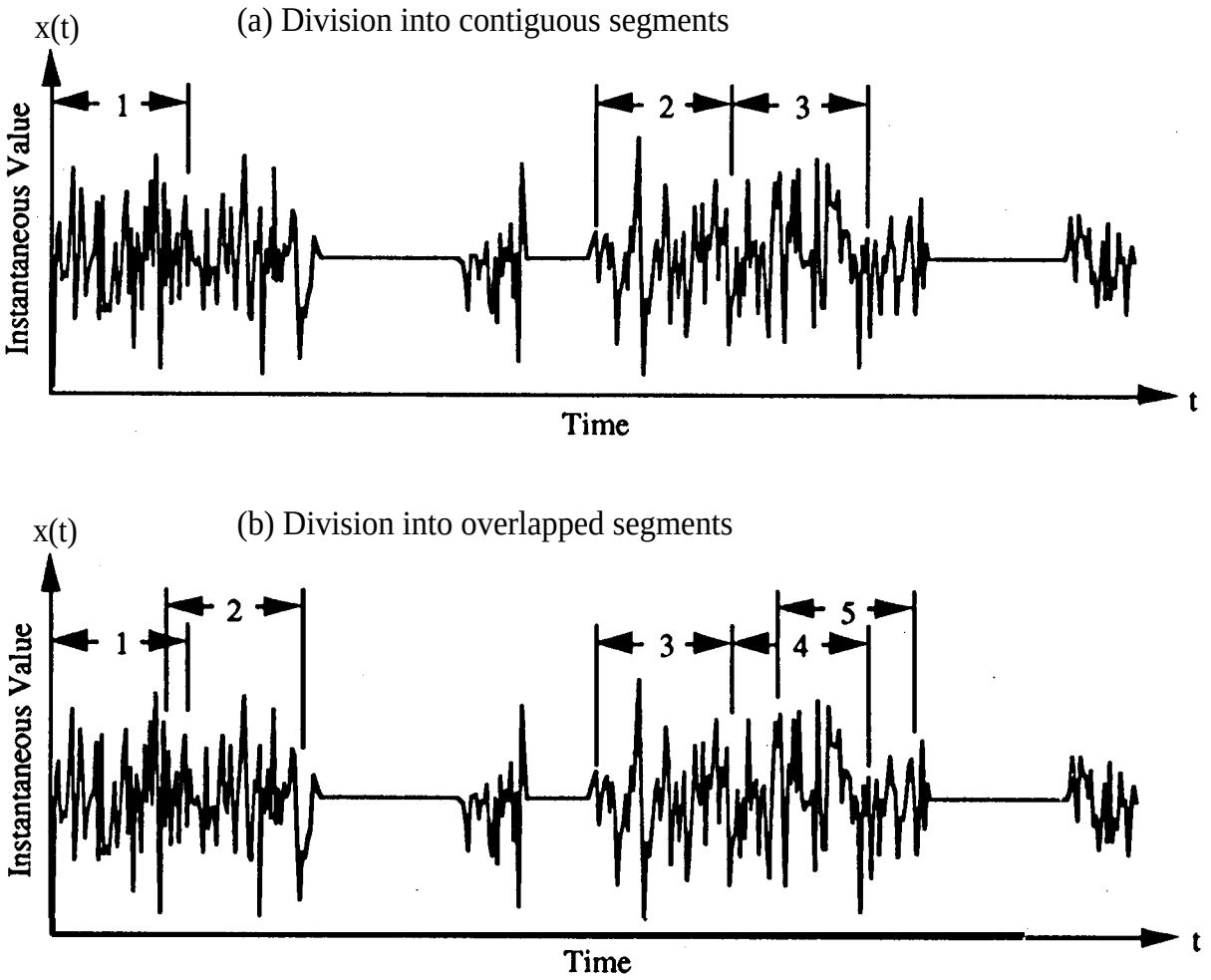

Figure 4.16. Selection of Time Segments for Spectral Analysis of Signals with Drop-Outs.

The same procedure can be used to compute spectra for periodic signal measurements with temporary drop-outs. However, if the periodicity is sufficiently stable to preclude sampling errors in the spectral computation (see Section 5.4.2.6), an adequate spectrum can usually be computed using any one segment of the signal between drop-outs.

4,7 Identification of Periodic Components. During the visual inspection of spectral data (see Section 4,5,2), there maybe cases where a sharply defined peak occurs in a narrowband spectrum at a frequency that cannot be correlated with a physical source, e.g., a rotating element or self-limiting instability. Such a peak might be due to an unknown periodic source that has physical significance. On the other hand, it could represent a lightly damped resonant response of a structure or acoustic cavity to random excitation, meaning the spectral peak represents a narrowband random signal rather than a periodicity. There are two basic procedures that can be employed to distinguish between these two types of signals. The first is a straightforward procedure using a narrowband spectral analysis, and the second is a more powerful procedure involving a bandlimited probability density analysis.

4.7.1 Narrowband Spectral Analysis, To distinguish between periodic and narrowband random components producing peaks in the spectrum of an otherwise broadband random signal, the spectrum should be recomputed using a finer frequency resolution (a narrower analysis bandwidth). Noting that sine waves theoretically have zero bandwidth, if the spectral peak is due to a periodic component, the width of the spectral peak will be the same as the resolution bandwidth of the analysis and, hence, will decrease as the analysis bandwidth is made smaller. If the spectral peak is due to a narrowband random component, it will have a finite bandwidth that will ultimately be identified as the resolution bandwidth of the analysis is made smaller. Assuming a linear spectrum is computed (see Section 5.4.2), if the spectral peak is due to a periodic component, the magnitude of the peak will not diminish as the resolution bandwidth is reduced, On the other hand, if the spectral peak is due to a resonant response to random excitation, the magnitude will ultimately diminish as the resolution bandwidth is made smaller. If an autospectrum is computed (see Section 5.4,3), the spectral peak due to a periodic component will increase as the resolution bandwidth is reduced, whereas the spectral peak due to a narrowband random response will ultimately show a negligible change as the resolution bandwidth is reduced (see Section 5.4.3.4).

4.7.2 Band-Limited Probability Density Analysis. There maybe cases where a peak in the spectrum of an otherwise broadband random signal is due to a deterministic phenomenon that is oscillatory, but not at a fixed frequency, e.g., the vibration induced by the unbalance of a rotating machine with varying rotational speed. In other cases, the spectral peak may be due to a periodic phenomenon with a randomly modulated amplitude, e.g., the pressure induced at the blade passage frequency in the plane of a propeller operating at a fixed rotational speed, but with a turbulent inflow. For such signals, sometimes referred to as quasi-periodic signals, the resulting peak in a

computed spectrum will have a finite bandwidth much like a narrowband random signal. Hence, the procedure discussed in Section 4.7.1 will not distinguish between the two cases,

A procedure that will distinguish between quasi-periodic and narrowband random signals is as follows:

(a) Isolate the frequency range of the signal around the spectral@ in question by filtering the original signal with a narrow bandpass filter (either analog or digital) having a center frequency at the mid-frequency of the spectral peak, and a bandwidth just wide enough to include the full bandwidth of the spectral peak.

(b) Compute a probability density function of the bandpass filtered signal using an averaging time T that is long compared to the reciprocal of the filter bandwidth B, i.e., $T > 10/B$.

If the spectral peak is due to a narrowband random signal, the probability density function of the bandpass filtered signal will be very close to the Gaussian form illustrated in Figure 4.13(a) [4.7]. If the spectral peak is due to a periodicity or quasi-periodicity, the probability density function of the bandpass filtered signal will have a valley centered at the mean value, as illustrated in Figure 4.13(b) [4.8].

4.8 Identification of Nonstationary Trends. The concept of stationarity is usually defined in the context of an ensemble of sample records forming a random process, where the process is stationary if the average properties of the process computed over the ensemble at any instant are invariant with time translations [4.5]. For an individual time history measurement, which constitutes a single physical realization of a random process, stationarity is interpreted as a lack of time dependence in the average properties computed over each of a sequence of contiguous, short time intervals. However, due to the statistical sampling errors inherent in computing average values of random data with a short averaging time (see Section 5.2,2.3), there is a problem in distinguishing between time variations in the sequence of computed averages and statistical sampling errors. This section details a simple statistical test that can be used to determine if the average properties of a measured time history computed from a sequence of short time averages vary significantly with time. The test is nonparametric and, hence, is applicable to all time histories, whether they are deterministic or random, and is independent of their probability density functions. The testis most powerful in detecting a monotonic trend in a parameter value of interest over the the measurement duration, and may be ineffective in detecting certain types of cyclical trends,

4.8.1 Basic Considerations. Nonstationary vibration and aeroacoustic data produced by aerospace vehicles commonly reveal a time-varying mean square (or rms) value, no matter what mechanism may be producing the nonstationary behavior. This occurs because the mean square value is determined by the mean value of the signal and its variance, i.e., the area under its auto-

spectrum. If a signal were to have a time-varying mean value and/or a time-varying spectrum, the mean square value could appear stationary only if the mean value and/or the spectrum varied with time in such a manner as to keep the sum of the square of the mean plus the variance a constant, Such nonstationary conditions are highly unlikely in vibroacoustic signals. Hence, a test for time variations of the mean square value alone will usually suffice as a test for stationarity. However, the statistical test to be described shortly can be applied to as many different parameters as desired to evaluate the stationary properties of the signal in greater detail.

4.8.2 Test Statistic. Consider a time history x(t) measured over a time interval, $O \leq t \leq T$,. Divide the measurement into a sequence of q contiguous (disjoint) segments, each of equal duration $T = T_r/q$. Compute an estimate for a parameter of interest (e.g., therms value) by time averaging over each of the segments to obtain the sequence of estimated values, y_i; i = 1, 2, ... q. Next, compute the quantities

$$h_{ij} = 1 \quad (y_i > y_j)$$
$$= O \quad (y_i \leq y_j) \qquad (4.\ la)$$

where $i < j$; i = 1, 2, ... q-1, and j = i+1, i+2, ..., q, Then compute

$$A_i = \sum_{j=i+1}^{q} h_{ij} \qquad (4.1b)$$

which are called the number of reverse arrangements for y_i. Finally, compute the total number of reverse arrangements for the entire sequence from

$$A = \sum_{i=1}^{q-1} A_i \qquad (4.1c)$$

If the signal parameter y of the measured time history x(t) is time invariant (stationary), the number of reverse arrangements A computed from the sequence of estimates, y_i; i = 1, 2,..., q, will be a random variable with an approximately normal distribution having a mean value and standard deviation given by [4.9]

$$\mu_A = \frac{q(q-1)}{4} \qquad (4.2a)$$

$$\sigma_A = \sqrt{\frac{q(2q+5)(q-1)}{72}} \qquad (4.2b)$$

4 . 8 . 3 Decision R- . The decision as to whether the parameter y of the measured time history x(t) can be accepted as stationary is accomplished by a conventional two sided, statistical hypothesis test [4.s], Specifically, for any desired level of significance α, the acceptance region for the hypothesis of stationarity is given by

$$A_{q;1-\alpha/2} < A \leq A_{q;\alpha/2} \tag{4.3}$$

where the values of $A_{q;1-\alpha/2}$ and $A_{q;\alpha/2}$ are given directly from Table 4.1. If the value of A computed in Equation (4.1) falls outside the bounds of Equation (4.3), this is considered to be adequate evidence (at the α level of significance) that the signal parameter being investigated is nonstationary. However, if the value of A falls within the bounds, then the signal parameter being investigated would be accepted as stationary.

Table 4.1. Percentage Points for the Reverse Arrangements Distribution,

q	$A_{q;1-\alpha/2}$			$A_{q;\alpha/2}$		
	$1-\alpha/2 = 0.99$	$1-\alpha/2 = 0{,}975$	$1-\alpha/2 = 0.95$	$\alpha/2 = 0.05$	$\alpha/2 = 0.025$	$\alpha/2 = 0.01$
10	9	11	13	31	33	35
12	16	18	21	44	47	49
14	24	27	30	60	63	66
16	34	38	41	78	81	85
18	45	50	54	98	102	107
20	59	64	69	120	125	130
25	100	108	114	185	191	200
30	152	162	171	263	272	282
40	290	305	319	460	474	489
50	473	495	514	710	729	751
60	702	731	756	1013	1038	1067
70	977	1014	1045	1369	1400	1437
80	1299	1344	1382	1777	1815	1860
90	1668	1721	1766	2238	2283	2336
100	2083	2145	2198	2751	2804	2866

Two issues in applying the test are the number of segments q over which estimates are made, and the level of significance α for the test. Assuming the data represent typical vibroacoustic measurements, the following rules are recommended for the selection of the number of segments q:

(1) The number of segments used for the estimates should never be less than q = 10, and preferably should be $q \geq 20$.

(2) If the total measurement duration is $20 < T_r \leq 100$ see, the number of segments should be increased appropriately to maintain a segment duration of T = 1 sec.

(3) If the total measurement duration is $T_r > 100$ sec, the segment duration T should be increased appropriately to maintain q = 100 segments.

The following rules are recommended for the selection of the level of significance u:

(1) For $q < 20$, use $\alpha = 0.10$.

(2) For $20 \leq q \leq 40$, use $\alpha = 0{,}05$.

(3) For $q > 40$, use $\alpha = 0.02$.

It should be mentioned that for $q > 40$, the testis extremely powerful and will detect minor time variations in the parameter value that may not be of physical significance.

4.8.4 **Illustration.** Figure 4,17 shows a sequence of rms value estimates for a 20 sec long random signal measurement, each computed over a 1 sec time interval to give a total of q = 20 estimates. Also shown in Figure 4.17 are the numerical values of the estimates. From Equation (4. 1), the reverse arrangements produced by this sequence of estimates are computed as follows:

$A_1 = 8$	$A_6 = 6$	$A_{11} = 7$	$A_{16} = 0$
$A_2 = 3$	$A_7 = 1$	$A_{12} = 6$	$A_{17} = 2$
$A_3 = 8$	$A_8 = 8$	$A_{13} = 0$	$A_{18} = 1$
$A_4 = 3$	$A_9 = 1$	$A_{14} = 0$	$A_{19} = 1$
$A_5 = 0$	$A_{10} = 4$	$A_{15} = 3$	

For example, y_1 is greater than y_2, y_4, y_5, y_7, y_9, y_{13}, y_{14}, and y_{16}; hence, $A_1 = 8$. the sum of the reverse arrangements is A = 62.

From Table 4.1 and Equation (4.3), the acceptance region for a test of q = 20 values at the 5% level of significance ($\alpha = 0{,}05$) is

$$64 < A \leq 125$$

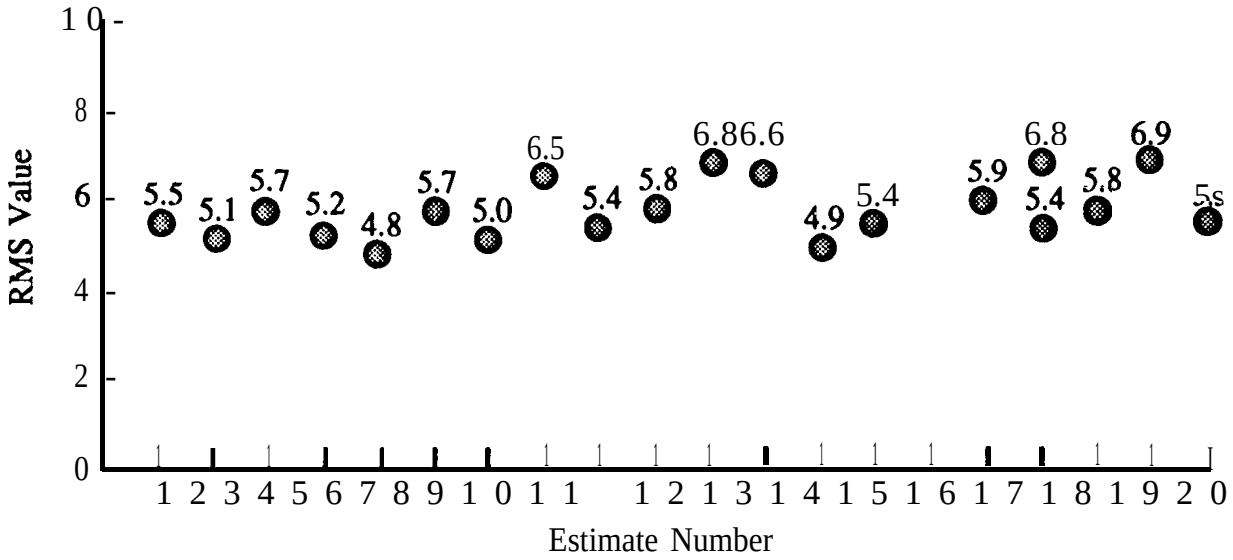

Figure 4,17. Sequence of Short Time-Averaged **RMS** Value Estimates of a Random Signal,

Since the computed value of the reverse arrangements is A = 62, the hypothesis of **stationarity** is rejected, and the rms value of the measurement is considered nonstationary. In fact, the estimates shown in Figure 4.17 were computed from a random signal that was generated with an rms value that gradually increased by about 15% over the 20 **sec** measurement duration. Hence, the test produced a statistically correct result.

4.9 References.

4.1 **Vellutini,** G. A., and Wright, C. P., "Knowledge-Based Systems for Test Data Acquisition/Reduction", ***Proc., 11th*** *Aerospace Testing* ***Seminar,*** pp. 85-103, Oct. 1988.

4.2 **Paez,** T. L., and **Smallwood,** D. O., "Statistical Measures of Clipped Random Signals", *Shock and Vibration Bull., No. 57, Pt 3,* pp. 165-177, Jan. 1987.

4,3 Nelson, D. B., "Critique of Ballistic Vehicle Vibration Measurements", *SAE Paper 871741,* **Oct.** 1987.

4.4 Wright, C. F., "Dynamic Data Invalidity Due To Measurement System Non-Linearity", ***Proc.,*** *Western Regional Strain Gage* ***Comm.,*** *Sot.* **Exper. Mech., Brookfield,** CT, Feb. 1985.

4,5 Bendat, J. S., and **Piersol,** A. G., *Random Data: Analysis and* ***Measurement*** *Procedures,* 2nd cd., Wiley, NY, 1986.

4.6 Otnes, R. K., and Enochson, L., *Applied Time Series Analysis,* Vol. 1, pp. 98-103, Wiley, NY, 1978.

4.7 Papoulis, A., "Narrow-Band Systems and Gaussianity", *RADC-TR-71* -225, Rome Air Development Center, Griffiss AFB, NY, Nov. 1971.

4.8 Rice, S. 0., "Mathematical Analysis of Random Noise", *Selected Papers on Noise and Stochastic Processes, (Ed: N.* Wax), Dover, Mineola, New York, 1954.

4.9 Kendall, M. G., and Stuart, A., *The Advanced Theory of Statistics,* Vol. 2, Hafner, NY, 1961.

THIS PAGE IS INTENTIONALLY LEFT BLANK

5. DATA ANALYSIS

5.1 Introduction. This section presents guidelines for dynamic data analysis instruments, procedures, and parameters. It is assumed the organization doing the analysis has a fast Fourier transform (FFT) digital signal processor or appropriate FFT software on a main-frame computer available for data analysis purposes. However, the guidelines are applicable to other types of signal processing procedures as long as the analysis parameters are equivalent. Such alternate procedures include correlation (so called "Blackman-Tukey") algorithms, digital bandpass filtering algorithms, and heterodyne techniques with a fixed filter. An outline of the data analysis procedures covered in this section is presented in Figure 5,1,

5.2 Time Histories. The signal analysis procedures discussed in this section are in addition to the evaluations previously detailed in Section 4 for data validation and editing purposes.

5.2.1 Instantaneous Values. Beyond the purposes of data validation and editing, certain applications may require an evaluation of instantaneous signal values, In particular, the general design of structures for low frequency loads is commonly based upon maximum value estimates made from signal time histories,

5,2,1,1 Analog Instruments. The most common analog- devices used to produce a hard copy record of a measured signal x(t); $O < t < T$, (commonly referred to as strip chart recorders) include [5. 1, 5.2]: (a) galvanometric pen recorders, (b) galvanometric light beam oscillograph recorders, (c) potentiometer recorders, (d) CRT recorders, (e) light array recorders, (f) x-y plotters, and (g) digital electrostatic recorders (which function like analog recorders even though they are basically digital devices). Of these available types of devices, the galvanometric light beam recorders and digital electrostatic recorders are considered the most desirable for dynamic data because of their high frequency response capabilities. Specifically, digital electrostatic recorders produce an output up to 15 kHz. Galvanometric light beam recorders work up to about 8 kHz (excluding the reduced deflection sensitivity of the galvanometers. The high frequency response of the most commonly used paper for galvanometric light beam recorders is about 5 kHz. If the data are FM tape recorded, signals at frequencies above 5 kHz can be brought within the upper frequency limit of the galvanometers and its paper by playing the tape back at a speed slower than the speed used to make the tape recording, e.g., 40 kHz data recorded at 60 ips can be reduced to 5 kHz at a playback speed of 7.5 ips, with no change in amplitude,

5.2.1.2 Digital Instruments. The most common digital devices used to produce a hard copy record of a digitized signal $x(n\Delta t)$; $n = 1, 2, ..., N$, include [5,2]: (a) incremental plotters, (b) x-y plotters, (c) dot matrix printers, (d) laser printers, and (e) thermal array recorders. High resolution dot matrix printers (at least 200 dots/in.), laser printers, and thermal array recorders are considered

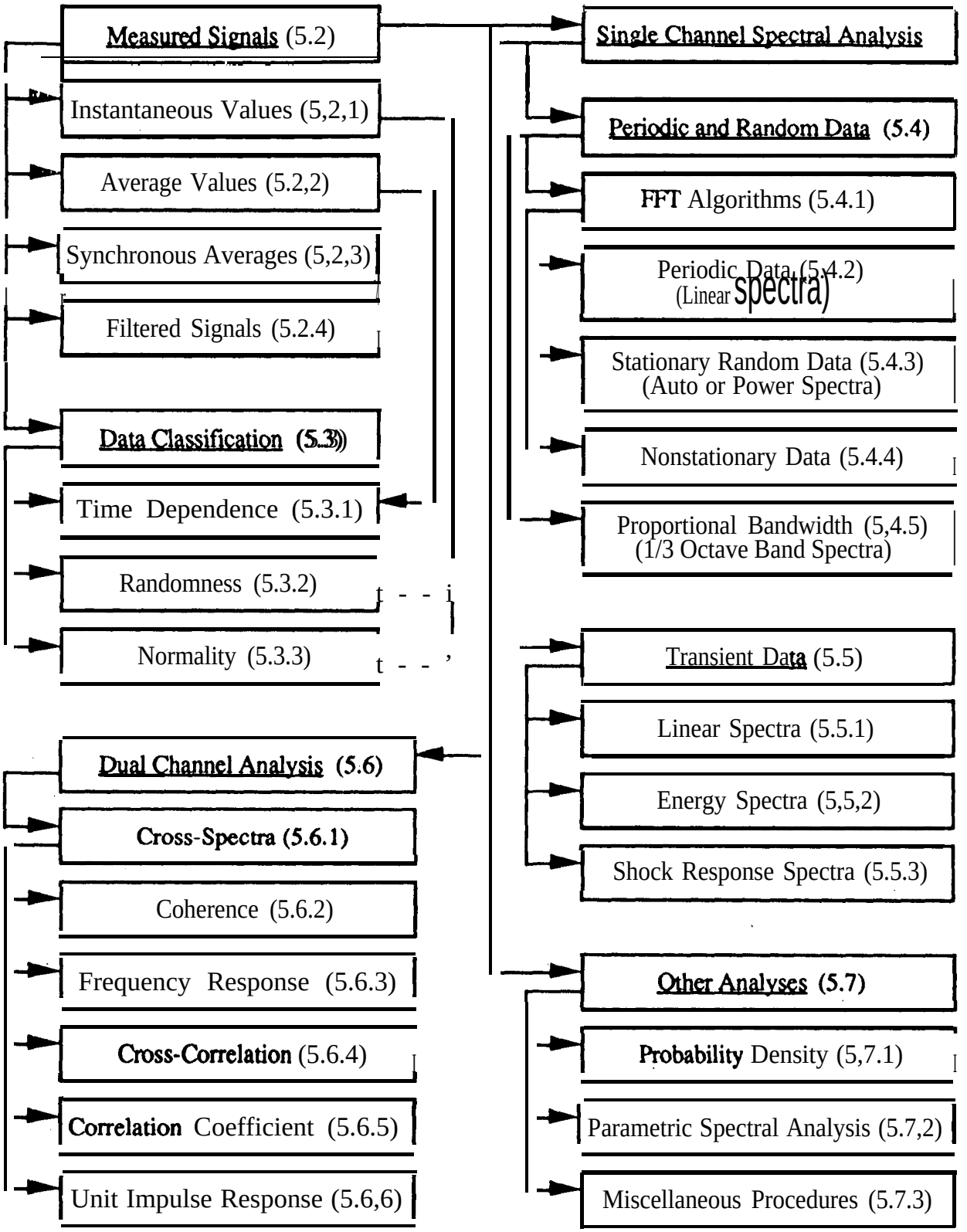

Figure 5.1. Outline of Data Analysis Procedures.

the most desirable for dynamic data. The magnitude resolution error associated with digital plotting devices is a function of the digital word size (see Section 3.7,1.3) and the time axis resolution, i.e., the number of digital values the plotter can generate over the length of the time axis.

5.2,2 Average Values. Various different average values (moments) of measured stationary signals might be computed, although the mean value μ_x and the standard deviation σ_x (or rms value ψ_x) are usually the average values of greatest interest. Estimates of the mean value and standard deviation of a signal x(t); $O \leq t \leq T$, maybe computed directly by either analog or digital devices using the following algorithms:

(a) Mean value: $$\hat{\mu}_x = \frac{1}{T}\int_0^T x(t)\,dt = \frac{1}{N}\sum_{n=1} x(n\Delta t) \tag{5.1}$$

(b) RMS value: $$\hat{\psi}_x = \left\{\frac{1}{T}\int_0^T x^2(t)\,dt\right\}^{1/2} = \left\{\frac{1}{N}\sum_{n=1}^{N} x^2(n\Delta t)\right\}^{1/2} \tag{5.2}$$

(c) Std. deviation: $$\hat{\sigma}_x = \left\{\frac{1}{T}\int_0^T [x(t) - \hat{\mu}_x]^2\,dt\right\}^{1/2} = \left\{\frac{1}{(N-1)}\sum_{n=1}^{N} [x(n\Delta t) - \hat{\mu}_x]^2\right\}^{1/2} \tag{5.3}$$

In Equations (5.1) through (5.3), T is the linear averaging time for analog signals, N is the number of data values for digital signals ($T = N\Delta t$), and the hat (A) denotes "estimate of", For most high frequency dynamic measurements, the transducer does not sense the static or DC component of the signal (see Section 3.2), whereas for most low frequency measurements (below 50 Hz), the DC component is included. Without the DC component, the mean value of the signal is zero and the rms value computation of Equation (5.2) will yield the standard deviation.

5.2.2.1 Instruments and Software. Both analog and digital DC voltmeters essentially compute the mean value of a signal, while true rms voltmeters (not to be confused with AC voltmeters) compute an approximation of the rms value of a signal. Most analog and digital voltmeters compute a continuous exponential weighted (RC) average, rather than a single linear average (see Section B.4.2 in Appendix B). The RC averaging time constant of the voltmeter, denoted by K, is often fixed at one or a few values ranging from K = 0.1 to 1 sec. The averaging time constant is a key parameter in establishing the accuracy of average value estimates for random signals, to be discussed shortly. The operations in Equations (5.1) through (5,3) are easily accomplished on a digital computer (either PC or main-frame) with simple software programs.

5.2.2,2 Types of Averaging. Although voltmeters usually compute a continuous exponentially-weighted average, computer programs can be written to average in any manner desired. The simplest programs compute a linear average over contiguous sets of N data values spaced At apart to

produce independent average value estimates every T = NAt see, as given in Equations (S. 1) through (5.3). For the case of stationary or steady-state signals (where the average value of interest does not change over the duration of the measurement), a single linear average over the entire measurement is recommended, For the case of nonstationary signals (where the average value of interest is changing over the measurement duration), an exponentially weighted average is recommended for analog signals, and a step-wise linear average is recommended for digital signals. A step-wise linear average (sometimes called a running average) can be produced by computing a series of average value estimates using N data values, where one new value is added to the end and one old value is discarded from the beginning of the N data values for each average. This will produce correlated average value estimates every At sec (see Appendix B).

5,2.2.3 Averaging Time and Sampling Errors. For periodic signals, the only error in an average value estima (beyond calibration errors) is the truncation error caused by the fact that the averaging operation may not cover an exact integer number of cycles of the signal. This truncation error becomes negligible as the linear averaging time becomes long relative to the period of the signal. For random signals, however, there will be a random sampling error in the average value estimate that is dependent on both the averaging time and the frequency bandwidth of the signal. The random errors for the estimates of the mean and rms values of random signals are summarized in terms of a normalized random error (coefficient of variation) in Figure 5,2. The normalized random error in the estimate of a parameter Φ is defined as

$$\varepsilon_r[\hat{\Phi}] = \frac{\sigma[\hat{\Phi}]}{\Phi} \tag{5.4}$$

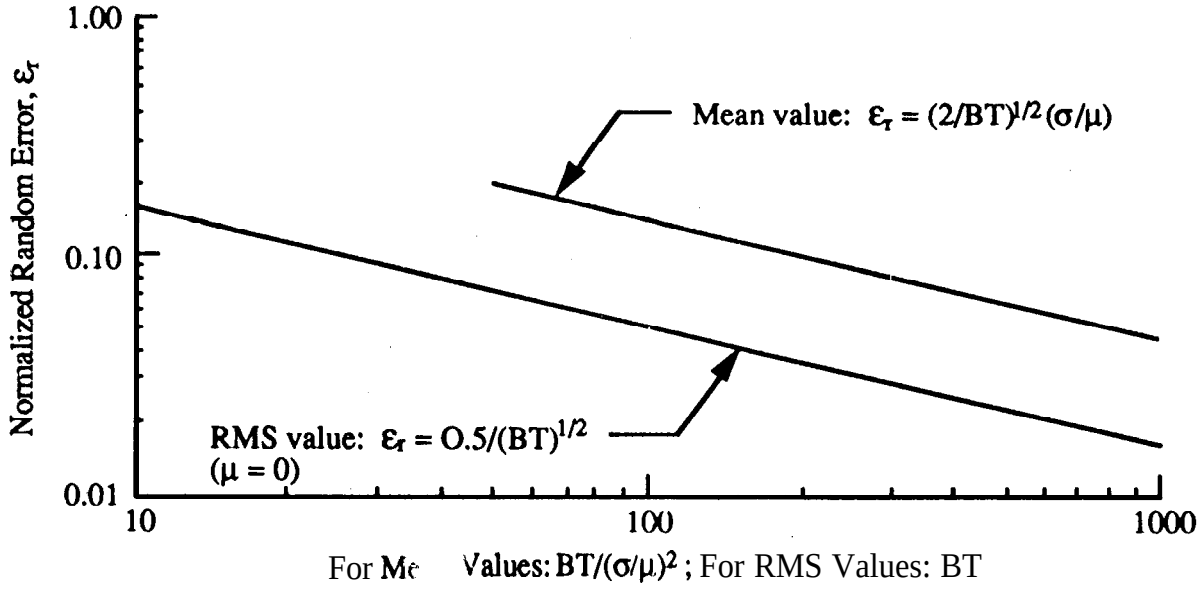

Figure 5,2. Normalized Random Errors for Mean and Mean Square Value Estimates.

where $\sigma[\hat{\Phi}]$ is the standard deviation of the estimate $\hat{\Phi}$. The quantity B in Figure 5.2 is the frequency bandwidth of the signal, assumed to have a uniform spectrum, and the quantity T is the linear averaging time used to make the estimate. For the case of exponentially-weighted averages with a time constant K, it can be assumed in Figure 5.2 that T = 2K [5.3]. See [5.4] for details on random errors in average value estimates.

5.2.3 Synchronous Averaging. Reciprocating and rotating machinery (including propellers and fans) operating under steady-state conditions produce periodic components (i.e., signals that exactly repeat themselves after a time interval T_1, called the period) such that

$$p(t) = p(t + iT_1);\ i = 1,2, 3,... \tag{5.5}$$

However, the periodic signal of interest is sometimes contaminated by random background noise and/or other independent data signals, producing a measured signal x(t) = p(t) + n(t), where n(t) is the noise and/or other independent signals. In such cases, the signal-to-noise level of the periodic signal of interest can be strongly enhanced by the procedure of synchronous averaging, where the measurement is divided into a collection of segments, xi(t); i = 1,2, ... q, each starting at exactly the same phase angle during a period of p(t). The collection of segments can then be ensemble averaged to extract p(t) from the background noise, as well as other periodic components which are not harmonically related to p(t), as follows:

$$p(t) \approx \frac{1}{q}\sum_{i=1}^{q} x_i(t) \tag{5.6}$$

5.2.3.1 Instruments and Software. Many of the modem special purpose signal processing computers produced for dynamic signal analysis provide a synchronous averaging mode. The primary requirement is that a trigger signal must be provided to the analyzer that will initiate new signal segments at a desired instant during a period of p(t). The averaging maybe accomplished directly on the signal segments, or in the frequency domain on the Fourier transforms of the segments. Simple software programs can be written to accomplish these same operations.

5.2,3.2 Triggering Procedures. Synchronous averaging is most effective when the trigger signal is a noise free indicator of the phase during each period of p(t). For reciprocating and rotating machines, a noise free trigger signal is commonly obtained using either an optical detector or a magnetic pulse generator on the reciprocating or rotating element of the machine. The time base accuracy of the trigger signal determines the accuracy of the magnitude of the resulting synchronous averaged signal, i.e., time base errors in the trigger signal cause a reduction in the indicated signal amplitude with increasing frequency [5.5].

5.2.3.3 **Signal-to-Noise Enhancement**. The signal-to-noise level enhancement for a synchronous averaged signal is shown in Figure 5.3, where q is the number of segments used in the ensemble averaging operation [5.4]. Letting σ_x and σ_n be the standard deviations of the signal and noise, respectively, the signal to noise level enhancement in dB is defined as

$$S/N_e = 10 \log_{10} [SNR_a/SNR_b] \tag{5.7}$$

where $SNR_a = (\sigma_x/\sigma_n)^2$ after the synchronous averaging, and SNR_b is the same ratio before the synchronous averaging,

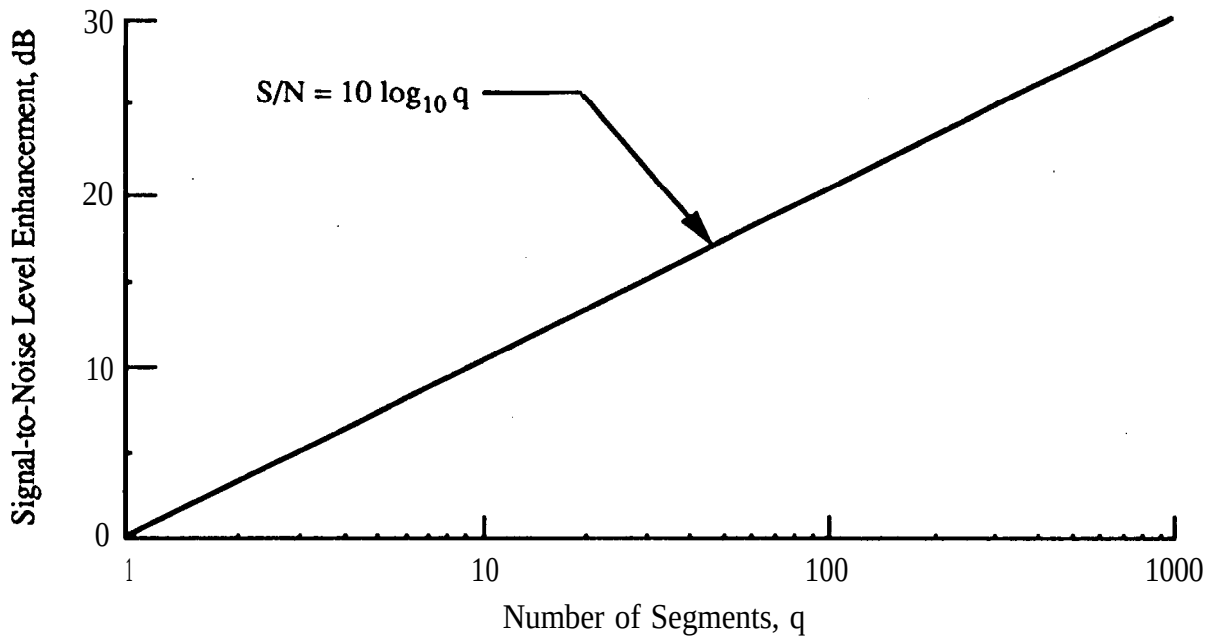

Figure 5.3. Signal-to-Noise Level Enhancement with Synchronous Averaging.

5.2.4 **Filtered Signals**. Vibration data are often acquired over a wider frequency range than may be of interest for certain applications, such as low frequency (usually below 50 Hz) dynamic loads analysis. It is common in such applications to lowpass filter the signals to obtain time histories representing only the low frequency portion of the signal. In a large number of cases, the low frequency signals are digitized and used as inputs to finite element computer models of structures to obtain time histories of internal dynamic loads (i.e., stresses or strains at critical locations) from which maximum values can be observed and compared to dynamic loads criteria. It should be mentioned that the practice of defining maximum low frequency loads using lowpass filtered signals involves a subjective judgment in that the resulting signal is heavily dependent on the cut-off frequency, roll-off rate, and phase shift of the lowpass falter.

Dynamic data signals are sometimes highpass filtered as well to AC couple the data. As for lowpass filters, the detailed characteristics of such highpass filters should be known, and their possible consequences on the interpretations of the resulting signals should be carefully assessed.

5.2.4.1 Analog Filtering. The simplest way to limit the frequency range of a signal is to lowpass filter the analog signal directly. If the signal is to be later digitized, the lowpass filtering can be easily accomplished using the anti-aliasing filter for the analog-to-digital converter (AD(2), as discussed in Section *3.7.3.* It must be remembered, however, that many analog anti-aliasing filters introduce a nonlinear phase shift near the filter cut-off frequency that may distort the signal time history.

5.2.4.2 Digital Filtering. The more desirable approach to lowpass filtering is to first digitize the signal with an ADC using a sampling rate and anti-aliasing filter appropriate for a substantially higher cut-off frequency than that of interest (at least ten times higher). The desired lowpass filterring can then be accomplished using a digital lowpass filter, Digital filters are highly stable and can be easily designed to have a near-linear phase shift, corresponding to a fixed time delay, thatwill not distort the signal time history. See Section 3.7.3 and [5.6, 5.7] for details.

5.3 Data Classification. Prior to a detailed analysis, it is necessary to establish certain basic characteristics of acquired dynamic signals that will influence the analysis procedures, The most important of these characteristics are (a) whether the signals are stationary, nonstationary, or transient, and (b) whether the signals are deterministic, random, or a mixture of both. For the case of stationary random signals, there may also be an interest in (c) whether the signal values are normally (Gaussian) distributed, In many cases, the basic characteristics of the signals can be determined or assumed from a knowledge of the experimental conditions that produced the data, as outlined in Section 4.2. In other cases, specific evaluations or tests maybe required to fully establish the basic characteristics of the signals, as detailed in Sections 4.7 and 4,8, Such evaluations and tests will usually be accomplished as part of the data validation and editing activities covered in Section 4, but additional considerations maybe warranted for data analysis purposes.

5.3.1 Time Dependence. The first issue of concern in dynamic data analysis is the possible time dependence of the signals, i.e., whether the signals are stationary (or steady-state), nonstationary, or transient. As part of the data validation procedures discussed in Section 4, each measurement should be identified with specific physical events that will separate the measured signals into time dependence categories, as follows:

5.3.1.1 Stationary or Steady-State Data. Stationary or steady-state signals are those whose average properties do not change with time, at least over the duration of the measurement, as illustrated previously in Figure 4.2. Nearly all laboratory tests and most field and aircraft flight tests can be designed to produce stationary or steady-state dynamic signals by simply keeping all the conditions

that influence the signals constant during the measurements. From a data analysis standpoint it is recommended that this be done whenever possible. However, there will be cases where the need for slowly changing test conditions may be more important than the data analysis considerations, e.g., swept sine tests used to identify resonance frequencies of structures.

5.3,1.2 Nonstationary Data. Nonstationary signals are those which are ongoing, but have at least one important average property that varies with time, as illustrated previously in Figure 4.3(b). In most cases, a time varying property of a measured signal can be anticipated from the characteristics of the experiment producing the signal, as discussed in Section 4.2.2,. However, there may be rare cases when the time dependence of a signal is in question, and a statistical test for stationarity like that described in Section 4.8 is warranted.

5.3.1.3 Transient Data. Transient signals are defined as those that have a clear beginning and end, and a relatively short duration, as illustrated previously in Figure 4.3(a). Common sources of transient dynamic data are summarized in Section 4.2.2.

5.3.1.4. Physical Considerations. For those cases where the final application of the dynamic data analysis is the determination of dynamic test requirements, the distinction between nonstationary and transient data should be viewed in a more physically relevant way. Specifically, nonstationary dynamic environments are usually simulated for testing purposes by a stationary excitation equivalent to the maximum levels that occur during the nonstationary dynamic event (see Appendix B). For this testing approach to be valid, the time variations in the nonstationary environment must be slow compared to the response characteristics of the item to be tested, so that the test item would essentially have a fully developed response at any instant during the nonstationary environment, as it will during the stationary test. Otherwise, a testing procedure using a transient excitation, rather than a stationary excitation, is essential to properly simulate the dynamic response of the test item to the environment. It follows that the distinction between nonstationary and transient data in this case is dependent on the response characteristics of the test itern.

An easy way to assess the response time of a test item to a nonstationary excitation is in terms of the mean square response time of a single degree-of-freedom system (see Section 3.2.2) to a step random excitation, given from [5.8] as

$$\tau \approx \frac{L}{4\zeta f_n} \tag{5.8}$$

where

τ = time required for single degree-of-freedom system to reach 95% of full mean square response

ζ = damping ratio of single degree-of-freedom system

f_n = undamped natural frequency of single degree-of-freedom system

To use Equation (5.8), estimate the lowest natural frequency and damping ratio of the test item, and solve for the response time. For example, if $f_n \approx 50$ Hz and $\zeta \approx 0.025$, $\tau \approx 0.2$ sec. If the time varying mean square value of a nonstationary signal varies from a minimum to a maximum in less than 0.2 see, then the signal should be viewed as a transient for testing purposes, and correspondingly should be analyzed as a transient, as outlined in Section *5.5. See* Appendix B for details on the estimation of time-varying mean square values for nonstationary signals.

5.3.2 Randomness. Dynamic signals may be either random or deterministic in character, or often a combination of the two, as discussed and illustrated for stationary signals in Section 4.2.1. For the case of nonstationary or transient dynamic signals, the distinction between random and deterministic characteristics is usually not critical, since the data analysis procedures are similar in both cases. However, for stationary random and steady state (usually periodic) deterministic signals, the distinction is important because (a) it helps define the physical mechanisms producing the dynamic environment being measured, and (b) the required data analysis procedures are different.

5.3.2.1 Identification of Periodic Components. Deterministic components in stationary dynamic data are usually periodic or almost periodic, and commonly originate from reciprocating or rotating machinery (including propellers and fans), or self-limiting structural or aeroacoustic instabilities. Such periodicities appear in a narrowband spectrum as sharply defined peaks at the frequencies of the periodic components. Hence, with a sufficient knowledge of the potential periodic sources, it is usually possible to associate sharply defined spectral peaks with specific physical sources, and in so doing, identify the spectral peaks as periodic components, It is also possible to identify periodic sources by signal processing procedures (see Section 4.7). In any case, the identification of spectral peaks that represent periodic components should be accomplished during the data validation and editing operations outlined in Section 4.2.1, but if not, it is recommended as an initial step prior to detailed data analysis.

5.3.2.2 Separation of Random and Periodic Components. Since different computational procedures and data displays are involved in the analysis of random versus periodic signals (to be detailed in Section 5.4), efforts are sometimes made to physically separate the random and periodic portions of a signal for separate analyses using digital filters and/or synchronous averaging operations (see Section 5.2.3). Assuming the ultimate applications of the analysis can be served by a spectrum, such a physical separation is not necessary, Instead, the spectral analysis can be accomplished simply by computing both a linear spectrum appropriate for periodic signals (see Section 5.4.2) and an autospectrum appropriate for random signals (see Section 5.4.3), and then interpreting the applicable spectrum at the specific frequencies of the periodic and random portions of the signal. The same result can be achieved by computing only a linear spectrum, and making appropriate corrections for the random portion of the signal, or vice-versa.

5.3.3 Normality. Situations may arise, particularly in failure prediction applications, where the probability structure of stationary random dynamic data is of concern (see Section 5.7.1). It is commonly assumed that random signals are normally distributed (or Gaussian), i.e., they have a probability density function given by

$$p(x) = \frac{1}{\sqrt{2\pi}\,\sigma_x} \exp\left[\frac{-(x-\mu_x)^2}{2\sigma_x^2}\right] \tag{5,9}$$

where μ_x and σ_x are the true mean value and standard deviation, respectively, of the signal, as estimated by Equations 5.1 and 5,3, However, there sometimes are significant deviations from normality in random signals, particularly when nonlinearities are involved in the structural or aero-acoustic elements producing the signals, which may have a direct bearing on their interpretations and applications [5.9], This possibility might be evaluated by simply computing a probability density function and comparing it to the normal probability density function given in Equation (5.9). In other cases, a statistical test for normality might be used.

5.3.3.1 Test for Normality. There are several different statistical tests for the normality of random data, but the most widely used is the chi-squared goodness-of-fit test, which is detailed in most engineering statistics textbooks, e.g., [5. 10]. The chi-squared test is most effective when applied to at least 200, but no more than 2000, statistically independent data values. Of course, the digitized values for dynamic data are generally correlated. As a rule of thumb in this case, the test should be applied over a sequence of digital data values such that $100 < BT < 1000$, where B is the approximate frequency bandwidth of the dominant dynamic data values, and T is the duration of the sequence of data values.

5.3.3.2 Spurious Deviations from Normality. When a probability density analysis or goodness-of-fit test is performed on a random signal, it is essential that the signal be stationary. If the signal is nonstationary, particularly when there is a time varying standard deviation, the probability density function computed by time averaging operations will appear non-Gaussian, even though the phenomenon producing the measurement may actually have a Gaussian distribution (see [5.4] for details). Hence, it is important that probability density computations and tests for normality be limited to measurements that are known to be stationary, or have passed a test for stationarity of the type outlined in Section 4.8.

5.4 Single Channel Spectral Analysis - Periodic and Random Data. The most common and useful presentation for individual dynamic measurements is some form of frequency decomposition or spectral analysis. Prior to 1965, such analyses were common] y performed using analog filtering instruments called wave analyzers. The use of digital computers for spectral analysis was limited prior to that time because the direct digital computation of spectra by Fourier transform procedures

was computationally inefficient. However, with the introduction of the so called "fast Fourier transform" (FFT) algorithms in 1965 [5.11], the calculation of spectra on digital computers immediately became highly efficient, and digital computational techniques rapidly replaced analog instruments. Also, due to the rapid development of integrated circuits at about the same time, a wide range of FIT-based special purpose digital signal processing instruments with front-end analog-to-digital converters (ADCs) came on the market, and rapidly evolved to provide the capability for fast, low cost data analysis with the same user control and convenience of the earlier analog instruments. Most narrowband spectral analysis of dynamic data is currently accomplished using special purpose FFT-based digital instruments or FIT-based software programs on main-frame computers and PCs.

5.4.1 FFT Algorithms. The finite Fourier transform of a measured signal x(t); $0 < t \leq T$, is defined as

$$X(f) = \int_0^T x(t)\, e^{-j2\pi ft}\, dt = \int_0^T x(t) \cos 2\pi ft\, dt - j \int_0^T x(t) \sin 2\pi ft\, dt \qquad (5.10a)$$

where X(f) is a function of both positive and theoretical negative frequencies in Hz, For digital computations, $x(t) = x(n\Delta t)$; n = O, 1, ... N-1, and the finite Fourier transform (usually called the discrete Fourier transform or DFT) is given by

$$X(k\Delta f) = At \sum_{n=0}^{N-1} x(n\Delta t) \exp[-j2\pi kn/N]; \; k = O, 1, ..., N-1 \qquad (5.10b)$$

where $Af = 1/T = 1/(N\Delta T)$. The variable being transformed, $x(t) = x(n\Delta t)$, can be a complex number, although it is usually a real number for the case of dynamic data signals. On the other hand, the output function, $X(f) = X(k\Delta f)$, generally is a complex number that includes both magnitude and phase information. The real part of the DFT is often called the cosine transform and the imaginary part is called the sine transform.

There are a family of computational algorithms, commonly called "fast Fourier transform" or "WI'" algorithms, that compute the DFT of a digital time series very efficiently. These FFT algorithms are the basis for most modern digital spectral analysis instruments and computer programs. The DFT essentially yields the Fourier series coefficients of the signal x(t); $0 < t \leq T$, under the assumption that x(t) is periodic with a period $T_1 = T$. See [5,4, 5.7, 5.11- 5.15] for detailed descriptions of FFT algorithms. The specific procedures used in this handbook to translate the DFT into the Fourier representation of a signal x(t) follow the conventions in [5.4].

5.4.1.1 Number of Data Values. The most common FFT algorithm used for dynamic data analysis requires that the number of data values to be analyzed be a power of two, i.e., $N = 2^p$, where p is an integer. Most of the special purpose FFT-based digital instruments operate with a fixed number of data values corresponding to values of p ranging from p = 8 (256 data values) to p = 12 (4096 data values). Software programs on large computers generally offer greater flexibility, but are still limited (even on virtual memory computers) by practical problems to sequences corresponding to $p \leq 16$ (65,536 data values). In any case, the sequence of data values operated on by a single FFT computation is referred to as a "block" of data. The number of data values in each block is called the block size N, and the duration of the block is called the block duration $T = N\Delta t$.

5.4.1.2 Redundant Components. Equation (5, 10b) shows that the DFT of a block of N data values, $x(n\Delta t)$; n = O, 1, ... N-1, will produce N discrete frequency values, $X(k\Delta f)$; k = O, 1, ... N-1. However, only the first [(N/2) + 1] frequency values in this sequence, from k = O to k = N/2 (representing non-negative frequency values), provide unique information (k = N/2 is the Nyquist frequency discussed in Section 3.7.2). The last [(N/2) - 1] frequency values, from k = [(N/2) + 1] to k = N-1 (which correspond to theoretical negative frequency values) are related to the earlier values by $X(k\Delta f) = X^*[(N-k)\Delta f]$, where the asterisk (*) denotes complex conjugate. Hence, it is usual to present only the fiist [(N/2) + 1] values of the DFT, with their magnitude multiplied by a factor of two (except for the k = O and N/2 values) to account for the contributions of the last [(N/2) - 1] values corresponding to the theoretical negative frequencies.

5.4.1.3 Leakage and Tapering. As noted in Section 5.4.1, the DFT computation essentially assumes the block of data values being analyzed represents one period of a periodic function, i.e., $NAt = T_1$. However, even when the signal being analyzed is truly periodic in form, it is unlikely that this condition can be satisfied in practice because the true period of the signal is usually not known in advance. Furthermore, the block size restrictions inherent in FFT algorithms (see Section 5.4. 1.1) generally rule out such precise selections for the number of data values needed to achieve this ideal situation. Hence, a truncation error occurs, due to the discontinuity between the beginning and the end of the block of data values being analyzed, that causes the computation of Fourier coefficients at a collection of frequencies, rather than at a single frequency, around the actual frequency of each spectral component in the periodic signal. Another way to view the problem is in terms of a time window u(t). Specifically, the signal being analyzed is actually a product of the signal of interest (extending over all time) and a rectangular time window, as shown in Figure 5.4(a). The resulting Fourier coefficients for a sine wave are then bounded by the Fourier transform of u(t), denoted by U(f), as shown in Figure 5.4(b).

The spectral function in Figure 5.4(b) constitutes the basic "spectral window" for the analysis, which includes a large main-lobe surrounded by side-lobes. These side-lobes allow power at frequencies outside the main-lobe to "leak through" and appear at the center frequency of the main-lobe. To suppress this leakage problem, the time window is modified by tapering the block of data

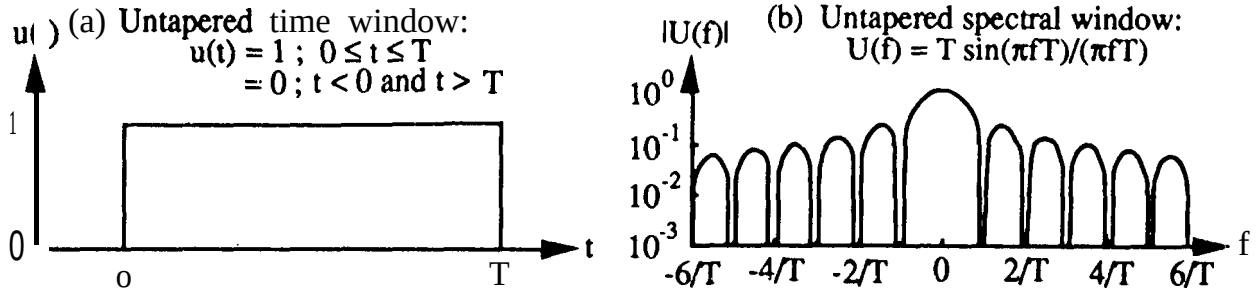

Figure 5.4. **Rectangular (Untapered)** Window for Spectral Analysis of Stationary Signals.

values to be analyzed such that the beginning and the end of the sequence will have the same value, Numerous different tapering functions have been proposed over the years, **but one of the earliest** and still widely used is the cosine-squared taper or Harming window defined in Figure 5.5(a). **The** Harming spectral window is shown in Figure 5.5(b). See [5.16, 5,17] for other windows with better side-lobe suppression characteristics.

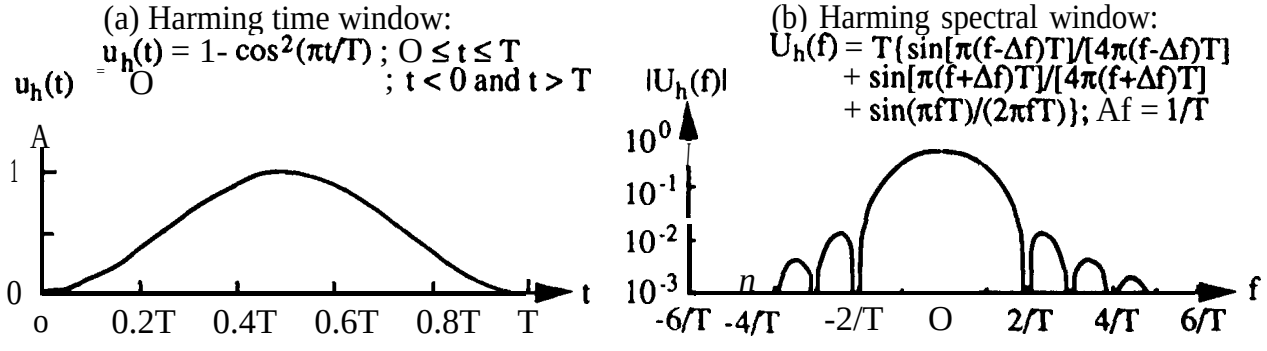

Figure 5.5. Harming Window for Spectral Analysis of Stationary Signals.

For random data, a side-lobe leakage problem always arises since the period of a random signal is theoretically infinite **and,** hence, a truncation error must always occur for any finite block size. See [5.4, 5.7, 5.16, 5.17] for details.

Although tapering operations are desirable to suppress side-lobe leakage, it should be emphasized that they alter the signal being anal**yzed** with the following additional consequences:

(1) The taper alters the mean square value of the signal, meaning the spectral values computed from the **tapered** signal must be appropriately scaled,

(2) The taper exaggerates the data values at the middle of the time window relative to the values near the beginning and the end of the window, meaning substantial errors may occur in **the** spectral values computed **from** the tapered signal if the data **are** nonstationary.

(3) The bandwidth of the spectral window produced by the taper is always wider than the bandwidth of the spectral window without tapering (see Section 5.4.1.4).

5.4,1.4 Spectral Bandwidth. The frequency resolution of a DFT computation (the frequency range between adjacent spectral components) is fixed by the block duration T, or the block size N, to $\Delta f = 1/T = 1/(N\Delta t)$. However, as introduced in the previous section, each spectral component represents a spectral window with a bandwidth B that is not necessarily equal to the resolution Δf. There are several ways to define the bandwidth of a spectral window, but the most common is the "half-power point" bandwidth. Given a spectral window U(f) centered at the frequency f_o, the half-power point bandwidth is $B_{hp} = f_a - f_b$, where f_a and f_b are those frequencies above and below f_o such that $|U(f_a)|^2 = |U(f_b)|^2 = |U(f_o)|^2/2$ The half-power point bandwidths of the spectral windows produced by the rectangular (untapered) and Harming time windows areas follows:

$$\text{Untapered: } B_{hp} = 0.89\,\Delta f = 0.89/T \qquad (5.11)$$
$$\text{Harming: } B_{hp} = 1.44\,\Delta f = 1.44/T$$

The half-power point bandwidths for the spectral windows produced by other tapering operations are detailed in [5.16].

For a given block duration T, it is seen from Equation (5. 11) that the Harming taper increases the half-power point bandwidth of the spectral window by about 62% over that for an untapered spectral window. Other tapering operations increase the half-power point bandwidth even more [5. 16]. It follows that tapering operations generally reduce the resolution of the DFT in terms of the ability of the main-lobe of the spectral window to distinguish between two closely spaced spectral components in the signaL However, the resolution that would have been obtained without tapering can be recovered by increasing the block duration T, and using overlapped processing (see Section 5.4.3.7).

5.4.2 Periodic Data. For a rigorous spectral analysis of periodic signals using a DFT, the block duration T = NAt in Equation (5. 10) should equal the period of the signal T_1 in Equation (5.5). For this case, the DFT will yield the exact Fourier series coefficients of the signal. In practice, however, it is common for $T \gg T_1$, and further for T not to be an integer multiple of T_1. Also, the phase information provided by the DFT is generally of no interest in single channel spectral analysis. Hence, the spectrum of a periodic signal is usually determined by

$$\begin{aligned} P_x(f) &= \frac{2}{T}|X(f)| \;;\; f > o \\ &= \frac{1}{T}(f)| \;;\; f = o \\ &= o \;;\; f < 0 \end{aligned} \qquad (5.12a)$$

For digital computations,

$$P_x(k\Delta f) = \frac{2}{N\Delta t}|X(k\Delta f)|; \quad k = 1, 2, \ldots, \frac{N}{2}-1$$
$$= \frac{1}{N\Delta t}|X(k\Delta f)|; \; k = O, \frac{N}{2} \qquad (5.12b)$$

where $|X(f)|$ and $|X(k\Delta f)|$ are the magnitudes of the DFT defined in Equation (5.10), and the factor of two for $f > 0$ is necessary to account for the theoretical negative frequency values. A plot of $P_x(f)$ has the units of amplitude (g, psi, etc.) versus frequency in Hz, and is often called a linear or line spectrum,

5.4.2.1 Instruments and Software. As discussed in Section 5.4, a wide range of FFT-based digital signal processing instruments are commercially available. All of these instruments have an operational mode for the spectral analysis of periodic signals using Equation (5.12). There is also a wide range of software packages, which can be purchased or leased, that accomplish the same computations. Beyond these commercial products, a program for periodic data analysis can be written using any one of the codes for FFT algorithms presented in many signal processing books, e.g., [5.18 - 5.21].

Beyond the above mentioned laboratory instruments and software, some manufacturers produce special-purpose analysis instruments that compute spectra on-line during flight experiments. Such instruments can provide substantial data compression and, hence, greatly reduce the bandwidth requirements for the telemetry system used for data retrieval (see Section 3.5.2), but they generally have a limited selection of analysis parameters. More important, since the actual data signal is not recovered, there is no way to correct errors in the original selection of analysis parameters, or to perform more detailed signal analysis operations after the fact.

5,4.2.2 Anti-Aliasing Filters. Analog lowpass filters should always be used prior to the digitizing of analog signals for linear spectra computations to avoid the possible aliasing errors discussed in Section 3.7.2. The recommended characteristics and cut-off frequencies for anti-aliasing filters are detailed in Section 3.7.3.

5.4.2.3 Leakage and Tapering. If feasible, periodic data analysis using a DFT computation should always be performed over a block duration equal to an integer multiple of one period of the signal being analyzed, i.e., $T = NAt = nT_1$; $n = 1, 2, 3, \ldots$ When this is not feasible, a tapering operation should be used to suppress the leakage due to the truncation error, as discussed in Section 5.4.1.3. The Harming window defined in Figure 5.5 is commonly used for this purpose, although the "flat-top" window [5.22] is considered more desirable for the analysis of periodic data because it produces a negligible amplitude error when the signal is truncated, i.e., $T \neq nT_1$, $n = 1, 2, 3, \ldots$ However, the spectral results produced by both the rectangular window (no taper) and the

Harming window can be corrected for amplitude and frequency errors using algorithms detailed in Section 5.4.2,5. See [5.7, 5.16, 5,17] for other windows that can be used for the spectral analysis of periodic signals.

If the Harming window is used to analyze periodic signals, it should be mentioned that the computed spectral components representing the harmonic components of the signal (the computed values of the linear spectrum at the frequencies closest to the actual frequencies of the spectral components of the periodic signal) are reduced in value by 50%. Hence, the resulting computed spectral components must be multiplied by a factor of two, i.e., $u_h(t)$ in Figure 5.5(a) should be multiplied by two for periodic data analysis. Note that this is different from the multiplier of $\sqrt{8/3}$ needed to correct the magnitude error caused by the application of the Harming window in the computation of autospectra for random signals (see Section 5,4,3.3).

5.4.2.4 Frequency Resolution. Theoretically, the harmonic spectral components of a periodic signal can be resolved if the frequency resolution for the analysis, given by $\Delta f = 1/T = 1/(N\Delta T)$, is less than the fundamental frequency of the signal given by $f_1 = 1/T_1$, i.e., $\Delta f < f_1$. In practice, assuming $T \neq nT_1$; n = 1, 2, 3, ... and the data are tapered to suppress leakage, it is recommended that the frequency resolution for the analysis be less than 10% of the fundamental frequency of the signal when the available duration of the measurement permits, i.e., $\Delta f < 0.1 f_1$.

5.4.2.5 Resolution Error Corrections. Again for the case where $T \neq nT_1$; n = 1, 2, 3, ... the computed spectral components with the largest magnitudes will be those nearest the actual harmonic components of the signal being analyzed, Hence, these largest computed components are usually interpreted as estimates for the frequency and amplitude of the actual harmonic components. There is both a frequency and amplitude error in this interpretation that can be reduced by performing the analysis with a narrower frequency resolution Δf. However, if Δf cannot be further reduced, a correction can be applied to the computed spectral components to obtain a more accurate estimate of the frequency and amplitude of the actual harmonic components. This correction is based upon the ratio of the largest spectral value to the second largest spectral value in the frequency region of each individual harmonic component. The correction factors for spectra computed with both a rectangular window (i.e., no tapering) [5.23] and a Harming window [5.24] are detailed in Figures 5.6 and 5.7. It should be emphasized that this correction procedure will be accurate only if the periodic signal is relatively free from background noise, and the resolution is adequate to provide at least five spectral analysis components between adjacent harmonic components in the signal.

5.4.2.6 Statistical Sampling Errors. There are no statistical sampling (random) errors associated with the spectral analysis of exact periodic signals. However, periodic signals in practice often include discrepancies from a precise periodic form, e.g., the tones in the pressure fields generated by propellers and fans at their blade passage frequencies often deviate from a rigorously defined peri-

odic signal due to random distortions in the inflow [5.25]. Hence, averaging a series of DFT spectral computations over the measurement duration is often desirable to suppress the influence of such discrepancies. An even better approach is to synchronous average the signal prior to the spectral computation, as discussed in Section 5.2,3, but this can be done only if a noise free indicator of the signal phase is available,

5.4,2.7 **Plotting**. The spectra for periodic signals commonly cover a wide dynamic range. Hence, it is recommended that the values be plotted on a logarithmic (or dB) scale, On the other hand, since the spectral components are harmonically related with a fixed frequency interval between spectral peaks, it is recommended that the frequency scale be linear.

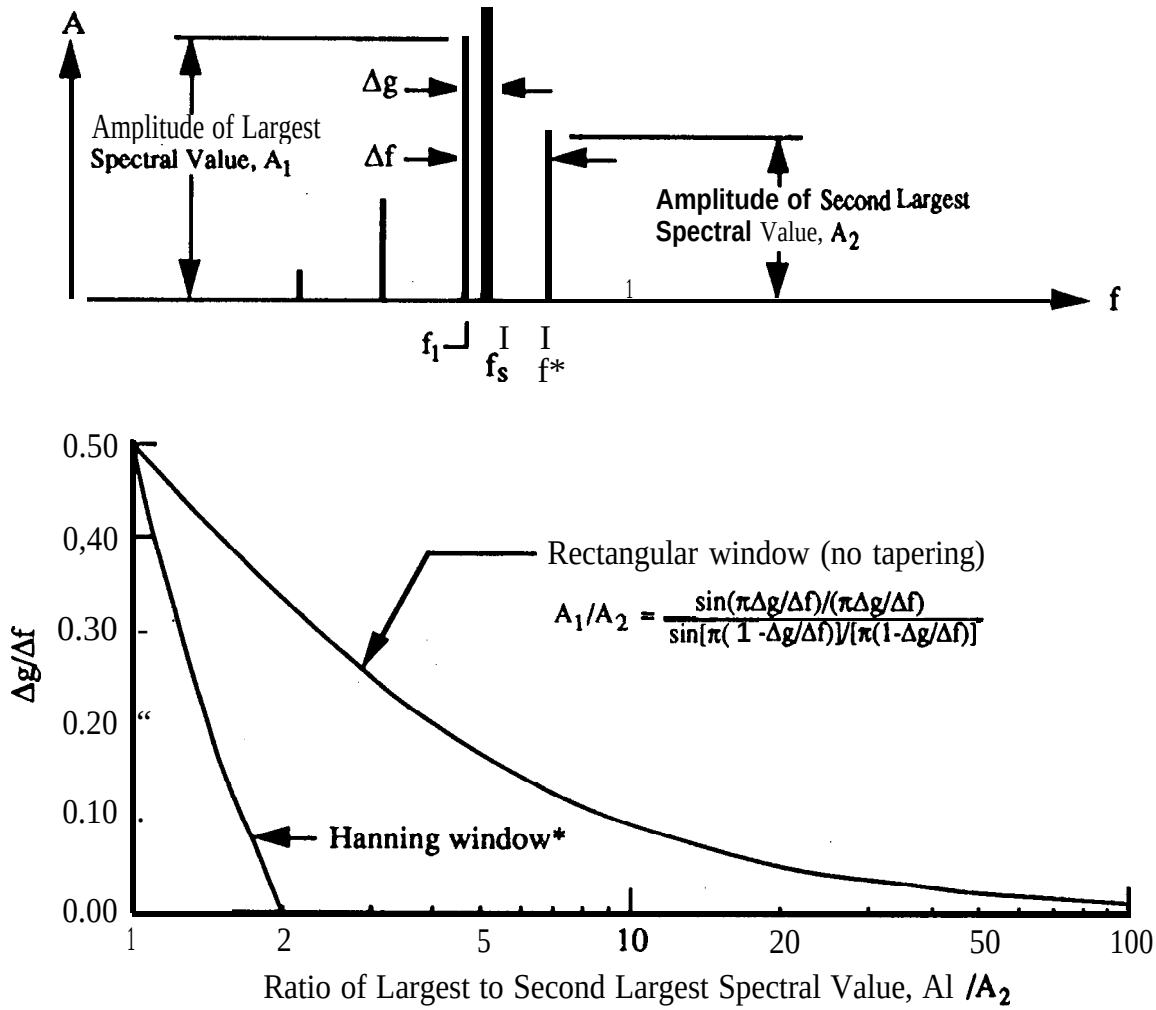

$$^{*}A_1/A_2 = \frac{\sin[\pi(\Delta g/\Delta f-1)/[4\pi(\Delta g/\Delta f-1)] + \sin(\pi\Delta g/\Delta f)/(2\pi\Delta g/\Delta f) + \sin[\pi(\Delta g/\Delta f+1)]/[4\pi(\Delta g/\Delta f+1)]}{\sin[\pi(-\Delta g/\Delta f)]/[4\pi(-\Delta g/\Delta f)] + \sin[\pi(1-\Delta g/\Delta f)]/[2\pi(1-\Delta g/\Delta f)] + \sin[\pi(2-\Delta g/\Delta f)]/[4\pi(2-\Delta g/\Delta f)]}$$

Figure 5.6. Frequency Correction for Periodic Component in Line Spectrum.

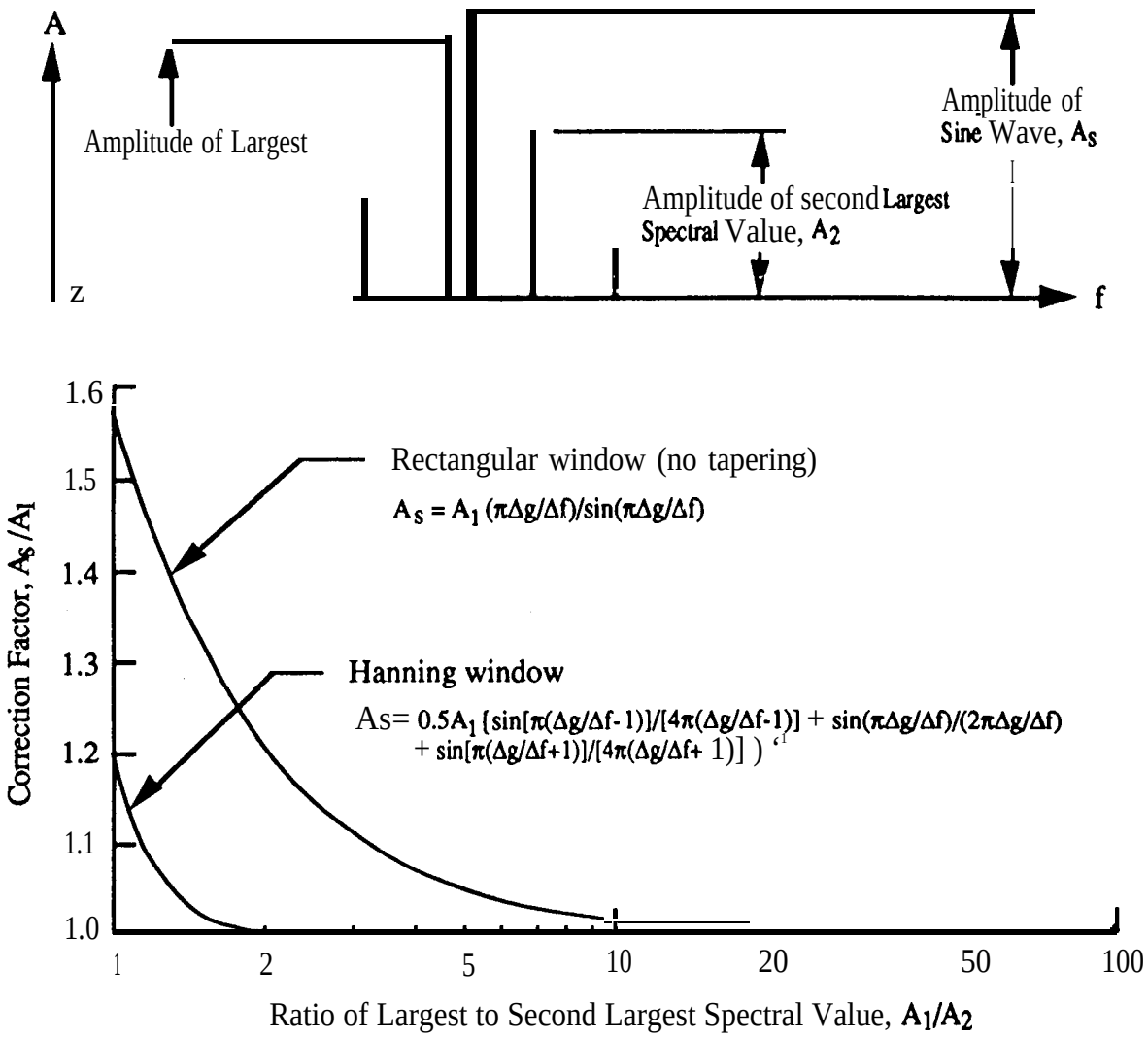

Figure 5.7. Amplitude Correction for Periodic Component in Line Spectrum.

5.4.3 **Stationary Random Data**. The spectra of stationary random signals should be computed using the autospectral density function (also called the power spectral density function), which is estimated by

$$\hat{G}_{xx}(f) = \frac{2}{n_d T}\sum_{i=1}^{n_d} |X_i(f)|^2 \; ; \quad f > 0$$

$$= \frac{1}{n_d T}\sum_{i=1}^{n_d} |X_i(f)|^2 \; ; \quad f = 0 \qquad (5.13a)$$

$$= 0 \; ; \quad f < 0$$

For digital computations,

$$G_{xx}(k\Delta f) = \frac{2}{n_d N\Delta t} \sum_{i=1}^{n_d} |X_i(k\Delta f)|^2 \quad ; \quad k = 1, 2, ..., \frac{N}{2} - 1$$

$$= \frac{1}{n_d N\Delta t} \sum_{i=1}^{n_d} |X_i(k\Delta f)|^2 \quad ; \quad k = 0, \frac{N}{2} \tag{5.13b}$$

In the above equations, X(f) and $X(k\Delta f)$ are as defined in Equation (5.10) and the hat (A) denotes "estimate of'. The summation over the index i indicates that the autospectrum must be estimated from an average of squared DFT computations over n_d disjoint (or statistically independent) blocks of data, each of a duration T = NAt. A plot of $G_{xx}(f)$ has the units of mean square value/Hz (g^2/Hz, psi^2/Hz, etc.) versus frequency in Hz, and is called an autospectrum, power spectrum, or power spectral density (PSD) plot.

It should be noted that the integral of the autospectrum (the area under the autospectrum) must always equal the mean square value (the square of the rrns value) of the signal from which it is computed; i.e.,

$$\hat{\psi}_x^2 = \int_0^\infty \hat{G}_{xx}(f)\, df = \Delta f \sum_{k=0}^{N/2} \hat{G}_{xx}(k\Delta f) \tag{5.14}$$

where $\hat{\psi}_x$ is defined in Equation (5.2). This relationship provides a good way to check autospectra computations by comparing the integral of the autospectrum to the square of the directly computed rms value of the signal.

5.4.3.1 Instruments and Software. Many of the commercial FIT-based digital signal processing instruments discussed in Section 5.4.2.1 have an operational mode for computing autospectra of random signals using Equation (5. 13), There is also a wide range of software packages, which can be purchased or leased, that accomplish the same computations. As with periodic signals, a program for the analysis of random signals is straight-forward to write using any available code for an FFT algorithm, e.g., [5.18 - 5.21]. Also, some manufacturers produce specialized instruments that compute spectra on-line during flight. experiments, as discussed previously in Section 5.4.2.1.

5.4.3.2 Anti-Aliasing Filters. Analog lowpass filters should always be used prior to the digitizing of analog signals for autospectra computations to avoid the possible aliasing errors discussed in Section 3.7.2. The recommended characteristics and cut-offfrequencies for anti-aliasing filters are detailed in Section 3.7.3.

5.4.3.3 Leakage and Tapering, As discussed in Section 5.4.1.3, the computation of a DFT from a block of random data values will always involve a leakage problem due to truncation. If the random signal king analyzed has a relatively smooth autospectrum, as is often true of boundary layer pressure and jet noise acoustic measurements, the leakage error will be negligible,However, if the signal being analyzed has an autospectrum that covers a wide dynamic range, as is common for structural vibration response measurements, then the leakage error can have a substantial influence on the smaller values of the resulting autospectral density estimate (see [5.4] for an illustration). Hence, a tapering operation should be used to suppress potential leakage errors, as discussed in Section 5.4.1.3. For consistency among different data analysis organizations, the cosine-squared or Harming window defined in Figure 5,5 is generally recommended, although other spectral windows [5.7, 5.16, 5.17] might be desirable for special applications and should be used if warranted. The application of the Harming window to random signals reduces the mean square value of each data block by a factor of 8/3 [5,4], Hence, the resulting computed spectral components must be multiplied by a factor of 8/3 to obtain a correct magnitude value, i.e., $u_h(t)$ in Figure 5.5(a) should be multiplied by $\sqrt{8/3}$ for random data analysis. Note that this is different from the multiplier of two needed to correct the magnitude error caused by the application of the Harming window in the spectral analysis of periodic signals, as discussed in Section 5.4.2.3.

5.4.3.4 Frequency Resolution. If the autospectrum of the random signal being analyzed displays sharply defined spectral peaks and/or notches, as is common for structural vibration measurements due to structural resonances, there will be a bias error in the spectral estimates at the frequencies of such peaks and/or notches due to the finite bandwidth of the analysis (see Section 5.4.1.4). This bandwidth bias error tends to reduce the indicated dynamic range of the autospectrum, i.e., it will make the peaks in the autospectrum estimate at resonance frequencies appear too low, and the notches at anti-resonance frequencies appear too high. The problem is most severe at the lower frequencies where the spectral peaks due to structural resonant responses tend to be very narrow in bandwidth, Specifically, the half-power point bandwidth of a spectral peak due to a structural resonance (hereafter referred to as the resonance bandwidth) can be approximated by [5.4]

$$B_r \approx 2\zeta f_r \tag{5.15}$$

where ζ is the estimated damping ratio (or fraction of critical damping) of the structural resonance, and f_r is the frequency of the structural resonance. The bandwidth bias error as a function of the ratio $\Delta f/B_r$ is shown for an autospectral density analysis using Equation (5.13) with a rectangular (untapered) and a Harming time window in Figure 5.8 [5.26], Also shown in this figure is the bandwidth bias error for an "ideal" window with a rectangular bandpass characteristic [5.27], which is approximated by a spectral analysis using digital filters or frequency averaged FFT computations discussed in Section B.5.2. 1.

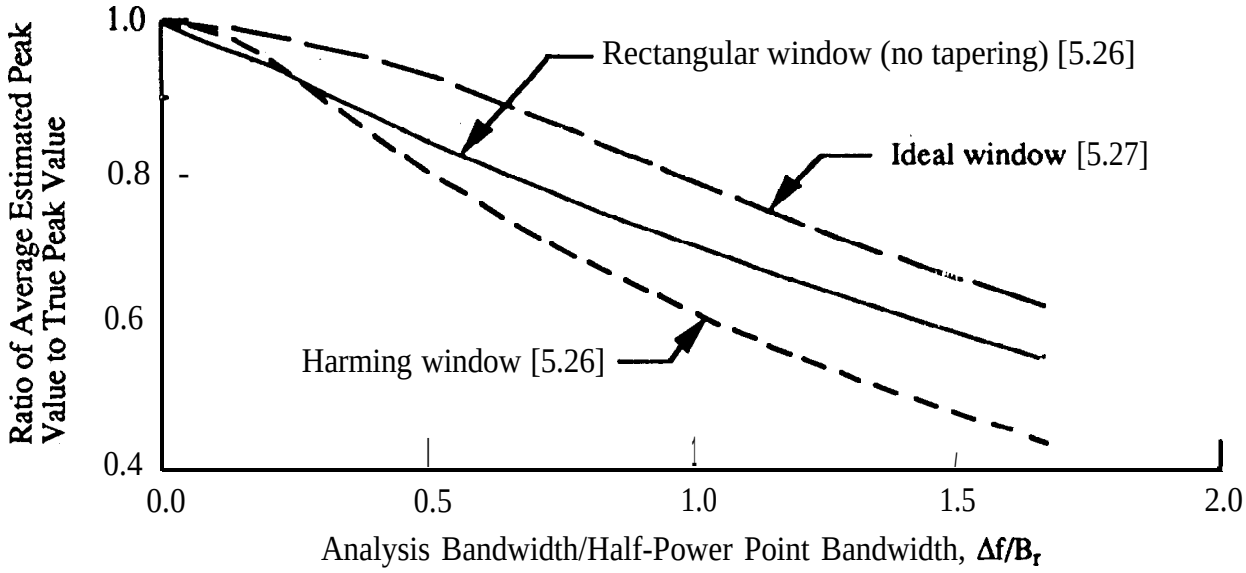

Figure 5,8. Frequency Resolution Bias Error for Peaks in Spectral Density Estimates.

If the available data are limited in duration to a few seconds or less, the "best" frequency resolution for an autospectrum estimate is one that will trade-off the bandwidth bias error and the statistical sampling (random) error (see Section 5.4.3.6) so as to minimize the total mean square error of the estimate, as detailed in [5.28]. However, if the measurement duration is unlimited so the random error can be made as small as desired, a "good" frequency resolution is one that will make the bandwidth bias error in Figure 5.8 negligible, say less than 5%. As a rule of thumb, this negligible error will be achieved if there are at least four spectral estimates between the half-power points of each peak or notch in the spectrum of the signal being analyzed, i.e., $\Delta f \leq B_r/4$. Unfortunately, this rule is often violated in practice. For example, the spectral analysis of high frequency aerospace vibration measurements is commonly performed over the frequency range from 20 to 2000 Hz with a frequency resolution of Δf = 5 Hz (corresponding to a DFT computation with N = 1024 data values per block, and a block duration of 0.2 see). From Equation (5.15), assuming the structure producing the vibration response measurement has a resonance at 50 Hz with a damping ratio of ζ = 0.025, the bandwidth of the resulting spectral peak would be B_r = 5 Hz. From Figure 5,8, for an analysis with a frequency resolution of Δf = 5 Hz, the spectral peak at this frequency would be under-estimated by 20 to 40%, depending on the spectral window for the analysis. Conversely, to make the bandwidth bias error negligible, the analysis would have to be performed with a frequency resolution of Δf = 1.25 Hz at this frequency (corresponding to a DFT computation with N = 4096 data values per block, and a block duration of T = 0.8 see).

To verify that a spectral resolution is adequate, two spectral analyses should be performed, one with a frequency resolution half the other. If the two spectral shapes are nearly identical (the magnitude and bandwidth of each spectral peak are similar in the two analyses), then no further analysis is required. On the other hand, if there are observable spectral differences, a zoom trans-

form (see Section *5.4.3.8)* should be applied to each spectral peak, using narrower and narrower frequency resolutions until no further changes in the spectral shape are observed. Finally, the frequency resolution of all autospectra computations should always be noted directly on the spectral plots, soothers can assess the degree of possible bandwidth bias errors in the results.

There are exceptions to the above recommended frequency resolution requirements. The most important involves spectra computed from signals that verify the equalization of a test facility used for a dynamic test, e.g., a vibration test on an electrodynamics shaker or an acoustic test in a reverberation chamber driven by electrodynamics air modulators. In these cases, the frequency resolution of the spectral analysis used to verify the test conditions should always be identical to the frequency resolution of the test facility equalization equipment. Otherwise, it may be impossible to verify the test equalization to within specified tolerances. A second possible exception applies to spectra computed for dynamic signals used to derive or verify vibration test criteria, where an enveloping operation is performed on the computed spectra. Due to practical considerations related to the mounting point impedance of the test item on a shaker as opposed to its actual support structure [5.29], it may not be appropriate to envelope the very narrow bandwidth spectral peaks in the signals used to establish the test levels. It follows that highly resolved spectral estimates may not be necessary or even desirable for this application.

5.4.3.5 Resolution Error Corrections. The bandwidth bias error discussed in Section 5.4.3.4 can always be suppressed by reanalyzing the data signal with a narrower frequency resolution (a longer block duration) using a zoom transform algorithm (see Section 5.4.3.8). However, a first order correction for the error can also be made at peaks and notches in the computed autospectrum using the inverse of the bias error plotted in Figure 5,8, as long as the frequency resolution is less than 1.5 times the resonance bandwidth ($\Delta f < 1.5\ B_r$). Further corrections for the bandwidth of the spectral peak can also be made, as detailed in [5.27].

5.4.3.6 Statistical Sampling Errors. An approximation for the normalized random error in autospectral density estimates is shown in Figure 5.9. Note that the random error is a function only of the number of disjoint averages n_d. If the data blocks being analyzed represent contiguous segments of the measured signal, the number of disjoint averages n_d will equal the number of analyzed data blocks N_b. However, when the analysis is performed using one of the commercial special purpose digital signal processing instruments, care must be exercised to properly count the number of disjoint averages. Specifically, most commercial instruments automatically overlap process the data when the time required by the instrument to compute the spectrum for each data block is shorter than the block duration $T = N\Delta t$. When the instrument is overlap processing, the number of averages performed by the instrument will be greater than the equivalent number of disjoint averages, because the data blocks being processed include redundant information. One way to determine the equivalent number of disjoint averages in an overlapped computation is from the relationship

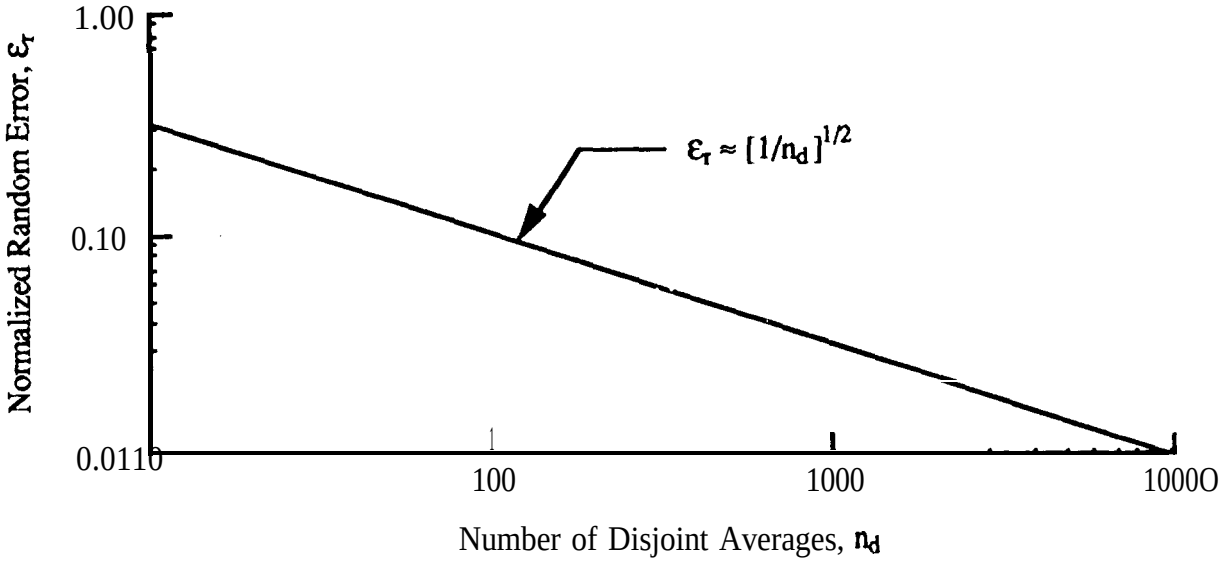

Figure 5.9. Normalized Random Error for Autospectral Density Estimates.

$$n_d = T_r \Delta f = \frac{T_r}{N\Delta t} \tag{5.16}$$

where T_r is the total duration of the analysis, and NAt is the block duration. A similar problem arises with software programs that intentionally overlap the data blocks being processed for reasons to be discussed shortly. In this case, however, the amount of overlap is generally specified, so the equivalent *number* of disjoint averages can be calculated from

$$n_d \approx (1 - P)\, N_b \tag{5.17}$$

where N_b is the number of blocks processed, and P is the fractional portion of each block that is used in the subsequent computation. See [S.4] for details.

5.4.3.7 Overlapped Processing. As discussed in Section 5.4.1.4, tapering operations to suppress side-lobe leakage in an autospectrum estimate also increase the bandwidth of the spectral window used for the analysis. If it is desired to maintain the same spectral bandwidth with tapering that would have been achieved without tapering, the block duration T (or block size N) for the analysis must be increased, However, assuming the total duration of the measurement Ţis fixed, this will reduce the number of disjoint averages n_d, and increase the random error of the spectral estimates. This increase in random error can be counteracted by simply computing the spectrum with overlapped blocks of data, rather than contiguous blocks, as detailed in [5.30, 5.31]. The greater the overlap, the greater the error reduction, but also the greater the number of computations. For autospectra computations on a main-frame computer, an overlap of 50% is recommended. This will eliminate over 90% of the increased random error due to most tapering operations, while

increasing the computations by a factor of only two. For computations using a commercial special purpose digital signal processing instrument, the data blocks should be overlapped by as much as is permitted by the real time rate of the instrument. The resulting normalized random error, in either case, can be approximated from Figure 5.9 using Equation (5.16) to estimate the equivalent number of disjoint averages,

5.4.3.8 Zoom Transforms. From Equation (5.13b), the upper frequency limit for a digital spectral estimate is the Nyquist frequency, $f_N = 1/(2\Delta t)$, while the resolution is $\Delta f = 1/(N\Delta t)$. It follows that the resolution of an analysis over a wide frequency range can be improved only by increasing the block size N. For software programs on a large main-frame computer, the block size N can usually be made long enough to accommodate most desired combinations of resolution and upper frequency limit. However, the block size employed for spectral computations by special purpose digital signal processing instruments is often fixed, meaning the resolution and upper frequency limit for an analysis are tied together. This limitation can be circumvented using so called "zoom transform" algorithms. Zoom transforms are usually accomplished through complex demodulation operations [5.4, 5.32], which essentially divide the full frequency range of the data signal into a collection of contiguous narrower frequency intervals that can be separately analyzed with all [(N/2) +1] spectral coefficients provided by a DFT with a fixed block size of N. Most commercial special purpose digital signal processing instruments are equipped with a zoom transform capability.

5.4.3.9 Plotting. Like periodic signal analysis, it is recommended that the spectral density values for random signals be plotted on a logarithmic scale due to the wide dynamic range of such data. However, unlike periodic signals, the peaks in the autospectra of random signals are usually due to resonant responses of a system (structural or acoustic) that tend to increase in bandwidth with increasing frequency, as suggested by Equation (5,15). Hence, a logarithmic scale is also recommended for the frequency axis in autospectra plots for random signals.

5.4.4 Nonstationary Data. Nonstationary data commonly occur when measurements are made during time-varying conditions. The resulting signals may be deterministic, random, or a combination of the two. As noted in Section 5.3,1.1, measurements under time-varying conditions should be avoided whenever possible. However, there are situations where they cannot be avoided, e.g., the data collected during the launch of a space vehicle. There is a rigorous methodology for the analysis of nonstationary data [5.4], but the analysis procedures require the computation of averages at specific instances of time over an ensemble of measurements obtained from repeated experiments performed under statistically equivalent conditions. The number of measurements required to accomplish a statistically meaningful ensemble average generally cannot be acquired in practice. Hence, the practical analysis of nonstationary signals is commonly accomplished using approximate spectral estimation techniques based upon time averaging operations.

5.4.4.1 Deterministic Signals. Nonstationary deterministic signals (excluding deterministic transients discussed in Section 5.5.1) are generally those signals that would have been periodic if the measurements had been made under steady-state conditions. A common and desirable method for analyzing such signals is to compute the DFT for each of a contiguous sequence of data blocks using Equation (5. 10), and presenting the results as a three-dimensional plot of amplitude versus frequency and time. Such plots are sometimes referred to as frequency-time spectra, order diagrams, waterfall plots, or Campbell diagrams. To obtain a clear identification of the spectral components of the time varying signal, the block duration for each computation must be short relative to the rate at which the average properties of the signal change. The optimum analysis is achieved by using the shortest block duration needed to obtain the minimum desired spectral resolution, and with no averaging of the spectra from adjacent blocks, i.e., $n_d = BT = 1$ for each time segment. All other considerations are as discussed in Section 5.4.2. See [5.32] for illustrations.

5.4.4.2 Random Signals. The computation of the frequency-time spectrum discussed for deterministic signals in Section 5.4.4.1 is sometimes applied to nonstationary random signals as well, e.g., [5.33]. Although this procedure can produce useful qualitative results in some cases (e.g., mapping the frequency of a time-dependent resonance), it generally is not effective for the analysis of random signals because of the sampling error defined in Figure 5.9. Specifically, the normalized random error in autospectra estimates of random data is an inverse function of $n_d = \sqrt{BT}$. For $n_d = 1$, as desired to obtain the maximum time and frequency resolution, the normalized random error is 100%, meaning errors of up to 3:1 in the spectral estimates at any frequency and time would be expected. Hence, more elaborate procedures based upon minimum mean square error criteria or parametric models are desirable for the analysis of nonstationary random signals. Such procedures for the analysis of Space Shuttle and Titan IV launch vibroacoustic data are recommended in Appendix B. Similar procedures could be derived for other types of nonstationary data.

5.4.4.3 Time Codes. All spectral analysis performed on nonstationary data requires the careful selection of the times of initiation and completion of the analysis time intervals. Detailed examination of the instantaneous time history of the signal, such as shown in Figure 4.4, is required for this selection. Experience has shown that the accurate initiation of the analysis time interval cannot be achieved manually, e.g., by the data analyst pressing a key at the designated time on the control keyboard of the analysis instrument. This situation has been identified as a major cause of error between organizations performing spectral analyses on supposedly identical data. To avoid this error, it is essential that the analysis interval be triggered by the time code originally applied to the data recorder or storage system during data acquisition (see Sections 2.7 and 3.6.6.3). The completion time of the spectral analysis is usually controlled by the computer storage constraints, which can be arranged to closely approximate the desired completion time.

5.4.5 Proportional Bandwidth Spectra. FFT algorithms inherently produce spectra with a constant frequency resolution, independent of the bandwidth center frequency. This is appropriate for

the analysis of periodic signals, where the frequency interval between harmonic components is a constant and the frequency bandwidth of the components is theoretically zero. For random dynamic signals, however, the sharply defiied peaks that may appear in an autospectrum are usually due to system resonances with finite bandwidths that increase with increasing frequency. Hence, a constant frequency resolution analysis using a DFT will tend to under-resolve spectral peaks that may appear at the lower frequencies and/or over-resolve spectral peaks at the higher frequencies. Referring to Equation (5.15), assuming the damping ratio is reasonably constant, a spectral analysis with a frequency resolution (spectral bandwidth) that is proportional to the center frequency, rather than a fixed bandwidth, has obvious merit as long as the bandwidth is sufficiently narrow.

5.4.5.1 1/3 Octave Band Spectra. Aeroacoustic data of all types have historically been analyzed using a constant percentage spectral resolution. The most widely accepted constant percentage resolution for this application is the 1/3 octave band (a frequency resolution bandwidth that is about 23% of the center frequency), for which an ANSI Standard exists [5.34]. This relatively coarse resolution is justified for acoustic signals because, in most cases, there spectra lack sharp peaks and notches. The presentation of the resulting spectra is usually in the form of rms values in 1/3 octave bands, but the results are sometimes presented in terms of average autospectral density values in 1/3 octave bands as well. Commercial instruments with analog 1/3 octave band filters are still in wide use, but these devices are rapidly being replaced with special purpose 1/3 octave band digital filtering instruments or comparable digital filtering software programs for main-frame computers and PCs. Although a 1/3 octave band resolution usually will not identify individual periodic components or narrow bandwidth random spectral peaks that may be present in a signal, such an analysis is considered acceptable for aeroacoustic environmental assessments. Any instrument with filters that meet the ANSI Standard [5,34] are recommended for this type of data analysis. Because of their wide use in describing aeroacoustic loads, 1/3 octave bandwidths are commonly used for aeroacoustic-induced vibration predictions, as well as for criteria verification purposes, e.g., [5.35 -5.371. This is an acceptable practice, as long as it is understood that the resulting spectra will include severe frequency resolution bias errors (see Sections 5.4.2.4 and 5.4.3.4) and, hence, will not accurately describe the sharp spectral peaks due to periodic components and random induced resonant responses in the vibration signal.

5.4.5.2 Other Proportional Bandwidth Spectra, Various other proportional bandwidth filters occasionally have been used over the years for the spectral analysis of both aeroacoustic and vibration data signals, including 1/1 octave, 1/6 octave, and 1/12 octave bands. For aeroacoustic data, to maintain consistency among the results produced by different organizations, it is recommended that all proportional bandwidth "spectra be computed using 1/3 octave bands only. For the case of vibration data where a proportional bandwidth analysis is performed, a 1/12 octave bandwidth is recommended (see Appendix B), although other proportional bandwidths might be warranted for special applications, e.g., a 1/3 octave bandwidth for comparison of vibration measurements to analytical predictions, or a 1/6 octave bandwidth for arriving at vibration test criteria.

5.5 Single Channel Spectral Analysis - Transient Data. There are two classes of data analysis that may be performed on transient signals: (a) a direct description of the transient in the frequency domain using linear spectra for deterministic transients or energy spectra for random transients, and (b) a description of the damaging potential of the transient as a function of natural frequency using shock response spectra, Analysis approach (a) is most appropriate for analytical applications, such as normal mode analysis and system identification problems, while approach (b) is better suited to provide general environmental descriptions for design criteria and test specification purposes. Both approaches assume the transient of interest can be measured over its entire duration (from its initiation to the termination of significant values). In addition, time histories of transient signals are often fed directly into computer models to obtain internal loads, as mentioned earlier in Section 5.2.4,

5.5.1 Fourier Spectra. For the case of a deterministic transient signal x(t) that is repeatable in detail from one flight or test to the next, a direct spectral description of the transient is provided by its Fourier transform X(f). Specifically, for a one-sided spectrum defined only for non-negative frequencies,

$$\begin{aligned} F_x(f) &= 2\,X(f)\ ; \quad f > 0 \\ &= x(f)\ ; \quad f = o \\ &= o\ ; \quad f < 0 \end{aligned} \tag{5.18}$$

where the factor of two for f > O is necessary to account for the theoretical negative frequencies in X(f). The desired Fourier transform is readily computed using an FFT algorithm to obtain the DFT defined in Equation (5. 10b). Assuming the block duration (T = NAt) equals or exceeds the duration of all significant values of the transient, the DFT in Equation (5.10b) from $k = 0$ to $N/2$ will essentially yield the exact Fourier transform of the transient. This follows because the values of the transient outside the time interval of the computation are presumed to be zero and, hence, all values of the Fourier transform of the transient from minus to plus infinity can be interpolated from the DFT. For single channel analysis applications, the phase portion of the Fourier transform is often ignored, and only the Fourier magnitude spectrum $|F_x(f)|$ is presented. A plot of $|F_x(f)|$ has the units of magnitude-see (g-see, psi-see, etc.) versus frequency in Hz. For more advanced applications, such as the computation of structural responses to transient loads, the Fourier phase spectrum must be maintained

It should be mentioned that Fourier spectra are sometimes computed for transients with a stochastic character, e.g., pyroshocks. However, since the Fourier spectrum is computed from only one signal segment, corresponding to $n_d = 1$, the random errors in the resulting estimate will be large (see Section 5.4.4.2). Hence, energy spectra are recommended for random transients, as discussed in Section 5.5.2.

5.5.1.1 Instruments and Software. The instruments and software used for the computation of Fourier spectra for deterministic transient signals are essentially the same as those discussed in Section 5,4.2.1 for periodic data analysis. When the analysis is done on-line with a special purpose digital signal processing instrument a threshold detector to initiate and capture a block of data for analysis is required. Such circuits are provided on most commercial FFT-based signal processing instruments, Of course, any software program with an FFT algorithm can also be used to compute Fourier Spectra.

5.5.1.2 Anti-Aliasing Filters. Analog lowpass filters should always be used prior to the digitizing of analog signals for Fourier spectra computations to avoid the possible aliasing errors discussed in Section 3.7,2. The recommended characteristics (magnitude and phase) and cut-off frequencies for anti-aliasing filters are detailed in Section 3.7.3.

5.5.1.3 Leakage and Tapering. If the block of data being analyzed includes all significant values of the entire transient signal, there will be no truncation causing leakage in the DFT computation, meaning no tapering of the data values is required. However, if the data block terminates before the transient signal has decayed to negligible values, then the resulting truncation will cause leakage in the spectral computation, as discussed in Section 5.4.1.3. This often occurs in transient signals with slow decay rates representing the response of lightly damped structures to an impulsive load. In general, any time window that has a value near unity at the maximum values of the transient, and decays to near zero at the end of the transient measurement, is acceptable to suppress leakage in transient data analysis, e.g., a window that is unity over the first half of the transient, and the second half of the Harming window in Figure 5.5(a) over the last half of the transient. For those cases where structural damping is to be estimated from the transient response signal, the tapering can be accomplished with an exponential time window that decays from a value of unity at the start of the data block (ideally initiating at the start of the transient) to a value of 0.001 (-60 dB) at the end of the data block, as illustrated in Figure 5.10(a). The corresponding spectral window for exponential tapering is shown in Figure 5.10(b). The exponential window detailed in Figure 5.10 is

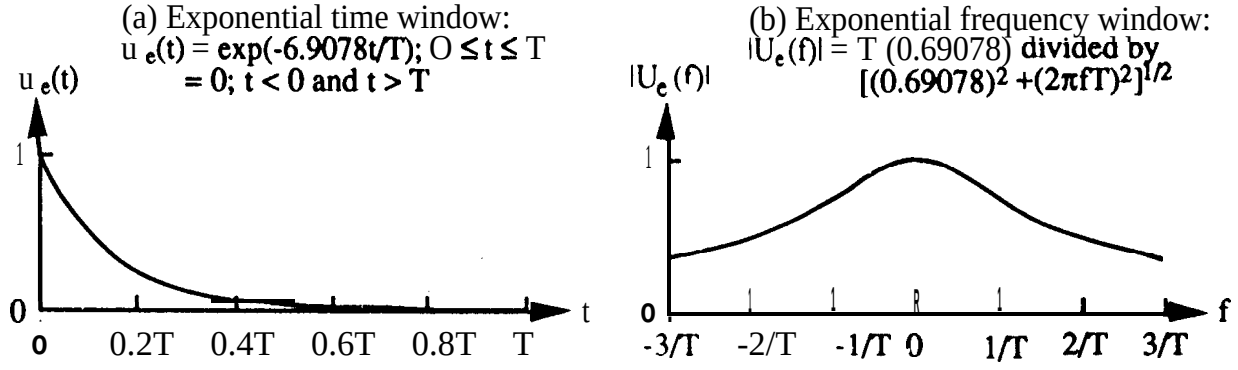

Figure 5.10. Exponential Window for Spectral Analysis of Transient Signals.

desirable because it appears in the resulting Fourier spectrum as additional, well defined linear darnping of the structural response and, hence, offers the opportunity to correct estimates of structural damping made from the Fourier spectrum for window effects.

5.5,1,4 Frequency Resolution. The frequency resolution for the computation of Fourier spectra is fixed by $\Delta f = 1/T = 1/(N\Delta t)$. However, if the data block being analyzed includes all significant values of the entire transient signal, then the continuous Fourier spectrum at all frequencies can be computed by interpolation techniques, or more simply by adding any desired number of zeros to the signal record prior to the DFT computation. For this case, the zeros constitute real data and, hence, will improve the frequency resolution of the analysis. In any case, given a final spectral resolution Af, and peaks and/or notches in the spectral data with a bandwidth B_r estimated by Equation (5. 15), there will be a bandwidth bias error that is approximated by one-half the value given in Figure 5.8.

5.5.1.5 Resolution Error Correction. Again for the case where the data block being analyzed includes all significant values of the entire transient signal, the bandwidth bias error discussed in Section 5.4.3.4 can be suppressed by reanalyzing the data signal with a narrower frequency resolution achieved by adding zeros, or by appropriate interpolation procedures. However, a first order correction for the error can also be made at peaks and notches in the computed Fourier spectrum using the inverse of one-half the error term plotted in Figure 5.8, as long as Af c 1.5&.

5.5.1.6 Statistical Sampling Errors. There are no statistical sampling errors in the computation of Fourier spectra for deterministic transient signals.

5.5.1.7 Plotting. As for stationary random signal analysis, it is recommended that the spectral magnitude values for deterministic transient signals be plotted as logarithmic magnitude versus logarithmic frequency, for the same reasons discussed in Section 5.4.3.9.

5.5.2 Energy Spectra. For the case of a transient signal x(t) that is random in character, it is common to describe the frequency content of the signal in terms of an energy spectral density function estimated by

$$\begin{aligned}
\hat{E}_{xx}(f) &= \frac{2}{n_d}\sum_{i=1}^{n_d} |X_i(f)|^2 \quad ; \quad f > 0 \\
&= \frac{1}{n_d}\sum_{i=1}^{n_d} |X_i(f)|^2 \quad ; \quad f = 0 \qquad (5.19a) \\
&= 0 \quad ; \quad f < 0
\end{aligned}$$

For digital computations,

$$\hat{E}_{xx}(k\Delta f) = \frac{2}{n_d}\sum_{i=1}^{n_d} |X_i(k\Delta f)|^2 \quad ; \quad k = 1, 2, \ldots, \frac{N}{2} - 1$$

$$= \frac{1}{n_d}\sum_{i=1}^{n_d} X_i(k\Delta f)|^2 \quad ; \quad k = 0, \frac{N}{2} \qquad (5.19b)$$

where X(f) and $X(k\Delta f)$ are as defined in Equation (5.10), and the hat (A) denotes "estimate of'. The summation over the index i indicates that the energy spectrum must be computed from an average of squared DFT computations over n_d transient measurements produced by repeated experiments performed under statistically equivalent conditions. By comparing Equation (S. 19) with Equation (5. 13), it is seen that the energy spectrum for transient random signals involves the same computations as the auto- (power) spectrum for stationary random signals, except there is no division by $T = N\Delta t$. The mathematical and physical significance of the energy spectrum is detailed in [5.4]. A plot of $E_{xx}(f)$ has the units of mean square value-sec/Hz (g^2-sec/Hz, psi^2-sec/Hz, etc.) versus frequency in Hz, and is called an energy spectrum or transient autospectrum.

5.5.2.1 Instruments and Software. The instruments and software used for the analysis of random transient signals in terms of energy spectra are essentially the same as those discussed in Section 5.4.3.1 for stationary random data analysis.

5.5.2.2 Anti-Aliasing Filters. Analog lowpass filters should always be used prior to the digitizing of analog signals for energy spectra computations to avoid the possible aliasing errors discussed in Section 3.7.2. The recommended characteristics and cut-off frequencies for anti-aliasing filters are detailed in Section 3.7.3.

5.5.2.3 Leakage and Tapering. As for deterministic transients, if the block of data being analyzed includes all significant values of the entire transient signal, there will be no truncation error causing leakage in the DFT computation and, hence, no tapering of the data values is required. However, if the data block terminates before the transient signal has decayed to negligible values, then the resulting truncation may cause leakage in the spectral computation, as discussed in Section 5.5.1.3. In such cases, some form of tapering, such as the exponential tapering detailed in Figure 5.10, is recommended.

5.5.2.4 Frequency Resolution. The frequency resolution considerations for energy spectra are the same as for Fourier spectra discussed in Section 5.5.1.4, except that the bandwidth bias error is approximated directly by the value given in Figure 5.8.

5.5.2.5 Resolution Error Corrections. For the case where the data block being analyzed includes all significant values of the entire transient signal, the bandwidth bias error discussed in Section 5.5.2.4 can always be suppressed by reanalyzing the signal with a narrower frequency resolution achieved by adding zeros, or by appropriate interpolation procedures. However, a first order correction for the error can also be made at peaks and notches in the computed energy spectrum using the inverse of the error term plotted in Figure 5.8.

5.5.2.6 Statistical Sampling Errors. The statistical sampling errors in energy spectra estimates are essentially the same as for autospectra estimates discussed in Section 5.4.3.6 (see Figure 5,8), except the n_d disjoint segments needed for the averaging operation must be obtained from repeated flights or tests performed under statistically equivalent conditions.

5.5.2,7 Plotting. As for stationary random signal analysis, it is recommended that the energy spectral density values for random transient signals be plotted as logarithmic spectral density versus logarithmic frequency, for the same reasons discussed in Section 5.4.3.9.

5,5.3 Shock Response Spectra. The shock response spectrum (SRS), sometimes called simply a shock spectrum or a response spectrum, represents a measure of the damaging potential of the transient, Specifically, the SRS is defined as the maximum response of the mass of a base-excited mechanical oscillator (single degree-of-freedom system) to the measured transient, as a function of the natural frequency and damping of the oscillator. The SRS is applicable to both deterministic and random transients, and can be defined for any input and response parameters of interest (displacement, velocity, or acceleration), For aerospace applications, it is common to define the input transient in terms of an acceleration at the oscillator base, and the response in terms of an absolute acceleration of the oscillator mass, as illustrated in Figure 5.11.

The absolute acceleration response $a_r(t)$ of the mass of an oscillator with a natural frequency f_n and damping ratio ζ to a transient acceleration $a_i(t)$ at the base of the oscillator is given by [5.38 - 5.40]

$$a_r(t) = 4\pi\zeta f_n \int_0^t a_i(\tau)\, e^{-2\pi\zeta f_n(t-\tau)} \cos[2\pi f_d(t-\tau)]\, d\tau$$

$$+ [(2\pi f_n)^2(1 - 2\zeta^2)/(2\pi f_d)] \int_0^t a_i(\tau)\, e^{-2\pi\zeta f_n(t-\tau)} \sin[2\pi f_d(t-\tau)]\, d\tau \qquad (5.20)$$

where

$$f_d = f_n(1-\zeta^2)^{1/2}$$

The SRS computation essentially consists of determining the maximum value of $a_r(t)$ as a function of f_n for a given damping ratio. The mechanical analog of the acceleration SRS computation is shown in Figure 5.11.

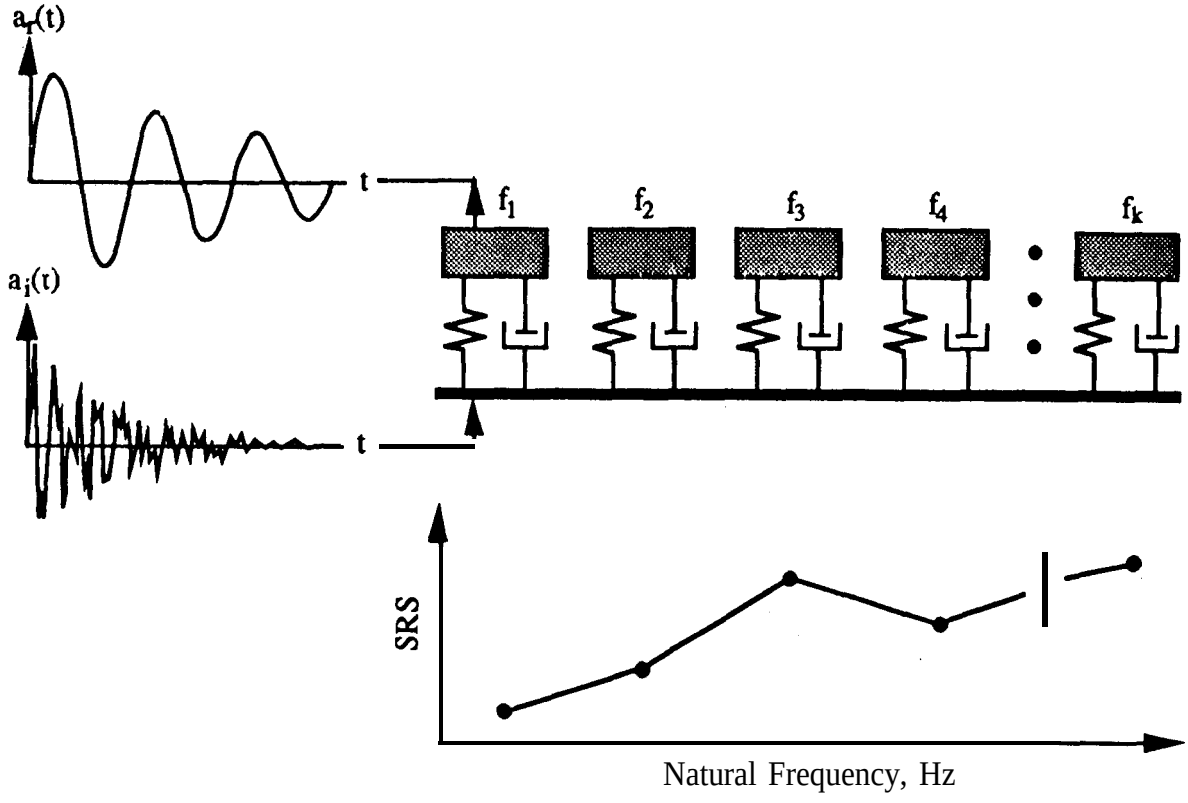

Figure 5.11. Mechanical Analog for Shock Response Spectrum Computation.

There are several SRS values that may be of interest for different applications, namely, the maximum absolute acceleration response of the oscillator mass versus f_n that occurs

(a) during the application of the transient, called the primary SRS denoted by $S_P(f_n)$,
(b) after the transient is over, called the residual SRS denoted by $S_R(f_n)$,
(c) in the positive direction, called the positive SRS denoted by $S^+(f_n)$,
(d) in the negative direction, called the negative SRS denoted by $S^-(f_n)$, or
(e) at any time in either direction, called the maximax SRS denoted by $S(f_n)$.

Each of the above SRS functions must also be identified with a specific value of damping assumed for the oscillator. Commonly assumed values of damping for SRS calculations in aerospace applications range from O to 5% of critical ($O \leq \zeta \leq 0.05$). A plot of $S(f_n)$ for an acceleration transient has the units of peak acceleration in g versus natural frequency in Hz.

5.5.3.1 Interpretation of SRS Results. The theory behind the use of the SRS for transient data analysis is as follows. If a mechanical component of interest has a single, dominant resonance frequency producing a linear response with a damping value ζ equal to the damping used to define the SRS, then the measured SRS identifies the maximum (peak) response of the component due to an

exposure to the transient. The actual frequency of the component resonance does not have to be known, since the SRS computation yields the maximum response for any resonance frequency that might exist within the frequency range of the analysis. For more advanced design applications, where the normal mode characteristics of the structure subjected to the transient are known, an estimate of the maximum system response based on the response of all structural modes can be computed from the SRS using the various assumptions discussed in [5.41, 5.42].

Two other properties of the absolute acceleration SRS related to its interpretation should be mentioned:

(1) The value of the SRS will approach the absolute maximum value of the transient acceleration $|a_i|_{max}$ as the natural frequency f_n of the oscillator exceeds the lesser of (a) the highest frequency in the Fourier spectrum of the transient, or (b) the upper frequency limit of the data acquisition system, denoted in either case by f_{max}. As a rule of thumb, $S_a(f_n) \approx |a_i|_{max}$ when $f_n \geq 5\ f_{max}$.

(2) Unlike the Fourier spectrum defined in Equation (5.18), the SRS does not have a unique relationship with the transient signal from which it is computed; i.e., it is possible for different transients to have the same SRS.

See [5.38 - 5.42] for further details on the measurement, analysis, and interpretation of SRS data for general transient signals. Discussions of the special problems associated with SRS measurements of pyroshock data are presented in Appendix A.

5.5,3.2 Presentation of SRS Results. The maximax SRS is often used as the criterion for equivalence between a measured transient environment and a laboratory simulation of that transient environment. However, as noted in Section 5.5.3.1(2), the maximax SRS alone does not provide a unique description of a transient. In particular, it is often possible to at least coarsely approximate the maximax SRS for a complex, multi-cycle transient environment by an appropriately shaped single pulse transient in the laboratory. Of course, the required single pulse used for the simulation will have a much higher maximum level than the actual environment, raising serious questions about the validity of the simulation. To avoid this potential problem, it is recommended that SRS data provided for laboratory simulation purposes be presented in one of the following forms:

(1) Present the maximax SRS along with the actual time history of the transient.

(2) Present the maximax SRS along with some measure of the duration of the transient signal, e.g., the approximate time interval from the start of the transient to that time when the envelope of the signal values is 10% of the maximum value. ‘

(3) Present two rnaximax SRSS computed with two widely different values of damping (Q), e.g., $\zeta = 0.05$ (Q = 10) and $\zeta = 0.005$ (Q = 100).

(4) Present the three dimensional SRS described in [S.39]. The three dimensional SRS is essentially a histogram of the peak values of the hypothetical oscillator response versus the oscillator natural frequency,

5.5.3.3 Instruments and Software. Specialized commercial instruments are available for the computation of SRS functions, but most SRS analysis is performed using software on general purpose computers. Commercial SRS software packages are available for both main-frame computers and PCs, e.g., [5.43].

5.5.3.4 Anti-Aliasing Filters. Analog lowpass filters should always be used prior to the digitizing of analog signals for SRS computations to avoid the possible aliasing errors discussed in Section 3.7,2, The recommendations for anti-aliasing filters in Section 3.7.3 apply, except it is suggested for SRS computations that the half-power point cut-off frequency of the anti-aliasing filter be 1.5 times the highest SRS natural frequency to be analyzed, This is needed to assure a full response of the highest frequency oscillator in the SRS computation to the transient energy within its bandwidth. Also, this will suppress the error in the SRS value at the highest naturalfrequency due to the possible nonlinear phase characteristics of the anti-aliasing filter [5.44].

As an alternative to setting the cut-off frequency of the anti-aliasing filter at 1.5 times the highest SRS natural frequency, a data normalization procedure, such as that described in [5.45], can be employed, Such procedures general] y involve Fourier transforming the digitized signal, dividing by the frequency response function of the anti-aliasing filter, and inverse transforming to obtain a signal corrected for the anti-aliasing filter magnitude and phase characteristics.

5.5.3.5 Sampling Rate. Unlike other spectral quantities evolving from DFT computations, the SRS is essentially a time domain quantity. Hence, the digital sampling rate, given by $R_s = 1/\Delta t$, introduces errors beyond those associated with aliasing about the Nyquist frequency, i.e., R_s must be high enough to accurately describe the response of the SRS oscillators. From [5.46], if R, = 2.56 f_h, where f_h is the highest natural frequency for the SRS computation, the error in the indicated maximum response of the highest frequency oscillator could exceed 60%. To minimize this potential error, it is recommended that SRS computations be performed with a sampling rate of $R_s \geq 10 f_h$, which will limit the magnitude error to less than 5% [5.46]. If the desired sampling rate of R_s 210 f_h is not achieved, but the sampling rate is at least, sayR$24 f_c, where f_c is the cut-off frequency for an anti-aliasing filter with a cut-off rate of at least 60 dB/octave, a digital-to-analog conversion could be performed to reconstruct the analog signal, which could then beresampled at the desired sampling rate. Of course, a similar result could be achieved using an appropriate digital interpolation algorithm, e.g., [5.47].

5.5,3.6 **Truncation Errors**. If the signal being analyzed has the form of a decaying oscillation, and the data block is not long enough to include all significant values of the entire transient signal, there will be a truncation error in the resulting SRS due to the step function at the end of the signal. As for the truncation problem discussed in Section 5.5.1.3, a tapering operation will help suppress this error. "In this case, however, the desired tapering operation should be performed only over the last 25% of the signal. Any smooth function that will make the last value in the signal equal zero is acceptable, e.g., the last half of the Harming window shown in Figure 5. 5(a). It should be mentioned that even with a tapering operation, signal truncation may still cause other problems (see Section 5.5.3.7).

5.5,3.7 **Initial Conditions**. The results of an SRS computation can also be significantly influenced by the initial conditions assumed for the data. To standardize results, the following recommendaions are made:

(1) For measurements on structures that experience no net velocity change due to the transient event, the signal should be forced to yield a net velocity change of zero from the beginning to the end of the transient event (called the AV = O criterion) before the SRS computation. The AV = O condition is achieved by calculating the average (mean) value of the acceleration signal, and subtracting this mean value from all data values.

(2) For measurements on structures that experience a net velocity change due to the transient event (i.e., deployed structures), the signal should be forced to have zero velocity preceding the pyroshock (called the initial V = O criterion) before the SRS computation.

(3) As an alternative to (2), if the net velocity change of the structure due to the transient event is precisely known, the signal may be forced to yield a net velocity change equal to the actual velocity change of the structure.

In establishing any of the above initial conditions, it is important that the zero baseline before the transient event be accurately established, if necessary, by avenging the signal prior to the event to suppress instrumentation noise.

A truncation error of the type discussed in Section 5.5.3.6 can complicate the selection of an appropriate initial condition. For example, the integration or double integration of a truncated signal representing the acceleration response of a structure might yield an unrealistic net velocity or displacement change of the structure. Hence, it is highly desirable to obtain transient measurements for SRS analyses that are sufficiently long to avoid significant truncations.

5.5.3.8 **Frequency Resolution**. Unlike Fourier, auto, and energy spectral computations, the resolution of an SRS computation is not dictated by the data block duration being analyzed; it is an in-

dependent variable established by the desired separation of the resonance frequencies of the hypothetical oscillators used for the SRS computation, as illustrated in Figure 5.11. For an SRS analysis with $\zeta = 0.05$, it is recommended that a logarithmic frequency resolution of 1/6 octave be employed (this is the approximate half-power point bandwidth of a 5% damped oscillator), A finer resolution may be warranted if a smaller value of darnping is assumed.

5.5.3.9 Resolution Error Corrections. There are no specific procedures for correcting resolution errors, other than to reanalyze the signal with a narrower resolution.

5.5.3.10 Statistical Sampling Errors. There are no statistical sampling errors in SRS estimates for deterministic transients, beyond those discussed in Section 5.5.3.7. The statistical sampling errors in SRS estimates for random transients due to variability from one event tothe next are not well defined. However, since the SRS value at a given natural frequent y represents the response of an oscillator to the energy spectral density values of the transient over the bandwidth of the oscillator, it follows that the statistical sampling error in the SRS should be substantially less than in energy spectral density estimates (see Section 5,5.2.6), Nevertheless, the averaging of SRS estimates computed from repeated experiments performed under statistically equivalent conditions is desirable, when feasible.

5.5.3.11 Plotting. Like energy spectra, it is recommended that the SRS values for transient signals be plotted as logarithmic SRS magnitude versus logarithmic frequency, for the same reasons discussed in Section 5.4.3.9.

5.5.3.12 Other SRS Computations. Although the computation of art absolute acceleration SRS is widely used in the aerospace industry, SRS computations using other output parameters are sometimes employed in other applications. For example, the relative displacement response to an acceleration input is often used in earthquake studies [5,42]. Specifically y, the displacement of the oscillator mass in Figure 5.11 relative to the base due to a base acceleration $a_i(t)$ is given by [5.39]

$$\delta(t) = \frac{1}{2\pi f_d} \int_0^t a_i(\tau)\, e^{-2\pi\zeta f_n(t-\tau)} \sin[2\pi f_d(t-\tau)]\, d\tau \qquad (5.21)$$

where f_d is defined in Equation (5.20). The relative displacement SRS, denoted by $S_\delta(f_n)$, is computed by solving for the maximum value of ii(t) in Equation (5,21) over the desired range of oscillator natural frequencies. The relative displacement SRS is often used to compute the "equivalent static acceleration" given by [5.39]

$$A_{eq} = \frac{(2\pi f_n)^2}{g} S_\delta(f_n) \qquad (5.22)$$

where g is the acceleration due to gravity. The equivalent static acceleration represents the steady acceleration (as a multiple of the acceleration due to gravity) that would produce the same relative displacement of the structure as the transient would produce for any given natural frequency.

Finally, there is a strong theoretical argument to define the SRS for structural responses in terms of relative velocity, rather than absolute acceleration or relative displacement, due to the inherent relationship between dynamic velocity and stress in simple structures [5.48, 5.49]. Furthermore, for hard impact and pyroshock transients, a relative velocity SRS generally covers a much narrower dynamic range than either an absolute acceleration or a relative displacement SRS. Such alternate parameters for SRS computations should be used where appropriate.

5.6 Dual-Channel Analysis. Many applications of dynamic data are served by the analysis of single-channel measurements, as covered in Sections 5.2 through 5.5. For more advanced applications, however, the joint analysis of two or more measurements may be required. This is usually accomplished directly in the frequency domain using cross-spectral density functions, and related functions such as coherence and frequency response functions. There are some applications where it is more convenient to present the desired information in the time domain using cross-correlation functions, and related functions such as correlation coefficient and unit impulse response functions.

5.6.1 Cross-Spectra. Given two signal measurements x(t) and y(t), any linear relationship between these two measurements will be extracted directly in frequency domain terms by the cross-spectral density function estimated by

$$\hat{G}_{xy}(f) = \frac{2}{n_d T} \sum_{i=1}^{n_d} X_i^*(f)\, Y_i(f) \quad ; \quad f > 0$$

$$= \frac{1}{n_d T} \sum_{i=1}^{n_d} X_i^*(f)\, Y_i(f) \quad ; \quad f = 0 \qquad (5.23a)$$

$$= 0 \quad ; \quad f < 0$$

For digital computations,

$$\hat{G}_{xy}(k\Delta f) = \frac{2}{n_d N \Delta t} \sum_{i=1}^{n_d} X_i^*(k\Delta f)\, Y_i(k\Delta f) \quad ; \quad k = 1, 2, \ldots, \frac{N}{2} - 1$$

$$= \frac{1}{n_d N \Delta t} \sum_{i=1}^{n_d} X_i^*(k\Delta f)\, Y_i(k\Delta f) \quad ; \quad k = 0, \frac{N}{2} \qquad (5.23b)$$

where X*(f) or $X^*(k\Delta f)$ is the complex conjugate of the DFT of x(t), and Y(f) or $Y(k\Delta f)$ is the DFT of y(t), as defined in Equation (5.10). As before, the hat (A) denotes "estimate of'. The summation over the index i indicates that the cross-spectral density function must be computed from an average of products of paired DFT computations over n_d disjoint blocks of data, each of a duration T = NAt. It should be mentioned that the cross-spectrum is sometimes defined as the average of $X(f)Y^*(f)$, which gives the complex conjugate of the definition in Equation (5.23),

The cress-spectral density function is generally a complex number which can be written as

$$G_{xy}(f) = C_{xy}(f) - jQ_{xy}(f) \tag{5.23c}$$

where the real part, denoted by $C_{xy}(f)$, is called the coincident spectral density function or co-spectrum, and the imaginary part, denoted by $Q_{xy}(f)$, is called the quadrature spectral density function or quad-spectrum: The cross-spectrum may also be expressed in terms of a magnitude and phase by

$$G_{xy}(f) = |G_{xy}(f)| e^{-j\phi_{xy}(f)} \tag{5.23d}$$

where

$$|G_{xy}(f)| = \sqrt{C^2_{xy}(f) + Q^2_{xy}(f)} \qquad \phi_{xy}(f) = \tan^{-1} \frac{Q_{xy}(f)}{C_{xy}(f)} \tag{5.23e}$$

A plot of $G_{xy}(f)$ has the units of x(t)y(t)/Hz (g^2/Hz, g-psi/Hz, etc.) versus frequency in Hz, and is called a cross-spectrum or cross-spectral density (CSD) plot.

5.6.1.1 Instruments and Software. Many of the commercial FFT-based digital signal processing instruments discussed in Section 5.4.3.1 are dual channel, and have an operational mode for computing cross-spectra of random signals using Equation (5.23) [some instruments compute the cross-spectrum in terms of the complex conjugate of Equation (5,23), which changes the sign of the phase term]. There is also a wide range of software packages that can be purchased or leased, which accomplish the same computations, Like autospectra, a program for the computation of cress-spectra is easy to write using any available code for an FFT algorithm [5.18 - 5.21].

5.6.1.2 Anti-Aliasing Filters. Analog lowpass filters should always be used prior to the digitizing of analog signals for cross-spectra computationsto avoid the possible aliasing errors discussed in Section 3,7.2. The recommended characteristics and cut-off frequencies for anti-aliasing filters are detailed in Section 3.7.3.

5.6.1.3 Leakage and Tapering. The requirements for tapering to suppress leakage errors are the same as discussed for autospectra in Section 5.4.3,3.

5.6.1.4 **Frequency Resolution**. The frequency resolution requirements are the same as presented for **autospectra** in Section 5.4.3.4, where the bandwidth bias error in Figure 5.8 applies to the magnitude of the cross-spectrum,

5,6.1.5 **Resolution Error Corrections**. The bandwidth bias error discussed in Section 5.4.3.4 can always be suppressed by reanalyzing the data signal with a narrower frequency resolution (i.e., a longer block duration). However, a **first** order correction for the error can also be made at peaks and notches in the computed cross-spectrum magnitude using the inverse of the error term plotted in Figure 5.8.

5.6.1.6 **Time Delay Bias Error**. Data acquisition systems generally collect **measured** signals on a common time base, unless special instructions are given to the contrary. In certain situations, a cross-spectrum may be computed between two signals x(t) and y(t), where there is a substantial physical propagation time τ from one signal to the other, e.g., as would occur if x(t) were an acoustic source and y(t) were the sound level measured at a substantial distance from the source, If the physical propagation time between x(t) and y(t) is a significant fraction of the analysis block duration T, a portion of y(t) will include information that is not represented in x(t). This produces a bias error that causes the estimated magnitude of the cross-spectrum at all frequencies to be too small, as presented in Figure 5.12. See [5.4, 5.26, 5.50, 5.51] for details. This time delay bias error can be eliminated by anticipating the propagation time, and inserting a compensating time translation (called a **pre-computational** delay) between x(t) and y(t) before computing the **cross-**spectrum. Such **pre-computational** delay algorithms are incorporated in most modern signal processing instruments and commercial software packages.

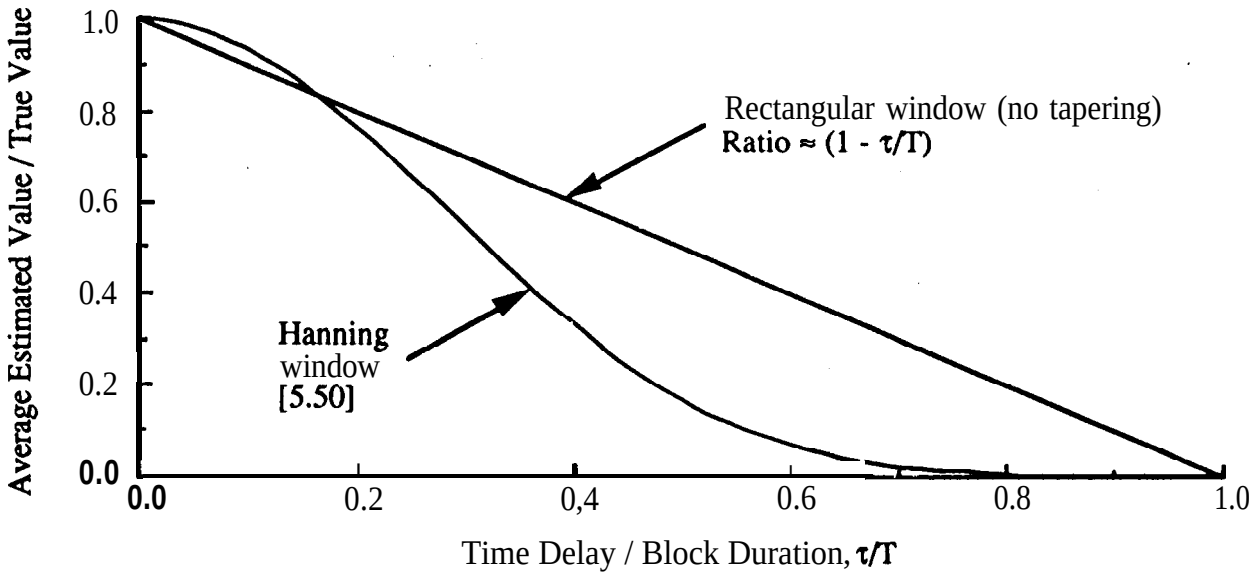

Figure 5.12. Time Delay Bias Error for Cross-Correlation, Cross-Spectral Density, and Frequency Response Magnitude Estimates.

5.6.1.7 Multiple Path (Reverberation) Bias Errors. As an extension of the time delay bias error in Section 5.6.1,6, when there are multiple propagation paths between two signals x(t) and y(t), each having a different physical propagation time, a time delay bias error occurs for each of the propagation paths. This is essentially the situation that exists when acoustic measurements are made in a reverberant enclosure. The resulting net time delay bias error cannot be corrected by pre-computational delay. Instead, the cross-spectrum must be computed using a block duration that is long compared to the propagation time through the longest significant path. From [5.50, 5.52], for a reverberant system, the block duration T must be longer than the reverberation time T_{rev} of the system, i.e., $T > T_{rev}$, where T_{rev} is the time required for the system response to a delta function to decay 60 dB. Data blocks of any desired duration, independent of frequency, can be achieved using zoom transforms discussed in Section 5.4.3,8.

5.6.1.8 Statistical Sampling Errors. Approximations for the normalized random error&r in cross-spectral density magnitude estimates and the standard deviation σ_r of the phase estimates are detailed in Figure 5.13 [5.4]. Note that the errors are functions only of the number of disjoint averages n_d and the coherence function $\gamma^2_{xy}(f)$ (see Section 5.6.2). As with autospectra estimates, if the data blocks being analyzed represented contiguous segments of the measured signal, the number of disjoint averages n_d would equal the number of analyzed data blocks N_b. However, when the analysis is performed using one of the commercial special purpose digital signal processing instruments or software programs operating in an overlapped processing mode, care must be exercised to properly count the number of disjoint averages, as discussed in Section 5.4.3.6.

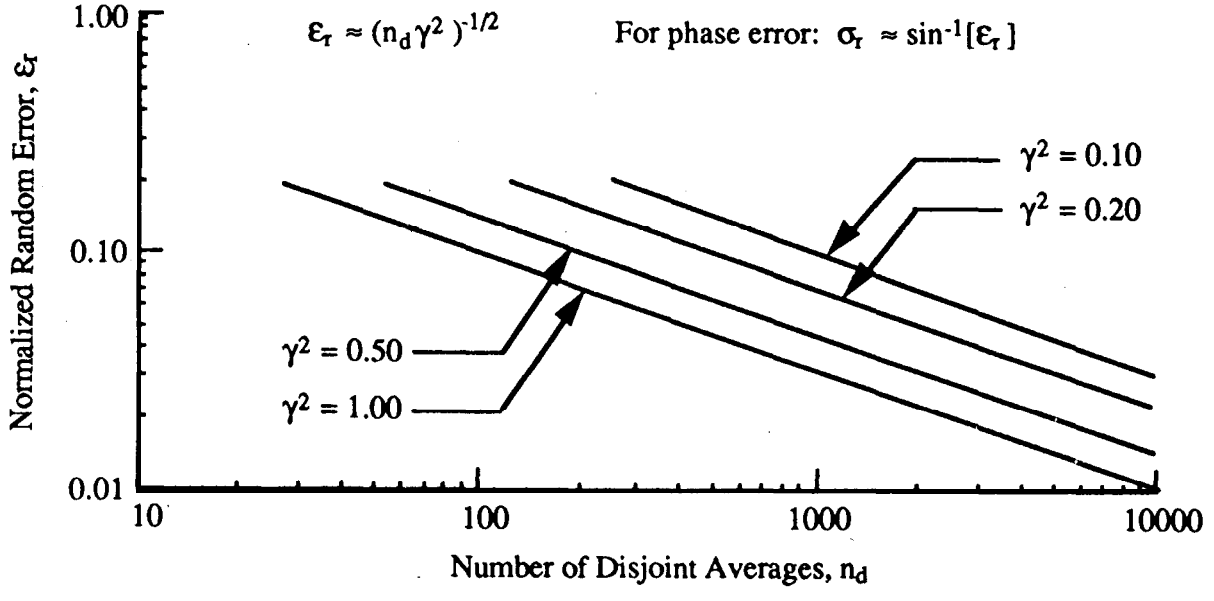

Figure 5.13. Normalized Random Error for Cross-Spectral Density Estimates.

5.6.1.9 Overlapped Processing. The requirements for overlapped processing are the same as discussed for autospectra in Section 5.4.3.7.

5.6.1.10 Zoom Transforms. The requirements for zoom transforms are the same as discussed for autospectra in Section 5.4,3.8.

5.6,1,11 Plotting. Like autospectra, it is recommended that cross-spectra magnitudes (or the co- and quad-spectra) be plotted as logarithmic spectral density magnitude versus logarithmic frequency. On the other hand, it is recommended that the cross-spectra phases be plotted as linear phase versus logarithmic frequency.

5,6.2 Coherence. It is often convenient to normalize the cross-spectral density magnitude to obtain a quantity called the coherence function (or sometimes coherency squared) given by

$$\gamma^2_{xy}(f) = \frac{|G_{xy}(f)|^2}{G_{xx}(f)\,G_{yy}(f)} \tag{5.24}$$

where $G_{xy}(f)$ is the cross-spectrum defined in Equation (5.23), and $G_{xx}(f)$ and $G_{yy}(f)$ are autospectra defined in Equation (5.13). The coherence function is bounded by $O \leq \gamma^2_{xy}(f) \leq 1$, and essentially identifies the degree of linear dependence (or correlation) between two measurements x(t) and y(t) as a function of frequency. Specifically, $\gamma^2_{xy}(f) = O$ means there is no linear relationship, and $\gamma^2_{xy}(f) = 1$ means there is a perfect linear relationship between x(t) and y(t) at frequency f. For values between zero and unity, the coherence can be interpreted as the fractional portion of $G_{yy}(f)$ that can be determined from a knowledge of G,X(f), or vice-versa, A plot of $\gamma^2_{xy}(f)$ is a dimensionless number versus frequency, and is called the coherence spectrum of x(t) and y(t).

5.6.2.1 Instruments and Software. Most of the commercial dual channel FIT-based digital signal processing instruments that compute cross-spectra will also compute coherence functions. The same is true of most commercial software packages designed to compute auto- and cross-spectra.

5.6.2.2 Anti-Aliasing Filters. The requirements for anti-aliasing filters are determined by the auto- and cross-spectra computations used to compute the coherence, as discussed in Section 3.7,3.

5.6.2,3 Leakage and Tapering. The requirements for tapering operations to suppress leakage are determined by the auto- and cross-spectra computations used to compute the coherence, as discussed in Section 5.4.3.3. It should be mentioned that the coherence function is very sensitive to leakage errors, as illustrated in [5.50].

5.6.2.4 **Frequency Resolution**. The frequency resolution requirements are determined by the auto- and cross-spectra used to compute the coherence, as discussed in Section 5.4.3.4. It should be mentioned that the coherence function is very sensitive to resolution bias errors, as illustrated in [5.50]. Further details concerning resolution bias errors are given in [5.26].

5,6.2.5 **Resolution Error Corrections**. Resolution bandwidth bias error corrections would be made in the auto- and cross-spectra used to compute the coherence, as discussed in Section 5.4.3.5.

5.6.2.6 **Time Delay Bias Errors**. Like cross-spectral density estimates, coherence estimates may involve a time delay bias error due to a physical propagation time between x(t) and y(t). The time delay bias error for coherence estimates is detailed in Figure 5.14. Note that the error for coherence estimates is the square of the error for cross-spectra estimates given in Figure 5.12. The procedure for suppressing the time delay bias error in coherence estimates is to use pre-computational delay, as discussed in Section 5.6.1.6.

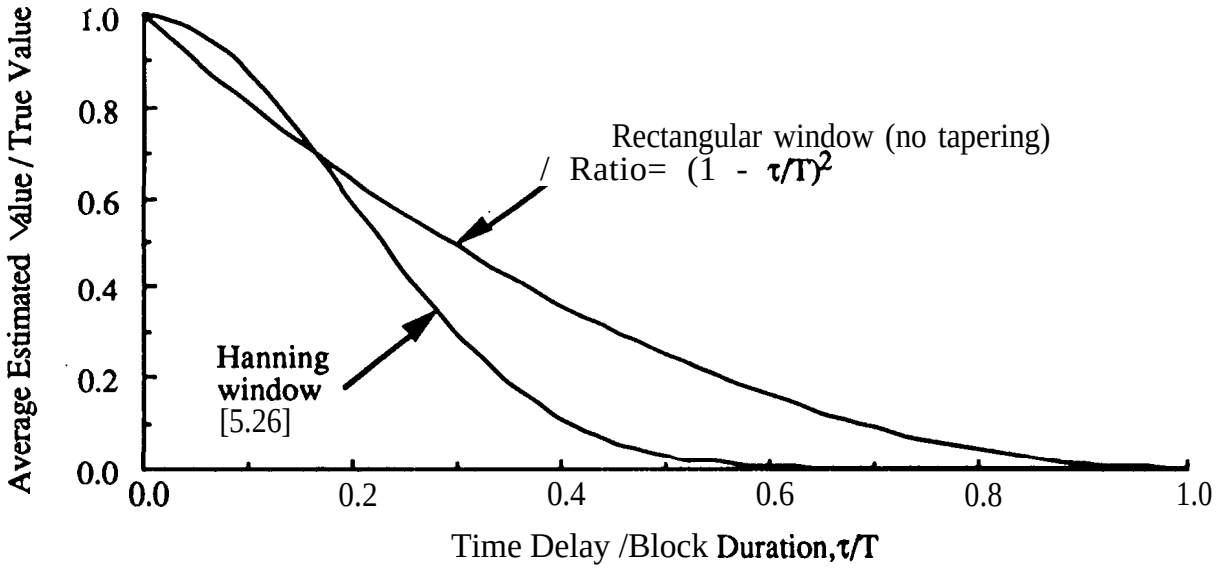

Figure 5.14. Time Delay Bias Error for Coherence Estimates.

5.6.2.7 **Multiple Path (Reverberation) Errors**. Coherence estimates may involve a multiple path time delay error, particularly for acoustic measurements in a reverberant environment, as discussed for cross-spectra estimates in Section 5.6.1.7. The procedure for suppressing this error in coherence estimates is the same as discussed in that section.

5,6.2.8 **Statistical Sampling Errors**. An approximation for the normalized random error in coherence estimates is detailed in Figure 5.15. Note that the random error is a function of the true co-

herence value $\gamma^2_{xy}(f)$ and the number of disjoint averages n_d in the computations of the auto- and cross-spectra used to compute the coherence, as discussed in Sections 5.4.3.6 and 5.6.1.8.

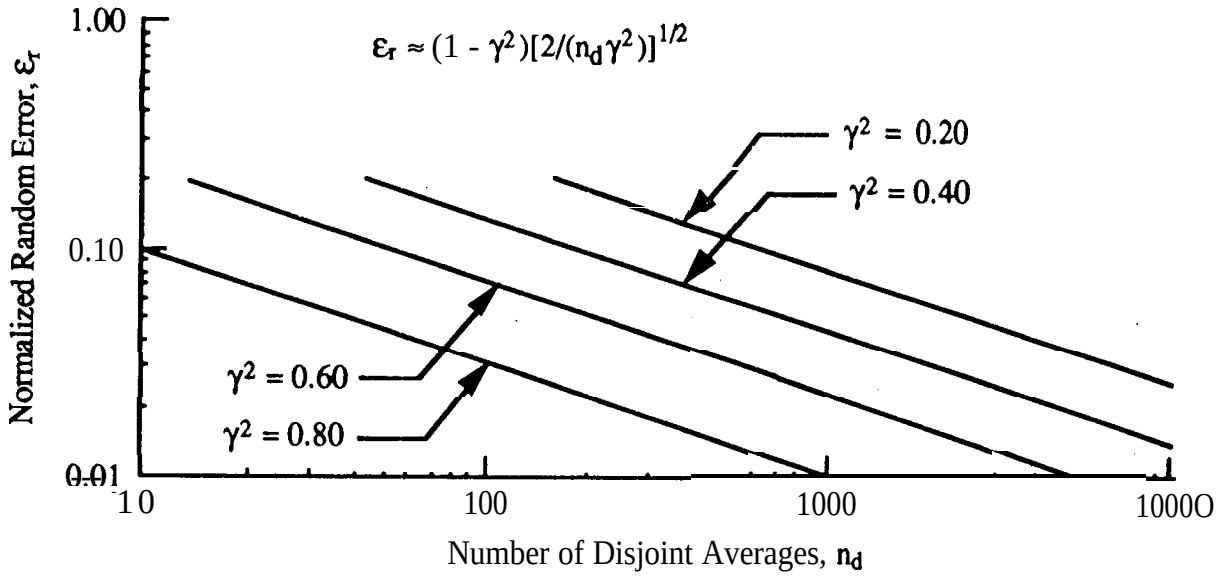

Figure 5.15. Normalized Random Error for Coherence Estimates.

5.6.2.9 Overlapped Processing. The requirements for overlapped processing are the same as discussed for autospectra in Section 5.4.3.7,

5.6.2.10 Zoom Transforms. The requirements for zoom transforms are the same as discussed for autospectra in Section 5.4.3.8.

5.6.2.11 Plotting. It is recommended that coherence estimates be plotted as linear coherence versus logarithmic frequency.

5.6.3 Frequency Response. A cress-spectrum is often computed as an intermediate step in the determination of a frequency response function given by

$$H_{xy}(f) = \frac{G_{xy}(f)}{G_{xx}(f)} \tag{5.25}$$

where $G_{xy}(f)$ is the cross-spectrum defined in Equation (5,23), and $G_{xx}(f)$ is the autospectrum defined in Equation (5.13). Noting that $G_{xy}(f) = C_{xy}(f) - jQ_{xy}(f)$, a complex quantity, the frequency response function can be written in terms of a magnitude and phase, as follows:

$$H_{xy}(f) = |H_{xy}(f)|\, e^{-j\phi_{xy}(f)} \tag{5.25a}$$

where

$$|H_{xy}(f)| = \frac{\sqrt{C_{xy}^2(f) + Q_{xy}^2(f)}}{G_{xx}(f)} \qquad \phi_{xy}(f) = \tan^{-1}\left[\frac{Q_{xy}(f)}{C_{xy}(f)}\right] \tag{5.25b}$$

The frequency response function of a system is the Fourier transform of the unit impulse response of the system (see Section 5.6.6), and essentially defines the linear gain $|H_{xy}(f)|$ and the phase shift $\phi_{xy}(f)$ between the system input and output signals x(t) and y(t) as a function of frequency. A plot of $H_{xy}(f)$ has the units of [y(t)/x(t)] (g/lb, in./psi, etc.) versus frequency in Hz, and is called a frequency response or FR plot. Frequency response functions are often called transfer functions, even though the "transfer function is a more detailed descriptor of the physical system given by the Laplace transform of the unit impulse response function [5.4]. Also, the phase factor is often defined as the negative of the value given by Equation (5.25 b).

5.6.3.1 Instruments and Software. Most of the commercial dual channel FIT-based digital signal processing instruments that compute cross-spectra will also compute frequency response functions. The same is true of most commercial software packages designed to compute auto- and cross-spectra.

5.6.3,2 Anti-Aliasing Filters. The requirements for anti-aliasing filters are determined by the signal auto- and cross-spectra used to compute the frequency response, as discussed in Section 3.7.3.

5.6.3,3 Leakage and Tapering. The requirements for tapering to suppress leakage errors are determined by the auto- and cross-spectra computations used to compute the frequency response, as discussed in Section 5.4.3.3.

5.6.3.4 Frequency Resolution. The frequency resolution requirements are determined by the auto- and cross-spectra computations used to compute the frequency response, as discussed in Section 5.4.3.4. It should be mentioned that the frequency response function is very sensitive to resolution bias errors, as illustrated in [5S0]. Further details concerning resolution bias errors in frequency response estimates are given in [5.26, 5.53].

5.6.3.5 Resolution Error Corrections. Resolution bandwidth bias error corrections would be made in the auto- and cross-spectra used to compute the frequency response, as discussed in Section 5.4.3.5.

5.6.3.6 Time Delay Bias Errors. Like cross-spectral estimates, frequency response estimates may involve a time delay bias error due to the physical propagation time between x(t) and y(t). The time delay bias error for frequency response estimates is the same as for cross-spectra estimates

shown in Figure 5.12. The procedure for suppressing the time delay bias error in frequency response estimates is to use pm-computational delay, as discussed in Section 5.6. 1.6.

5.6.3.7 Multiple Path (Reverberation) Errors. Frequency response estimates for multiple path systems may involve the same bias error problem discussed for cross-spectra estimates in Section 5.6,1,7. The procedure for suppressing this error in frequency response estimates is the same as discussed in that section.

5.6.3,8. Statistical Sampling Errors. Approximations for the norms.lizcxl random error ε_r in frequency response magnitude estimates and the standard deviation σ_r of the phase estimates are detailed in Figure 5.16 [5.4]. Note that the errors are functions of the true coherence value $\gamma^2_{xy}(f)$ and the number of disjoint averages n_d in the computations of the auto- and cross-spectra used to calculate the frequency response, as discussed in Sections 5.4.3.6 and 5.6.1.8.

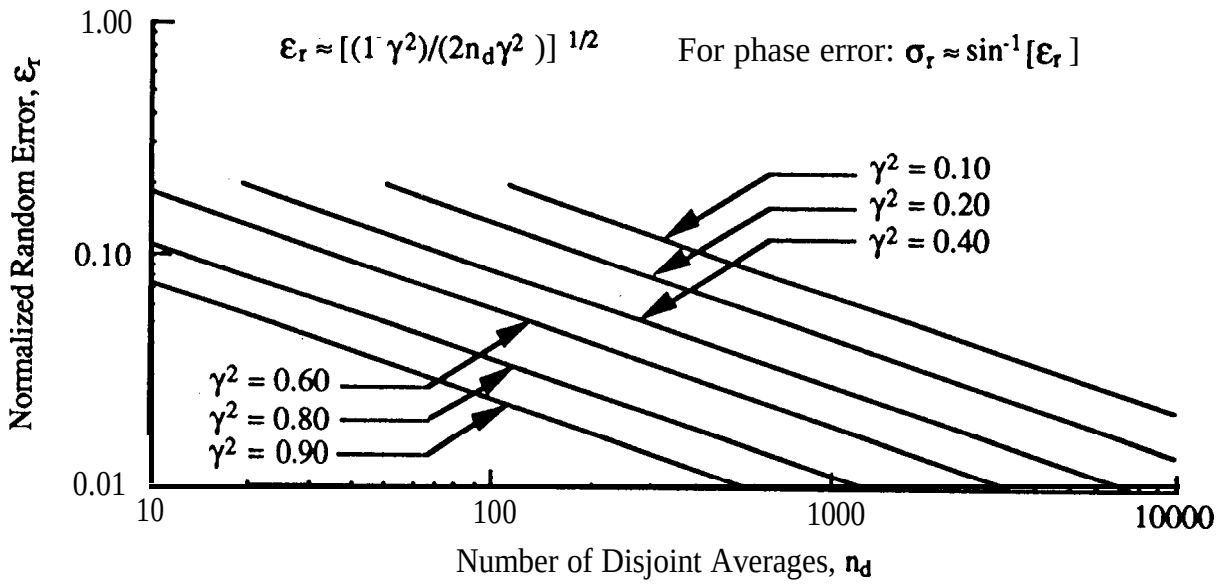

Figure 5,16. Normalized Random Error for Frequency Response Estimates.

5.6.3,9 Overlapped Processing. The requirements for overlapped processing are the same as discussed for autospectra in Section 5.4.3.7.

5.6.3.10 Zoom Transforms. The requirements for zoom transforms are the same as discussed for autospectra in Section 5.4.3.8.

5.6.3.11 Plotting. It is recommended that frequency response magnitude estimates be plotted as logarithmic magnitude versus logarithmic frequency, and that frequency response phase estimates be plotted as linear phase versus logarithmic frequency.

5.6.4 Cross-Correlation. Given two signal measurements x(t) and y(t), any linear relationship between these two measurements will be extracted in time domain terms by the cross-correlation function estimated by

$$\hat{R}_{xy}(\tau) = \frac{1}{T-\tau}\int_0^{T-\tau} x(t)y(t+\tau)dt \qquad (5.26a)$$

For digital computations,

$$\hat{R}_{xy}(m\Delta t) = \frac{1}{N-m}\sum_{n=0}^{N-m} x(n\Delta t)y([n+m]\Delta t) \;;\; m < N \qquad (5.26b)$$

where the hat (^) denotes "estimate of'. It can be shown [S.4] that the cross-correlation function is the inverse Fourier transform of the cross-spectral density function given by Equation (5.23) and, hence, contains no information that is not available from a cross-spectrum. However, the time domain character of the cross-correlation may sometimes present information in a more desirable format for engineering evaluations. This is particularly true of applications involving time delay estimates [5.4, 5.50]. Because of the computational efficiency of FFT algorithms, most modern software and special purpose signal processing instruments compute cross-correlation estimates by first computing a cross-spectrum and then inverse Fourier transforming the result. This approach involves a number of special operations and corrections to avoid circular effects in the results [5.4, 5.7,5.12- 5.14], but is very efficient on the computer. A plot of $R_{xy}(\tau)$ has the units of x(t)y(t) (g^2, g-psi, etc.) versus time delay in sec, and is called a correlation plot or correlogram.

5,6,4.1 Instruments and Software. Many of the commercial dual channel FIT-basal digital signal processing instruments that compute cross-spectra will also compute cross-correlation functions. The same is true of most commercial software packages designed to compute cross-spectra.

5.6.4.2 Anti-Aliasing Filters. The requirements for anti-aliasing falters are determined by the upper frequency limit desired for the cross-correlation estimate, just as for auto- and cross-spectra calculations, as discussed in Section 3.7.3.

5.6.4.3 Leakage and Tapering. There are no leakage errors in cross-correlation estimates, even when they are computed through the cross-spectrum. Furthermore, tapering operations will distort the cross-correlation and, hence, should never be used.

5.6.4.4 Time Resolution. The time resolution of a cross-correlation estimate is fixed by At, the sampling interval for the data.

5,6.4,5 **Time Delay Bias Errors**. Like cross-spectra estimates, cross-correlation estimates may involve a time delay bias error due to the physical propagation time between x(t) and y(t). The time delay bias error for cross-correlation estimates is the same as for cross-spectra estimates shown in Figure 5.12. The procedure for suppressing the time delay bias error in cross-correlation estimates is to use **pre-computational** delay, as discussed in Section 5.6.1.6.

5.6.4.6 **Statistical Sampling Errors**. An approximation for the normalized random **error** in **cross-**correlation estimates is detailed in Figure 5.17. Note that the random error is a function of the correlation coefficient value (see Section 5.6.5), the number of data values per block N, and the number of disjoint averages n_d (for those cases where the cross-correlation is computed from a **cross-**spectrum computation).

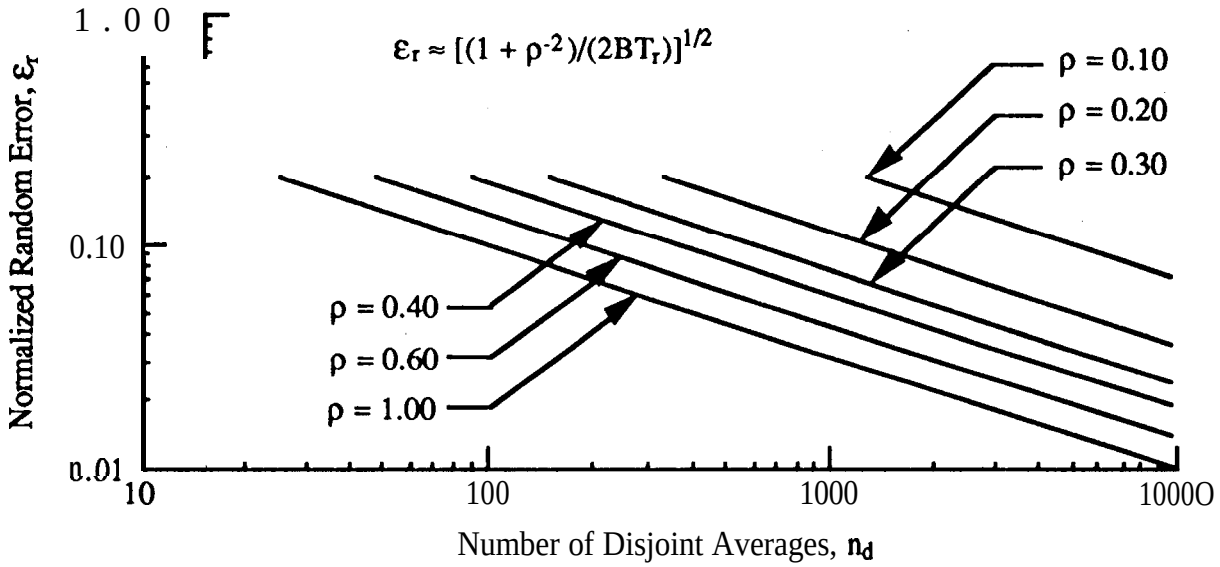

Figure 5.17. **Normalized** Random Error for Cross-Correlation Estimates.

5.6.4.7 **Overlapped Processing**. When computed from a cross-spectrum estimate, no overlapping of data blocks should be used.

5.6.4.8 **Plotting.** It is recommended that cross-correlation estimates be plotted as linear correlation versus linear time delay.

5.6.5 **Correlation Coefficient**. For some applications, it is more convenient to estimate a normalized cress-correlation function, called the correlation coefficient function, given by

$$\rho_{xy}(\tau) = \frac{R_{xy}(\tau)}{\sigma_x \sigma_y} \tag{5.27}$$

where σ_x and σ_y are the standard deviations of x(t) and y(t), respectively, as defined in Equation (5.3). The quantity $\rho^2_{xy}(\tau)$ is bounded by zero and unity, and defines the fraction of the variance of y(t) that is linearly related to x(t), i.e., $\rho^2_{xy}(\tau) = 0$ means there is no linear relationship, and $\rho^2_{xy}(\tau) = 1$ means there is a perfect linear relationship between x(t) and y(t) at the time delay τ. The correlation coefficient function is the time domain analogy to the coherence function in the frequency domain. The various considerations concerning the computation of the correlation coefficient function are the same as discussed for the cross-correlation function in Section 5.6.4.

5.6.6 Unit Impulse Response. The unit impulse response of a physical system, denoted by $h_{xy}(\tau)$, is defined as the response of the system to a delta function input, i.e., y(t) when $x(t) = \delta(t)$. It is the inverse Fourier transform of the frequency response function given by Equation (5.25). Noting from Equation (5.25) that the frequency response function is simply the cross-spectrum divided by the autospectrum, it follows that the unit impulse response function can be interpreted as a cross-correlation function between the signals x(t) and y(t) when the autospectrum of x(t) is unity at all frequencies, i.e., $G_{xx}(f) = 1$. Modem software and special purpose signal processing instruments compute the unit impulse response function exactly as they compute the cross-correlation function in Section 5.6.4, except the cross-spectrum is divided by the autospectrum before the inverse transform is computed. The various considerations concerning the computation of the unit impulse response function are the same as discussed for the cross-correlation function in Section 5.6.4.

5.7 Other Analyses. Sections 5.2 through 5.6 of this document cover the most common data analysis procedures applied to measured dynamic signals. There are many other data analysis procedures that might be required on occasions for specialized applications. Also, there are other techniques for computing the spectral characteristics of measured signals that may sometimes be warranted by special circumstances.

5.7.1 Probability Density. Given a stationary random signal x(t), the signal value at any instant can be described only in probability terms using a probability density function. Such descriptions of signal magnitudes are often of interest in reliability y and failure prediction applications involving extreme values [5.54], as well as for data validation purposes (see Section 4.5.1). There are two categories of probability density functions that may be of interest: (a) those related to the instantaneous values of the signal, and (b) those related to the peak values of the signal.

5.7.1.1 Instantaneous Probability Density. Given a stationary random signal x(t); $0 \le t \le T$, the instantaneous probability density function is estimated by

$$\hat{p}(x) = \frac{T_x}{T\Delta x}; \quad x_{min} \le x < x_{max} \tag{5.28a}$$

where T is the total duration of the measured signal, T_x is the time spent by the signal inside a narrow magnitude interval Ax centered on the magnitude value x, and the hat (A) denotes "estimate of'. For digital computations where x(t) = $x(n\Delta t)$; n = 1, 2, 3, ,.., N,

$$\hat{p}(i\Delta x) = \frac{N_x}{N\Delta x} \; ; \; x_{min} \leq i\Delta x < x_{max} \tag{5.28b}$$

where N is the total number of data values in the measured signal, N_x is the number of data values that fall inside the magnitude interval Ax centered on the magnitude value iAx, and i is an integer. The detailed digital procedure for estimating instantaneous probability density functions is presented in [5.4]. To obtain accurate estimates at large positive and negative values of x(t), very long measurement durations are required.

The estimation of instantaneous probability density functions will involve both a magnitude resolution bias error due to the finite amplitude interval Ax, and a statistical sampling (random) error due to the finite measurement duration T (or block size N), as detailed in [5.4]. To minimize these errors, it is recommended that digital computations of instantaneous probability density functions be performed using the parameters Ax$\leq 0.1\sigma_x$ and N 210,000, where σ_x is the standard deviation of the measured signal.

The use of the instantaneous probability density function for data evaluation purposes is addressed in Sections 4.5.1 and 4.7.2. Tests for normality of random data are discussed in Section 5.3.3.1. The role of probability density functions in extreme value predictions is outlined in [5.54], and applications to nonlinear signal analysis problems are detailed in [5.9, 5.50]. A plot of p(x) has the units of (I/x) versus magnitude x, It is recommended that probability density estimates be plotted either as linear or logarithmic probability density versus linear magnitude. A simple algorithm for the computation of probability density functions is given in [5.4].

5.7.1.2 <u>Peak Probability Density</u>. Again given a stationary random signal x(t); O $\leq$ t $\leq$ T, the peak probability density function is estimated by

$$\hat{p}_p(x) = \frac{N_{p_x}}{N_p \Delta x} \tag{5.29}$$

where N_p is the total number of peaks in the measured signal, N_{p_x} is the number of peaks inside a narrow magnitude interval Ax centered on the magnitude value x, and the hat (A) denotes "estimate of'. It follows that the estimation of a peak probability density function reduces to a peak counting problem, where the definition of a peak is critical. When estimated by digital procedures, the easiest way to define a peak is by any data value X_p that falls in an interval Ax centered on x, which is immediately preceded and followed by data values of x $\leq x_p$ - nAx; n = 1, 2, ... For those cases where the signal is not symmetric about the mean value, it may be desirable to estimate the proba-

bility density function for notches (downward peaks) as well, in which case a notch is defined as any data value x_{-p} that falls in an interval Ax centered on x, which is immediately preceded and followed by data values of $x \geq x_{-p} + nAx$; n = 1, 2, ...

The estimation of peak probability density functions will involve both a magnitude resolution bias error due to the finite amplitude interval Ax, and a statistical sampling (random) error due to the finite measurement duration T (or block size N), which in turn is a function of the autospectrum of the signal. To control these errors, it is recommended that digital computations of peak probability density functions be performed using the parameters $Ax \leq 0.1\ \sigma_x$ and $N_p \geq 1O(K)$, where a peak value x_p is defined as any value or series of values in the signal that are preceded and followed by a value $x \leq (x_p - Ax)$, and σ_x is the standard deviation of the measured signal. A plot of $p_p(x)$ has the units of (l/x) versus magnitude x, It is recommended that peak probability density estimates be plotted as either linear or logarithmic probability density versus linear magnitude.

The peak probability density function for a stationary random signal with a normal (or Gaussian) instantaneous probability density function is determined solely by the autospectrum of the signal [5.55]. For this case, assuming $\mu_x = O$,

$$p_p(x) = \frac{\sqrt{1-\alpha}}{\sqrt{2\pi}\,\sigma_x} \exp\left[\frac{-x^2}{2(1-\alpha)\sigma_x^2}\right] + \frac{x\sqrt{\alpha}}{2\sigma_x^2}\left\{1 + \operatorname{erf}\left[\frac{x\sqrt{\alpha}}{\sqrt{2(1-\alpha)}\,\sigma_x}\right]\right\} \exp\left[\frac{-x^2}{2\sigma_x^2}\right] \tag{5.30a}$$

where

$$\alpha = \frac{\left[\int f^2 G_{xx}(f)\,df\right]^2}{\sigma_x^2 \int f^4 G_{xx}(f)\,df} \cdot \left[\frac{\text{number of upward zero crossings/sec}}{\text{number of maxima/sec}}\right]^2 \tag{5.30b}$$

In the above equations, σ_x and $G_{xx}(f)$ are the standard deviation and autospectrum, respectively, of the signal x(t), and erf[ ] is the error function of [ ]. The peak probability density functions of Gaussian data for various values of *a are* shown in Figure 5.18. Whenever a stationary random signal can be assumed to have a normal instantaneous probability density function defined in Equation (5.9), it is recommended that the peak probability density function be estimated from Equation (5.30) using an estimate of the autospectrum (see Section 5,4.3).

Peak probability density functions have been widely applied to problems involving the prediction of fatigue damage in structures subjected to random vibration [5.54]. In recent years, however, other procedures [5.56, 5.57] have largely replaced the use of peak probability density functions for low cycle fatigue predictions.

5.7.2 <u>Parametri Spectral Analysis Procedures</u>. Sections 5.3 through 5.5 of this document cover only conventional spectral analysis procedures which involve DFTs that inherently produce spectral estimates with a minimum frequency resolution of Af = 1/T, where T is the duration of the data

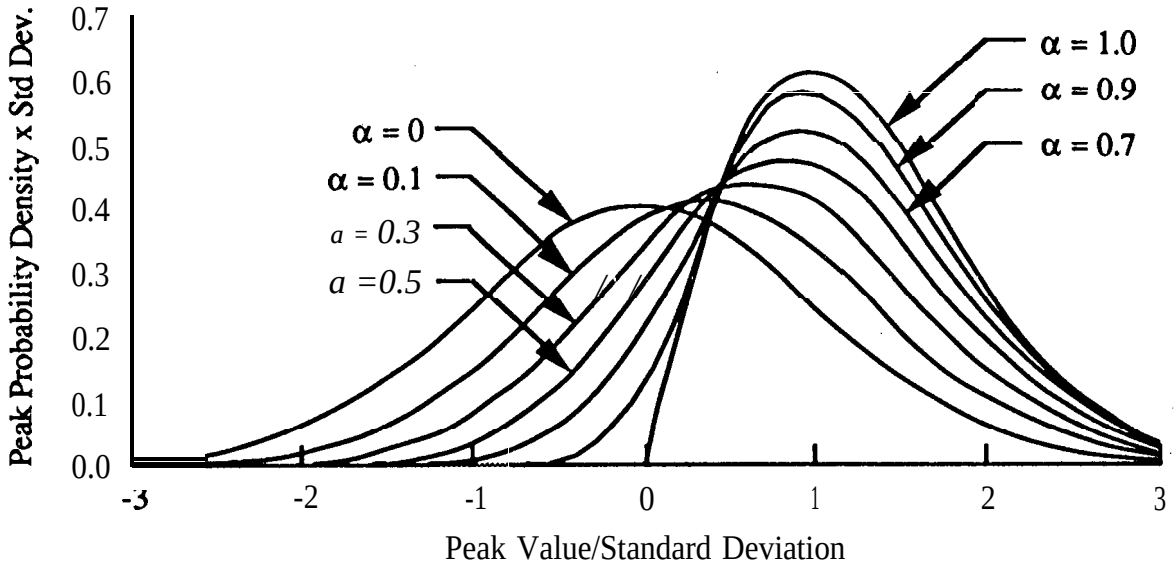

Figure 5.18. Probability Density Functions of Peak Values in Gaussian Random Signals versus Spectral Parameter α.

block. There may be situations where it is difficult or impossible to acquire a sufficiently long measurement to ensure the resolution needed for a proper analysis. In such cases, spectral estimation techniques based on modeling procedures (often referred to as parametric or modern spectral estimation techniques) might be employed. Included here are moving average (MA) procedures leading to "maximum entropy" spectral analysis, autoregressive (AR) procedures leading to "maximum likelihood" spectral analysis, and autoregressive moving average (ARMA) procedures. See [5.58 - 5,61] for details. Although these procedures are not recommended for general data analysis, nothing in this document should be interpreted to rule out the use of such techniques when warranted by limited measurement durations.

5,7.3 Miscellaneous Signal Processing Procedures. Other signal processing procedures that may sometimes be required include the computation of the following functions:

(a) Conditioned spectral density functions, including multiple and partial coherence functions, for correlated source studies [5.4, 5,50].

(b) Coherent output power functions for source identification studies [5.4, 5.50].

(c) Hilbert transforms for the generation of envelope functions and causality studies [5.4, 5.7].

(d) Peak value counting functions, such as "rain flow" counts, for structural fatigue studies [5,56, 5.57].

(e) Higher order moments, such as the third (skewness) moment and the fourth (kurtosis) moment, for nonlinear response analysis [5.9] and other data evaluations [5,62].

(f) Quadratic, cubic, and hyper-coherence functions for nonlinear signal studies [5.9, 5.50,5.63 - 5.65].

(g) Higher order spectral density functions (bispectra and trispectra) for the analysis of non-Gaussian signals in Gaussian random noise [5.63, 5.66, 5.67].

(h) Generalized and instantaneous spectral density functions for the analysis of nonstationary random signals [5.4 and Appendix B].

In these cases, the required data analysis techniques are too closely associated with the specific requirements of the application to permit the formulation of standard procedures. See the noted references for guidance.

5.8 References.

5.1 Doebelin, E. O., *Measurement Systems Application and Design, 4th cd.,* McGraw-Hill, NY, 1990.

5.2 Beauchamp, K. G., and Yuen, C. K., *Data Acquisition For Signal Analysis,* George Allen & Unwin, London, 1980.

5.3 Bendat, J. S., and PierSol, A, G., *Measurement and Analysis of Random Data,* Wiley, NY, 1966.

5.4 Bendat, J. S., and Piersol, A. *G., Random Data: Analysis and Measurement Procedures,* 2nd cd., Wiley, NY, 1986.

5.5 Sun, M., et al, "An Analysis of the Effects of Jitter in Data Acquisition on Synchronous Averaging", *IEEE Trans. Systems, Man, and Cybernetics,* Vol. 21, No. 2, pp. 456-463, Mar. /Apr. , 1991.

5.6 Hamming, R. W., *Digital Filters,* 2nd cd., Prentice-Hall, Englewood Cliffs, NJ, 1983.

5.7 Otnes, R. K., and Enochson, L., *Applied Time Series Analysis,* Wiley, NY, 1978.

5.8 Barnoski, R. L., and Maurer, J. R., , T. K., "Mean-Square Response of Simple Mechanical Systems to Nonstationary Random Excitation", *J. Appl. Mech.*, Vol. 36, No. 2, pp. 221-227, June 1969.

5.9 Bendat, J. S., *Nonlinear System Analysis from Random Data,* Wiley, NY, 1990.

5.10 Ross, S. M., *Introduction to Probability and Statistics for Engineers and Scientists,* Wiley, NY, 1987.

5.11 Cooley, J. W., and Tukey, J. W., "An Algorithm for the Machine Calculation of Complex Fourier Series", *Mathematics of Computation,* Vol. 19, p. 297, Apr. 1965.

5.12 Oppenheim, A.' V., and Schafer, R. W., *Discrete-Time Signal Processing,* Prentice-Hall, Englewood Cliffs, NJ, 1989.

5.13 Brigham, E. O., *The Fast Fourier Transform and Its Applications,* Prentice-Hall, Englewood Cliffs, NJ, 1988,

5.14 DeFatta, D. J., Lucas, J. G., and Hodgkiss, W. S., *Digital Signal Processing,* Wiley, NY, 1988.

5.15 Broth, J. T., Principles of Experimental Frequency Analysis, Elsevier, NY, 1990.

5.16 Harris, F, J., "On the Use of Windows for Harmonic Analysis with the Discrete Fourier Transform", *Proc., IEEE,* Vol. 66, pp. 51-83, Jan. 1978.

5.17 Nuttall, A. H., "Some Windows with Very Good Sidelobe Behavior", *IEEE Trans., Acoustics, Speech, and Signal Processing,* Vol. ASSP-29, No. 1, pp. 84-91, Feb. 1981.

5.18 Anon, *Programs for Digital Signal Processing,* IEEE Press, (distribution Wiley, NY, 1979).

5.19 Chen, C. H., *Signal Processing Handbook, Marcel* Dekker, New York, 1988.

5,20 Stearns, S. D., and David, R. A., *Signal Processing Algorithms,* Prentice-Hall, NJ, 1988,

5.21 Stearns, S. D., and Hush, D. R., *Digital Signal Analysis,* 2nd ed., Prentice-Hall, Englewood Cliffs, NJ, 1990.

5.22 Anon, "Key Parameters-Currently Used Windows", DSP-03 12, Spectral Dynamics, San Diego, CA, Feb. 1989.

5.23 Thompson, J. K., and Tree, D. R., "Leakage Error in Fast Fourier Analysis", *J. Sound* and *Vibration,* Vol. 71, No. 4, pp. 531-544, 1980.

5.24 Randall, R. B., *Frequency* Analysis, 3rd ed., Bruel & Kjaer, Naerum, Denmark, 1987.

5.25 PierSol, A. G., Wilby, E. G., and Wilby, J. F., "Evaluation of Aero Commander Propeller Acoustic Data", *NASA CR-158919,* May 1978.

5.26 Schmidt, H., "Resolution Bias Errors in Spectral Density, Frequency Response and Coherence Function Measurements", *J. Sound and Vibration,* Vol. 101, No. 3, pp. 347-427, 1985.

5.27 Forlifier, W. R., "The Effects of Filter Bandwidth in Spectrum Analysis of Random Vibration", *Shock* and *Vibration Bull.,* No. *33,* Pt *2,* pp. 273-278, Feb. 1964.

5.28 Piersol, A. G., "Optimum Resolution Bandwidth for Spectral Analysis of Stationary Random Vibration Data", *J. Shock and Vibration,* Vol. 1, No. 1, pp. 33-43, 1993/1994.

5.29 Scharton, T. D., Boatman, D. J., and Kern, D, L., "Dual Control Vibration Testing", *Proc., 60th Shock and Vibration Symp.,* Vol. IV, pp. 199-217, Virginia Beach, VA, Nov. 1989.

5.30 Welch, P. D., "The Use of Fast Fourier Transform for the Estimation of Power Spectra: A Method Based on Time Averaging Over Short, Modified Periodograms", *IEEE Trans. Audio and Electroacoustics,* Vol. AU-15, No. 2, pp. 70-73, June 1967.

5.31 Nuttall, A. H., "Spectral Estimation By Means of Overlapped Fast Fourier Transformed Processing of Windowed Data", *Naval Underwater Systems Center TR-4169, New* London, CT, Oct. 1971.

5.32 Randall, R. B., "Vibration Measurement Equipment and Signal Analysis", Ch. 13, *Shock and Vibration Handbook,* 3rd ed. (Ed: C. M. Harris), McGraw-Hill, NY, 1988.

5.33 Keegan, W. B., et al, "Payload Bay Acoustic and Vibration Data from STS-1 Flight", *NASA/GSFC DATE Report 002,* June 1981,

5.34 Anon, "American National Standard, Specification for Octave-Band and Fractional-Octave-Band Analog and Digital Filters", *ANSI Std S1.11-1986.*

5.35 Wilby, J. F., and PierSol, A. G., "Analytical Predictions of Aerospace Vehicle Vibration Environments", *ASME Paper 81-DET-29*, Sep. 1981.

5.36 Barnoski, R. L., et al, "Summary of Random Vibration predictions procedures", NASA CR-1302, 1969.

5.37 Himelblau, H., Fuller, C. M., and Scharton, T. D., "Assessments of Space Vehicle Aero-acoustic-Induced Vibration Prediction, Design, and Testing",*NASA CR-IS%,* July 1970.

5.38 Kelly, R. D., and Richman, G., *Principles and Techniques of Shock Data Analysis,* SVh4-5, Shock and Vibration Information Analysis Center, Arlington, VA, 1969.

5.39 Rubin, S., "Concepts in Shock Data Analysis", Ch. 23, *Shock and Vibration Handbook,* 3rd ed. (Ed: C. M. Harris), McGraw-Hill, NY, 1988.

5.40 Jacobsen, L. S., and Ayre, R. S., *Engineering Vibrations,* McGraw-Hill, NY, 1958.

5.41 Anon, "Combining Modal Responses and Spatial Components in Seismic Response Analysis", *Nuclear Regulatory Guide 1.92,* Rev. 1, Feb. 1976.

5.42 Wilson, E. L., DerKiureghian, A., and Bayo, E. P., "A Replacement for the SRSS Method in Seismic Analysis", *Earthquake Engineering aria' Structural Dynamics*, Vol. 9, pp. 187-194, 1981.

5.43 Smallwood, D. O., "An Improved Recursive Formula for Calculating Shock Response Spectra", *Shock and Vibration Bull., No. 56, Pt 1,* pp. 279-287, 1986.

5.44 Nelson, D. B., "Effect of Filter Frequency Response on Pyroshock Data Analysis", *Proc., Spacecraft Dynamic Environment TIM,* Vol. 2, pp. 255-283, The Aerospace Corp., El Segundo, CA, June 1990.

5.45 Smith, S., and Hollowell, W., "Techniques for the Normalization of Shock Data", *Proc.,* 62nd *Shock and Vibration Symp.*, Vol. II, pp. 403-411, Get. 1991.

5.46 Wise, J. H., "The Effects of Digitizing Rate and Phase Distortion Errors on the Shock Response Spectrum", *Proc., Inst. Envir. Se.,* pp. 36-43, Apr. 1983.

5.47 Ellis, T. M., and McLain, D. H., "Algorithm 514., A New Method of Cubic Curve Fitting Using Local Data [E2]", *Trans. Mathematical Software*, Vol. 3, No. 2, pp. 175-178, June 1977.

5.48 Gaberson, H. A., and Chalmers, R, H., "Modal Velocity as a Criterion of Shock Severity", *Shock and Vibration Bull., No. 40,* Pt *2,* pp. 31-49, Dec. 1%9.

5.49 Ungar, E. E., "Damping of Panels", Ch. 14, *Noise and Vibration Control* (Ed: L. L. Beranek), McGraw-Hill, NY, 1971.

550 Bendat, J. S., and Piersol, A. G., *Engineering Application of Correlation and Spectral Analysis,* 2nd cd., Wiley, NY, 1993.

5.51 Trethewey, M. W., and Evensen, H. A., "Time-Delay Bias Errors in Estimating Frequency Response and Coherence Functions From Windowed Samples of Continuous and Transient Signals", *J. Sound and Vibration,* Vol. 97, No. 4, pp. 531-540, 1984.

5.52 Verhulst, K., and Verheij, J. W., "Coherence Measurements in Multi-Delay Systems", J. Sound *and Vibration,* Vol. 62, No. 3, pp. 460-463, 1979.

5.53 Walker, A. W., "The Effect of Bandwidth on the Accuracy of Transfer Function Measurements of a Single Degree of Freedom System Response to Random Excitation", *J. Sound and Vibration,* Vol. 74, No. 2, pp. 251-263, 1981.

5.54 Crandall, S. H., and Mark, W. D., *Random Vibration in Mechanical Systems,* Academic Press, NY, 1963.

5,55 Rice, S. O., "Mathematical Analysis of Random Noise", *Selected Papers on Noise and Stochastic Processes (Ed: N.* Wax), Dover, Mineola, NY, 1954.

5,56 Dowling, N. E., "Fatigue Failure Predictions for Complicated Stress-Strain Histories", *J. Materials,* Vol. 7, No. 1, pp. V-1 to V-17, 1972.

5.57 Rice, R. C., *Fatigue Design Handbook,* 2nd cd., Sot. Auto. Engrs, Warrendale, PA, 1988.

5.58 Childers, D. G., *Modern Spectral Analysis,* IEEE Press, NY, 1978.

5.59 Robinson, E. A., and Treitel, S., *Geophysical Signal Analysis,* Prentice-Hall, Englewood Cliffs, NJ, 1980.

5,60 Marple, L. S., *Digital Spectral Analysis with Applications,* Prentice-Hall, Englewood Cliffs, NJ, 1987.

5.61 Kay, S, M., *Modern Spectral Estimation: Theory and Application,* Prentice-Hall, Englewood Cliffs, NJ, 1988.

5.62 Connon, W. H. III, "Comments on Kurtosis of Military Vehicle Vibration Data", *Proc., Inst. Envir. Se.,* pp. 440-442, May 1991.

5.63 Bendat, J. S., and Piersol, A. G., "Spectral Analysis of Non-Linear Systems Involving Square-Law Operations", *J.Sound and Vibration,* Vol. 81, No. 2, pp. 199-213, 1982.

5.64 Bendat, J. S., and Piersol, A. G., "Decomposition of Wave Forces into Linear and Non-linear Components", *J. Sound and Vibration,* Vol. 106, No. 3, pp. 391-408, 1986.

5.65 Jong, J.-Y., Coffin, T., and Jones, J. H., "A Non-Linear Hyper-Coherence Filter for Damage Assessment in Noisy Environments", Model Determination for Large Space Systems Workshop (Ed: J.-C. Chen), *JPL Dec. D-5576,* Vol. 3, pp. 1129-1142, Mar. 1988.

5.66 Nikias, C. L., and Raghuveer, M. R., "Bispectrum Estimation: A Digital Signal Processing. Framework", *Proc., IEEE,* Vol. 75, No. 7, pp. 869-891, July 1987.

5.67. Mendel, J. M., "Tutorial on Higher-Order Statistics (Spectra) in Signal processing and System Theory: Theoretical Results and Some Applications", *Proc., IEEE,* Vol. 79, No. *3, pp.* 278-305, Mar. 1991.

THIS PAGE IS INTENTIONALLY LEFT BLANK

APPENDIX A
PYROSHOCK DATA ACQUISITION AND ANALYSIS

A.1 Introduction. The term pyroshock (or pyrotechnic shock) generally refers to the severe mechanical transients caused by the detonation of an ordnance device on a structure. Such devices, including flexible linear shaped charges (El-SC), explosive nuts, pin pullers, and cable cutters, are widely used to accomplish the in-flight separation of structural elements on aerospace vehicles [Al], "and are a significant cause of flight failures [A.2]. It follows that the measurement of pyroshocks for the purpose of developing equipment design and test criteria is of major importance in the aerospace industry, as well as in other applications where pyrotechnic devices are used.

Pyroshocks are commonly measured using accelerometer because of their small size and weight, and wide frequency range capabilities. A typical pyroshock time history signal measured with an accelerometer is shown in Figure A. 1. However, the basic characteristics of the pyroshock phenomenon often exceed the capabilities of commercially available accelerometers. Specifically, pyroshocks are similar to the ballistic shocks caused by the impact of non-penetrating projectiles on a hard structure [A.3] in that they produce a near-instantaneous velocity change of the structure at the moment of impact, corresponding to art acceleration response that approaches a delta function. The result is the generation of intense stress waves with rapid rise times (on the order of 10 μsec [A.4]) that travel throughout the structure with various modes of propagation [A.5]. Discontinuities in the structural propagation path (in particular, bolted or riveted joints and structural boundaries) tend to reflect, attenuate, and/or scatter the propagating waves, causing a rapid Auction in the structural response accelerations with increasing distance from the source. Also, the dispersive character of some of the propagating waves, particularly the bending waves at the higher frequencies, causes them to spread in time with increasing distance from the source, reducing the sharpness of the wave front. On the other hand, if the measurement is made close to the source, the

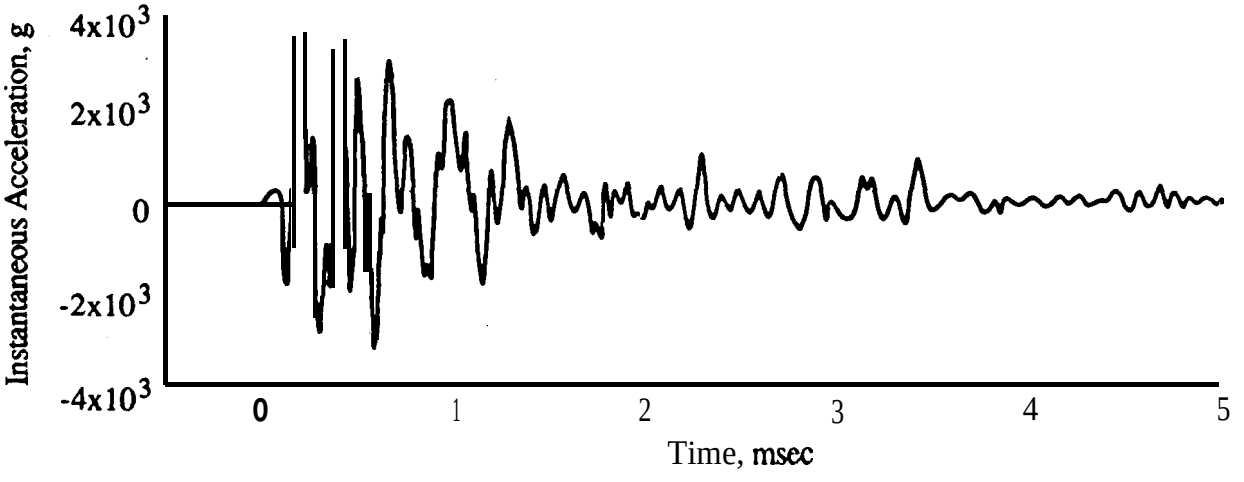

Figure A. 1. Typical Pyroshock Acceleration Signal Measured with 20kHz Bandwidth.

initial acceleration pulse associated with the near-instantaneous velocity change of the structure (called the "pm-pulse" in [A.6] and the "pre-shock" in [A.7]) often excites the natural frequencies of the accelerometer and/or overloads its sensing element. Although difficult to detect with an accelerometer, this near-field pulse can be identified with a velocity transducer, as illustrated in Figure A.2, which is taken from [A.7]. This figure shows the velocity response of a one-half inch thick steel plate measured by a laser vibrometer (which directly measures velocity) with the target directly over a line of primer cord (25 grains/ft) detonated on the opposite side of the plate. The measured initial velocity change is about 5.6 m/s (220 in./sec) in 3 μsec, which corresponds to an acceleration of almost 200,000 g.

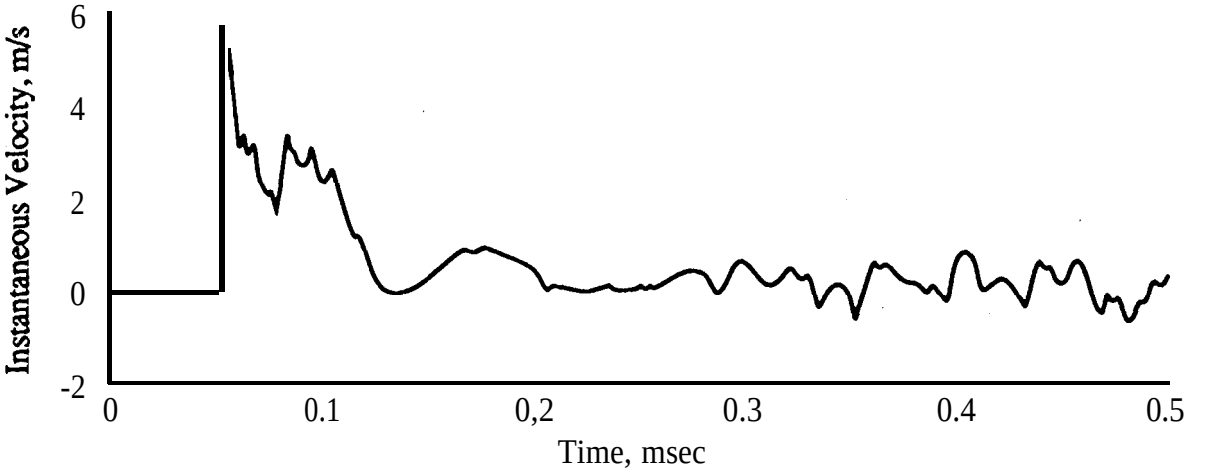

Figure A.2. Near-Field Pyroshock Velocity Signal Measured with 1 MHz Sampling Rate [A.7].

The purpose of this appendix is to clarify the basic problems related to the measurement of pyroshocks using accelerometers, and to recommend procedures to suppress these problems and evaluate the quality of the resulting acceleration signals. A summary of the major data acquisition and analysis problems is presented in Section A.2, and specific guidelines and recommendations are detailed in Section A.3. Alternate pyroshock measurement procedures are briefly outlined in Section A.4. Many examples of actual pyroshock data are presented in these sections to illustrate various measurement problems. It should be mentioned that the pyroshock signals shown in these examples were digitally converted from hard copies of actual data, and replotted using a computer graphics program. This process somewhat suppressed the higher frequency content of the time history signals shown in the examples.

A.2 Summary of Data Acquisition and Analysis Problems. The basic instrumentation needed to acquire and analyze pyroshock data consists of (a) a transducer, (b) a signal conditioner, (c) sometimes an analog tape recorder, (d) an analog lowpass anti-aliasing filter, (e) an analog-to-digital converter (ADC), (f) a digital storage device, and (g) a signal processing instrument or computer

with appropriate analysis software. Background discussions of these data acquisition and analysis system instruments and procedures are presented Sections 3 and 5.5.3.

A.2. 1 Transducers. Most pyroshock measurements are made using either piezoelectric or piezoresistive type accelerometers (see [A.8] and Section 3.2.6.1) with special features to enhance their ability to measure mechanical shocks, specifically, a higher than usual sensing element resonance frequency (often in excess of 100 kHz) and a high maximum acceleration limit (up to 200,000 g). Nevertheless, the capabilities of the accelerometer are often exceeded in pyroshock measurements made near the source of excitation.

A.2.1.1 Accelerometer Resonances. Whether piezoelectric or piezoresistive, accelerometers used for pyroshock measurements have sensing elements that are very lightly damped, i.e., the damping ratio is generally ζ <0.005. To restrict the accelerometer output to no more than 5% above its nominal sensitivity, the upper frequency limit of the accelerometer should be no more than about 20% of the resonance frequency of the sensing element (see Section 3.2.3.2). Above this frequency limit, the accelerometer output will be increasingly exaggerated with increasing frequency. Worse yet, if there is significant excitation in the frequency range of the sensing element resonance, the element will "ring" causing a strong output signal at its resonance frequency, which may be much higher than the true acceleration input over all frequencies. The resonance frequencies of the accelerometer case will cause the same effect, Resonances of the accelerometer to excitations along transverse axes may also occur, causing additional problems.

Unfortunately, due to the impulsive character of pyroshocks, the spectrum of the structural response near shock sources often extends to extremely high frequencies (the theoretical spectrum of a true impulse or delta function covers an infinite frequency range [A.9]). Hence, it is common for pyroshock measurements to be contaminated by transducer resonances. This is illustrated in Figure A.3, which shows the acceleration signal measured by a commercial accelerometer (designed for shock measurements) during a typical pyroshock test [A. 10]. Note that the measured acceleration signal is dominated by a response component with a frequency of about 37 kHz, which corresponds to the frequency of a case (rather than a sensing element) resonance of the accelerometer. Of course, even when transducer resonances are excited, if the maximum acceleration limit is not excited and the dynamic range of the data acquisition system is adequate, the system responds linearly and the shock signal at frequencies below resonance will still be accurate. However, the resonance response often causes (a) the maximum acceleration limit to be exceeded, or (b) saturation of the signal conditioning amplifier or other some other component of the data acquisition system. Then the system response is nonlinear, causing a loss of information at all frequencies.

The manufacturers of accelerometers produced for shock measurement applications have attempted to circumvent the above noted problem by designing accelerometers with the highest feasible sensing element and case resonance frequencies (advertised to as high as 1 MHz). However, the evidence is clear that all currently available accelerometers will reveal a strong resonant response of

either the sensing element or the case if measurements are made (without a mechanical falter) sufficiently close to a pyrotechnic source. Such a resonant response should be assumed to exist in all pyroshock measurements made near the source of excitation, even though the frequency response range of the analysis equipment may not extend to a sufficiently high frequency to see that resonant response.

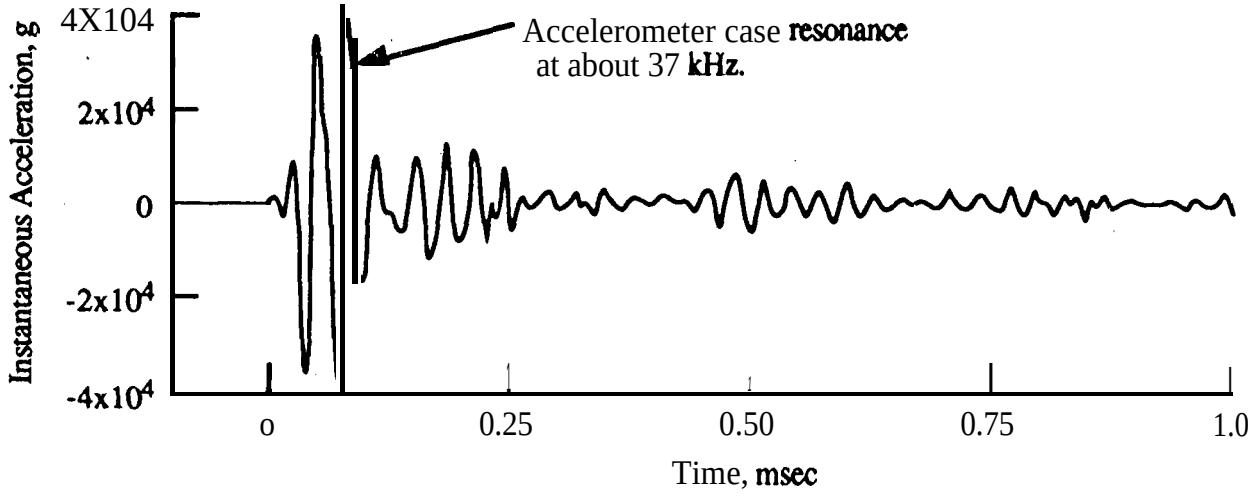

Figure A.3. Pyroshock Acceleration Signal Measured with 80 kHz Bandwidth Showing Accelerometer Case Resonance [A. 10].

A.2.1.2 Accelerometer Overload. For some piezoresistive accelerometers, an excessive input acceleration often breaks the sensing element, causing an instant termination of the output signal. For piezoelectric accelerometers, however, there is the possibility that the accelerometer will continue putting out a signal even though the sensing element was overloaded by the initial acceleration pulse. Such a momentary overload of the sensing element commonly causes a zero-shift in the output signal with a rapid recovery time (usually less than 5 msec), as illustrated in Figure A.4. In some cases, a zero-shift with a much longer recovery time (usually greater than 20 msec) will occur due to an accelerometer malfunction called "crystal domain-switching" [A. 11], as illustrated in Figure A-5, but such a result could also be indicative of saturation in the accelerometer amplifier (see Section A.2.2). In any case, if a pyroshock signal reveals a zero-shift, the measurement generally should be considered invalid (see Section A.2.2 for possible exceptions). It should be emphasized that altering the initial conditions of the measured signal for analysis purposes (e.g., applying the AV = O criterion discussed in Section 5.5.3.7) will not correct the problems indicated by a zero-shift.

A.2.1.3 Accelerometer M o u -. For pyroshock measurement purposes, it is most desirable to mount accelerometers directly to the structure. Nevertheless, accelerometers are often mounted on rectangular blocks attached to one side of the structure, as illustrated in Figure A.6(a). This arrangement facilitates the mounting of accelerometers for measurements of in-plane motions. Also,

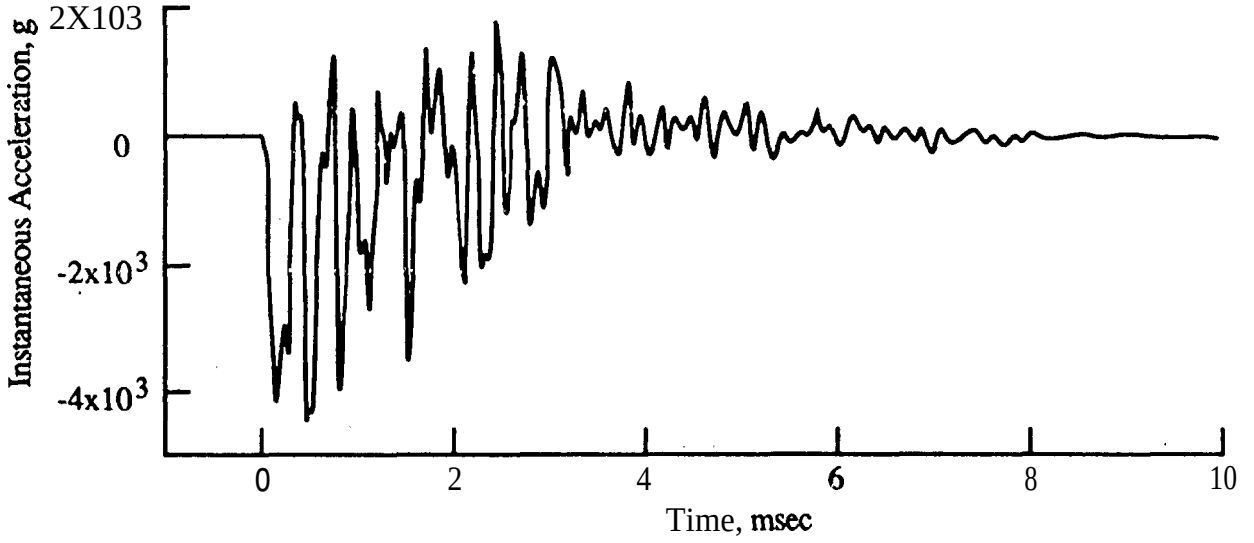

Figure A. 4. Pyroshock Acceleration Signal with Zero-Shift due to Saturation of Accelerometer Piezoelectric Element.

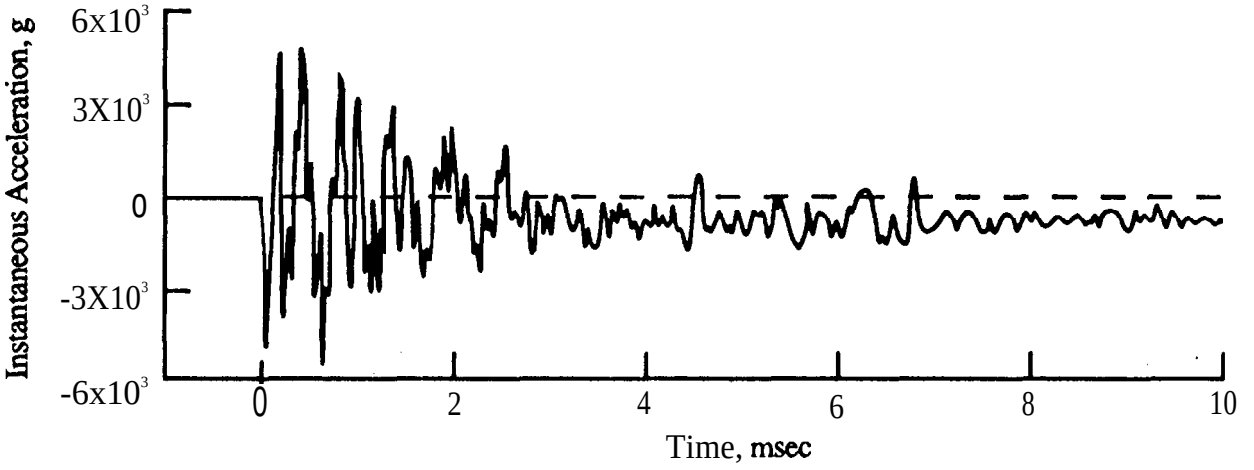

Figure A.5. Pyroshock Acceleration Signal with Zero-Shift due to Accelerometer Malfunction and/or Amplifier Saturation.

the mounting block generally reduces the problem of spurious accelerometer outputs due to base strain. On the other hand, the rectangular mounting block arrangement in Figure A.6(a) introduces two problems, as follows:

(1) The mounting block adds both mass and stiffness to the structure that will distort the high frequency dynamic response of the structure, producing errors in the measurements of the structural response along all three orthogonal axes (see Section 3,2.5.2 for mass loading corrections),

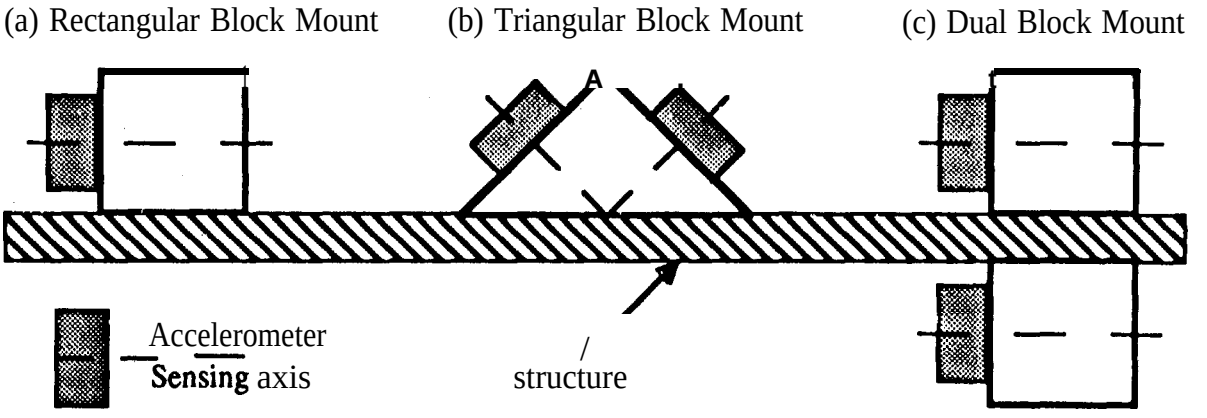

Figure A.6. Accelerometer Mounting Procedure for In-Plane Pyroshock Measurements.

(2) The inertial load of the mounting block introduces a spurious rotational motion of the structure at the mounting block location, producing major errors (often in excess of 100%) in the measurements of the structural response, particularly along the in-plane axes (see [A. 12]).

For measurements on relatively heavy and stiff structures, such as bulkheads, the errors introduced by rectangular mounting blocks maybe minor. However, the mounting block induced errors are often substantial for measurements made on thin panel structures.

The influence of rotational motions on in-plane measurements can be minimized by the use of triangular mounting blocks, as suggested in [A, 12]. In a triangular mounting block arrangement, two accelerometers are mounted with their sensing axes at 45 degrees to the orthogonal axes of the structure, as illustrated in Figure A.6(b). The acceleration response normal to the structure is then determined by summing the two accelerometer signals and dividing by $\sqrt{2}$, while the in-plane response is determined by subtracting the two accelerometer signals and dividing by $\sqrt{2}$. This theoretically allows the in-plane motion to be measured correctly at the surface of the structure, independent of rotational motions of the structure. However, to be effective, the sensitivity and phase of the two accelerometer channels must be very accurately matched. A carefully calibrated and highly stable digital data acquisition system is usually required to achieve the necessary accuracy.

An alternate procedure for suppressing in-plane measurement errors due to rotational motions is to use two in-plane accelerometers, one on each of two identical blocks mounted on both sides of the structure at the same location (assuming such a mounting arrangement is possible), as illustrated in Figure A.6(c). The sum of the two accelerometer signals divided by two will yield an in-plane acceleration measurement free of rotational effects. Also, the mass symmetry of the mounting blocks will suppress mounting block induced rotational motions. However, to be effective, the two accelerometer channels must be very accurately matched, as discussed above for the triangular mounting block arrangement. See Section 3,2.6.3 for further details on accelerometer mountings.

A. 2.1.4 Other Problems. Other potential problems associated with accelerometer measurements of pyroshocks include the following:

(1) The accelerometer connectors may break, or momentarily open circuit causing severe noise contamination of the signal, particularly with piezoelectric accelerometers. Connector prob lems can be largely eliminated by soldering the cables directly to the accelerometer lead wires.

(2) Accelerometers mounted using a glue may break free. Accelerometers mounted by a stud or through a bolted mounting block may loosen or momentarily separate from the structure during the shock.

(3) The shock may cause sufficient base strain to the accelerometer to produce a spurious output due to a deformation of the sensing element.

(4) Accelerometers that are not electrically isolated and are attached to the structure with a glue may ground and cause severe noise contamination due to ground loops,

(5) The accelerometer output may be influenced by the electromagnetic radiation (EMR) pulse generated by the pyrotechnic detonating device.

(6) The accelerometer output may include a response to the acoustic noise produced by the pyro-shock.

(7) The accelerometer output may include contributions from a transverse accelerometer reso-nance.

(8) The accelerometer performance may be influenced by heat transients produced by the detona-tion of the ordnance causing the pyroshock (see Section 3.2.4.2).

These various problems can be largely eliminated by a proper selection and use of accelerometers for pyroshock applications [A. 13-A. 17], and good measurement procedures, as recommended in Section A.3.

A.2.2 Signal Conditioners. Both piezoelectric and piezoresistive accelerometers must be used with a signal conditioner (amplifier and/or power supply), as described in Section 3.3. For piezo-electric accelerometers, which are essentially charge-generating devices with a very high source impedance, the first stage of the "signal conditioner is a charge converter, as illustrated in Figure 3.37. The transfer of the accelerometer signal through cables to the charge amplifier is vulnerable to losses due to the cable capacitance, as well as noise contamination, if the cables become very long (see Section 3.3.5). To avoid these problems, some manufacturers build piezoelectric ac-

celerometers with electronic circuits integrated within the accelerometer that convert the charge signal into a voltage signal with a relatively low source impedance.

In any case, the signal conditioner has a finite dynamic range arid slew rate limits that may not be adequate to cover the full dynamic range of the pyroshock signal generated by the accelerometer. Specifically, the high frequency portion of pyroshock signals is commonly very intense due to the response of lightly damped high frequency modes of the structure subjected to the pyrotechnic source. This may not be immediately apparent because the high frequency portion of the signal often exceeds the upper frequency limit of the data analysis equipment, The result can be a saturation of the signal conditioner amplifier (charge converter) due to an input gain setting that is inadequate to accept these unseen high magnitude, high frequency signals. Amplifier saturation appears in the signal conditioner output signal in many ways, but most commonly as a zero-shift in the signal time history followed by a slow recovery (usually in excess of 20 msec). An example of severe amplifier saturation is shown in Figure A.7. Less extreme amplifier saturation might appear as illustrated in Figure A.5. However, as discussed in Section A.2. 1.2, the signal shown in Figure A.5 could also be caused by a malfunction of the accelerometer.

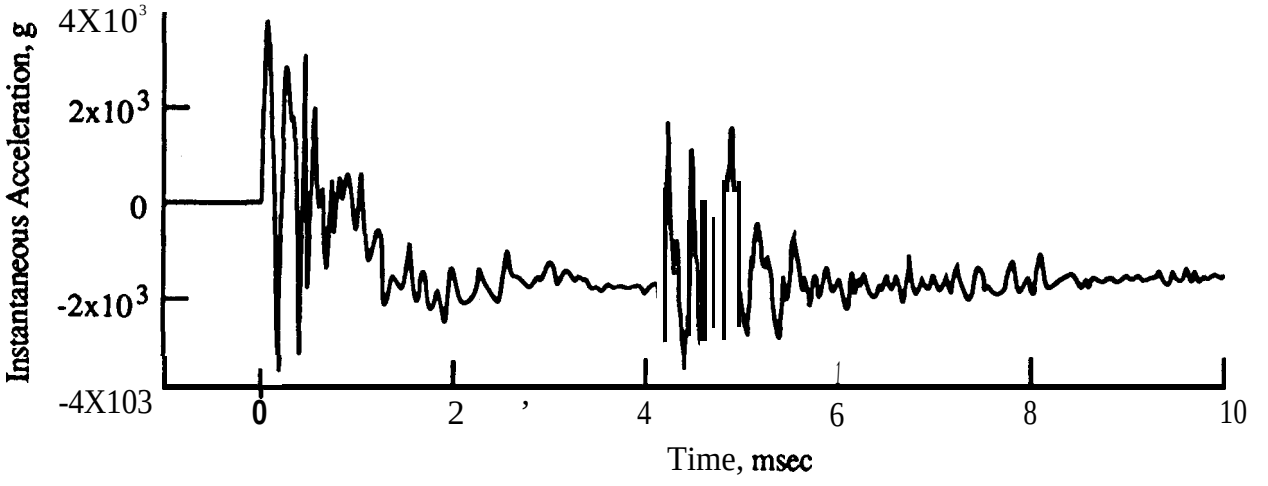

Figure A.7. Pyroshock Acceleration Signal with Zero-Shift due to Amplifier Saturation.

Generally, a zero-shift due to amplifier saturation should be viewed the same as a zero-shift due to accelerometer saturation or other malfunctions, namely, the data should be considered invalid [A. 18]. In some cases, however, limited information might be recovered if certain assumptions concerning the exact nature of the amplifier overload are justified [A. 19]. Again, it should be emphasized that altering the initial conditions of the measured signal for analysis purposes (e.g., applying the AV = O criterion discussed in Section 5.5.3.7) will not correct the problems indicated by a zero-shift. See Section 3.3.2 for further details on amplifiers.

A.2.3 Electrical Lowpass Filters. The signal conditioners used with both piezoelectric and piezoresistive accelerometers often include an electrical lowpass filter with a selectable upper cut-off frequency, ranging from 2 kHz to 20 kHz, immediately before the charge converter or first amplifier stage. Passive lowpass pre-filters are also sometimes used in the cable before the signal conditioner (see Section 3.3.3.3). The purpose of these filters is to allow the user to suppress the high frequency content of the measured pyroshock signal before further signal conditioning, voltage amplification, and recoding operations are performed. Since the high frequency portion of a pyroshock acceleration signal is typically very intense, removing that portion of the signal early in the data acquisition process can allow a higher gain setting to the signal conditioner and, hence, greatly enhance the signal-to-noise level in later data processing. However, such lowpass filtering may in some cases result in a loss of relevant information, depending on the application of the data [A. 15]. Also, filters with nonlinear phase characteristics may distort the pyroshock signal at frequencies near the cut-off frequency of the filter (see Section *3.7.3.4).*

The use of electrical lowpass filters and/or pre-filters would appear to provide a solution to the dynamic range problems caused by the usually intense high frequency portion of pyroshock acceleration signals, as well as the spurious signals due to resonant responses within the accelerometer. However, experience suggests the dynamic range problem is not so easily resolved. Studies of various different piezoelectric accelerometer/signal conditioning systems [A. 10] indicate that the lowpass filters in at least some commercial signal conditioners appear to malfunction when the upper cut-off frequency is set below about 20 kHz. Similar anomalies in the performance oflowpass falters in commercial signal conditioners have been observed in carefully controlled laboratory tests with synthesized transient signal inputs [A.20].

A.2.4 Mechanical Lowpass Filters. The obvious solution to the dynamic range problem in pyroshock measurements, as well as the accelerometer ringing problem discussed inSection A.2. 1.1, is to prevent the high frequency portion of the shock from reaching the accelerometer. This can be accomplished by inserting a mechanical lowpass filter between the accelerometer and its mounting point, where the upper cut-off frequency of the mechanical filter is well below the lowest resonance frequency of the accelerometer. Such mechanical filters have been commercially available for many years (e.g., [A.21]), and various configurations of mechanical falters have been evaluated for pyroshock measurement applications (e.g., [A.22]). To achieve a flat gain factor of near unity at frequencies below their cut-off frequency, mechanical filters are or should be constructed with a damping ratio of $\zeta \approx 0.7$. This introduces a phase shift into the acceleration sensed by the accelerometer at all frequencies, but the phase shift is nearly linear with increasing frequency (corresponding to a fixed time delay) and, hence, does not distort the measured acceleration signal. On the other hand, the filters must be "tuned" for specific accelerometer weights, and used within a narrow temperature range to avoid variations from the desired damping value. Furthermore, they may "bottom" when subjected to an intense pyroshock, and sometimes have poor transverse response characteristics.

At least one major manufacturer of piezoelectric transducers has introduced an accelerometer that incorporates a mechanical lowpass filter in the support of the sensing element. This approach is attractive in that it reduces the size and weight of the transducer installation, and assures the falter is properly "tuned". However, the other potential problems discussed above still apply.

A.2.5 Data Recorders, Reproducers, and Storage. When feasible, it is desirable to digitally, capture and store measured pyroshock signals on-line directly out of the signal conditioner. Digital capture devices are now available with sampling rates exceeding 10 MHz, and real time storage capabilities exceeding 1 million sample values. The analog-to-digital converters (ADC's) for such instruments usually employ at least a 12 bit word size, meaning they provide a maximum dynamic range (as defined in Section 3.7.1.3) of DR = 72 dB.

Unfortunately, there are many cases where it may not be feasible (or at least not convenient) to use direct digital capture and storage devices, particularly when a large number of accelerometer measurements are being made simultaneously. Hence, pyroshock signals are commonly recorded on analog tape recorders for storage and later analysis. For FM tape recorders that meet the requirements of IRIG Standard 106-93 [A.23], the rms signal-to-noise ratio of the recorded signals is a maximum of about S/N= 48 dB.

For any type of recording, since there is usually considerable uncertainty about the peak acceleration value that will occur during a pyroshock event, it is often necessary to set the recorder input gain to a conservative value (provide "head-room") to assure against an overload. This means that the useful dynamic range of the recorded signals may be very much less than the maximum dynamic range of the recorder. This head-room problem can be suppressed by simultaneously recording each pyroshock signal on two or more recorder channels set with different sensitivities. Of course, this approach increases the instrumentation requirements, and usually is not necessary if a direct digital capture device is used. See Section 3.6 for further details on data recording.

A.2.6 Anti-Aliasing Filters and Analog-to-Digital Converters. Essentially all pyroshock data analysis is currently accomplished using digital data analysis procedures. When digital capture and storage devices arc used for data acquisition, the pyroshock signals are converted directly into a digital format. Otherwise, the recorded data signals are digitized by an ADC on the front end of the data analysis instrument, or by a "stand-alone" ADC tied to a computer, as described in Section 3.7. In any case, the anti-aliasing filter and ADC sampling rate requirements for pyroshock data are essentially the same as those detailed for general transient data in Section 5.5.3.

It should be mentioned that aliasing errors can be particularly severe for the case of pyroshock data because of the intense high frequency energy in such data, and the possible ringing of the accelerometer at frequencies above the Nyquist frequent y. For example, consider the acceleration in Figure A.3, where there is a dominant component at about 37 kHz due to an accelerometer case

resonance. If this signal had been acquired with a digital sampling rate of, say, Rs =40 ksps, producing a Nyquist frequency of f_N = 20 kHz, the 37 kHz component would have been aliased down to appear in all data analysis at 3 kHz (see Section 3.7.2). From this illustration, the potential for serious misinterpretations of digitally acquired pyroshock data due to aliasing is clear. It should also be mentioned that electrical lowpass filtering in the signal conditioner or mechanical lowpass filtering in the transducer will help suppress aliasing, assuming the cut-off frequency is no higher than that of the anti-aliasing filter, but such filtering should never be used as a substitute for anti-aliasing filters.

A.2.7 Analysis Proc -. As noted in Section 5.5.3, the shock response spectrum (SRS) has become widely accepted as the primary descriptor for transient signal measurements, including pyroshock measurements [A.24]. However, the application of the SRS to pyroshock measurements is often the source of controversy for various reasons, including the following:

(1) The SRS for a given pyroshock is not unique, i.e., there are numerous different transient time histories that will produce the same SRS.

(2) Since the SRS represents the response of single degree-of-freedom systems to the measured transient, it does not yield the peak acceleration that might occur in the response of a multi-mode component (a multiple degree-of-freedom system) subjected to the measured pyroshock. Hence, it is not indicative of the damage potential of the pyroshock to such cases.

(3) The linearity assumption in the SRS is sometimes questionable, particularly for components subjected to high intensity transients like pyroshocks.

(4) The SRS is highly sensitive to the assumed damping value for multi-cycle transients like pyroshocks.

A.2.7.1 Sensitivity to Damping Value. The last problem noted above is the most serious from the viewpoint of pyroshock simulations for testing purposes. Specifically, the values of the SRS for a single cycle transient (e.g., a half-sine pulse) can never exceed twice the peak acceleration of the transient, no matter what damping value is assumed [A.25, A.26]. However, as the number of cycles in the transient increases, the SRS values approach the steady-state response of the hypothetical oscillators producing the SRS. This point is illustrated for a sinusoidal-like transient in Figure A.8, which is taken directly from [A.25]. The results in Figure A.8 are for zero damping and, hence, the SRS will approach infinity as the number of half-cycles N in the transient becomes large. With nonzero damping, the SRS approaches a limiting value of Q = 1/(2{), where ζ is the assumed damping ratio (see Section 3.2.2). Referring to Figure A. 1, pyroshocks typically include a large number of cycles, meaning the sensitivity of pyroshock SRS computations to the assumed damping can be substantial.

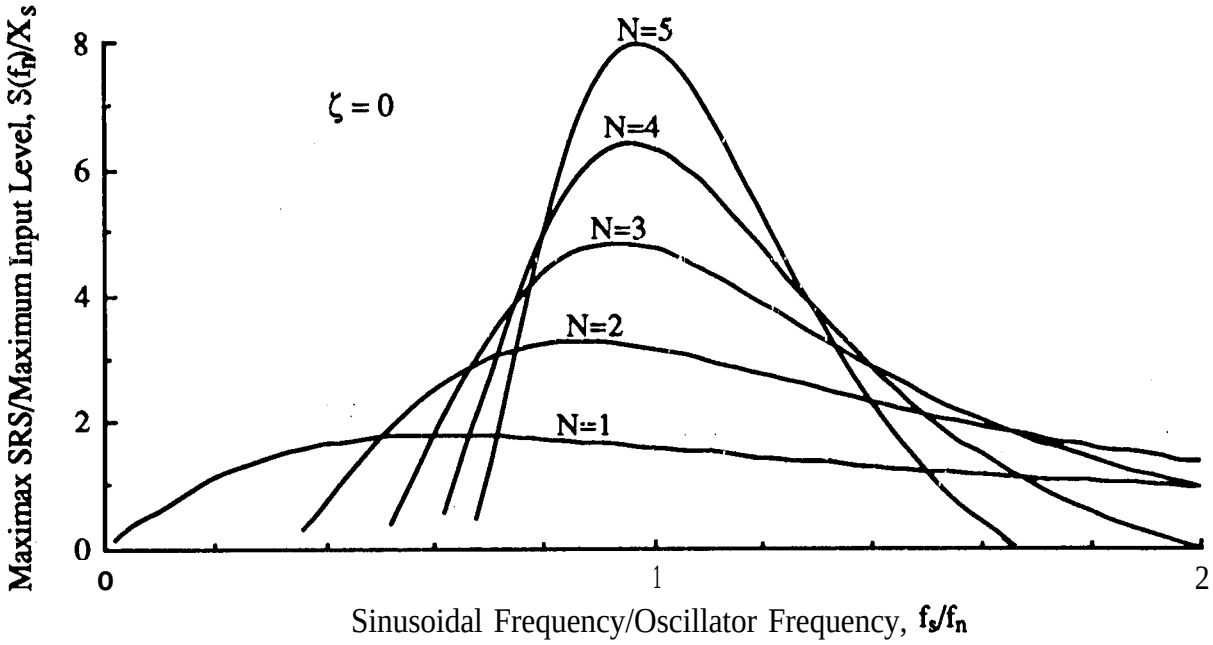

Figure A.8. Maximax Shock Response Spectra for Sinusoidal Forcing Function, $X_s \sin(2\pi f_s t)$; $0 < t \leq [N/(2f_s)]$ versus Number of Half-Cycles, N [A.25].

From the viewpoint of test validation, errors due to the sensitivity of the SRS to the assumed damping can be suppressed by using the same darnping for the test simulation analysis as was used to evaluate the actual pyroshock event. This approach will be effective only if the test simulation is accomplished using a pyroshock excitation, or a reasonable simulation thereof [A.24]. For example, the SRS for a given pyroshock could be crudely approximated by a single cycle transient having a properly designed waveform. However, the required peak acceleration of that single cycle transient would be very much larger than the actual peak acceleration of the pyroshock, raising serious questions about the accuracy of the test simulation from a damage potential viewpoint. Procedures for preventing this type of misuse of the SRS are detailed in Section 5.5.3.2.

A.2.7.2 Dynamic Range. The acceleration SRSS for pyroshock measurements commonly cover a wide dynamic range. This is illustrated by the typical pyroshock acceleration SRS in Figure A.9. Even if the Fourier spectrum of the structural acceleration response to the pyroshock were uniform with frequency, the SRS acceleration values would rise with natural frequency at a rate approaching 6 dB/octave. This follows from the fact that, for zero damping, the residual shock response spectrum $S_R(f_n)$ is proportional to frequency times the magnitude of the Fourier spectrum $|X(f)|$ of the structural response, i.e., $S_R(f_n) = 2\pi f\,|X(f)|$ [A.26]. In many cases, the smoothed Fourier spectrum of the structural acceleration response to a pyroshock excitation actually increases with frequency. This occurs because the bandwidth of the modes of the structure subjected to the pyroshock generally increase with frequency. The net result is the substantial increase in SRS values going from low to high natural frequencies seen in Figure A.9.

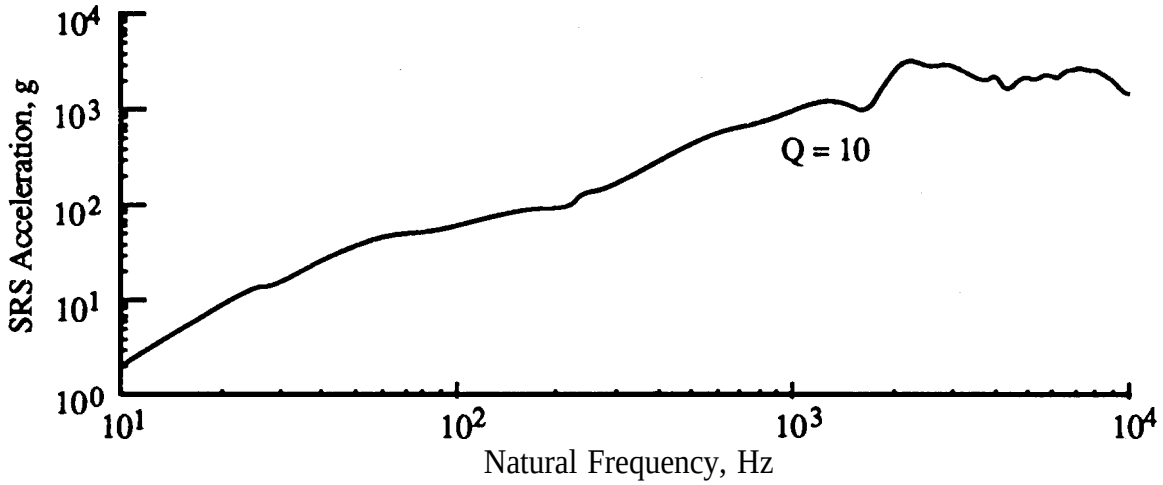

Figure A.9. **Typical Maximax** Acceleration Shock Response Spectrum for Pyroshock on Heavy Aluminum Structure.

A.2.7.3 **Other Analysis Techniques**. There are other techniques for analyzing and evaluating transient **data,** including pyroshock data. The two most common alternatives are the Fourier spectrum and the energy spectrum (see Sections 5.5.1 and 5.5.2, respectively). These two functions provide a description of the transient environment itself, rather than the effect of the transient on a hypothetical component modeled by simple oscillators. They also yield rigorous input/output relationships **[A.9]** that are not provided by the SRS. The energy spectrum is the more applicable of the two functions for the description of stochastic transients, such as pyrotechnic and ballistic shocks. Its use has been explored for such applications **[A.27],** but has been found lacking in two important ways, as follows:

(1) To achieve, statistical stability, the computation of an energy spectrum requires an averaging operation over several repeated shocks, or over frequency in a manner that restricts the resolution of the analysis (see Section 5.5.2).

(2) The energy spectrum does not define peak accelerations for either the transient or a hypothetical component subjected to the transient.

See **[A.28]** for **other** analysis techniques that might be suitable for special applications.

A.3 **Guidelines and Recommendations**. The following guidelines **are** recommended for the acquisition and analysis of pyroshock data.

A.3.1 Measurement Locations. For those cases where pyroshock measurements are being made to define the input loads to a specific item of system hardware, the measurement locations for accelerometers should be as close as feasible to the attachment points of the hardware, with either

the actual hardware or an accurate simulation of the hardware present. In those cases where the measurement locations are not dictated by the attachment points for specific hardware items, the following guidelines are recommended:

(1) For structures that are homogeneous between the pyrotechnic source and measurement location, never select a measurement location within 6 in. of the source.

(2) Always select measurement locations that are as far from the pyrotechnic source as feasible to still acquire meaningful engineering information.

(3) When applicable, select measurement locations that are separated from the source by a structural path with discontinuities, e.g., riveted or bolted joints, or isolation elements.

Common sense dictates that the above guidelines should apply to the installation of system hardware as well.

The above recommendations evolve from the fact that essentially all pyroshock measurements made in the past using an accelerometer mounted within 6 in. of a pyrotechnic source on a structure with a homogeneous path (i.e., no joints or isolation elements) between the source and the measurement location have proven, under careful inspection, to be highly questionable. Even out to 12 in. from the source on a homogeneous structural path, accurate pyroshock data are difficult to acquire using accelerometers. Hence, if circumstances arise where near-field pyroshock measurements are required in violation of the above recommendations, the use of transducers other than accelerometers should be considered (see Section A.4).

A.3.2 Accelerometers. Although some investigators tend to favor piezoresistive over piezoelectric accelerometers for pyroshock measurements (e.g., [A. 15]), current piezoelectric accelerometers are considered acceptable if they are properly used. In either case, however, only those accelerometers designed specifically for shock measurement applications should be employed.

A.3.2.1 Electrical Isolation. Most modern piezoelectric and piezoresistive accelerometers incorporate electrical isolation, but many older models do not. In these cases, great cam must be exercised to avoid background noise problems due to ground loops and the electromagnetic radiation (EMR) pulse generated by the ignition of the ordnance device producing the pyroshock, as follows:

(1) If the accelerometers do not incorporate electrical isolation, they must be mounted to the structure through electrically isolated studs, or with a glue that provides electrical insulation.

(2) The accelerometers should be checked with an ohmmeter for possible grounding to the structure before each test. The only ground should be at the signal conditioner or end instrument.

(3) If possible, the accelerometers should again be checked with an ohmmeter for possible grounding to the structure after each test, to confirm that the electrical isolation did not fail due to the pyroshock.

(4) For piezoelectric accelerometers without integrated electronics, all cables between the accelerometers and their charge amplifiers should be continuous, noise-treated coaxial cable. No junction boxes or twisted pairs cabling should ever be used.

(5) Rather than using connectors, it is desirable to directly solder the cables to the accelerometer leads, when feasible.

(6) To suppress EMR contamination and cable damage, the cables should not be attached to the structure beyond the accelerometer connection, and should be carried away from the accelerometer in the opposite direction from the pyrotechnic source. A special stand might be needed to support the cables off the structure.

(7) To check for possible EMR contamination of accelerometer signals during a test, an inert accelerometer (an accelerometer with an inactive sensing element, but otherwise identical to the measurement accelerometers) should be attached to the structure near the measurement accelerometers, and wired to a nearly-identical signal conditioner with the same gain setting. A significant output from the signal conditioner for the inert accelerometer due to the pyroshock event will indicate an EMR noise interference problem. Most accelerometer manufacturers sell inert versions of their transducers.

(8) If an inert accelerometer is not available, the next best check for EMR contamination is to freely suspend an additional accelerometer adjacent to, but not touching, the structure and wire it to a nearly-identical signal conditioner with the same gain setting. Again, a significant output from the signal conditioner for the freely suspended accelerometer due to the pyroshock event will indicate an EMR noise interference problem.

A.3.2.2 Accelerometer Mountings. The use of mounting blocks to attach accelerometers to the structure is discouraged for the reasons noted in Section A.2. 1.3. However, if mounting blocks are required, attention should be given to avoiding mounting block resonance and separation problems, as follows:

(1) The mounting blocks should be aluminum, magnesium, or preferably beryllium if funding allows, with no dimension greater than 0.75 in. on a side. This will usually assure a resonance frequency of the mounting block, loaded with the accelerometer, in excess of 40 kHz.

(2) For the measurement of very intense pyroshocks (peak values in excess of 5,000 g), the mounting blocks should be both glued and bolted to the structure, if feasible, to reduce the risk of separation during the pyroshock. The organization responsible for assessing the integrity of the structure to which the accelerometer is mounted should be consulted before any bolt holes are drilled in the structure. For less intense pyroshocks, a glue bond alone will usually be adequate.

(3) If the mounting blocks are both bolted and glued to the structure, the bolts should be loosened following each pyrotechnic event to determine if the blocks are still bonded to the structure by the glue. A broken glue bond would indicate the mounting block separated during the shock.

(4) For in-plane measurements, if a digital data acquisition system is used that can provide the necessary accuracy, two accelerometers on either the triangular or dual mounting block arrangement shown in Figure A.6 should be considered.

See [A.29] for further details on the use of mounting blocks and comparisons of various mounting glues.

A.3.2.3 Mechanical Lowpass Filters. The use of a mechanical lowpass filter between the accelerometer and the structure is acceptable if the specific filter being used has been thoroughly evaluated and verified to be effective for the measurement of pyroshock signals. This recommendation with the same caveat also applies to accelerometers with incorporated mechanical filters. The principal concerns in the evaluation of such filters should be as follows:

(1) The mechanical filter cut-off frequency should beat least 1.5 times the highest natural frequency for subsequent SRS computations.

(2) There should be no “bottoming” or other nonlinearity of the mechanical falter when subjected to a pyroshock of the magnitude to be measured

(3) The gain of the mechanical filter near its resonance frequency should not reveal a substantial peak due to inadequate damping.

(4) There should be no significant transverse resonances of the mechanical filter causing an unacceptable sensitivity to off-axis acceleration inputs.

Improvised mechanical filters (i.e., wood, hard rubber, or other "soft mount” materials) are not recommended due to the large uncertainties in their performance characteristics.

A.3.3 Signal Conditioners. Pyroshock measurements with piezoelectric accelerometers should always be made using a charge amplifier, unless the accelerometer has integrated electronics. Electrical filtering prior to the amplifier should be limited as follows:

(1) LowPass filters should not be used with a cut-off frequency of less than *20 kHz,* unless a filter with a lower cut-off frequency has been thoroughly evaluated to be effective for the measurement of the pyroshocks of interest (see Section A.2.3). In any case, the cut-off frequency of lowpass filters should always be at least 1.5 times the highest natural frequency for subsequent SRS computations.

(2) There is no objection to using highpass filters to remove electrical offsets and/or drift in the transducer instrumentation. However, the cut-off frequency of the highpass filters should be no more than 20 Hz or 0.1 % of the highest SRS computation frequency, whichever is lower. A cut-off frequency above this limit might remove a temporary zero-shift indicative of an invalid measurement due to accelerometer and/or amplifier saturation (see Sections A.2. 1.2 and A.2.2).

(3) The signal conditioner filters (lowpass and/or highpass) can be of any type, as long as their cut-off frequencies are no greater than 0.67 f_l for highpass filters and no less than 1.5 f_h for lowpass filters, where f_l and f_h are the lowest and highest natural frequencies, respectively, for subsequent SRS computations. These cut-off frequency selections will minimize the errors in the lowest and highest SRS oscillator responses, as well as the errors due to the possible nonlinear phase characteristics of the filters [A.30].

(4) The gain of signal conditioner filters (low-pass and/or highpass) should be flat to within ± 5% within the frequency range from f_l to f_h.

A.3.4 Data Recorders. Although on-line digital data acquisition and storage is desirable to achieve a maximum dynamic range (see Section A.2.5), the use of tape recorders is often necessary when a large number of accelerometer measurements are required. To maintain the interchangability of tape recorders used for the playback of the recorded pyroshock signals, such data recordings should be made as follows:

(1) Only laboratory-quality IRIG standard 14-channel or 28-channel FM tape recordings with extended range (Wideband I or Wideband II) heads are recommended, although IRIG standard PCM recordings are acceptable if they have a frequency range of O to 40 kHz.

(2) The tape speed for FM tape recordings should be at least 60 in./sec (ips), giving a frequency range with Wideband I electronics of at least O to 40 kHz. It is acceptable to playback the data recordings at a reduced speed for digital conversion and data analysis.

A.3.5 Data Sampling and Editing. Special purpose instruments are sometimes used for pyroshock data analysis that have fixed sampling rates and automatically compute an SRS after the sampling operation, However, when the available instrumentation permits, the data signals should be sampled and edited as follows:

A.3.5.1 Anti-Aliasing Filters and SamDll-. All measured pyroshock signals must be lowpass filtered for anti-aliasing purposes before digital conversion. This is true even when lowpass filters "are used at the accelerometer (see Section A.3.2.3) and/or at the input to the signal conditioner (see Section A.3.3) during data acquisition. The recommendations presented in Section 3.7.3 and extended in Section 5.5.3.4 apply to the selection of anti-aliasing filters and their cut-off frequency. The recommendations presented in Section 5.5.3.5 apply to the selection of the sampling rate.

A.3.5.2 Data Editing. All digitized pyroshock time history signals should be inspected for errors by an experienced analyst prior to the SRS computation. This should include a visual inspection for the following common anomalies:

(1) Obvious wild points, dropouts, magnitude limitations, or other anomalies that are clearly indicative of an ADC malfunction or clipping (see Section 4.4).

(2) Signal terminations indicative of an accelerometer failing or coming off the structure.

(3) Sharp randomly-occurring spikes in the signal indicative of noise due to a loose connector or other intermittent noise sources (see Section 4.4).

(4) Zero-shifts indicative of saturation in the accelerometer or signal conditioner. See Figures A.4, A.5, and A.7 for illustrations.

(5) Asymmetry between positive and negative values indicative of one-sided clipping or saturation in the accelerometer or signal conditioner. See Figure A.4 for an illustration.

It should be noted that knowledge-based computer programs for automated data editing of pyroshock signals have been developed by some organizations (e.g., [A.31]). The use of such automated data editing systems is endorsed if their effectiveness has been thoroughly verified by experience, and an experienced analyst is available to perform a cursory review of the edited results.

A.3.5.3 Velocity Validation. Beyond the above visual checks by an experienced analyst (or an automated data editing program), all pyroshock acceleration signals should be further checked for validity by computing a running integration to obtain an instantaneous velocity signal, as summarized below. In applying the velocity validation procedure, it should be mentioned that a low fre-

quency trend (usually one or fewer cycles over the analysis duration) might occur in the integration of any random signal due to the integrated low frequency noise. Care must be exercised to distinguish between the more rapid trends indicative of a spurious acceleration signal, and the slower trends due to a normal integrated noise problem,

(1) For measurements on structures that experience no net velocity change due to the pyroshock event, and the AV = O criterion in Section 5.5.3.7 is imposed, a clean, accurate pyroshock acceleration signal should integrate to a velocity signal that looks like a lowpass filtered version of the acceleration signal with a zero velocity value at the end of the data block, as illustrated in Figure A. 10(a). If the velocity signal reveals a rapid shift in its mean value to unreasonably high velocity values, particularly during the early part of the transient where the shock magnitude is intense, this is indicative of a serious defect in the acceleration measurement. An illustration is shown in Figure A. 10(b) where a noise spike is present in the acceleration signal. Excluding spurious trends due to integrated noise, if the mean value of the velocity signal exceeds the peak-to-peak range of the fluctuating portion of the velocity signal, the data should be considered invalid. Fortunately, serious defects in measured pyroshock acceleration signals commonly cause zero-shifts in the instantaneous velocity signal far greater than the above recommended limit.

(2) For measurements on structures that experience a net velocity change due to the pyroshock event (e.g., deployed structures), and the initial V = O criterion in Section 5.5.3.7 is imposed, a clean, accurate pyroshock acceleration signal should integrate to a velocity signal that looks like a lowpass filtered version of the acceleration signal with a velocity value at the end of the data block equal to the net velocity change of the structure. Excluding spurious trends due to integrated noise, if the velocity signal at the end of the data block differs from the net velocity change of the structure by more than 2:1, the data should be considered invalid. As in (1), serious defects in measured pyroshock acceleration signals commonly cause errors in the terminal velocity signal far greater than the above recommended limit.

A.3.6 Data Analysis. The SRS is considered to provide the most useful description of pyroshock data from the viewpoint of establishing test specifications and design criteria (see Section 5.5.3). Absolute acceleration is the most commonly used SRS response parameter for these applications, but relative displacement or velocity can also be used. Other forms of data analysis, primarily Fourier and energy spectra, should be considered for other applications, such as the estimation of structural frequency response functions.

A.3.6.1 Analysis Durations. To avoid truncation errors (see Section 5.5.3.6), the signals acquired for pyroshock data analysis must be long enough to cover all significant signal values above the background noise of the measurements. To suppress potential noise problems in the later analysis, however, the analysis block durations should be limited as follows:

(a) Valid pyroshock measurement.

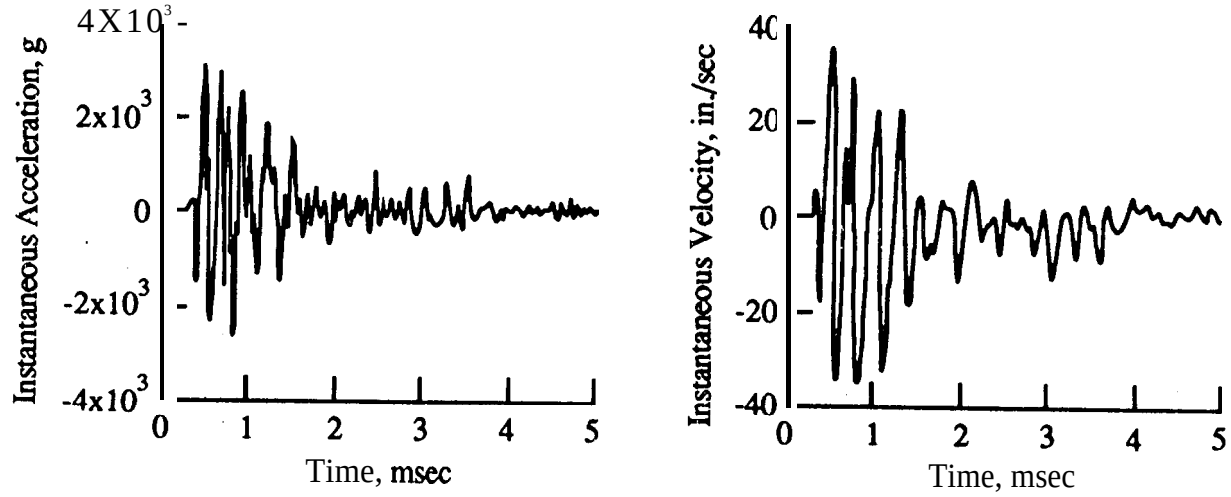

(b) Invalid pyroshock measurement.

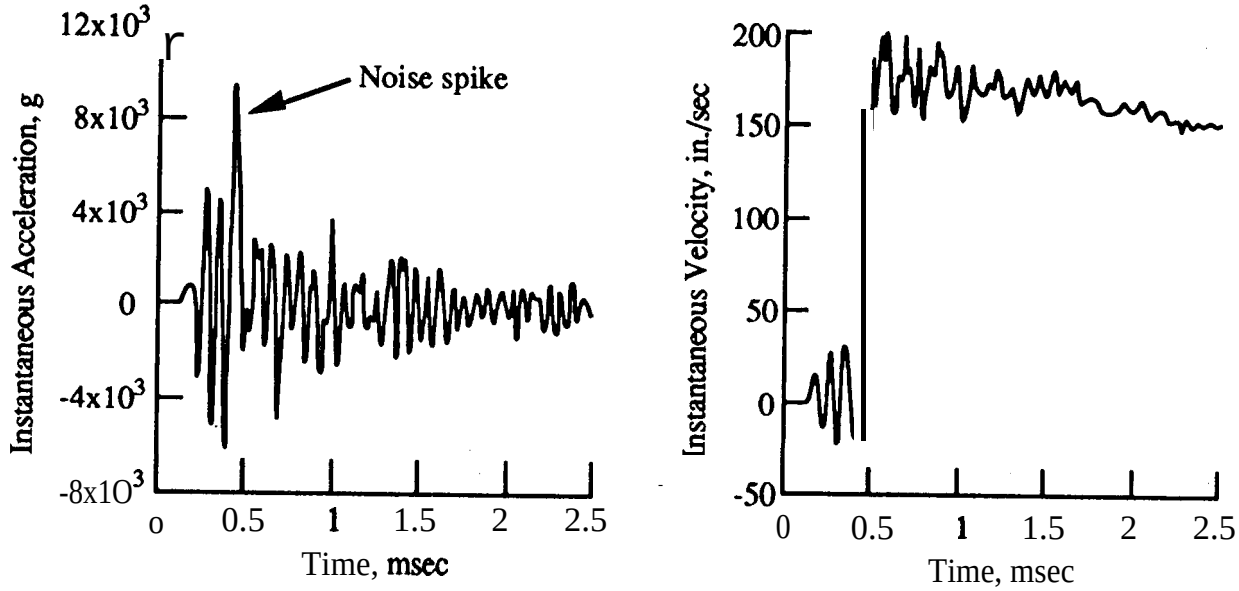

Figure A. 10. **Pyroshock** Acceleration and Velocity Signals for Valid and Invalid Measurements **(Courtesy McDonnell-Douglas** Astronautics Company, **St.** Louis, MO).

(1) The measured signal prior to the initiation of the acceleration transient obviously represents background noise and should be deleted **from** the data used to compute the pyroshock SRS, i.e., the time history values for the analysis should start at the last data point with a near-zero value prior to the **pyroshock.** The **deleted** portion of the signal should be retained in storage for the computation of a noise SRS (see Section A.3.6.4).

(2) If the background noise is substantial, the zero value in **(1)** should be established from the average of the signal values prior to the initiation of the transient. To eliminate the potential

error in this zero value estimate due to power line pickup, the average should be computed over a time interval $T = n/f_{pl}$; $n = 1, 2, \ldots$ where f_{pl} is the power line frequency (60 Hz in the U. S.)

(3) The measured signal after the acceleration transient has clearly diminished into the instrumentation background noise floor should also be deleted from the data used to compute the pyroshock SRS. The last data point should have a value as near as possible to the average value of the signal after the transient. If the background noise is substantial, the average value of the signal after the transient should be determined as in *(2). The* deleted portion of the signal should be retained in storage for the possible computation of a noise SRS (see Section A.3.6.4)

The last recommended action requires judgment. In applying this judgment, it is better to make the analysis duration too long rather than too short, since an excessive truncation of the signal will usually distort the analysis results more severely than additional noise (see Section 5.5.3.6).

A.3.6.2 Damping Ratio. The results of an SRS analysis of pyroshock data are influenced by the damping ratio assumed in the computation (see Section A.2.7. 1). To standardize data analysis results, the following recommendations are made:

(1) Except for applications involving special circumstances, the damping ratio for SRS computations should be $\zeta = 0.05$ (Q = 10).

(2) If the SRS is being determined to establish test criteria for a laboratory simulation using other than a pyroshock excitation, all SRS computations should be performed twice with two different damping ratios, namely, $\zeta = 0.05$ (Q= 10) and $\zeta = 0.01$ (Q= 50). This will allow an assessment of how accurately the laboratory excitation simulates the pyroshock environment (see Section 5.5.3.2),

(3) If the SRS is being determined to establish design criteria, other damping values may be used that better match the known damping characteristics of specific hardware items.

A.3.6.3 Initial Conditions. The results of an SRS computation can also be significantly influenced by the initial conditions assumed for the data. Again to standardize results, the use of the initial conditions detailed in *Section 5,5.3.7* is recommended.

A.3.6.4 Background Noise. Due to the low sensitivity of shock accelerometers, and other factors limiting dynamic range (see Section A.2.5), measured pyroshock acceleration signals commonly include substantial background noise. The effects of this noise on the SRS analysis can be suppressed somewhat by a judicious selection of the actual time history segment used for the analysis,

as detailed in Section A.3.6. 1. However, the noise superimposed on the transient signal may still influence the SRS computation, particularly at the lower frequencies where the actual shock signal is not very intense. Hence, it is recommended that all measured pyroshock signals be checked for the possible influence of background noise by computing a "noise" SRS from a segment of the measured signal preceding each transient. The duration of the segment used to compute the noise SRS should be identical to the analysis duration used to compute the pyroshock SRS. If a sufficient segment of the signal is not available prior to the initiation of the transient, the noise SRS should be computed from a segment of the signal measured after the transient has diminished into the noise, again with the same duration as the signal segment used to compute the pyroshock SRS.

A.3.6.5 EMR Generated Noise. As noted in Section A.3.2. 1, the EMR generated by the pyrotechnic source might cause spurious signals that will be detected by the inert or freely suspended accelerometer discussed in that section. Hence, it is recommended that the SRS for the output of the inert or freely suspended accelerometer be computed to check for EMR contamination of the pyroshock signals. The starting time and duration of the segment used for this SRS computation should be identical to that used to compute the SRSS for the actual pyroshock measurements on the structure. If there is significant EMR noise in the measurements, the SRS for the inert or freely suspended accelerometer will often approach the pyroshock SRS values at some or all natural frequencies.

A.3.6.6 Positive versus Negative SRS. Experience indicates that valid pyroshock measurements generally produce similar positive and negative SRS values at all natural frequencies. Conversely, anomalous pyroshock measurements usually result in substantial differences between the positive and negative SRS values, at least at some natural frequencies. This is illustrated for valid and invalid pyroshock measurements in Figures A, 11 and A. 12, respectively. These figures also show the velocity checks for the two measurements, which confirm the anomalous character of the pyroshock in Figure A. 12. Hence, it is recommended that the positive and negative SRS, along with any other desired SRS, be computed for all pyroshock measurements as a final check on their validity.

A.3.6.7 SRS Evaluations. As a final assessment of the validity of the computed SRS results, the following evaluation criteria are recommended

(1) The SRS results should be considered invalid at those natural frequencies where the SRS computed for the background noise discussed in Section A.3.6.4 is less than 6 dB below the pyroshock SRS.

(2) The SRS results should be considered invalid at those natural frequencies where the SRS computed for the inert or freely suspended accelerometer discussed in Section A.3.6.5 is less than 6 dB below the pyroshock SRS.

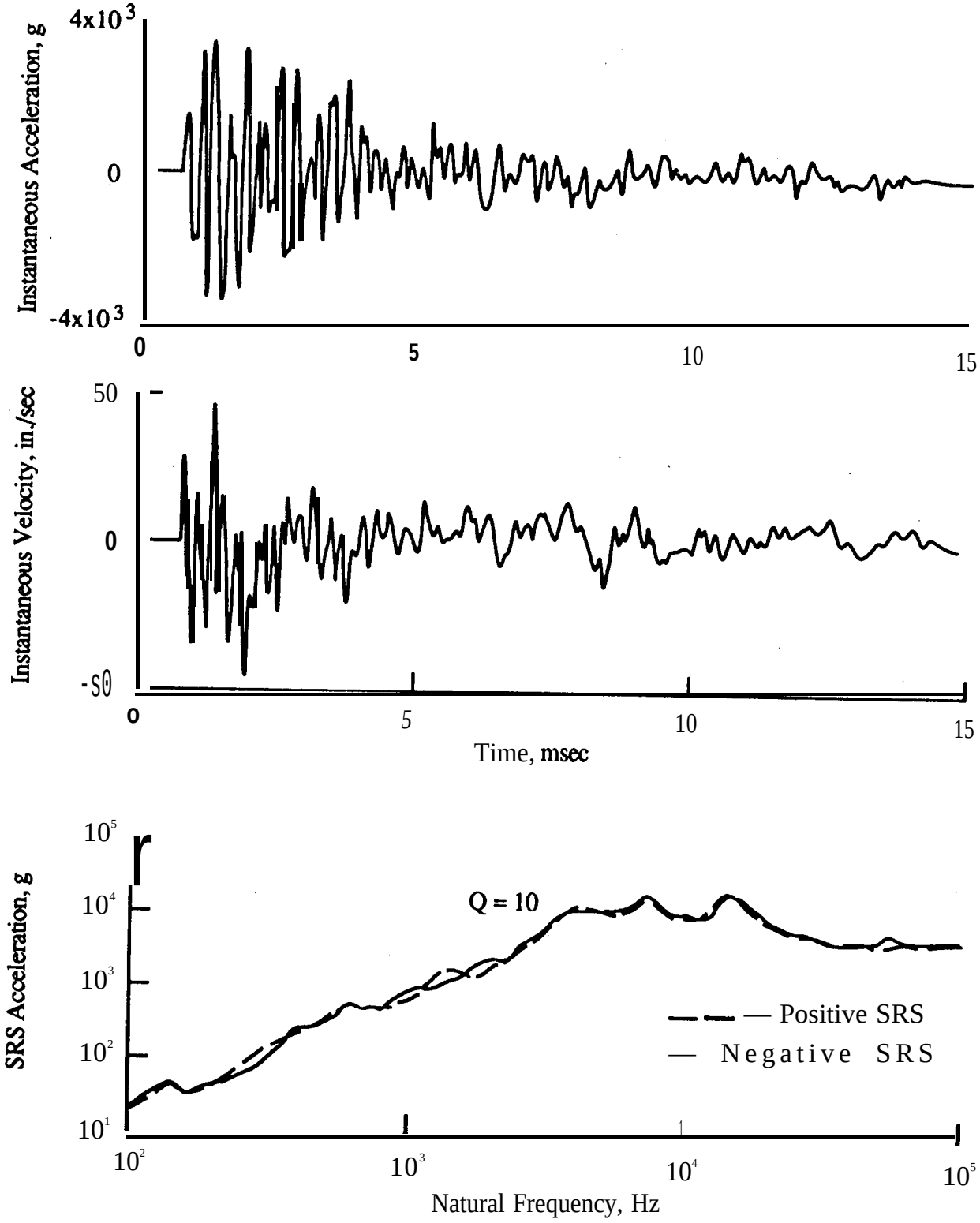

Figure A. 11. Pyroshock Acceleration and Velocity Signals, and Positive and Negative Acceleration Shock Response Spectra for Valid Data (Courtesy McDonnell-Douglas Astronautics Company, St. Louis, MO).

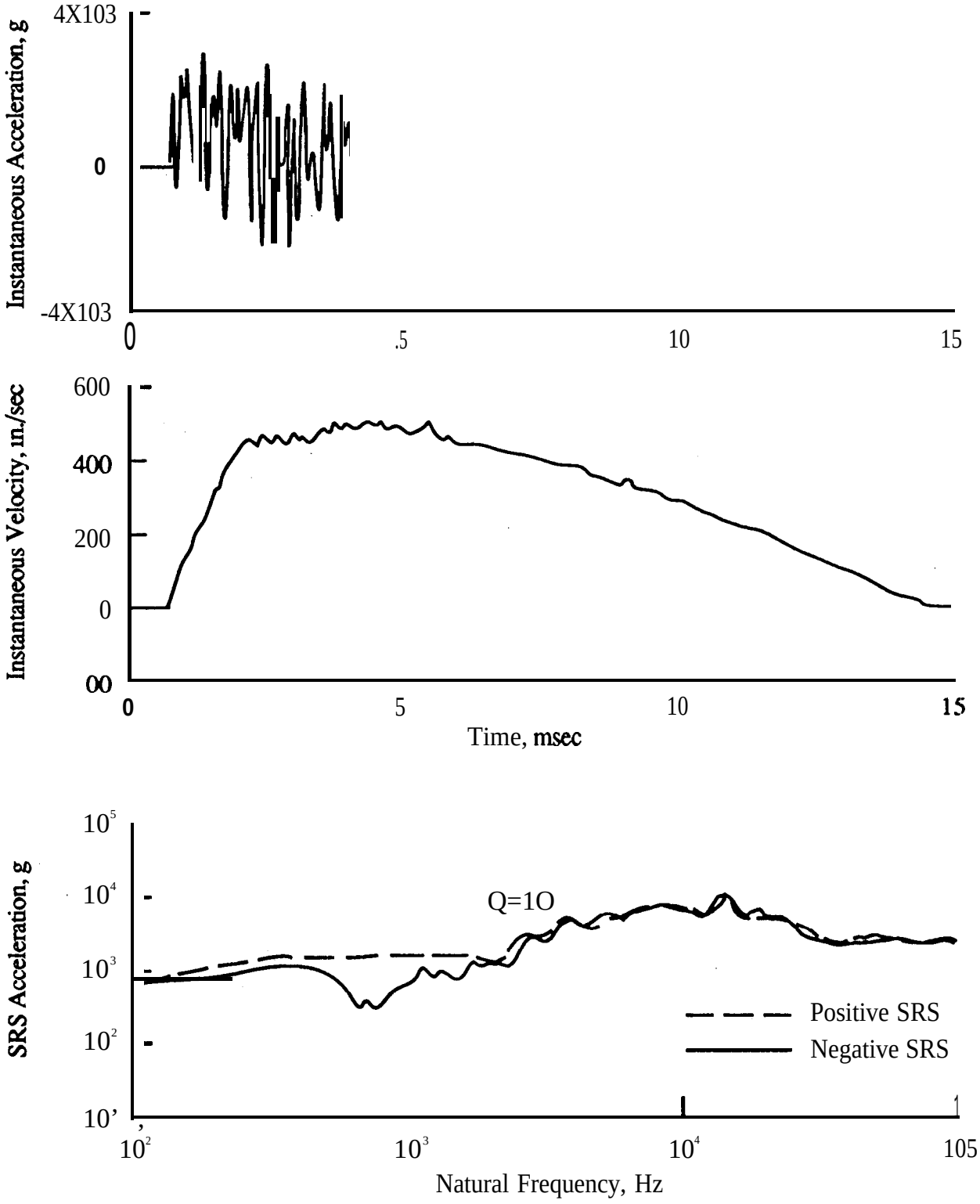

Figure A.12. Pyroshock Acceleration and Velocity Signals, and Positive and Negative Acceleration Shock Response Spectra for Invalid Data (Courtesy McDonnell-Douglas Astronautics Company, St. Louis, MO).

(3) The SRS results should be considered invalid at all natural frequencies if the slope of the SRS at frequencies well below the first normal mode of the structure is significantly less than 6 dB/ octave. See Figure A. 12 for an illustration and [A.32] for details.

A.4 Other Pyroshock Measurement Procedures. As noted in the Section A. 1, accelerometers are widely used for the measurement of pyroshocks, primarily because of their convenience, even though they can introduce serious problems when used for near-field pyroshock measurements. However, there are other types of transducers that might be used in place of accelerometers for near-field measurements. The three most common alternatives are as follows:

(1) Strain gages (see Section 3.2.8) can be used to measure intense, near-field pyroshocks with few problems [A.4, A.33], and are recommended when the actual surface strain in a structure is of interest. However, surface strain measurements on a structure are difficult to translate into the orthogonal motions needed to arrive at design and test criteria for equipment mounted on that structure.

(2) Laser Doppler vibrometers (see Section 3.2.6,2.2) constitute an attractive alternative to accelerometers for laboratory pyroshock measurements in that they (a) directly measure motion, (b) make no physical contact with the structure, and (c) have no resonance problems. Laser vibrometers have been successful y used to measure pyroshocks within 1 inch of the source, where the shock magnitude exceeds 80,000 g (see Figure A.2 and [A.7]). Some laser vibrometers directly measure velocity (e.g., [A.34]), while others measure displacement (e.g., [A.35]). In either case, an acceleration signal can be obtained, if desired, by differentiating a velocity signal once or a displacement signal twice, Of course, laser vibrometers cannot be used in flight experiments, or other experiments where there is not a firm, motionless location for the laser source and receiver.

(3) Magnetic velocity pickups (see Section 3.2.6.2.1) have been used successfully for high frequency impact measurements [A.36], and might be useful for pyroshock measurements at frequencies well above the magnetic suspension frequency of the transducer moving element. They can be used in both laboratory and flight experiments, and require very little support electronics because they self-generate a signal with a low source impedance. Magnetic velocity pickups directly generate a velocity signal, but this can be differentiated to obtain an acceleration signal, if desired. On the other hand, magnetic velocity pickups are mechanical devices with potential resonance problems that can be troublesome.

A.5 References.

A.1 Kalbfleisch, K, C., "Review Of Pyre-Shock Generating Devices And Source Levels", *Proc., Inst. Envir. Se.,* Pyrotechnic Shock Tutorial Session, 1985.

A.2 Moening, C. J., "Views Of The World Of Pyroshock", *Shock and Vibration Bull., No. 56,* Pt *3,* pp. *3-28, 1986.*

A.3 Walton, W. S., "Shock Measurement During Ballistic Impact Into Armored Vehicles", *Shock and Vibration Bull., No. 50,* Pt *2,* pp. 45-55, 1980.

A.4 Neubert, V. H., and Parker, R. P., "Timewise Outputs of Pyrotechnic Bolts", *Shock and Vibration Buff., No. 44,* Pt 1, pp. 101-110, Oct. 1973.

A.5 Walton, W. S., "Propagation of Ballistic Shock in a Flat Steel Plate", *Proc., 61st Shock and Vibration Symp.,* Vol. 3, pp. 181-190, Oct. 1990..

A.6 Galef, A, E., "The Pre-Pulse In Pyroshock Measurement And Analysis", *Shock and Vibration Bull., No. 56, Pt. 3,* pp. 29-32, 1986.

A.7 Valentekovich, V. M., and Goding, A, C., "Characterizing Near Field Pyroshock With a Laser Doppler Vibrometer", *Proc., 61st Shock and Vibration Symp.,* Vol. II, pp. 205-221, Oct. 1990.

A.8 Eller, E. E., and Whittier, W. H., "Piezoelectric And Piezoresistive Transducers", Ch. 12, *Shock And Vibration Handbook,* 3rd ed. (Ed: C. M. Harris), McGraw-Hill, NY, 1988.

A.9 Bendat, J. S., and Piersol, A. G., *Random Data: Analysis And Measurement Procedures,* 2nd cd., Wiley, NY, 1986.

A.1O Powers, D, R., "Charge Amplifier Characteristics When Subjected To Pyrotechnic Shock", *MDAC Report TM-TMHK-ENV-R7484,* McDonnell Douglas Astronautics Co., Huntington Beach, CA, 14 Jan. 1987.

A l1 Chu, A., "Zero-Shift of Piezoelectric Accelerometers in Pyroshock Measurements", *Shock and Vibration Bull., No. 57,* Pt I, pp. 71-80, 1987,

A.12 Hollowell, W., and Smith, S., "In-Plane Shock Response Measurement", *Proc., 61st Shock and Vibration Symp.,* Vol. H, pp. 223-232, 1990.

A.13 Powers, D. R., "Pyroshock Instrumentation", *Proc., Spacecraft Dynamic Environment TIM,* Vol. II, Presentation No. 24, JPL, Pasadena, CA, Sept. 1989.

A.14 Wilson, J. S., "Accelerometers For Pyroshock Measurements", *Proc., Inst. Envir. Se., pp. 263-267, 1986.*

A.15 Smith, J. S., "Effects of Variables Upon Pyrotechnically Induced Shock Response Spectra", *Vol. 1- NASA TP-2603,* May 1986, *Vol. 2- NASA TP-2872, Nov. 1988.*

A.16 Wilson, J. S., "State-Of-The-Art Accelerometer Characteristics For Pyrotechnic Shock Measurement", *Shock and Vibration Bull., No. 56, Pt 3,* pp. 71-73, 1986.

A.17 Sill, R. D., and Leonhardt, P. M., "Instrumentation For Measuring Pyroshock", *Proc., Inst. Envir. Se.,* Pyrotechnic Shock Tutorial Session, 1985.

A.18 Galef, A. E., "Zero-Shifted Accelerometer Outputs", *Shock and Vibration Bull., No. 56, Pt 3, pp. 77-80, 1986.*

A.19 Galef, A. E., "Some Successes and Caveats in Massaging Pyroshock Data", *Proc., Spacecraft Dynamic Environment TIM,* Vol. II, Presentation No. *30,* JPL, Pasadena, CA, Sept. 1989.

A.20 Chu, A., "A Shock Amplifier Evaluation", *Proc., Inst. Envir. SC..* pp. 708-719, 1990.

A.21 Broth, J. T., *Mechanical Vibration and Shock Measurements,* 2nd ed., p. 126, Bruel & Kjaer, Naerum, Denmark, 1984.

A,22 Bateman, V. I., Bell, R. G., and Davie, N. T., "Evaluation of Shock Isolation Techniques for Piezoresistive Accelerometers", *Proc., 60th Shock and Vibration Symp., Pt* 1, pp. 273-292, Nov. 1989.

A.23 "Telemetry Group, Range Commanders Council, Telemetry Standards", *IRIG Std 106-93,* Jan. 1993.

A.24 Rubin, S., "Pyrotechnic Shock", *Shock and Vibration Bull., No. 56, Pt 3,* pp. 1-2, 1986.

A.25 Jacobsen, L. S., and Ayre, R. S., *Engineering Vibrations,* McGraw-Hill, NY, 1958.

A.26 Rubin, S., "Concepts In Shock Data Analysis", Ch. 23, *Shock and Vibration Handbook,* 3rd ed. (Ed: C. M. Harris), McGraw-Hill, NY, 1988,

A.27 PierSol, A. G., "Evaluation Of The Harpoon Missile Shock Environment During Ejection Launch By Aircraft Launchers", *NWC TP-5880*, Naval Weapons Center, China Lake, CA, Jan. 1977.

A.28 Baca, T. J., "Alternate Shock Characterization for Consistent Shock Test Specification", *Shock and Vibration Bull., No. 54, Pt 2,* pp. 109-130, 1984.

A.29 Landerville, J. B., and Urashima, K. P., "Accelerometer Bonding Study", *Proc., 12th Aerospace Testing Seminar,* pp. 95-105, Mar. 1990.

A.30 Nelson, D. B., "Effect of Filter Frequency Response on Pyroshock Data Analysis", *Proc., Spacecraft Dynamic Environment TIM,* Vol. 2, pp. 255-283, The Aerospace Corp., El Segundo, CA, June 1990.

A.31 Vellutini, G. A., and Wright, C. P., "Knowledge-Based Systems For Test Data Acquisition/Reduction", *Proc., 11th Aerospace Testing Seminar,* pp. 85-103, Ott, 1988..

A.32 Smallwood, D. O., "The Shock Response Spectrum At Low Frequencies", *Shock and Vibration Bull., No. 56, Pt* 1, pp. 279-287, 1986.

A.33 Evans, M. J., Neubert, V. H., and Bement, L. J., "Measurement, Data Analysis, and Prediction of Pyrotechnic Shock from Pin-Pullers and Separation Joints", *Shock and Vibration Bull., No. 57, Pt 2,* pp. 121-133, Jan. 1987.

A.34 Valentekovich, V. M., Navid, M., and Goding, A. C., "Laser Doppler Vibrometer Measurements of Pyrotechnically Induced Shock", *Proc., 60th Shock and Vibration Symp.,* Pt 1, pp. 259-271, Nov. 1989.

A.35 Lieberman, P., Czajkowski, J., and Rehard, J., "Optical System for Measurement of Pyrotechnic Test Accelerations", *J. IES,* Vol. XxXV, No. 6, pp. 25-39, Nov./Dec. 1992.

A.36 Walton, W. S., "New Ballistic Shock Protection Requirement for Armored Combat Vehicles", *Proc., 61th Shock and Vibration Symp.,* Vol. 1, pp. 299-309, 1989.

APPENDIX B
NONSTATIONARY RANDOM VIBROACOUSTIC DATA ANALYSIS

B.1 Introduction. Referring to Section 5.4.4 in the main text, the spectral analysis of individual nonstationary signals is relatively straightforward if the signals are deterministic (e.g., a sine wave with a slowly varying magnitude and/or frequency). Specifically, repeated FFTs can be computed over short, contiguous time segments with no averaging (BT = 1) to obtain a meaningful time-varying spectrum of the signal [B. 1]. However, this approach is not applicable to the spectral analysis of nonstationary random signals, because statistical sampling (random) errors occur that require BT >> 1 to obtain an accurate spectral estimate at a specific frequency and time. For aero-acoustic data, which are commonly analyzed with specified resolution bandwidths (i.e., 1/3 octave bands), this requirement introduces a conflict between a time resolution bias error and the random error in the 1/3 octave band spectral estimates at specific center frequencies and times. For vibration data, which are usually analyzed in terms of narrowband auto- (power) spectra, a third error is involved, namely, a frequency resolution bias error. The goal in the spectral analysis of nonstationary random vibroacoustic data is to select analysis parameters that will provide an acceptable compromise between the bias and random errors in the resulting spectral estimates.

Before proceeding with any analysis of a nonstationary random signal representing vibroacoustic data, it is important to identify and separate nonstationary events produced by different physical mechanisms. This matter is discussed in Section B.2. The recommended spectral representation for nonstationary random vibroacoustic signals is the maximax spectrum, which is defined in Section B.3. Procedures for computing the maximax spectra for nonstationary random vibro-acoustic signals are recommended in Sections B.4 and B .5. Alternate nonstationary random data analysis procedures are outlined in Section B.6.

B.2 **Nonstationary Time Intervals**. Referring to Section 4.2.2, the first step in nonstationary data analysis is to identify and separate nonstationary events in the data that are due to different physical mechanisms. Of special importance is the identification of "transients" events, as defined in Section 5.3.1.4. Transient data should be analyzed by the procedures detailed in Section 5.5. Even after removing transients, the remaining data may involve a sequence of nonstationary events due to widely different physical phenomena. For example, the launch of a space vehicle generally reveals three primary events producing nonstationary vibroacoustic data due to time-varying random excitations, as follows:

(a) The acoustic pressures generated by the rocket motors during lift-off.
(b) The fluctuating pressures generated by shock wave-boundary layer interactions during transonic flight.
(c) The fluctuating pressures generated by the turbulent aerodynamic boundary layer during flight through the region of maximum dynamic pressure (max q).

In most cases, it is desirable to analyze individual nonstationary events separately. In some cases, only a single maximax spectrum (defined in the next section) for the entire nonstationary environment is desired. Such judgments depend on the end application of the data analysis, and should be resolved prior to the data analysis,

B.3 Maximax Spectrum. The recommended spectral representation for nonstationary vibroacoustic data is a spectrum that defines the maximum spectral value in each frequency resolution bandwidth during the nonstationary event, independent of when the maximum value occurs. Such a spectral description, referred to hereafter as the maximax spectrum, generally will not represent the instantaneous spectrum of a measurement at any specific time [B.2]. However, since aerospace structure and equipment failures tend to be frequency-dependent, the maximax spectrum does provide a conservative measure of the dynamic environment from the viewpoint of its damage potential to structures and equipment. This assumes, of course, that the unit impulse response functions of the exposed structures and equipment decay rapidly compared to the underlying time variations of the nonstationary environment, i.e., the nonstationary environment is not "transient", as defined in Section 5.3.1,4. Transient dynamic data should be analyzed and described by the procedures detailed in Section 5.5 and Appendix A.

It should be mentioned that the maximax spectrum for a nonstationary vibroacoustic load is often interpreted for design and testing purposes as the autospectrum of an equivalent stationary load that would produce the same responses of exposed structures and equipment as the maximum of the nonstationary load at each frequency. However, the maximum nonstationary load at each frequency occurs only momentarily. Since structure and equipment failure mechanisms are commonly related to the duration of a dynamic load, as well as its spectral magnitude, there is clearly a problem in properly relating the damage potential of nonstationary vibroacoustic loads to stationary design and test criteria. The resolution of such issues is beyond of the scope of this Handbook.

B.4 Nonstationary Aeroacoustic Data Analysis. Stationary aeroacoustic data are usually analyzed in 1/3 octave bands and presented in terms of sound pressure or fluctuating pressure levels in dB (both referred to hereafter as SPL), i.e.,

$$L_x(f_i) = 10 \log \left[\frac{\psi_x(f_i)}{\psi_{ref}} \right]^2 ; \; i = 1, 2, \ldots \qquad \text{(B.1)}$$

where

f_i = 1/3 octave band center frequency (in Hz)

$L_x(f_i)$ = SPL (in dB) in 1/3 octave band centered at f_i

$\psi_x(f_i)$ = rms value of acoustic or fluctuating pressure (in Pa or psi; 1 Pa = 1.45×10^{4} psi) in 1/3 octave band centered at f_i [note that $\psi_x(f_i) = \sigma_x(f_i)$ since $\mu_x = 0$]

ψ_{ref} = rms value of standard reference pressure (in air) = 20 μPa = 2.90×10^{-9} psi

A similar equation relates the overall SPL, denoted by L_x, to the overall rms value of the acoustic or fluctuating pressure, ψ_x.

For the case of nonstationary random aeroacoustic measurements, a time-varying spectrum of the SPL is usually estimated from a running average of the mean square pressure in each 1/3 octave band to obtain a time-varying rms value given by

$$\hat{\psi}_x(f_i,t) = \left[\frac{1}{T}\int_{t-\frac{T}{2}}^{t+\frac{T}{2}} x^2(f_i,t)\,dt\right]^{\frac{1}{2}} \tag{B.2}$$

where the hat (A) denotes "estimate of", and $x^2(f_i,t)$ is the instantaneous squared value of the signal passed by the ith 1/3 octave band filter. From [B.3], this time-varying estimate of the rms value in each 1/3 octave band involves a time resolution bias error and a random error, which can be approximated in normalized terms by

$$\text{Bias error: } \varepsilon_b\left[\hat{\psi}_x(f_i,t)\right] = \frac{b[\hat{\psi}_x(f_i,t)]}{\psi_x(f_i,t)} \approx \frac{T^2}{48}\,\frac{d^2[\psi_x^2(f_i,t)]/dt^2}{\psi_x^2(f_i,t)} \tag{B.3}$$

where

$\hat{\psi}_x(f_i,t)$ = estimate of $\psi_x(f_i,t)$

$b\left[\hat{\psi}_x(f_i,t)\right] = E\left[\hat{\psi}_x(f_i,t)\right] - \psi_x(f_i,t)$ = bias error of estimate $\hat{\psi}_x(f_i,t)$

$d^2[\psi_x^2(f_i,t)]/dt^2$ = second derivative of $\psi_x^2(f_i,t)$ with respect to t

and

$$\text{Random error: } \varepsilon_r\left[\hat{\psi}_x(f_i,t)\right] = \frac{\sigma[\hat{\psi}_x(f_i,t)]}{\psi_x(f_i,t)} \approx \frac{1}{2\sqrt{B_i T}} \tag{B.4}$$

where

$\sigma\left[\hat{\psi}_x(f_i,t)\right]$ = standard deviation of estimate $\hat{\psi}_x(f_i,t)$

B_i = bandwidth (in Hz) of 1/3 octave band centered at f_i ($B_i \approx 0.23\, f_i$)

T = averaging time of analysis (in sec)

The approximation for the time resolution bias error in Equation (B.3) generally reaches a maximum when the rms value reaches a maximum [B.3]. Also, it is clear from the random error in Equation (B.4) that therms value estimates will be least accurate in the lowest 1/3 octave band, since it has the smallest bandwidth B_i.

From Equation (B.4), if the random aeroacoustic signal king analyzed were stationary, all 1/3 octave band levels could be computed with any desired degree of accuracy by simply increasing the averaging time T. On the other hand, for nonstationary signals, increasing T will increase the time resolution bias error approximated in Equation (B.3). This is illustrated in Figure B. 1, which dis-

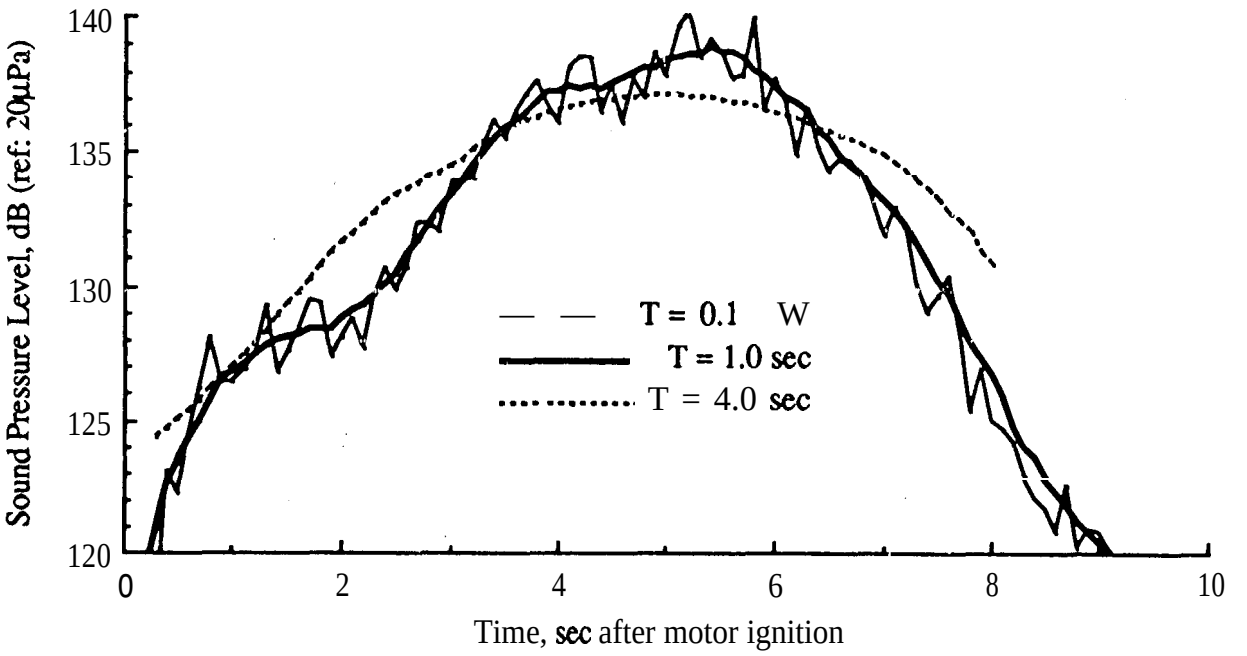

Figure B. 1. Ruining Averages of Overall SPL Inside Titan IV Payload Shroud During Lift-Off.

plays the running average of the overall SPL measured inside the Titan IV payload fairing during lift-off, where the SPL is computed with three different averaging times.It is seen in Figure B. 1 that an averaging time of T = 0.1 sec produces an excessive random error, while T = 4.0 sec produces a clear bias error that causes the maximum SPL to be underestimated. The averaging time of T = 1.0 sec appears to provide a reasonable compromise between these bias and random errors. In more quantitative terms, the total mean square error for a time-varying rms value estimate can be formulated by summing the squares of the errors defined in Equations (B.3) and (B.4). That averaging time To that will minimize this total mean square error in the estimated 1/3 octave band' rms values is derived in [B.3] to be

$$T_{0i} \approx \left[\frac{144}{B_i C_T(f_i,t)}\right]^{0.2} \tag{B.5}$$

where

$$C_T(f_i,t) = \left[\frac{d^2[\psi_x^2(f_i,t)]/dt^2}{\psi_x^2(f_i,t)}\right]^2 \tag{B.6}$$

and all other terms are defined in Equations (B.3) and (B.4). Note in Equation (B.5) that T_{0i} varies inversely with the 0.2 power of B_i, which means the optimum averaging time is not very sensitive to the variations in the 1/3 octave bandwidth. For the overall rms value of the signal, Equation (B.5) still applies, except the bandwidth term B_i is replaced by an equivalent overall bandwidth B_s given by [B.3]

$$B_s \approx \frac{\left[\int_0^\infty \overline{G}_{xx}(f)\,df\right]^2}{\int_0^\infty [\overline{G}_{xx}(f)]^2 df} \approx \frac{\left[\overline{\psi_x^2}\right]^2}{\int_0^\infty [\overline{G}_{xx}(f)]^2 df} \tag{B.7}$$

where $\overline{G}_{xx}(f)$ and $\overline{\psi_x^2}$ are the average autospectrum and mean square value, respectively, of the overall signal x(t) around the time that the rms value reaches a maximum.

The problem in practice is to determine $C_T(f_i,t)$, as defined in Equation (B.6). This term generally varies with time and center frequency, but for space vehicle lift-off aeroacoustic data, $C_T(f_i,t)$ usually reaches a maximum value near the time t_m when the SPL is a maximum, and its variation with frequency is small [B.3]. Hence, to determine an accurate maximax spectrum, a single value of $C_T(t_m)$ can be used in Equation (B.5) for all 1/3 octave bands, where $C_T(t_m)$ is determined from the overall acoustic signal. Appropriate values of $C_T(t_m)$ for the acoustic levels inside the Titan IV payload fairing and the Space Shuttle payload bay during lift-off have been empirically computed in [B.4]. For other launch events and vehicles, or other types of nonstationary acoustic data, $C_T(t_m)$ can be estimated from a running average of the time-varying overall SPL by [B.3]

$$C_T(t_m) \approx \left[\frac{2\pi}{3T_{hp}}\right]^4 \tag{B.8}$$

where 'T_{hp}' is the half-power duration of the maximum in the overall SPL; i.e., the difference in the times before and after t_m when the SPL is 3 dB below the maximum SPL. For example, using the time-varying SPL estimate in Figure B. 1 computed with T = 1.0 see, the 3 dB down points occur at about $t_1 \approx 3.5$ sec and $t_2 \approx 6.5$ see, meaning $T_{hp} \approx 3$ sec. It follows from Equation (B.8) that $C_T(t_m) \approx 0.24$ sec^{-4} for the time-varying SPL inside the Titan IV payload fairing during lift-off.

B.4.1 General Data Analysis proc-, The following procedure is recommended for the analysis of nonstationary aeroacoustic signals in 1/3 octave bands:

(1) For each measurement, compute the time-varying SPL over the nonstationary event of interest in each of the 1/3 octave bands within the desired analysis frequency range using a running average. The running average may be computed by either of the two procedures defined in Section B.4.2. The averaging time should be determined by the procedures detailed in Section B.4.3.

(2) From the time-varying SPL values computed in Step (1), determine the maximum value in each of the 1/3 octave bands, independent of when the maximum value occurs.

(3) Plot the maximum SPL values determined in the individual 1/3 octave bands in Step (2) as a function of the 1/3 octave band center frequency to obtain the **maximax SPL** spectrum.

It should be **emphasized** that the above analysis procedure will not produce valid results if the non-stationary signal includes "transient" events, as defined in Section 5.3.1.4.

B.4.2 Averaging Procedures. Given an analog time history measurement x(t); $O \leq t \leq T_r$, with a mean value of zero, a common way to estimate a running average of the mean **square** value is with a continuous, exponentially-weighted average given by

$$\hat{\psi}_x^2(t) = \frac{1}{K}\int_0^t x^2(\tau)\, e^{-(t-\tau)/K}\, d\tau \qquad \textbf{(B.9)}$$

where K is the averaging time constant. For a digitized measurement **x(nΔt);** n = 1, 2, ... the equivalent of a running average can be computed using a step-wise, unweighed (or linear) average over N data points (T = NAt) given by

$$\hat{\psi}_x^2(\,[iM+(N/2)]\ At\,) \left[= \frac{1}{N}\sum_{n=iM+1}^{iM+N} x^2(n\Delta t)\right] \qquad (B,1O)$$

where i = O, 1,2,... , $(n_s - 1)$, n_s = number of steps, and M = size of the step (the number of data values between each step). For example, if M = 1, a new average is initiated for every new data point (i.e., every At see), producing the closest approximation to a continuous average. If M = N, then a new average is initiated at the end of the previous average (i.e., every NAt see), producing average values over contiguous segments of the signal.

Most data **processing is presently accomplished using digital procedures, so the step-wise linear averaging procedure defined in Equation (B.** 10) is the more commonly **used.**

B.4.3 General Averaging Time Selection Procedure. The desired averaging time for a running or step-wise estimate of the time-varying SPL is that value of K in Equation **(B.9),** or that value of T = NAt in Equation (B. 10), which is as long as feasible without causing a significant time resolution bias error. An optimum value for this averaging time can be determined by the analytical **procedures** summarized in Equations **(B.5)** through (B .8). Otherwise, a near-optimum averaging time can be established by trial-and-error procedures, as follows:

(1) Compute the running or step-wise average of the SPL of x(t) with a very short averaging time relative to the time variations in the average properties of the data.

(2) Recompute the running or step-wise average repeatedly with an incrementally increased averaging time (say by a factor of two) until there is a clear smoothing of the basic trend in the SPL versus time. This operation is demonstrated in Figure B. 1, where the step-wise linear averages are computed with a step size in Equation (B. 10) of M = 0.1 N (O. 1 sec).

(3) That averaging time which just initiates a clear smoothing of the basic trend in the SPL versus time constitutes a good averaging time that approximates the optimum averaging time T_0 for the data analysis outlined in Section B.4. 1, e.g., in Figure B. 1, a good averaging time is about T = 1 sec.

The above operations theoretically should be carried out independently on the filtered signals in each 1/3 octave band of interest, However, in lieu of a time consuming evaluation of all the 1/3 octave band signals, the averaging times for the 1/3 octave band levels can be chosen as follows:

(1) Approximate the optimum averaging time T_0 with a step-wise linear average, or the optimum averaging time constant K_0 with an exponentially-weighted running average, for the overall SPL, as detailed above and illustrated in Figure B. 1.

(2) For the overall and all 1/3 octave bands with center frequencies above 250 Hz, use the averaging time of T_0 or K_0 determined for the overall,

(3) For all 1/3 octave bands with center frequencies at 250 Hz and below, use an averaging time of $2T_0$ or $2K_0$.

(4) For the case of step-wise averages computed from digital data using Equation (B. 10), the recommended step size is M < 0.2N.

The above simplified procedure for selecting 1/3 octave band averaging times is based upon studies of the averaging time needed to minimize the mean square errors in the 1/3 octave band estimates of Titan IV lift-off acoustic measurements relative to the optimum averaging time for the overall value estimates [B.4]. Hence, the recommendations may not be optimal for other launch events or vehicles, or other types of nonstationary acoustic data.

B.4.4 Procedures for Titan IV and Space Shuttle Lift-Off Acoustic Data. For the special case of Titan IV and Space Shuttle lift-off acoustic data analysis, the recommended averaging times for overall and 1/3 octave band SPL estimates are

Overall and all 1/3 octave bands above 250 Hz; $T_0 = 1.0$ or $K_0 = 0.5$
All 1/3 octave bands at 250 Hz and below; $T_0 = 2.0$ or $K_0 = 1.0$ (B.11)

From [B.4], for the Space Shuttle lift-off acoustic data only, a small reduction in the mean square error of sound level estimates can be achieved using an averaging time that is about 50% longer than given in Equation (B. 11). For the case of step-wise averages computed from digital data using Equation @.10), the recommended step size is M < 0.2N. It should be emphasized that the averaging times in Equation (11) are optimal only for Titan IV and Space Shuttle lift-off acoustic data, and may not be appropriate for other launch events and vehicles, or other types of nonstationary acoustic data.

B.5 Nonstationary Vibration Data Analysis, Vibration data are usually analyzed in narrow frequency bandwidths and presented in terms of auto- (power) spectral density functions (autospectra), as defined in Section 5.4.3. As for the 1/3 octave band analysis of nonstationary random aeroacoustic data, a time-varying autospectrum for a nonstationary random vibration signal can be estimated by

$$\hat{G}_{xx}(f,t) = \frac{1}{BT}\int_{t-\frac{T}{2}}^{t+\frac{T}{2}} x^2(t,B,f)\,dt \qquad \text{(B.12)}$$

where $x^2(t,B,f)$ is the instantaneous squared value of the signal passed by a narrow bandpass filter with a bandwidth B centered at frequent y f. The computational analog for Equation (B. 12) is illustrated in Figure B.2.

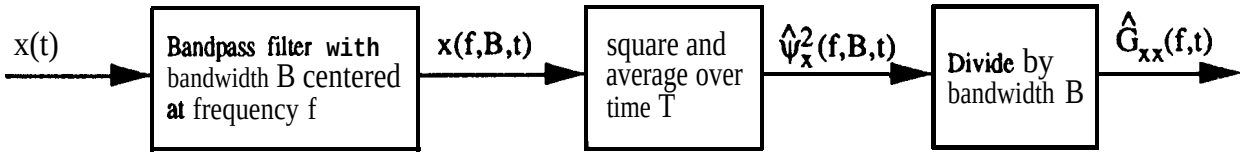

Figure B.2. Procedure for Estimating Time-Varying Autospectral Density Function.

Unlike the analysis of aeroacoustic data in Section B.4 where the resolution bandwidth is specified, the spectral analysis of nonstationary random vibration data involves a selectable bandwidth B that introduces a frequency resolution bias error in the analysis, on top of the time resolution bias and random errors. From [B.3], these errors can be approximated in normalized terms by

Frequency resolution bias error: $$\varepsilon_{b_f}[\hat{G}_{xx}(f,t)] = \frac{b_f[\hat{G}_{xx}(f,t)]}{G_{xx}(f,t)} \approx \frac{B^2}{12(\sim fr)2} \qquad \text{(B.13)}$$

Time resolution bias error: $$\varepsilon_{b_t}[\hat{G}_{xx}(f,t)] = \frac{b_t[\hat{G}_{xx}(f,t)]}{G_{xx}(f,t)} \approx \frac{T^2}{24}\,\frac{d^2[G_{xx}(f,t)]/dt^2}{G_{xx}(f,t)} \qquad \text{(B.14)}$$

Random error: $$\varepsilon_r[\hat{G}_{xx}(f,t)] = \frac{\sigma[\hat{G}_{xx}(f,t)]}{G_{xx}(f,t)} \approx \frac{1}{\sqrt{BT}} \qquad \text{(B.15)}$$

where

$b[\hat{G}_{xx}(f,t)] = E[\hat{G}_{xx}(f,t)] - G_{xx}(f,t)$ = bias of estimate $\hat{G}_{xx}(f,t)$

$\sigma[\hat{G}_{xx}(f,t)]$ = standard deviation of estimate $\hat{G}_{xx}(f,t)$

ζ = damping ratio of structural resonance at frequency f_r

B = frequency resolution bandwidth for the spectral estimate

T = time resolution (averaging time) for the spectral estimate

The approximation for the frequency resolution bias error in Equation (B. 13) applies at those frequencies where the autospectrum displays a sharp peak due to a resonant response of the structure on which the measurement is made, and assumes there is only one resonance within the bandwidth B. The approximation for the time resolution bias error in Equation (B. 14) evolves from the same considerations that produced Equation (B.3), and will generally be a maximum when the spectral density value at each frequency reaches a maximum during the nonstationary event.

Assuming it is the spectral estimates at the resonance frequencies of the vibrating structure that are of greatest concern, the total mean square error is given by the sum of the squares of the normalized errors in Equations (B, 13) through (B. 15). That frequency resolution bandwidth B_0 and averaging time T_0 that will minimize this total mean square error in the estimated autospectral density values are derived in [B.3] to be

$$B_0 \approx 2.29\ C_T^{1/24}(f,t)/C_B^{5/24}(f) \text{ and } T_0 \approx 2.29\ C_B^{1/24}(f)/C_T^{5/24}(f,t) \qquad \text{(B.16)}$$

where

$$C_B(f) \approx \frac{4}{(\zeta f_r)^4} \text{ and } C_T(f,t) = \left[\frac{d^2[G_{xx}(f,t)/dt^2}{G_{xx}(f,t)}\right] \qquad \text{(B.17)}$$

and all other terms are as defined following Equation (B. 15),

The term $C_B(f)$ in Equation (B. 17) is dependent on the damping ratio of each resonant mode of the vibrating structure on which the measurement is made. In practice, however, a single value of damping is usually assumed for all resonant modes of the structure. For aerospace vehicle structures, $\zeta = 0.05$ is recommended.

The term $C_T(f,t)$ in Equation (B. 17) may vary with both time and frequency. However, as for the aeroacoustic data in Section B.4, $C_T(f,t)$ at all frequencies can usually be approximated by a single value $C_T(t_m)$, which is determined from the overall vibration signal at that time t_m when the rms value is a maximum. This term has been determined empirically for the payload vibration levels during lift-offs of the Titan IV and the Space Shuttle in [B.5]. For other launch events and vehicles, or other types of nonstationary vibration data, $C_T(t_m)$ can be estimated from the overall vibration signal using Equation (B.8).

It should be mentioned that the $C_B(f)$ term in Equation (B. 17) is an approximation that is acceptably accurate only for nonstationary random vibrations at frequencies above 20 Hz where the time-variation of the overall value is relatively slow, i.e., from Equation (B.8), $C_T(t_m) < 0.25\ sec^{-4}$, corresponding to a half-power duration of about $T_{hp} \geq 3$ sec. The lift-off vibration environments for Titan IV and Space Shuttle comply with this restriction at frequencies down to f = 20 Hz. However, for other nonstationary random vibration environments where the half-power duration is $T_{hp} < 3$ sec and/or the lowest frequency of interest is f < 20 Hz, Equation (B. 16) may substantially under-estimate the optimum frequency resolution bandwidth B_0, as detailed in [B.6]. For example, if $C_T(t_m) = 20\ sec^{-4}$ ($T_{hp} \approx 1$ see) and f = 20 Hz, B_o = 3.3 Hz as opposed to 1.9 Hz predicted by Equation (B. 16). See [B.6] for a more accurate determination of the optimum spectral analysis parameters for nonstationary random vibration data.

B.5.1 General Data Analysis p r -. The following procedure is recommended for the analysis of nonstationary random vibration data:

(1) For each measurement, compute the time-varying autospectrum over the nonstationary event of interest in each of the analysis bands within the desired analysis frequency range using a running average. The resolution bandwidths should be as recommended in Section B.5.2. The running average can be computed by any of the procedures defined in Section B.5.3. The averaging time should be determined by the procedures detailed in Section B.5.4.

(2) From the time-varying autospectrum computed in Step (l), determine the maximum spectral density value in each of the resolution bandwidths, independent of when the maximum value occurs.

(3) Plot the maximum autospectra values determined in the individual resolution bandwidths in Step (2) as a function of the resolution bandwidth center frequency to obtain the maximax autospectrum.

As an alternate to the above procedure, a rnaximax spectrum can be approximated by a single spectral computation over an averaging interval centered on the time when the overall value of the vibration signal reaches a maximum. The resolution bandwidth and averaging time should be as recommended in Sections B.5.2 and B.5.4. This approach to approximating the maximax spectrum is simpler and requires less computation, but is vulnerable to errors if the time-varying spectral values at some frequencies reach maxima at times outside the selected averaging interval. In any case, it should be emphasized that the recommended analysis procedures will not produce valid results if the nonstationary signal includes "transient" events, as defined in Section 5.3.1.4.

B.5.2 Frequency Resolution Bandwidth. When $C_B(f)$ in Equation (B. 17) is substituted into the expression for B. in Equation (B. 16), it is seen that B.= $(\zeta f)^{5/6}$. Assuming the damping ratios of

all structural resonances are approximately equal, it follows that the optimum bandwidth for the spectral analysis of vibration data is nearly proportional to frequency; i.e., B.= f. From [B.5], assuming $\zeta \approx 0.0$s, the proportional bandwidth that will produce a near-minimum mean square error for the spectral anal ysis of Titan IV and Space Shuttle lift-off vibration data is a 1/12 octave bandwidth (B = 0.058 fHz) modified below 43 Hz to a constant bandwidth of 2.5 Hz; i.e.,

$$f < 43 \text{ Hz}; B_0 = 2.5 \text{ Hz}$$
$$f243 \text{ Hz}; B_0 = 0.058 \text{ f Hz} \qquad \text{(B.18)}$$

Although derived for special cases, it is believed that the bandwidth in Equation (B.18) constitutes a good selection for the analysis of most space vehicle launch vibration data.

B.5.2.1 Proportional Resolution Bandwidth. A spectral analysis with the proportional resolution bandwidth recommended in Equation (B. 18) can be achieved using either a digital filteringalgorithm or an FFT algorithm with frequency averaging, as follows:

(1) If the spectral analysis is performed using a digital filtering algorithm, compute the autospectrum over the averaging time T_0 with the modified 1/12 octave band resolution defined in Equation (B. 18).

(2) If the spectral analysis is performed using an FFT algorithm, compute a raw autospectrum over an averaging time T to obtain a set of discrete spectral components separated by Af = 1/T (this computation should be performed with a rectangular time window; i.e., there should be no tapering of the signal to suppress side-lobe leakage). Then average together adjacent spectral components as required to obtain a frequency resolution bandwidth that approximates the modified 1/12 octave band resolution defined in Equation (B. 18). Due to limitations on the number of values that can be transformed by FFT algorithms (Section 5.4.1,1), it may be necessary to (a) compute frequency averaged autospectra from two or more overlapped segments, each of duration NAt = T < T_0, and (b) ensemble average the autospectra for the overlapped segments to obtain the average autospectrum over T_0.

B.5.2.2 Fixed Resolution Bandwidth. The most common way to compute an autospectrum for vibration data is to use FFT procedures where (a) the time interval of interest is divided into n_d disjoint segments, each of duration T, (b) a raw spectrum is computed for each segment, and (c) the raw spectra are ensemble-averaged to obtain the average autospectrum for the time interval $n_d T$ (see Section 5.4.3). This procedure inherently involves a constant resolution bandwidth; i.e., the resolution bandwidth can be changed only by recomputing the autospectrum with a different segment duration T. It is shown in [B.3] that a spectral analysis "with an acceptable mean square error over a frequency range from 20 to 2,000 Hz can be achieved using three constant bandwidths, namely,

$$
\begin{aligned}
20 \le f < 100\ \text{Hz};\quad & B=3\text{Hz} \\
100 \le f < 400\ \text{Hz};\quad & B=10\text{HZ} \\
400 \le f \le 2{,}000\ \text{Hz};\quad & B=30\text{Hz}
\end{aligned}
\tag{B.19}
$$

In Equation (B. 19), B is the half-power point bandwidth of the spectral window provided by the ensemble averaged FFT analysis, which is a function of the tapering operation used to suppress side-lobe leakage (see Section 5.4.1.3 and [B.7]), e.g., for a Harming taper, $B = 1.44\Delta f = 1.44/T$.

B.5.2.3 Other Frequency Resolution Bandwidth Selections. The spectral analysis of nonstationary vibration data sometimes must be performed in compliance with a Military Standard (e.g., MIL-STD- 1540) or some other governing document, which may specify a resolution bandwidth that is in conflict with the recommendations in Sections B.5.2.1 and B.5.2.2. Also, as discussed in Section 5.4.3,4, the end use of the spectral data may warrant a resolution bandwidth that differs from the recommendations in Sections B.5.2. 1 and B.5.2.2. In such cases, the requirements imposed by the specification or the desired end use of the data should prevail.

B.5.3 Averaging Procedures. The following averaging procedures are recommended to create a ruining average of the time-varying autospectrum for a nonstationary random vibration signal.

(1) For a spectral analysis using digital filters, as described in Section B.5.2.1(1), the averaging operations detailed in Section B.4.2 apply.

(2) For an analysis using a single FFT computation followed by frequency averaging, as described in Section B.5.2. 1 (2), the FFT should be computed over the desired averaging time $T = N\Delta t$. To simulate a running average, the computations should be repeated in a step-wise manner with a new average initiated every 0.2T sec or less; i.e., with $M < 0.2N$ where M is the step size.

(3) For an analysis using conventional FFT computations with ensemble averaging as described in Section B.5.2.2, the total time duration for the ensemble-averaged computations should be $T_0 = n_d T = n_d N\Delta t$. To simulate a running average, the ensemble-averaged computations should be repeated in a step-wise manner with a new average initiated every $0.2 n_d T$ or less; i.e., with M c $0.2 n_d N$ where M is the step size.

B.5.4 General Averaging Time Selection Procedure. When $C_B(f)$ in Equation (B.17) is substituted into the expression for T_0 in Equation (B, 16), it is seen that $T_0 \propto (\zeta f)^{-1/6}$. This means the optimum averaging time is only weakly dependent on the analysis frequency and, hence, a fixed averaging time for the spectral analysis at all frequencies will provide acceptably accurate results (see [B.3] for details), Given a measured nonstationary random vibration signal, the recommended procedure to select this fixed averaging time for a spectral analysis is as follows:

(1) Approximate an optimum averaging time T_0 with a step-wise linear average, or an optimum averaging time constant K_0 with an exponentially-weighted running average, for the overall rms value of the vibration signal using the analytical or trial-and-error procedures detailed in Section B.4.3.

(2) Use an averaging time of 2T0 or $2K_0$ for the spectral computations in all frequency bands.

The above recommendations are based upon studies of the averaging time needed to minimize the mean square errors in autospectra estimates of Space Shuttle lift-off vibration measurements relative to the optimum averaging time for the overall value estimates [B.5]. Hence, the recommendations may not be optimal for other launch events and vehicles, or other types of nonstationary vibration data.

B.5.5 Procedures for Titan IV and Space Shuttle Lift-Off Vibration Data. For the special case of Titan IV and Space Shuttle lift-off vibration data, if a running or step-wise estimate of the rms value for the overall vibration level during lift-off is desired, the recommended averaging time is

$$T_0 = 1 \text{ sec or } K_0 = 0.5 \text{ sec} \tag{B.20}$$

For autospectra estimates, the recommended frequency resolution bandwidths are as detailed in Section B.5.2, and the recommended linear averaging time is derived in [B.5] to be

$$T_0 = N\Delta t \approx 2 \text{ sec} \tag{B.21}$$

With a linear averaging time of T_0 = 2 see, the number of averages required to obtain the desired resolution bandwidth for autospectra estimates computed using FFT procedures are as follows:

(1) For autospectra estimates computed using the frequency averaged FFT procedure in Section B.5.2. 1(2), let the following assumptions apply (see Section 3.7 for definitions and details):

Highest frequency of interest; f = 2,000 Hz
Anti-aliasing filter cut-off frequency; f_c = 2,000 Hz
Nyquist frequency; f_N = 2,500 Hz
Sampling rate; R_s = 5,000 sps
Block size for FFT algorithm; N = 8,192 (p = 13)
Block duration; T = 1.64 sec
Frequency resolution of raw spectral estimates; Af = 0.61 Hz

Under these assumptions, a spectral analysis with a *2* sec averaging time will require two overlapped FFTs, each with a duration of 1.64 sec (8, 192 data points), and an overlap of

1,28 sec (6,400 data points). For the raw autospectrum computed from each of the two FFTs, the number n_k of adjacent spectral components centered at frequency f_k that should be averaged together is as follows:

$$f_k < 43\ \text{Hz},\ n_k = 4$$
$$f_k \geq 43\ \text{Hz},\ n_k = 0.058\, f_k\, T = 0.095\, f_k \qquad \text{(B.22)}$$

where n_k should be rounded off to the next highest frequency. For example, at f_k = 20, 250, and 2,000 Hz, n_k = 4, 24, 191, respectively. The two frequency averaged spectra should then be ensemble averaged to obtain the final autospectrum estimate for the 2 sec duration.

(2) For autospectra estimates computed using the ensemble-averaged FFT procedure in Section B.5.2.2, the number n_d of disjoint signal segments in each frequency range that should be averaged together is as follows:

$$20 \leq f < 100\ \text{Hz}\ (B = 3\ \text{Hz});\ n_d = 6$$
$$100 \leq f < 400\ \text{Hz}\ (B = 10\ \text{Hz});\ n_d = 20 \qquad \text{(B.23)}$$
$$400 \leq f \leq 2{,}000\ \text{Hz}\ (B = 30\ \text{Hz});\ n_d = 60$$

If overlapped processing procedures are used to compute ensemble-averaged autospectra estimates (see Section 5.4.3.7), the number of FFT computations will be larger than the value of n_d in Equation (B.23) by a factor of 1/(1 - P), where P is the fractional portion of overlap.

It should be emphasized that the averaging time and number of averages recommended in Equations (B.20) through (B.23) are optimal only for Titan IV and Space Shuttle lift-off vibration data, and may not be appropriate for other launch events and vehicles, or other types of nonstationary vibration data.

For the case of step-wise averages computed from digital data using Equation (B. 10), the recommended step size is M < 0.2N for the digital filtering and FFT frequency averaging procedures in Section B.5.2.1, or M < $0.2 n_d N$ for the FFT ensemble averaging procedure in Section B.5.2.2. As an alternate to the step-wise averaging procedure, a maximax spectrum can be approximated by a single spectral computation over an averaging interval centered on the time when the overall value of the vibration signal reaches a maximum. However, this simplified analysis approach is vulnerable to the errors discussed in Section B.5. 1.

B.6 Alternate Nonstationary Data Analysis Procedures. Beyond the running (or step-wise) averaging techniques covered in Sections B.4 and B.5, there are other approaches to the analysis of nonstationary random acoustic and vibration data, including (a) curve fitting techniques (regression analysis) using time-dependent polynomial functions. and (b) special analysis procedures using

parametric models [B.3]. Curve fitting techniques are based upon classical regression analysis procedures that can substantially reduce estimations errors, but they tend to be computationally intensive and require considerable skill in selecting an appropriate order for the analysis. An application of the curve fitting analysis procedure to the computation of the time-varying overall sound level inside a Titan IV Payload Fairing during lift-off is presented in [B.3].

The most common parametric model used for the analysis of nonstationary launch vehicle acoustic and vibration data is the "locally stationary" model [B.8], which allows the computation of a time-varying spectrum to be decomposed into two separate operations, one to define the time-varying mean square value of the signal, and the other to define the spectral properties of the signal. Specifically, the time-varying mean square value of the signal is computed using the entire signal bandwidth, meaning the averaging time can be made short without causing a large random error. Conversely, the basic spectral character of the signal is computed using the entire signal duration, meaning the frequency resolution bandwidth can be made small without causing a large random error. A parametric model tailored to provide an optimum spectral analysis of Space Shuttle launch vibration data during lift-off, transonic flight, and max "q" flight is detailed in [B.9].

B.7 References.

B.1 Bendat, J. S., and Piersol, A. G., *Random Data: Analysis and Measurement Procedures,* 2nd cd., Wiley, NY, 1986.

B.2 Piersol, A. G., "The Analysis of Nonstationary Vibration Data", *NASA CP-2488,* Vol. 1, pp. 3-25, Oct. 1987.

B.3 Bendat, J. S., and Piersol, A. G., *Engineering Applications of Correlation and Spectral Analysis,* 2nd cd., Wiley, NY, 1993.

B.4 Piersol, A. G., "Optimum Data Analysis Procedures for Titan IV and Space Shuttle Payload Acoustic Measurements During Lift-Off', *JPL Subcontractor Report 99.50-136S,* Jet Propulsion Laboratory, Pasadena, CA, Dec. 1991.

B.5 PierSol, A. G., "Optimum Data Analysis Procedures for Titan IV and Space Shuttle Payload Vibration Measurements During Lift-Off", *JPL Subcontractor Report 9950-1372,* Jet Propulsion Laboratory, Pasadena, CA, Feb. 1992.

B.6 PierSol, A. G., "Optimum Parameters for the Spectral Analysis of Nonstationary Random Vibration Data", *Proc., 64th Shock and Vibration Symp.,* Vol. 1, pp. 379-388, Oct. 1993.

B.7 Harris, F. J., “On the Use of Windows for Harmonic Analysis with the Discrete Fourier Transform”, *Proc., IEEE,* Vol. 66, pp. 51-83, Jan. 1978.

B.8 Silverman, R. A., "Locally Stationary Random Processes’, Trans. *IEEE, Info. Theory,* Vol. IT-3, p. 182-187, Sept. 1957.

B.9 Himelblau, H., and Piersol, A. G., “Evaluation of a Procedure for the Analysis of Nonstationary Vibroacoustic Data”, *J. Inst. Envir. Sc.,* Vol. XXXII, No. 2, pp. 35-42, Mar./Apr. 1989.

INDEX

Accelerometer, 37,41,63
installation, 77,262, 273
mass correction, 60
piezoelectric, 63
piezoresistive, 70
phase shift, 40,
pyroshock applications, 261,272
servo, 72
variable capacitance, 72
Aeroacoustic noise, 8,45,288
Aliasing, 136
anti-aliasing filters, 137,234,268
errors, 137
Amplifiers, see signal conditioners
Analog-to-digital converters, 133
aliasing, 136
anti-aliasing filters and errors, 137
cut-off frequency, 137,234,268
digital formats, 134
dynamic range, 134
instruments, 133
magnitude errors, 138
multiple channel, 140
Nyquist (folding) frequency, 136
oversampling, 138
phase errors, 138, 140, 141
Anti-aliasing falters, 137,234
pyroshock applications, 268,276
Autospectrum, 218
analysis errors, 220
analysis procedures, 218
data editing applications, 186
nonstationary data, 224,294
zoom transforms, 224
Average values, 203
averaging time and sampling errors, 204
running averages, 204, 289, 292, 294
synchronous averaging, 174$205

Base strain, 58,265

Cabling, 103
Calibration, 16, 141
end-to-end electrical, 144
end-to-end mechanical, 72, 148
laboratory, 141
linearity, 152
signal, 144
step, 151
Clipping, 170, 184
Coherence, 241
analysis errors, 242
analysis procedures, 241
calibration applications, 143
Communication links, 121
FDM telemetry, 122
land lines, 121
PCM telemetry, 121
radio frequency telemetry, 121
Cross-axis sensitivity, 41,274
Cross-correlation, 246
analysis errors, 246
analysis procedures, 246
Cross-spectra, 237
analysis errors, 239
analysis procedures, 237
data editing applications, 143

Data analysis, 201
dual channel analysis, 237
FFT algorithms, 211
nonstationary data, 224,287,291
periodic data, 214
single channel, 210
stationary random data, 218
time histories, 201
transient data, 227, 277,283, 2%

Data classifications, 207
identification of events, 165,287
nonstationary trends, 168, 194
nonstationary versus transient, 208
periodic components, 165,193,209
randomness, 165, 209
Data editing, 189,276
corrections for instrument noise, 189
removal of noise spikes, 190
removal of signal drop-outs, 191
removal of spurious trends, 191
Data recording, 123,268,275
ancillary signals, 130
data capacity, 124
environmental degradation, 131
frequency response, 124
recording modes, 125
tape copying, 131
tape storage, 131
Data validation, 165,276
identification of physical events, 165
visual inspection of analog time histories, 170
visual inspection of analyzed data, 184
visual inspection of digital time histories, 181
Digital-to-analog converters, 141
Drop-outs, 180, 186, 191
Dynamic range, 10, 134

Electrodynamic transducers, 30
Electro-optical transducers, 30,283
Energy spectrum, 229
analysis errors, 230
analysis procedures, 229
Environmental effects, 46
contamination, 57
corrosion, 56
humidity, 56, 132
radiation, 57
static pressure, 54
temperature, 46, 132
thermal shock, 54
vacuum, 54, 132
vibroacoustics, 58
Errors, 15
autospectrum analysis, 220
budgets, 15
coherence analysis, 241
ems-correlation analysis, 247
cross-spectrum analysis, 238
energy spectrum analysis, 230
Fourier spectrum analysis, 229
frequency response analysis, 244
line spectrum analysis, 216
major causes, 18
shock spectrum analysis, 234,279
time delay bias, *239*

Filters, 100,206
anti-aliasing applications, 137,234
mechanical, 102, 267, 274
pyroshock applications, 267,268
Flutter compensation, 119, 130
Force transducers, 92
piezoelectric, 93
strain gage, *88*
Fourier spectrum, 227
Frequency resolution, 214
autospectrum analysis, 220
coherence analysis, 242
cross-spectrum analysis, 239
energy spectrum analysis, 230
Fourier spectrum analysis, 229
frequency response analysis, 244
line spectrum analysis, 216
shock response spectrum analysis, 235
Frequency response function, 243
analysis errors, 244
analysis procedures, *243*

Gaussian distribution, see normal distribution
Grounding, 105, 272
Guard band, 107

Headroom, 11,268

Inclusions and exclusions, 1
Intermittent noise, 174, 184,190
IRIG standards, 18, 107-130

Leakage and tapering, 212
  autospectral analysis, 220
  coherence analysis, 241
  cross-spectral analysis, *238*
  energy spectral analysis, 230
  Fourier spectral analysis, 228
  frequency response analysis, 244
  line spectral analysis, 215
Log sheets, 155

Maximax spectrum, 288
Mean square value, 203,289
Mean value, 203
Mechanical filters, 102,267,274
Microphone, 43
  capacitive, 29
  electret, 29
  piezoelectric, 83
  piezoresistive, 83
Modulation, 107
  ADARIO, 118
  frequency (FM), 107
  pulse amplitude (PAM), 117
  pulse code (pCM), 112
Modulation index, 112
Multi-channel measurement 14, 140
Multiple path (reverberation) errors, 240,242
Multiplexers and demultiplexers, 106
  frequency division (FDM), 107,119
  time division (TDM), 107, 112, 119

NIST tractability, 141
Nonstationary data, 194,208,224,287
Normal distribution, 210,250
  spurious deviations from, 184,210
  test for, 210
Nyquist (folding) frequency, 136

1/3 Octave band spectrum, *226,288*
Overlapped processing, 192,223
OverSampling, 138

Parametric procedures, 250
  nonstationary data analysis, 301
  spectrum analysis, 250
Peak probability density, 249
Periodic data, 165,210,214
  calibration applications, 146, 150
  identification, 165, 193,209
Phase shift, 40, %
  anti-aliasing falters, 138,234
  calibration applications, 143
Physical properties, 59
  size, 59
  stiffness, 62
  weight, 60
Planning, 3
  data events, 3, 168,287
  dynamic range, 10, 134
  error budgets, 15
  frequency range, 9
  headroom, 11
  instrumentation systems, 3
  measurement duration, 13
  measurement locations and directions, 7
  multi-channel measurements, 14
  number of measurements, 7
  telemetry, 3
  time codes, 15
Power line pickup, 176, 186
Power spectral density, see autospectrum

Pressure transducers, 43,82
condenser microphones, 83
electret microphone, 84
installation, 84
metallic and piezoresistive gages, 83
piezoelectric microphones, 83
piezoresistive transducers, 83
Probability density, 248
data editing applications, 174,184,193
normal (Gaussian), 210
Proportional bandwidth analysis, 225
Pyroshock, 259
acquisition and analysis problems, 260
recommended procedures, 269,271
transducers, 283

Random data, 165,209
Record keeping, see log sheets
Recorders, 123
hard Copy, 201
magnetic tape, 123
Recording modes, 125
Regression analysis, 153
calibration applications, 153
removal of spurious trends, 191
Root-mean-square (rms) value, 203
nonstationary data, *289*

Sensing element, 25
capacitive, *29*
electrodynamic, 30
electro-optical, 30
other, 30
piezoelectric, 25
servo control, 30
strain sensitive, 25
Shields, 106
Shock response spectrum, 231
analysis errors, 234
analysis procedures, 231
pyroshock applications, 277
recommended presentation, 233
Signal conditioners, 94
amplifiers, 96
cabling, 103
filters, 100
power supplies, 95, 103
pyroshock applications, 265,275
strain gage conditioners, 94
Signal enhancement, 205
Signal-to-noise ratio, 10
analog-to-digital converters, 134
FDM telemetry, 122
synchronous averaging, 206
Single-degree-of-freedom system, 31
Sinusoidal data, see periodic data .
Slew limiting, 96
Spurious trends, 178, 183, 191
Standard deviation, 203
Stationarity, 194,207
Stationary random data analysis, 218
Strain gage, 86
conditioners, 94
frequency limits, 38
installation, 90
load cell application, 88
structural applications, 46,86
transducer applications, 90
System gain settings, 153

Tape recorders, see recorders
Tape speed control, 119, 130
Telemetry, 3, 121
Time codes, 15, 130,225
Time delay bias error, 239
coherence analysis, 242
cross-correlation analysis, 246
cross-spectrum analysis, 239
frequency response analysis, 245
multiple path, 240

Transducers, 25
base strain, 58
environmental effects, 46
magnitude characteristics, 39
phase shift, 40
physical properties, 59
sensitivity, 35
transverse (cross-axis) sensitivity, 41
useful frequency range, 36
Transfer function, see frequency response function
Transverse sensitivity, 41
mechanical filters, 267,274
Triboelectric noise, 104

Unit impulse response, 248

Velocity transducers, 37,73
electrodynamics, 30
installation, 77
laser Doppler, 74
pyroshock applications, 283

Whetstone bridge, 28
calibration, 28
strain gage applications, 94,99
Wild points, 182, 186, 190

zoom transforms, 224
autospectrum analysis, 221,224
coherence analysis, 243
cross-spectrum analysis, 241
frequency response analysis, 245